WIND ATLAS FOR EGYPT

Measurements and Modelling 1991-2005

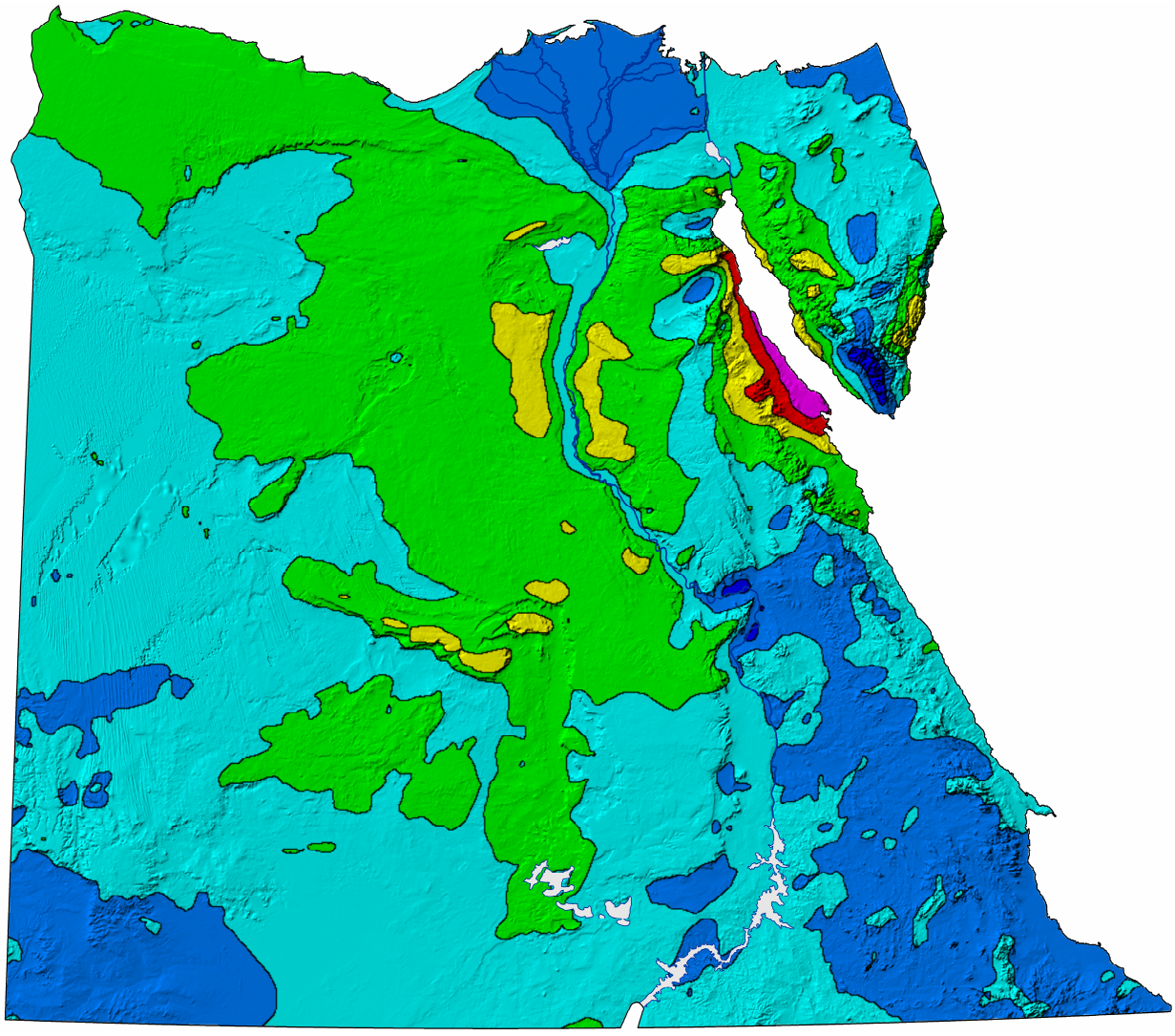

New and Renewable Energy Authority
Egyptian Meteorological Authority
Risø National Laboratory

Cairo and Roskilde
December 2005

WIND ATLAS FOR EGYPT

WIND ATLAS FOR EGYPT

Measurements and Modelling 1991-2005

Niels G. Mortensen (editor)
Jens Carsten Hansen
Jake Badger
Bo H. Jørgensen
Charlotte B. Hasager

RISØ NATIONAL LABORATORY

Laila Georgy Youssef
Usama Said Said
Ashour Abd El-Salam Moussa
Mohammad Akmal Mahmoud

NEW AND RENEWABLE ENERGY AUTHORITY

Ahmed El Sayed Yousef
Adel Mahmoud Awad
Mahmoud Abd-El Raheem Ahmed
Mohamed A.M. Sayed
Mohamed Hussein Korany
Metwally Abd-El Baky Tarad

EGYPTIAN METEOROLOGICAL AUTHORITY

Roskilde
December 2005

The Wind Atlas for Egypt 1991-2005 is a result of the Egyptian-Danish project *Wind Atlas for Egypt*. The Danish contribution to this project and the publication of the atlas are funded by the Danish Ministry of Foreign Affairs through Danida.

The sample wind resource map on the front cover shows the mean wind speed at 50 m above ground level over Egypt, see the Atlas for details. The elevation map on the back cover was constructed from Shuttle Radar Topography Mission data.

Printed by Pitney Bowes Management Services Danmark A/S.

ISBN 87-550-3493-4
Printed in Denmark 2006

Table of Contents

Executive summary

The Wind Atlas for Egypt presents the results of a comprehensive eight-year wind resource assessment programme covering the entire land area of Egypt. The aim of the programme has been to establish the meteorological basis for the assessment of the wind energy resources all over Egypt, in particular in six designated regions: the Northwest Coast, the Northeast Coast, the Gulf of Aqaba, the Gulf of Suez, the Red Sea and the Western Desert.

The main objective has been to provide reliable and accurate wind atlas data sets for evaluating the potential wind power output from large electricity-producing wind turbine installations. In addition, the Wind Atlas provides an overview of the Egyptian wind resource based on mesoscale modelling – as well as data and some guidelines for the meteorological aspects of the detailed siting of large and small wind farms.

The study employs wind speed and direction measurements taken in the period 1991 to 2005 at 22 wind atlas stations located in most parts of Egypt. In addition, data from eight standard meteorological stations have been analysed. The twenty-two 25-m masts were erected specifically for the wind study, but provide information on other climate characteristics as well: atmospheric pressure, solar insolation, air temperature, air temperature gradient, atmospheric stability, wind speed profiles, extreme wind speeds, gust and lull wind speeds and turbulence intensity.

The wind data from the 30 stations are analysed using the Wind Atlas Analysis and Application Program (WAsP), following the procedures and guidelines of the European Wind Atlas (Troen and Petersen, 1989). The roughness (land-use) of the terrain has been assessed from topographical maps, aerial photographs, satellite imagery, as well as during site visits. The height variations of the terrain – used for assessing the influence of the orography on the wind measurements and wind climate estimations – are described in digital terrain models, which have been obtained by digitisation of standard topographical maps or have been generated from Shuttle Radar Topography Mission elevation data. The magnitude of the regional wind climate at the locations of the 30 stations is shown in the figure overleaf.

In addition to the measurements, the wind climate of Egypt has been modelled using the Karlsruhe Atmospheric Mesoscale Model (KAMM). Maps of the predicted mean wind speed and power density at 50 meters above ground level are presented, as well as maps and data describing the regional wind climate of Egypt. The KAMM simulations capture the main features of the observed wind climate; even though the mean wind speed and energy flux density are sometimes under-predicted.

The Atlas updates and details our view of the wind-climatological conditions over Egypt and provides a consistent and coherent picture of the variation of the wind resource over the country and adjoining sea and land areas. The coloured map overleaf is an example of a wind resource map of Egypt, based on mesoscale modelling; it shows the mean wind speed in metres per second at a height of 50 m above the actual land surface. It should be borne in mind that the horizontal resolution in this map is 7.5 km, so it only shows the wind resource in broad outline and terrain features on a smaller scale may give higher wind speeds locally.

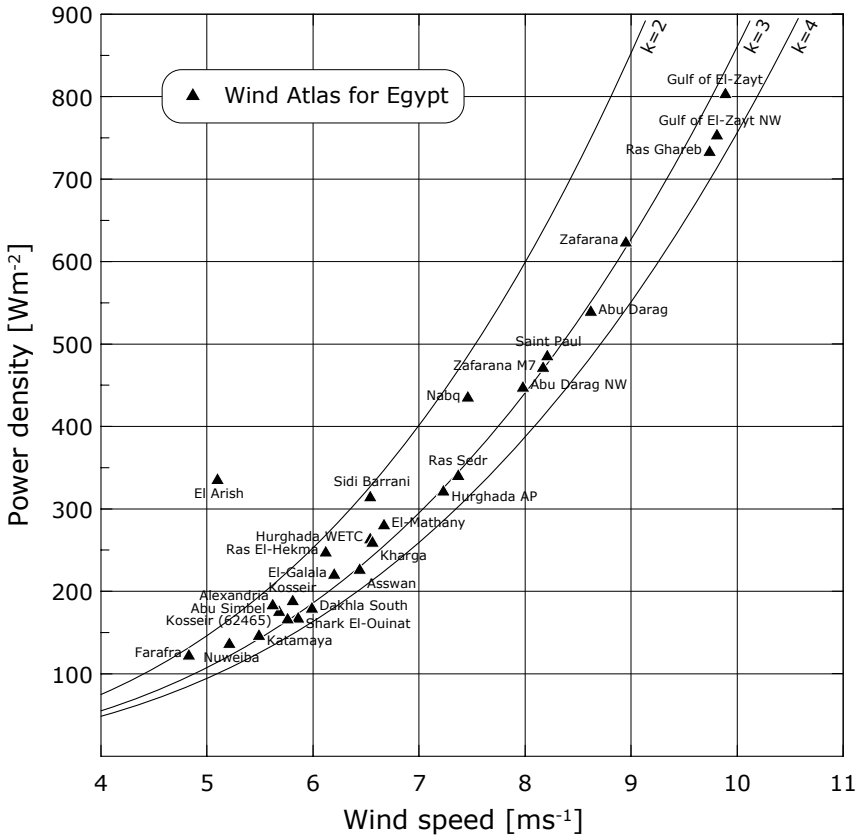

Mean wind speeds and power densities at a height of 50 m above ground level over roughness class 1 (z_0 = 0.03 m) for 30 stations in the Wind Atlas for Egypt.

The Wind Atlas for Egypt confirms the existence of a widespread and particularly high wind energy resource along the Gulf of Suez. With mean wind speeds and mean power densities of 7–10.5 ms^{-1} and 350–900 Wm^{-2}, respectively, estimated for a height of 50 m over roughness class 1 (roughness length of 0.03 m), the wind resources are comparable to those of the most favourable regions in NW-Europe. The resources, however, are not evenly distributed over the region and large horizontal gradients in the wind resource have been found. The magnitude and variation of the wind resource in this region has been verified by comparison to the wind measurements.

The Wind Atlas further indicates that the wind energy resource in large regions of the Western and Eastern Desert – in particular west and east of the Nile valley between 27°N and 29°N, but also north and west of the city of Kharga – are much higher than hitherto assumed. The mean wind speeds predicted here are between 7 and 8 ms^{-1} and the power densities between 300 and 400 Wm^{-2}. There are no meteorological stations for verification in these regions; however, comparisons elsewhere in the Western Desert of predictions derived from the mesoscale modelling to those derived from measurements suggest that the mesoscale model is indeed able to resolve and predict the wind resource in this type of terrain.

Parts of the Sinai Peninsula also feature relatively high wind energy resources, in particular along the coast of the Gulf of Aqaba and along the mountain ridge to the west of the Ajmah Mountain (Gebel El Tih). These local maxima in the wind resource have not been verified directly from measurements because of the lack of meteorological stations in the interior of Sinai.

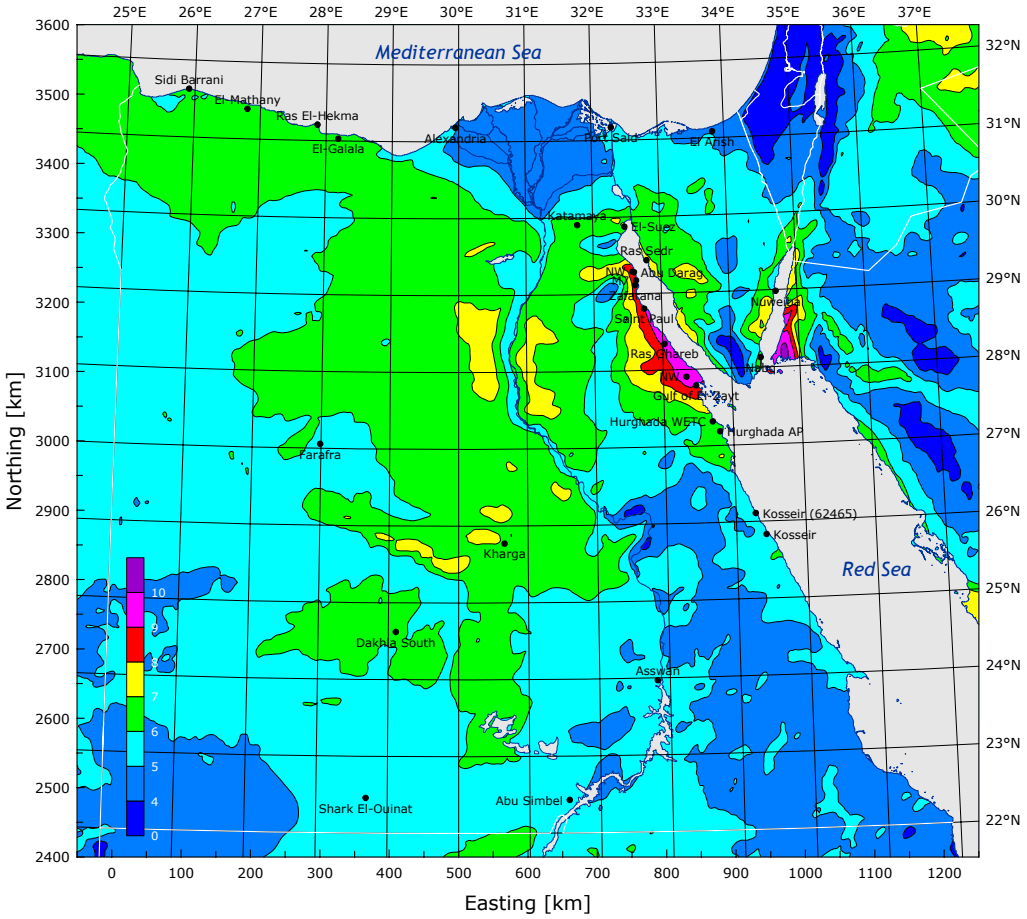

The predicted wind climate over Egypt determined by mesoscale modelling. The map shows the mean wind speed in [ms^{-1}] at a height of 50 m over the actual land surface. Black dots show the locations of the meteorological stations used for the Atlas.

The north-western part of the Mediterranean coast, from Sallum to Alexandria, seems to be a region of somewhat lower wind resource than was previously assumed. The highest resource is likely to be found on the coastal hills and escarpments and further along the escarpment that constitutes the north-western rim of the Qattara Depression. Likewise, the coastal tracts of the Red Sea region seem less windy than was hitherto assumed.

Finally, the existence of a large, windy region in the south-westernmost part of the Western Desert (the Gilf Plateau) has not been confirmed. This has not been verified by measurements at ground level in the region due to logistical difficulties in erecting and operating a meteorological station in this remote, mountainous area.

The Wind Atlas for Egypt represents a significant step forward in the application of the wind atlas methodology in Egypt. Not only does it provide a coherent and consistent overview of the wind resource over the entire land (and sea) area of Egypt, the results of the mesoscale modelling are further available in a database (numerical wind atlas) that may be employed for detailed wind resource assessment and siting of wind turbines and wind farms. Utilising this database together with elevation maps derived from Space Shuttle radar measurements and land-use maps constructed from satellite imagery, the actual wind resource and likely power production of a given wind farm can be estimated in a matter of hours – anywhere in Egypt.

Application of the numerical wind atlas for any site in Egypt consists of the following steps: First, the regional wind climate is extracted from the database of wind atlas data sets provided by the Atlas. These data sets are available with a resolution of about five km for all of Egypt and can be employed directly with the WAsP model, which is the software that calculates the predicted wind climate and power production. Secondly, an elevation map of about 20×20 km^2 is constructed from Shuttle Radar Topography Mission data; these are also readily available for all of Egypt. Thirdly, a land-use (roughness length) map is constructed from a topographical map or satellite imagery, e.g. Google Earth. Finally, the climatological, topographical and site-specific wind turbine data are entered into the WAsP software, which is then able to calculate the predicted wind climate and estimated wind farm power production.

The numerical wind atlas methodology will not meet bankable accuracy in resource estimates, but will typically provide good indications of the geographical distribution of the wind resource and will also be very useful for decision making, identification of future measurement sites, and planning of feasibility studies and of actual project preparation.

In regions where wind measurements are available at a nearby meteorological station, the exact same procedure can be carried out, but in this case using the wind atlas data set from the meteorological station instead of the data set from the numerical wind atlas. A database of wind atlas data sets based on measurements at the 30 stations of the Wind Atlas has been established as part of the project. This observational wind atlas methodology will provide reliable resource estimates provided it is applied following up-to-date engineering practices.

The wind atlas methodology, originally developed for wind resource assessment and siting in Europe, has proven useful, even in the extreme climatic conditions of the desert. Applied with care, and further employing the results of the mesoscale modelling, it can provide reliable predictions of the wind climate at candidate sites for wind turbines and wind farms all over Egypt. An even higher degree of reliability may be obtained in the six regions that have been investigated in detail and where wind measurements have been collected at the meteorological stations. The experience obtained can be used in other places with a similar climatology and geography.

The reliability of wind power calculations based on the statistics in the Wind Atlas for Egypt depends on the reliability of the data from the particular station from which the statistics have been derived, i.e. on the quality of the data and the amount of information available. Secondly, it depends on the complexity of the terrain at the meteorological station as well as at the sites of interest. Finally, the temporal and geographical variability of the wind resource will necessarily add to the uncertainty of the estimates, even if this variation can be taken into account by employing the results of the mesoscale model.

Preface and acknowledgements

The *Wind Atlas for Egypt – Measurements and Modelling 1991-2005* is the result of an investigation of the climatic wind conditions over the entire land area of Egypt.

The investigation was conducted from January 1998 to the date of publication by the New and Renewable Energy Authority, the Egyptian Meteorological Authority and Risø National Laboratory – under the sponsorship of the governments of Egypt and Denmark.

The Atlas is an attempt to provide an updated overview of the wind-climatological conditions of Egypt, based on reliable wind data and using contemporary models. It further seeks to provide an up-to-date methodology for applying the data and model results for the purpose of wind resource assessment.

The Atlas concludes and reports on the findings of a comprehensive wind resource assessment programme – known as the *Wind Atlas for Egypt* project – which has had three main components:

- Component A: Wind Atlas for the Gulf of Suez (NREA and Risø)
- Component B: Preliminary Wind Atlas for Egypt (EMA and Risø)
- Component C: Wind Atlas for Egypt (NREA, EMA and Risø)

In addition to the Wind Atlas for Egypt itself, the results of Component C comprise the following main outputs:

- 11 wind atlas measurement stations in operation
- A database of wind atlas data files in WAsP format
- A database of all meteorological measurements
- Training courses for technicians and professional staff
- A cup anemometer rehabilitation and calibration facility
- Additional hardware for the wind atlas stations, including safety features
- A satellite-based, on-line data transmission system for three stations
- Software packages for wind data analysis and wind flow modelling
- Mesoscale modelling of Egypt and six regions using the KAMM model
- A database of KAMM modelling results

The wind resource assessment programme has been supervised and managed by a Project Implementation Unit (PIU) with representatives from the three organizations involved. At the time of writing, the PIU consisted of Laila Georgy Youssef from NREA, Ahmed El Sayed Yousef from EMA and Niels G. Mortensen from Risø – with Jens Carsten Hansen from Risø acting as PIU secretary. During the course of the project A.M. El-Asrag, Mohamed M. El-Bakry and Rabie S. Foulie have also represented the Egyptian Meteorological Authority in the PIU.

We are indebted to many of our colleagues for their help and support during the course of this project and in finalizing the Atlas. At Risø we would especially like to thank Ole F. Hansen and Anker B. Andersen for designing and manufacturing the meteorological stations, Karen Enevoldsen for implementing and operating the satellite-based data transmission system, Søren W. Lund and Jan Nielsen for training and assistance in instrumenting the stations, Gunnar Jensen for data management and calibration of meteorological sensors, Cyril Nedaud for digitising and quality assurance of some of the station terrain descriptions, and Erik L. Petersen and Ib Troen for permission to publish excerpts from the European Wind Atlas.

The establishment and maintenance of the meteorological stations, the data of which form the very basis of this Atlas, was performed by NREA and EMA professional staff. Special thanks are due to NREA technicians Samir Lashien, Raafat Hendy, Hamed Omar, and Amr Mohammad Moustafa for station maintenance and data retrieval.

Over the years, many more people at NREA, EMA, Risø and elsewhere have made suggestions for improvements of the Atlas, offered constructive criticism of our work, or simply made the task easier through their help and encouragement. While these contributions have all served to enhance and improve the Atlas, the responsibility for any omissions, errors and misinterpretations naturally remains with the authors.

Cairo and Roskilde, December 2005

1 Introduction to the Wind Atlas

The aim of the Wind Atlas for Egypt is to establish the meteorological basis for the assessment of wind energy resources all over Egypt, with special emphasis on those regions where the wind resource is particularly high. The main objective is to provide suitable data for evaluating the potential wind power output from large electricity-producing wind turbine installations. In addition, the Wind Atlas provides data and some guidelines for the meteorological aspects of the detailed siting of large and small wind turbines.

An important characteristic of wind energy is that the power output of a wind turbine is proportional to the third power of the wind speed. Therefore, the precision requirements of wind speed statistics for energy assessments are higher than for most other purposes.

Another noteworthy characteristic of the wind is the seasonal and year-to-year variations of the wind conditions. An accurate determination of wind climatologies must take account of these variations; therefore, several full years of wind data must be used in the analysis.

Hence, the application of wind measurements to wind power calculations demands long time series of high-quality wind data. The main wind atlas stations used for the present study have provided more than ten years of wind data, where a high quality has been secured by wind tunnel calibration of the anemometers and rehabilitation and recalibration of the anemometers at a dedicated calibration facility, see Appendix C.

The wind speed measured at a meteorological station is determined mainly by two factors: the overall weather systems, which often have an extent of several hundred kilometres, and the nearby topography out to a few tens of kilometres from the station. Strictly speaking, the direct use of measured wind speed data for wind resource calculations results in power estimates that are representative only for the actual position of the wind-measuring instruments. The application of measured wind speed statistics to wind energy resource calculations in a region therefore requires methods for the transformation of wind speed statistics.

The representativity and usefulness of the regional wind climates determined by employing the wind atlas methodology may be severely reduced in regions where mesoscale effects become important. In principle, this can be solved by increasing the density of meteorological stations in the region, but in practice this is rarely feasible.

An efficient method of predicting and mapping the regional wind climate in such cases is to combine a mesoscale model with the micro-scale models. The mesoscale model simulates the wind flow over a much larger area; like the flow over and around mountain ranges and in large valleys or the flow over an entire country. The model domain may be large enough to cover e.g. the entire Gulf of Suez and adjoining areas; however, the spatial resolution is only about 5 km and features smaller than this grid size are thus not taken into account. The micro-scale model is therefore used to calculate the speed-up and sheltering by hills, local obstacles, and local roughness conditions, as described above. Such a procedure is described by Frank (2000) and

Frank and Landberg (1997). It is illustrated in detail in Chapter 4, where the Karlsruhe Atmospheric Mesoscale Model (KAMM) is used to model the mesoscale effects on the wind flow over Egypt and over several smaller, regional domains.

The mesoscale model KAMM can thus be combined with the micro-scale model WAsP: KAMM calculates the mesoscale wind field using as input a description of the synoptic-scale climatology, as well as suitable orography and roughness maps. The climatology of the post-processed simulated wind fields and the local orography and roughnesses are subsequently used by WAsP to predict the local wind climate.

The accuracy and reliability of the KAMM-WAsP methodology may be evaluated by comparison to meteorological measurements and observed wind climates at surface stations, see Chapter 6.

1.1 Wind atlas analysis

In the Wind Atlas for Egypt, what has become known as the *wind atlas methodology* has been applied. This comprehensive set of models for the horizontal and vertical extrapolation of wind data and the estimation of wind resources was developed for the analyses presented in the European Wind Atlas (Troen and Petersen, 1989). The actual implementation of the models is now known as the *Wind Atlas Analysis and Application Program* – or WAsP for short, see Appendix D.

The models are based on the physical principles of flows in the atmospheric boundary layer and they take into account the effect of different surface conditions, sheltering effects due to buildings and other obstacles, and the modification of the wind imposed by the specific variations of the height of ground around the meteorological station in question. Figure 1-1 illustrates the use of these models on measured wind data to calculate a regional wind climatology; this is referred to as the *analysis part* and is shown by the up-arrow in Figure 1-1.

The figure also illustrates the so-called *application part* of the methodology, following a procedure in which the regional wind climatologies are used as input to the same models to produce site-specific wind climatologies and, given the power curve of a wind turbine, production estimates. The models are described briefly in Chapter 5. For more detailed information on the models and the WAsP program, the reader is referred to the European Wind Atlas (Troen and Petersen, 1989) and the WAsP User's Guide (Mortensen et al., 2005), respectively.

Regional wind climatologies have been calculated for 18 wind atlas stations, where long-term time-series have been obtained, as well as from 12 stations where only 1-2 years of wind data have been measured. These results are presented in Part III of the Atlas: *Wind climates and wind conditions*. The station locations are shown in Figure 1-2 below and their exact coordinates given in Table 7-1 in Chapter 7.

For each of the 18 reference stations time-series of wind speeds and directions were analyzed, taken every ten minutes or third hour over a period of 3-14 years, between 1991 and 2005. For the short-term stations data were taken every ten minutes over a period of one year, from June 2004 to May 2005.

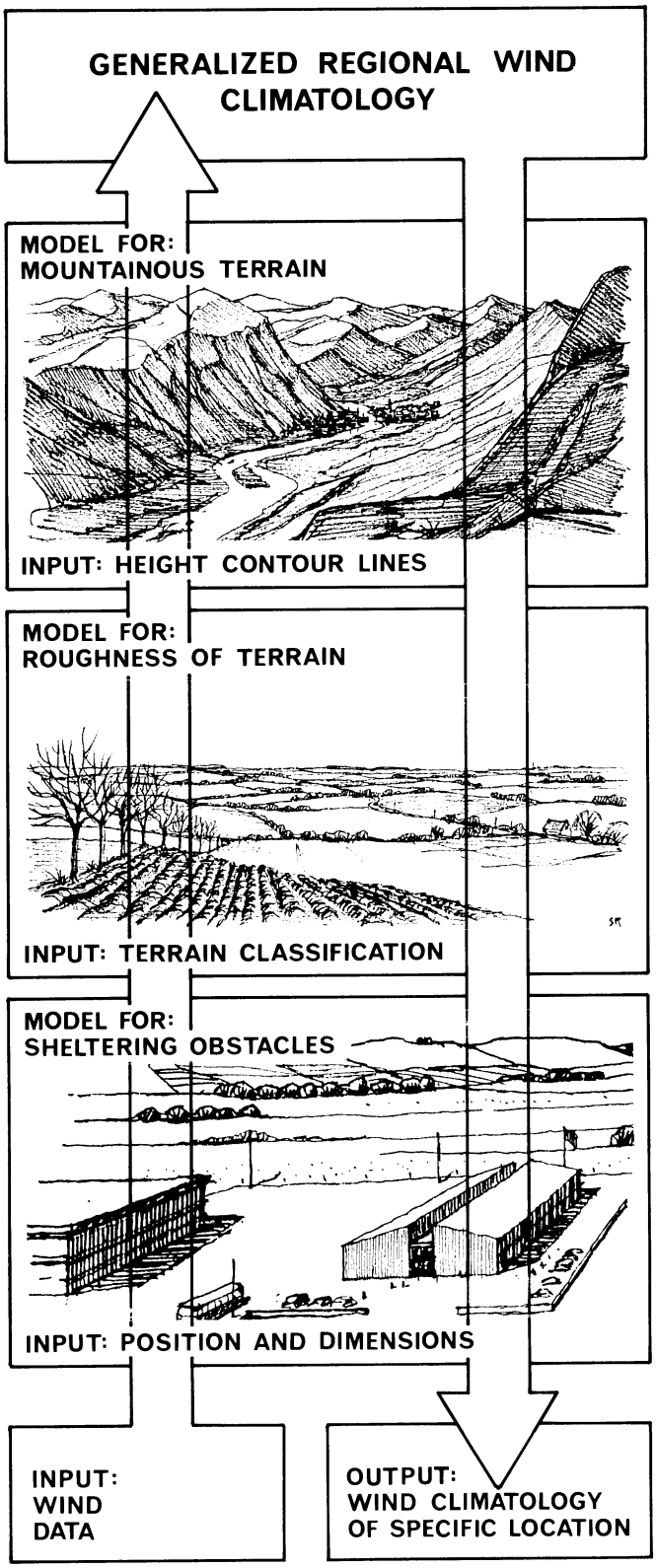

Figure 1-1. The wind atlas methodology of WAsP. Meteorological models are used to calculate the regional wind climatology from the raw data – the analysis part. In the reverse process – the application of wind atlas data – the wind climate at any specific site may be calculated from the regional climatology.

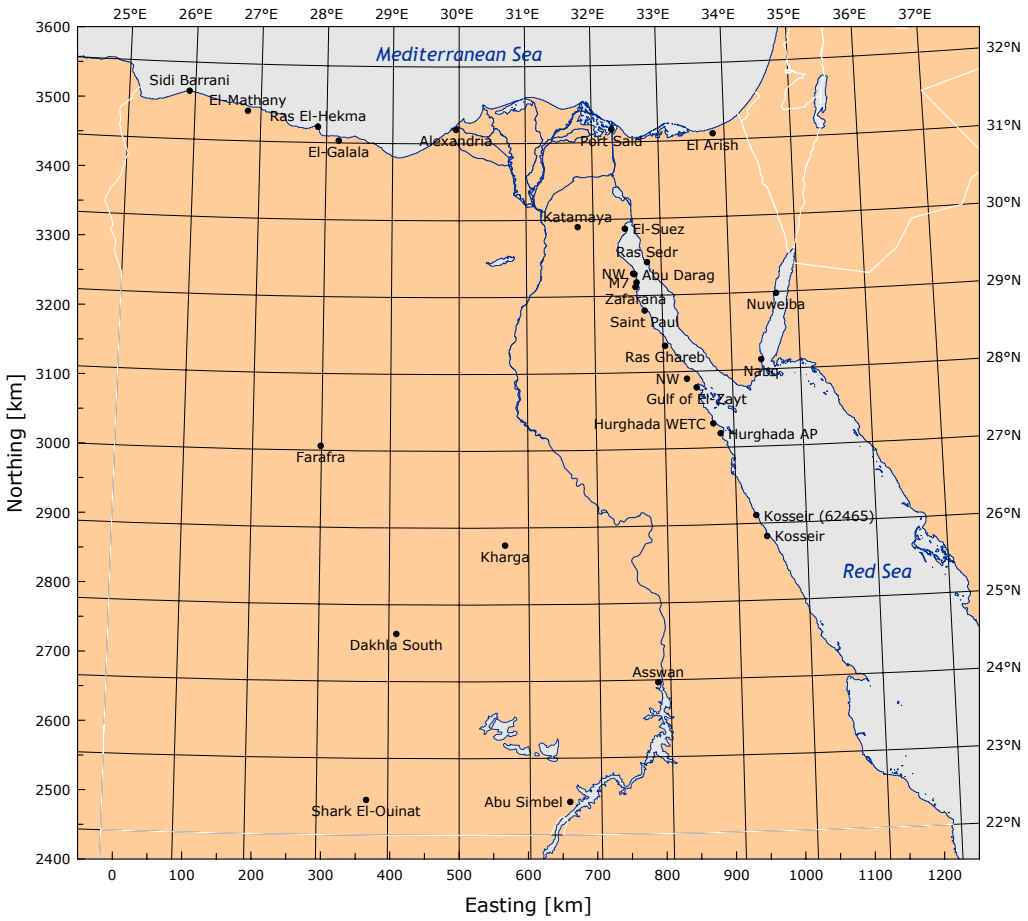

Figure 1-2. Meteorological stations in Egypt. Latitude and longitude, as well as the Cartesian UTM coordinates, are referenced to World Geodetic System 1984 (WGS84).

In addition, accurate descriptions of each station and its surroundings were collected from databases, maps, aerial photographs, satellite imagery and during field trips, which included:

- terrain roughness, i.e. water areas, built-up areas, desert surfaces etc.
- nearby sheltering obstacles, such as buildings
- terrain elevation variations (orography)

For the calculation of regional climatologies, the station descriptions and the models were used to transform the measured data sets of wind speeds and directions from each station to what would have been measured at the location of the station if the surroundings were as follows:

- flat and homogeneous terrain,
- no nearby obstacles,
- and measurements had been taken at heights of 10, 25, 50, 100, and 200 m above ground level.

As an example, one of the transformed data sets represents wind speed and direction distributions at 25 metres above open water.

With four roughness classes and five standard heights, the measured wind data set (observed wind climate) from each station is thus transformed into 20 generalized data sets. These 20 data sets from each of the stations form the basis of the regional wind climatology, because through the transformation procedure the data sets were – to the extent that the models can adequately describe the flow – freed from the influence of local topography to become *regionally representative*.

How regionally representative a transformed data set (the regional wind climate) is depends on the complexity of topography and obstacles surrounding the meteorological station. The representativeness of a station is severely reduced with increasing complexity of the surrounding orography. However, for most of the stations in Egypt the applicability of the wind atlas data to estimate the wind climate of the surrounding regions is not limited by the complexity of the near-by terrain. Here, the representativeness is determined mainly by the spatial variation in the overall wind climate, caused by the large-scale terrain features of Egypt.

While the wind flow aloft may be fairly uniform over distances which are large compared to the size of the study areas, the geography of parts of Egypt like the Gulf of Suez – with mountains reaching more than 1000 m on both sides of the Gulf – and, indeed, the wind measurements themselves, suggest that mesoscale effects play an important role in this area. These effects are not taken into account by the wind atlas models applied in the data analysis and the density of meteorological stations is too low to assess in detail the spatial variation of the wind climate. The transformed statistics from the stations should therefore be applied with care when estimating the wind climate at some distance from the stations – in particular when going inland from the coastal stations, since the gradients in the wind climate are likely to be large perpendicular to the Gulf and to the mountain ranges.

It must be emphasized that the regional wind climates, i.e. the 20 transformed data sets obtained from each station, are based on data measured at low levels, usually at 25 or 10 metres height. Not only might the transformation and use of such data for horizontal extrapolation lead to large uncertainties, but also the transformation up to greater heights is associated with errors. The physical theories which have been used to construct the vertical transformation procedures have proven their validity up to heights of approximately 100 metres through comparisons with data sets from many meteorological towers, situated mostly in temperate climates. In Egypt, large daily variations in the heat flux occur, leading to large variations in atmospheric stability and in the vertical profiles of horizontal mean wind speed. The station situated at the Wind Energy Technology Center (WETC) in Hurghada feature wind measurements at both 10 and 25 metres above ground level (a.g.l.). Although the evidence presented by Mortensen et al. (2003) shows good agreement between measured and modelled data at these two levels, the statistics derived for larger heights are associated with larger uncertainties than the uncertainties pertaining to the measurement level.

The most important statistic to be derived from a wind speed data set for use in wind energy resource estimation is the *probability distribution function*. This is because when this function has been determined for a given site, the calculation of the average yearly power production of any wind turbine installed at the site is only a matter of integrating the product of this function and the power curve of the wind turbine.

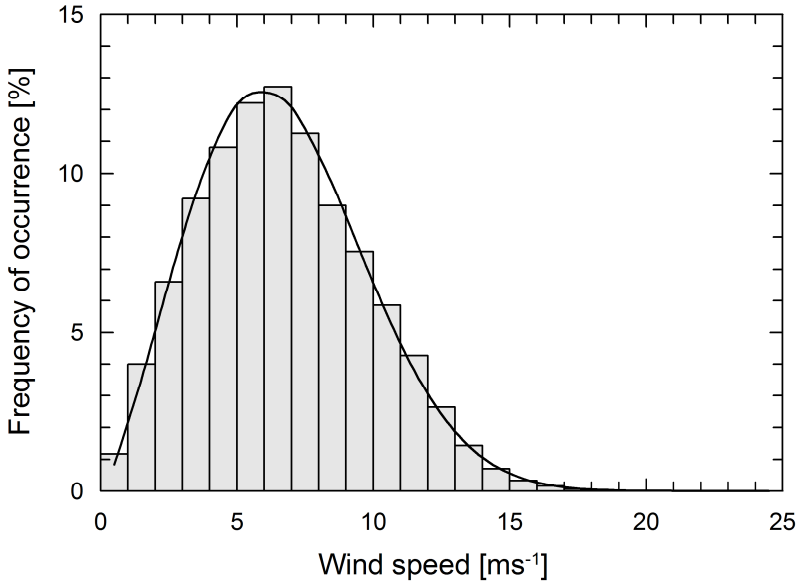

Figure 1-3. Histogram of measured wind speed data and the corresponding fitted Weibull distribution function for the 25-m level at Hurghada WETC, 1992-2001. The Weibull distribution is characterized by two parameters: the scale parameter A is related to the mean value of the wind speed and the shape parameter k determines the shape of the Weibull curve; here A = 7.56 and k = 2.32.

A basic hypothesis of the Wind Atlas is that wind speed data are distributed according to the *Weibull distribution*, which is shown in Figure 1-3 and explained further in Chapter 5. The Weibull distribution usually gives a good fit to observed wind speed data and this has also been found to be true for most of the stations in Egypt. Chapter 7 provides both the raw data histograms and the fitted Weibull distribution curves.

The Weibull parameters fitted to the 20 transformed wind data sets are found in the *Total* columns of the station statistics, see Chapter 7. For the purpose of determining the wind resource at other sites in which the roughness class changes with the wind direction – for example a coastal site – each of the 20 wind data sets has been divided into 12 further data sets according to wind direction. The parameters of the Weibull distribution function fitted to the wind speed/wind direction data sets are also given in the station statistics. Finally, the station statistics include a table with mean wind-speed values and the corresponding mean power density of the wind for four roughness classes and the five standard heights.

The reliability of wind power calculations based on the station statistics in the Wind Atlas for Egypt depends on the reliability of the data from the particular station from which the statistics have been derived, i.e. on the quality of the data and the amount of information available. An appraisal of the data quality for the stations can be made by means of the station descriptions and the figures and tables given in Chapter 7. The meteorological sensors and data acquisition systems used for the Wind Atlas stations are described in detail in Appendix A, including an assessment of the accuracy of the wind speed measurements. Appendix D describes the methodology and facility used for calibration of the wind speed sensors.

1.2 Mesoscale modelling

The conventional method used to produce estimates of the wind resource on national scales is to analyse wind measurements made at a number of sites around the country as in for example the European Wind Atlas (Troen and Petersen, 1989). In order for this method to work there needs to be a sufficient quantity of high quality data, covering the country. This criterion is sometimes difficult to satisfy and therefore other methods are required – methods that will not meet bankable accuracy in resource estimates, but on the other hand that will typically give good indications of the geographical distribution of the wind resource and that will be very useful for decision making and planning of feasibility studies and of actual project preparation.

Numerical wind atlas methodologies have been devised to solve the issue of insufficient wind measurements. One such methodology is the so-called KAMM/WAsP method developed at Risø National Laboratory (Frank and Landberg, 1997).

In this methodology an approach called *statistical-dynamical downscaling* is used (Frey-Buness et al, 1995). The basis for the method is that there is a robust relationship between meteorological situations at the large scale and meteorological situations at the small scale.

Information about the large-scale meteorological situation is freely available from the NCEP/NCAR reanalysis data-set. This data-set has been created by assimilating measurement data from around the globe in a consistent fashion from 1948 to the present day. The primary purpose for the generation of this data-set is to provide a reference for the state of the atmosphere and to identify any features of climate change. Another application of the data set is as a long term record of large-scale wind conditions. The NCEP/NCAR data is used to create around 100 different large-scale wind situations, called wind classes that represent the large-scale wind climate.

In order to make these wind classes meaningful at a smaller scale, a mesoscale model is used to find out how the large-scale wind forcing is modified by regional scale topography. Therefore for each wind class a mesoscale model simulation is performed using the Karlsruhe Atmospheric Mesoscale Model (KAMM, Adrian and Fiedler, 1991).

Post-processing of the results from all the simulations yields a wind resource map at the resolution of the model simulations. Further analysis of the results from the simulations with consideration to the topography as described in the mesoscale model, yields wind atlas maps for generalized surface conditions. Files containing detailed information about the wind speed and direction distributions can also be generated that are directly compatible with the WAsP software, the wind industry standard for site resource assessment calculations.

Creating a numerical wind atlas demands a large computational effort, and this computation effort increases with the size of the region to be mapped. Egypt's large size means that it is not possible to perform the numerical wind atlas calculations for the whole country at a reasonable resolution in one go. Therefore it was decided to split the numerical wind atlas effort into several calculation domains. These domains

have been chosen with assistance from NREA and EMA, so that the principle areas of interest in the country are covered.

The domains used for numerical wind atlas calculation are shown in Figure 1-4. There are six domains: two large Western and Eastern Egypt domains, a Red Sea domain, a Western Desert domain, a Northwest coast domain, and the Gulf of Suez domain from the earlier numerical wind atlas study.

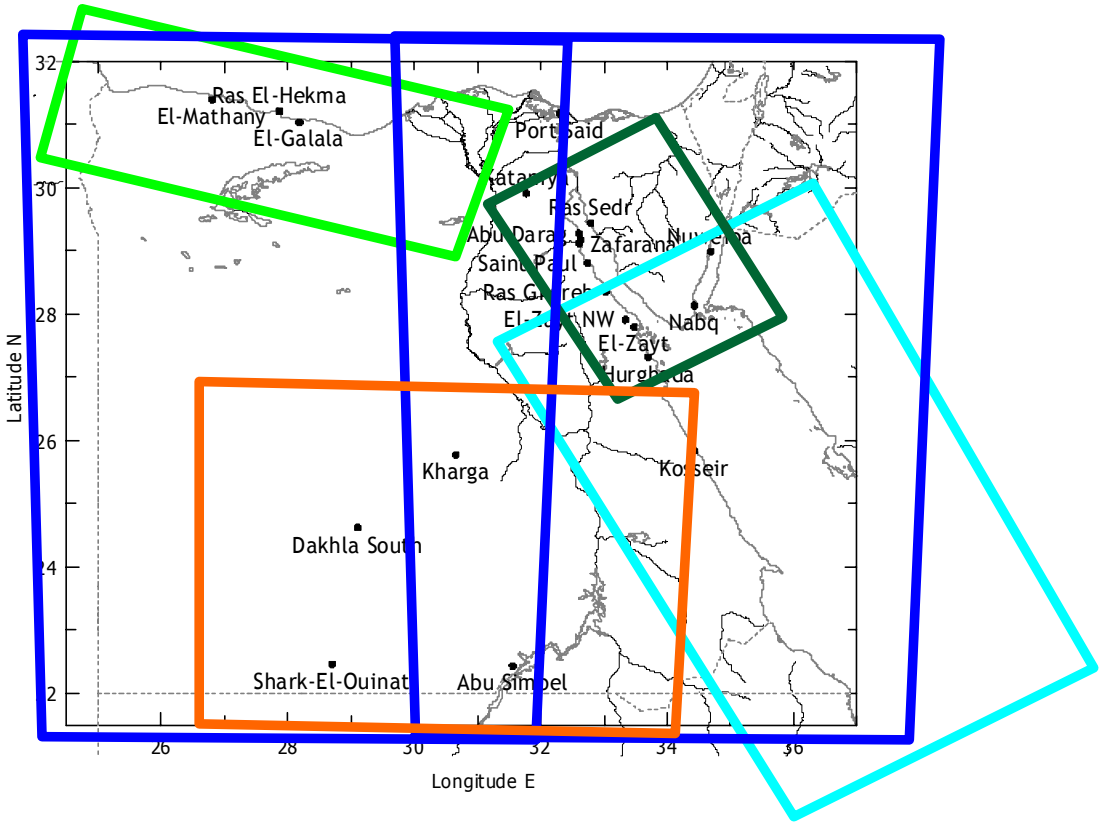

Figure 1-4. Map of Egypt showing the various modelling domains being used. A complete numerical wind atlas calculation is made for each domain.

An appraisal of the reliability of wind power calculations based on the statistics of the numerical wind atlas can be made by means of the comparisons given in Chapter 6. Here, regional mean wind climate values based on the KAMM/WAsP methodology are compared with values based on observations and WAsP.

PART I
THE WIND RESOURCE

2 Wind resources of Egypt

This chapter presents an overview of the wind climate and wind resources in Egypt, from the general circulation of the subtropical atmosphere to the wind measurements made at each station. The main results of the wind resource assessment programme are given in detail in Chapters 4 and 7.

2.1 General circulation

The mean meridional circulation of the atmosphere provides some insight into the wind characteristics that may be expected over Egypt. The forces driving the circulation originate in the differential heating of the earth by the sun, which causes a temperature gradient to develop between the equator and the northern pole. The associated density and pressure gradients would, if the earth did not rotate, lead to a poleward flow of air in the upper atmosphere and flow towards the equator at lower levels. However, while such a simple circulation does exist, it is confined to low latitudes because of the rotation of the earth. Figure 2-1 shows this so-called Hadley cell circulation between the equator and approximately 30°N.

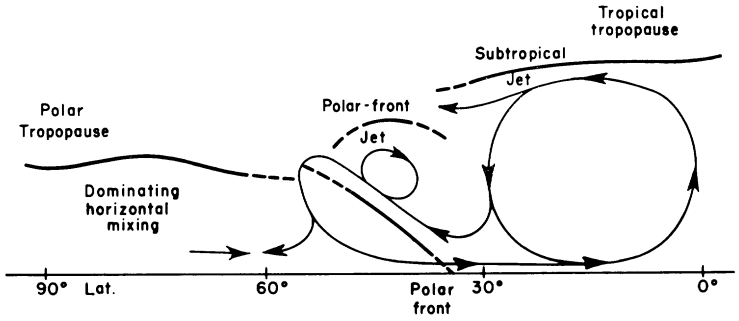

Figure 2-1. Schematic representation of the mean meridional circulation over the Northern Hemisphere during winter according to Palmén (1951). Reproduced from Lockwood (1974).

The poleward flow aloft results in the formation of a subtropical jet stream around 30°N, below which widespread subsidence of the air takes place. This subsidence leads to clear skies and, consequently, little or no rainfall. At ground level the subtropical jet corresponds to the well-known high-pressure systems (anticyclones) found around 30°N (and S). Between these and the relatively low pressure near the equator the winds are northerly and north-easterly in the Northern Hemisphere. The trade winds, noted for their constancy in both speed and direction (Lockwood, 1974), form part of this return flow of the Hadley circulation. The low latitude circulation changes only little with season, the subtropical anticyclones being nearest to the equator in winter.

Even though this picture of the meridional circulation may be oversimplified, it sets the scene for the interpretation of the meteorological data collected at the stations. As an example, the seasonal change in the position of the high-pressure systems is clearly seen in the pressure measurements at Hurghada (Mortensen et al., 2003). Also, the winds over Egypt are predominantly northerly and fairly steady – and the desert landscape testifies to the generally clear skies and lack of precipitation.

2.2 Previous investigations

The overall climate of Egypt is described in various textbooks and climatologies, of which the work by Griffiths and Soliman (1972) go into some detail. Their description encompasses the pressure distribution and general circulation, radiation, sunshine, temperature, precipitation, snow, thunderstorms, hail, evaporation, relative humidity, and surface wind – with reference also to earlier work by others. Their descriptions are presumably based upon the measurements made at standard meteorological stations in the synoptic network. The surface wind conditions are summarized (Griffiths and Soliman, 1972) in an isovent map of Egypt, see Figure 2-2.

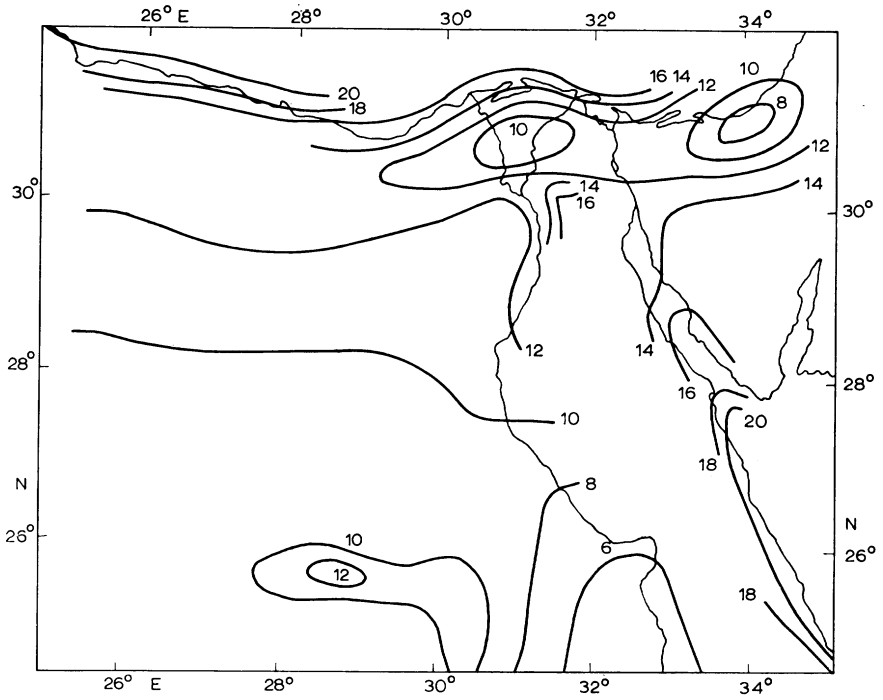

Figure 2-2. Annual mean wind speeds over Egypt in km h^{-1} according to Griffiths and Soliman (1972). One km h^{-1} corresponds to 0.28 ms^{-1}.

This map indicates that the highest wind speeds are found in the western part of the Mediterranean coast, along the Gulf of Suez, and in the northern part of the Red Sea. While this is roughly in accordance with more recent studies, the wind speed values shown in the map for e.g. the Gulf of Suez are apparently far too low, and the geographical variation within the Gulf can only be partly confirmed. No information is given on the exact measuring procedure or height above the ground, so the reason for this is not known.

The need for a more precise quantification and mapping of the wind climate of Egypt was recognized early and a number of wind resource assessment studies were initiated in the 1970's and 1980's. These activities were summarized by Renne et al. (1986) and Elliott et al. (1987), who also published a map showing the distribution of seven wind power classes over Egypt, see Figure 2-3.

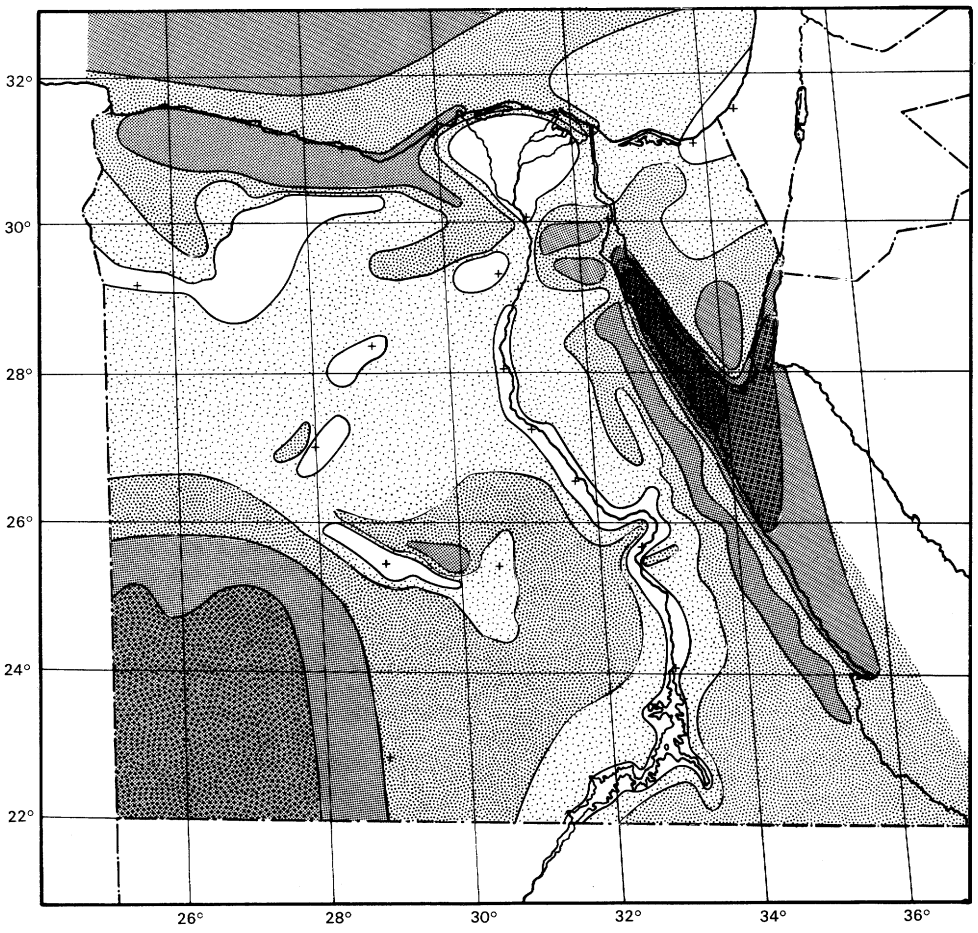

Figure 2-3. Annual average wind power estimates for Egypt according to Elliott et al. (1987). The distribution of six so-called wind power classes are shown in the map, class 1 being all white and class 6 almost black:

Power Class	Wind speed [ms^{-1}]	Power density [Wm^{-2}]	Power Class	Wind speed [ms^{-1}]	Power density [Wm^{-2}]
1	< 4.4	< 100	4	5.6-6.0	200-250
2	4.4-5.1	100-150	5	6.0-6.4	250-300
3	5.1-5.6	150-200	6	6.4-7.0	300-400

The wind speeds and power densities correspond to a height of 10 m. A seventh class with $U > 7.0$ ms^{-1} and $E > 400$ Wm^{-2} is also defined, but cannot be identified in this map. Mean wind speed is based on Rayleigh speed distribution of equivalent mean wind power density. Wind speed is for standard sea-level conditions.

Elliott et al. (1987) reanalysed existing wind data obtained at met. stations run by the Egyptian Meteorological Authority (indicated by '+' symbols in the map) and then verified and detailed these resource estimates through additional wind measurements at key locations. For this purpose a number of wind monitoring stations were erected along the Mediterranean and Red Sea coastlines. Their analysis further used climatological data on winds aloft and maps of pressure patterns and airflow, as well as topographical maps in estimating the wind resources of the data-sparse areas. The resource estimates were calculated from measured distributions of mean wind speed

or, in cases where only average wind speeds were available, by assuming that the wind speeds are distributed according to the Rayleigh distribution[1].

The wind power estimates given in Figure 2-3 apply to "areas free of local obstructions to the wind and to terrain features that are well exposed to the wind, such as open plains, plateaus, and hilltops. Within mountainous areas, the wind resource estimates apply to exposed ridge crests and mountain summits" (Renne et al., 1986). The topography of the terrain is thus taken into account in the drawing of Figure 2-3, albeit in a qualitative way.

The Gulf of Suez and northern Red Sea were identified as having a particularly high wind resource. The wind climate of the Gulf of Suez range from class 3 (5.1-5.6 ms^{-1}) in the northernmost part of the Gulf to class 6 (6.4-7.0 ms^{-1}), this class covers the southern-most three quarters of the Gulf. At one station, Ras Ghareb, the data even indicate class 7 (7.0-9.4 ms^{-1}), but this is attributed to the location of the station on a well-exposed ridge (Renne et al., 1986) and may not be representative of the terrain of the region in general.

For the Sinai Peninsula, wind data have further been collected and summarized by Manes et al. (1980). A summary of these data was referenced in the international literature by Nof and Paldor (1994). Average annual wind speeds for stations along the east shore of the Gulf of Suez reported by Nof and Paldor (1994) are: 6.0 ms^{-1} close to the city of Suez, 8.9 ms^{-1} at Ras Sedr (200 m a.s.l.), and 7.6-7.7 ms^{-1} close to El-Tor in the southern part of the Gulf. These average wind speeds were based on 2-7 years of data and are consistent with the picture shown in Figure 2-3.

Two other regions in Egypt were identified as having a fairly high and widespread wind resource: the Mediterranean coast and the most south-westerly part of the Western Desert. Most of the Mediterranean coastal region is shown to be of Class 4, this estimate was partly based on met. stations in this area. However, in the Western Desert, very few met. stations exist and the estimates are necessarily more uncertain.

A wealth of internal reports and data summaries exist with respect to the various wind resource assessment studies carried out in Egypt from the 1970's and onwards. Much of this information is summarized by Mobarak et al. (1982) and Mobarak (1992). The Egyptian Meteorological Authority has further published monthly mean wind roses for 20 stations all over Egypt in its *Climatic Atlas of Egypt* (1996); these roses show both the distribution of wind directions and the distribution of seven classes of wind speed in each sector.

In 1990, the available wind data for the Gulf of Suez were re-evaluated by the New and Renewable Energy Authority and Risø National Laboratory (Larsen and Hansen, 1991; Hansen and Larsen, 1991) with the purpose of making the data useful for wind atlas analysis. Following the methodology provided by the European Wind Atlas (Troen and Petersen, 1989), the sites where wind data had been collected were described with respect to the distribution of roughness areas and the occurrence of sheltering obstacles, and regional wind climatologies for these stations were established.

[1] The Rayleigh distribution is identical to a Weibull distribution with $k = 2$.

This survey concluded that the wind conditions in the Gulf of Suez indeed seemed very favourable for wind energy utilization, but recommended that three new stations be established to improve the estimates of the wind energy potential at the two most promising and probable sites for construction of large wind farms. Met. masts were therefore erected at Abu Darag, Zafarana and Hurghada in the spring of 1991. Later, an additional mast was erected just west of the Gulf of El-Zayt. A presentation and analysis of the data collected at these four stations, as well as at five historical stations, were presented in a *Wind Atlas for the Gulf of Suez* by Mortensen and Said (1996).

Since 1997-98, the wind resource assessment activities in Egypt have to a large extent been carried out in the Wind Atlas for Egypt project. The work has been organised in three main components:

- Component A: Wind Atlas for the Gulf of Suez
- Component B: Preliminary Wind Atlas for Egypt
- Component C: Wind Atlas for Egypt

A *Wind Atlas for the Gulf of Suez – Measurements and Modelling 1991-2001* was published by the New and Renewable Energy Authority and Risø in 2003 (Mortensen et al. 2003) and a *Preliminary Wind Atlas for Egypt* was published internally by the Egyptian Meteorological Authority and Risø in 2004 (Mortensen et al., 2004). The main results of these atlases are contained in the present Wind Atlas.

2.3 The wind climate of Egypt

The wind climate of Egypt has been investigated by two different, complementary methodologies: mesoscale modelling based on long-term reanalysis data and micro-scale modelling based on measurements from 30 meteorological stations all over Egypt. The mesoscale modelling is described in detail in Chapter 4, including an overview of the results obtained for six modelling domains: Western Egypt, Eastern Egypt, the Northwest Coast, the Gulf of Suez, the Red Sea and the Western Desert.

For the detailed results of the wind resource assessment programme the reader is referred to Chapter 7 which contains a summary of the observed and regional wind climates based on the wind measurements. The meteorological stations and the meteorological sensors employed for the Atlas are described in Appendix A; the organization of the data is accounted for in Appendix B. In addition to the mean wind statistics, Chapter 8 presents some additional wind statistics – referred to as design wind conditions – which have been obtained during the measuring campaign and in subsequent analyses.

Observed wind climates

An overall summary of the wind climates observed at the 30 meteorological stations is given in Table 2-1. The stations are listed according to the region in which they are located. As shown in Chapter 7, the terrain-induced corrections to the measured wind climates are most often fairly small, so some characteristics of the wind climates may already be deduced from these tables. Figure 2-4 shows the variation of the observed mean wind direction and mean wind speed over Egypt. Mean wind direction is shown as arrows oriented in the direction of the mean wind vector; the size of the arrows is proportional to the mean wind speed.

Table 2-1. Summary of wind observations at the met. stations: Data-collecting period, data recovery rate (R), Weibull A- and k-parameters, mean wind speed (U), mean power density (E), and direction (D_U) and magnitude ($|\mathbf{U}|$) of the mean wind vector.

Region/Station	Period	R	A	k	U	E	D_U	$\|U\|$
		[%]	[ms^{-1}]		[ms^{-1}]	[Wm^{-2}]	[deg]	[ms^{-1}]
Northwest Coast								
Sidi Barrani (62301)	10 y	n/a	7.0	2.16	6.2	254	324	2.8
El-Mathany	1 y	99.5	6.4	2.33	5.7	190	284	2.0
Ras El-Hekma	1 y	99.8	7.2	2.23	6.4	275	309	3.1
El-Galala	1 y	97.2	6.7	2.41	5.9	206	324	2.6
Alexandria (62318)	10 y	n/a	5.2	2.42	4.6	99	329	2.9
Northeast Coast								
Port Said	1 y	66.2	5.3	2.32	4.7	105	301	1.6
El Arish (62337)	10 y	n/a	3.0	1.44	2.8	37	303	1.0
Gulf of Aqaba								
Nuweiba	1 y	80.9	6.2	2.58	5.6	161	027	4.0
Nabq	1 y	97.6	7.7	2.04	6.8	367	009	5.9
Gulf of Suez								
Katamaya	1 y	79.5	6.0	2.66	5.4	143	357	2.8
El-Suez (62450)	10 y	n/a	6.2	3.17	5.5	140	350	3.9
Ras Sedr	5 y	84.1	8.5	3.06	7.6	368	341	6.0
Abu Darag NW	3 y	82.3	9.6	3.34	8.6	519	352	6.9
Abu Darag	14 y	82.5	10.1	3.50	9.1	598	355	7.6
Zafarana M7	7 y	79.1	11.1	3.57	10.0	788	356	8.4
Zafarana	14 y	85.2	10.2	3.19	9.1	626	358	7.0
Saint Paul	5 y	82.7	9.4	3.25	8.5	498	332	7.0
Ras Ghareb	5 y	85.5	11.0	3.40	9.9	775	322	8.7
Gulf of El-Zayt NW	5 y	82.0	11.8	3.70	10.7	950	313	9.4
Gulf of El-Zayt	7 y	83.8	11.5	3.29	10.3	900	322	9.0
Red Sea								
Hurghada WETC	11 y	79.6	7.6	2.32	6.7	308	322	4.9
Hurghada (62463)	10 y	n/a	7.6	2.66	6.7	285	325	5.4
Kosseir (62465)	4 y	97.1	5.1	2.03	4.6	178	334	3.5
Kosseir	1 y	88.7	6.4	2.28	5.64	187	321	4.3
Western Desert								
Farafra (62423)	2 y	98.6	3.9	1.79	3.5	53	342	2.0
Kharga	1 y	99.8	7.4	2.57	6.6	268	345	5.8
Dakhla South	1 y	81.5	7.3	3.31	6.6	229	352	5.5
Shark El-Ouinat	3 y	100.0	7.2	3.29	6.5	222	355	5.5
Asswan (62414)	10 y	n/a	5.4	2.61	4.8	102	346	3.8
Abu Simbel	1 y	99.9	6.4	2.76	5.7	166	356	4.8

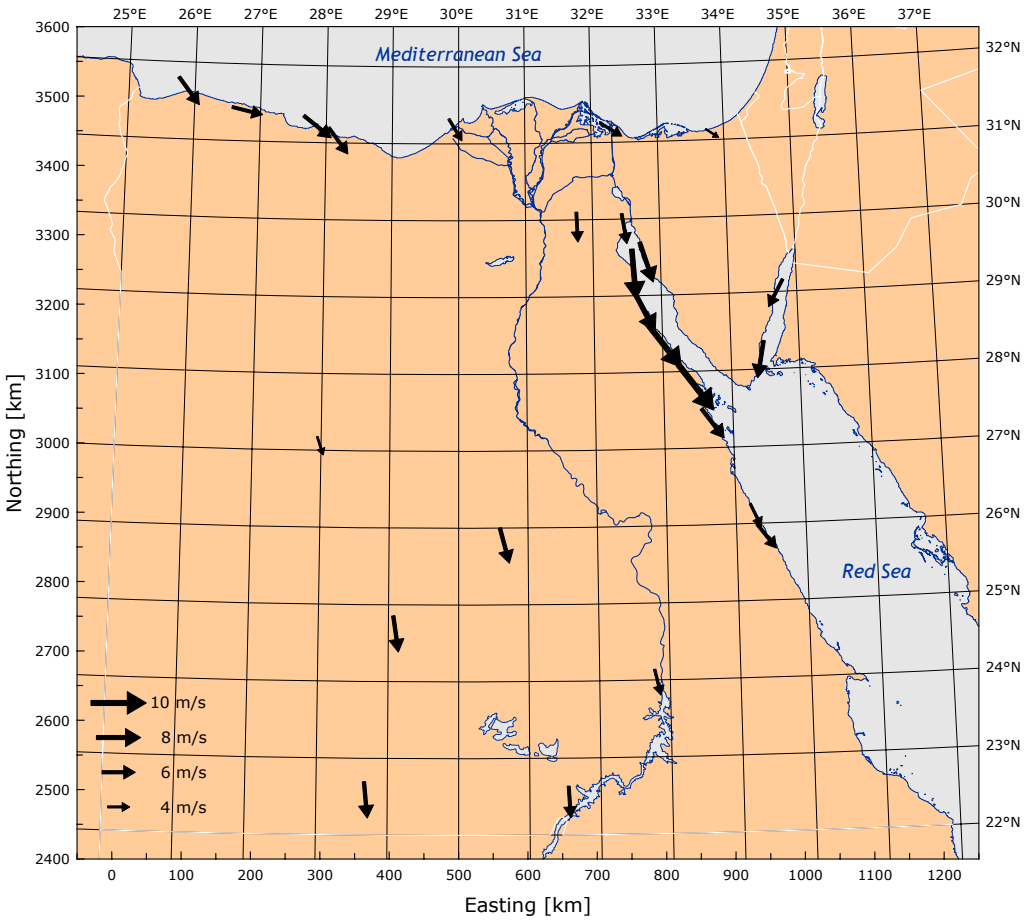

Figure 2-4. Mean observed wind direction at selected stations. The direction of the arrows corresponds to the direction of the mean wind vector; the size of the arrow is linearly proportional to the mean wind speed.

As might be expected from the description given in Section 2.1, the winds are northerly and north-westerly over most of Egypt. In the Gulfs of Suez and Aqaba, the wind direction is strongly influenced by the wide valleys in which the stations are situated.

Summaries of the wind observations at each of the 30 stations are given in Chapter 7, including tables and graphs showing the wind rose, the distribution of wind speeds, and the daily, yearly and year-to-year variations of mean wind speed. Descriptions of the measurement conditions and surrounding terrain are also given.

Regional wind climates

The brief overview of the wind climates given above is based on the measured wind speed and direction data – the observed wind climates. In this section we compare the generalized wind atlas data sets – i.e. the regional wind climates – the construction of which was described briefly in Chapter 1. In Chapter 4, we describe how the regional wind climates can also be determined by mesoscale modelling.

As an example, Figure 2-5 shows corresponding values of mean wind speed and mean power density for all 30 stations in the Wind Atlas. The mean values were calculated from the generalized data sets given in Chapter 7 for roughness class 1 (z_0 = 0.03 m) at a height of 50 m above ground level.

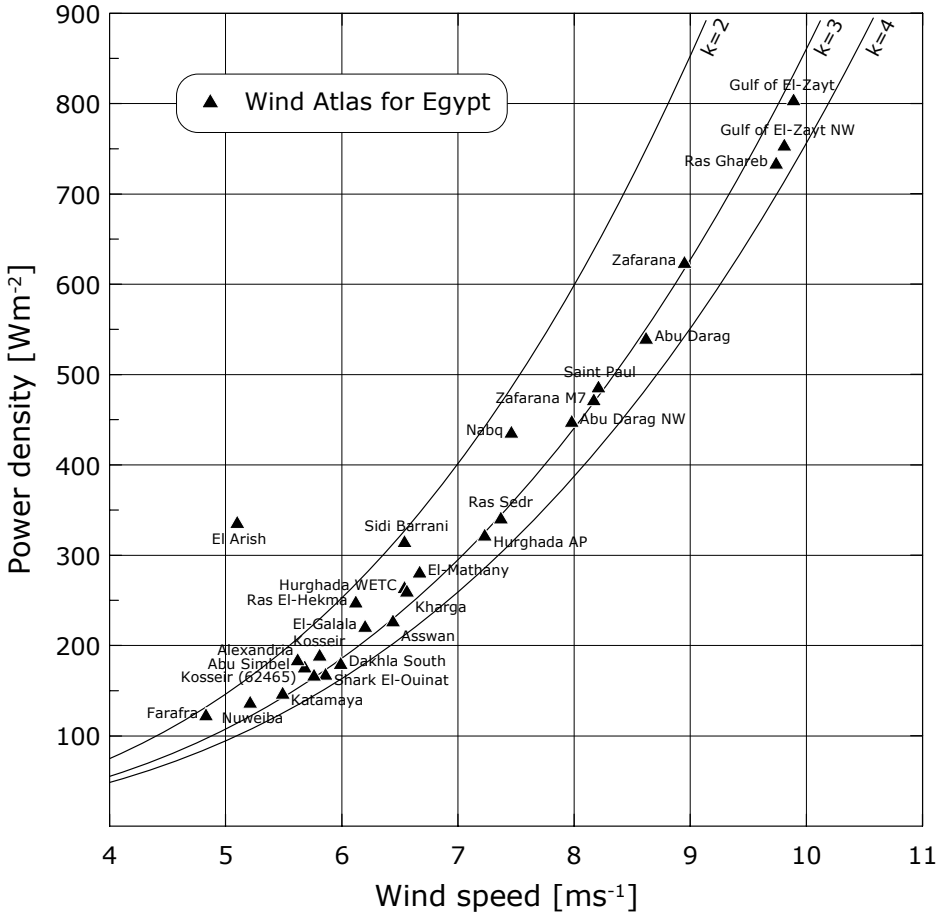

Figure 2-5. Mean wind speeds and power densities at a height of 50 m over roughness class 1 (z_0 = 0.03 m) for the 30 stations in the Wind Atlas for Egypt.

Figure 2-5 thus shows what *would* have been measured at the location of the stations at a height of 50 m if the surroundings were simply a uniform land surface with z_0 = 0.03 m. The differences in corresponding mean wind speed and power density values are related to the different Weibull *k*-parameters of the wind speed distributions. Note that a roughness length of 0.03 m is higher than what is found for most sites in the desert, so the actual wind climate is often higher than is shown above.

Referencing the wind climates to these standard conditions makes it possible to show and compare the different stations in a common framework. It should be borne in mind, that the data shown in Figure 2-5 are of slightly varying quality and, in addition, may not be equally representative. The climatic variability will add to the uncertainty of the intercomparison; the data from the stations were obtained for different periods where the wind climate may have been slightly different. This further raises another important question: to what extent is the period covered representative for the longer-term climate and how large a deviation must be expected in future decades?

These reservations notwithstanding, there seem to emerge a fairly clear picture which is in accordance with the wind atlas maps shown in Figure 2-6 and Figure 2-7. The maps show the regional wind climate of Egypt – as mean wind speeds and power densities, respectively – modelled by the mesoscale model. A closer comparison of the regional wind climate values derived from the measurements and those derived from the mesoscale modelling is given in Chapter 6.

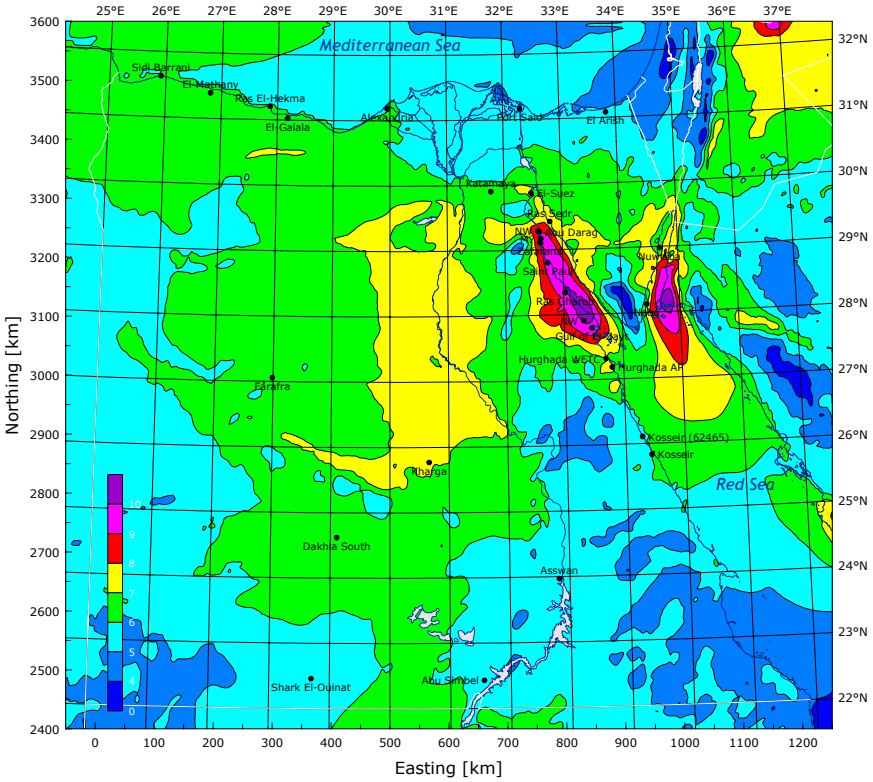

Figure 2-6. The regional wind climate of Egypt determined by mesoscale modelling. The map shows the mean wind speed in [ms^{-1}] at a height of 50 m over a flat, uniform land surface of roughness class 0 (z_0 = 0.0002 m).

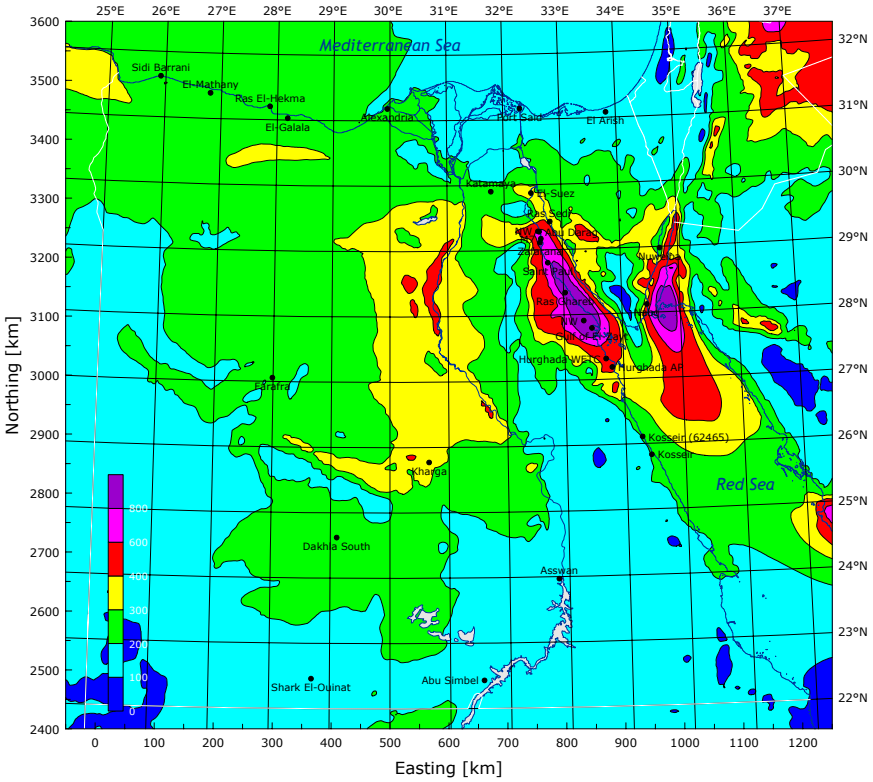

Figure 2-7. The regional wind climate of Egypt determined by mesoscale modelling. The map shows the mean power density in [Wm^{-2}] at a height of 50 m over a flat, uniform land surface of roughness class 0 (z_0 = 0.0002 m).

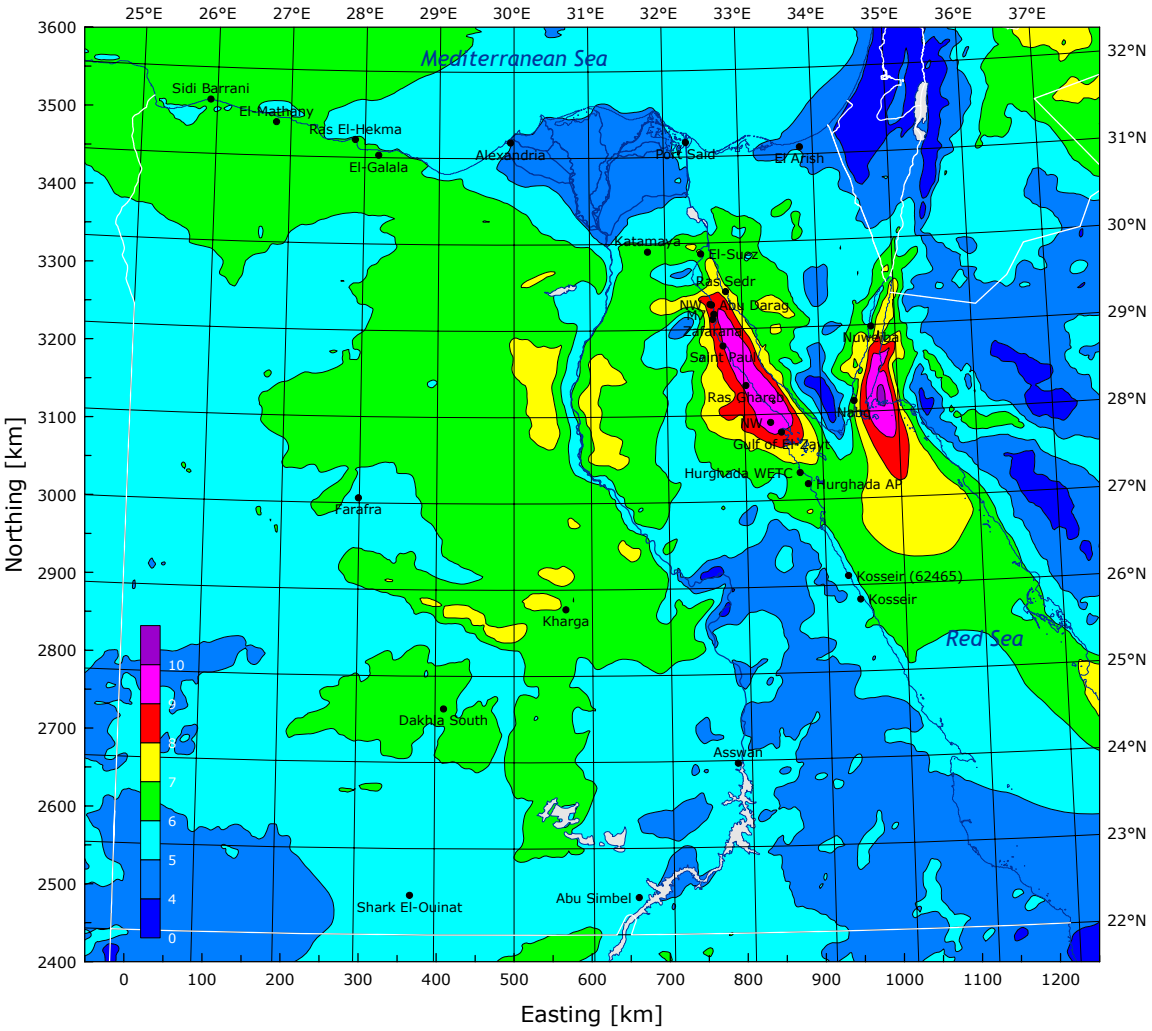

Figure 2-8. The predicted wind climate of Egypt determined by mesoscale modelling. The map shows the mean wind speeds in [ms^{-1}] at a height of 50 m over the actual (model) land surface. The horizontal grid point resolution is 7.5 km.

Predicted wind climates

The mesoscale modelling results can be utilised to construct wind resource maps of Egypt, i.e. maps showing the predicted wind climate at some height above ground level, based on the values in the grid points of the mesoscale model. Figure 2-8 and Figure 2-9 are examples of such wind resource maps: they show the mean wind speed [ms^{-1}] and mean power density [Wm^{-2}], respectively, for a height of 50 metres above the actual land surface. The maps were constructed by combining the results of the two large domains covering Egypt, see Chapter 4. The horizontal grid point resolution in these maps is 7.5 km, so they only show the wind resource in broad outline and terrain features on a smaller scale may give rise to larger wind resources locally. More detailed maps with a resolution of 5 km can be made of the six smaller domains.

It is not possible to compare the maps in Figure 2-8 and Figure 2-9 directly to the map shown in Figure 2-3, which shows the wind speeds and power densities at 10 m a.g.l. for seven wind power classes. Not only are the classes of wind speed and power not identical, several assumptions would also have to be made in extrapolating the wind speed from 10 to 50 meters. And, more importantly, the influence of the terrain on the predicted winds is evaluated in entirely different ways.

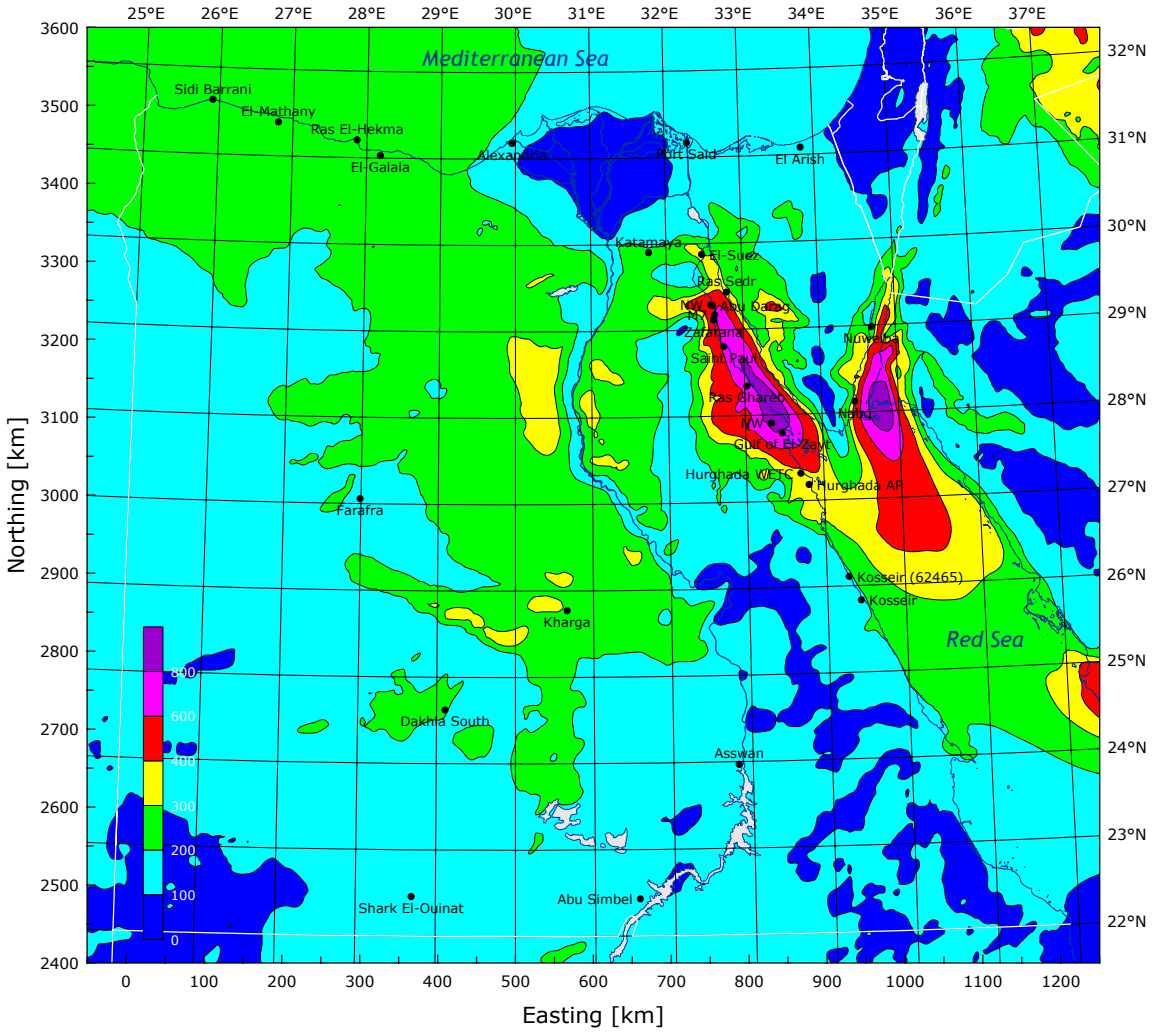

Figure 2-9. The predicted wind climate of Egypt determined by mesoscale modelling. The map shows the mean power density in [Wm^{-2}] at a height of 50 m over the actual (model) land surface. The horizontal grid point resolution is 7.5 km.

The wind power estimates given in Figure 2-3 apply to well-exposed sites, situated on open plains, hilltops, ridges, escarpments and ridge crests and mountain summits (Renne et al., 1986). Many such terrain features are not resolved by the KAMM mesoscale model with a grid point resolution of 7.5 km (or even 5 km), but would have to be modelled in detail using WAsP or a similar microscale model. Figure 2-10 provides an example of this near the Ras El-Hekma meteorological station.

The map in Figure 2-3 indicates five regions with relatively high wind resources: the Northwest Coast, the Gulf of Aqaba, the Gulf of Suez, the northern Red Sea and the south-westernmost part of the Western Desert. This map was part of the basis used in the planning of the measurements and modelling in the Wind Atlas for Egypt. The present study presents the following updated picture, see above:

For the *Northwest Coast* region, the wind resources seem to be somewhat lower than indicated by Figure 2-3, even when taking the speed-up over hills and escarpments and the coastal effects into account: most of this region is Class 2 and 3, rather than Class 4 (Figure 2-3). The highest wind power potential is not along the coast, but on top of the escarpment that constitutes the north-western rim of the Qattara Depression.

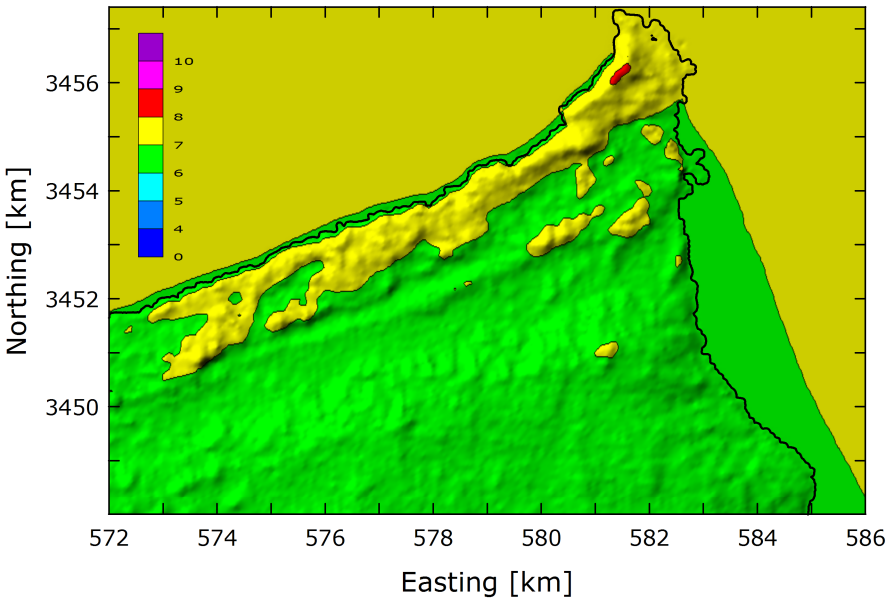

Figure 2-10. Predicted wind climate of the Ras El-Hekma peninsula determined by WAsP modeling. The map shows the mean wind speed in [ms^{-1}] at a height of 50 m over the actual land surface. The horizontal resolution in the modelling is 100 m.

For the *Gulf of Aqaba* region, the resources are indeed relatively high, in particular offshore and on the eastern coast of the Gulf. The onshore resource changes significantly along the western coastline. The highest resource here seems to be confined to a 50-km long coastal stretch between Nuweiba in the north and Nabq in the south.

The *Gulf of Suez* region is the region with the highest wind resource in Egypt; the present investigation confirms that the wind resource is even higher that was hitherto assumed. Fairly large areas with mean wind speeds in excess of 10 ms^{-1} at a height of 50 m a.g.l. exist from Abu Darag in the north to Gulf of El-Zayt in the south.

The high wind resource areas in the northern *Red Sea* occur mostly offshore and the high resource found in the southern part of the Gulf of Suez does not extend very far into the Red Sea. This fact is supported by the observed wind climates in this region. The gradient from north to south in the wind climate is very pronounced just south of the station at Gulf of El-Zayt.

The most obvious difference between the maps in Figure 2-3 and Figure 2-8 is perhaps seen in the south-westernmost part of the *Western Desert*. Here, the wind resource seems to be much lower than the huge area of Class 5 indicated in Figure 2-3. This area is characterised by fairly low winds of Class 1-2 (or even lower).

The two investigations both indicate that large parts of the Western Desert, the Nile Valley and the Sinai Peninsula have a relatively low wind resource. However, the present investigation has identified a huge area in the Western Desert – on both sides of the Nile Valley between 27°N and 29°N – where the wind resource is significantly higher. These rather flat regions were previously classified as Class 1 and 2, but seem to belong to Class 3 and 4.

3 Application of the Wind Atlas

Estimation of the wind resource ranges from overall estimates of the mean energy content of the wind over a large area – called *regional assessment* – to the prediction of the average yearly energy production of a specific wind turbine or wind farm at a specific location – called *siting*. The information necessary for siting generally needs to be much more detailed than in the case of regional assessment. However, both applications make use of the general concepts of topography analysis and regional wind climatologies.

The main objective of the Wind Atlas is to provide suitable data for evaluating the potential power output from single wind turbines as well as large-scale wind farms. This is accomplished through accurate measurements of wind speed and direction at several locations, followed by the calculation of regional climatologies for these stations. The models used for this analysis may also serve as a tool for the application of wind atlas data sets to produce site-specific wind climatologies and power production estimates.

Mesoscale effects – e.g. the forcing of the wind flow by mountains and wide valleys – are very pronounced in the Gulf of Suez. Consequently, the regional or geostrophic wind climate may change rapidly over short distances. The wind atlas methodology cannot adequately resolve these variations because the number of stations in the Gulf of Suez is limited. The KAMM/WAsP methodology is therefore introduced in order to alleviate the shortcomings of the wind atlas methodology.

The KAMM mesoscale model can furthermore be used for regional assessment, i.e. to estimate the overall variation of the wind resource over Egypt – based on the long-term climatology of the atmosphere.

The WAsP micro-scale model can also be used for siting purposes, i.e. to estimate the expected annual energy production of single wind turbines and wind farms at specific locations – based on wind measurements at nearby meteorological stations.

The KAMM/WAsP methodology can be used for siting purposes at locations far from existing meteorological stations, i.e. the predictions of annual energy production are adjusted to take into account the variation of the wind climate on the mesoscale. For this purpose,

3.1 The wind-climatological inputs

The wind-climatological inputs are treated extensively in the remainder of the Wind Atlas. For application purposes – like the use of a wind atlas data set for estimation of the power production of a wind farm over the next 20 years or so – it should be borne in mind that the data sets provided in the Atlas represent very different time periods. It is essential in each project to evaluate how representative the chosen data set is for the long-term climatology of the site in question. Reliable wind index information is not readily available for Egypt, so the predictions must be referenced to any and all long-term data sets available.

3.2 The topographical inputs

The terrain features that influence the wind flow close to the ground – and thereby determine how the regional wind climate is transformed into the site-specific wind resource – are often categorized in three broad classes:

- The geometry of the terrain surface (elevation, slope, ruggedness, etc.)
- The surface characteristics of the terrain (land use or roughness length)
- Near-by sheltering obstacles (houses, trees, shelter belts, etc.)

The coordinate systems used with these topographical inputs are described briefly at the end of this section.

Terrain surface elevation – height contour maps

An accurate description of the overall geometry of the terrain surface is a prerequisite for reliable modelling of the wind flow over the terrain. The most important feature is the elevation of the terrain surface above mean sea level.

The wind atlas model requires a digital height contour map for the flow modelling. This can be obtained by digitising the height contours from a standard topographical map; however, this is a labour-intensive and somewhat tedious process. Moreover, it may be impossible to find reliable and up-to-date maps for a given wind farm site.

Shuttle Radar Topography Mission (SRTM, 2005) elevation data has recently become available, see section 9.1. This data set consists of elevation values for the node points in a 3 arc-second (~93 m) grid. The data cover all of Egypt, although some fairly large areas in the Western Desert are filled with voids. Figure 3-1 shows examples of elevation maps derived from the SRTM data set.

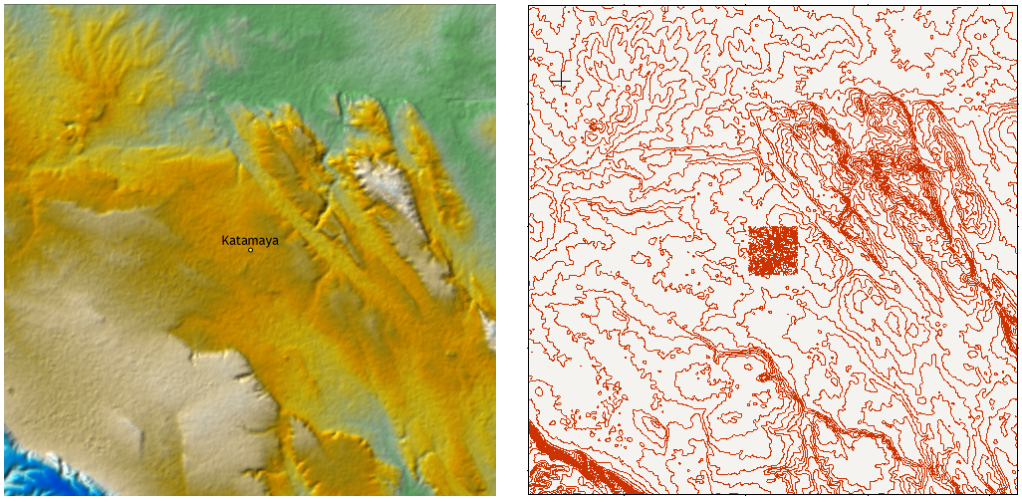

Figure 3-1. Elevation maps of the area around the meteorological station Katamaya. The maps cover an area of 20×20 km^2. Both maps were constructed from SRTM elevation data, the height contour map to the right is used for the flow modelling.

Preliminary investigations show that maps derived from SRTM data are sufficiently detailed and accurate for most wind flow modelling purposes. However, the height contours should be compared to a reliable map of the area, if one exists.

When it comes to actual planning and construction of a wind farm, more detailed maps may be required. These can be established by a number of other techniques; an example of a detailed elevation map of a wind farm site is given in Figure 3-2.

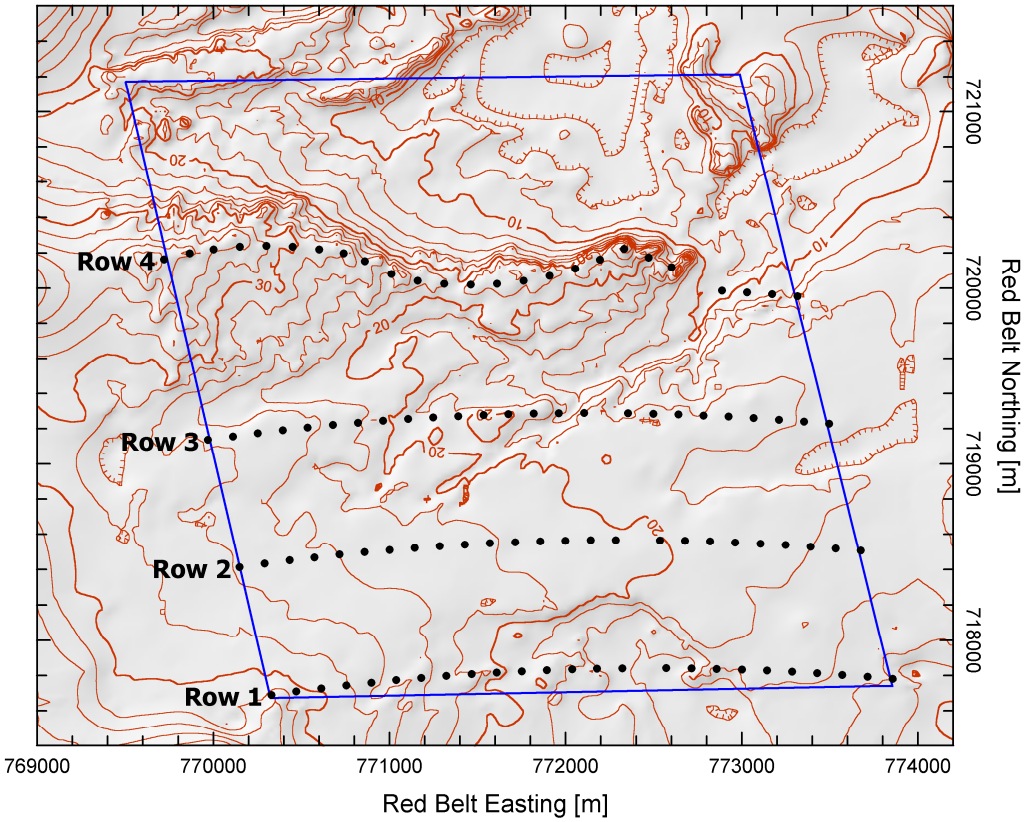

Figure 3-2. Elevation map of the NREA/Danida wind farm site close to Zafarana. The map was established by a site-specific survey employing kinematic GPS techniques. The height contour interval in the map above is 2 m, but it is possible to draw 1-m contours as well. Four sample wind turbine groups, each consisting of 25 600-kW wind turbines, are indicated by black dots.

In general, it is possible to establish digital maps with 10-m height contours in most of Egypt. If spot heights are considered as well, it may be possible to detail such maps in certain areas, but if a more detailed elevation description is needed, a site-specific survey of the terrain is required.

The influence of the detail in the elevation description on the modelling of the wind flow – and thereby the estimation of the annual energy production – can be illustrated by using different maps of the same area; with different height contour intervals. An example is given in Table 3-1 where predictions for the four different wind farm rows shown in Figure 3-2 have been calculated for maps with different height contour intervals: 1, 2, 5, 10 and 20 meters. The regional wind climate and wind turbine type used for the predictions are the same in all 5 scenarios. The hub height of the turbine is 40 m a.g.l. and the wake interactions between the four farms have not been taken into account in this example.

In the flat areas (Row 1 and 2), the height contour interval has little influence on the estimated AEP. In the more hilly areas (Row 3 and 4), the contour interval has some influence on the estimated AEP, especially in more hilly terrain (Row 4).

Table 3-1. Estimated annual energy production for four different 15-MW wind farms, for different height contour intervals in the digital terrain model. The AEP production figures given for each farm correspond to an index of 100.

Wind farm	AEP [GWh]	Height contour interval in map				
		20 m	10 m	5 m	2 m	1 m
Row 1	68.178	99.4	99.7	99.7	99.8	100.0
Row 2	68.709	99.4	99.6	99.7	100.0	100.0
Row 3	68.833	98.5	99.1	98.9	99.8	100.0
Row 4	72.534	94.1	96.6	98.6	99.8	100.0

With a small height contour interval, the hills and valleys (wadis) become more well-defined and the speed-up/slow-down of the modelled winds more pronounced. This leads to higher estimated AEP values because the wind turbines are typically situated on top of the hills and ridges. In the case of the Row 4 wind farm, the AEP seems to be underestimated by about 3-4% if standard 10-m contours are used for the flow modelling. In all cases, a contour interval of about 2 m seems to be sufficient for accurate flow modelling.

Land-use and roughness length – roughness maps

An accurate description of the land use and roughness lengths of the terrain surface is another prerequisite for reliable modelling of the wind flow over the terrain. The most important land-use classes in Egypt are: the sea surface, various desert surfaces, the mountains and the built-up areas. Natural vegetation and agricultural areas play little or no role in most places. The coastline represents the most pronounced and important change of roughness and this should always be taken into account.

The overall land-use pattern of a particular area can be established from topographical maps, aerial photographs or satellite imagery. Because of the existence of land mines, field mapping and verification is in some regions (e.g. the Gulf of Suez) limited to what can be seen from public roads or by climbing meteorological masts or buildings.

The most up-to-date and readily available information on the type and distribution of land-use classes stems from satellite imagery. An example is shown in Figure 3-3, where a satellite image is used to classify and digitize the land-use or roughness classes close to the anemometer in Nouzha Airport, Alexandria. The image is geo-referenced by the three fixed points A, B and C; the 'real world' coordinates of which are known. The coastline was obtained from the SRTM Water Body Data set.

The most common land-use type, corresponding to the back-ground roughness length, consists of desert surfaces. It may be difficult to estimate the roughness length of such surfaces; however, it should be borne in mind that this estimate is most critical if the meteorological mast is low and less critical the higher the mast. Preferably, the anemometer used for predicting the wind turbine production should be mounted at a height comparable to the hub height of the proposed wind turbine.

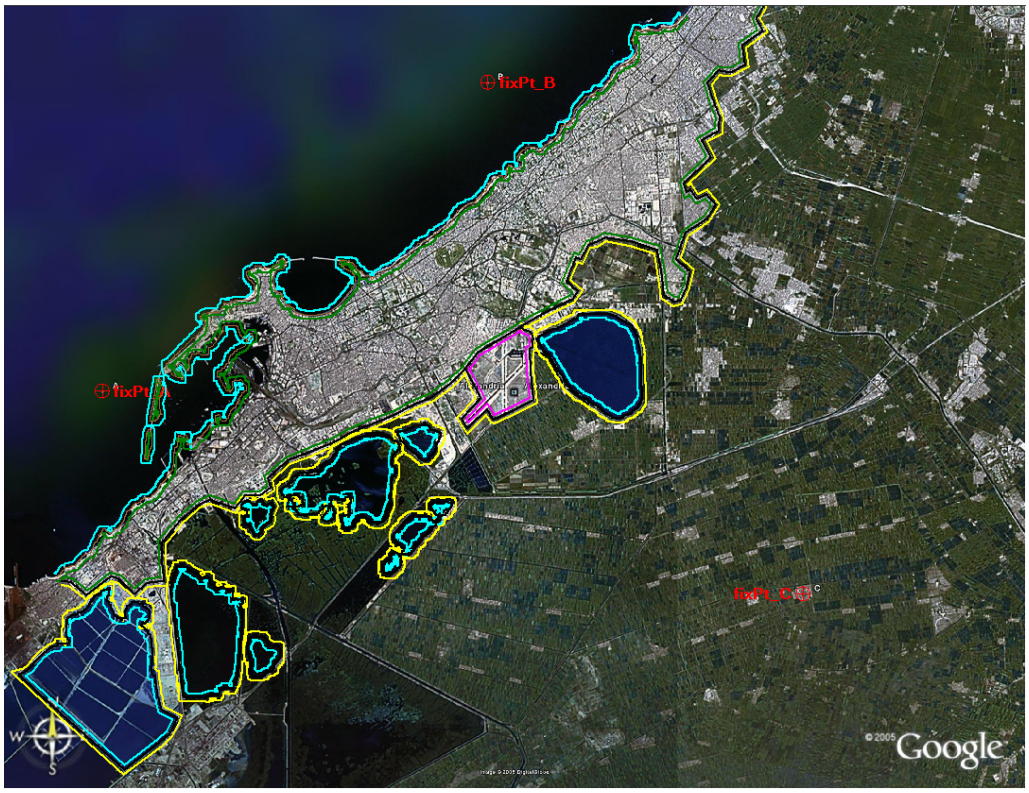

Figure 3-3. Classification and digitization of major roughness classes close to the meteorological station in Nouzha Airport, Alexandria. The classes identified here are: the sea, some lakes, the built-up areas of Alexandria, the airport runway area and the rural areas of the Nile delta (Image © DigitalGlobe and Google).

The influence of the detail and accuracy in the roughness description on the wind flow modelling can be illustrated using different maps of the wind farm area; with different roughness classifications. An example is given in Table 3-2, where predictions for the four different wind farms shown in Figure 3-2 have been calculated for maps with entirely different roughness classifications: land only, land/sea only and the full description. The regional wind climate has also been recalculated since the meteorological station Abu Darag is in the same map. However, the wind turbine type used for the predictions is the same in all three scenarios. The hub height of the turbine is 40 m a.g.l. and wake interactions between the four farms have not been taken into account.

Table 3-2. Estimated annual energy production for four 15-MW wind farms, for three different roughness descriptions in the digital terrain map. The production figures given for each farm correspond to an index of 100.

Wind farm	AEP [GWh]	Roughness description		
		'Land only'	'Coast line'	'Complete'
Row 1	68.169	102.6	97.6	100.0
Row 2	68.707	102.4	97.5	100.0
Row 3	68.830	102.5	97.6	100.0
Row 4	72.531	102.6	98.0	100.0

In the “land” case, the entire modelling domain consists of a uniform land surface with a roughness length of 2 mm; here the power production is overestimated somewhat. In the “coast” case, the surface is divided in two classes only: land (z_0 = 2 mm) and sea; here the AEP is underestimated. Finally, in the “full” case, a detailed roughness length description based on interpretation of aerial photographs and site visits is employed.

Effect of the coastline

Many candidate sites for wind turbine installations in the Gulf of Suez are situated close to the coastline. The effect of this on the mean power production is illustrated in Figure 3-4, where the annual energy production of a 450-kW wind turbine is estimated as a function of distance to the coastline in the Zafarana area. The production is calculated along a 20-km horizontal transect, from 10 km inland to 10 km offshore, using the wind atlas data set from Zafarana. Mesoscale effects have not been taken into account. The transect is roughly perpendicular to the coastline and to the prevailing wind direction. For comparison, calculations for a similar 20-km transect near Vindeby, Denmark, are also shown. The world's first offshore wind farm was constructed here in 1990-91 and the Vindeby transect is also roughly perpendicular to the local coastline and to the prevailing wind direction.

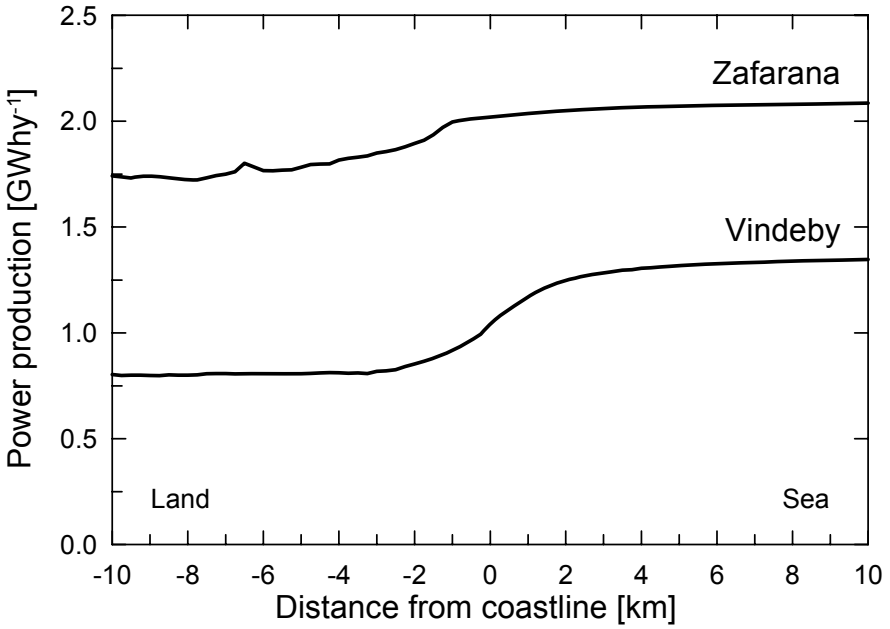

Figure 3-4. Estimated mean power production of a 450-kW wind turbine in the Gulf of Suez and in Denmark. The power productions are calculated at 250-m intervals along a 20-km transect perpendicular to the coastline.

Over sea, the production in the Zafarana area is estimated to be around 55 per cent higher than for a similar offshore site in Denmark. Over land, the production in Zafarana decreases to about 80 per cent of the offshore value, whereas the energy production in the Danish example falls to about 60 per cent of the corresponding Danish offshore value. The inland potential in Zafarana is therefore twice as high as the inland potential close to Vindeby. The different ratios of inland-to-offshore wind potential are mainly due to the different surface roughnesses of the Egyptian desert and open Danish farmland, respectively; the desert being much smoother to the wind flow.

Sheltering obstacles

Sheltering obstacles in Egypt are almost exclusively man-made structures like houses, walls or fences. However, the height of typical obstacles and their distance to possible wind farm areas suggest that it will only rarely be necessary to model these structures as obstacles. Instead, the towns, villages and summer cottage areas are treated as adding to the roughness of the areas in question.

The following rule of thumb may serve as a guideline when deciding whether to include obstacles in the terrain as sheltering obstacles or as roughness elements:

- if the point of interest (anemometer or wind turbine hub) is closer than about 50 obstacle heights to the obstacle and closer than about three obstacle heights to the ground, the object should probably be included as a sheltering obstacle. In this case the obstacle should not at the same time be considered as adding to the roughness of the terrain.
- if the point of interest is further away than about 50 obstacle heights or higher than about three obstacle height, the object should most likely be included in the roughness description. In this case the obstacle should not at the same time be considered as a sheltering obstacle.

A wind turbine with a hub height of 40-50 m a.g.l. and sited well away from buildings will therefore rarely experience shelter effects. Conversely, the shelter effects may be quite severe for a meteorological station with a 10-m mast sited close to built-up areas.

Coordinate systems

Most of the information used in regional wind resource assessment and siting – and indeed much of the information presented in the Wind Atlas – is geo-referenced. The location of a given meteorological station, the elevation of the terrain, the extent and shape of significant land-use or roughness classes and the layout of a wind farm can only be described accurately by referring to the exact position or coordinates of the feature in question. Wind flow modelling requires accurate and reliable information on the coordinates of the inputs used.

Two coordinates systems (projections) are used in the Atlas: the usual geographic coordinates (latitude, longitude) and the Cartesian Universal Transverse Mercator (UTM) system. Both systems are referenced to the World Geodetic System 1984 (WGS 84) datum.

Figure 3-5 shows the geographical coordinate system used – lines of equal latitude and longitude – for Egypt. This system is not Cartesian and therefore not suited for wind flow modelling or planning purposes. However, several input data are provided in this system, e.g. Google Earth images, other satellite images, Shuttle Radar Topography Mission elevation data, SRTM Water Body Data, Coastline Extractor data, etc.

Figure 3-6 shows the Cartesian UTM systems used. Because Egypt spans more than 11 degrees of longitude, three different UTM zones must be used; these are shown by the grid lines in Figure 3-6. For the meteorological stations of the Atlas, it is only necessary to use zones 35 and 36.

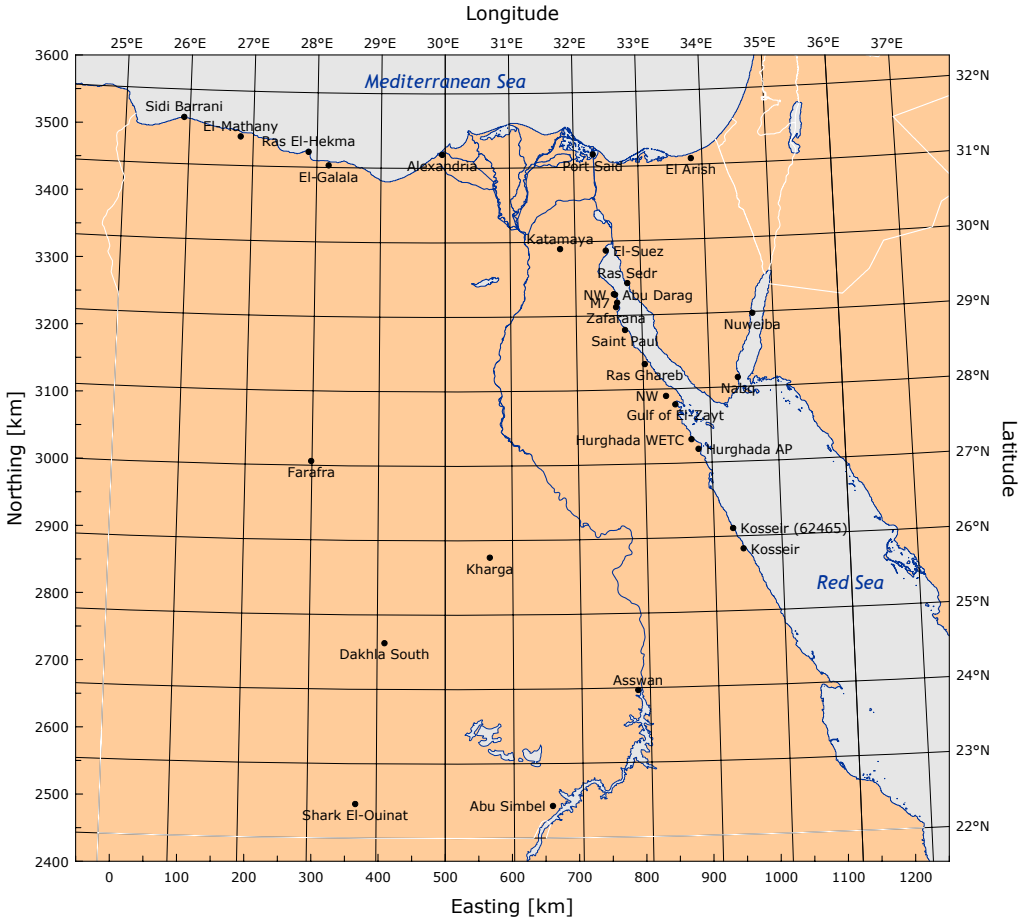

Figure 3-5. Coastline map of Egypt showing a geographic coordinate grid – latitude and longitude lines in degrees north and degrees east, respectively. The coastline map and graticule are drawn in a Cartesian coordinate system representing a Transverse Mercator projection with the central meridian 30°E.

Each zone has a local *x*-axis originating 500 km W of the central meridian of the zone. The *y*-axis originates at the Equator for all three zones. The meteorological station coordinates in the Wind Atlas are referenced to either UTM zone 35 or 36.

Ordinary paper maps in Egypt are drawn in yet another system: a Transverse Mercator projection with zones that are four degrees wide. These systems are referred to as the 'Purple Belt', 'Red Belt' and 'Green Belt' coordinates, and are referenced to the 'Old Egyptian 1907' map datum.

Transformation between different coordinate systems is quite complicated and must be performed using specialised software. The WAsP Map Editor (Rathmann, 2005) and the Geo-Projection Transformer (Rathmann, 2005) are two software packages that can transform single points, lists of points and entire WAsP map files – using several different map projections and almost 150 different map datums.

Global Positioning System (GPS) devices also refer to a specific coordinate system. The default system in most receivers is (latitude, longitude) referred to WGS84, but this can be changed in a set-up menu. Coordinates downloaded from the GPS using some software may be referenced to WGS84, regardless of the setting of the GPS.

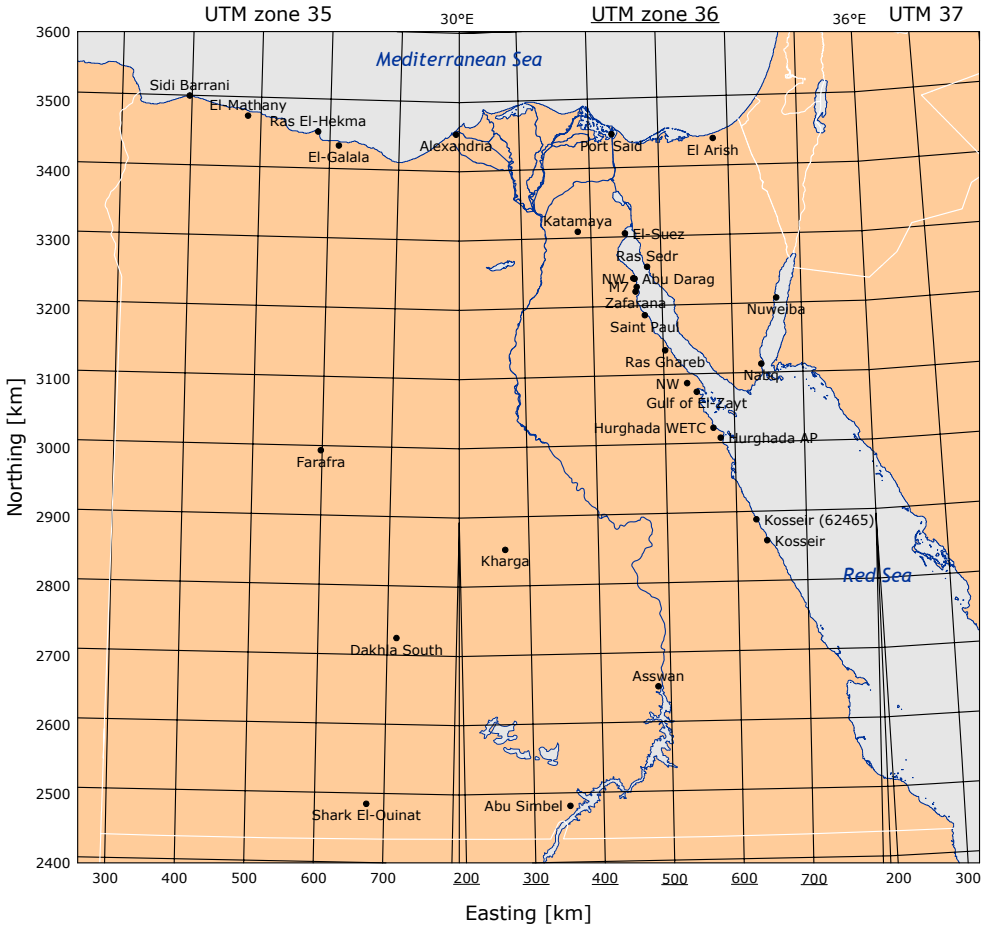

Figure 3-6. Coastline map of Egypt showing the three UTM zones covering Egypt: 35, 36 and 37. Each zonal coordinate system is Cartesian and the coordinates can be given in [m] or [km]. The coastline map and coordinate grids are drawn in a Cartesian coordinate system representing a Transverse Mercator projection with the central meridian 30°E.

3.3 Wind resource mapping

For a given wind farm site, the regional wind climate derived from the numerical wind atlas or a near-by meteorological station can be used to map the wind resource over the site. An example is given in Figure 3-7, where the annual energy production (AEP) of a 600-kW wind turbine has been estimated by means of the WAsP model. The wind farm site is located close to Zafarana and the regional wind climate from the meteorological station Abu Darag was used for the modelling.

Even within this fairly small and homogeneous site, the estimated production varies by more than 20%, from 0.92 to 1.13 times the mean value over the site, respectively. The accuracy of the resource map has been verified by wind measurements at nine of the positions (meteorological masts M1-M9) indicated in the map (Hansen et al., 1999). The main reasons for this variation are the distance to the coast of the Gulf of Suez and the terrain height variations within the site.

Wind resource maps for any area in Egypt can be established in the same manner by using the regional wind climate statistics from the numerical wind atlas. Such maps are likely to be less detailed and reliable than the map shown in Figure 3-7.

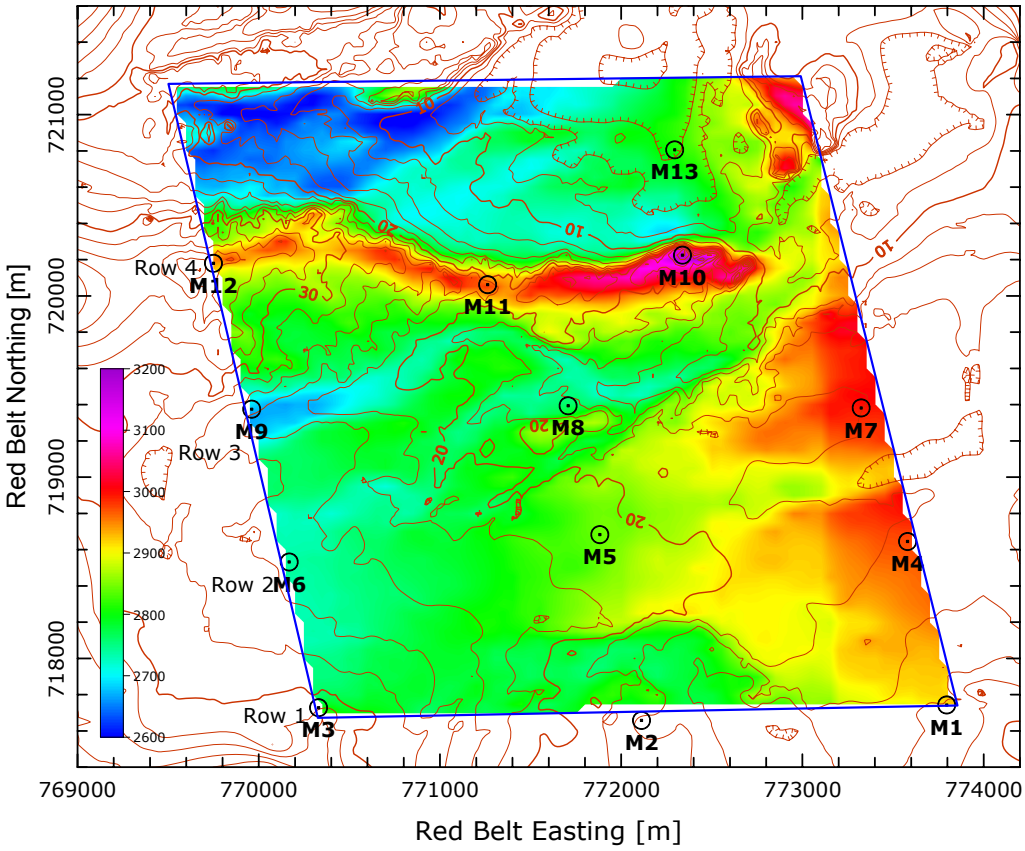

Figure 3-7. Estimated Annual Energy Production in [MWh] for a 600-kW wind turbine at the NREA/Danida wind farm site close to Zafarana. The hub height is 45 m a.g.l. and the power production was calculated in a regular grid with a grid point spacing of 50 m. Height contour interval is 2 m. M1 to M13 are meteorological stations with 47-m masts used for verification purposes.

3.4 Wind farm calculations

The wind resource map is one of the basic inputs in the wind turbine siting procedure and in the construction of the wind farm layout. Figure 3-8 shows a sample layout for a 60-MW wind farm in the Zafarana site mentioned above. The sample wind farm consists of one hundred 600-kW wind turbines, where the wind farm layout was designed to maximise wind farm production and minimize wind farm wake effects – while at the same time also being aesthetically pleasing.

Once the wind farm layout and turbine type have been chosen, the wind atlas methodology (WAsP) can be used to estimate the actual annual energy production from the wind farm, including wake effects. For this calculation to be reliable, it is important to use site-specific power and thrust curves for the wind turbine in question. Information on the average annual air density at the site is required; this may be calculated from site measurements of atmospheric pressure and air temperature. If such measurements are not available, the annual average values of atmospheric pressure and air temperature may be estimated from the *Climatic Atlas of Egypt* (Egyptian Meteorological Authority, 1996).

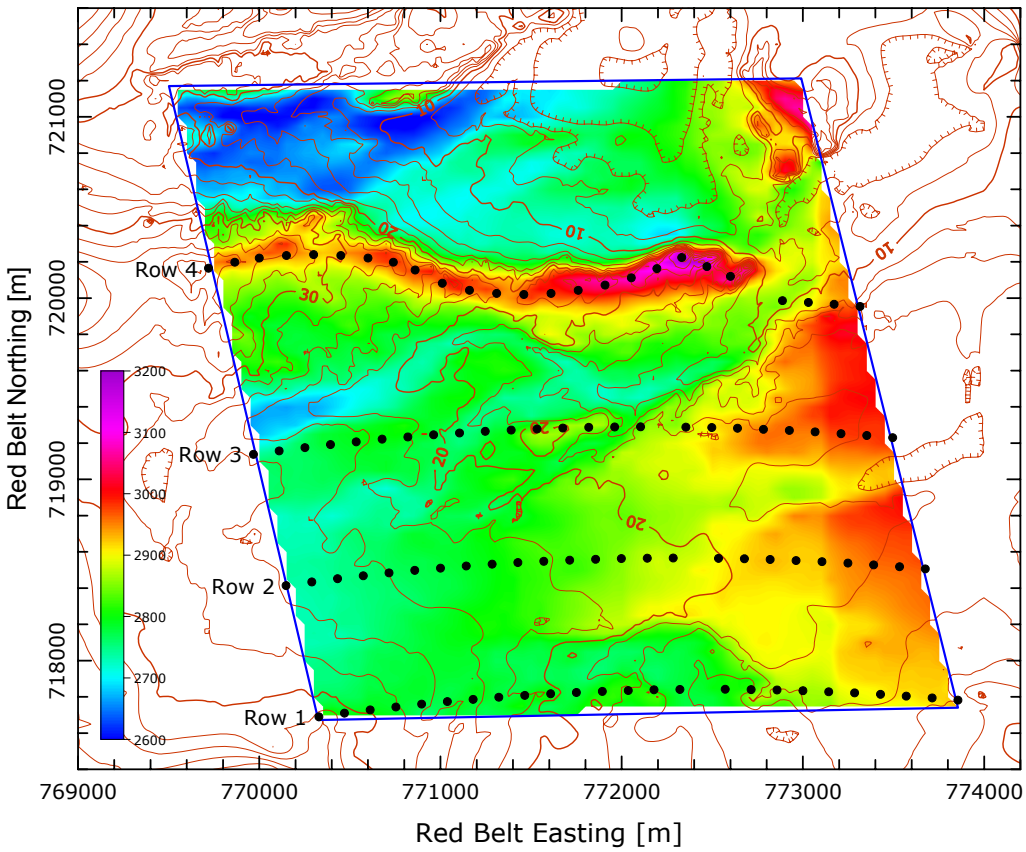

Figure 3-8. Sample layout for a 60-MW wind farm in the NREA/Danida wind farm site close to Zafarana. The farm consists of one hundred 600-kW wind turbines. Each turbine position is indicated by a dot, the diameter of which is proportional to the rotor diameter.

3.5 Design wind conditions

In addition to the predicted wind climate – the distribution of wind directions (wind rose) and the sector-wise distributions of mean wind speed – other wind conditions may be important for the design of a wind farm. Some of these characteristics have been measured directly at the wind atlas stations; others must be estimated from the meteorological data. Chapter 8 provides a brief summary of the extreme wind speeds, the gustiness of the wind and the turbulence intensity estimated from measurements in the database. For extrapolation of these wind conditions to wind turbine sites and for estimations at sites where no stations exist, other models must be employed, e.g. the WAsP Engineering model (Jørgensen et al., 2005).

3.6 Reliability of wind resource estimates

The reliability of wind power calculations, such as those presented above, depends first of all on the reliability of the data from the meteorological station from which the wind statistics have been derived; i.e. the accuracy of the wind speed and direction measurements and the amount of data available. Secondly, it depends on the complexity of the terrain; at the meteorological station as well as around the sites of interest. Finally, the geographical variability of the wind resource will necessarily add to the uncertainty of the estimates.

The reliability of the wind data can be assessed from the statistical tables and graphs given for each station in Chapter 7. Furthermore, the meteorological measurements are stored in a database and the data are thus available for additional analyses, see Appendix B.

The complexity of the terrain around the meteorological stations can be assessed from the maps given in Chapter 7, as well as from other readily available information, such as standard 1:50,000 topographical maps, SRTM elevation data and Google Earth views of the landscape.

The spatial variation of the wind resource can be assessed in quite some detail from the results of the mesoscale modelling of Egypt and the six detailed modelling domains presented in Chapter 4. These results may not be sufficiently detailed and accurate for micro-siting and production calculations, but provide a fairly reliable picture of the large-scale spatial variations of the wind resource.

The similarity principle

Current knowledge about the uncertainties in WAsP wind resource assessment may be summarised in the so-called *similarity principle*: Accurate predictions of wind climate and annual energy production based on observed wind climates require that the meteorological station (predictor) and the turbine site (predicted site) should be as similar as possible with respect to:

- Topographical setting
    - ruggedness (RIX index)
    - elevation and exposure
    - distance to significant roughness changes (coastline)
    - background roughness lengths
- Climatic conditions
    - regional wind climate (synoptic and mesoscale)
    - general forcing effects
    - atmospheric stability

With respect to WAsP, accurate predictions using the WAsP BZ-flow model – and indeed most other wind resource assessment and siting models – may be obtained (Bowen and Mortensen, 1996) provided:

- the meteorological station and wind turbine site are subject to the same overall weather regime, i.e. that mesoscale effects are not significant or, if present, the two sites are affected in the same way,
- the prevailing weather conditions are close to being neutrally stable, and
- the surrounding terrain (of both sites) is sufficiently gentle and smooth to ensure mostly attached flows.

The latter requirement in particular has a significant impact on the accuracy of WAsP predictions in complex terrain.

PART II
THE MODELS AND THE ANALYSIS

4 Mesoscale modelling

4.1 Model description

The Karlsruhe Atmospheric Mesoscale Model (KAMM) is a 3D, non-hydrostatic, and incompressible mesoscale model. It is described in Adrian and Fiedler (1991), and Adrian (1994). Spatial derivatives are calculated in the model by central differences on a terrain following grid. The turbulent fluxes are modelled using a mixing-length model with stability dependent turbulent diffusion coefficients in stably stratified flow, and a non-local closure for the convective mixed layer. Lateral boundary conditions assume zero gradients normal to the inflow sides. On outflow boundaries, the horizontal equations of motion are replaced by a simple wave equation allowing signals to propagate out of the domain without reflection. Gravity waves can penetrate the upper boundary outward using the boundary condition of Klemp and Durran (1983).

KAMM is able to run as a "stand-alone" model, i.e. the model can be run by using only the large scale forcing in the form of a single vertical profile of geostrophic wind and virtual potential temperature. Hence, it is not necessary to nest the mesoscale model within a larger model domain that must supply the boundary conditions. At regional scales the mesoscale model is used to model atmospheric flows in domains of order 500 km × 500 km × 5 km.

4.2 Topographic data

Data concerning the surface elevation comes from the United States Geological Survey (USGS) GTOPO30 global topographic dataset; see Chapter 9 for the web page reference. This data uses a longitude-latitude projection at 30 arc-second resolution. The elevation data is manipulated first to change it to a UTM coordinate system and then to change the resolution appropriately for the mesoscale simulations.

Data concerning the surface roughness is derived from the United States Geological Survey (USGS) Global Land Cover Classification (GLCC); see Chapter 9 for the web page reference. This data is given using the Lambert azimuthal projection. The land cover data is converted to the UTM coordinate system and then to the appropriate resolution. It is also converted from land cover data to surface roughness data. This is done by using a look-up table that relates specific land cover classifications to specific terrain surface roughnesses.

4.3 Initial meteorological data

Atmospheric data is obtained from the NCEP/NCAR reanalysis data set. Data is given on a longitude-latitude grid with a resolution of 2.5 × 2.5 degrees at various isobaric surfaces through the atmosphere. This data needs to be converted into geostrophic wind and potential temperature values for different heights in meters in the atmosphere. The data is compiled into long time-series data for use in the wind class generation programs. The Climate Diagnostics Centre provides access to the NCEP/NCAR reanalysis data; see Chapter 9 for the web page reference. The NCEP/-NCAR data from 1965 to 1998 has been used for the numerical wind atlas studies described in this chapter.

4.4 Classification system

The time-series data of wind and temperature profiles derived from NCEP/NCAR reanalysis data is used to determine approximately 80 to 120 wind classes. These wind classes form a representative set of wind conditions for the region. The wind classes represent different wind speeds, wind directions, atmospheric stability or shear.

A way to measure the likely impact of an obstacle, such as a hill, on the flow is to calculate the Froude number. The Froude Number is $U/(h \times N)$, where U is a velocity scale, h is a height scale of the obstacle and N is the Brunt-Väisälä frequency, where $N^2 = (g/\theta_0)(\mathrm{d}\theta/\mathrm{d}z)$.

For cases where the Froude number is below one, the flow tends to flow around obstacles. For cases where the Froude number is above one, the flow tends to flow over obstacles. More stable conditions tend to lead to lower Froude number flow behaviour, in which channelling between or around obstacles is more prevalent, as well as lee effects to be more persistent. The figures of the example simulated wind fields that follow for the different computational domains also show examples of different Froude number flow for similar wind speeds.

The inverse Froude number squared is used in the wind class classification system to differentiate meteorological situations that have similar wind speed and direction but different thermal stratification. The height scale used is 1500 m, the height difference between the first and second level in the wind class profile.

4.5 Post-processing

After the mesoscale simulations are complete for all of the wind classes, the results are compiled in the post-processing stage of the methodology.

First, a weighted mean of the wind class simulations results is calculated. This yields a simulated resource map. Second, for each wind class simulation, effects of elevation and roughness variation are removed with modules similar to those used in the WAsP software. Then the weighted mean of the adjusted result from the wind simulations is made. This yields a wind atlas map, or generalized wind map for flat, uniform surface conditions of a specified roughness. Figure 4-1 shows a schematic diagram of the wind class simulations and the post-processing steps.

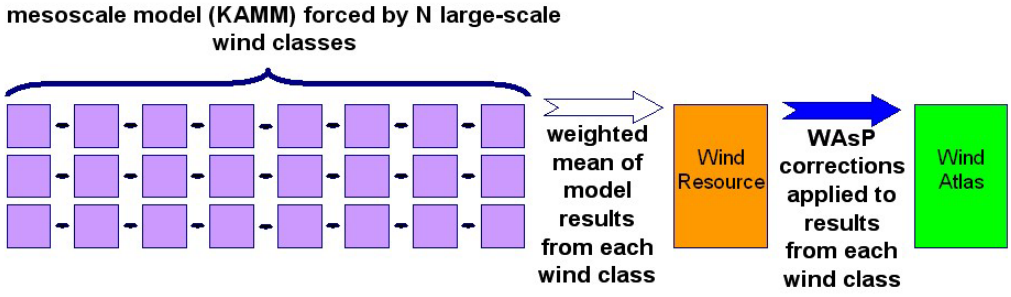

Figure 4-1. A schematic diagram showing the KAMM/WAsP numerical wind atlas methodology.

The calculation of the wind atlas values uses a logarithmic profile with friction velocity U_* determined from a stability-dependent geostrophic drag law. Here, the Monin-Obukhov length scale is set to be large, $L_* = 10^9$. This disables the stability correction. Thus, when comparing to a wind atlas based on measurements, it may be appropriate to disable the stability correction of WAsP when processing the measured data.

4.6 Modelling domains

Creating a numerical wind atlas demands a large computational effort, and this computation effort increases with the size of the region to be mapped. Egypt's large size means that it is not possible to perform the numerical wind atlas calculations for the whole country at a reasonable resolution in one go. Therefore it was decided to split the numerical wind atlas effort into several calculation domains. These domains have been chosen with assistance from NREA and EMA, so that the principle areas of interest in the country are covered.

The domains used for numerical wind atlas calculation are shown in Figure 4-2. There are 6 domains: two large Western and Eastern Egypt domains, a Red Sea domain, a Western Desert domain, a Northwest Coast domain, and the Gulf of Suez domain from the earlier numerical wind atlas study.

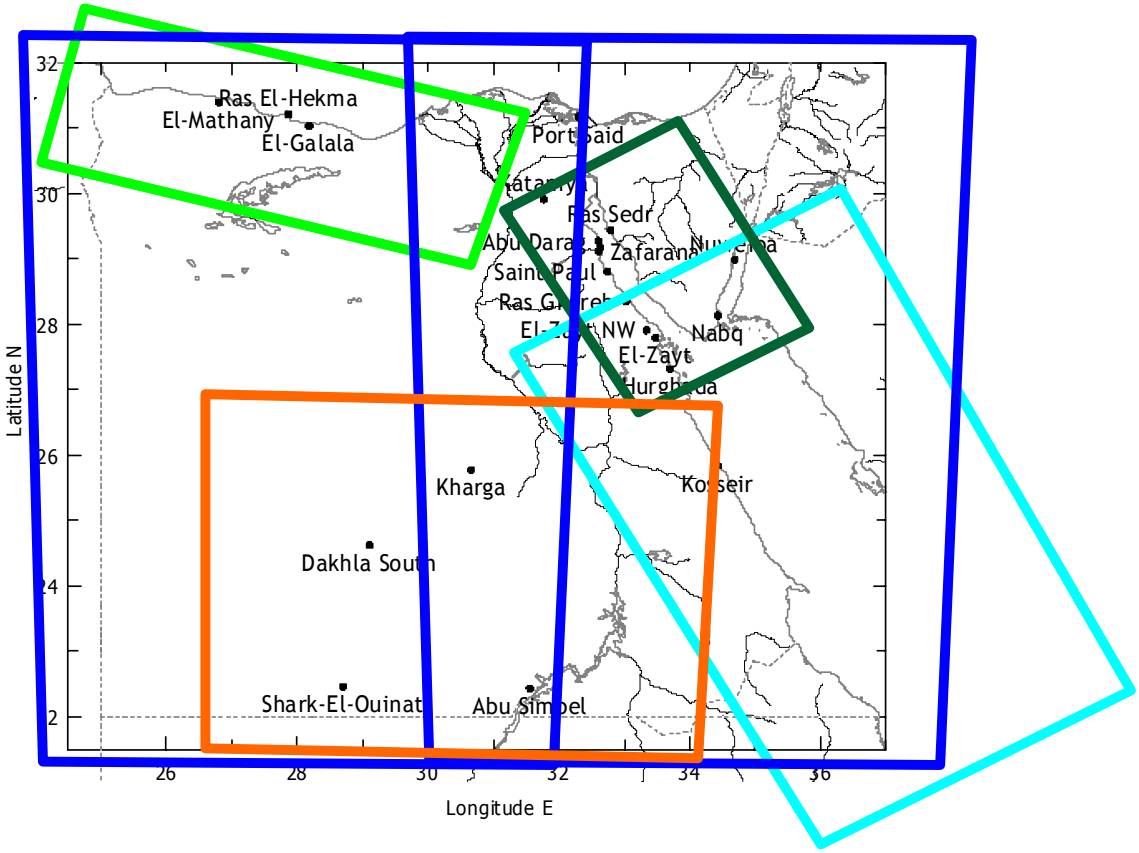

Figure 4-2. Map of Egypt showing the various modelling domains being used. A complete numerical wind atlas calculation is made for each domain.

In all modelling domains the land and sea temperatures are set higher than the air temperature by 8.0°C and 3.0°C, respectively.

Western and Eastern Egypt

The purpose of constructing a wind atlas to cover Egypt in two parts is to gain a whole impression of the wind resources in Egypt. The disadvantages of this approach are that the resolution cannot be very high and that the wind classes are not very location-specific. This means that there is a risk that large-scale wind features that may occur in specific regions of Egypt will not be represented very well in the wind classes. It is for these reasons that the smaller-domain numerical wind atlas calculations are also performed. Because these two domains are larger than usual, further information specific to them is given below.

The advantage of this method is that a map for all of Egypt is recreated that can be used as prospecting tool, whereby areas of the country can be assessed for the wind resource in an approximate way. In this way new areas of promising wind resource may be discovered.

The size of each of the Western Egypt and Eastern Egypt domains is 810 km × 1230 km. At a grid resolution of 7.5 km, 109 × 165 grid points on each model level are used. In the vertical 25 model levels are used.

Wind classes

The calculation domain is very large for the Western and Eastern Egypt modelling, therefore the way in which the large-scale wind forcing classes are determined is rather different compared to the standard method. Normally, geostrophic winds at a single location would be used to determine wind class limits. Then the wind class vertical profiles of wind speed and temperature would be evaluated using the same single location. In this case however, there is a danger that if one location was used to create wind class limits and wind class vertical profiles that the wind classes will reflect wind conditions specific to that single location. The typical wind classes in the north of the large domain may well be different from the typical wind classes for the south of the domain.

In order to overcome this problem two differences to the standard method are employed. First, wind class limits are distributed systematically over 12 direction sectors, using wind speed limits of 4, 6, 8, 10, 14 and 20 ms^{-1}. This gives 84 wind classes. The class limits are applied at the 100-m geostrophic wind. In the standard method the wind class limits would be determined optimally using the geostrophic winds at one location.

Secondly, the geostrophic winds at 36 regularly spaced locations around Egypt are used to determine the wind class vertical profiles. In the standard method the wind class profiles would be determined using the geostrophic winds at one location.

As in the standard method, the varying importance of each wind class for different parts of the domain is accounted for by calculating the frequency of occurrence of the wind classes at the regularly spaced locations throughout the domain.

Each of the wind class profiles comprises of the westerly and southerly components of the geostrophic wind and the virtual potential temperature at 100, 1500, 3000, 5500 meters. The mesoscale model is run with a fixed simulation time of 8 hours and 23 minutes.

Smaller regional domains

Descriptions of the smaller, regional domains covering the Northwest Coast, the Western Desert, the Gulf of Suez and the Red Sea are given in the sections below. These sections also contain descriptions and illustrations of the geostrophic wind classes used for the analyses.

4.7 Domain set-up and results

In this section, the important specific set-up parameters and results are given for the 6 domains. Each domain summary is printed on three pairs of facing pages. The first opening contains set-up information and input data used for the modelling

- calculation domain orography
- calculation domain surface roughness
- wind classes, speeds and directions and inverse Froude number squared

The second opening contains examples of single wind class simulations

- simulated wind at 50 m a.g.l. for 4 wind classes

The third opening contains examples of weighted mean results for the domain

- mean simulated wind speed at 50 m a.g.l.
- mean generalized wind speed at 50 m above flat, uniform terrain with a surface roughness of 0.0002 m.
- mean simulated power density at 50 m a.g.l.
- mean generalized power density at 50 m above flat, uniform terrain with a surface roughness of 0.0002 m.

For practical reasons, the maps of western Egypt, eastern Egypt and the Red Sea have been rotated 90° counter-clockwise, so that the north direction is to the left.

WESTERN EGYPT DOMAIN

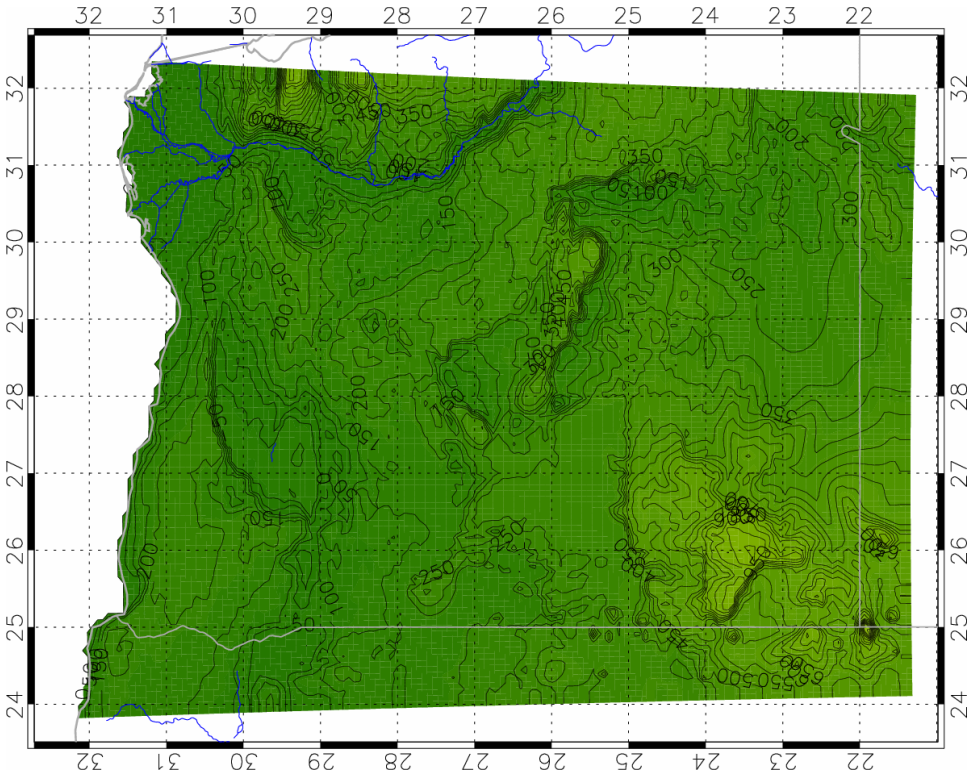

Figure 4-3. The computational domain orography. The contour interval is 50 m. Note, that the north-direction is to the left.

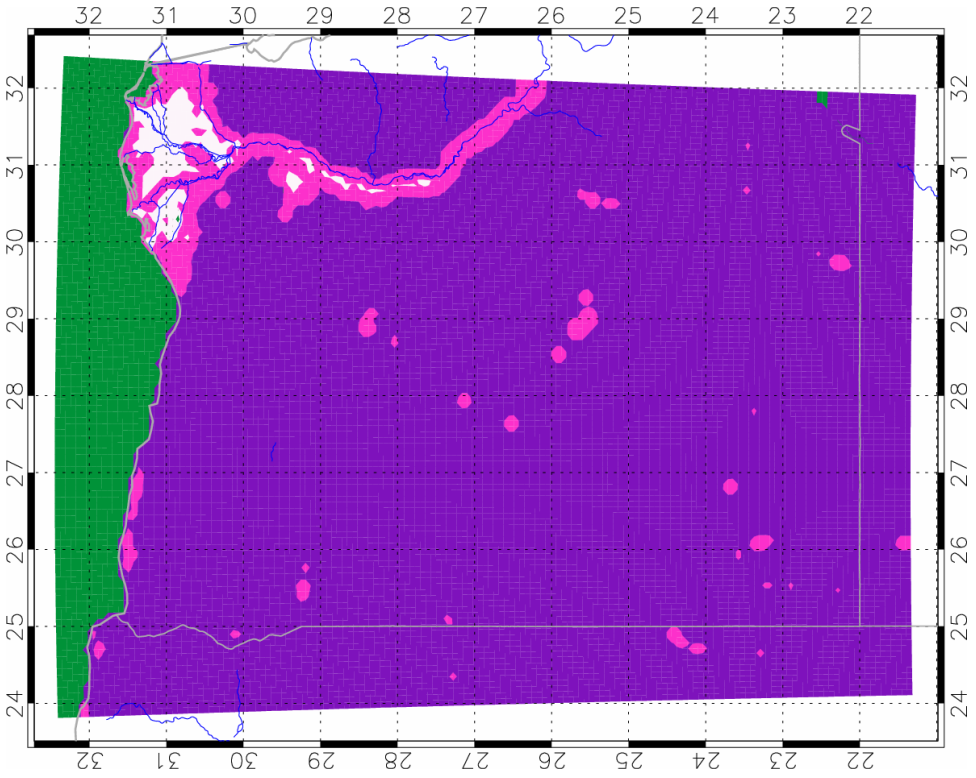

Figure 4-4. The computational domain roughness. Colour key: green 0 m < z_0 ≤ 0.0002 m, purple 0.0002 m < z_0 ≤ 0.002 m, pink 0.002 m < z_0 ≤ 0.1 m, white 0.1m < z_0.

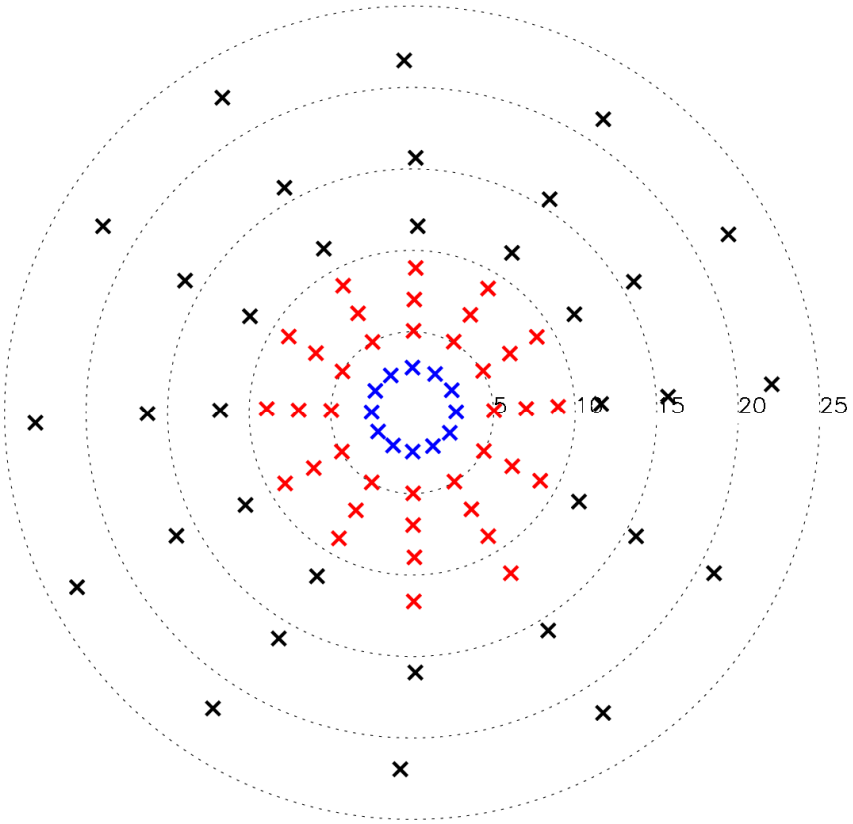

Figure 4-5. The geostrophic wind classes used as forcing for the simulations. Each cross represents a forcing wind speed (distance from the centre of the diagram) and direction. The speed scale is in ms^{-1}. The colours indicate the inverse Froude number squared (IFNS), black IFNS < 1.5, red 1.5 < IFNS < 3.5, green 3.5 < IFNS < 5.5, dark blue 5.5 < IFNS < 7.5, light blue 7.5 < IFNS.

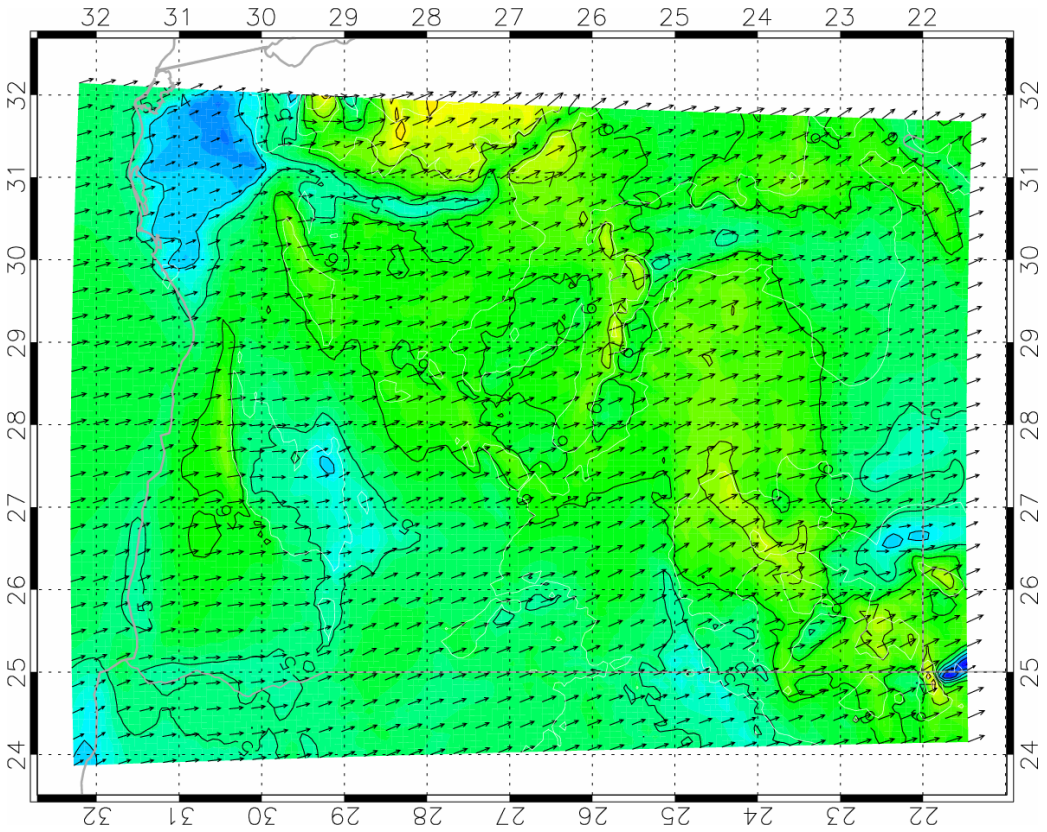

Figure 4-6. Wind vectors and speed at 50 m a.g.l. for a 1 degree 7.0 ms^{-1} forcing. The contour interval is 1 ms^{-1}. Note, that the north-direction is to the left.

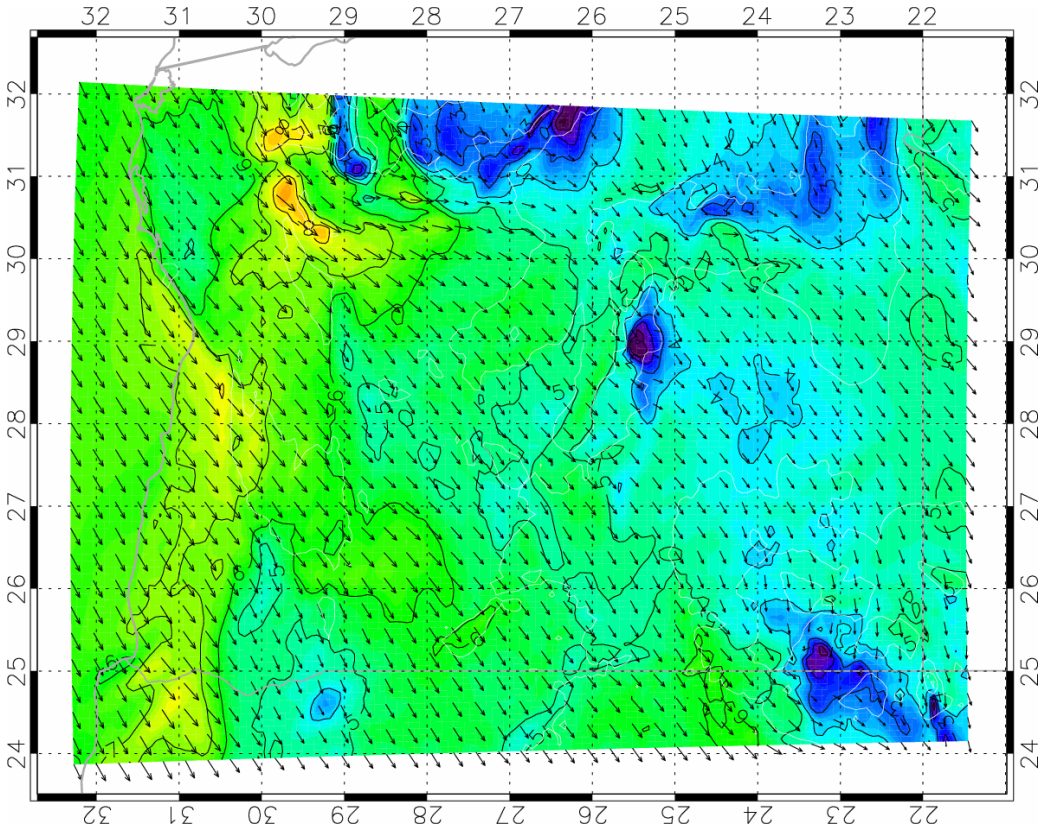

Figure 4-7. Wind vectors and speed at 50 m a.g.l. for a 88 degree 7.0 ms^{-1} forcing. The contour interval is 1 ms^{-1}. Note, that the north-direction is to the left.

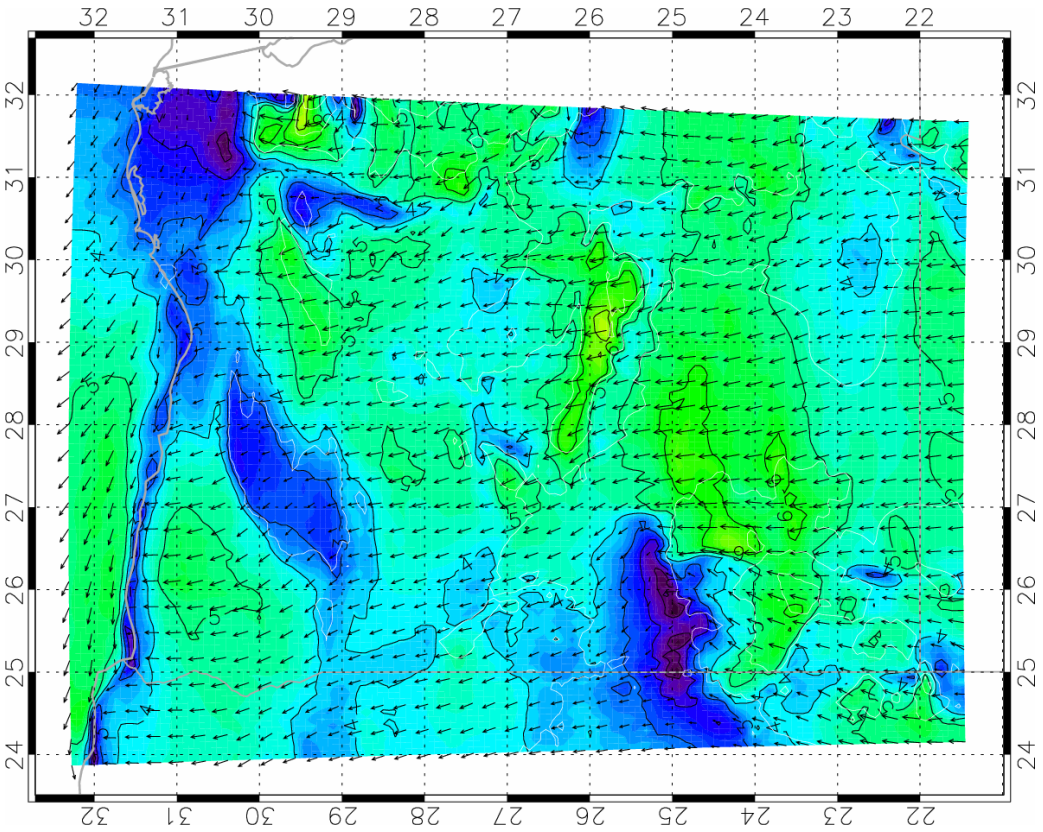

Figure 4-8. Wind vectors and speed at 50 m a.g.l. for a 180 degree 6.9 ms^{-1} forcing. The contour interval is 1 ms^{-1}. Note, that the north-direction is to the left.

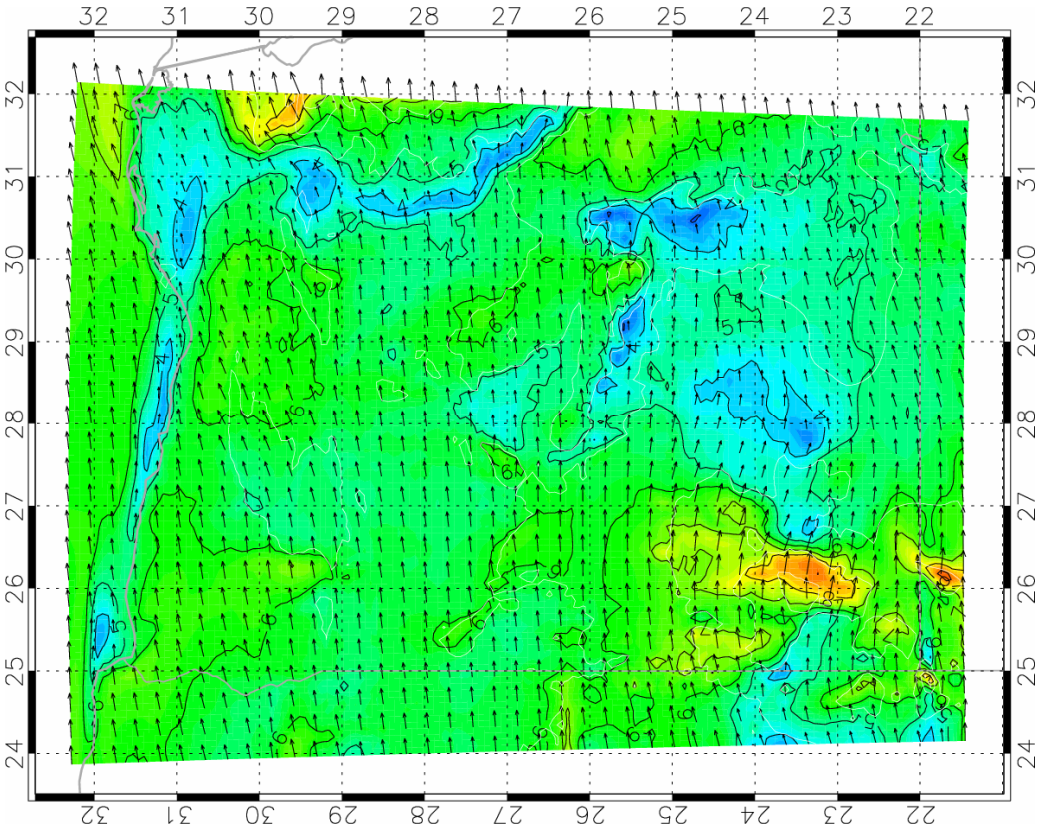

Figure 4-9. Wind vectors and speed at 50 m a.g.l for a 271 degree 7.0 ms^{-1} forcing. The contour interval is 1 ms^{-1}. Note, that the north-direction is to the left.

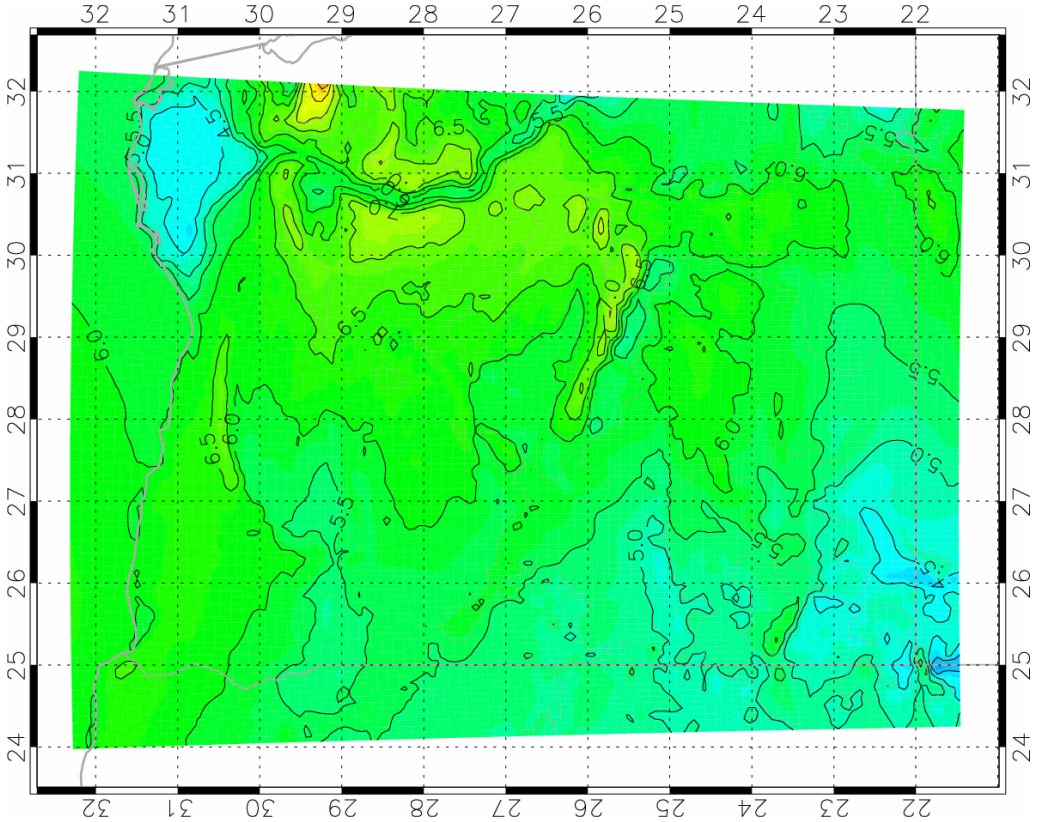

Figure 4-10. Mean simulated wind speed at 50 m a.g.l. The contour interval is 0.5 ms^{-1}. Note, that the north-direction is to the left.

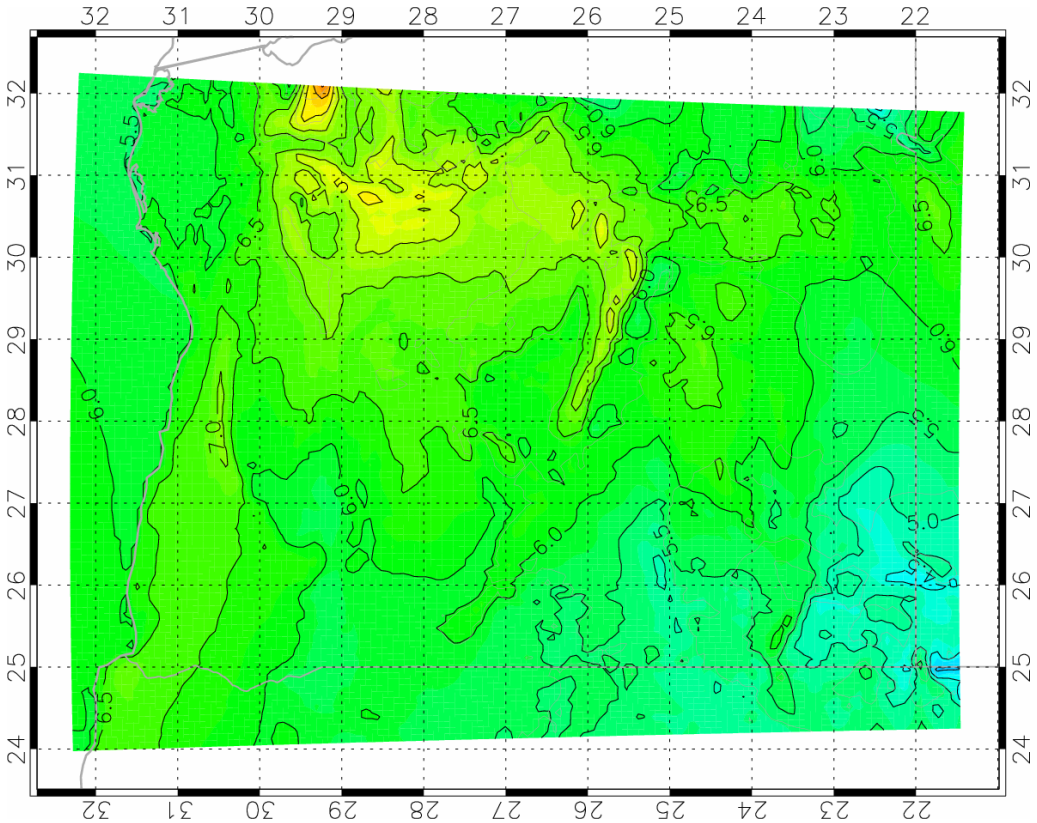

Figure 4-11. Mean generalized wind speed at 50 m a.g.l. for 0.0002 m roughness. The contour interval is 0.5 ms^{-1}. Note, that the north-direction is to the left.

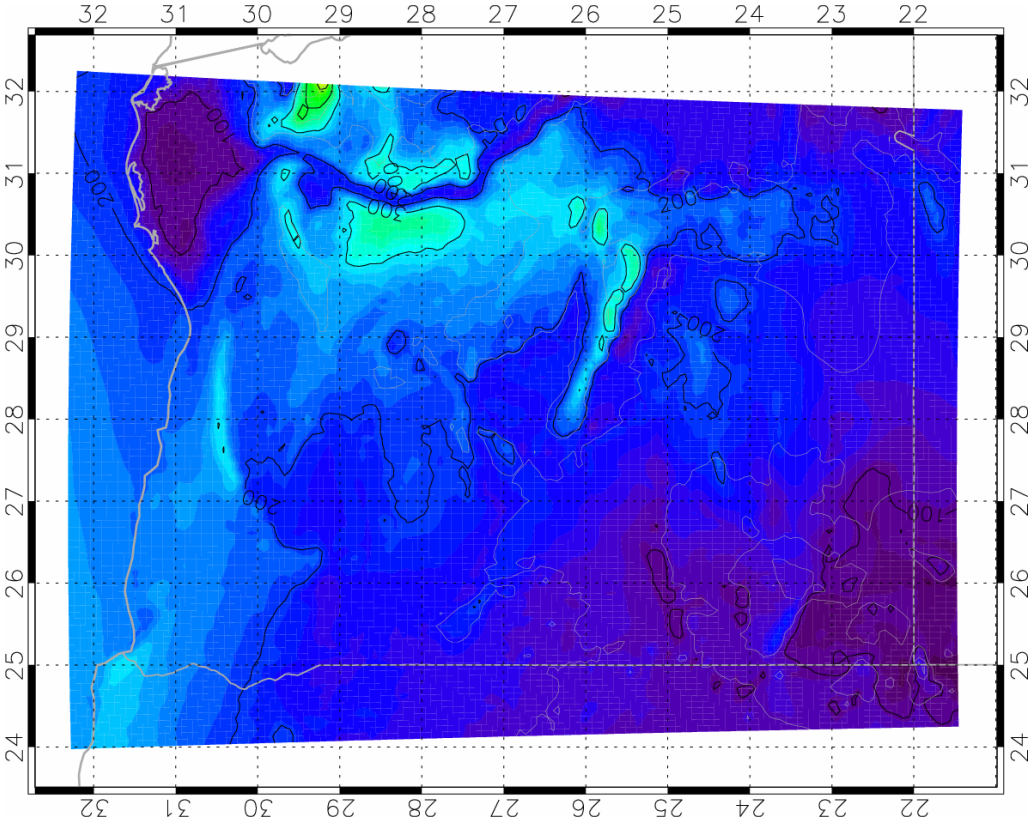

Figure 4-12. Mean simulated wind power density at 50 m a.g.l. The contour interval is 100 Wm^{-2}. Note, that the north-direction is to the left.

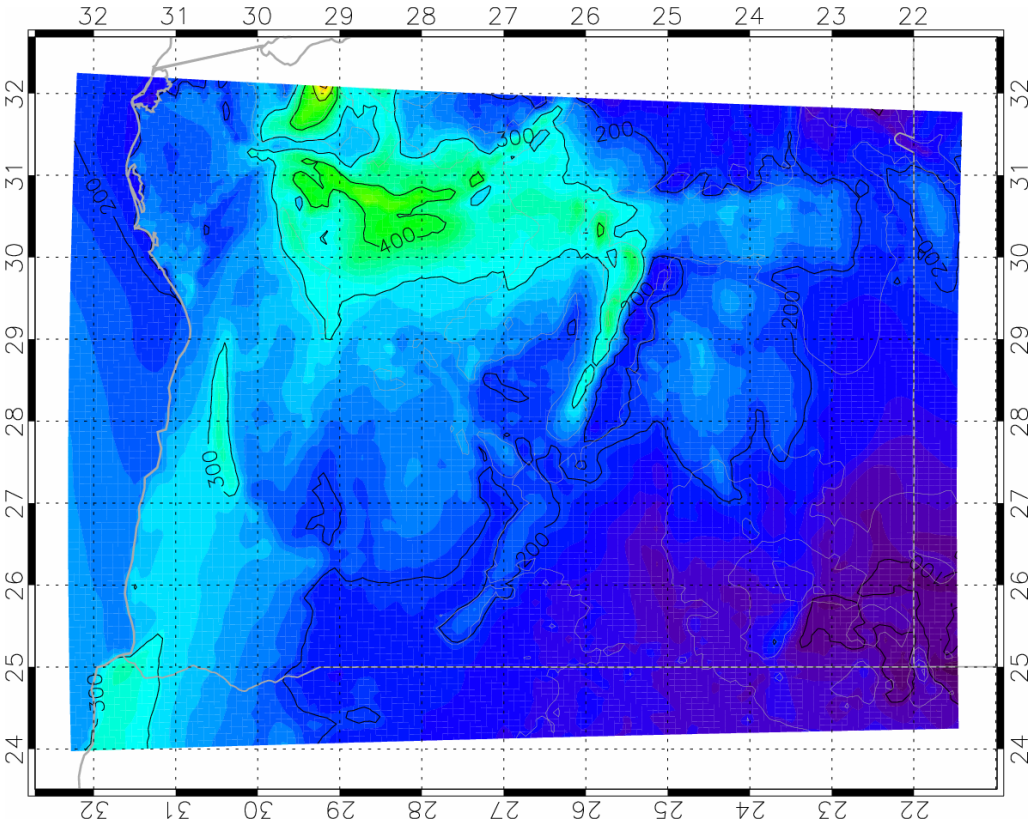

Figure 4-13. Mean generalized wind power density at 50 m a.g.l. for 0.0002 m roughness. The contour interval is 100 Wm^{-2}. Note, that the N-direction is to the left.

EASTERN EGYPT DOMAIN

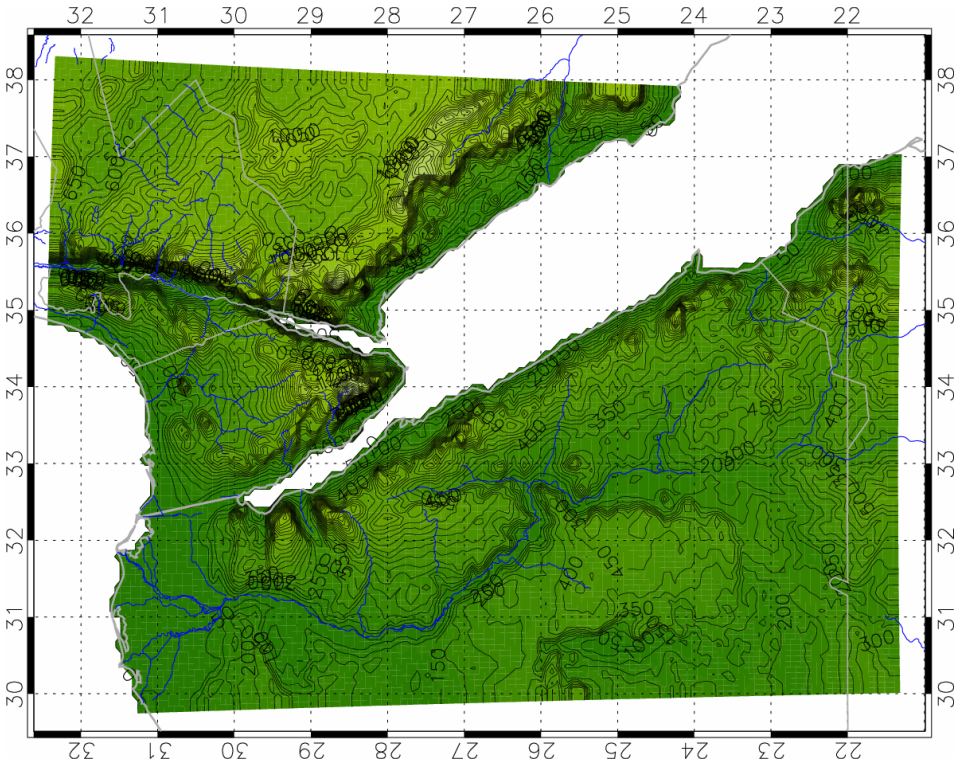

Figure 4-14. The computational domain orography. The contour interval is 50 m. Note, that the north-direction is to the left.

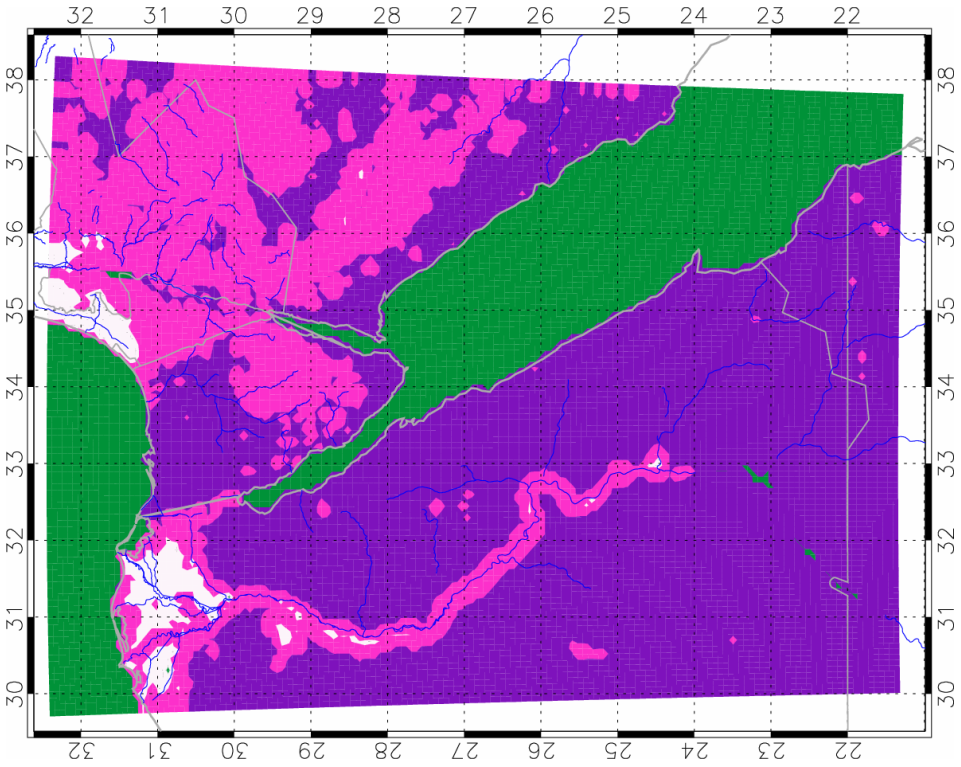

Figure 4-15. The computational domain roughness. Colour key: green 0 m < z_0 ≤ 0.0002 m, purple 0.0002 m < z_0 ≤ 0.002 m, pink 0.002 m < z_0 ≤ 0.1 m, white 0.1m < z_0.

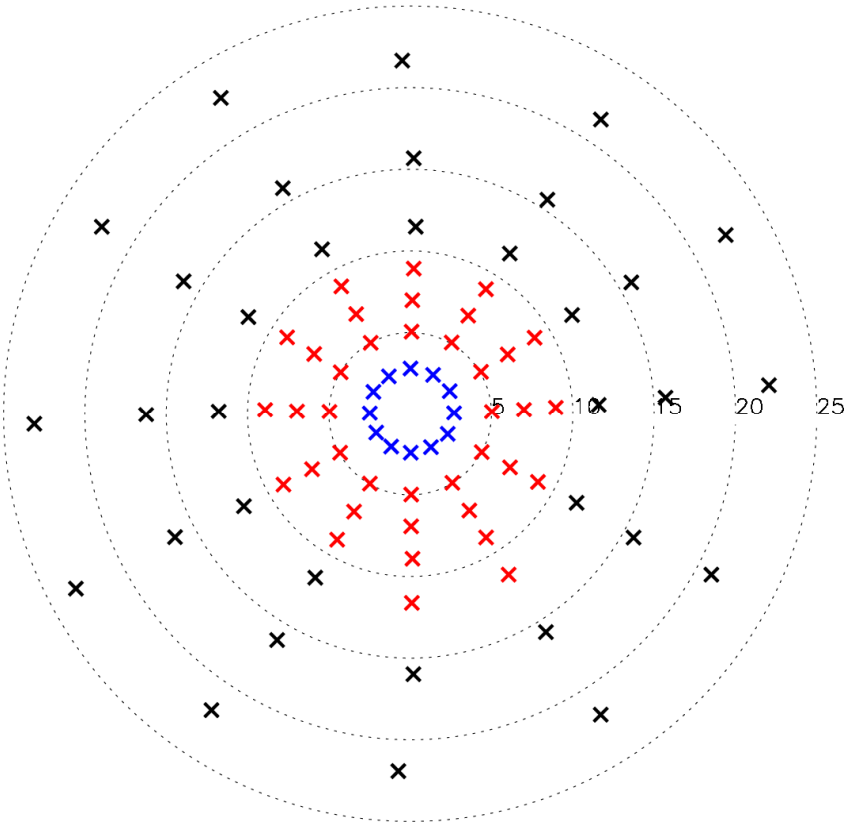

Figure 4-16. The geostrophic wind classes used as forcing for the simulations. Each cross represents a forcing wind speed (distance from the centre of the diagram) and direction. The speed scale is in ms^{-1}. The colours indicate the inverse Froude number squared (IFNS), black IFNS < 1.5, red 1.5 < IFNS < 3.5, green 3.5 < IFNS < 5.5, dark blue 5.5 < IFNS < 7.5, light blue 7.5 < IFNS.

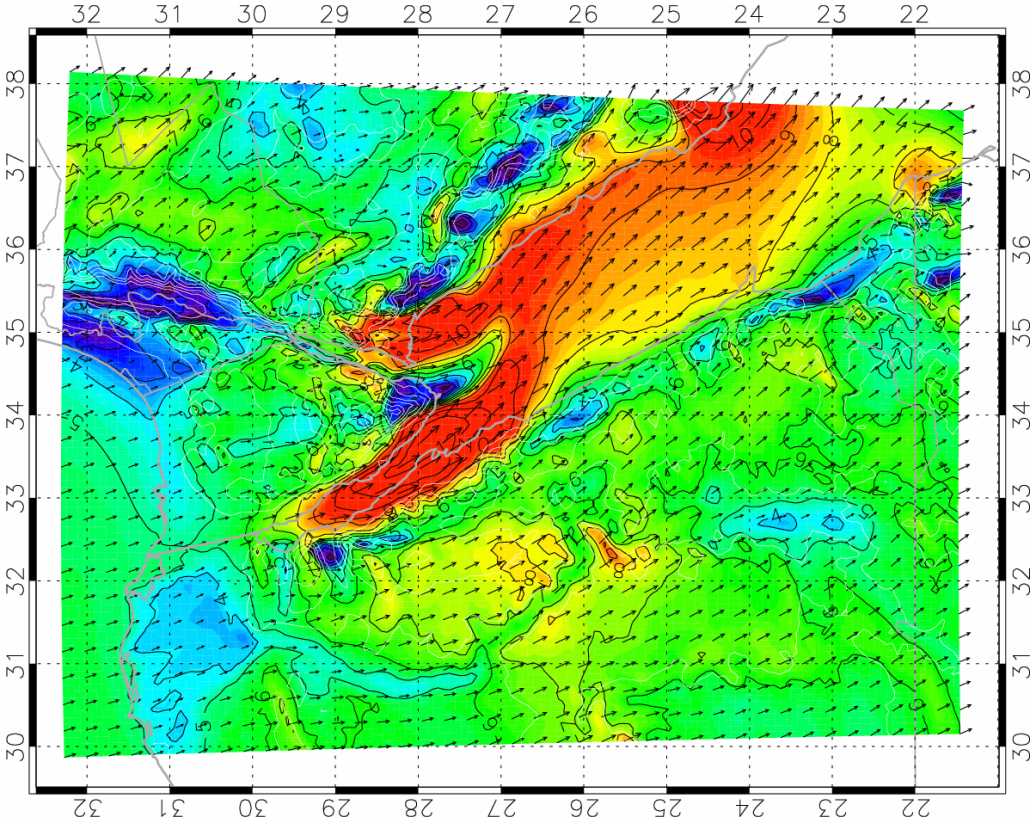

Figure 4-17. Wind vectors and speed at 50 m a.g.l. for a 1 degree 7.0 ms^{-1} forcing. The contour interval is 1 ms^{-1}. Note, that the north-direction is to the left.

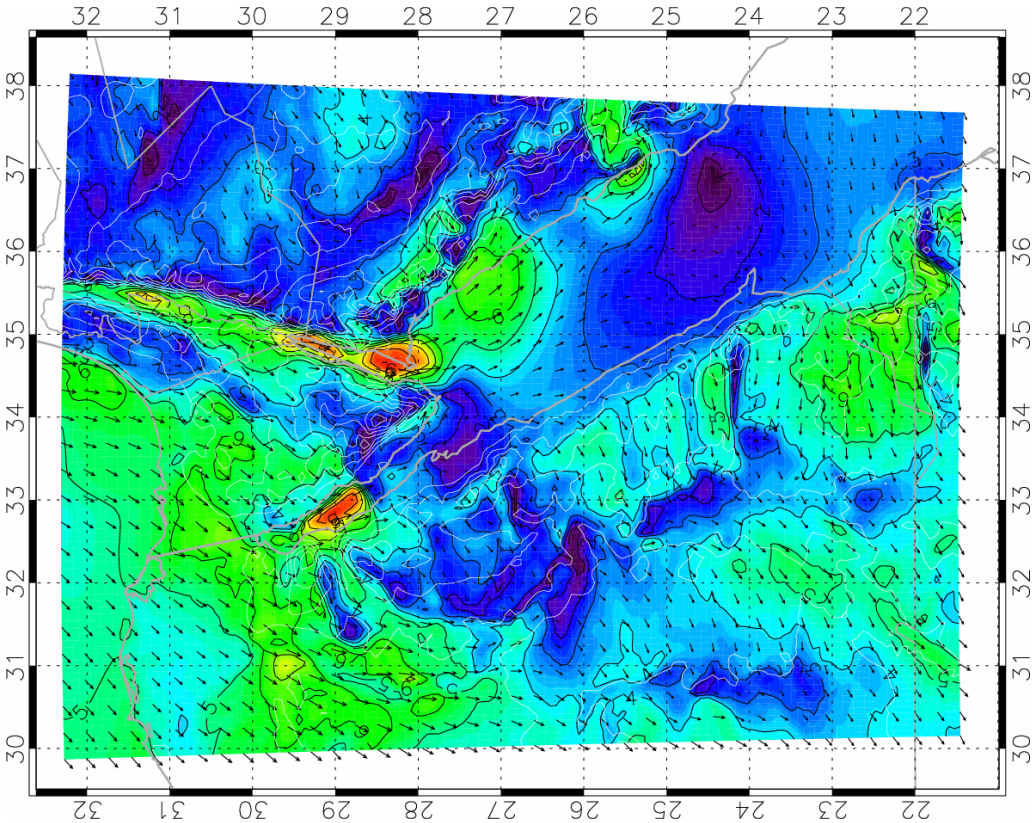

Figure 4-18. Wind vectors and speed at 50 m a.g.l. for a 88 degree 7.0 ms^{-1} forcing. The contour interval is 1 ms^{-1}. Note, that the north-direction is to the left.

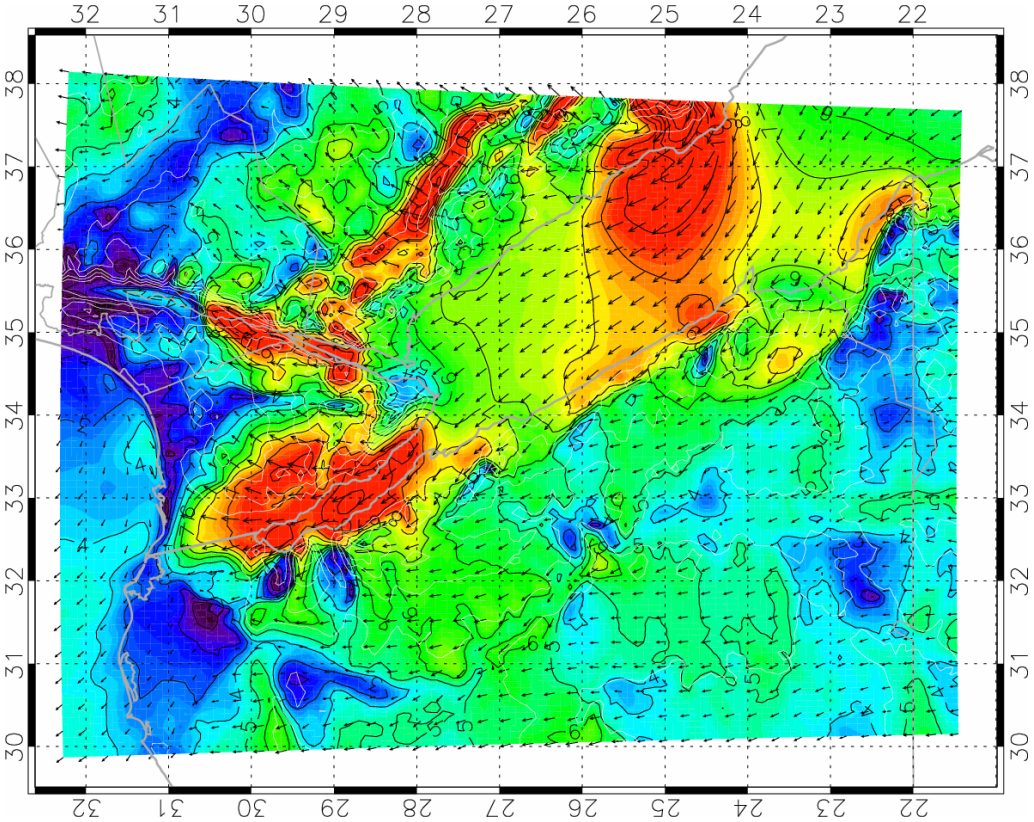

Figure 4-19. Wind vectors and speed at 50 m a.g.l. for a 180 degree 6.9 ms^{-1} forcing. The contour interval is 1 ms^{-1}. Note, that the north-direction is to the left.

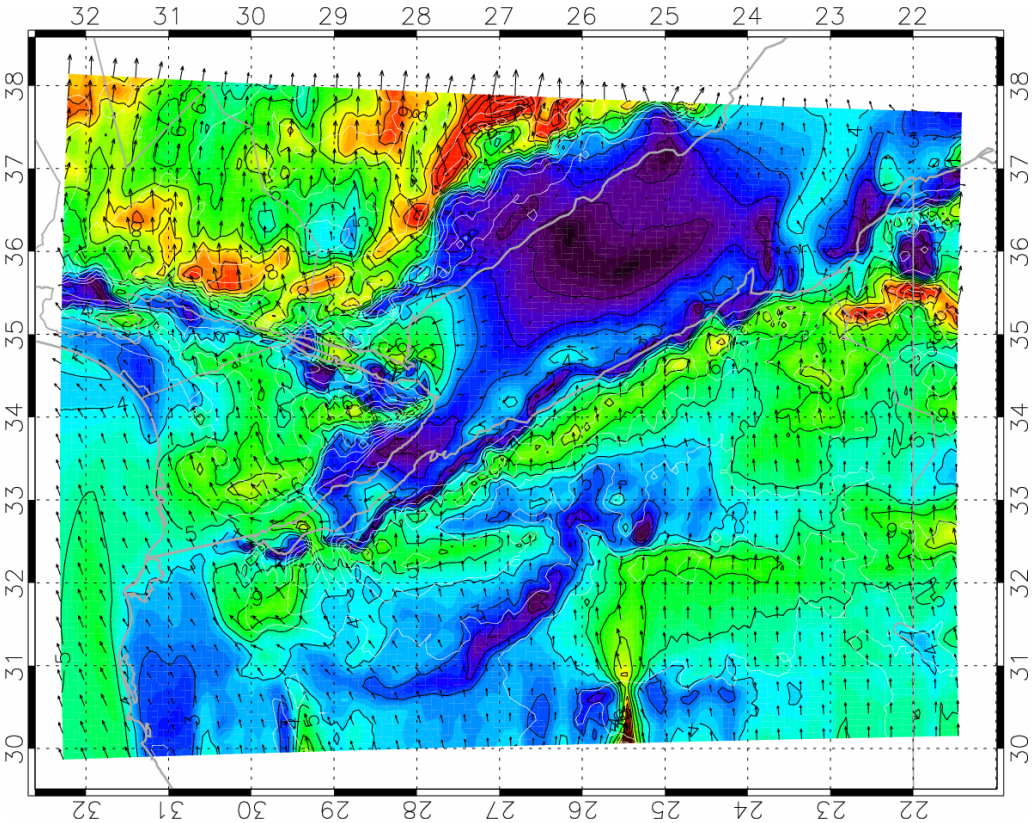

Figure 4-20. Wind vectors and speed at 50 m a.g.l. for a 271 degree 7.0 ms^{-1} forcing. The contour interval is 1 ms^{-1}. Note, that the north-direction is to the left.

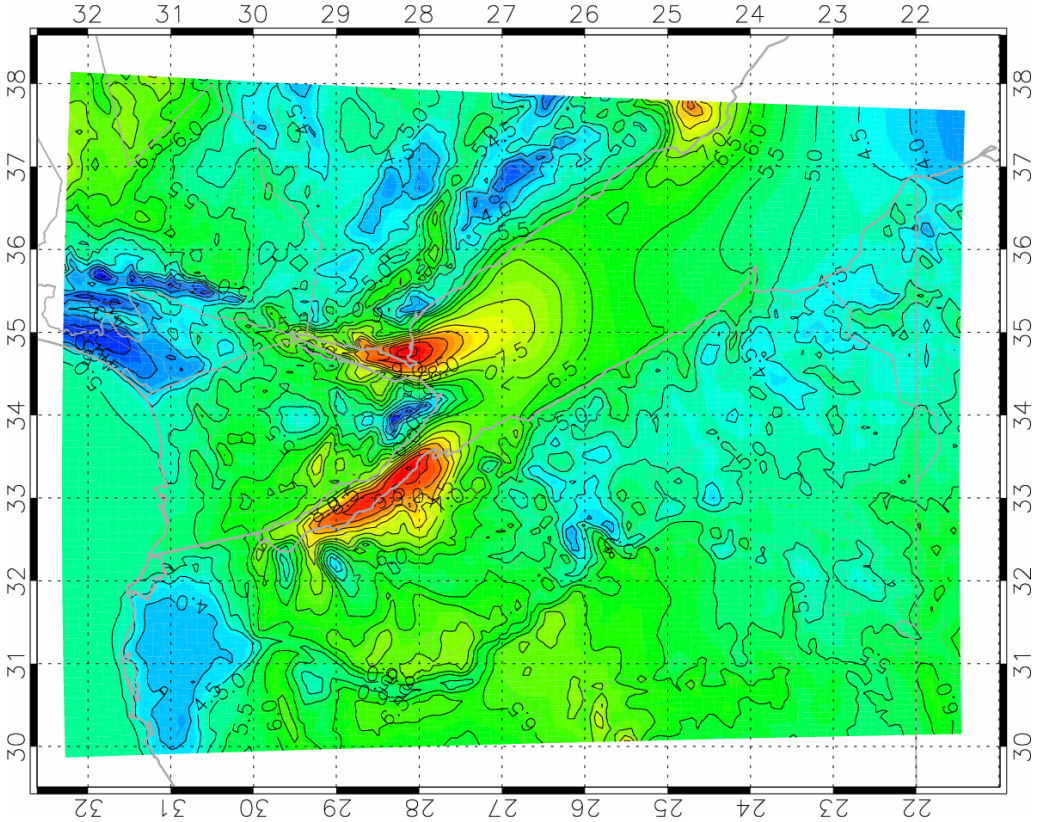

Figure 4-21. Mean simulated wind speed at 50 m a.g.l. The contour interval is 0.5 ms^{-1}. Note, that the north-direction is to the left.

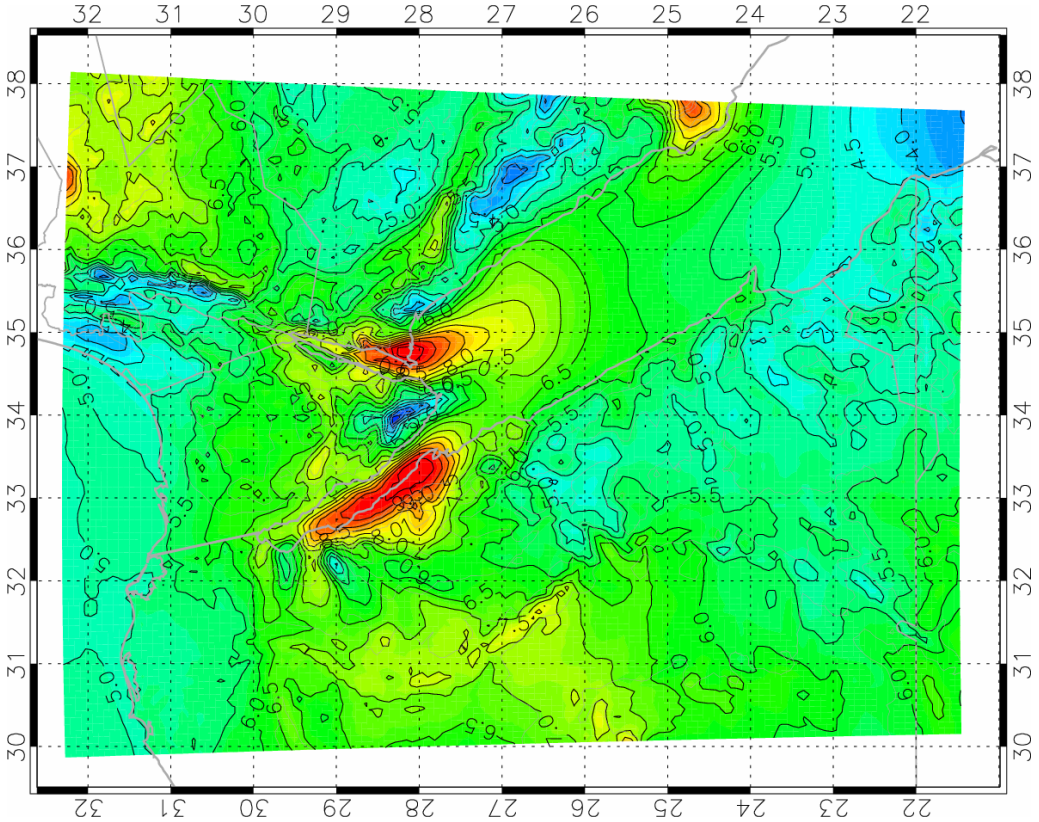

Figure 4-22. Mean generalized wind speed at 50 m a.g.l. for 0.0002 m roughness. The contour interval is 0.5 ms^{-1}. Note, that the north-direction is to the left.

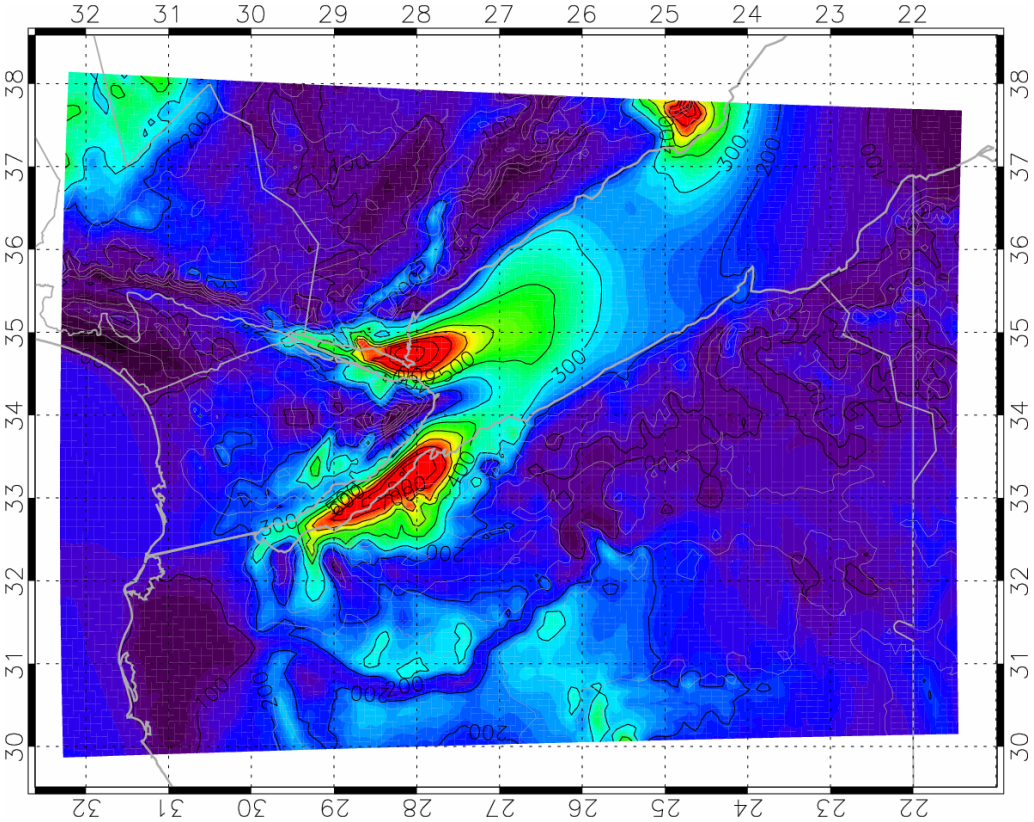

Figure 4-23. Mean simulated wind power density at 50 m a.g.l. The contour interval is 100 Wm^{-2}. Note, that the north-direction is to the left.

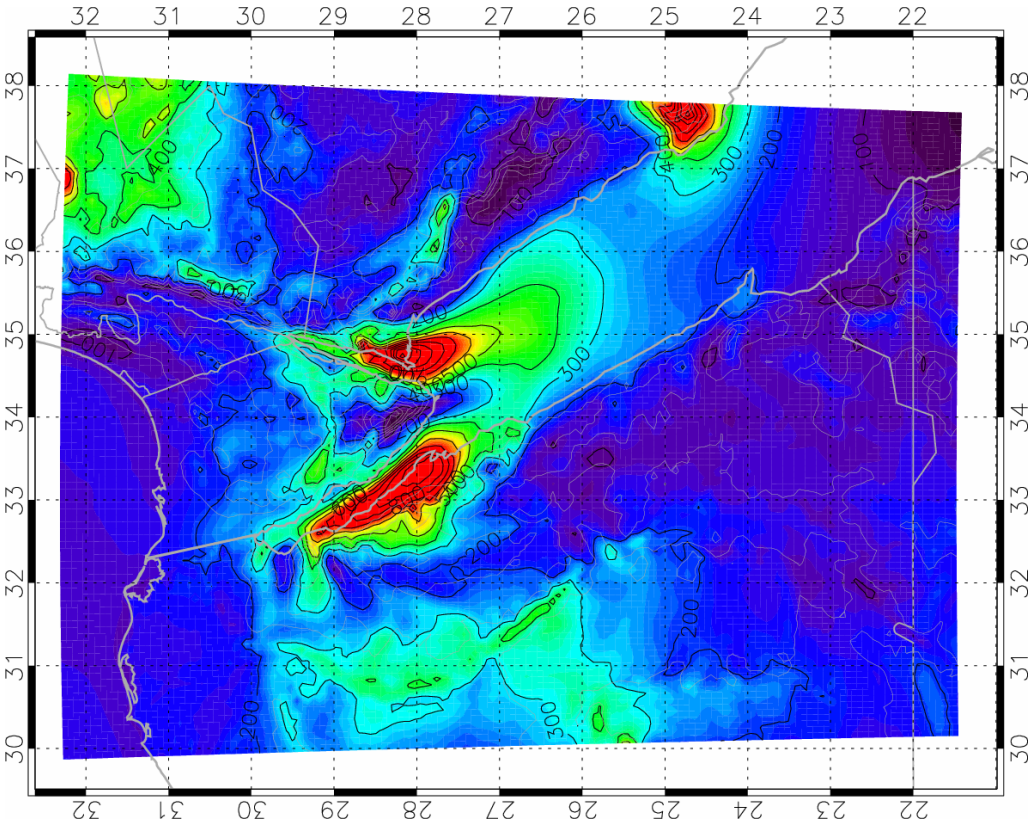

Figure 4-24. Mean generalized wind power density at 50 m a.g.l. for 0.0002 m roughness. The contour interval is 100 Wm^{-2}. Note, that the N-direction is to the left.

NORTHWEST COAST DOMAIN

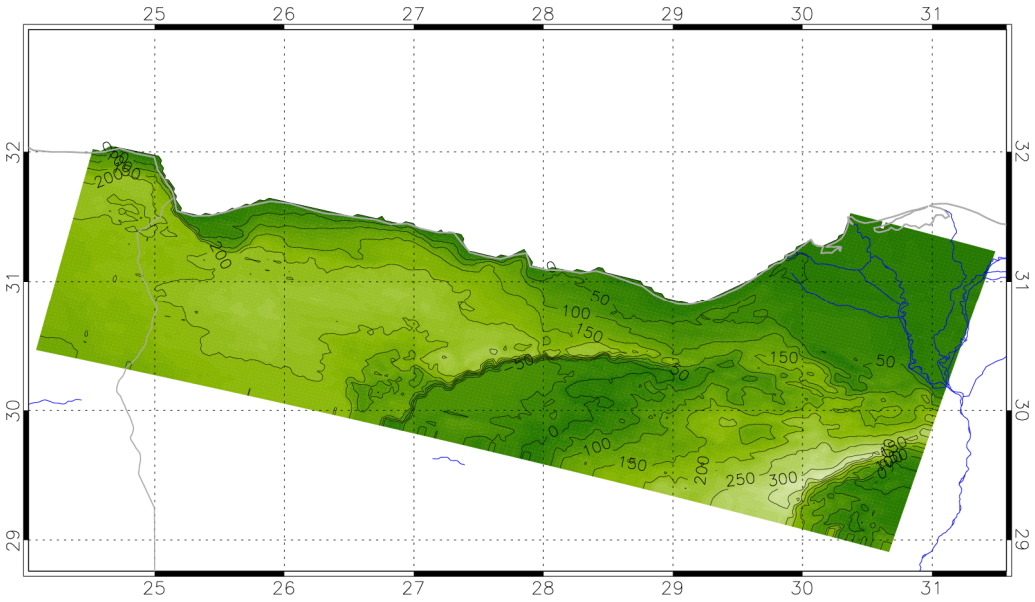

Figure 4-25. The computational domain orography. The contour interval is 50 m.

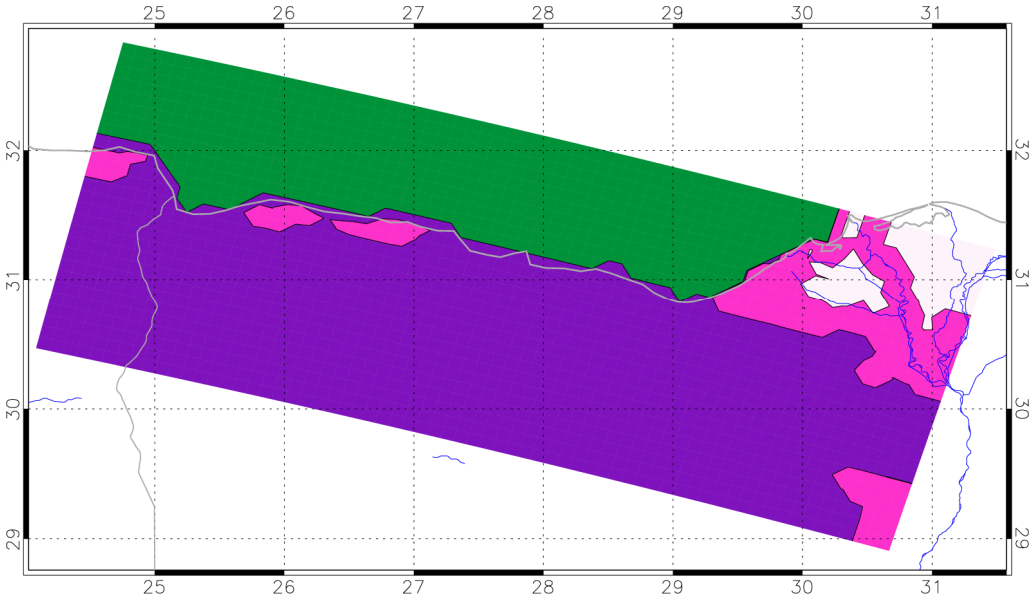

Figure 4-26. The computational domain roughness. Colour key: green 0 m < z_0 ≤ 0.0002 m, purple 0.0002 m < z_0 ≤ 0.002 m, pink 0.002 m < z_0 ≤ 0.1 m, white 0.1m < z_0.

The Northwest Coast domain contains the stations at El-Mathany, Ras El-Hekma and El-Galala. The size of the domain is 660 km × 270 km. At a grid resolution of 5 km, 133 × 55 grid points on each model level are used. In the vertical, 25 model levels are used. The grid has been rotated 15 degrees clockwise in order to align the major axis of the domain with the coastline.

Wind classes

The wind class limits and profiles have been evaluated at the location 28.75°E 31.25°N. The automatic procedure produced 110 wind classes. The class limits were applied at 0 m, and the wind class profiles comprise of the westerly and southerly components of the wind and the virtual potential temperature at 0, 1500, 3000, 5500 meters. The mesoscale model is run with a fixed simulation time of 7 hours and 13 minutes. In the post processing, variable class frequencies have been used.

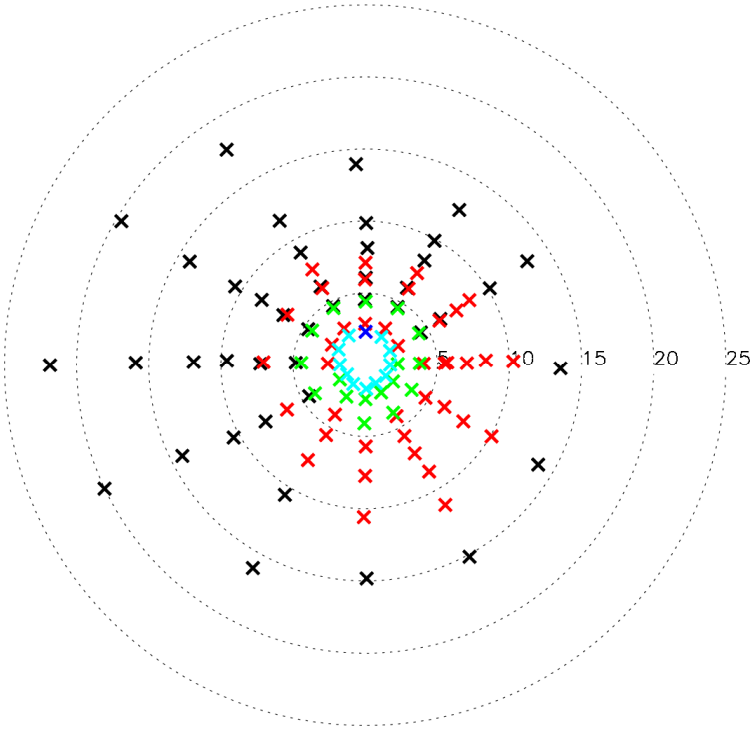

Figure 4-27. The geostrophic wind classes used as forcing for the simulations. Each cross represents a forcing wind speed (distance from the centre of the diagram) and direction. The speed scale is in ms^{-1}. The colours indicate the inverse Froude number squared (IFNS), black IFNS < 1.5, red 1.5 < IFNS < 3.5, green 3.5 < IFNS < 5.5, dark blue 5.5 < IFNS < 7.5, light blue 7.5 < IFNS.

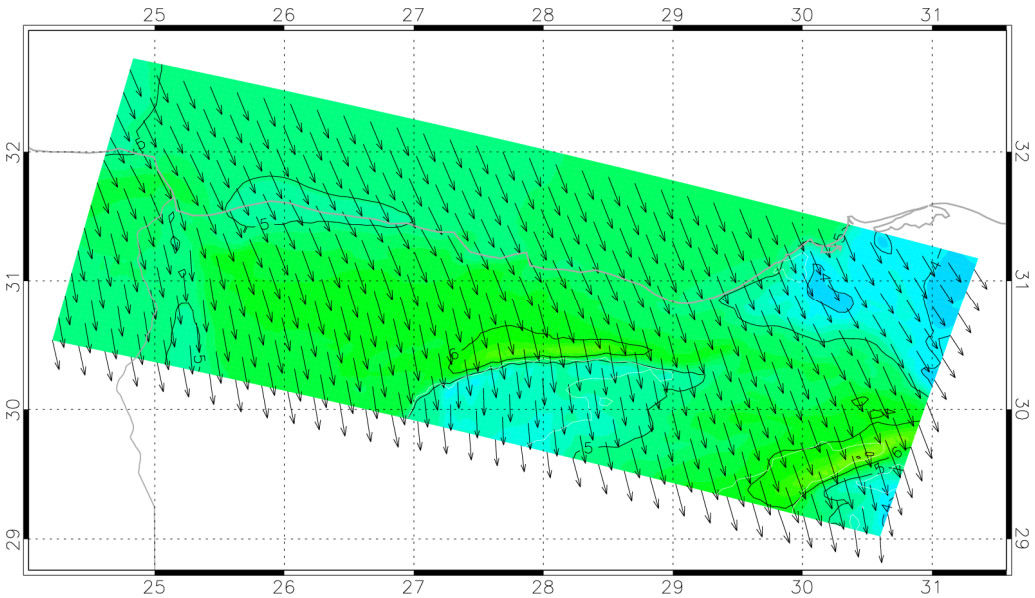

Figure 4-28. Wind vectors and speed at 50 m a.g.l. for a 0 degree 5.9 ms^{-1} low Froude number forcing. The contour interval is 1 ms^{-1}.

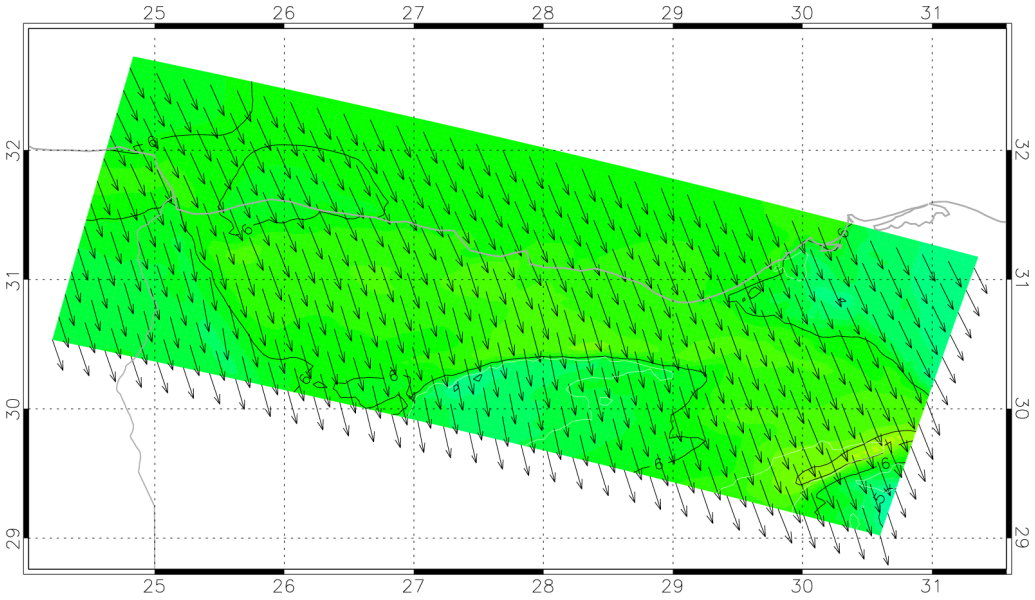

Figure 4-29. Wind vectors and speed at 50 m a.g.l. for a 0 degree 6.1 ms^{-1} high Froude number forcing. The contour interval is 1 ms^{-1}.

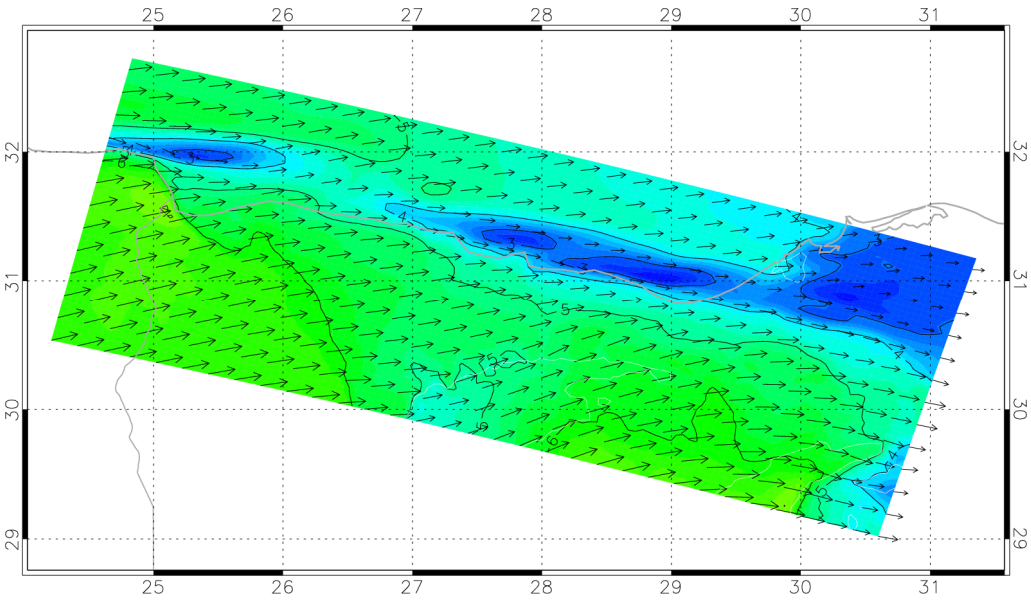

Figure 4-30. Wind vectors and speed at 50 m a.g.l. for a 272 degree 7.0 ms^{-1} low Froude number forcing. The contour interval is 1 ms^{-1}.

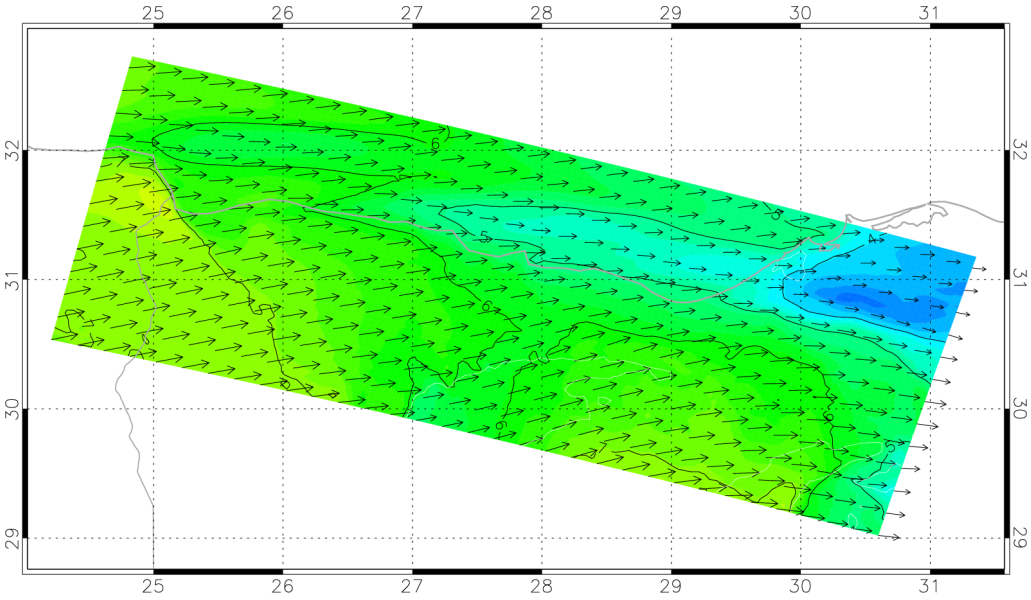

Figure 4-31. Wind vectors and speed at 50 m a.g.l. for a 271 degree 7.3 ms^{-1} high Froude number forcing. The contour interval is 1 ms^{-1}.

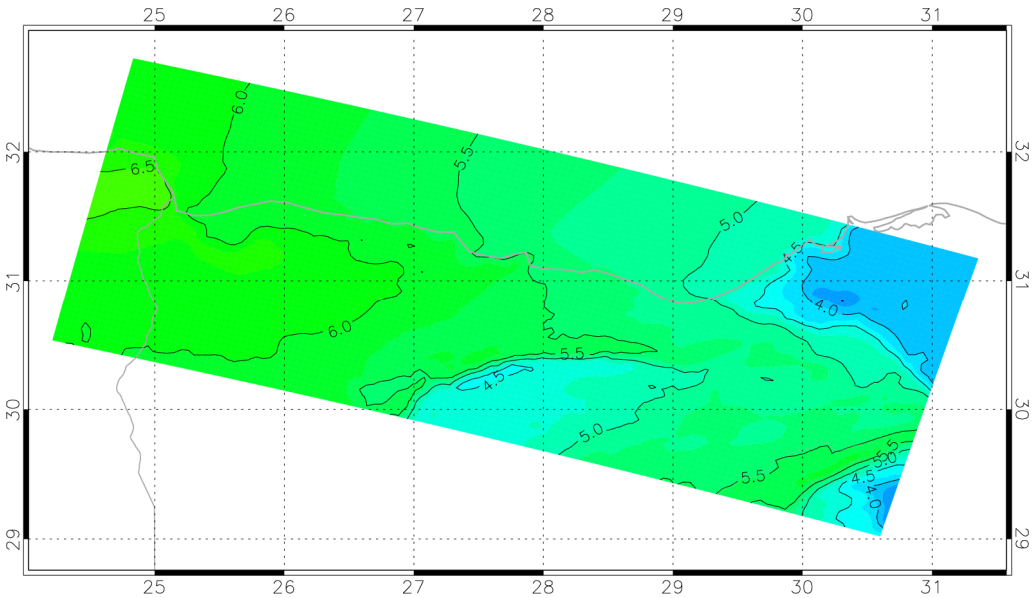

Figure 4-32. Mean simulated wind speed at 50 m a.g.l. The contour interval is 0.5 ms^{-1}.

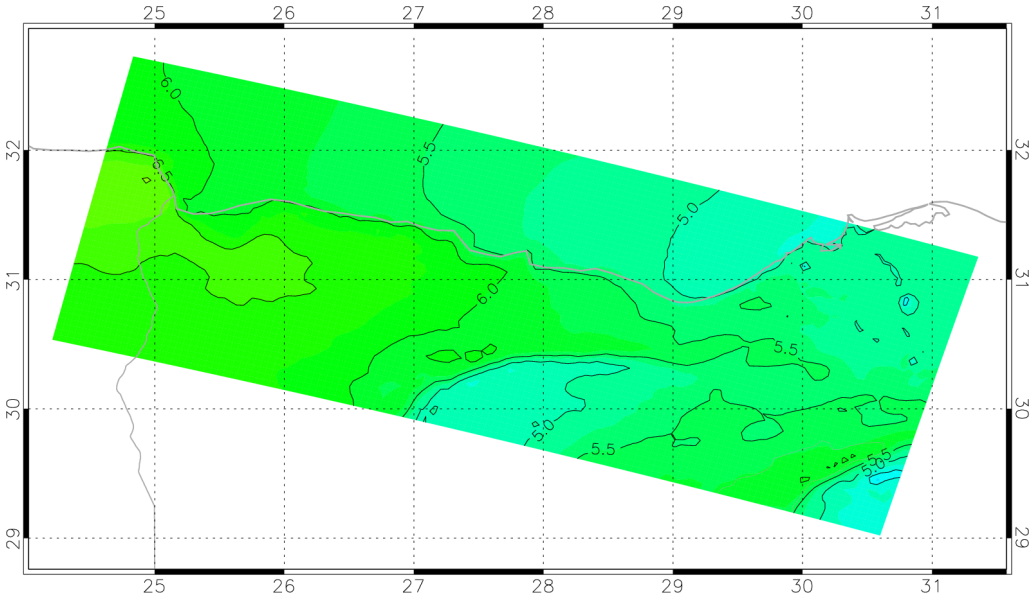

Figure 4-33. Mean generalized wind speed at 50 m a.g.l. for 0.0002 m roughness. The contour interval is 0.5 ms^{-1}.

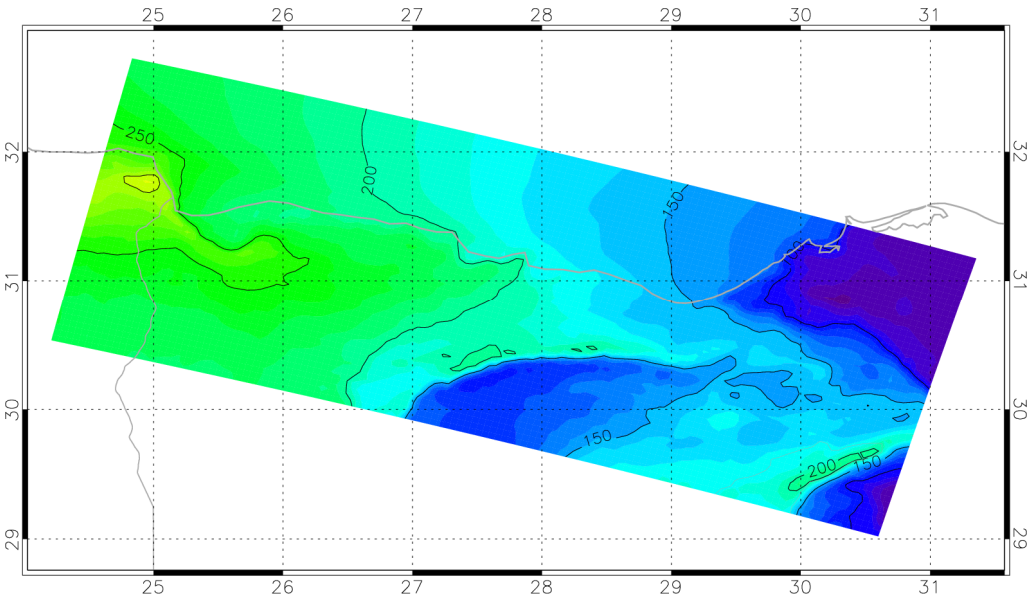

Figure 4-34. Mean simulated wind power density at 50 m a.g.l. The contour interval is 50 Wm^{-2}.

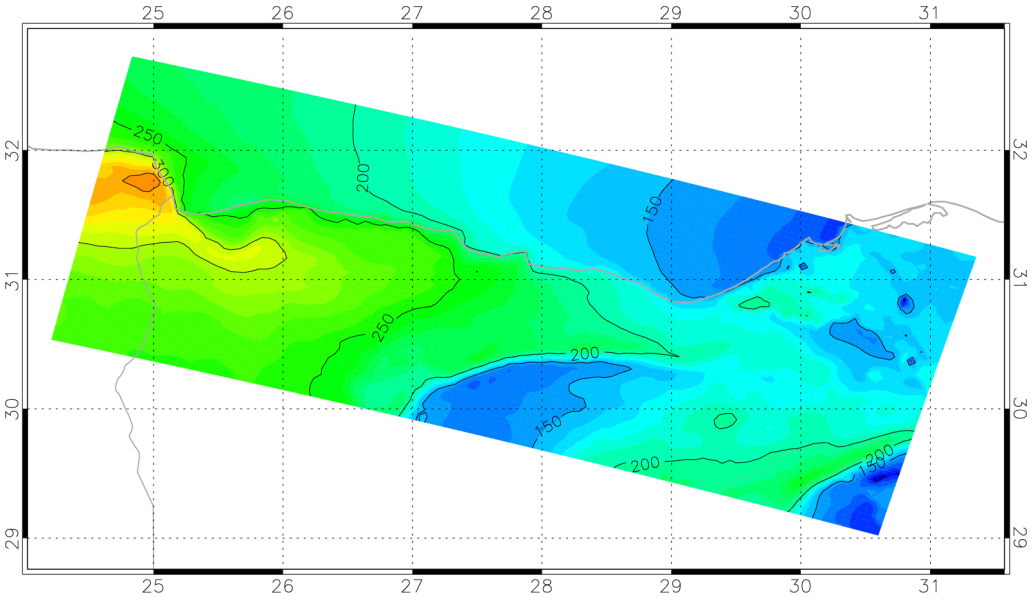

Figure 4-35. Mean generalized wind power density at 50 m a.g.l. for 0.0002 m roughness. The contour interval is 50 Wm^{-2}.

WESTERN DESERT DOMAIN

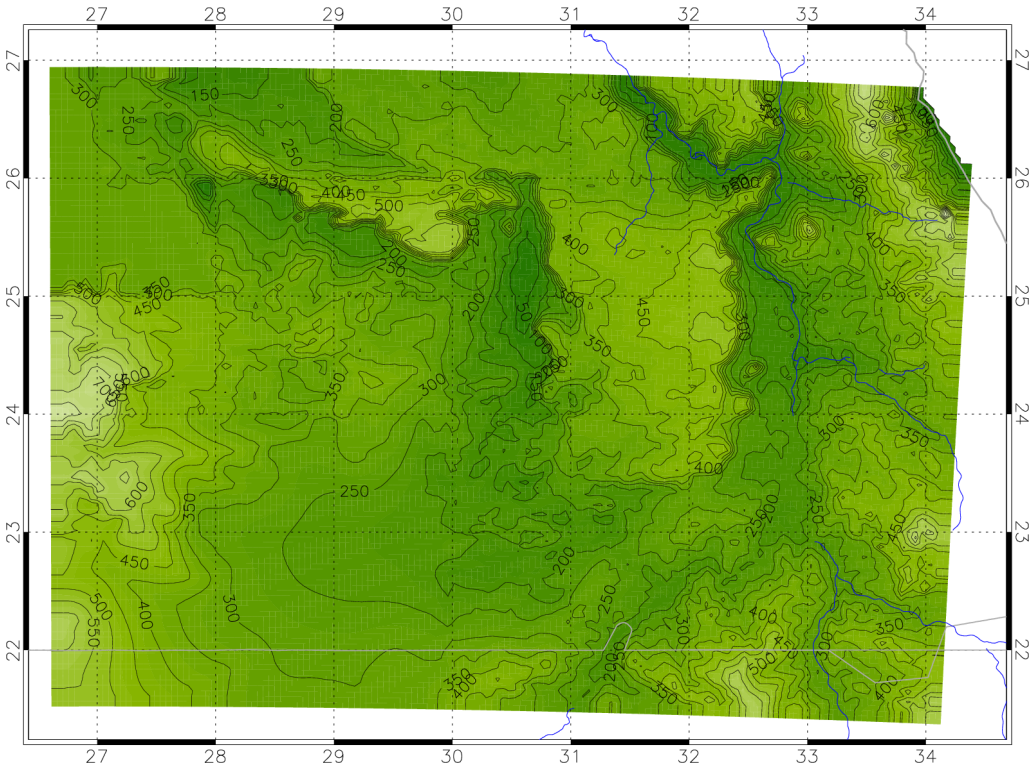

Figure 4-36. The computational domain orography. The contour interval is 50 m.

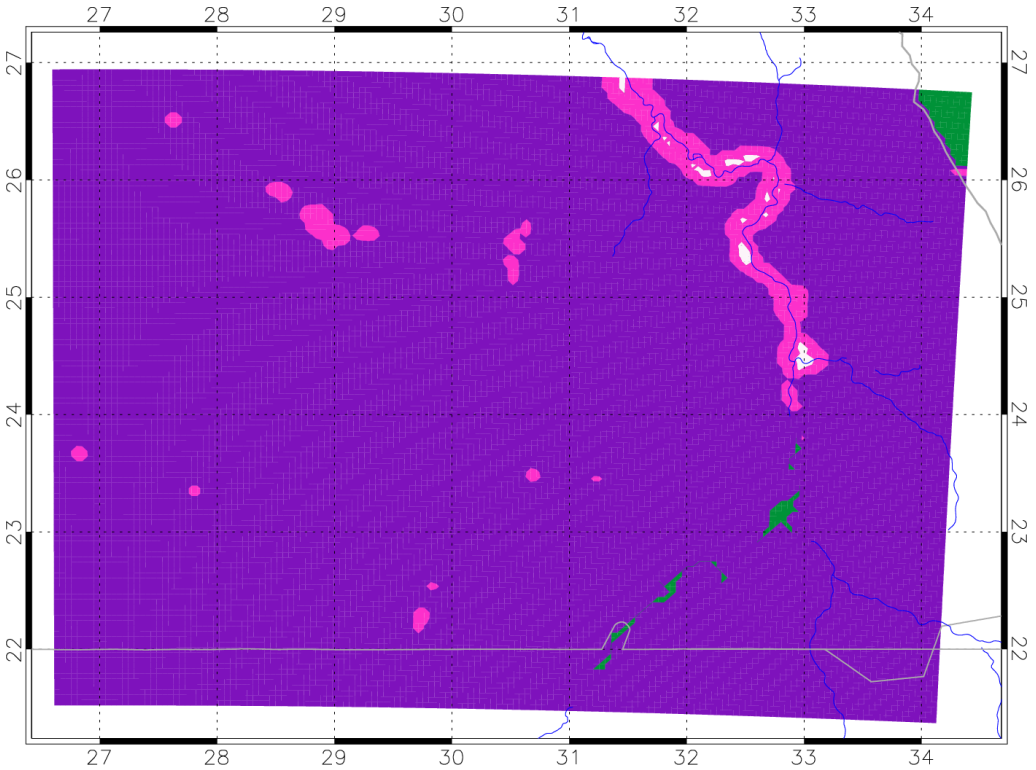

Figure 4-37. The computational domain roughness. Colour key: green 0 m < z_0 ≤ 0.0002 m, purple 0.0002 m < z_0 ≤ 0.002 m, pink 0.002 m < z_0 ≤ 0.1 m, white 0.1m < z_0.

The Western Desert domain contains the stations at Shark El-Ouinat, Abu Simbel, Dahkla South and Kharga. The size of the domain is 780 km × 600 km. At a grid resolution of 5 km, 157 × 121 grid points on each model level are used. In the vertical 25 model levels are used.

Wind classes

The wind class limits and profiles have been evaluated at the location 31.25°E 23.75°N. The automatic procedure produced 68 wind classes. The class limits were applied at 0 m, and the wind class profiles comprise of the westerly and southerly components of the wind and the virtual potential temperature at 0, 1500, 3000, 5500 meters. The mesoscale model is run with a fixed simulation time of 9 hours and 28 minutes. In the post processing, variable class frequencies have been used.

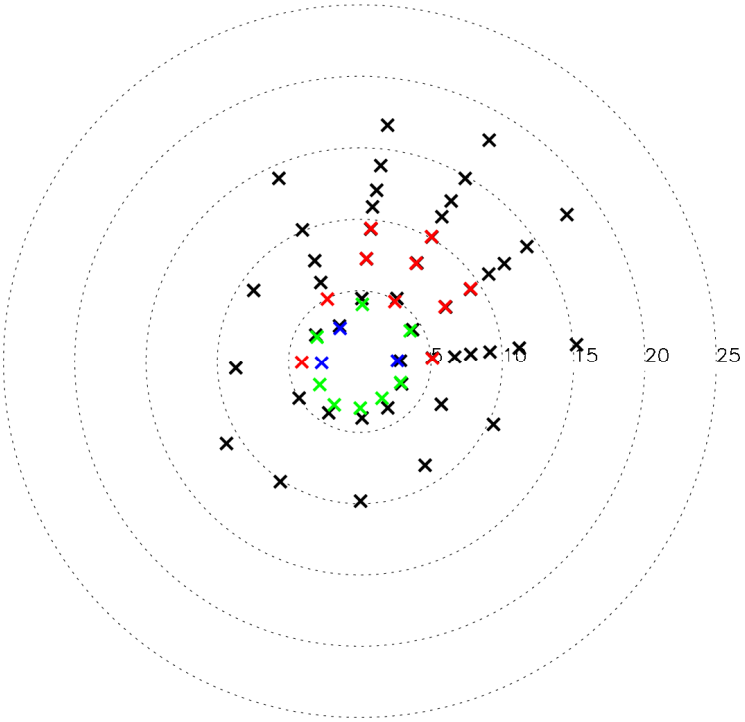

Figure 4-38. The geostrophic wind classes used as forcing for the simulations. Each cross represents a forcing wind speed (distance from the centre of the diagram) and direction. The speed scale is in ms^{-1}. The colours indicate the inverse Froude number squared (IFNS), black IFNS < 1.5, red 1.5 < IFNS < 3.5, green 3.5 < IFNS < 5.5, dark blue 5.5 < IFNS < 7.5, light blue 7.5 < IFNS.

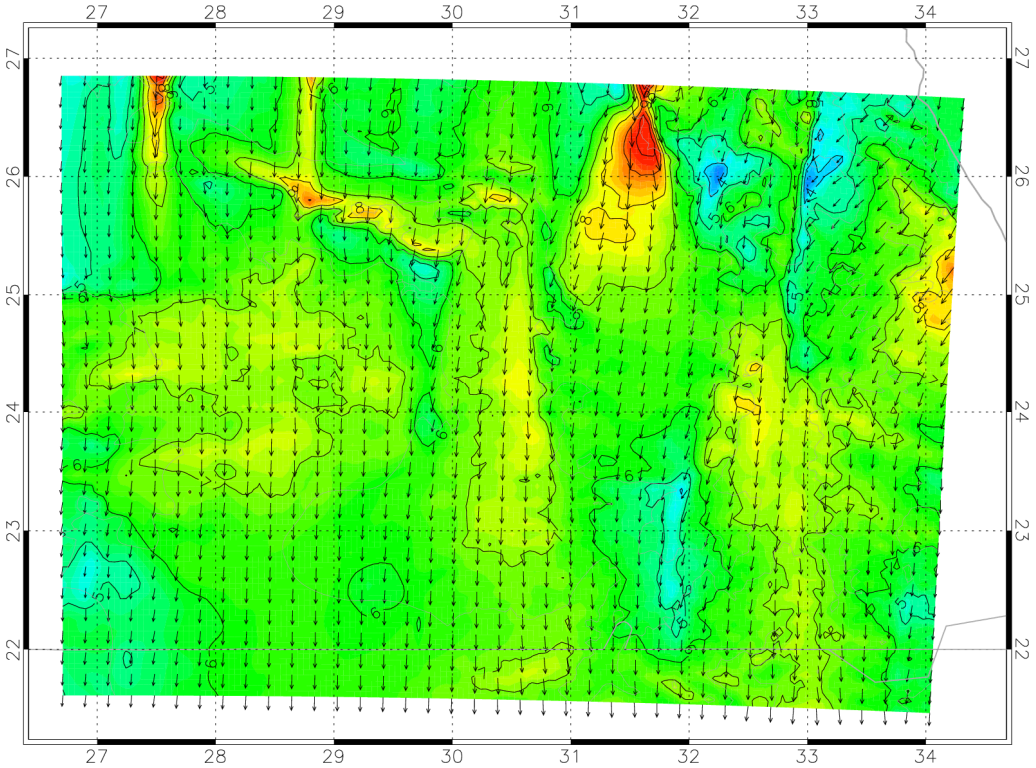

Figure 4-39. Wind vectors and speed at 50 m a.g.l. for a 30 degree 10.1 ms^{-1} low Froude number forcing. The contour interval is 1 ms^{-1}.

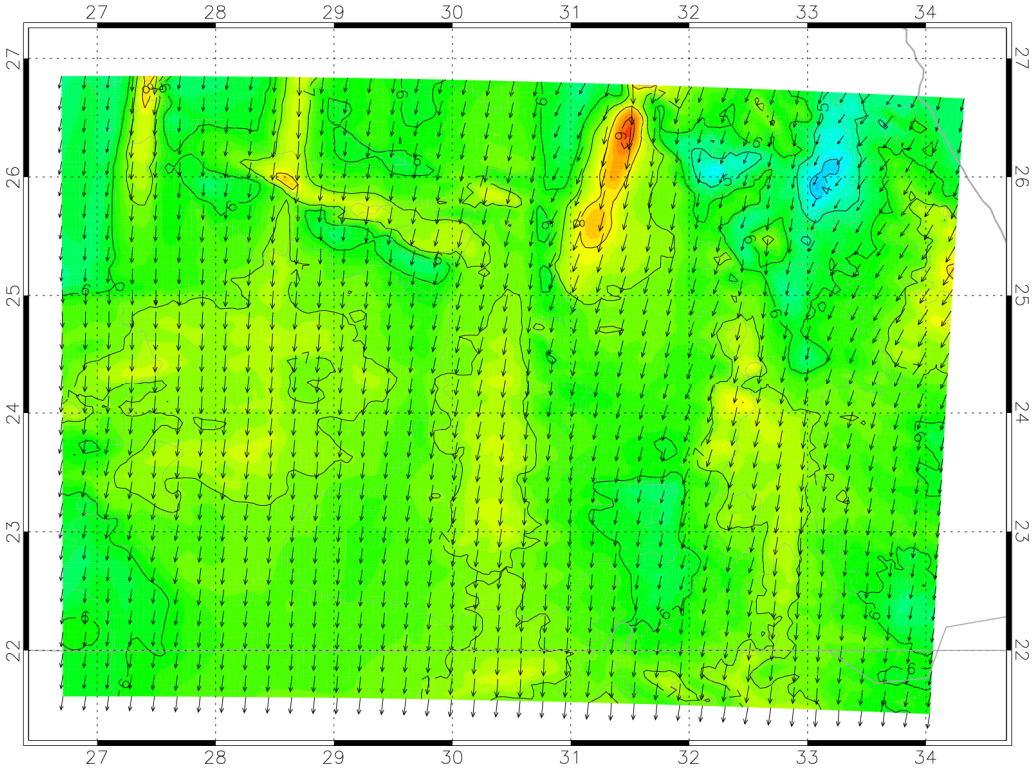

Figure 4-40. Wind vectors and speed at 50 m a.g.l. for a 30 degree 10.2 ms^{-1} high Froude number forcing. The contour interval is 1 ms^{-1}.

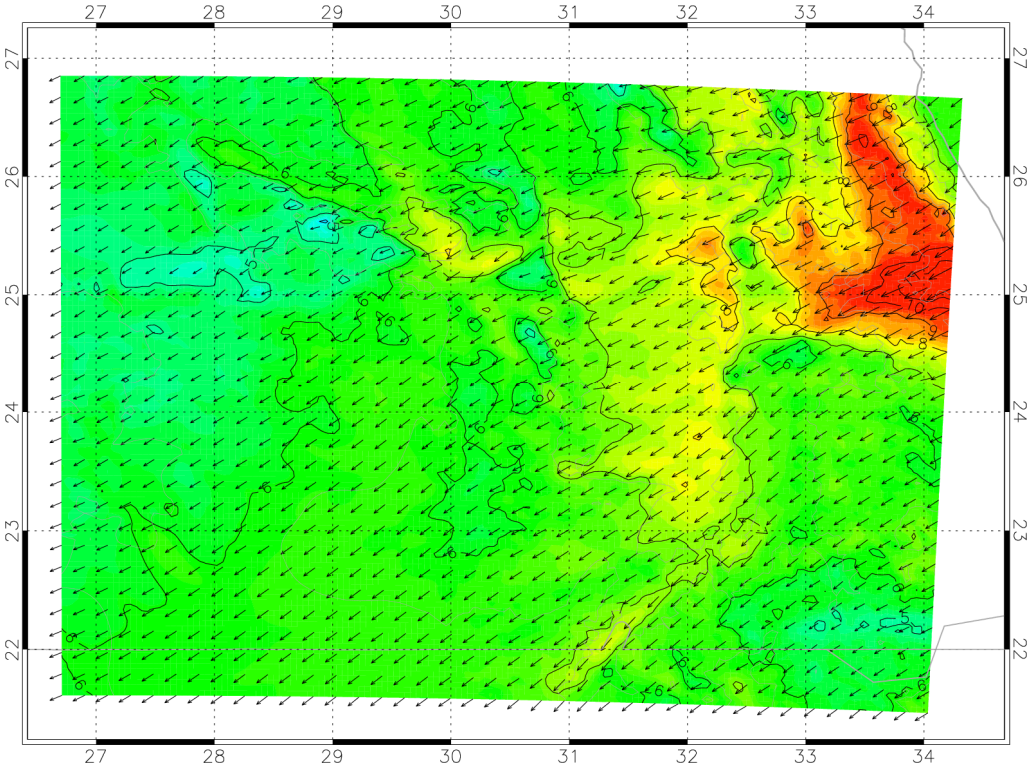

Figure 4-41. Wind vectors and speed at 50 m a.g.l. for a 085 degree 11.2 ms^{-1} forcing. The contour interval is 1 ms^{-1}.

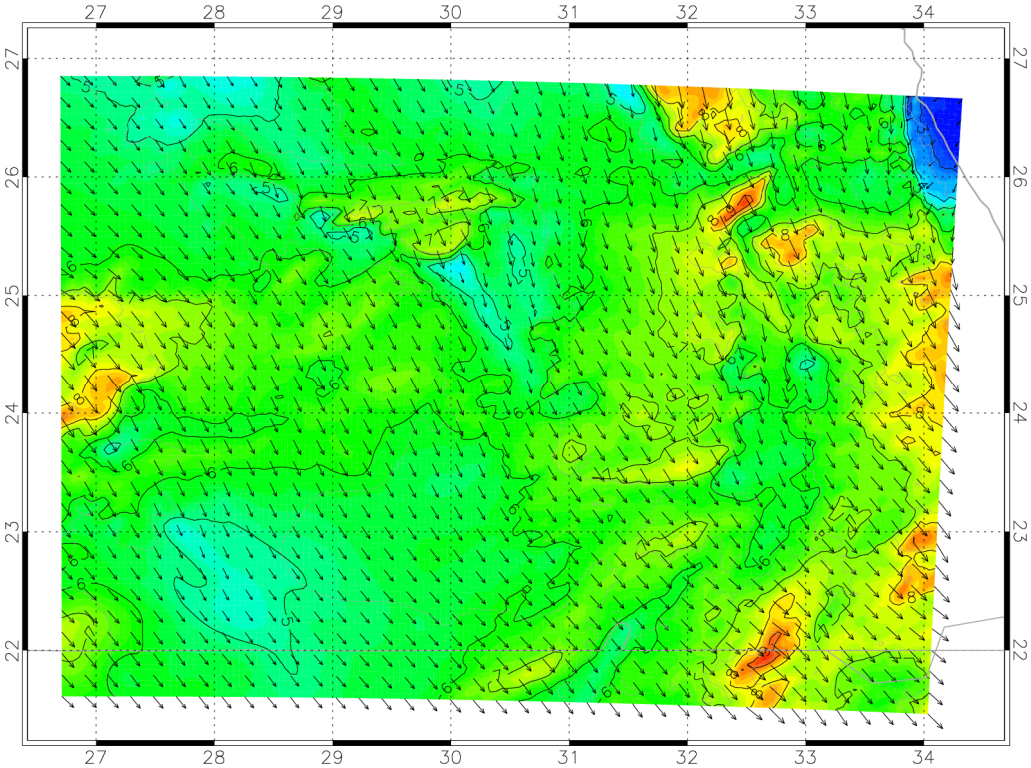

Figure 4-42. Wind vectors and speed at 50 m a.g.l. for a 337 degree 10.1 ms^{-1} forcing. The contour interval is 1 ms^{-1}.

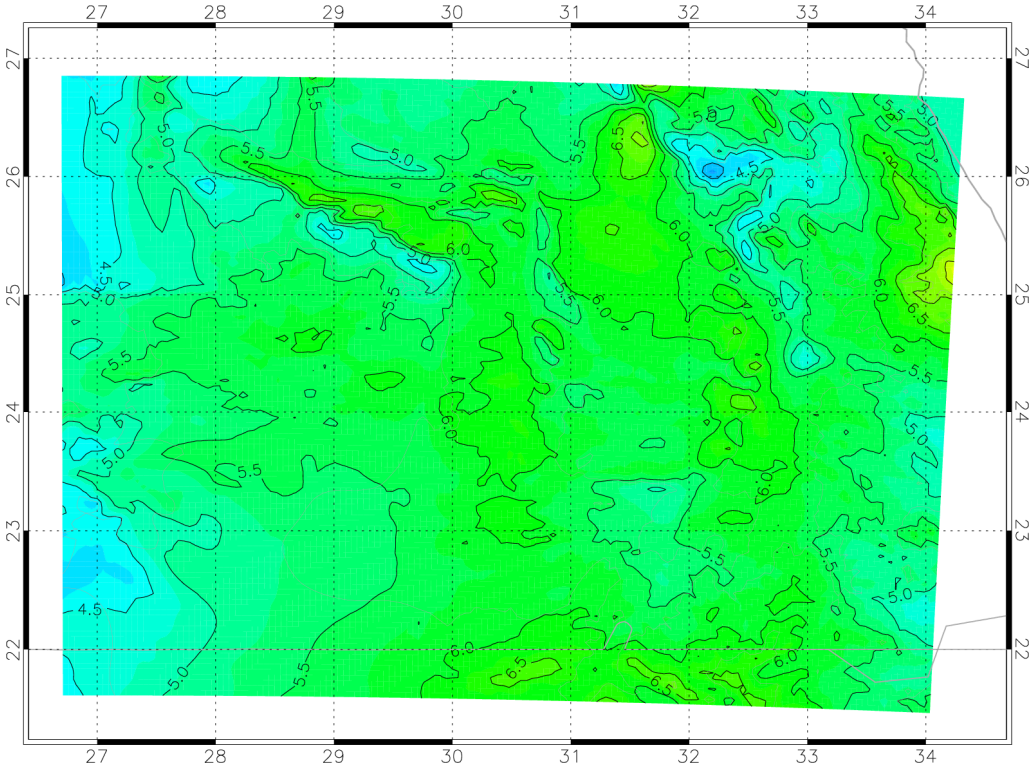

Figure 4-43. Mean simulated wind speed at 50 m a.g.l. The contour interval is 0.5 ms^{-1}.

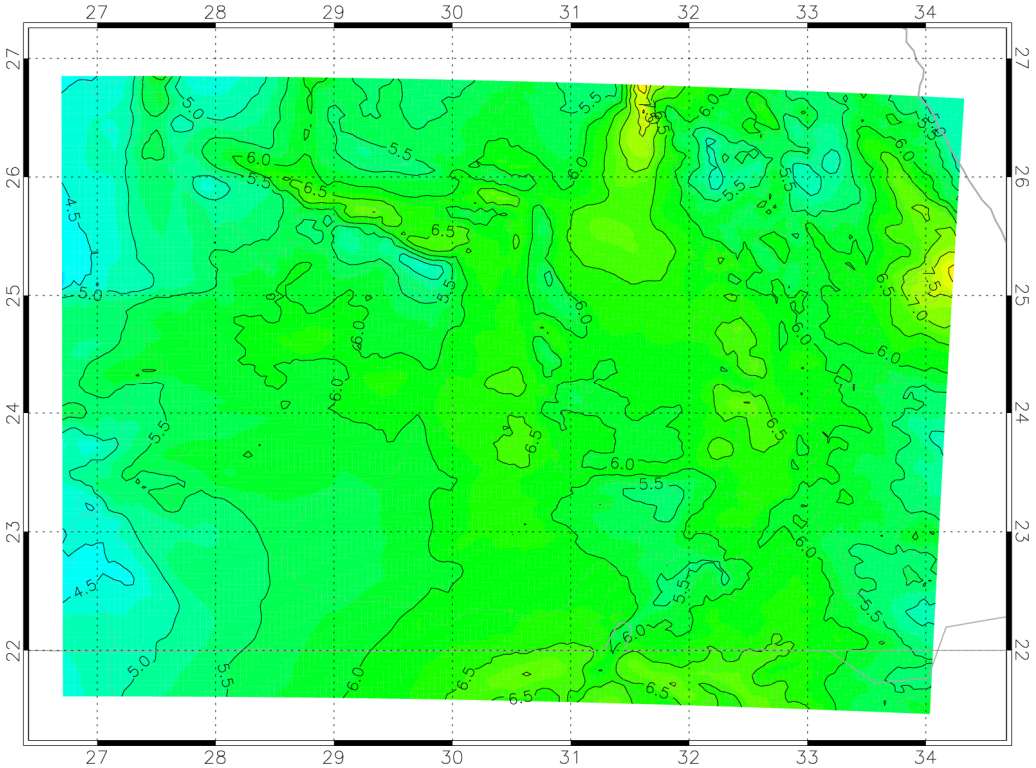

Figure 4-44. Mean generalized wind speed at 50 m a.g.l. for 0.0002 m roughness. The contour interval is 0.5 ms^{-1}.

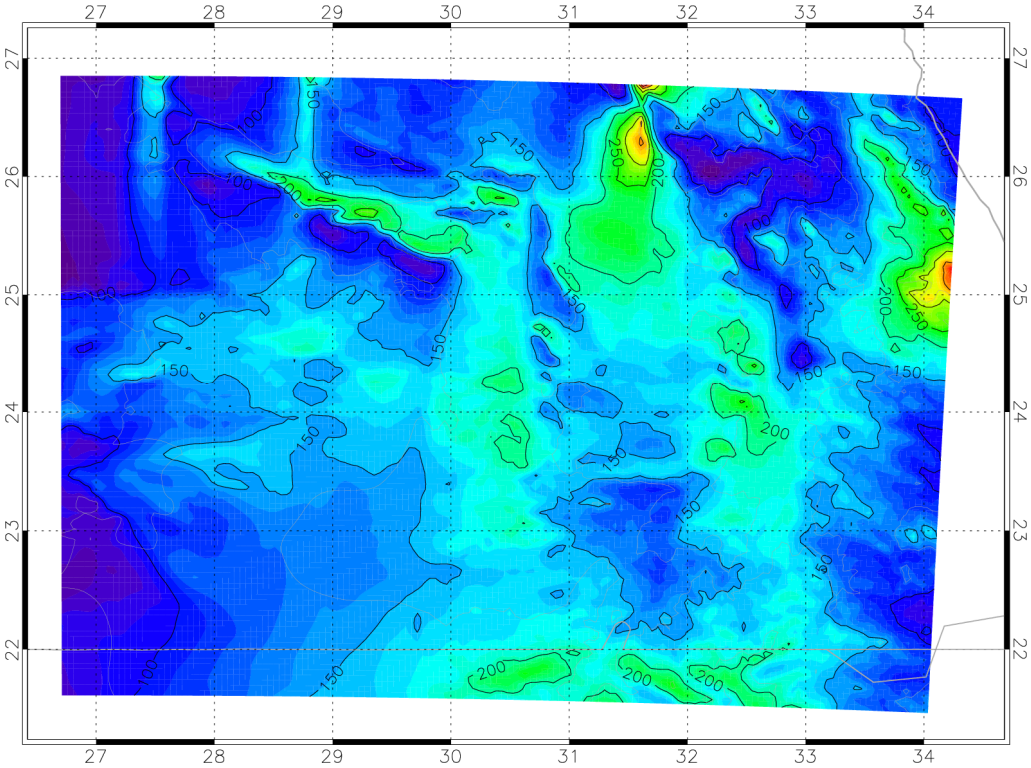

Figure 4-45. Mean simulated wind power density at 50 m a.g.l. The contour interval is 50 Wm^{-2}.

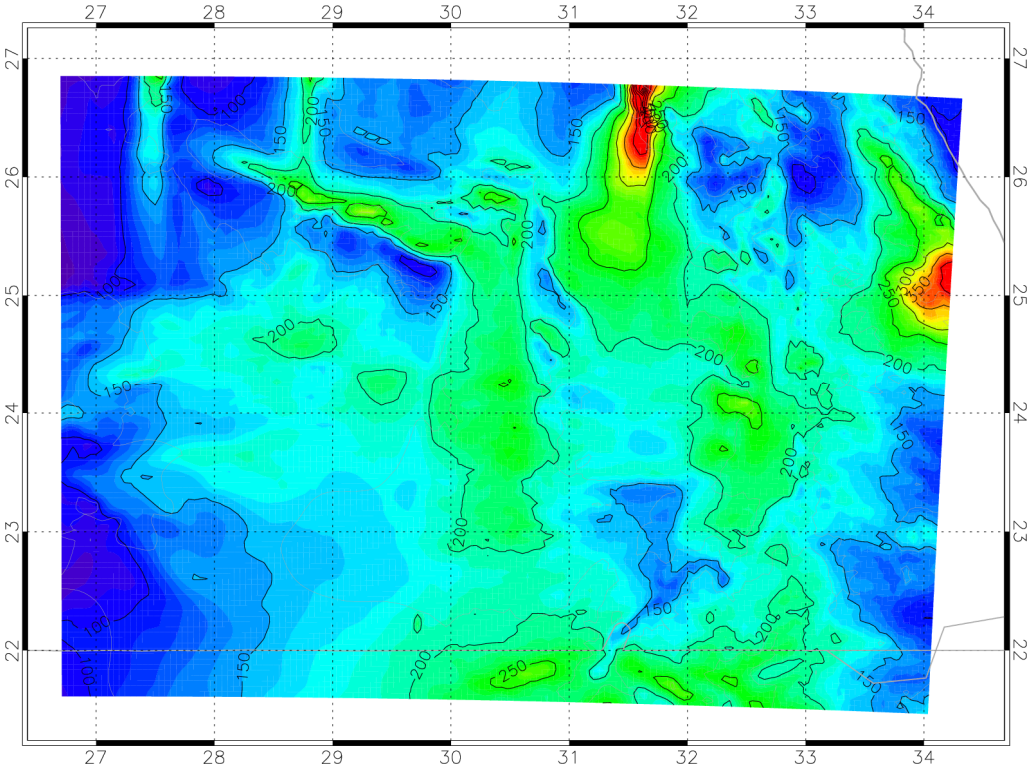

Figure 4-46. Mean generalized wind power density at 50 m a.g.l. for 0.0002 m roughness. The contour interval is 50 Wm^{-2}.

GULF OF SUEZ DOMAIN

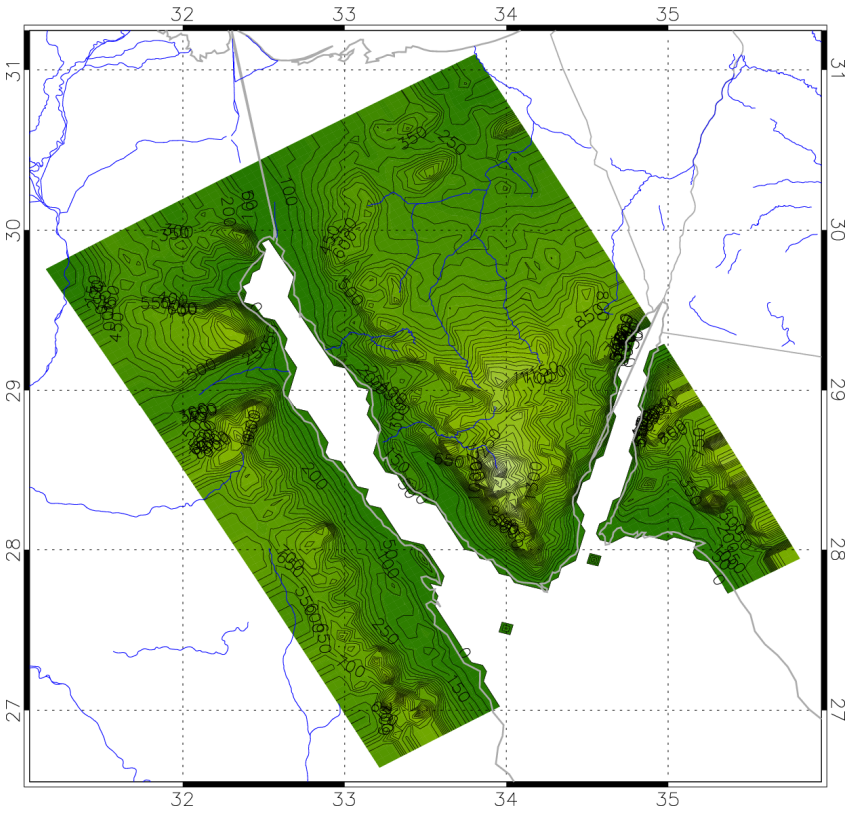

Figure 4-47. The computational domain orography map. The contour interval is 50 m.

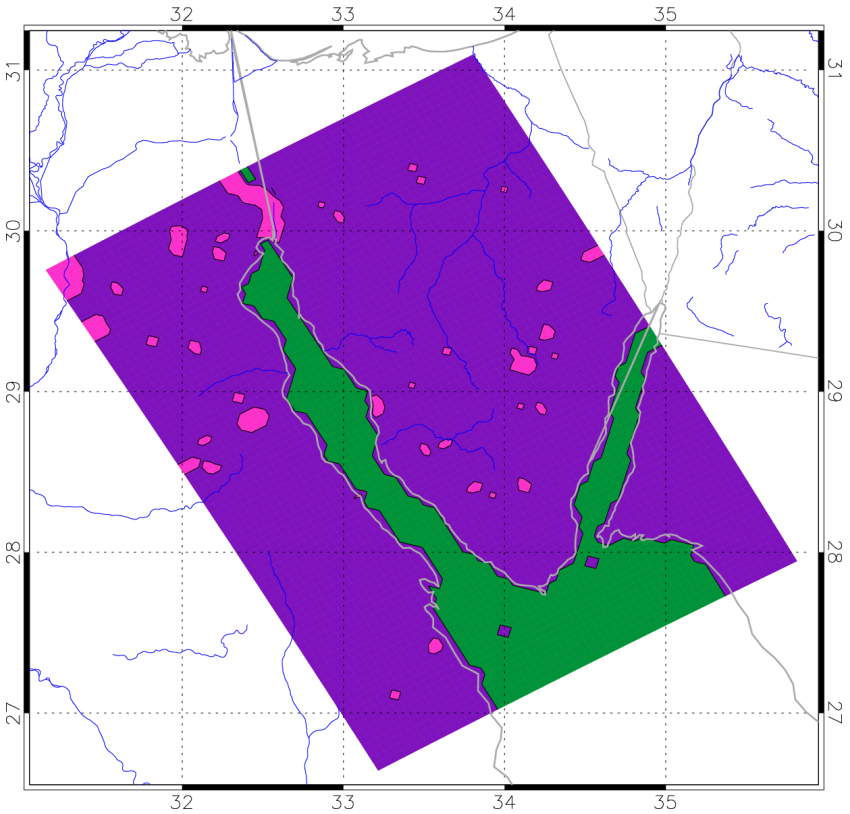

Figure 4-48. The computational domain roughness. Colours: green 0 m < z_0 ≤ 0.0002 m, purple 0.0002 m < z_0 ≤ 0.002 m, pink 0.002 m < z_0 ≤ 0.1 m, white 0.1m < z_0.

For the Gulf of Suez, the same domain was chosen as previously used by Helmut Frank in the mesoscale model calculations reported by Mortensen et al. (2003). The grid of 60 × 81 points covers an area of 295 km × 400 km at a horizontal resolution of 5 km. The map is rotated 30 degrees anticlockwise in order to align the axis of the Gulf with the domain boundaries without cutting through steep terrain. The model uses 28 vertical levels from the surface to a constant height of 6000 m. Since vertical stretching is applied, the bottom levels are located close to each others (order of 40 m) while the top levels are located at greater distances from each other (order of 400 m).

Wind classes

The wind class generation should be configured so that the wind classes are distinctly divided according to stability. In the previous simulations of Helmut Frank, a lot of emphasis was placed on shear, i.e. the classes were divided according to positive or negative shear. Equally successful results have been obtained with the current class generation configuration, also using shear. In addition, the current simulations show that one may classify according to positive or negative stability, instead of shear, resulting in a nearly identical classification. The classification procedure must be configured to allow a large number of class divisions according to stability. A resulting set of 126 classes was generated for the Gulf of Suez. The input profiles of geostrophic wind and virtual potential temperature are defined at 0, 1500, 3000 and 5500 m. For the Gulf of Suez, the input profiles of the geostrophic wind were calculated from the NCEP/NCAR reanalysis data for the point at 33.75°E, 28.75°N. However, to be able to apply the bottom point of the initialization profile to a model level above the terrain, the input profile was applied in the model initialization point of 33.00°E, 29.00°N. The mesoscale model is run with variable simulation time determined by $T = \max\{390,\ 870 \times \exp(-0.065 U_g)\}$. In the post processing, the class frequencies are fixed across the domain.

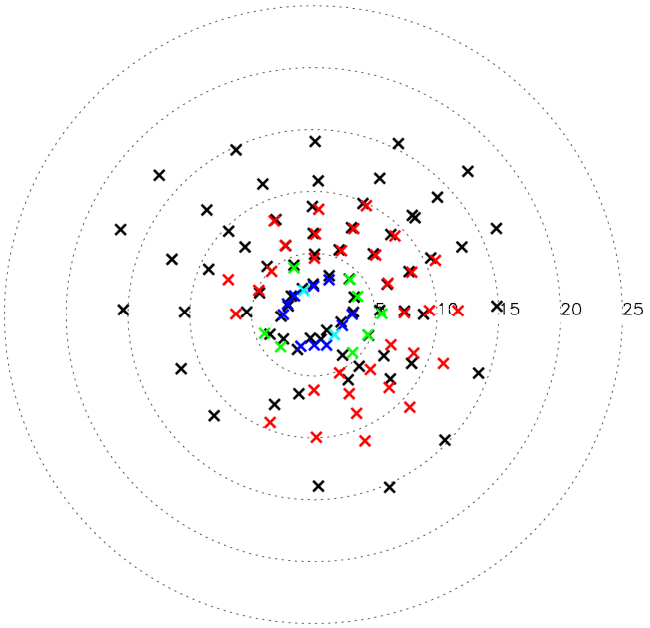

Figure 4-49. The geostrophic wind classes used as forcing for the simulations. Each cross represents a forcing wind speed (distance from the centre of the diagram) and direction. The speed scale is in ms^{-1}. The colours indicate the inverse Froude number squared (IFNS), black IFNS < 1.5, red 1.5 < IFNS < 3.5, green 3.5 < IFNS < 5.5, dark blue 5.5 < IFNS < 7.5, light blue 7.5 < IFNS.

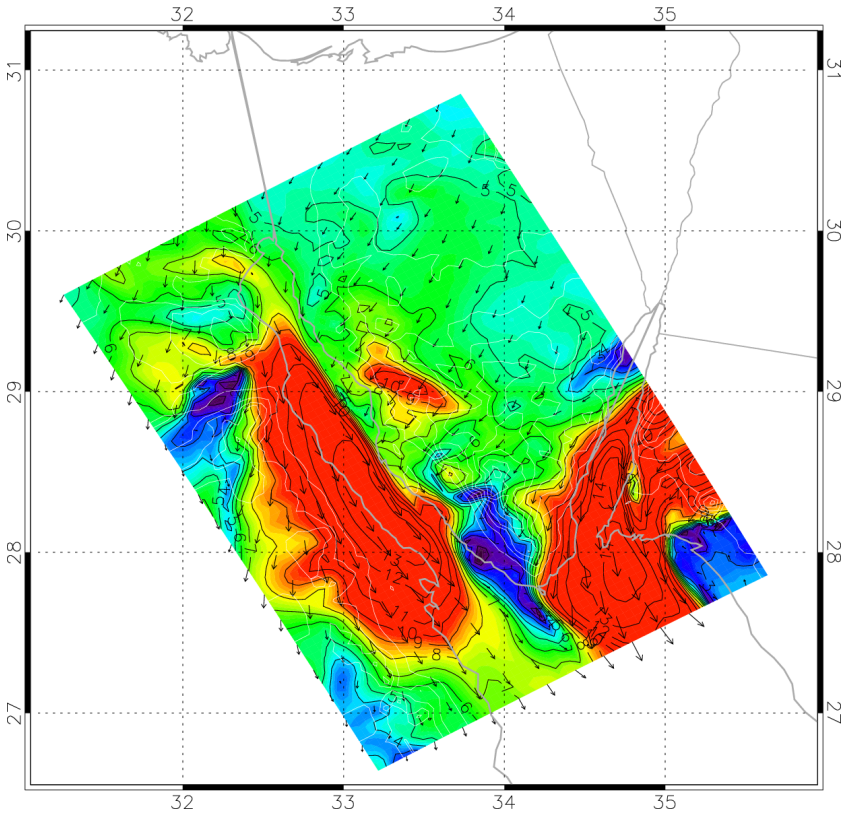

Figure 4-50. Wind vectors and speed at 50 m a.g.l. for a 46 degree 9.2 ms^{-1} forcing. The contour interval is 1 ms^{-1}.

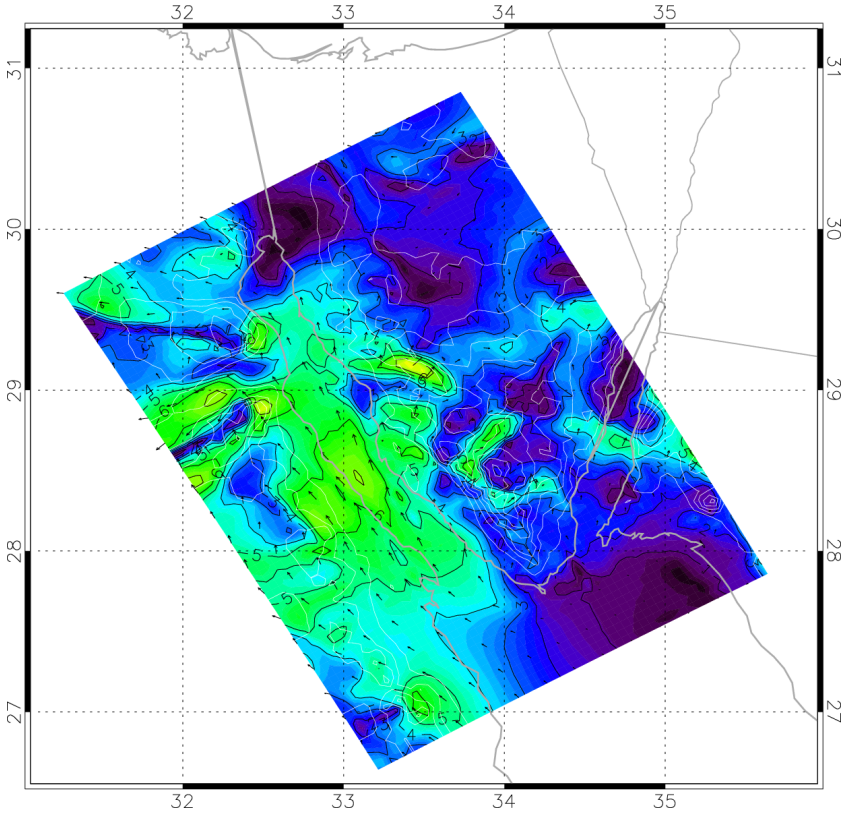

Figure 4-51. Wind vectors and speed at 50 m a.g.l. for a 134 degree 6.4 ms^{-1} forcing. The contour interval is 1 ms^{-1}.

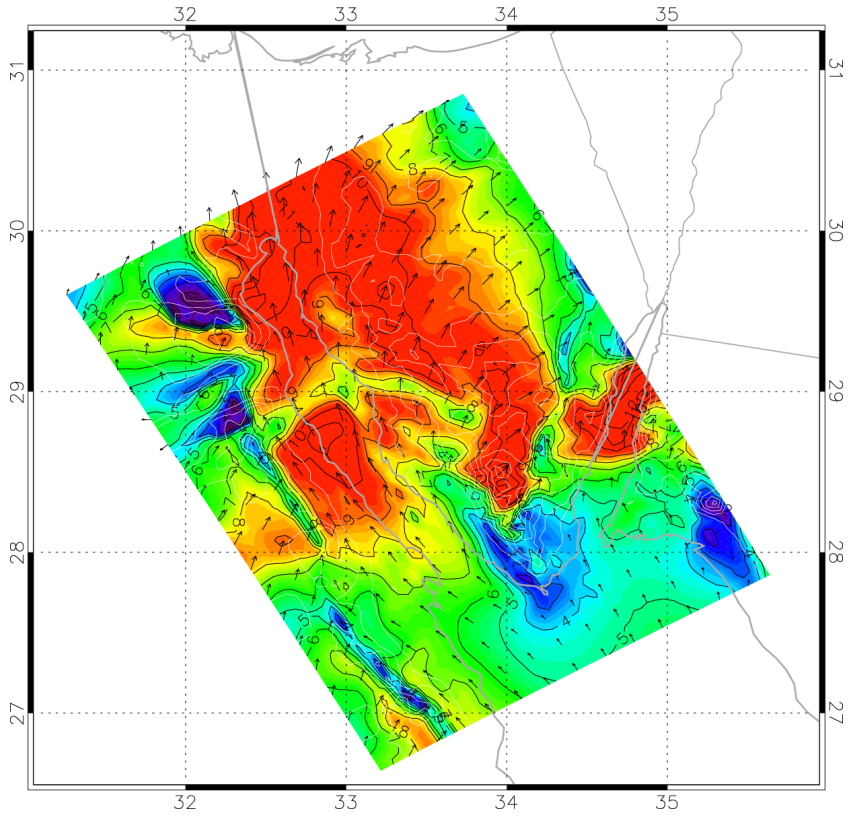

Figure 4-52. Wind vectors and speed at 50 m a.g.l. for a 202 degree 9.4 ms^{-1} forcing. The contour interval is 1 ms^{-1}.

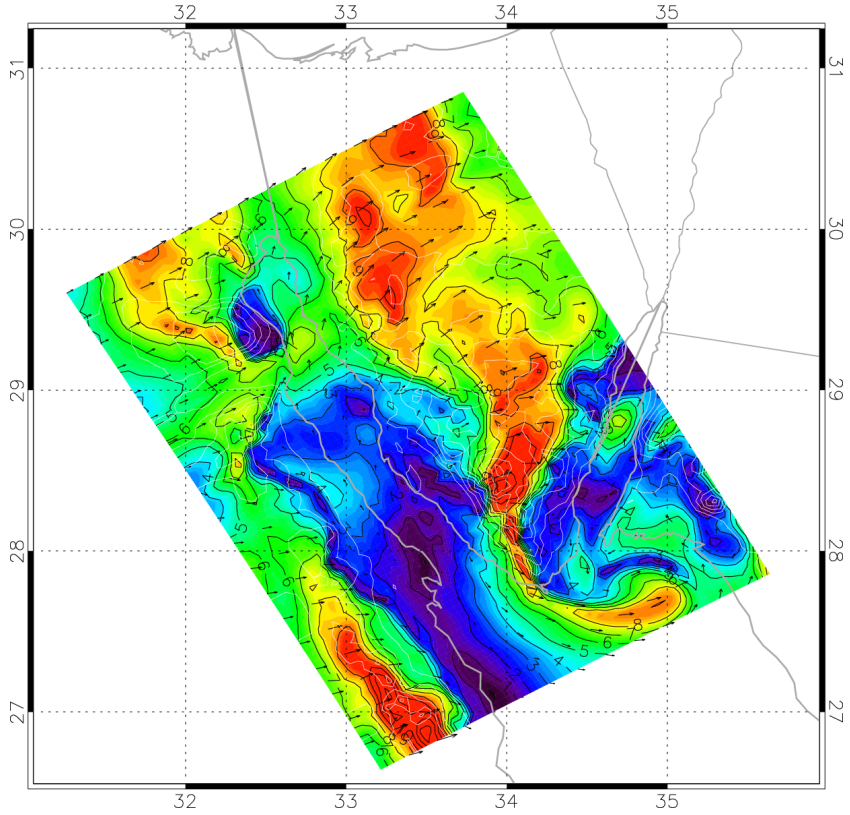

Figure 4-53. Wind vectors and speed at 50 m a.g.l. for a 271 degree 6.3 ms^{-1} forcing. The contour interval is 1 ms^{-1}.

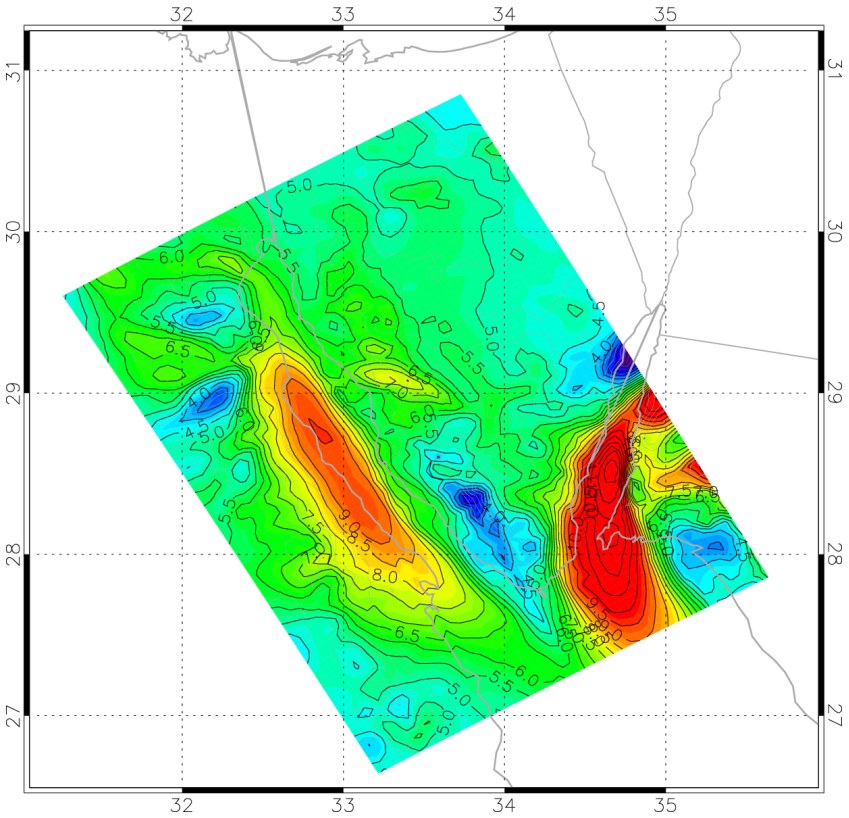

Figure 4-54. Mean simulated wind speed at 50 m a.g.l. The contour interval is 0.5 ms^{-1}.

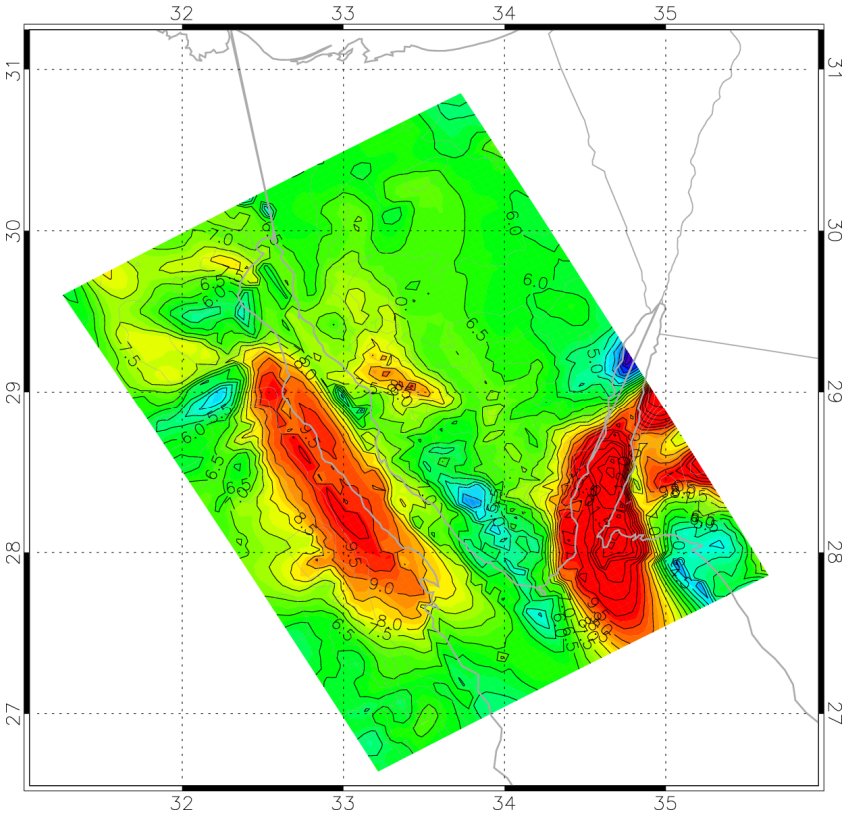

Figure 4-55. Mean generalized wind speed at 50 m a.g.l. for 0.0002 m roughness. The contour interval is 0.5 ms^{-1}.

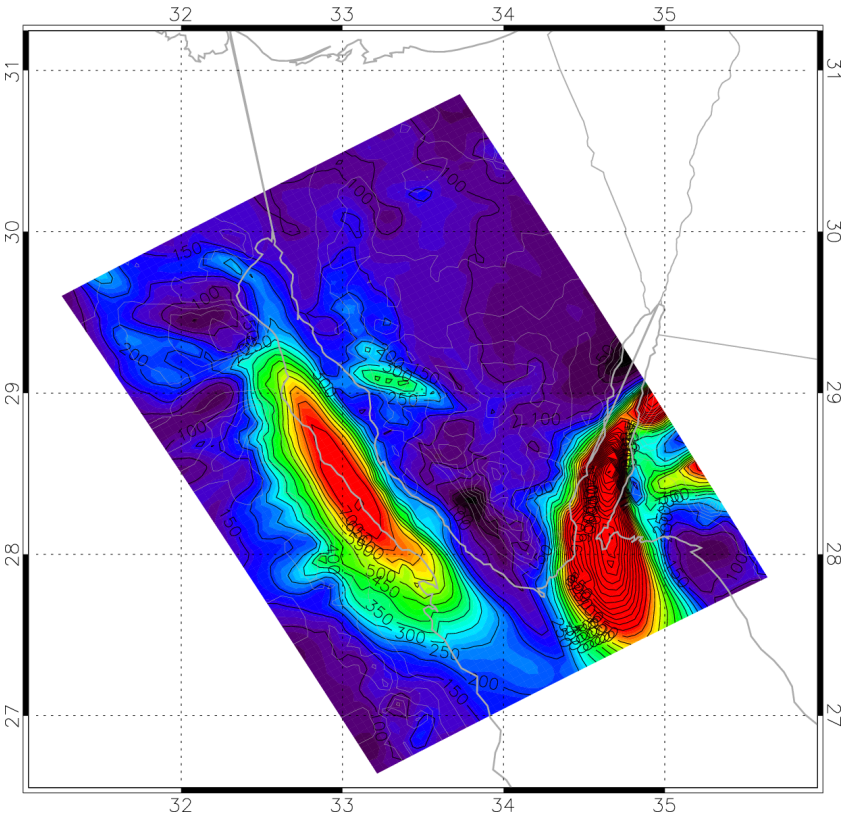

Figure 4-56. Mean simulated wind power density at 50 m a.g.l. The contour interval is 50 Wm^{-2}.

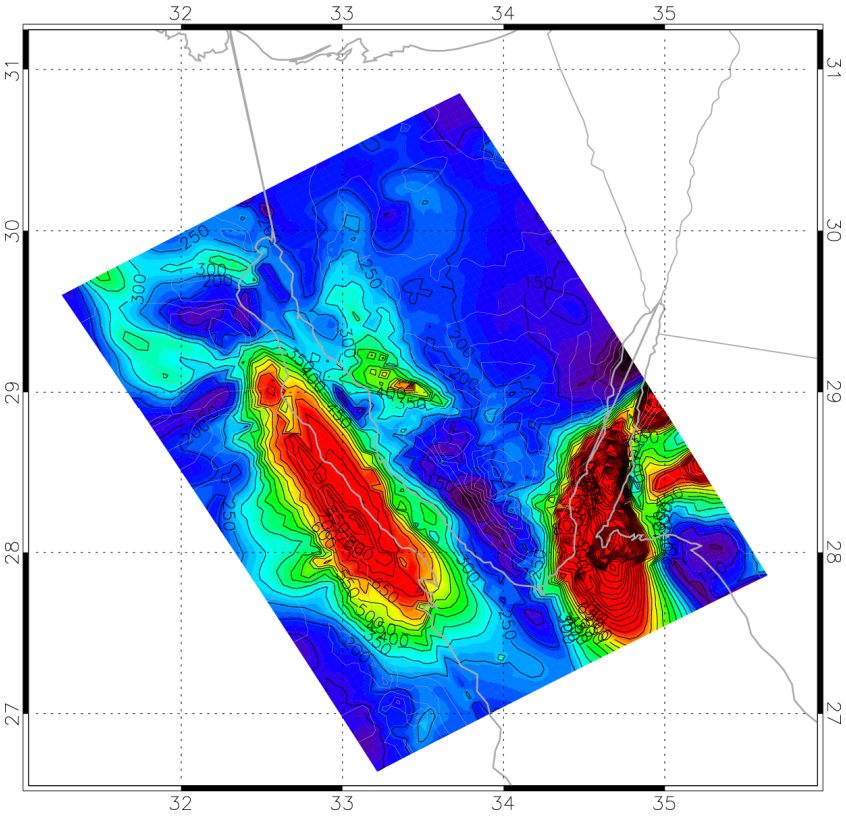

Figure 4-57. Mean generalized wind power density at 50 m a.g.l. for 0.0002 m roughness. The contour interval is 50 Wm^{-2}.

RED SEA DOMAIN

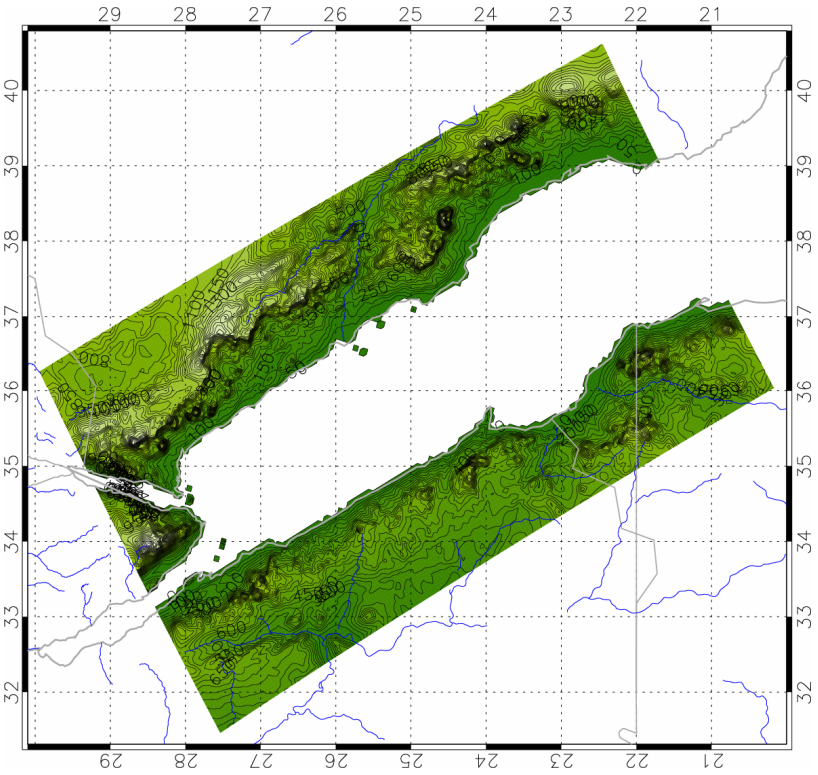

Figure 4-58. The computational domain orography. The contour interval is 50 m. Note, that the north-direction is to the left.

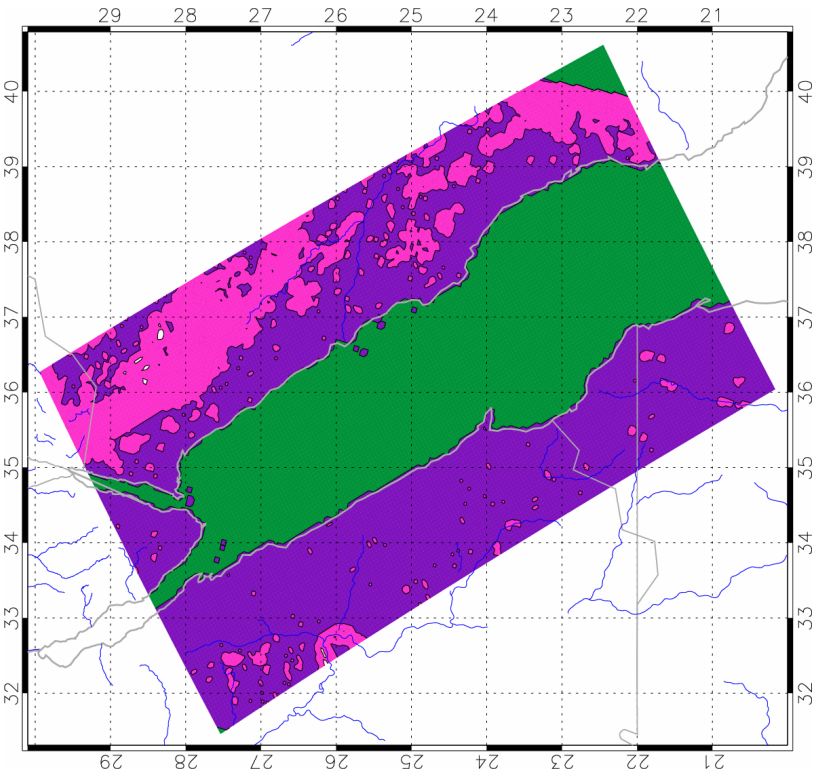

Figure 4-59. The computational domain roughness. Colour key: green 0 m $< z_0 \leq$ 0.0002 m, purple 0.0002 m $< z_0 \leq$ 0.002 m, pink 0.002 m $< z_0 \leq$ 0.1 m, white 0.1m $< z_0$.

For the Red Sea area, a domain covering 560 km × 960 km has been used. The domain is rotated 30 degrees anticlockwise. This covers both sides of the Red Sea. It reaches far enough inland to include the high elevations in the western part of the domain. In addition, it also reaches far enough inland in the eastern part across the water to include the high elevations, which are expected to strongly influence the wind climate in the area of interest. As the Sinai Peninsula, the Gulf of Suez and the Gulf of Aqaba also influence the wind climate in the area of interest, the domain must extend quite far north. As it is desired that the domain should cover an area of interest down to 22°N, the result is a rather large domain.

Utilizing the mesoscale modelling experience from the Gulf of Suez, 28 vertical levels are used. At 5 km resolution, the domain yields $N_X \times N_Y \times N_Z = 113 \times 193 \times 28 = 607{,}488$ grid points. The current limit with 2 GB memory per processor allows up to 800,000 grid points in KAMM. Based on past experience, the best model results for the area of interest can only be obtained for a horizontal resolution with grid cells down to 5 km. Otherwise the domain must be smaller. This will cause the influence of the high elevations near the water to be lost or the boundaries will cut through steep terrain thereby hampering the boundary conditions of KAMM. Also, 5-km grid cells should be sufficiently large in order to avoid too much diffusion being added in the turbulence parameterization of KAMM. Simulations have been performed at 20 km, 10 km and 5 km.

Wind classes

The modelling experience from the Gulf of Suez was reused in the calculations for the Red Sea. A resulting set of 113 classes was generated. The input profiles were calculated at the point 33.75°E, 26.25°N. The model initialization point was chosen as 34.50°E, 26.25°N. This point is located at sea, thus allowing the bottom level of the input profile to be applied in the model. Like in the case of Gulf of Suez, the mesoscale model is run with variable simulation time determined by $T = \max\{390, 870 \times \exp(-0.065 U_g)\}$. In the post processing, the class frequencies are fixed across the domain.

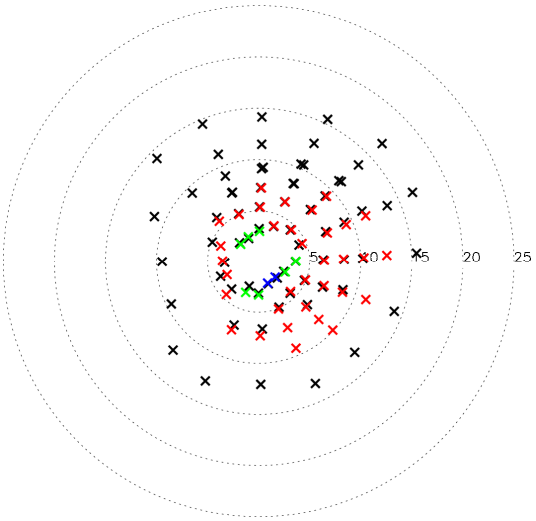

Figure 4-60. The geostrophic wind classes used as forcing for the simulations. Each cross represents a forcing wind speed (distance from the centre of the diagram) and direction. The speed scale is in ms^{-1}. The colours indicate the inverse Froude number squared (IFNS), black IFNS < 1.5, red 1.5 < IFNS < 3.5, green 3.5 < IFNS < 5.5, dark blue 5.5 < IFNS < 7.5, light blue 7.5 < IFNS.

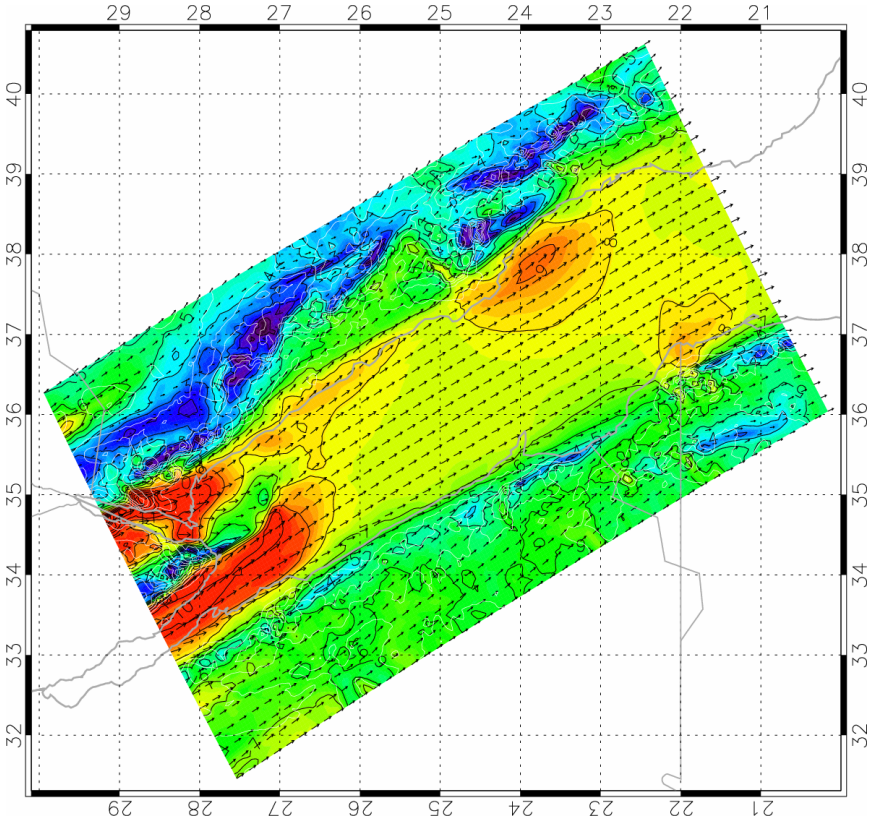

Figure 4-61. Wind vectors and speed at 50 m a.g.l. for a 3 degree 9.3 ms^{-1} forcing. The contour interval is 1 ms^{-1}. Note, that the north-direction is to the left.

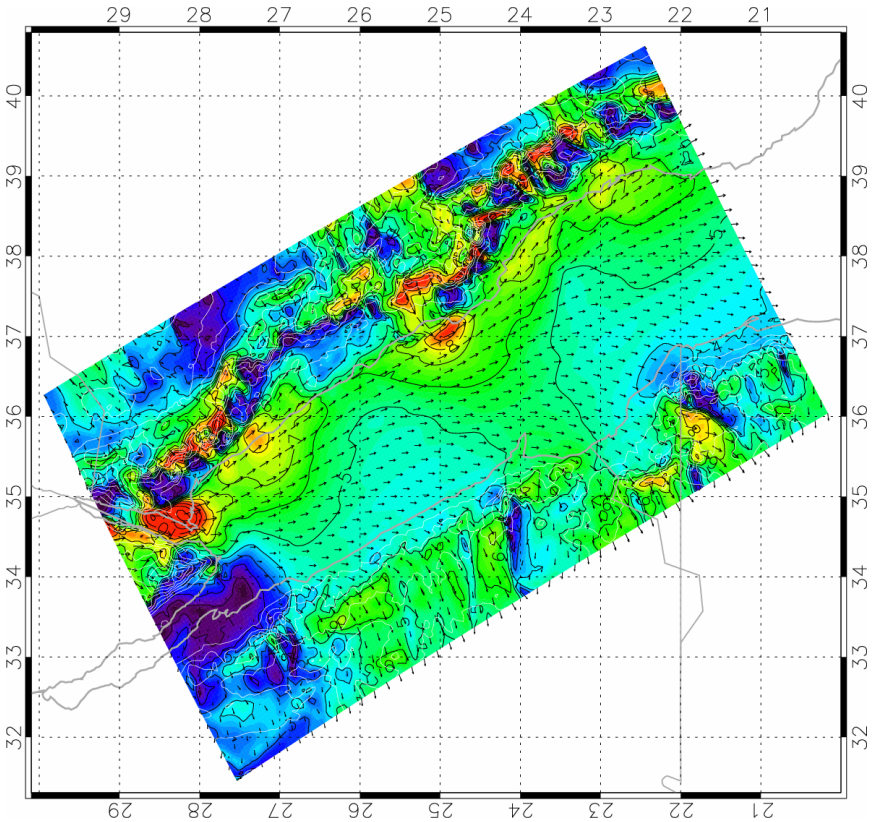

Figure 4-62. Wind vectors and speed at 50 m a.g.l. for a 88 degree 10.3 ms^{-1} forcing. The contour interval is 1 m/s. Note, that the north-direction is to the left.

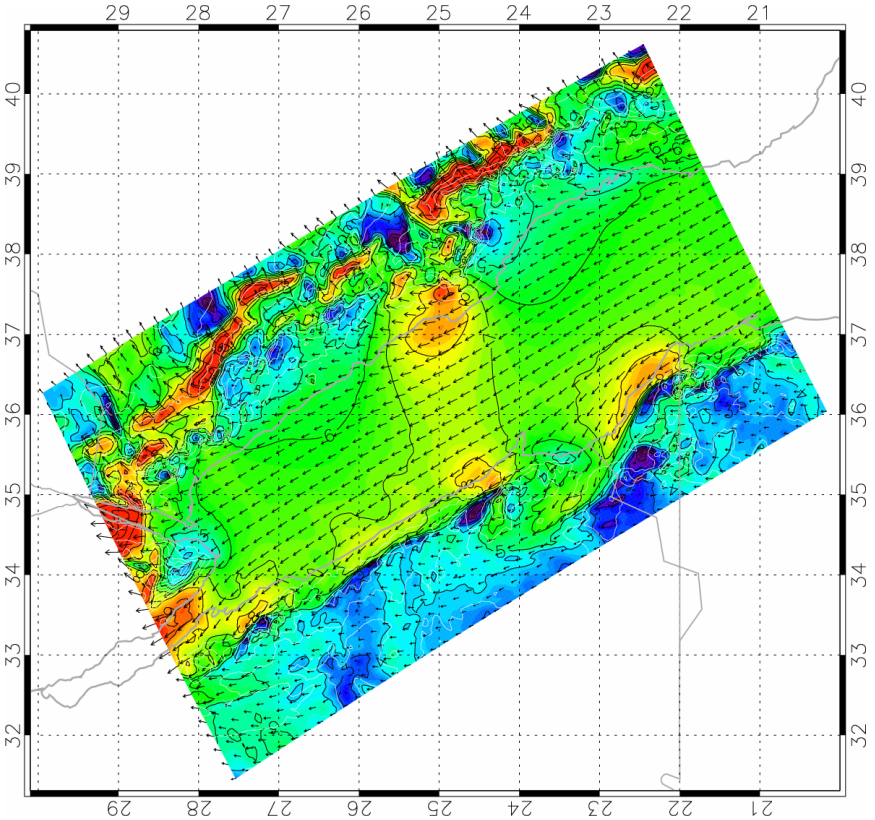

Figure 4-63. Wind vectors and speed at 50 m a.g.l. for a 179 degree 7.3 ms^{-1} forcing. The contour interval is 1 ms^{-1}. Note, that the north-direction is to the left.

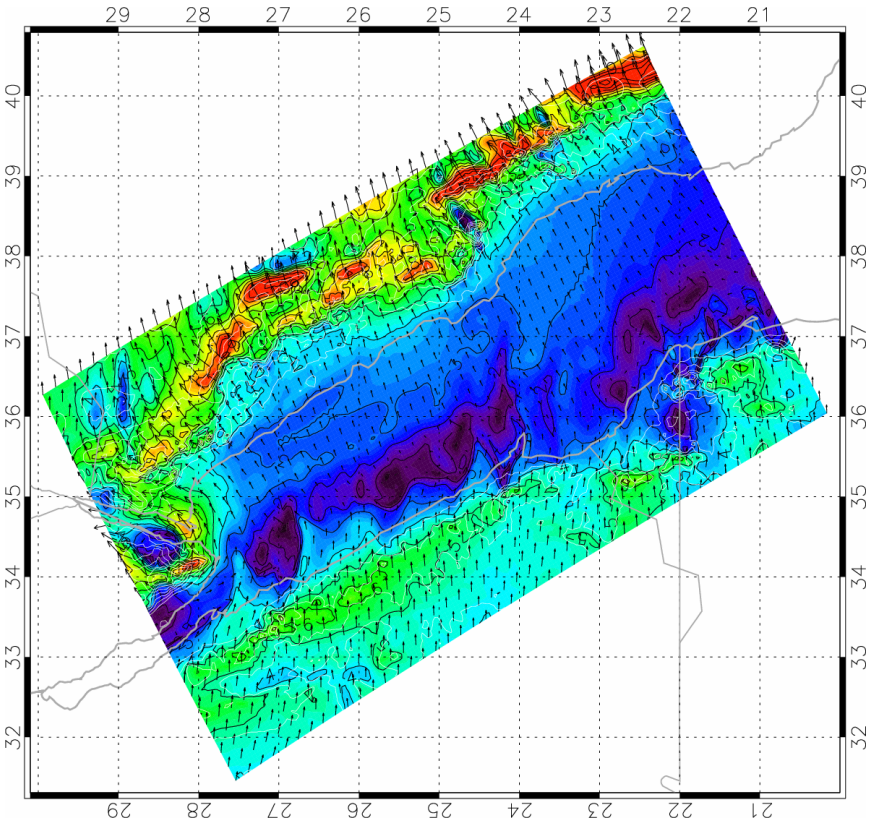

Figure 4-64. Wind vectors and speed at 50 m a.g.l for a 268 degree 3.3 ms^{-1} forcing. The contour interval is 1 ms^{-1}. Note, that the north-direction is to the left.

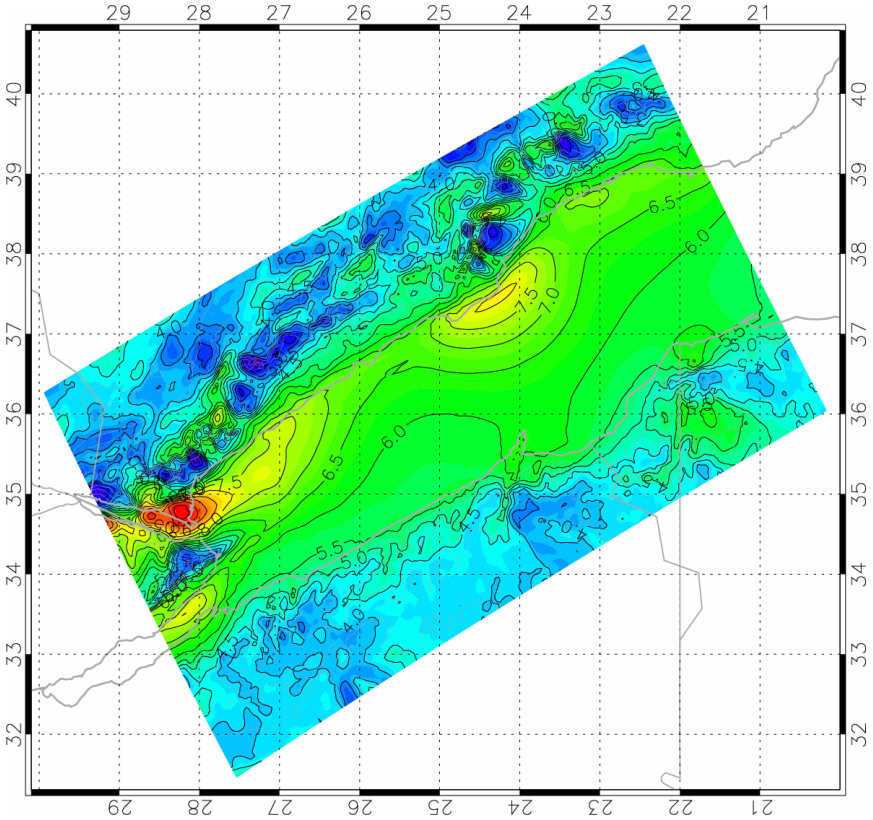

Figure 4-65. Mean simulated wind speed at 50 m a.g.l. The contour interval is 0.5 ms^{-1}. Note, that the north-direction is to the left.

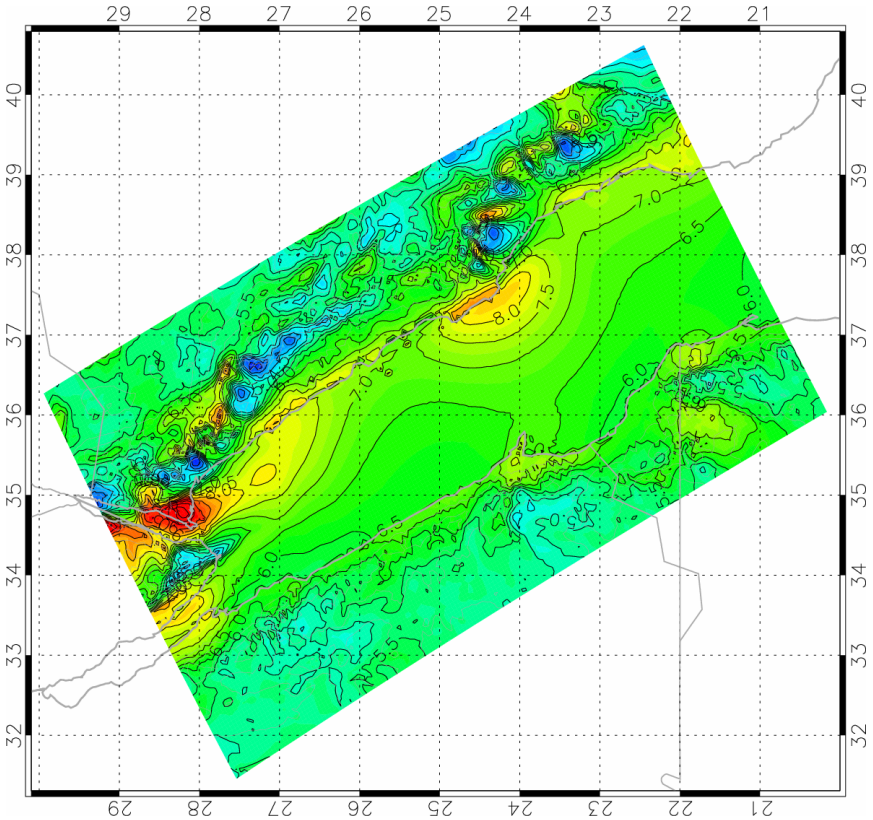

Figure 4-66. Mean generalized wind speed at 50 m a.g.l. for 0.0002 m roughness. The contour interval is 0.5 ms^{-1}. Note, that the north-direction is to the left.

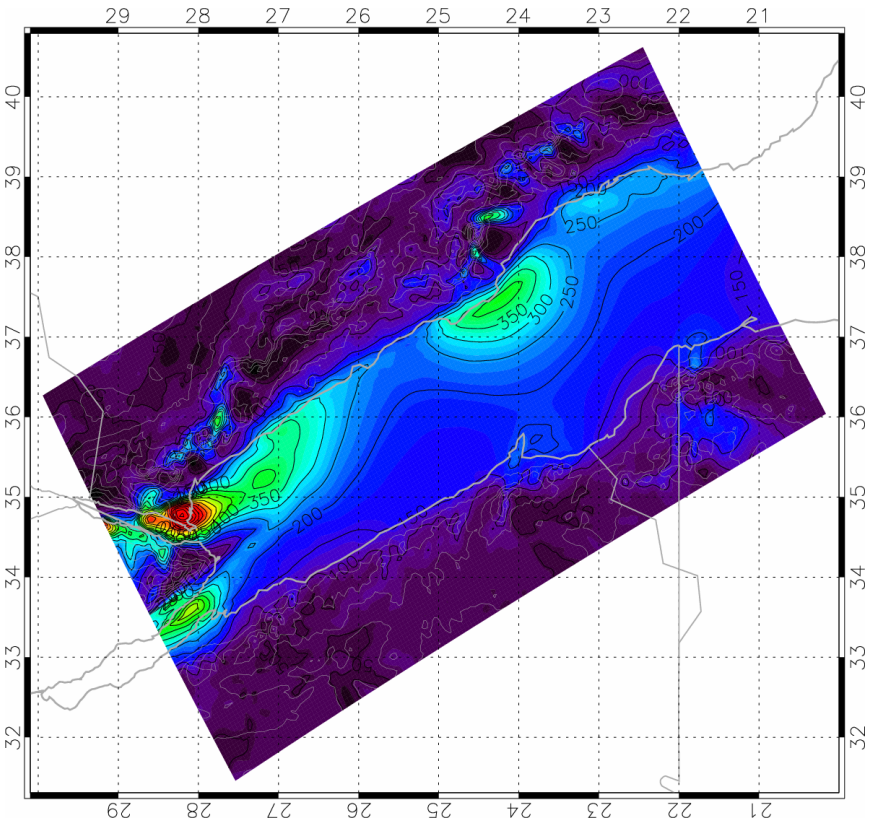

Figure 4-67. Mean simulated wind power density at 50 m a.g.l. The contour interval is 50 Wm^{-2}. Note, that the north-direction is to the left.

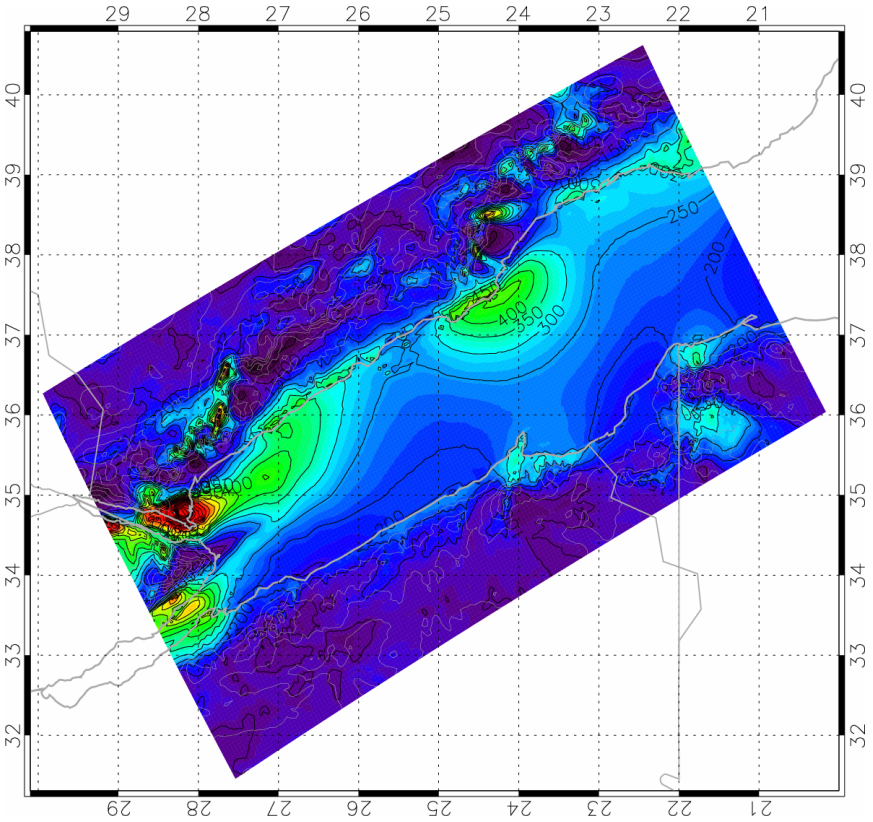

Figure 4-68. Mean generalized wind power density at 50 m a.g.l. for 0.0002 m roughness. The contour interval is 50 Wm^{-2}. Note: the north-direction is to the left.

Intentionally left blank

5 The Wind Atlas methodology

This chapter presents a brief survey of the physical and statistical models employed for the Atlas. A more thorough description of the different physical and statistical modelling tools, as well as the practical details related to data handling and the preparation of descriptions of anemometric conditions are given in the European Wind Atlas (Troen and Petersen, 1989). This volume also contains a general discussion of uncertainties and possible errors in the meteorological data and in the model.

5.1 The physical basis

As described in the introduction to this report, the Wind Atlas concept builds upon the use of a set of models for the correction of measured wind data and an analysis of the corrected data in terms of their frequency distributions. The integrated computer model used in the analysis is called the *Wind Atlas Analysis and Application Program* (WAsP). The sub-models are described briefly below – for more detailed information on the models and the WAsP-program, the reader is referred to the European Wind Atlas (Troen and Petersen, 1989) and the WAsP User's Guides (Mortensen *et al.*; 2004, 2005), respectively.

Surface-layer similarity laws

The layer closest to the ground is called the atmospheric boundary layer. The layer extends up to about 100 m on clear nights with low wind speeds and up to more than 2 kilometres on a fine summer day. The lowest part of this layer is called the surface layer, which is sometimes defined as a fixed fraction; say 10% of the boundary layer depth. For the purpose of climatology relevant to wind power utilization, we can neglect the lowest wind speeds so only situations where the atmospheric boundary layer extends to approximately 1 km and surface-layer physics apply in the lowest 100 m of the layer are of concern.

At high wind speeds the wind profile over flat and reasonably homogeneous terrain is well modelled using the logarithmic law:

$$u(z) = \frac{u_*}{\kappa} \ln\left(\frac{z}{z_0}\right) \tag{5-1}$$

where $u(z)$ is the wind speed at height z above ground level, z_0 is the surface roughness length, κ is the von Kármán constant, taken here as 0.40, and u_* is the so-called friction velocity related to the surface stress τ through the definition:

$$|\tau| = \rho \cdot u_*^2 \tag{5-2}$$

where ρ is the air density. Even at moderate wind speeds, deviations from the logarithmic profile occur when z exceeds a few tens of metres. Deviations are caused by the effect of buoyancy forces in the turbulence dynamics; the surface roughness is no longer the only relevant surface characteristic but has to be supplemented by parameters describing the surface heat flux. With surface cooling at nighttime, turbulence is lessened causing the wind profile to increase more rapidly with height; conversely, daytime heating causes increased turbulence and a wind profile more constant with height. Similarity expressions for these more general profiles are given by:

$$u(z) = \frac{u_*}{\kappa}\left(\ln\left(\frac{z}{z_0}\right) - \Psi\left(\frac{z}{L}\right)\right) \tag{5-3}$$

where Ψ is an empirical function (Businger, 1973; Dyer, 1974). The new parameter introduced in this expression is the so-called Monin-Obukhov length L:

$$L = -\frac{T_0}{\kappa g}\frac{\rho c_p u_*^3}{H_0} \tag{5-4}$$

where T_0 and H_0 are the surface absolute temperature and heat flux, respectively, c_p is the heat capacity of air at constant pressure, g the acceleration of gravity and the remaining quantities are defined above.

The stability modifications of the logarithmic wind profile are often neglected in connection with wind energy, the justification being the relative unimportance of the low wind speed range. The WAsP model treats stability modifications as small perturbations to a basic neutral state (Troen and Petersen, 1989). In order to take into account in an approximate manner the effects of varying the surface heat flux without the need for detailed modelling of each individual wind profile, a simplified procedure is adopted which only requires input in the form of the climatological average and root-mean-square of the surface heat flux.

The geostrophic drag law and the geostrophic wind

The winds in the atmospheric boundary layer can be considered to arise from pressure differences caused mainly by "synoptic" activity, i.e. the passing of high and low pressure systems. As the boundary layer structure has a rather rapid response to changes in pressure forcing, an approximate balance is found between the pressure gradient force and the frictional force at the surface of the earth. This balance can be theoretically derived under idealised conditions of stationarity, homogeneity and barotrophy (the pressure gradient being constant over the depth of the boundary layer). For conditions of neutral stability, the balance was already described by Rossby and Montgomery (1935). The result is usually expressed as a relation – called the geostrophic drag law – between the surface friction velocity u_* and the so-called geostrophic wind G:

$$G = \frac{u_*}{\kappa}\sqrt{\left(\ln\left(\frac{u_*}{fz_0}\right) - A\right)^2 + B^2} \tag{5-5}$$

$$\sin\alpha = -\frac{Bu_*}{\kappa G} \tag{5-6}$$

in which α is the angle between the near-surface winds and the geostrophic wind, f is the Coriolis parameter and A and B are empirical constants (here A = 1.8, B = 4.5). The geostrophic wind can be calculated from the surface pressure gradient and is often close to the wind speed observed by radiosondes above the boundary layer. The geostrophic drag law can be extended to conditions of non-neutral stability in which case the above constants A and B become functions of the stability parameter μ defined by:

$$\mu = \frac{\kappa u_*}{fL} \tag{5-7}$$

5.2 The roughness change model

The logarithmic wind profile applies only if the upwind terrain is reasonably homogeneous. If this is not the case, deviations will be observed and it is not possible to assign a unique roughness length to the terrain. Even though "effective"' roughness lengths can be assigned by different methods, these will depend on the height of observation. An exception to this is the effective roughness length implicitly defined by the geostrophic drag law.

The average surface stress and surface wind speed must depend on surface conditions only up to a certain upstream distance; distant obstacles are "forgotten"' by the tendency of the boundary layer to approach equilibrium between the pressure gradient force and friction. The distance scale involved is proportional to the Rossby radius G/f and is of the order of 10-100 km. For the wind frequency distribution it is assumed here that it is sufficient to consider surface conditions out to distances of the order of 10 km. From simple considerations pertaining to the surface layer, it is possible in the case of small-scale terrain inhomogeneities to model the change of surface stress which occurs when wind flows from a surface characterized by a roughness length z_{01} to another surface with a roughness of z_{02}. In this case an internal boundary layer (IBL) grows downwind from the roughness change; considering a point at a distance x downwind from the change, the IBL has grown to a height h given by (Panofsky, 1973):

$$\frac{h}{z_0'}\left(\ln\frac{h}{z_0'}-1\right)=\text{constant}\cdot\frac{x}{z_0'} \tag{5-8}$$

where $z_0' = \max(z_{01}, z_{02})$. Above h no change is felt whereas the wind profile has been perturbed in the layer below h. The value of the constant is here 0.9. It is empirically found that the change of surface friction velocity is well modelled using the following relation which can be derived from matching of neutral wind profiles at the height h:

$$\frac{u_{*2}}{u_{*1}}=\frac{\ln(h/z_{01})}{\ln(h/z_{02})} \tag{5-9}$$

where u_{*2} is the surface friction velocity at the point considered and u_{*1} the surface stress upwind from the change. The wind profile is perturbed in the IBL and the surface friction velocity cannot be calculated from observed wind speeds using the logarithmic profile. However, experimental evidence (Sempreviva et al., 1990), as well as results from numerical models (Rao *et al.*, 1974), show that the perturbed profile can be well modelled with three logarithmic parts:

$$u(z)=\begin{cases} u'\dfrac{\ln(z/z_{01})}{\ln(c_1h/z_{01})} & \text{for } z\geq c_1h \\ u''+(u'-u'')\dfrac{\ln(z/c_2h)}{\ln(c_1/c_2)} & \text{for } c_2h\leq z\leq c_1h \\ u''\dfrac{\ln(z/z_{02})}{\ln(c_2h/z_{02})} & \text{for } z\leq c_2h \end{cases} \tag{5-10}$$

where $u'=(u_{*1}/\kappa)\ln(c_1h/z_{01})$, $u''=(u_{*2}/\kappa)\ln(c_2h/z_{02})$ and $c_1 = 0.3$, $c_2 = 0.09$.

From this equation and with the aid of Eq. (9) the surface friction velocity u_{*2} corresponding to a measured wind speed can be related to the friction velocity upstream of a change in surface roughness. For more roughness changes Eq. (9) can be applied in sequence, and thus a measured wind speed can be used for calculating the surface friction velocity far upstream. However, successive roughness changes must not occur too close to each other and therefore the following distance rule is applied. If x_n is the distance to the nth change in surface roughness, then the upstream roughness must be estimated as an average covering the area between the distance x_n and $2x_n$ in the azimuth sector considered. The factor 2 is somewhat arbitrary, and the rule may be deviated from in cases where clear roughness boundaries are found, e.g. at a coastline.

Moving further upstream, the roughness change model just described will give results deviating from reality because it does not incorporate the above-mentioned boundary layer approach to equilibrium. As was the case with stability corrections, the discrepancies are considered to be small perturbations and a simple model is constructed by considering the asymptotic behaviour. The far-upstream surface conditions must lose importance as x/D becomes large, where D is the chosen equilibrium distance (here taken to be 10 km) and also the above surface layer relations must apply for x much smaller than D. This behaviour is obtained by a simple weighting of the roughness changes by a factor W_n:

$$W_n = \exp\left(-\frac{x_n}{D}\right) \tag{5-11}$$

Instead of considering a change from z_{0n} to z_{0n+1} at distance x_n the value $\ln(z_{0n}) + W_n \ln(z_{0n+1}/ z_{0n})$ substitutes $\ln(z_{0n+1})$. By application of this weighting in sequence, a value of the surface friction velocity far upstream is obtained together with a value of the corresponding equilibrium surface roughness to which the geostrophic drag law applies.

5.3 The shelter model

The frictional effect of a land surface is caused by drag on surface-mounted obstacles ranging from individual sand grains, grass, leaves etc. to large trees and buildings. Their collective effect is modelled through the surface roughness length as described in the section above.

Close to an individual obstacle, at distances comparable to the height of the obstacle and at heights likewise comparable to the height of the obstacle, the wind profile is perturbed, particularly in the downstream wake, and the object must be treated separately. In the wake immediately behind a blunt object, such as a row of trees or a house (less than five object heights downstream and at heights less than twice the height of the object) the details of the object exert a critical influence on the effects. The wake behind a building depends for example on the detailed geometry of the roof and the incidence angle of the wind, to mention two parameters. In addition, wakes from other nearby objects may interfere, causing the problem to become very complicated.

The main reason for addressing the problem here is that some of the meteorological data sets used in previous studies come from meteorological stations at which the wind data are influenced by nearby obstacles. As far as the analyses of the four

stations in the present study and the application of the Wind Atlas in siting are concerned, the problems are negligible.

The shelter model incorporated in WAsP should be seen as a tool for correcting data influenced by single obstacles that are sufficiently far away to make the perturbations small and to avoid the intricacies of the nearby wakes.

For simple two-dimensional semi-infinite obstacles such as long rows of trees, walls, or hedges, the expressions given by Perera (1981) obtained from wind-tunnel studies are used:

$$\frac{\Delta u}{u} = 9.8\left(\frac{z_a}{h}\right)^{0.14} \frac{x}{h}(1-p)\eta \exp(-0.67\eta^{1.5}) \tag{5-12}$$

where

$$\eta = \frac{z_a}{h}\left(\frac{0.32}{\ln(h/z_0)}\frac{x}{h}\right)^{-0.47} \tag{5-13}$$

and P is the porosity (open area/total area) of the obstacle, h is the height of the obstacle, z_a is the height considered (e.g. the anemometer height), and x is the down-stream distance.

With finite obstacle lengths and skew incidence of the wind, the sheltering of an obstacle will in general be different. In the European Wind Atlas (Troen and Petersen, 1989) some simple guidelines are indicated; however, the model actually used in the analysis is slightly more refined.

For each of a number of radial lines or rays originating from the point considered, the distances to and heights of objects crossed by the ray are noted. If a single ray crosses several obstacles each of these crossings is initially treated as a single semi-infinite obstacle. Starting with the most distant one, the shelter on all downstream obstacles is calculated in sequence. If objects are so close to each other that their zones of separation join, the downstream sheltering is reduced by the relative area of the downstream obstacle which is embedded in the separation zone of the upstream obstacle. In this connection the separated zone upwind of a two-dimensional obstacle is considered to be limited by a straight line from the top of the obstacle down to the surface at a distance twice the height of the obstacle, and similarly downstream to a distance of five times the height.

Subsequent to this calculation of the shelter at the point considered from the sequence of objects, the sheltering for each ray is mixed with neighbouring values. This is done to model the actual mixing of momentum deficit at the edge of the wake. Finally, the average shelter is calculated over an azimuth sector by summing up the sheltering calculated on each ray in the azimuth sector. Here eight rays are used per 30° azimuth sector and an effective lateral spreading over an angle of 12°.

5.4 The orographic model

Like the change-of-roughness and shelter models, the orographic model is used to correct measured wind data for the effect of local terrain inhomogeneities; in the present case this means differences in terrain elevation around the meteorological stations. Emphasis is placed on the effects of terrain undulations with horizontal scales up to several tens of kilometres, and the model was especially developed to serve this purpose. It has strong similarities with the MS3DJH family of models based on the analysis of flow over hills by Jackson and Hunt (1975). Readers who wish to become acquainted with these models should consult the papers by Walmsley et al. (1982), Troen and de Baas (1986). The model is different, however, in a number of respects, the most important being the high resolution and polar representation.

The first step in the model is the calculation of the potential flow perturbation induced by the terrain and corresponding to a unit wind vector in the undisturbed wind direction. This proceeds as follows: the velocity perturbation is related to the potential by:

$$\vec{u} = \nabla\chi \tag{5-14}$$

where χ is the potential and $\vec{u}$ the three-dimensional vector of velocity perturbations $\vec{u} = (u, v, w)$.

If vanishing potential is assumed at a given outer model radius *R*, a general solution to the potential flow problem in polar coordinates can be expressed as a sum in terms of the form:

$$\chi_j = K_{nj} J_n\left(c_j^n \frac{r}{R}\right)\exp(in\phi)\exp\left(-c_j^n \frac{z}{R}\right) \tag{5-15}$$

where K_{nj} are arbitrary coefficients, J_n the *n*th order Bessel function, *r* radius, ϕ azimuth, *z* height, and c_j^n are the *i*th zero of J_n. For a specific problem, the coefficients are determined by the boundary conditions, which are here the surface kinematic boundary condition:

$$w_0 = \frac{\partial}{\partial z}\chi\Big|_{z=0} = \vec{u}_0 \cdot \nabla h(r, \phi) \tag{5-16}$$

where w_0 is the terrain-induced vertical velocity, $\vec{u}_0$ the basic state velocity vector and *h* the height of terrain. The functions $J_n\left(c_j^n \frac{r}{R}\right)$ form an orthogonal set of radial functions (Fourier-Bessel series) for each *n*, and the azimuth representation $\exp(in\phi)$ likewise forms an orthogonal set (Fourier series). The coefficients K_{nj} can therefore be calculated independently by projecting the right-hand side of Eq. (16) onto this basis of functions. The mathematical details of these transforms are described in Oberhettinger (1973).

The polar representation has important advantages over the more common Cartesian as used in the above-mentioned models, while maintaining the advantages of spectral decomposition. By defining the model centre to coincide with the point of interest, it is possible to concentrate the model resolution there and also to restrict the calculations

to the perturbation at this point. For the centre point $r = 0$, the following solution is found:

$$\nabla\chi_j = \frac{1}{2}(1,i)K_{1_j}\frac{c_j^1}{R}\exp\left(-c_j^1\frac{z}{R}\right) \tag{5-17}$$

The final result of the first step in the model is thus a series of coefficients k_{1_j} from which the solution of the potential flow perturbation is given as a sum of the terms stated in Eq. (17). Each term has an associated horizontal scale $L_j = R/c_j^1$, which is also the characteristic depth to which the perturbation penetrates.

The second step in the model consists of a modification of the potential flow solution to accommodate in an approximate sense the effects of surface friction.

Potential flow implies a balance between the pressure gradient force and advection of momentum in the equations of momentum and vanishing turbulent momentum transfer. Near the surface the turbulent transfer cannot be neglected. The deviation from the potential flow behaviour is restricted to a layer whose depth is of the order ℓ_j with $\ell_j << L_j$. In the present model the value of ℓ_j is determined following Jensen et al. (1984) as:

$$\ell_j = 0.3 \cdot z_{0j}\left(\frac{L_j}{z_{0j}}\right)^{0.67} \tag{5-18}$$

where z_{0j} is the surface roughness length of the scale considered. For homogeneous conditions $z_{0j} = z_0$. For inhomogeneous sites the surface roughness length is taken as an exponentially weighted average from $r = 0$ to $r = 5\ L_j$ in the upwind direction (weighting $\ln(z_0)$).

For heights much smaller than ℓ_j, turbulent transfer forces a balance between stress and wind shear, leading to a logarithmic profile of the velocity perturbation. For heights comparable with ℓ_j maximum flow perturbation occurs, and this perturbation exceeds the value predicted from potential flow. In the present model the perturbation profile is modelled for each term in the above expansion by assigning a perturbation to the height z of magnitude Δu_j:

$$\frac{\Delta\vec{u}_j(z)}{|u_0(z)|} = \frac{|u_0(L_j)|^2}{|u_0(z_j')|^2}\nabla\chi_j \tag{5-19}$$

where $u_0(z)$ is the basic state velocity at height z and z_j' is equal to $\max(z, \ell_j)$.

The calculation of the coefficients k_{1_j} through the projection method involves numerical integrations over azimuth and radius. This is performed on a grid illustrated in Figure 5-1.

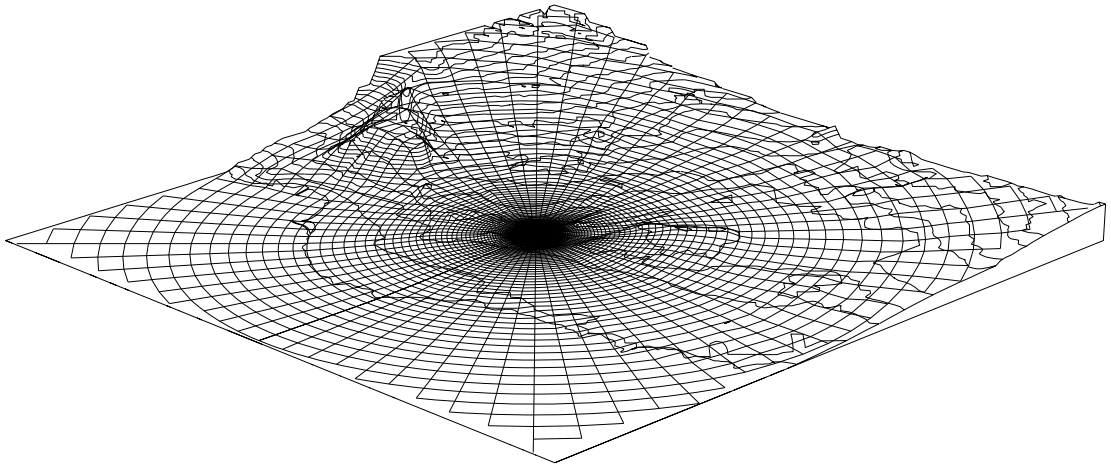

Figure 5-1. The polar zooming grid employed by the model for the calculation of flow in complex terrain. Part of the terrain around Zafarana is seen from a point above the Gulf of Suez, looking towards SW. The grid is superimposed on the terrain and centered on the meteorological station Zafarana. The side length is 20 km.

The radial grid size is smallest at the centre and is increased by a constant factor (=1.06) outwards for each grid cell. In principle, the necessary input is the height of terrain at each grid point, but a much more convenient representation of the terrain height is the contour lines (lines of constant height) as given on standard topographical maps. The model was designed, therefore, to directly accept arbitrarily chosen contour lines as input and integrates the estimation of grid-point values and the numerical integrations in one process. The grid consists of 100 radial stations and the resulting resolution near the centre is approximately 2 m for a model with R = 10 km, and approximately 10 m for R = 50 km, etc. Therefore resolution is limited in practice only by the accuracy and density of the contour data from the topographical maps.

5.5 The statistical basis

The presentation of wind data makes use of the Weibull distribution (Weibull, 1951) as a tool to represent the frequency distribution of wind speed in a compact form. The two-parameter Weibull distribution is expressed mathematically as:

$$f(u) = \frac{k}{A}\left(\frac{u}{A}\right)^{k-1} \exp\left(-\left(\frac{u}{A}\right)^{k}\right) \tag{5-20}$$

where $f(u)$ is the frequency of occurrence of wind speed u (as elsewhere in the Atlas the indication of mean value $\langle u \rangle$ is not shown explicitly). The two Weibull parameters thus defined are usually referred to as the scale parameter A and the shape parameter k. The influence on the shape of $f(u)$ for different values of the shape parameter is illustrated in Figure 5-2. For $k > 1$ the maximum (modal value) lies at values $u > 0$, while the function decreases monotonically for $0 < k \leq 1$.

The Weibull distribution can degenerate into two special distributions, namely for k = 1 the exponential distribution and for k = 2 the Rayleigh distribution. Since observed wind data, especially in the Westerlies, exhibit frequency distributions which are often well described by the Rayleigh distribution, this one-parameter distribution is sometimes used to represent wind data; here, however, the more general two-parameter

Weibull distribution is used throughout. Inspection of the *k*-parameter for individual stations in the Atlas shows that the values cover the range from two to four; the two-parameter distribution will therefore provide much better fits to the data than the Rayleigh distribution.

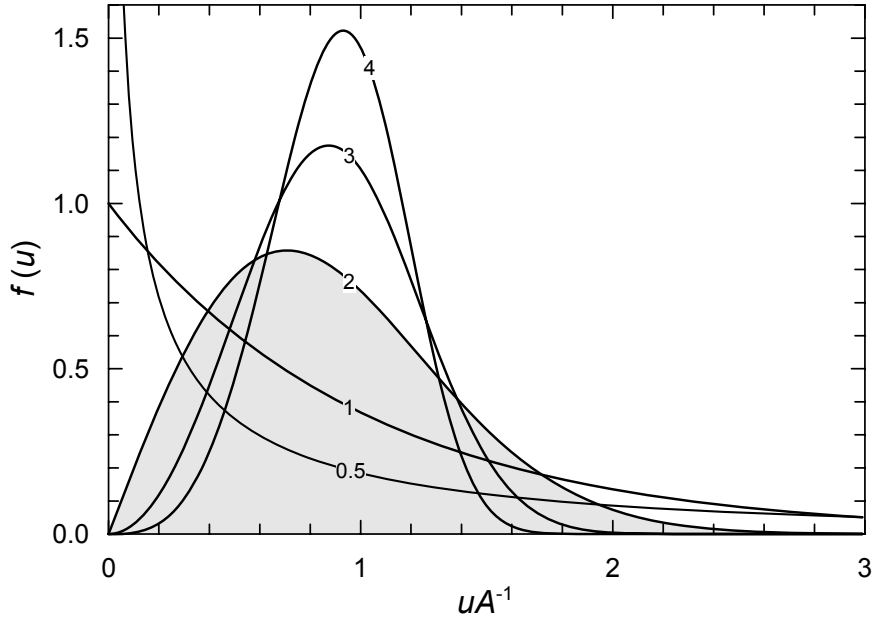

Figure 5-2. The shape of the Weibull distribution function for different values of the shape parameter: k = 0.5, 1, 2, 3, 4.

The cumulative Weibull distribution $F(u)$ gives the probability of the wind speed exceeding the value u and is given by the simple expression:

$$F(u) = \exp\left(-\left(\frac{u}{A}\right)^k\right) \tag{5-21}$$

The Weibull distribution generates Weibull-distributed higher powers: if u is Weibull-distributed with parameters A and k, then u^m is Weibull-distributed with the parameters A^m and k/m.

Moments and other important characteristics of Weibull distributions are easy to derive; a list of the more common characteristics is given here for reference:

$$\begin{aligned}
&\text{mean value} : A\Gamma(1+1/k)\\
&\text{mean square} : A^2\Gamma(1+2/k)\\
&\text{mean cube} : A^3\Gamma(1+3/k)\\
&\text{mean } m\text{th power} : A^m\Gamma(1+m/k)\\
&\text{variance} : A^2\left[\Gamma(1+2/k)-\Gamma^2(1+1/k)\right]\\
&\text{modal value} : A\left(\frac{k-1}{k}\right)^{1/k}\\
&\text{median} : A(\ln 2)^{1/k}
\end{aligned} \tag{5-22}$$

where $\Gamma(x)$ is the gamma function. The available wind power density is proportional to the mean cube of the wind speed:

$$E = \frac{1}{2}\rho A^3 \Gamma\left(1+\frac{3}{k}\right) \tag{5-23}$$

where E is power density (Wm^{-2}), ρ is air density (1.225 kg m^{-3} for a temperature of 15°C and a standard pressure of 1013.25 hPa).

The wind speeds at which the highest power density is available is given by:

$$u_m = A\left(\frac{k+2}{k}\right)^{1/k} \tag{5-24}$$

Thus, for a Rayleigh distribution, the wind speed which contains the highest energy on the average is twice the most frequent speed (modal value).

Many different methods can be used for the fitting of the two Weibull parameters to a histogram giving the frequency of occurrence of wind speed in a number of intervals (bins). If the observed data are well represented by the Weibull distribution over the whole range of speeds, then the fitting procedure can be chosen at will. In general, however, observed histograms will show deviations due to a number of causes, and a fitting procedure must be selected which focuses on the wind speed range relevant to the application. Here the emphasis is on the higher wind speeds and a moment fitting method is used which focuses on the higher but not the extreme wind speeds.

For each azimuthal sector, the two Weibull parameters are determined by the requirements that: 1) the total wind power in the fitted Weibull distribution and the observed distribution are equal, and 2) the frequencies of occurrence of wind speeds higher than the observed average speed are the same for both distributions. The combination of these two requirements leads to an equation in k only, which is solved by a standard root-finding algorithm.

Most difficulties in fitting to observed data are related to the treatment of very low and very high wind speeds. The highest wind speeds, say the uppermost percentile of observations, are statistically very uncertain and special methods (i.e. Gumbel, 1958) must be employed in extreme wind analysis, see Chapter \ref{sec-4}. This analysis is not included in the WAsP program, and the Weibull distributions given here should not be used for the estimation of frequencies of occurrence much below 0.01.

At low wind speeds, limitations in instrument response, reporting practices and data truncation can in general lead to substantial errors in the frequency of occurrence. Sometimes such errors give rise to an abnormally high frequency of recorded calms. For wind power applications, the precise form of the frequency curve for wind speeds lower than the average is of little concern and the present fitting method is designed with this in mind. It should be noted, however, that for meteorological stations with mean speeds of ~3 ms^{-1} or lower, located in a reasonably windy climate, but locally heavily sheltered, the calculated regional wind climate from such stations becomes inaccurate because of these difficulties. In addition, the physical models used in the analysis are deficient at low wind speeds. Fortunately, none of the stations reported in the present atlas are of this type.

The fitting method described above is used to estimate the Weibull parameters for each of the observed azimuth sectors and for the sector-wise fitting of model-derived (or transformed) frequency distributions. The parameters pertaining to the associated total or azimuth-independent wind distributions are obtained from the sector-wise distributions fitting to the sums of the first and third moments.

5.6 The Wind Atlas analysis model

The model is composed of the submodels described in the preceding sections. By means of measured wind data, descriptions of local terrain roughness, sheltering obstacles and topographical height data, a regional wind climatology is calculated in the form of Weibull parameters pertaining to standard conditions. For each of the meteorological stations used in the Atlas, the input to the model is summarized on the three first pages and the model output is given on the last page in the station statistics in Chapter 7. A schematic representation of the analysis model is shown in Figure 5-3.

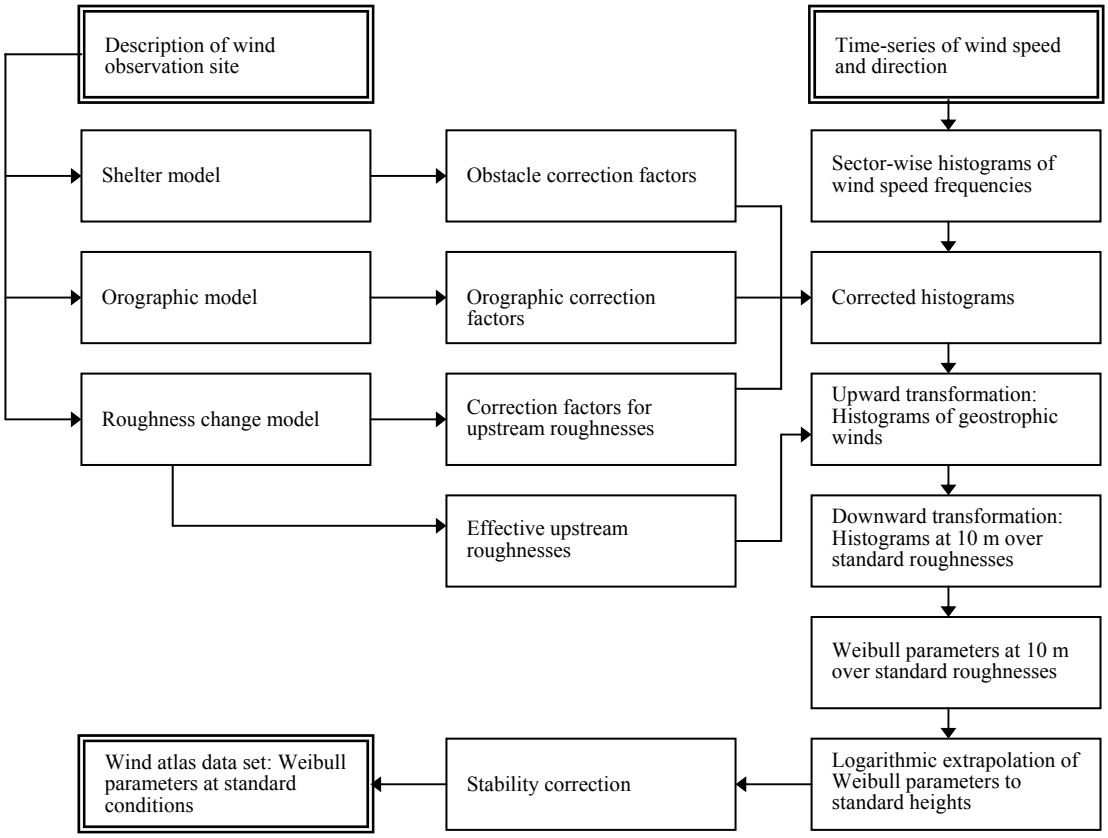

Figure 5-3. A schematic representation of the Wind Atlas analysis model.

The calculation procedure can be summarized as follows: input data are in the form of histograms for each of 12 azimuth sectors, giving the frequency of occurrence of wind speeds in bins of 1 ms^{-1} width.

First, wind speed-independent correction factors are calculated for each azimuth sector. Three sets of factors are considered:

- The obstacle correction factors, calculated using the shelter model, here denoted C^j_{obs} for the *j*th azimuth sector.
- The roughness change factors C^j_{rou} .The roughness change model relates the velocity at the station to the velocity upstream of the specified roughness changes. In addition, the area weighting of surface roughness gives an effective upstream surface roughness z^j_{0e} .
- The orography correction factors, calculated by application of the orographic model. The model is applied using as input a wind profile with direction in the centre of each sector. As described in Section 5.4 the actual surface roughnesses are taken into account as parameters in the orographic model. From this C^j_{oro} and D^j_{oro} are obtained, where D^j_{oro} is degrees of turning of the wind vector calculated by the orographic model.

Secondly, each combined azimuth and wind-speed bin is transformed using these factors. Considering the *j*th sector and the wind-speed bin from $u^{(k)}$ to $u^{(k+1)}$, application of the obstacle correction factor C^j_{obs} gives the corresponding values which would pertain if the obstacles were removed. Similarly, the orographic corrections and the roughness change corrections are applied to transform the bin boundaries to values for upstream conditions. For the turning of the azimuthal boundaries, the orographic turning angles are applied using the average of the two values nearest the boundary considered.

The effective surface roughness z^j_0 is used with each of the new bin boundaries in the geostrophic drag law, Eq. (5), to calculate the corresponding boundaries $G^{k,j}$ and $G^{k+1,j}$ with associated directions D^{kj}_{low} and D^{kj}_{high} from the low and high side of the original azimuth bin. In this transformation process the frequency of occurrence in the bin is conserved. The geostrophic wind could be used as a means of representation of the regional climatology, but the transformation process is instead continued to obtain the wind distributions over the standard values of surface roughness. Again using the geostrophic drag law, u_*-values for the standard surface roughness are obtained from the above $G^{k,j}$, $G^{k+1,j}$ and wind directions from the *D*-values above. From the logarithmic profile (Eq. 1) the corresponding values for the wind speeds at the lowest standard level (10 m) are obtained. At this stage the contributions to each of the "standard" azimuth (30°) and speed (1 ms^{-1}) bins are calculated.

This procedure is repeated for each azimuth/speed bin in the input data and the result is four sets of histograms of the same form as the input histograms, but pertaining to the lowest standard level of 10 metres and to each of the four roughness classes. For each azimuth sector, the corresponding frequency of occurrence is extracted and the Weibull parameters are determined using the fitting procedure described in Section 5.5. The Weibull parameters corresponding to the higher standard levels z_n are then calculated as described in Section 5.1, using a modification of the logarithmic profile which takes into account the effects of the variation of surface heat flux. The average and root-mean-square heat fluxes are specified independently for over-land and over-sea conditions. The following standard values from the European Wind Atlas (Troen and Petersen, 1989) are adopted for all the analysed stations:

Average heat flux over land	-40 Wm^{-2}
Average heat flux over sea	15 Wm^{-2}
Root-mean-square heat flux over land	100 Wm^{-2}
Root-mean-square heat flux over sea	30 Wm^{-2}

The European Wind Atlas (Troen and Petersen, 1989) further gives factors of "contamination" by the stability effects on mean values and standard deviations, respectively. These expressions are evaluated for contamination in the input data using the anemometer height, distance to the coast, and upstream equilibrium surface roughness in each azimuth sector. Similarly, the contamination is calculated for the different standard heights, and the ratios of these values to those on input are used to correct the Weibull parameters calculated using a logarithmic profile. The corresponding means and standard deviations are calculated using the expressions given in Eq. (22), the corrections are applied, and an inverse calculation is performed to determine the Weibull parameters corresponding to corrected values for means and variances. In this calculation, roughness class 0 refers to conditions over water and the three other roughness classes are corrected to conditions well inland beyond any coastal influence.

5.7 The Wind Atlas application model

For the construction of the Atlas itself, the analysis model described in the preceding section is complete. Equally important, however, is the model built to enable an inverse calculation of site-specific wind speed distributions from the regional climatology. The model is shown schematically in Figure 5-4. Such a model can be used to check the calculated regional statistics and can also be offered as a siting tool to the Wind Atlas user.

The model incorporated in WAsP is designed to be as close as possible to the inverse of the analysis model. The correction factors for local shelter, orography, and roughness changes are calculated exactly as in the analysis model, now of course using the obstacle list, roughness description, and orographic data pertaining to the site where the Atlas data are to be applied.

For the height considered, the Wind Atlas table is referenced and the appropriate Weibull parameters A_j and k_j for each azimuth sector are extracted in addition to the sector frequency f_j. For heights different from the standard heights and for surface roughnesses different from the standard values, a logarithmic interpolation is used. The surface roughness values used for each sector are the values calculated in the roughness change model z_{0e} (Section 5.2). The correction factors are applied to the A-parameter for each sector while keeping the k-parameter values at the table values. Finally, the stability correction is performed in the manner described above.

For a given height above the terrain and from a specification of terrain roughnesses, sheltering obstacles, and orographic details, the model therefore calculates values for the sector-wise Weibull parameters, and sector frequencies for a chosen regional climatology. Internal consistency is checked by calculating the station climatology using the regional climatology derived from the same station via the analysis model.

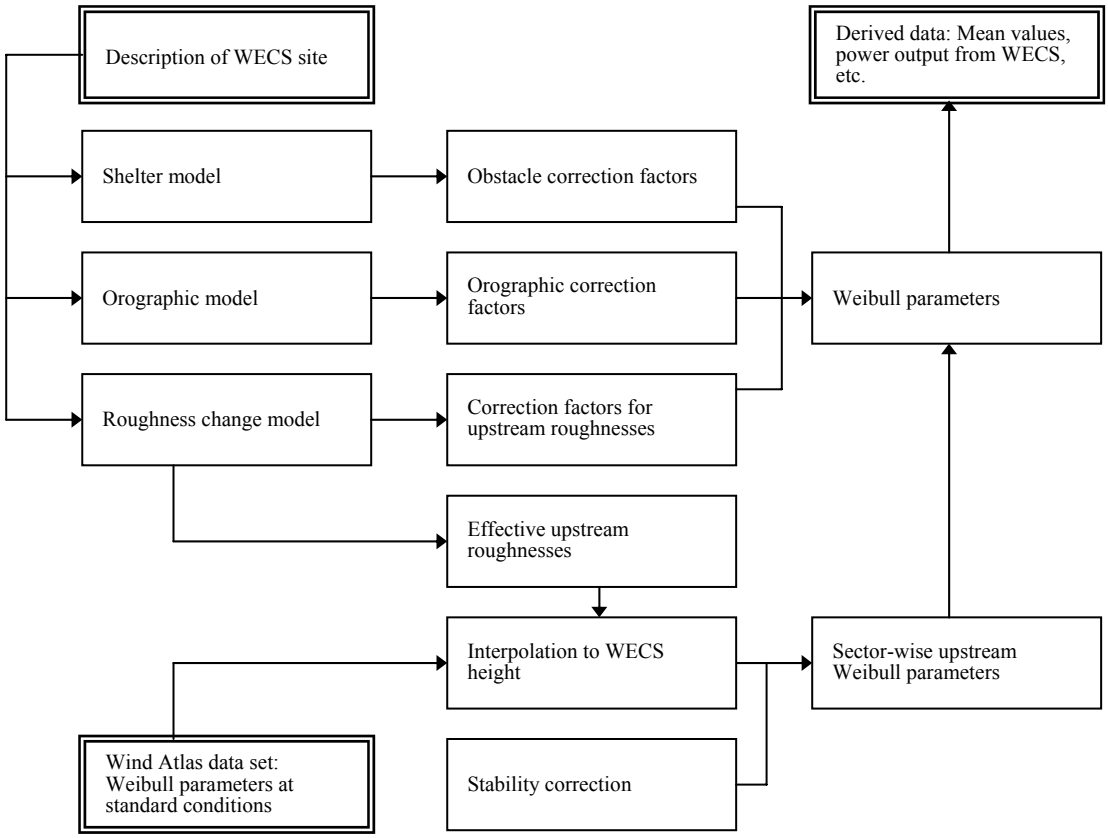

Figure 5-4. A schematic representation of the Wind Atlas application model.

Of more interest is the intercomparison using the regional climatology from one station to predict the local climatology of another nearby station. This intercomparison exercise is described in Chapter 6.

5.8 Meteorological data and station descriptions

The meteorological data originate from two sources: 25-m met. masts erected specifically for the project (see Appendix A) and standard (10 m) met. stations operated by the Egyptian Meteorological Authority. Data were analysed according to Troen and Petersen (1989) and Mortensen et al. (2005). The data cover periods of between one and 14 years; no attempt has been made to relate the data sets to a common reference period. The coverage and representativity of each data set are apparent from the data summaries given in Chapter 7. Stations with no night-time observations – or with no data for a particular season – were omitted in the wind atlas analysis.

Elevation descriptions covering areas of 20×20 km^2 were obtained by digitisation of ordinary 1:50,000 topographical maps (10-m contours and spot heights) or constructed from version 2 of the SRTM 3 arc-second data set.

Roughness descriptions were obtained by digitisation of topographical maps, aerial photographs or satellite imagery (e.g. Google Earth Pro). The descriptions have been verified during site visits, which also provided information on the existence of near-by sheltering obstacles. As can be seen in Chapter 7, a few stations are severely sheltered and the situation is outside the operational envelope of the shelter model.

6 Verification of the wind atlas methodology

6.1 Station intercomparisons

A judgement as to whether the regional statistics calculated by means of a particular station are in fact adequate for the determination of wind speed distributions – with sufficient accuracy for wind energy estimates – in the region around the station, has to be based on comparisons between predictions and measurements. In general, such verification can be attempted by intercomparing stations which are mainly situated in the same basic wind-climatological conditions and are separated by a distance of approximately 50 km or less. Most of the stations in Egypt, however, are separated by much larger distances and this method of verification is not possible here.

In parts of the Gulf of Suez, the distances between stations are much smaller than 50 km, but here the regional wind climate changes significantly over distances of a few kilometres only. This is illustrated in Table 6-1 below which shows the results of a station intercomparison in the Zafarana area.

Table 6-1. Comparison of four stations in the Zafarana area. The rows contain predicted mean wind speed and power density for each station; each column corresponds to a predicting station. The right-most column contains the wind climates observed at the stations. The diagonal line of bold face figures indicates the stations predicting themselves.

Station		Abu Darag	Mast 7	Zafarana	Z. West	Measured
Abu Darag	[ms^{-1}]	**8.83**	8.96	9.40	7.98	8.82
	[Wm^{-2}]	**584**	523	750	502	586
Mast 7	[ms^{-1}]	9.15	**9.14**	9.58	8.07	9.21
	[Wm^{-2}]	654	**657**	785	512	664
Zafarana	[ms^{-1}]	8.60	8.47	**8.91**	7.55	8.97
	[Wm^{-2}]	554	526	**626**	416	630
Z. West	[ms^{-1}]	8.66	8.63	9.08	**7.64**	7.48
	[Wm^{-2}]	560	555	664	**433**	429

The four stations lie within an area which is only about 10 km E-W and 19 km N-S. Abu Darag and Zafarana M7 are both situated close to the coastline, about 12 km apart, in similar topographical settings. These two stations predict each other very well. Zafarana and Zafarana West are situated about 5 km and 14 km from the coastline, respectively, in a wide valley oriented west-east. Here, the overall wind climate changes rapidly due to mesoscale effects and the stations cannot be used to accurately predict each other or any of the coastal stations.

In conclusion, the mesoscale modelling results may be used as a guideline as to how far from a given met. station the WAsP application procedure can be expected to provide reliable predictions.

6.2 KAMM- and WAsP-modelled regional wind climates

In this section a comparison is made between the wind atlas wind speed values derived from the numerical wind atlas method (KAMM/WAsP) and the WAsP method using observations. For a given location a wind atlas file can be used to give an expected wind speed for a set of standard heights above a set of standard terrain roughnesses.

In Figure 6-1 to Figure 6-6 the mean wind speeds at 10, 25, 50, 100 and 200 m above a flat, uniform terrain surface with a roughness length z_0 of 0.03 m are used for the comparison. The legend to the right of each plot shows the names of the stations used. Each figure shows the comparison within a single modelling domain. There is overlap of domains and therefore stations may appear in more than one of the plots. Where there is good agreement between KAMM/WAsP and observation and WAsP, the plotted points lie close to the one-to-one line in each plot.

In many cases there is good agreement between the wind atlases derived from KAMM modelling and observations. The agreement at the station locations adds confidence to the KAMM-derived wind data for locations away from stations.

There are several possibilities why there may be poorer agreement between KAMM- and observation-derived wind atlases.

Close to the KAMM domain boundaries a less accurate wind atlas is usually derived. This is an unavoidable consequence of limited area modelling. The effect can be minimized by careful selection of the domain, keeping points of interest well within the domain and including the dominant topographic features in the domain as much as possible.

The complexity of the flow modification by the topography influences the agreement between the KAMM results and the observations. For the Gulf of Suez and the Red Seas domains, the topography tends to be higher and have a stronger influence on the flow. For the Northwest Coast and Western Desert domains, the topography is less complex, and the flow modification due to terrain is less pronounced.

Correct selection of the wind classes used to force the mesoscale model has a very strong influence on the accuracy of the KAMM results. The use of more location-specific wind classes in the smaller domains tends to reduce the error from this source.

Other causes of error may be found within the WAsP analyses. The correct choice of surface roughness for instance has an influence on the wind atlas values. Also some of the stations are relatively close to sheltering obstacles. Obstacles can be difficult to model correctly. Comparison of the wind direction distributions also would help to highlight causes of errors, including errors due to incorrectly modelled influence of obstacles.

Finally, the observed data sets have not been referenced to the same standard period of time so the scatter in Figure 6-1 to Figure 6-6 also simply reflect the climatic variability in the wind regimes.

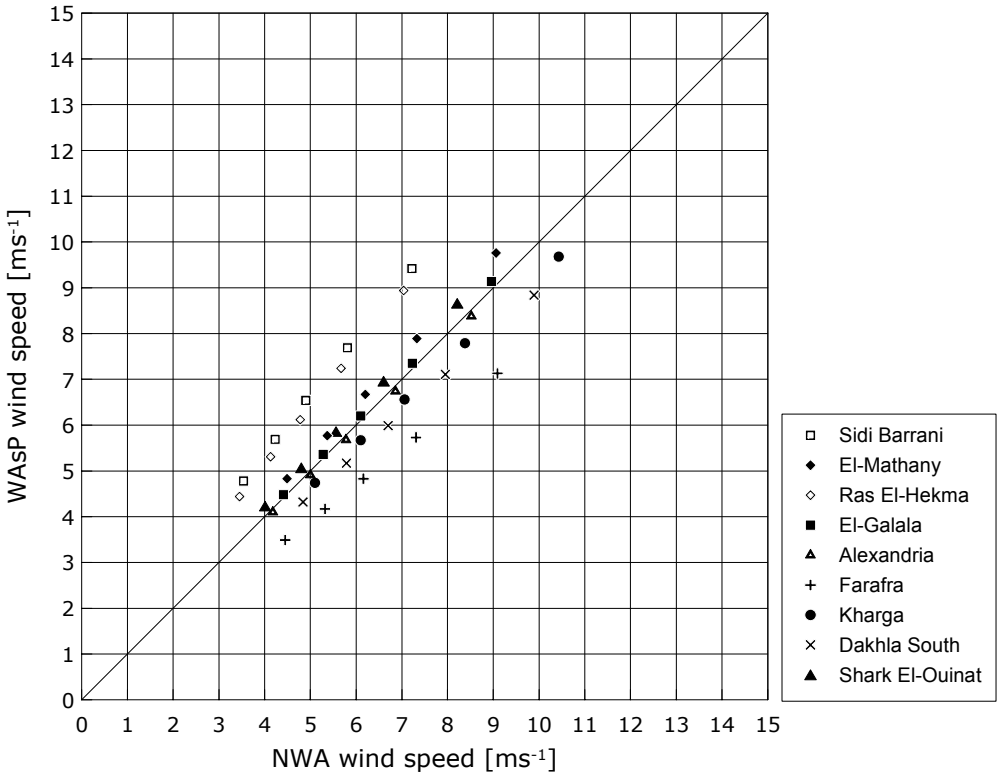

Figure 6-1. Western Egypt domain comparison of atlas wind speed values at 10, 25, 50, 100, 200 m calculated using KAMM/WAsP (x-axis) and observations/WAsP (y-axis), roughness is 0.03 m.

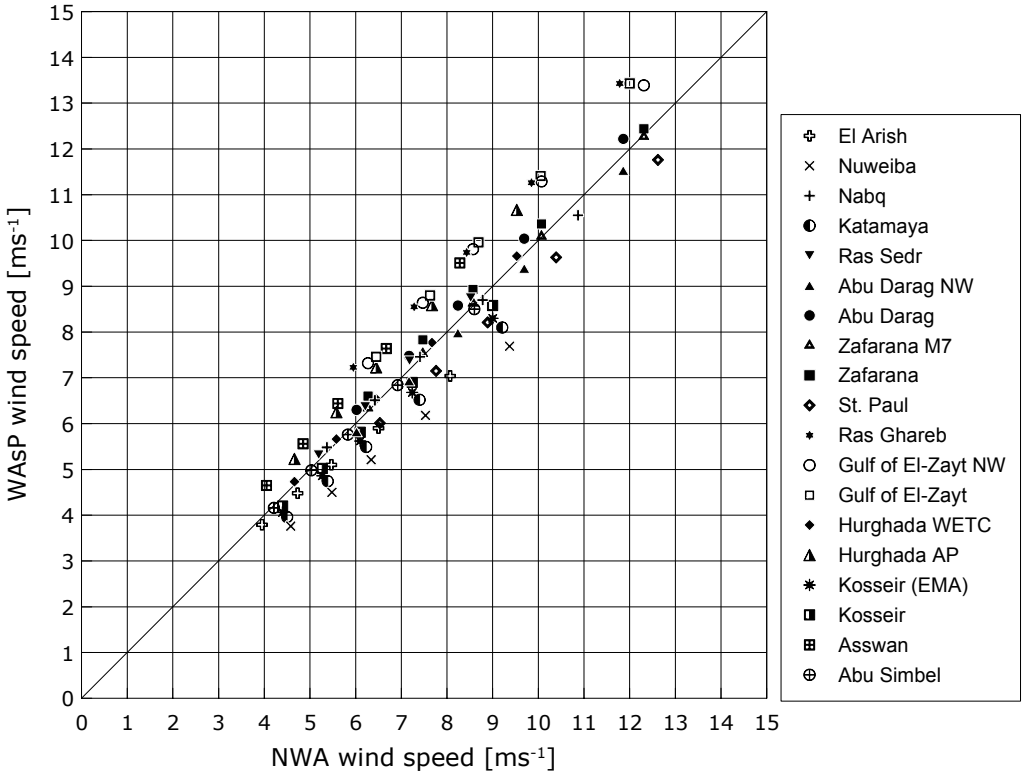

Figure 6-2. Eastern Egypt domain comparison of atlas wind speed values at 10, 25, 50, 100, 200 m calculated using KAMM/WAsP (x-axis) and observations/WAsP (y-axis), roughness is 0.03 m.

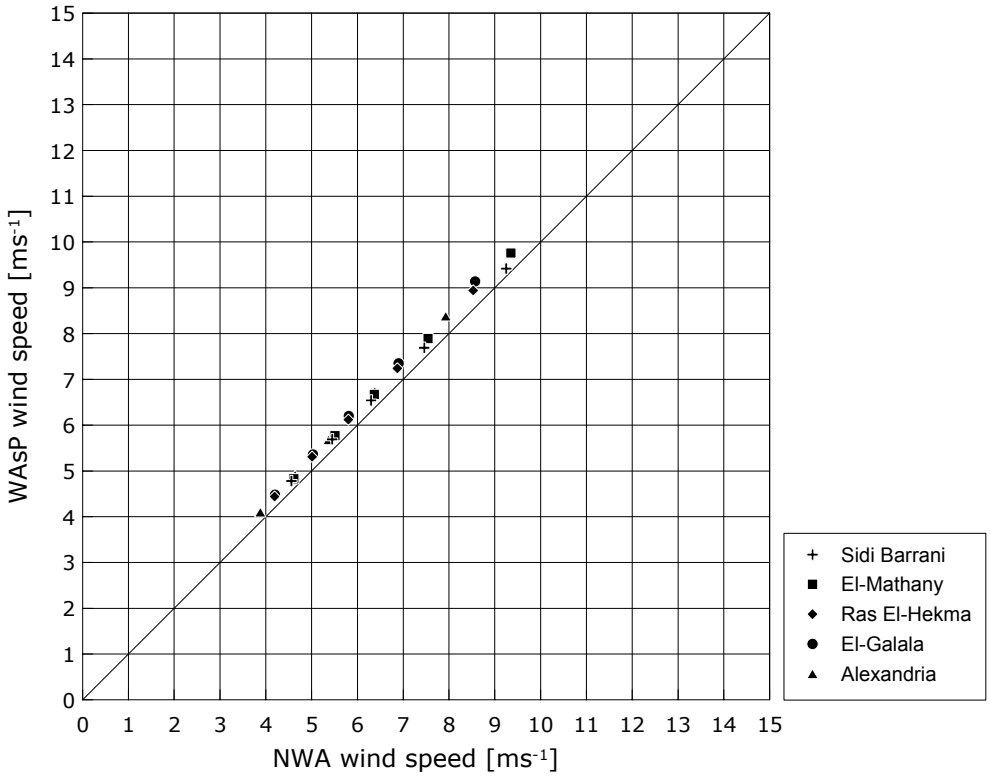

Figure 6-3. Northwest Coast domain comparison of atlas wind speed values at 10, 25, 50, 100, 200 m calculated using KAMM/WAsP (x-axis) and observations/WAsP (y-axis), roughness is 0.03 m.

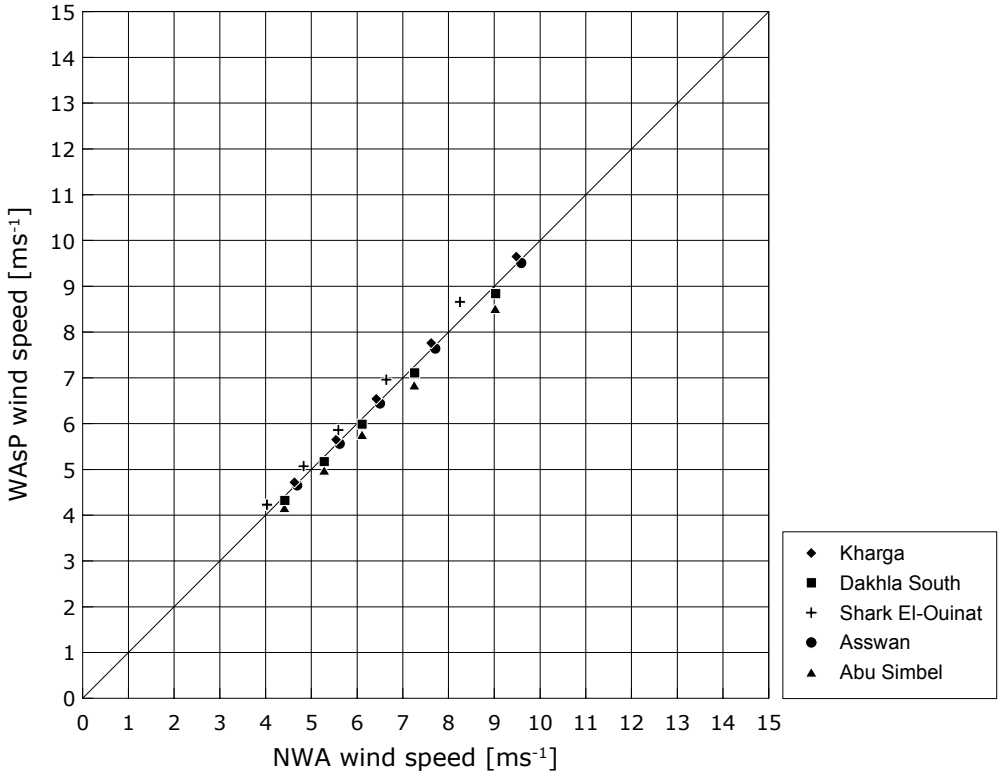

Figure 6-4. Western Desert domain comparison of atlas wind speed values at 10, 25, 50, 100, 200 m calculated using KAMM/WAsP (x-axis) and observations/WAsP (y-axis), roughness is 0.03 m.

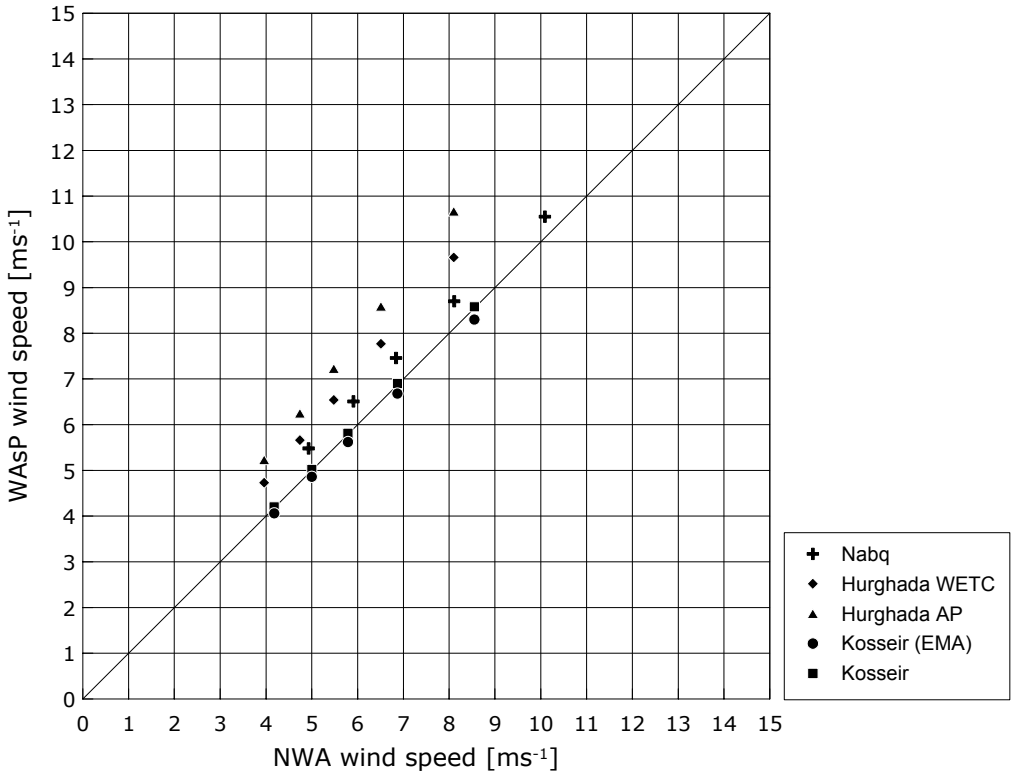

Figure 6-5. Red Sea domain comparison of atlas wind speed values at 10, 25, 50, 100, 200 m a.g.l. calculated using KAMM/WAsP (x-axis) and observations/WAsP (y-axis), roughness is 0.03 m.

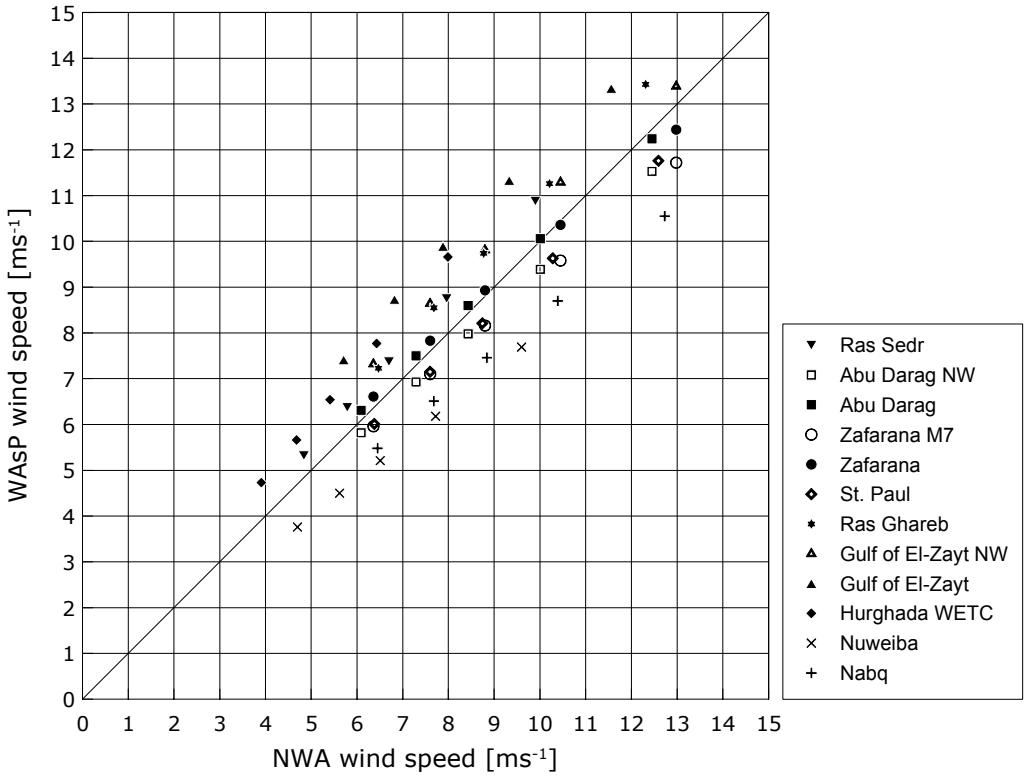

Figure 6-6. Gulf of Suez domain comparison of atlas wind speed values at 10, 25, 50, 100, 200 m calculated using KAMM/WAsP (x-axis) and observations/WAsP (y-axis), roughness is 0.03 m.

Table 6-2 summarises the comparisons between the KAMM- and WAsP-modelled regional wind climates. The absolute error is calculated as the difference between the two estimates (for the height of 50 m a.g.l.) divided by their mean value, and expressed as a percentage. The right-most column shows the mean absolute error for a subset of stations in the Red Sea and the Gulf of Suez.

Table 6-2. Comparison of atlas wind speed values at 50 m a.g.l. and a roughness of 0.03 m, calculated using KAMM/WAsP and observations/WAsP.

Domain	**Grid size**	**Mean absolute error**	**Mean absolute error**
		All stations	Selected stations
	[km]	[%]	[%]
Western Egypt	7.5	12.4	n/a
Eastern Egypt	7.5	7.6	n/a
Northwest Coast	5.0	5.2	n/a
Western Desert	5.0	3.1	n/a
Gulf of Suez	5.0	9.4	5.6
Red Sea	5.0	10.5	4.4

The scatter plots shown in Figure 6-5 and Figure 6-6 indicate that the largest differences between the KAMM- and WAsP-modelled regional wind climates are found for stations located close to the southern entrance of the Gulf of Suez. If Hurghada WETC and Hurghada AP are disregarded in the Red Sea comparison, the mean absolute error decreases from 10.5% to 4.4%. Likewise, if the Gulf of El-Zayt NW and Gulf of El-Zayt stations are disregarded in the Gulf of Suez comparison, the mean absolute error decreases from 9.4% to 5.6%. The typical mean absolute error is then about 10% for the large domains and about 5% for the small domains.

PART III
STATION STATISTICS AND CLIMATOLOGIES

7 Observed and regional wind climates

In this chapter, the climatological data for the meteorological stations used in the study are presented in tables and graphs. For each station, the tables give the calculated regionally representative wind climatology – the *regional wind climate* – obtained from the station data by applying the Wind Atlas analysis, together with a summary of the raw data – the *observed wind climate* – and the measuring conditions. The raw data and some derived quantities are furthermore shown graphically in so-called wind climatological fingerprints (Troen and Petersen, 1989). Each station summary is printed on two pairs of facing pages. The first opening contains

- the station description
- the station topography
- the topographical model corrections
- several raw data summaries and graphs

and the second opening gives

- the wind climatological fingerprint
- the seasonal and year-to-year variations of wind speed
- the calculated regionally representative Weibull parameters
- the calculated regional mean wind speeds and power densities

The presentation of the data is explained in detail in the following sections.

7.1 The station description

The station description comprises the geographical location, a description of the setting and surroundings of the station, a station topographical map, and a summary of the corrections derived from the WAsP analysis.

Name of station

The names of the stations are those used on topographical maps or in previous reports and they are spelled accordingly. The name of the region or modelling domain is also given: Northwest Coast, Northeast Coast, Gulf of Aqaba, Gulf of Suez, Red Sea or the Western Desert.

Geographical coordinates

The latitude and longitude of each station are given in degrees, minutes and seconds. The horizontal datum is the World Geodetic System 1984 (WGS84). The positions have been determined using a GPS (Global Positioning System) receiver and verified by plotting the position on a topographical map, satellite image or aerial photograph.

Grid coordinates

The Cartesian grid coordinates consist of the Universal Transverse Mercator (UTM) Easting (E) and Northing (N) in full metres. The number of the UTM zone (Z), to which these coordinates refer, is also given. Positions west of 30°E are referenced to UTM zone 35; positions east of this meridian to UTM zone 36. The horizontal datum is the World Geodetic System 1984 (WGS84).

Elevation
The elevation of the station is given in metres above mean sea level (m a.s.l.). Vertical datum is determined by the WGS84 Earth Gravitational Model (EGM96) or the mean sea level Alexandria 1906.

Station description
The overall setting of each station is described, i.e. major terrain features such as distance from the sea, lakes, rivers, forests, mountains, etc. Major obstacles close to the anemometer mast are also mentioned as well as other information regarded as significant for the interpretation of the station statistics.

Station topographical map
The topographical map shows the terrain elevations in a 10×10-km^2 area around the station – with the station approximately in the middle of the map. The height contour interval is 10 m in most cases, though a larger contour interval is used for stations in mountainous terrain. 100-m contours are shown with thick lines and labelled with the elevation value. The contour lines used in the orographic flow model may be more detailed (1- or 2-m contours close to the station) and usually cover a much larger area (say, 20×20 km^2). Some areas of different roughness length may be indicated as well, in particular land, sea and lake areas.

The elevation information was obtained from version 2 (the 'finished' data set) of the Shuttle Radar Topography Mission (SRTM) data set. Additional information for the Gulf of Suez was obtained by digitisation of first edition Egyptian Series 1:50,000 maps; compiled from aerial photography taken in 1988 and completed and verified in 1989. Information on land use and thereby roughness length of the terrain surface was obtained from satellite imagery (e.g. Google Earth Pro), topographical maps, aerial photographs and from field visits to the sites.

Topographical model corrections
The wind speed correction factors (in per cent) and wind direction correction angles – to allow for sheltering obstacles and the effects of roughness change and orographic forcing – applied in the calculation of the Wind Atlas tables are given in a separate table below the station topographical map. If a station has been corrected for effects of sheltering and roughness change only, there are no corrections to the wind directions.

7.2 Raw data summaries
The raw data summary comprises the distributions of the wind measurements in tabular and graphical form, as well as tables of the daily, seasonal and year-to-year variations of mean wind speed.

Distribution of wind measurements
This table gives the sector-wise distribution of the raw wind speed measurements and the distribution of wind speeds within each sector. The frequency of occurrence of the winds in the sectors is given in per cent, whereas the distribution of wind speeds is given in per mille (tenths of per cent), i.e. normalized to 1000 within each sector. The table pertains to the anemometer height in metres above ground level (m a.g.l.) and the measurement period listed above the table as CCYY-CCYY, i.e. 1992-2001 means from 1 January 1992 to 31 December 2001.

A Weibull distribution function has been fitted to the wind speed distribution in each sector. The resulting Weibull *A*- [ms^{-1}] and *k*-parameters are listed in the last two columns of the table.

Wind rose and histogram

The wind rose shows the distribution of wind direction in the processed time-series. Wind direction is divided in twelve 30°-sectors; the angular axis is given in degrees from 0° to 360° clockwise, the units on the radius axis is per cent.

The histogram shows the total distribution of observed wind speeds (bar graph) in the processed time-series. A Weibull distribution function has been fitted to the data and is shown with a full line. The units on the *x*-axis is ms^{-1}, on the *y*-axis per cent.

Daily and annual variation of wind speed

This table gives the mean wind speed as a function of time of day and month of year. The time of day is given as Egyptian Standard Time (LST), equivalent to Universal Coordinated Time (UTC) + 2 hours. The table corresponds to the period (10 years or less) used in the wind-climatological fingerprint, see below.

7.3 The wind climatological fingerprint

The purpose of the graphical presentations of wind data given on the left-hand side of the second opening is to give a compact and informative overview of the wind data used for the Atlas. The first line states the name of the meteorological station and the period over which the data were collected. This is followed by the height above ground level where measurements were taken, the mean value, the standard deviation and the mean value of the cube of the measured wind speeds. The fingerprint is limited to 10 years of data; if the data series is longer, the 10-y period with the highest data recovery rate has been used. The graphical presentation consists of five graphs:

The mean year

The average seasonal variation of the measured wind speed (full line) and cube of wind speed (dashed line) is shown in the top left graph. All data associated with the same calendar month are averaged and the results plotted at the midpoint in each of the indicated monthly intervals. The unit on the ordinate is ms^{-1} for mean speeds and m^3s^{-3} for the mean of the cube of the wind speed. Values read from the graph must be multiplied by the scale factor given to the right. The continuous curves are obtained by interpolation using a periodic cubic spline. The speed data are also contained in the tables on the station description pages.

The mean days

The average daily variation of the measured wind speed for the months of January and July is shown in the top right graph. The average hourly variation of wind speed is shown in full lines for January and July and for the cube of wind speed dashed lines are used. Data from all months of January (July) associated with the same time of day are averaged. Results obtained for each of the indicated standard hours are plotted using an interpolating smooth curve (periodic cubic spline). The mean ordinate for each curve is identical to the ordinate on the corresponding mean year curve (top left graph) at the January (July) points. The unit on the ordinate is ms^{-1} for mean speeds and m^3s^{-3} for the mean of the cube of speed. Values read from the graph must be

multiplied by the scale factor given to the left. Mean days for each calendar month are calculated and define – for each calendar month – a mean or reference day that is used as reference in calculating the spectrum below. The speed values are contained in the tables in the station descriptions.

The wind rose

The relative frequencies of winds coming from each of twelve sectors are shown in the middle left graph as the radial extent of the circle segments spanning the sectors (thick lines). The contributions from each sector to the total mean speed and to the total mean cube of speed are given as the narrower segments and the central segments respectively. For each quantity the normalization is such that the largest segment extends to the outer dotted circle. The corresponding value for each of the three quantities is given in the small box in per cent (numbers given to the nearest integer). The inner dotted circle corresponds to half of this value.

The spectrum

The contribution to the total variance of wind speed for a range of periods is shown by the full curve in the middle right graph. The vertical scale is arbitrarily adjusted to centre the curve. The abscissa gives the periods on a logarithmic scale. The curve is calculated from the total time series by first subtracting the monthly mean day values from each day data, hour by hour. The monthly mean days for all twelve months were calculated as described for January and July above. The mean days are in this context considered deterministic in contrast to the calculated time series of deviations which form the stochastic part. This is followed by a Fourier transform of the deviations and the spectral estimates are squared and block averaged over bands of equal relative bandwidth corresponding to the widths of the steps in the curve.

The full vertical bar on the left side gives the contribution to the standard deviation of wind speed in the whole set of data from periods which fit into one year. This is calculated as the standard deviation of the *mean year* (top left). The adjacent dashed bar gives similarly the mean year contribution to the standard deviation of the cube of wind speed. Units are per cent of the total standard deviation of the data. Similarly the bars on the right give the contributions to the standard deviations of speed and cube of speed by periods which fit into one day, i.e. 24, 12, 8 and 6 hours in the present case of basic 3-hourly data. The numbers listed at the top left inside the graph are the contribution to the total standard deviation in per cent by the random variations contained in the variance spectrum, divided into the part with periods longer than one year, periods between one year and one day, and periods smaller than one day (the sum of squares of the contributions of the three random parts together with the contributions from the deterministic mean year and mean day adds to unity). The numbers in the small box below the graph give the relative standard deviation for speed and cube of speed for the mean January day (first two numbers) and the mean July day (last two numbers).

The time print

The month-by-month relative deviation from the mean months is shown in the bottom graph. For each month the average speed and cube of speed is calculated and the expected value from the corresponding calendar month in the *mean year* (top left) is subtracted. The relative deviation is shown by the jagged lines – where the full line corresponds to speed and the dashed line corresponding to the cube of speed. The

smoother full line shows the year-by-year relative deviation of mean speed from the total average. Each point on this curve gives the relative deviation in the period extending backwards and forwards one half year (centred block averages). The centre value for each calendar year thus gives the deviation for that particular year. The open circles show similarly the relative deviation of the mean cube of speed for each calendar year. The numbers to the right give the root mean square of the calendar year deviations in per cent for speed (lower number) and cube of speed (upper number). The vertical scale is linear from -1 to +1, and shifts at +1 to a coarser linear scale which is adjusted to accommodate the largest deviations.

Year-to-year and annual variations of wind speed

The table below the wind climatological fingerprint gives the mean wind speed as a function of year and month of year. There may be more years listed in this table than is used for the fingerprint, which covers a period of 10 years or less only.

7.4 Regional climatology and mean values

The Wind Atlas tables give the calculated Weibull *A*- and *k*-parameters for 12 sectors, 5 heights and 4 roughness classes. In addition, the sector-wise frequency of occurrence of wind speed is given in per cent for each roughness class. The Weibull *A*-parameters are given in [ms^{-1}].

Estimated mean wind speed and mean power

The last table on the right-hand page gives the estimated (calculated) mean wind speed [ms^{-1}] and total mean power density of the wind [Wm^{-2}] for each of the five standard heights and four roughness classes. These are calculated using the Weibull parameters of the Wind Atlas tables.

Note, that the four roughness classes correspond to uniform surfaces with a roughness length of 0.0002 m, 0.003 m, 0.03 m, and 0.10 m, respectively. Compared to the European Wind Atlas (Troen and Petersen, 1989), an intermediate class (i.e. z_0 = 0.003 m) is used here, because of the generally low roughness of the desert surfaces.

7.5 Station statistics and climatologies

The station statistics and climatologies given below were compiled and modelled in 2005 – using data collected from the period January 1992 to May 2005. The wind atlas data were calculated using the available information at the time of writing and the results might change in subsequent analyses. The 30 stations included in the atlas are listed in Table 7-1 and their locations are shown on the map in Figure 7-1. This map further shows the elevations of Egypt, derived from the “Shuttle Radar Topography Mission Data Set" (SRTM30), which contains spot heights of the node points in a grid with 30 arc-second resolution (926 m or less). Overall summaries of the wind measurements are given in Chapter 2.

Table 7-1. Meteorological stations used in the Wind Atlas. The met. stations are listed according to region. Grid coordinates and elevations are given in meters. The UTM zone number is given under the heading 'Z'.

Region/Station	**Latitude N**			**Longitude E**			**Easting**	**Northing**	**Z**
Northwest Coast									
Sidi Barrani (62301)	31°	37'	36.5"	25°	54'	29.8"	396,462	3,499,587	35
El-Mathany	31°	23'	25.9"	26°	48'	2.5"	481,051	3,472,901	35
Ras El-Hekma	31°	12'	21.4"	27°	52'	0.3"	582,568	3,452,750	35
El-Galala	31°	1'	43.6"	28°	10'	59.7"	612,930	3,433,392	35
Alexandria (62318)	31°	10'	55.2"	29°	57'	7.2"	781,337	3,453,527	35
Northeast Coast									
Port Said	31°	10'	5.8"	32°	18'	4.6"	433,412	3,448,462	36
El Arish (62337)	31°	4'	57.7"	33°	49'	41.0"	578,984	3,439,060	36
Gulf of Aqaba									
Nuweiba	28°	58'	53.2"	34°	41'	6.8"	664,183	3,207,100	36
Nabq	28°	7'	45.2"	34°	25'	46.3"	640,395	3,112,343	36
Gulf of Suez									
Katamaya	29°	54'	21.2"	31°	46'	8.4"	381,156	3,308,994	36
El-Suez (62450)	29°	52'	27.8"	32°	28'	18.8"	449,002	3,304,985	36
Ras Sedr	29°	25'	57.8"	32°	47'	25.5"	479,672	3,255,947	36
Abu Darag NW	29°	17'	15.0"	32°	34'	53.4"	459,351	3,239,911	36
Abu Darag	29°	16'	49.4"	32°	36'	3.3"	461,235	3,239,117	36
Zafarana M7	29°	10'	22.2"	32°	37'	44.9"	463,938	3,227,191	36
Zafarana	29°	6'	48.7"	32°	36'	38.9"	462,134	3,220,626	36
Saint Paul	28°	48'	12.6"	32°	44'	23.5"	474,615	3,186,243	36
Ras Ghareb	28°	20'	25.7"	33°	1'	37.0"	502,641	3,134,920	36
Gulf of El-Zayt NW	27°	54'	21.5"	33°	20'	10.5"	533,090	3,086,832	36
Gulf of El-Zayt	27°	47'	23.9"	33°	28'	23.3"	546,610	3,074,027	36
Red Sea									
Hurghada WETC	27°	18'	59.3"	33°	42'	3.5"	569,352	3,021,683	36
Hurghada (62463)	27°	11'	5.1"	33°	48'	7.9"	579,462	3,007,152	36
Kosseir (62465)	26°	6'	44.0"	34°	15'	21.5"	625,582	2,888,716	36
Kosseir	25°	49'	56.2"	34°	25'	33.0"	642,905	2,857,885	36
Western Desert									
Farafra (62423)	27°	3'	29.3"	27°	59'	20.7"	598,085	2,993,260	35
Kharga	25°	46'	20.3"	30°	39'	40.1"	265,442	2,852,551	36
Dakhla South	24°	37'	19.0"	29°	6'	22.8"	713,227	2,724,721	35
Shark El-Ouinat	22°	27'	31.2"	28°	41'	51.1"	674,669	2,484,585	35
Asswan (62414)	23°	57'	55.1"	32°	49'	30.4"	482,207	2,650,398	36
Abu Simbel	22°	25'	49.1"	31°	33'	25.7"	351,509	2,481,171	36

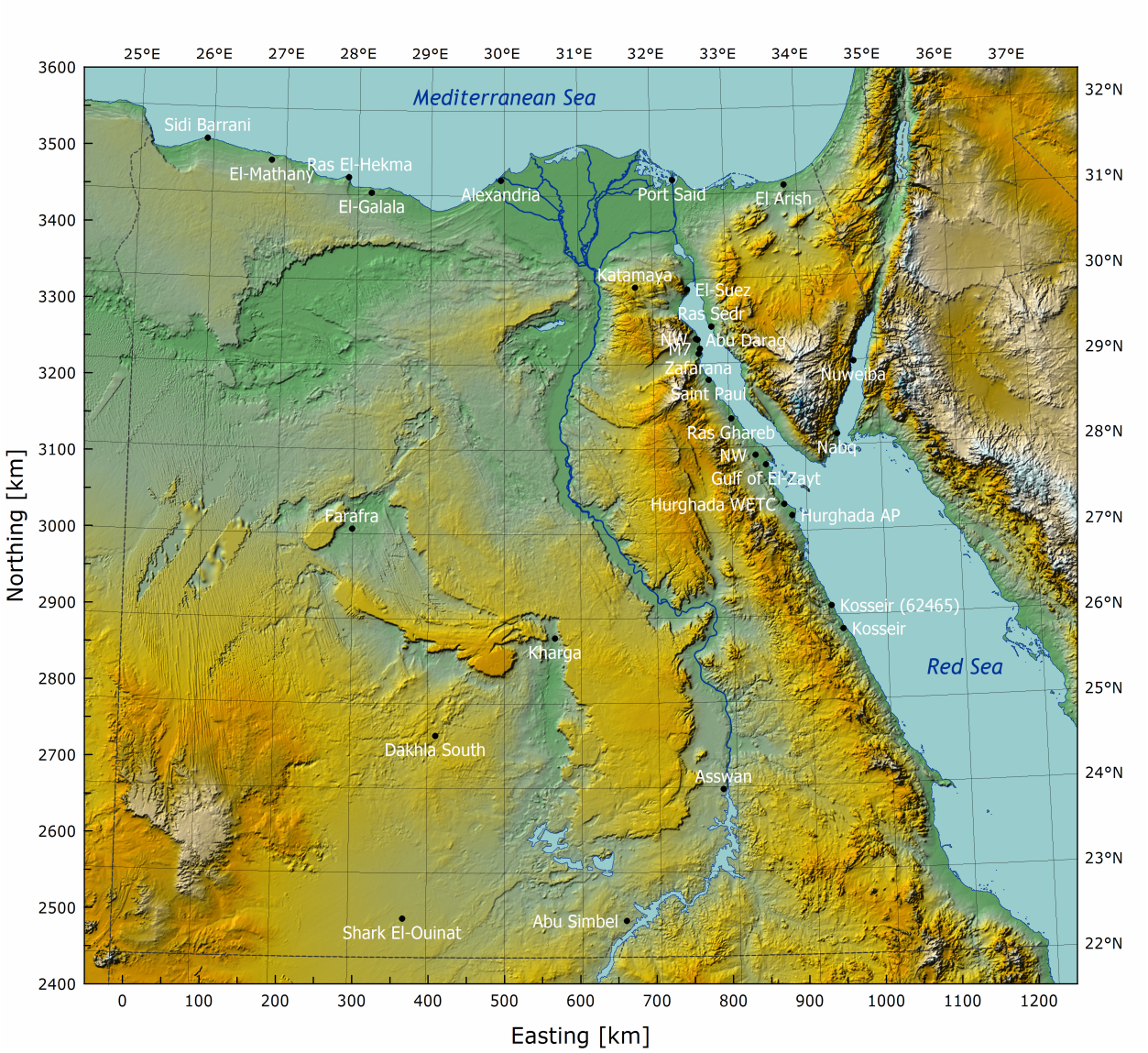

Figure 7-1. Elevation map of Egypt showing the meteorological stations used for the Wind Atlas. The geographic and Cartesian (UTM) coordinates are referenced to the World Geodetic System 1984 (WGS84).

Site and station selection

The 30 sites were selected to cover six regions in Egypt where previous investigations had indicated that the magnitude of the wind resource might be feasible for implementation of wind power systems. In each region, the wind atlas project has erected from one to eight 25-m lattice masts. In addition, a number of long-term EMA stations were selected, between one and three for each region. These stations can be identified in Table 7-1 and the tables below by the WMO identification number given in parentheses after the name of the station. Altogether, the project has operated 22 wind atlas stations and employed eight standard EMA stations. The met. stations are shown in the elevation map of Egypt given in Figure 7-1.

Sidi Barrani (62 301) Northwest Coast

31° 37′ 36.5″ N 25° 54′ 29.8″ E	UTM 35 E 396 462 m N 3 499 587 m	2 m

The Sidi Barrani mast is situated a few kilometers NW of the town of Sidi Barrani. The shortest distance to the coastline of the Mediterranean Sea is a few hundred meters in a northerly direction. The coastline is rocky and consists of a small cliff or escarpment. There are a few low sheltering obstacles (the met. station buildings) S and SE of the mast. The surface consists mostly of rocks and bare soil with a roughness length of about or less than 0.01 m.

Observed data from a nearby airport indicate that the mean wind speed in the 12-month period 2004-06 to 2005-05 is 98.6% of the mean value over the 10-year period 1995-2004.

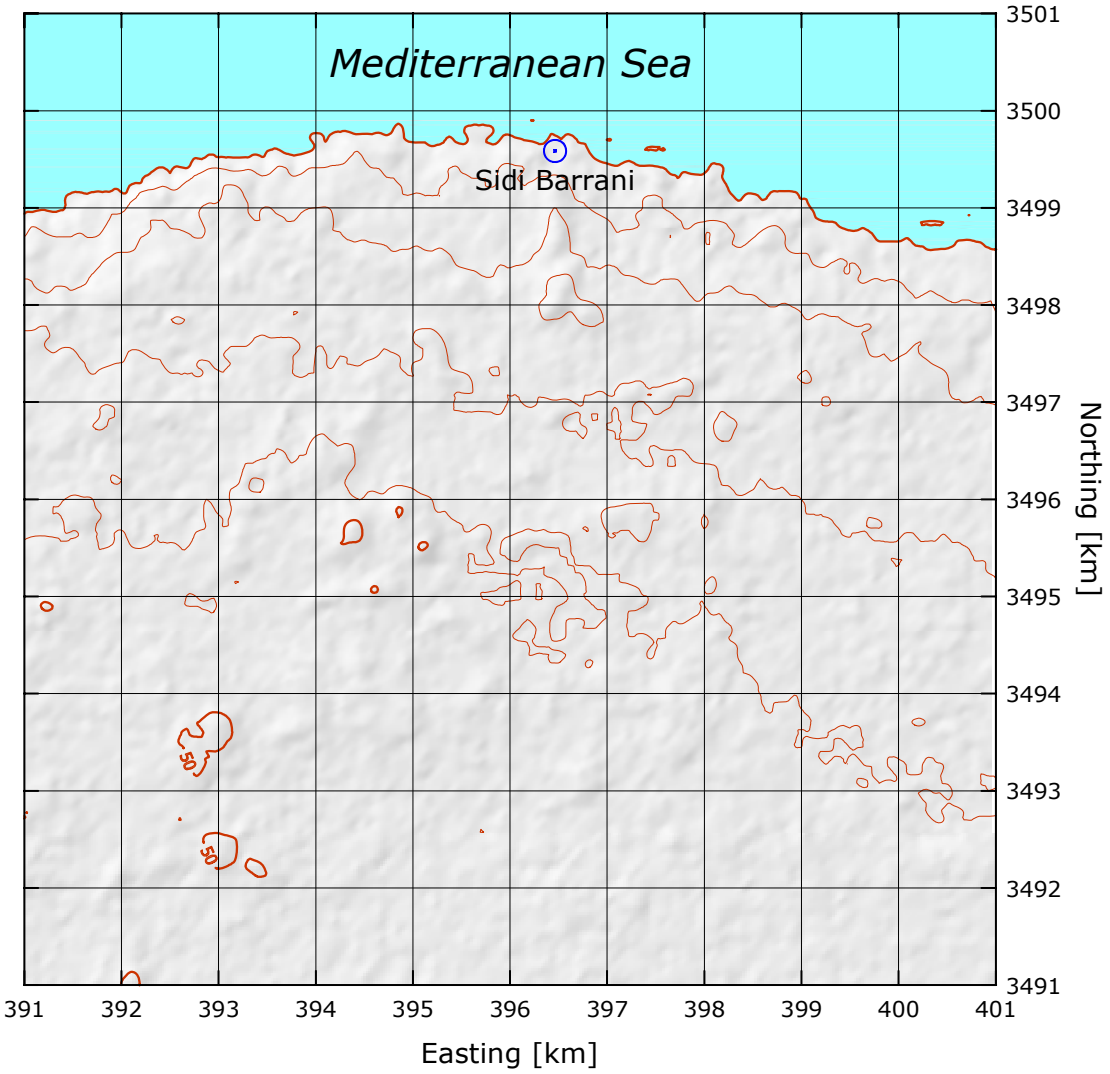

Sector	Input		Obstacles		Roughness		Orography		z_{0m}
0	0.0	0.0	0.0	0.0	0.0	0.0	−3.0	−0.4	0.0000
30	0.0	0.0	0.0	0.0	0.0	0.0	−3.2	0.2	0.0000
60	0.0	0.0	0.0	0.0	0.0	0.0	−2.5	0.5	0.0000
90	0.0	0.0	0.0	0.0	−1.2	0.0	−1.7	0.4	0.0000
120	0.0	0.0	−23.0	0.0	0.0	0.0	−1.4	−0.3	0.0050
150	0.0	0.0	−31.7	0.0	0.0	0.0	−2.5	−0.8	0.0050
180	0.0	0.0	0.0	0.0	0.0	0.0	−3.7	−0.5	0.0050
210	0.0	0.0	0.0	0.0	0.0	0.0	−4.0	0.3	0.0050
240	0.0	0.0	0.0	0.0	0.0	0.0	−2.9	0.8	0.0050
270	0.0	0.0	0.0	0.0	−5.9	0.0	−1.7	0.5	0.0000
300	0.0	0.0	0.0	0.0	0.0	0.0	−1.3	−0.2	0.0000
330	0.0	0.0	0.0	0.0	0.0	0.0	−2.0	−0.5	0.0000

Height of anemometer: 10.0 m a.g.l. 1995–2004

Sect	Freq	< 1	2	3	4	5	6	7	8	9	11	13	15	17	>17	*A*	*k*
0	13.4	34	41	83	133	178	187	133	89	53	44	18	5	1	1	6.0	2.29
30	9.0	43	38	105	170	208	173	102	72	40	34	11	3	0	0	5.5	2.17
60	6.1	34	29	65	127	164	164	134	109	67	72	24	9	2	0	6.4	2.22
90	4.6	27	22	59	101	117	142	163	99	103	102	44	19	1	1	7.2	2.38
120	3.0	39	27	61	97	132	156	131	96	88	124	32	8	6	3	7.0	2.22
150	2.5	81	36	93	119	123	117	111	124	64	66	36	17	8	3	6.5	1.94
180	3.4	29	29	59	114	108	113	102	149	85	113	55	26	12	8	7.7	2.19
210	5.1	23	25	53	120	112	131	134	107	85	111	49	29	16	4	7.4	2.02
240	5.4	23	16	61	96	96	124	139	103	113	134	45	28	15	8	7.8	2.13
270	6.6	26	23	41	81	102	129	128	108	88	136	80	25	20	14	8.0	2.03
300	15.7	17	16	41	73	118	129	157	143	109	119	50	16	10	3	7.7	2.47
330	25.1	20	20	49	95	137	162	168	126	95	84	27	10	4	4	7.1	2.41
Total	100.0	28	25	61	107	139	152	143	113	84	89	35	14	6	4	7.0	2.16

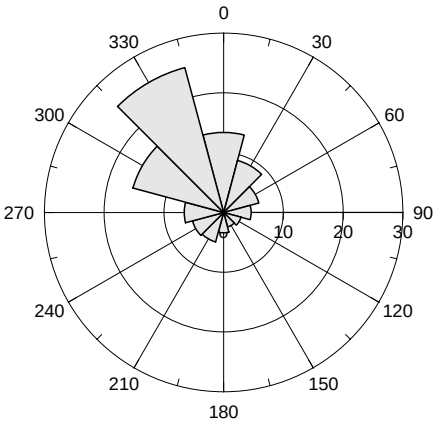

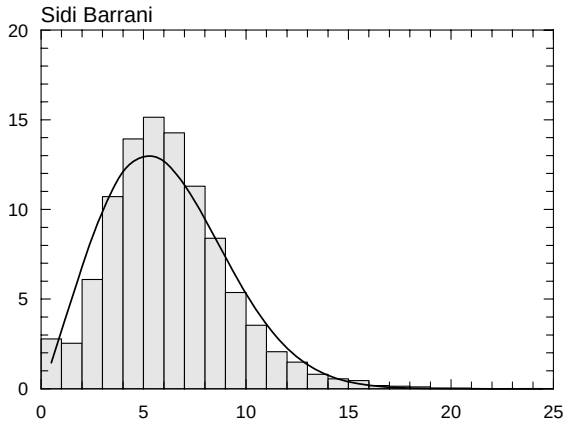

	Jan	Feb	Mar	Apr	May	Jun	Jul	Aug	Sep	Oct	Nov	Dec	Year
0	—	6.7	—	—	—	2.0	2.8	3.8	2.7	3.4	2.9	6.3	3.2
3	—	6.7	—	—	—	2.7	3.3	4.5	3.0	3.6	3.2	6.3	3.7
6	7.0	7.4	6.7	6.3	4.7	4.9	5.3	4.9	4.7	4.9	6.2	7.1	5.9
9	7.0	7.5	7.2	7.2	5.7	5.7	6.2	5.7	5.5	5.4	6.4	7.2	6.4
12	7.1	7.3	7.2	7.2	6.0	6.0	6.3	6.3	6.0	5.8	6.5	7.4	6.6
15	6.7	6.9	6.8	7.2	6.1	5.6	6.0	6.3	6.2	5.7	5.9	6.3	6.3
18	6.4	6.6	6.6	6.4	5.1	4.7	4.9	5.1	5.4	5.2	5.6	6.2	5.7
21	—	5.7	—	—	—	2.4	3.3	4.0	3.5	3.4	3.8	6.3	3.6
Mean	6.8	7.1	6.9	6.9	5.6	5.2	5.6	5.6	5.4	5.3	6.0	6.8	6.1

	Jan	Feb	Mar	Apr	May	Jun	Jul	Aug	Sep	Oct	Nov	Dec	Year
1995	7.1	6.5	6.0	6.5	5.0	4.6	4.6	5.0	6.5	5.3	7.0	7.5	6.0
1996	7.8	8.2	7.5	8.1	5.9	5.7	7.4	6.2	5.6	6.3	6.6	7.0	6.9
1997	6.6	7.7	7.9	7.8	5.9	6.5	6.9	6.3	5.8	6.2	6.3	7.6	6.8
1998	7.5	7.0	8.4	7.7	7.1	7.2	6.3	6.2	6.2	6.5	6.9	7.8	7.1
1999	7.1	7.4	7.4	6.7	5.6	7.0	6.8	5.9	5.1	6.0	6.7	6.9	6.5
2000	7.9	6.7	7.8	7.3	6.0	6.4	6.5	7.2	5.6	5.5	5.3	5.9	6.5
2001	4.6	6.5	4.3	5.2	4.2	3.0	4.3	3.8	5.1	4.3	5.8	7.4	4.9
2002	6.2	5.2	5.4	5.3	4.7	4.5	4.6	5.6	5.8	4.3	4.9	5.9	5.2
2003	6.1	9.4	8.3	8.1	4.4	—	—	—	—	—	—	6.9	7.5
2004	7.6	6.3	5.9	6.0	6.0	2.9	3.8	4.6	3.8	3.8	5.0	5.6	4.8
Mean	6.8	7.1	6.9	6.9	5.6	5.2	5.6	5.6	5.4	5.3	6.0	6.8	6.1

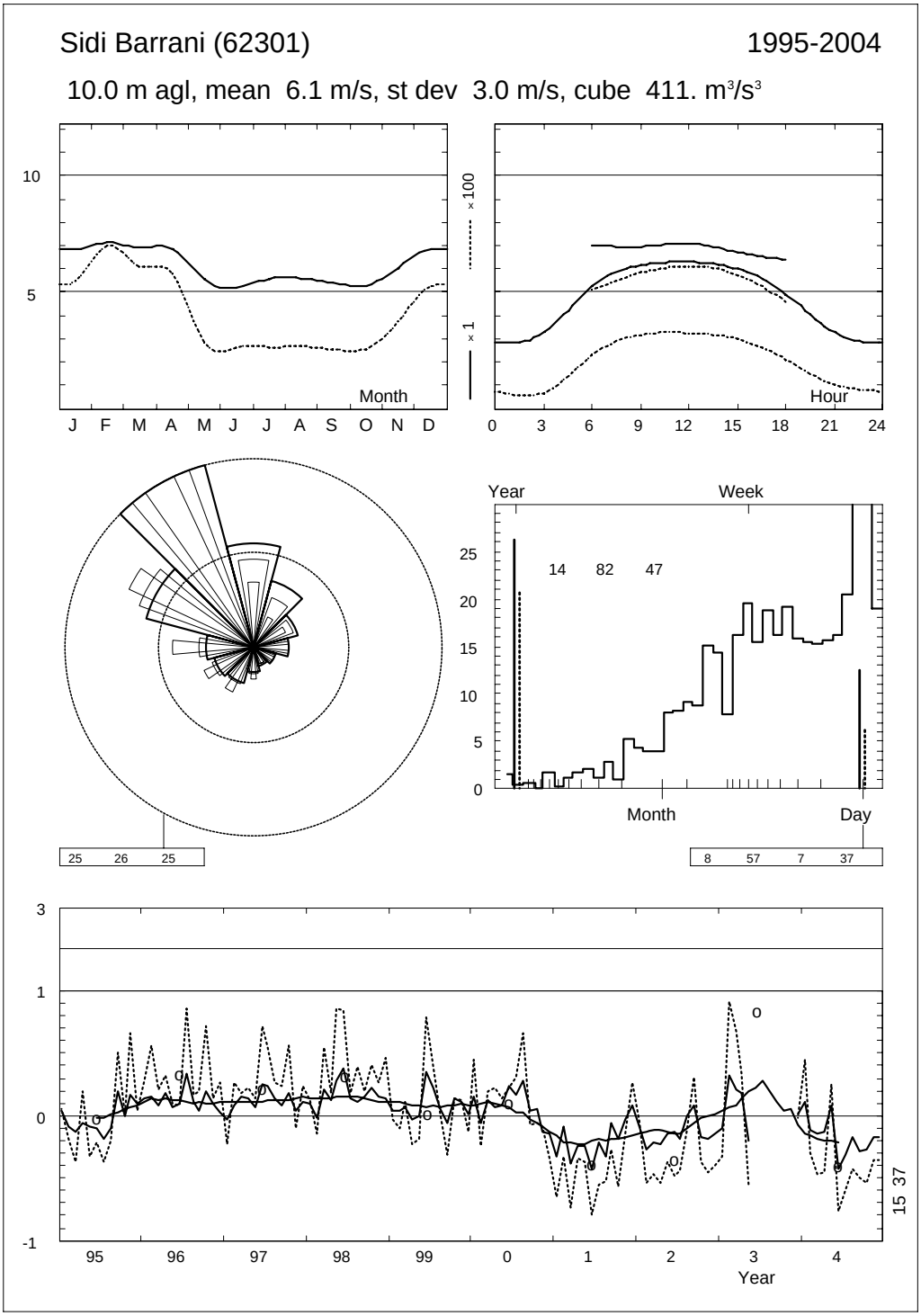
Sidi Barrani (62301)
1995-2004
10.0 m agl, mean 6.1 m/s, st dev 3.0 m/s, cube 411. m³/s³
10
5
Month
J F M A M J J A S O N D
× 100
× 1
Hour
0 3 6 9 12 15 18 21 24
Year
Week
14 82 47
25
20
15
10
5
0
Month
Day
25 26 25
8 57 7 37
3
1
0
-1
95 96 97 98 99 0 1 2 3 4
Year
15 37

Roughness Class 0 ($z_0 = 0.0002$ m)

z	0	30	60	90	120	150	180	210	240	270	300	330	Total
10	6.3	5.7	6.6	7.4	10.9	11.8	9.9	9.6	9.9	9.2	7.8	7.2	7.7
	2.26	2.17	2.19	2.33	2.41	2.10	2.41	2.32	2.45	2.15	2.43	2.39	2.04
25	6.9	6.3	7.2	8.1	11.9	12.9	10.9	10.4	10.8	10.0	8.6	7.9	8.5
	2.33	2.23	2.25	2.41	2.44	2.12	2.46	2.37	2.50	2.19	2.51	2.46	2.08
50	7.4	6.7	7.7	8.6	12.7	13.7	11.6	11.1	11.5	10.7	9.2	8.5	9.1
	2.39	2.29	2.31	2.47	2.50	2.15	2.53	2.43	2.57	2.25	2.58	2.53	2.13
100	8.1	7.3	8.3	9.4	13.6	14.6	12.4	12.0	12.4	11.5	10.0	9.2	9.8
	2.32	2.22	2.24	2.39	2.47	2.15	2.47	2.38	2.51	2.21	2.49	2.45	2.11
200	8.9	8.1	9.2	10.4	14.6	15.6	13.5	13.0	13.5	12.6	11.1	10.2	10.8
	2.19	2.10	2.12	2.26	2.40	2.11	2.39	2.29	2.42	2.12	2.36	2.32	2.05
Freq.	14.3	9.4	6.3	4.7	3.0	2.5	3.4	5.1	5.4	6.5	15.0	24.4	100.0

Roughness Class 1 ($z_0 = 0.0300$ m)

z	0	30	60	90	120	150	180	210	240	270	300	330	Total
10	4.3	4.0	4.7	5.4	8.0	8.1	6.9	6.7	6.9	6.1	5.3	4.9	5.4
	1.89	1.79	1.89	1.81	2.17	1.88	2.13	2.04	2.13	1.86	2.04	1.98	1.78
25	5.2	4.8	5.6	6.4	9.4	9.5	8.1	8.0	8.2	7.2	6.3	5.9	6.4
	2.04	1.94	2.04	1.96	2.24	1.93	2.25	2.15	2.24	1.98	2.20	2.14	1.90
50	6.0	5.6	6.5	7.4	10.6	10.6	9.2	9.1	9.3	8.3	7.3	6.8	7.4
	2.30	2.18	2.30	2.20	2.35	2.00	2.44	2.32	2.42	2.18	2.47	2.40	2.07
100	7.1	6.7	7.7	8.8	11.9	11.9	10.6	10.4	10.7	9.7	8.7	8.1	8.7
	2.45	2.32	2.45	2.34	2.53	2.14	2.62	2.49	2.60	2.34	2.63	2.56	2.24
200	8.8	8.3	9.6	11.0	13.8	13.5	12.7	12.5	12.8	11.8	10.8	10.1	10.6
	2.34	2.22	2.34	2.24	2.46	2.09	2.52	2.40	2.51	2.24	2.52	2.45	2.22
Freq.	12.9	8.5	5.8	4.2	2.9	2.7	3.7	5.3	5.7	8.2	17.2	22.9	100.0

Roughness Class 2 ($z_0 = 0.1000$ m)

z	0	30	60	90	120	150	180	210	240	270	300	330	Total
10	3.7	3.6	4.1	4.8	7.0	6.9	5.9	5.9	6.0	5.2	4.6	4.3	4.7
	1.88	1.83	1.87	1.78	2.15	1.88	2.10	2.09	2.15	1.87	2.05	1.98	1.79
25	4.6	4.4	5.1	5.9	8.5	8.3	7.2	7.2	7.3	6.4	5.7	5.3	5.8
	2.01	1.96	2.00	1.91	2.22	1.92	2.20	2.19	2.25	1.99	2.20	2.12	1.89
50	5.4	5.2	5.9	6.9	9.7	9.5	8.4	8.3	8.5	7.4	6.6	6.2	6.7
	2.22	2.17	2.21	2.11	2.31	1.99	2.36	2.34	2.41	2.17	2.43	2.35	2.05
100	6.4	6.2	7.1	8.3	11.1	10.8	9.7	9.7	9.9	8.8	7.9	7.4	8.0
	2.44	2.38	2.43	2.32	2.51	2.12	2.59	2.57	2.64	2.38	2.67	2.58	2.25
200	7.9	7.6	8.7	10.2	12.8	12.4	11.6	11.6	11.7	10.7	9.7	9.1	9.7
	2.34	2.28	2.33	2.22	2.45	2.10	2.50	2.48	2.55	2.29	2.56	2.47	2.23
Freq.	12.5	8.3	5.7	4.0	2.8	2.8	3.9	5.3	5.8	8.9	18.1	22.0	100.0

Roughness Class 3 ($z_0 = 0.4000$ m)

z	0	30	60	90	120	150	180	210	240	270	300	330	Total
10	2.9	2.8	3.3	3.9	5.5	5.2	4.6	4.7	4.7	4.0	3.6	3.3	3.7
	1.83	1.79	1.92	1.75	2.13	1.87	2.10	2.10	2.13	1.90	2.04	1.98	1.80
25	3.8	3.8	4.3	5.1	7.2	6.8	6.0	6.1	6.1	5.2	4.7	4.4	4.8
	1.94	1.90	2.03	1.84	2.19	1.91	2.19	2.19	2.21	2.02	2.16	2.10	1.88
50	4.6	4.5	5.2	6.2	8.5	8.0	7.2	7.2	7.3	6.3	5.7	5.3	5.8
	2.11	2.06	2.21	1.99	2.26	1.97	2.32	2.31	2.35	2.19	2.35	2.28	2.01
100	5.6	5.5	6.3	7.4	9.9	9.4	8.5	8.6	8.6	7.6	6.8	6.4	7.0
	2.40	2.35	2.51	2.26	2.40	2.08	2.56	2.55	2.59	2.49	2.67	2.60	2.24
200	6.8	6.7	7.7	9.0	11.5	10.9	10.2	10.2	10.3	9.3	8.3	7.8	8.5
	2.31	2.26	2.42	2.18	2.44	2.12	2.53	2.53	2.56	2.40	2.58	2.50	2.23
Freq.	11.9	7.9	5.5	3.8	2.8	2.9	4.1	5.3	5.9	10.0	19.2	20.7	100.0

z	Class 0		Class 1		Class 2		Class 3	
m	ms^{-1}	Wm^{-2}	ms^{-1}	Wm^{-2}	ms^{-1}	Wm^{-2}	ms^{-1}	Wm^{-2}
10	6.8	369	4.8	145	4.2	95	3.3	46
25	7.5	472	5.7	228	5.1	166	4.3	98
50	8.0	569	6.5	316	6.0	243	5.2	160
100	8.7	726	7.7	479	7.1	370	6.2	250
200	9.5	986	9.4	886	8.6	672	7.5	444

El-Mathany — Northwest Coast

31° 33′ 25.9″ N 26° 48′ 02.5″ E	UTM 35 E 481 051 m N 3 472 901 m	114 m

The El-Mathany mast is situated in one of five NREA sites established in connection with a Dutch wind/diesel project. The shortest distance to the coastline of the Mediterranean Sea is about 7 km in a NNE direction. The site is located in an agricultural area, SE of a small village. Where the surface is not used for farming it consists of low scrub vegetation on a stony and sandy surface. The site and the surroundings are very flat with significant roughness areas occurring to the S, SW, W and NW.

Observed data from the airports in Sidi Barrani and Alexandria indicate that the mean wind speeds in the 12-month period 2004-06 to 2005-05 are approx. 99% of the mean values over the 10-year period 1995-2004. The data recovery rate at El-Mathany is 99.5%.

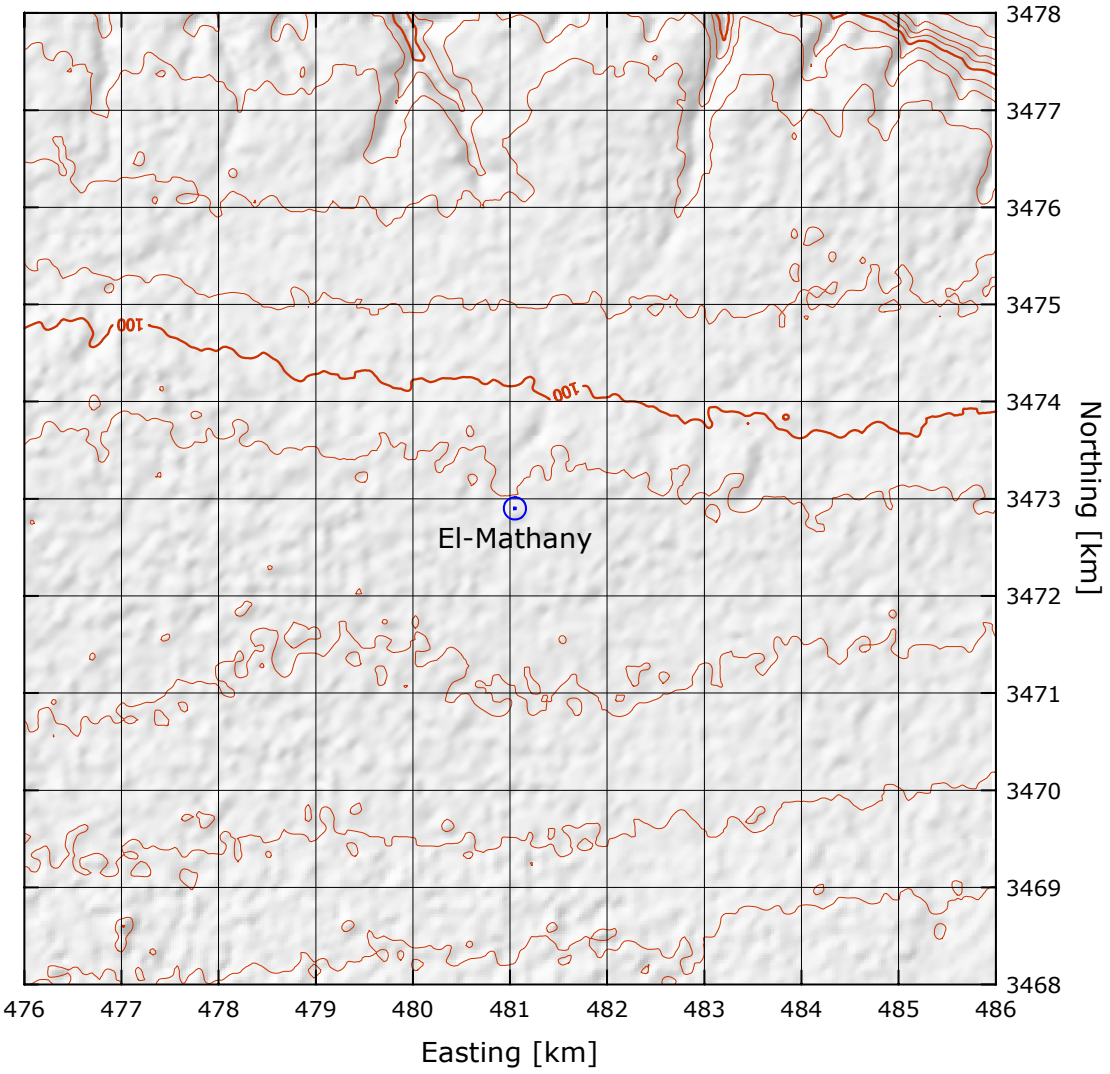

Sector	Input		Obstacles		Roughness		Orography		z_{0m}
0	0.0	0.0	0.0	0.0	−10.8	0.0	3.1	0.2	0.0020
30	0.0	0.0	0.0	0.0	−10.7	0.0	2.8	−0.5	0.0020
60	0.0	0.0	0.0	0.0	−6.9	0.0	1.7	−0.6	0.0100
90	0.0	0.0	0.0	0.0	−3.7	0.0	0.9	−0.2	0.0240
120	0.0	0.0	0.0	0.0	0.0	0.0	1.2	0.5	0.0500
150	0.0	0.0	0.0	0.0	0.0	0.0	2.4	0.7	0.0500
180	0.0	0.0	0.0	0.0	0.0	0.0	3.3	0.2	0.0500
210	0.0	0.0	0.0	0.0	0.0	0.0	3.0	−0.5	0.0500
240	0.0	0.0	0.0	0.0	0.0	0.0	1.8	−0.7	0.0500
270	0.0	0.0	0.0	0.0	0.0	0.0	0.9	−0.2	0.0500
300	0.0	0.0	0.0	0.0	−1.9	0.0	1.2	0.5	0.0340
330	0.0	0.0	0.0	0.0	−8.9	0.0	2.4	0.6	0.0050

Height of anemometer: 24.5 m a.g.l. 2004-05

Sect	Freq	<1	2	3	4	5	6	7	8	9	11	13	15	17	>17	*A*	*k*
0	8.5	21	54	73	142	270	237	128	56	16	3	1	0	0	0	5.3	3.42
30	6.1	46	111	106	162	194	175	118	50	19	17	2	0	0	0	5.1	2.57
60	3.8	14	66	102	171	170	131	127	117	54	29	19	0	0	0	5.7	2.27
90	3.1	8	54	97	127	161	145	168	73	56	92	18	1	0	0	6.3	2.40
120	4.2	15	40	82	78	137	166	157	160	94	55	10	4	2	0	6.7	2.92
150	5.4	5	35	49	47	64	95	124	142	127	158	101	36	6	10	8.7	2.57
180	4.9	3	32	59	83	92	100	119	131	118	141	68	46	7	0	8.2	2.54
210	5.5	7	42	76	90	96	87	167	159	119	105	31	10	10	2	7.6	2.79
240	13.2	4	27	63	106	176	208	169	85	54	73	26	6	2	0	6.4	2.30
270	11.4	7	41	110	171	220	157	106	55	30	60	32	8	1	0	5.6	1.79
300	19.5	3	22	54	96	147	152	181	159	101	69	14	2	0	0	6.9	3.23
330	14.3	12	28	50	105	191	242	176	97	48	43	7	1	0	0	6.2	2.99
Total	100.0	10	40	71	115	170	172	151	107	67	65	23	7	2	1	6.4	2.33

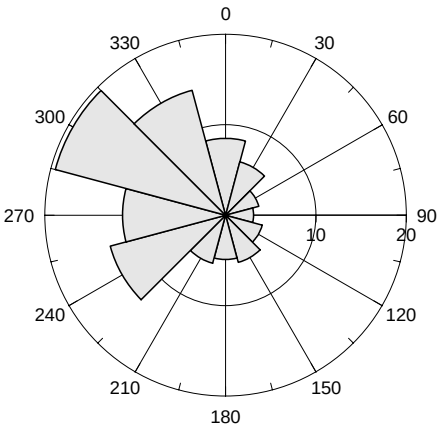

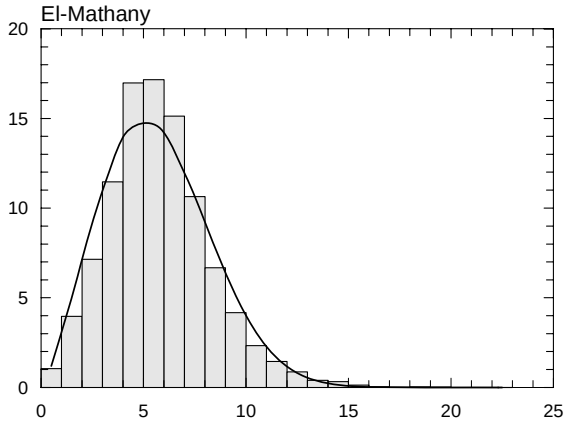

	Jan	Feb	Mar	Apr	May	Jun	Jul	Aug	Sep	Oct	Nov	Dec	Year
0	7.1	6.4	5.3	5.4	4.6	4.7	4.6	4.2	3.9	3.9	6.0	5.3	5.1
1	7.2	6.5	5.7	5.0	4.5	4.6	4.8	4.2	4.5	4.0	6.2	5.0	5.2
2	7.4	6.3	6.0	5.2	4.7	5.1	4.8	4.2	4.5	4.1	6.4	5.2	5.3
3	7.6	6.1	6.2	5.6	4.8	5.3	5.0	4.3	4.7	4.2	6.1	5.0	5.4
4	7.4	6.3	6.1	5.4	4.9	5.2	4.9	4.4	4.8	4.4	6.0	4.8	5.4
5	7.4	6.3	6.2	5.9	4.9	5.0	4.9	4.5	5.1	4.5	6.1	5.4	5.5
6	7.6	6.0	6.3	5.5	4.8	4.9	4.7	4.3	5.1	4.8	6.1	5.5	5.5
7	7.9	6.3	6.2	4.9	4.3	4.7	4.4	4.2	4.7	4.6	6.2	5.6	5.3
8	7.7	6.2	5.6	5.5	4.9	5.3	4.7	4.8	4.6	4.2	6.2	5.5	5.4
9	7.7	6.5	6.6	5.8	5.0	5.0	4.8	5.2	5.0	4.5	6.6	5.4	5.7
10	7.5	7.2	6.8	6.5	5.0	5.3	4.7	5.3	5.3	4.7	7.0	5.8	5.9
11	8.0	7.8	6.4	6.6	5.4	5.7	5.3	5.6	5.4	4.9	6.9	6.0	6.2
12	8.4	8.1	6.2	7.0	5.7	6.2	5.9	6.3	5.8	5.4	7.4	6.3	6.6
13	8.6	7.9	6.5	7.3	6.3	6.2	6.1	6.8	6.2	5.7	7.5	6.3	6.8
14	8.4	7.8	6.5	7.2	6.9	6.7	6.5	7.2	6.6	6.1	7.5	6.3	7.0
15	8.5	7.9	6.7	7.3	6.8	6.8	6.6	7.4	6.6	6.0	7.4	6.0	7.0
16	8.1	7.6	6.6	7.1	7.0	6.7	6.6	7.4	6.8	5.9	7.4	5.7	6.9
17	6.9	6.8	6.3	7.2	6.5	6.6	6.5	7.2	6.4	5.3	6.6	5.4	6.5
18	6.6	5.8	6.0	6.8	6.3	6.1	6.2	6.7	6.0	4.7	5.7	4.9	6.0
19	6.3	5.9	5.0	5.9	5.7	5.7	5.6	6.0	5.2	4.4	5.5	4.8	5.5
20	6.6	5.8	4.8	5.5	4.8	4.9	4.8	5.3	4.8	4.2	5.5	5.1	5.2
21	6.4	5.8	4.6	5.3	4.5	4.5	4.2	4.7	4.4	3.9	5.2	5.4	4.9
22	6.6	5.9	4.9	4.7	4.5	4.5	4.2	4.4	3.9	3.9	5.7	5.3	4.9
23	6.9	6.2	5.0	5.0	4.5	4.4	4.3	4.1	3.9	3.8	5.7	5.5	4.9
Mean	7.4	6.6	5.9	6.0	5.3	5.4	5.2	5.4	5.2	4.7	6.4	5.5	5.7

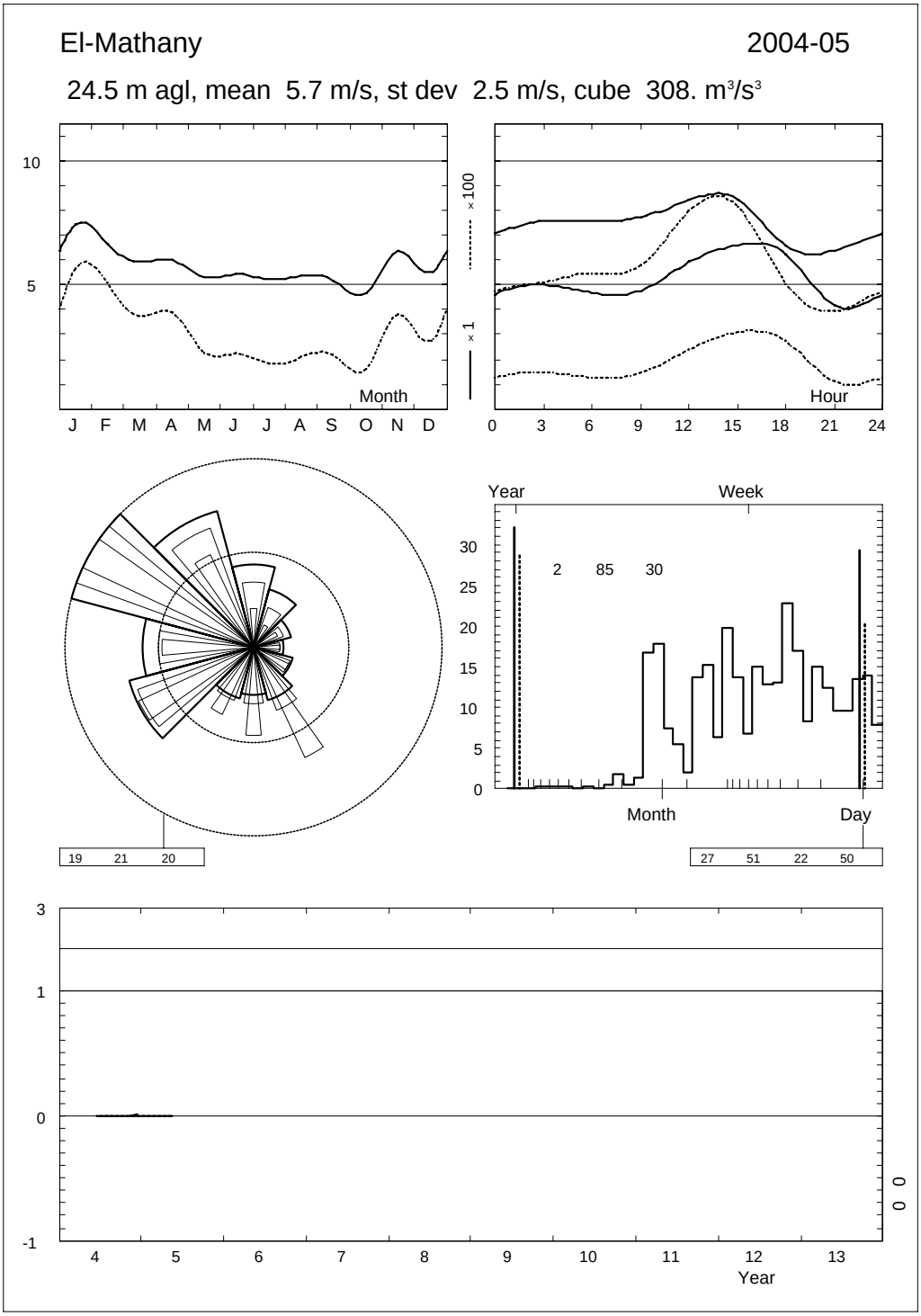

	Jan	Feb	Mar	Apr	May	Jun	Jul	Aug	Sep	Oct	Nov	Dec	Year
2004	—	—	—	—	—	5.4	5.2	5.4	5.2	4.7	6.4	5.5	5.4
2005	7.4	6.6	5.9	6.0	5.3	—	—	—	—	—	—	—	6.3
Mean	7.4	6.6	5.9	6.0	5.3	5.4	5.2	5.4	5.2	4.7	6.4	5.5	5.7

Roughness Class 0 ($z_0 = 0.0002$ m)

z	0	30	60	90	120	150	180	210	240	270	300	330	Total
10	6.2	5.7	6.4	7.4	8.3	10.3	10.1	9.4	8.1	7.3	8.3	7.4	7.8
	3.15	2.80	2.47	2.58	3.06	2.72	2.77	2.94	2.55	2.14	3.24	3.10	2.51
25	6.8	6.2	7.0	8.1	9.1	11.3	11.1	10.3	8.9	8.0	9.1	8.1	8.6
	3.26	2.89	2.55	2.66	3.16	2.78	2.83	3.02	2.63	2.21	3.35	3.20	2.57
50	7.3	6.7	7.5	8.7	9.7	12.0	11.8	11.0	9.5	8.6	9.8	8.7	9.2
	3.34	2.96	2.62	2.73	3.25	2.85	2.91	3.10	2.71	2.26	3.43	3.28	2.63
100	7.9	7.2	8.2	9.5	10.6	12.9	12.8	12.0	10.3	9.4	10.6	9.4	10.0
	3.24	2.87	2.54	2.65	3.14	2.79	2.84	3.01	2.62	2.19	3.32	3.18	2.57
200	8.8	8.0	9.1	10.5	11.7	14.1	13.9	13.2	11.4	10.3	11.7	10.5	11.0
	3.06	2.72	2.40	2.50	2.97	2.69	2.73	2.86	2.48	2.08	3.15	3.01	2.47
Freq.	9.6	6.5	4.3	3.3	4.0	5.2	4.9	5.3	11.5	12.0	18.0	15.3	100.0

Roughness Class 1 ($z_0 = 0.0300$ m)

z	0	30	60	90	120	150	180	210	240	270	300	330	Total
10	4.1	3.9	4.7	5.3	5.9	7.5	7.0	6.4	5.6	5.0	5.9	4.9	5.5
	2.81	2.12	2.11	2.21	2.63	2.44	2.38	2.47	2.16	1.74	2.89	2.65	2.16
25	4.9	4.7	5.7	6.4	7.0	8.9	8.3	7.6	6.6	5.9	7.0	5.9	6.5
	3.04	2.29	2.28	2.39	2.84	2.55	2.52	2.67	2.33	1.88	3.12	2.86	2.31
50	5.7	5.4	6.5	7.4	8.1	10.1	9.4	8.8	7.7	6.9	8.1	6.8	7.5
	3.41	2.58	2.56	2.69	3.20	2.74	2.75	3.00	2.62	2.11	3.51	3.22	2.55
100	6.7	6.4	7.7	8.7	9.6	11.5	10.9	10.4	9.1	8.2	9.5	8.1	8.9
	3.63	2.74	2.72	2.86	3.40	2.95	2.95	3.19	2.79	2.25	3.74	3.43	2.72
200	8.4	7.9	9.6	10.9	11.9	13.7	13.2	13.0	11.3	10.2	11.9	10.0	11.0
	3.47	2.62	2.60	2.73	3.25	2.85	2.84	3.05	2.66	2.15	3.57	3.27	2.65
Freq.	8.3	6.0	3.8	3.2	4.3	5.4	4.8	5.6	13.1	11.9	19.6	14.1	100.0

Roughness Class 2 ($z_0 = 0.1000$ m)

z	0	30	60	90	120	150	180	210	240	270	300	330	Total
10	3.6	3.4	4.2	4.7	5.2	6.5	6.0	5.4	4.8	4.4	5.1	4.3	4.8
	2.88	2.15	2.11	2.22	2.51	2.43	2.37	2.38	2.14	1.83	2.81	2.67	2.17
25	4.4	4.2	5.1	5.8	6.5	7.9	7.4	6.7	5.9	5.5	6.2	5.3	5.9
	3.08	2.29	2.26	2.38	2.69	2.53	2.49	2.56	2.29	1.96	3.01	2.86	2.30
50	5.2	5.0	6.0	6.8	7.6	9.1	8.5	7.8	6.9	6.4	7.3	6.2	6.8
	3.41	2.54	2.50	2.63	2.98	2.70	2.70	2.83	2.54	2.17	3.33	3.17	2.51
100	6.1	5.9	7.1	8.0	9.0	10.6	10.0	9.3	8.3	7.7	8.6	7.3	8.1
	3.74	2.79	2.75	2.90	3.27	2.96	2.97	3.11	2.79	2.38	3.66	3.48	2.74
200	7.6	7.3	8.8	9.9	11.1	12.6	12.1	11.4	10.2	9.4	10.6	9.1	10.0
	3.58	2.67	2.63	2.77	3.13	2.87	2.86	2.97	2.67	2.28	3.51	3.33	2.67
Freq.	8.1	5.8	3.7	3.3	4.4	5.3	4.9	6.3	13.0	12.5	19.2	13.6	100.0

Roughness Class 3 ($z_0 = 0.4000$ m)

z	0	30	60	90	120	150	180	210	240	270	300	330	Total
10	2.8	2.7	3.3	3.7	4.3	5.1	4.7	4.1	3.8	3.6	3.9	3.3	3.7
	2.60	2.06	2.09	2.29	2.41	2.45	2.39	2.27	2.13	2.02	2.76	2.75	2.18
25	3.7	3.6	4.3	4.9	5.6	6.6	6.1	5.4	4.9	4.8	5.1	4.4	4.9
	2.76	2.19	2.22	2.42	2.55	2.54	2.51	2.41	2.26	2.14	2.93	2.92	2.29
50	4.4	4.3	5.2	5.9	6.7	7.9	7.3	6.5	5.9	5.8	6.2	5.3	5.9
	2.99	2.37	2.41	2.63	2.78	2.69	2.69	2.62	2.45	2.33	3.18	3.17	2.47
100	5.3	5.2	6.3	7.1	8.1	9.3	8.7	7.8	7.2	6.9	7.4	6.3	7.1
	3.41	2.71	2.74	3.00	3.16	2.95	3.02	2.98	2.79	2.65	3.62	3.61	2.76
200	6.5	6.4	7.7	8.7	9.9	11.1	10.5	9.6	8.8	8.5	9.1	7.8	8.7
	3.29	2.61	2.64	2.89	3.04	2.93	2.94	2.87	2.69	2.55	3.49	3.47	2.71
Freq.	7.8	5.5	3.7	3.4	4.5	5.3	5.0	7.2	12.8	13.4	18.6	12.9	100.0

z	Class 0		Class 1		Class 2		Class 3	
m	ms^{-1}	Wm^{-2}	ms^{-1}	Wm^{-2}	ms^{-1}	Wm^{-2}	ms^{-1}	Wm^{-2}
10	7.0	325	4.8	123	4.2	81	3.3	39
25	7.6	419	5.8	198	5.2	144	4.3	85
50	8.2	510	6.7	282	6.1	216	5.2	141
100	8.9	658	7.9	448	7.2	342	6.3	228
200	9.8	907	9.8	863	8.9	645	7.7	418

Ras El-Hekma — Northwest Coast

31° 12′ 21.4″ N 27° 52′ 00.3″ E	UTM 35 E 582 568 m N 3 452 750 m	23 m

The Ras El-Hekma mast is situated in one of five NREA sites established in connection with a Dutch wind/diesel project. The shortest distance to the coastline of the Mediterranean Sea is a few hundred metres in an easterly direction. The site is located on a fairly steep hill along the eastern coastline of the Ras El-Hekma peninsula. The surrounding terrain is fairly complicated with respect to roughness and elevation.

Observed data from the airports in Sidi Barrani and Alexandria indicate that the mean wind speeds in the 12-month period 2004-06 to 2005-05 are approx. 99% of the mean values over the 10-year period 1995-2004. The data recovery rate at Ras El-Hekma is 99.8%.

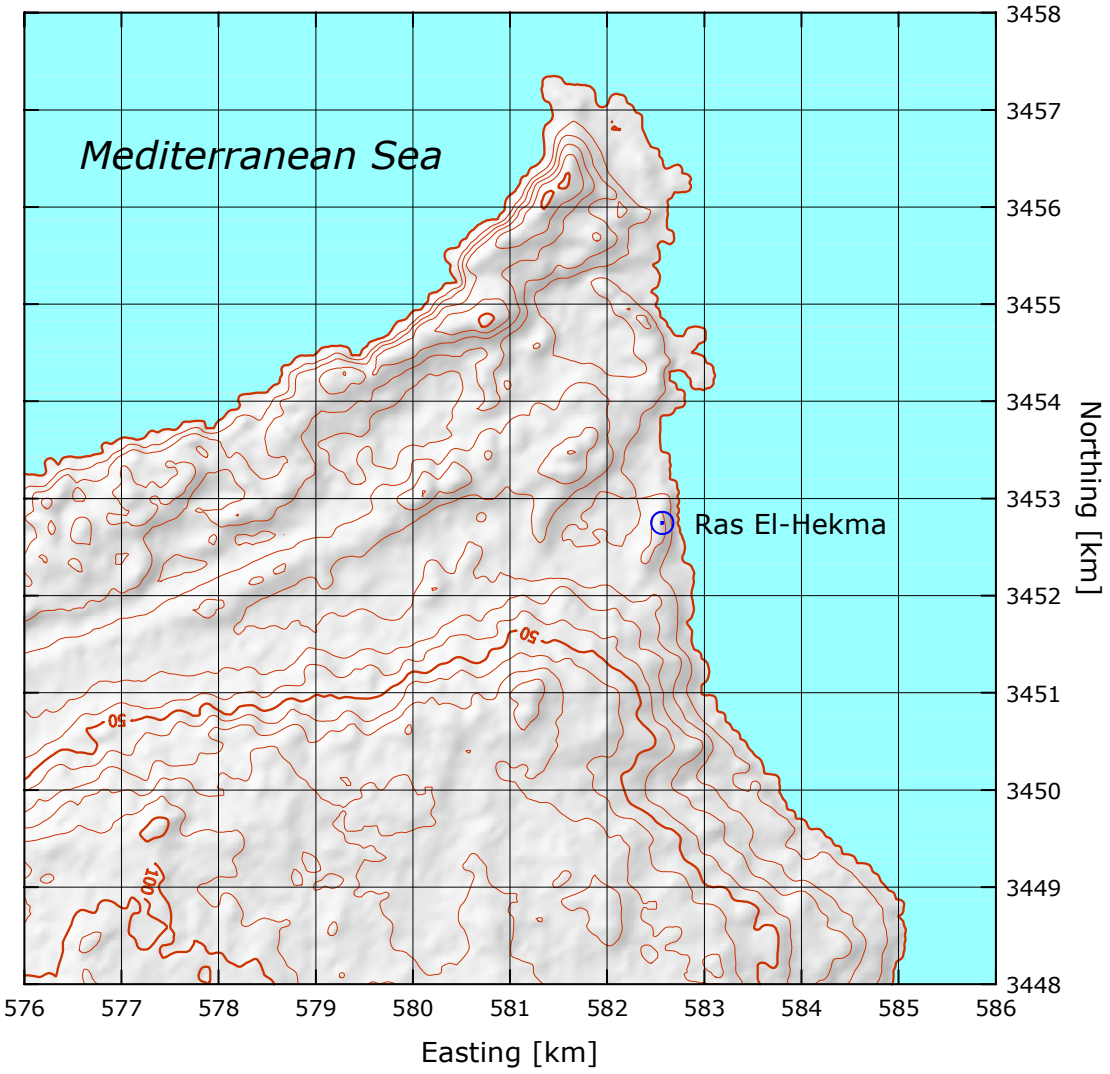

Sector	Input		Obstacles		Roughness		Orography		z_{0m}
0	0.0	0.0	0.0	0.0	−6.4	0.0	1.7	−1.2	0.0010
30	0.0	0.0	0.0	0.0	0.0	0.0	3.3	2.6	0.0000
60	0.0	0.0	0.0	0.0	0.0	0.0	9.5	3.4	0.0000
90	0.0	0.0	0.0	0.0	0.0	0.0	14.0	0.9	0.0000
120	0.0	0.0	0.0	0.0	0.0	0.0	12.8	−2.3	0.0000
150	0.0	0.0	0.0	0.0	1.7	0.0	7.0	−3.7	0.0010
180	0.0	0.0	0.0	0.0	0.0	0.0	1.3	−1.4	0.0300
210	0.0	0.0	0.0	0.0	0.0	0.0	2.8	2.8	0.0300
240	0.0	0.0	0.0	0.0	0.0	0.0	10.2	3.9	0.0300
270	0.0	0.0	0.0	0.0	−9.4	0.0	15.9	1.2	0.0030
300	0.0	0.0	0.0	0.0	−11.0	0.0	14.8	−2.6	0.0010
330	0.0	0.0	0.0	0.0	−11.6	0.0	7.7	−3.9	0.0010

Height of anemometer: 24.5 m a.g.l. 2004-05

Sect	Freq	< 1	2	3	4	5	6	7	8	9	11	13	15	17	>17	*A*	*k*
0	10.9	6	29	81	173	249	225	130	60	23	20	3	1	0	0	5.5	2.85
30	6.3	18	41	124	194	157	135	135	110	64	20	3	0	0	0	5.6	2.46
60	3.6	1	55	118	165	133	126	151	101	89	51	8	1	0	0	6.1	2.53
90	4.1	10	51	95	127	126	120	129	90	69	108	45	23	7	0	6.9	2.02
120	3.4	9	53	84	125	165	132	108	85	93	97	34	7	7	0	6.5	2.01
150	4.9	2	24	38	85	105	156	224	152	109	80	12	6	6	0	7.2	3.08
180	2.3	9	32	51	49	81	91	116	67	81	170	89	105	56	5	9.5	2.31
210	2.6	1	37	56	83	60	32	52	50	56	153	198	130	80	12	11.0	3.13
240	7.2	5	20	43	59	78	132	127	124	109	166	92	39	3	3	8.4	2.59
270	9.4	4	20	51	78	104	107	129	115	110	151	66	39	22	4	8.3	2.29
300	19.5	1	11	22	40	104	167	157	165	147	137	33	10	4	2	7.9	3.08
330	25.8	3	13	33	76	171	193	167	119	73	95	46	9	1	0	7.0	2.34
Total	100.0	5	23	53	93	141	159	147	117	90	102	43	18	8	1	7.2	2.23

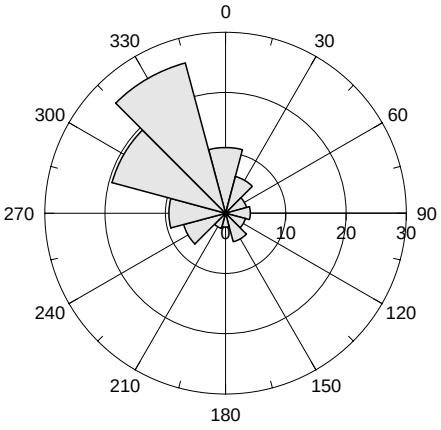

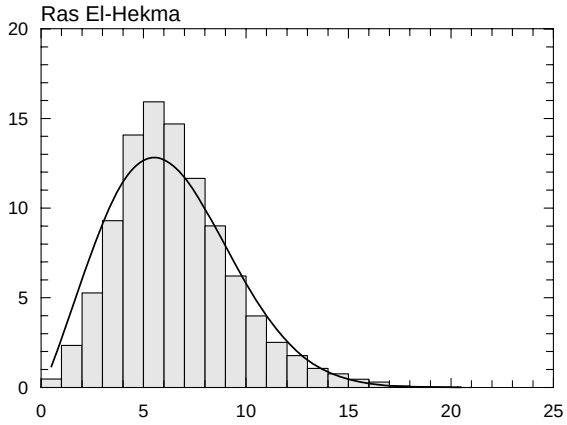

	Jan	Feb	Mar	Apr	May	Jun	Jul	Aug	Sep	Oct	Nov	Dec	Year
0	8.8	6.8	5.9	6.1	5.3	5.3	5.3	5.3	5.3	4.4	6.9	6.4	6.0
1	9.1	6.9	6.5	6.4	5.5	5.7	5.5	5.4	5.4	4.4	7.2	6.4	6.2
2	8.8	7.1	6.6	6.4	5.5	5.5	5.6	5.6	5.4	4.6	7.4	6.4	6.2
3	9.0	7.6	6.7	6.4	5.6	5.6	6.0	5.7	5.5	5.0	7.7	6.3	6.4
4	9.6	7.7	6.7	6.9	5.7	5.9	6.2	5.6	5.3	5.1	7.5	6.5	6.5
5	9.5	7.9	6.4	6.6	5.7	6.2	6.4	5.8	5.2	4.8	7.4	6.5	6.5
6	9.2	8.1	6.7	6.4	5.5	6.1	6.0	5.9	5.3	5.0	7.7	6.9	6.6
7	9.6	7.9	7.0	6.6	5.5	5.9	6.0	5.5	5.0	5.3	7.5	6.7	6.5
8	9.1	7.6	6.9	6.3	5.5	6.4	6.3	6.0	4.9	5.2	7.2	6.9	6.5
9	9.2	7.1	7.1	6.3	5.6	6.6	6.2	6.3	5.2	5.1	6.9	6.6	6.5
10	8.8	7.8	7.2	6.7	5.8	6.5	6.5	6.4	5.2	5.1	6.8	6.6	6.6
11	9.1	7.7	7.0	7.1	6.1	6.6	6.4	6.6	5.4	4.9	7.2	6.5	6.7
12	9.1	8.0	7.0	7.4	6.3	6.8	6.6	6.6	6.0	5.2	7.0	6.7	6.9
13	9.1	7.8	7.1	7.6	6.8	6.8	6.6	7.0	6.4	5.5	7.2	6.3	7.0
14	9.7	7.8	7.1	7.8	6.8	6.8	7.0	7.4	6.6	5.7	7.5	6.6	7.2
15	8.9	8.0	7.3	7.8	6.7	6.9	6.9	7.6	7.2	5.7	7.2	6.6	7.2
16	8.5	7.9	7.1	7.8	6.7	6.6	7.1	7.4	7.2	5.6	7.2	6.6	7.1
17	8.0	7.5	6.9	7.4	6.4	6.5	6.9	7.3	6.6	5.4	7.5	6.5	6.9
18	7.4	6.4	6.7	7.0	6.0	6.2	6.3	6.8	6.3	5.3	7.4	6.6	6.5
19	7.0	6.2	6.2	6.6	5.6	5.9	5.6	6.3	6.0	5.1	7.3	6.4	6.2
20	7.7	6.4	6.4	6.2	5.3	5.5	5.3	5.9	5.5	4.9	7.4	6.2	6.1
21	7.6	6.5	5.8	6.5	5.3	5.4	5.3	5.5	5.4	4.9	7.1	6.2	5.9
22	8.3	6.7	5.7	6.5	5.3	5.4	5.4	5.4	5.2	4.5	6.9	6.1	5.9
23	8.2	6.5	5.8	6.3	5.3	5.4	5.3	5.5	5.1	4.5	6.9	6.4	5.9
Mean	8.7	7.3	6.7	6.8	5.8	6.1	6.1	6.2	5.7	5.0	7.3	6.5	6.5

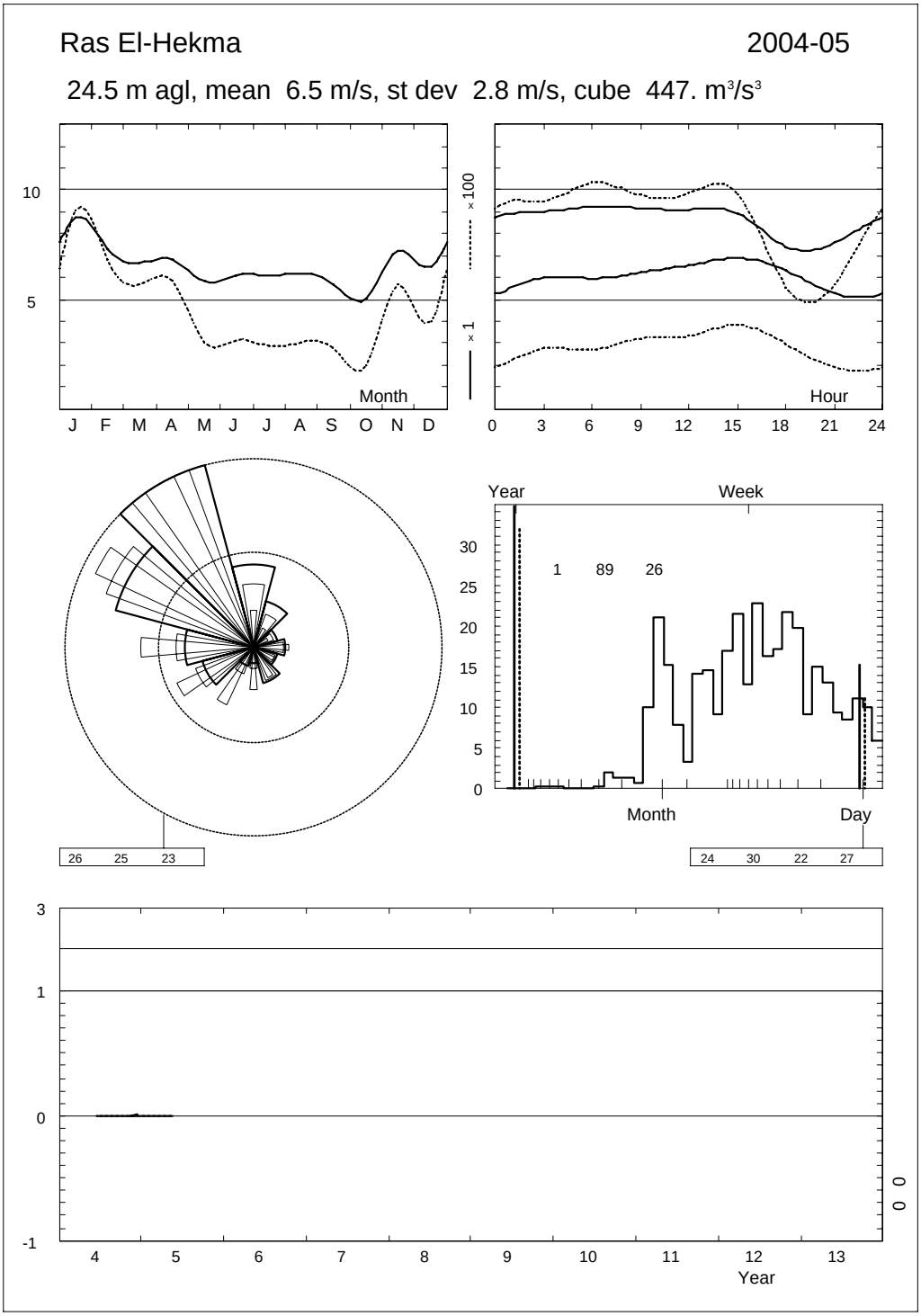

	Jan	Feb	Mar	Apr	May	Jun	Jul	Aug	Sep	Oct	Nov	Dec	Year
2004	—	—	—	—	—	6.1	6.1	6.2	5.7	5.0	7.3	6.5	6.1
2005	8.7	7.3	6.7	6.8	5.8	—	—	—	—	—	—	—	7.1
Mean	8.7	7.3	6.7	6.8	5.8	6.1	6.1	6.2	5.7	5.0	7.3	6.5	6.5

Roughness Class 0 ($z_0 = 0.0002$ m)

z	0	30	60	90	120	150	180	210	240	270	300	330	Total
10	6.0	5.2	5.1	5.5	5.4	6.3	10.0	12.0	9.4	8.4	7.5	7.2	7.2
	2.35	2.46	2.34	1.97	1.96	2.88	2.07	2.85	2.74	2.49	2.90	2.36	2.12
25	6.5	5.7	5.6	6.0	5.9	6.9	10.9	13.1	10.2	9.2	8.2	7.9	7.9
	2.42	2.53	2.41	2.03	2.02	2.98	2.10	2.89	2.82	2.57	2.99	2.43	2.17
50	7.0	6.1	6.0	6.5	6.3	7.4	11.6	13.9	11.0	9.9	8.8	8.4	8.5
	2.49	2.60	2.47	2.08	2.08	3.06	2.15	2.96	2.90	2.64	3.07	2.49	2.22
100	7.6	6.6	6.5	7.0	6.8	8.1	12.4	14.9	11.9	10.7	9.6	9.2	9.2
	2.41	2.52	2.40	2.02	2.01	2.96	2.12	2.92	2.82	2.56	2.97	2.42	2.19
200	8.4	7.3	7.2	7.8	7.6	8.9	13.4	16.1	13.1	11.8	10.6	10.1	10.1
	2.28	2.38	2.27	1.91	1.90	2.80	2.06	2.85	2.68	2.42	2.81	2.29	2.12
Freq.	14.4	7.2	3.8	3.7	3.2	4.6	2.9	3.3	6.9	8.3	16.8	24.9	100.0

Roughness Class 1 ($z_0 = 0.0300$ m)

z	0	30	60	90	120	150	180	210	240	270	300	330	Total
10	4.0	3.5	3.6	3.8	3.9	4.7	7.8	8.0	6.3	5.7	5.2	4.9	5.0
	2.08	2.01	1.86	1.63	1.81	1.94	2.13	2.32	2.31	2.15	2.37	1.93	1.86
25	4.8	4.2	4.3	4.6	4.7	5.6	9.1	9.4	7.6	6.8	6.2	5.9	6.0
	2.24	2.17	2.01	1.76	1.96	2.10	2.21	2.41	2.50	2.33	2.56	2.08	1.98
50	5.5	4.9	5.0	5.3	5.4	6.4	10.3	10.6	8.7	7.8	7.1	6.8	6.9
	2.52	2.44	2.26	1.97	2.20	2.35	2.33	2.55	2.80	2.62	2.88	2.34	2.17
100	6.6	5.8	6.0	6.3	6.4	7.7	11.6	12.0	10.3	9.3	8.4	8.1	8.2
	2.68	2.60	2.41	2.10	2.34	2.51	2.50	2.74	2.99	2.79	3.06	2.49	2.32
200	8.2	7.2	7.4	7.9	8.0	9.5	13.5	14.0	12.8	11.5	10.5	10.0	10.1
	2.56	2.48	2.30	2.01	2.24	2.39	2.43	2.66	2.85	2.66	2.92	2.38	2.29
Freq.	12.3	6.1	3.6	3.6	3.4	4.4	2.8	3.9	7.4	9.8	18.7	23.9	100.0

Roughness Class 2 ($z_0 = 0.1000$ m)

z	0	30	60	90	120	150	180	210	240	270	300	330	Total
10	3.5	3.1	3.2	3.3	3.5	4.0	6.8	6.7	5.5	4.9	4.5	4.2	4.4
	2.11	1.97	1.85	1.65	1.91	1.66	2.17	2.23	2.28	2.20	2.31	1.93	1.86
25	4.3	3.8	3.9	4.1	4.3	5.0	8.3	8.1	6.7	6.0	5.5	5.2	5.4
	2.26	2.11	1.99	1.76	2.04	1.78	2.24	2.31	2.44	2.35	2.47	2.07	1.96
50	5.0	4.4	4.6	4.8	5.1	5.9	9.5	9.3	7.9	7.0	6.4	6.1	6.3
	2.50	2.34	2.20	1.95	2.26	1.97	2.35	2.44	2.71	2.61	2.74	2.29	2.13
100	6.0	5.3	5.5	5.8	6.0	7.0	10.9	10.7	9.4	8.4	7.7	7.3	7.5
	2.75	2.57	2.42	2.14	2.48	2.16	2.56	2.66	2.97	2.87	3.01	2.51	2.33
200	7.4	6.5	6.8	7.2	7.4	8.7	12.6	12.6	11.6	10.3	9.5	9.0	9.2
	2.63	2.46	2.31	2.05	2.38	2.07	2.49	2.58	2.85	2.74	2.88	2.40	2.29
Freq.	11.7	5.8	3.6	3.6	3.5	4.2	2.9	4.3	7.6	10.6	19.4	22.9	100.0

Roughness Class 3 ($z_0 = 0.4000$ m)

z	0	30	60	90	120	150	180	210	240	270	300	330	Total
10	2.7	2.4	2.5	2.6	2.8	3.3	5.4	5.0	4.2	3.8	3.5	3.3	3.4
	2.08	2.01	1.78	1.65	1.98	1.60	2.23	2.19	2.26	2.28	2.27	1.96	1.87
25	3.6	3.2	3.3	3.5	3.7	4.4	7.0	6.5	5.6	5.0	4.6	4.3	4.5
	2.20	2.13	1.88	1.75	2.10	1.69	2.29	2.26	2.39	2.41	2.40	2.07	1.96
50	4.3	3.9	4.0	4.2	4.4	5.3	8.3	7.8	6.7	6.0	5.6	5.2	5.4
	2.39	2.31	2.05	1.90	2.28	1.84	2.38	2.38	2.60	2.62	2.61	2.25	2.10
100	5.2	4.7	4.8	5.1	5.3	6.5	9.8	9.2	8.1	7.2	6.7	6.3	6.6
	2.72	2.63	2.33	2.16	2.60	2.09	2.55	2.58	2.96	2.99	2.97	2.56	2.34
200	6.3	5.7	5.9	6.2	6.5	7.9	11.4	10.8	9.9	8.8	8.2	7.7	8.0
	2.62	2.54	2.25	2.08	2.50	2.01	2.58	2.58	2.86	2.88	2.87	2.47	2.31
Freq.	10.9	5.4	3.6	3.5	3.7	3.9	2.9	4.7	7.7	11.7	20.4	21.5	100.0

z	Class 0		Class 1		Class 2		Class 3	
m	ms^{-1}	Wm^{-2}	ms^{-1}	Wm^{-2}	ms^{-1}	Wm^{-2}	ms^{-1}	Wm^{-2}
10	6.4	286	4.4	111	3.9	73	3.0	35
25	7.0	368	5.3	177	4.8	129	4.0	76
50	7.5	446	6.1	249	5.6	190	4.8	125
100	8.1	573	7.2	388	6.6	296	5.8	199
200	8.9	789	8.9	740	8.1	555	7.1	361

El-Galala

Northwest Coast

31° 01′ 43.6″ N 28° 10′ 59.7″ E	UTM 35 E 612 930 m N 3 433 392 m	59 m

The El-Galala mast is situated in one of five NREA sites established in connection with a Dutch wind/diesel project. The shortest distance to the coastline of the Mediterranean Sea is about 5 km in a NNE direction. The site is located on a low, smooth hill S and SE of the small town of El-Galala. The only significant roughness areas are the town to the N, some scattered bushes and trees to the N and NW and the sea to the N.

Observed data from the airports in Sidi Barrani and Alexandria indicate that the mean wind speeds in the 12-month period 2004-06 to 2005-05 are approx. 99% of the mean values over the 10-year period 1995-2004. The data recovery rate at El-Galala is 97.2%.

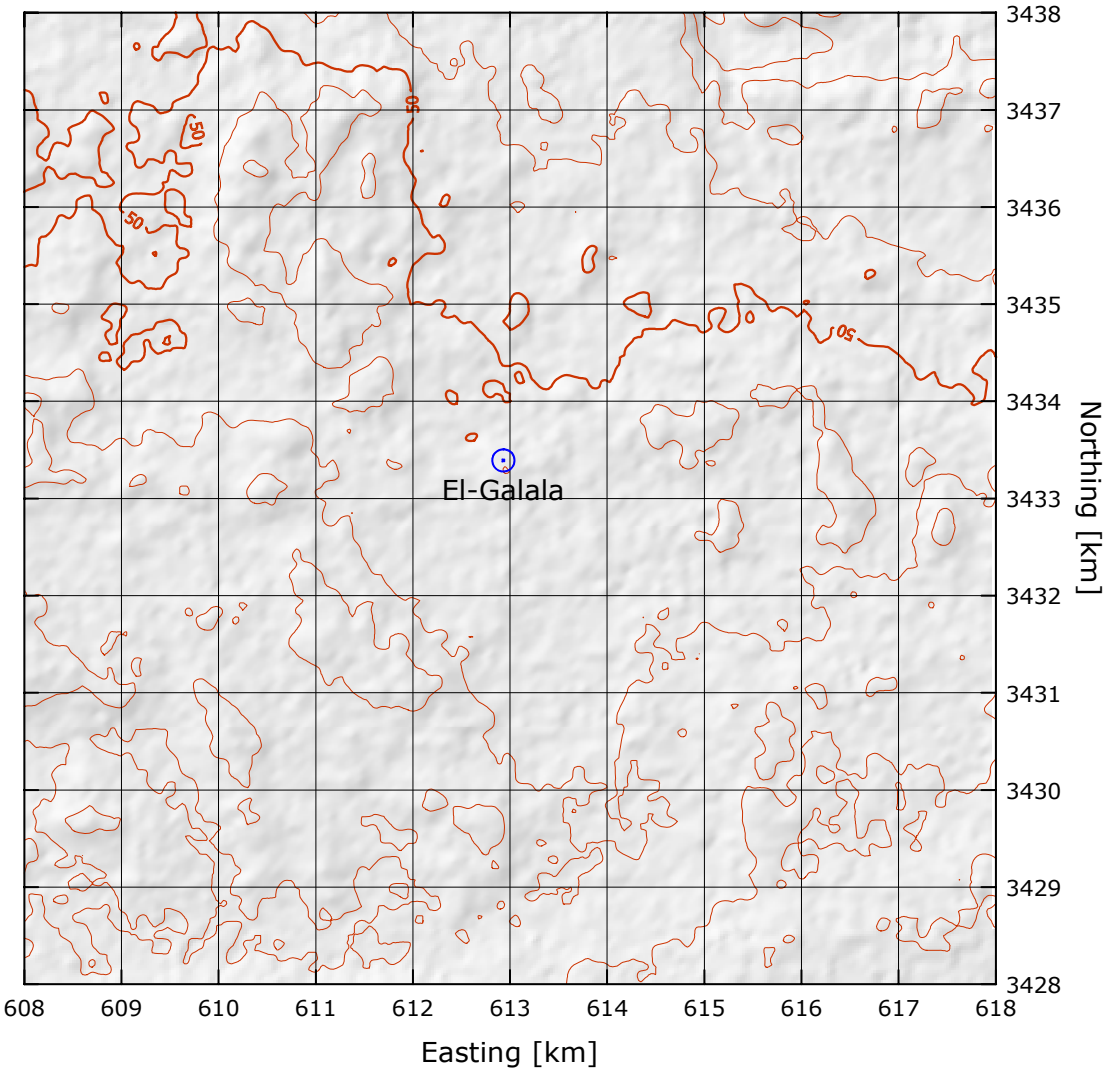

Sector	Input		Obstacles		Roughness		Orography		z_{0m}
0	0.0	0.0	0.0	0.0	−7.5	0.0	3.4	0.3	0.0020
30	0.0	0.0	0.0	0.0	−6.0	0.0	3.3	−0.3	0.0010
60	0.0	0.0	0.0	0.0	−3.5	0.0	2.4	−0.7	0.0030
90	0.0	0.0	0.0	0.0	0.0	0.0	1.3	−0.3	0.0100
120	0.0	0.0	0.0	0.0	0.0	0.0	1.3	0.4	0.0100
150	0.0	0.0	0.0	0.0	0.0	0.0	2.4	0.7	0.0100
180	0.0	0.0	0.0	0.0	0.0	0.0	3.5	0.3	0.0100
210	0.0	0.0	0.0	0.0	0.0	0.0	3.5	−0.4	0.0100
240	0.0	0.0	0.0	0.0	0.0	0.0	2.4	−0.7	0.0090
270	0.0	0.0	0.0	0.0	0.0	0.0	1.3	−0.3	0.0100
300	0.0	0.0	0.0	0.0	−3.1	0.0	1.3	0.4	0.0080
330	0.0	0.0	0.0	0.0	−7.6	0.0	2.4	0.7	0.0020

Height of anemometer: 24.5 m a.g.l. 2004-05

Sect	Freq	< 1	2	3	4	5	6	7	8	9	11	13	15	17	>17	*A*	*k*
0	13.6	8	29	51	101	180	232	172	107	47	50	21	3	0	0	6.3	2.61
30	7.1	19	66	88	129	173	199	191	77	41	17	0	0	0	0	5.7	3.25
60	3.5	17	60	104	146	142	170	158	95	65	35	1	1	5	2	6.0	2.57
90	4.6	4	47	66	126	210	192	165	97	42	40	10	0	0	0	6.0	2.66
120	4.9	10	75	107	149	128	158	129	105	64	61	15	0	0	0	6.0	2.42
150	5.1	6	27	77	104	149	156	154	142	98	72	12	2	1	0	6.7	2.87
180	3.5	3	16	58	94	149	177	144	107	82	98	50	19	2	0	7.0	2.20
210	2.9	3	25	47	117	131	117	100	107	75	117	79	51	28	2	7.9	1.98
240	4.1	9	23	48	71	119	119	150	171	113	112	54	10	2	0	7.6	2.90
270	10.1	8	35	70	123	150	142	120	119	82	93	45	9	4	1	6.8	2.20
300	13.5	4	20	48	108	160	185	130	106	94	97	30	14	5	1	6.9	2.20
330	27.2	3	16	37	84	147	189	172	130	102	95	22	3	0	0	7.0	2.82
Total	100.0	7	31	58	106	156	181	154	116	80	77	25	7	2	0	6.7	2.41

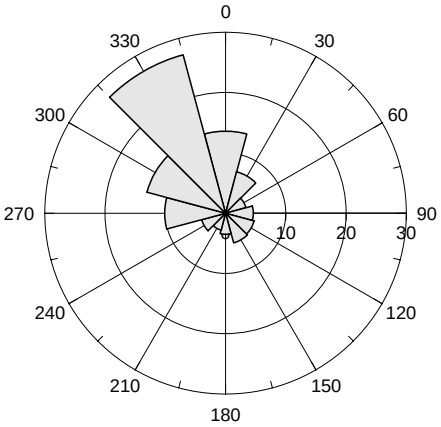

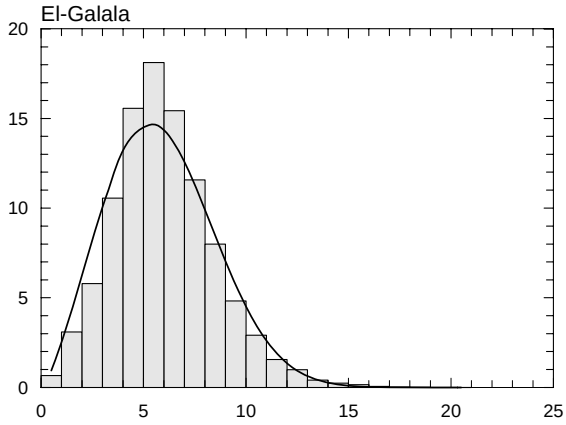

	Jan	Feb	Mar	Apr	May	Jun	Jul	Aug	Sep	Oct	Nov	Dec	Year
0	7.1	6.3	5.2	5.5	4.7	4.4	4.6	4.1	4.8	4.4	6.3	5.9	5.3
1	7.5	6.2	5.4	5.4	4.5	4.6	4.4	4.2	5.0	4.7	6.5	5.7	5.3
2	7.4	6.0	5.3	5.5	4.6	4.4	4.6	4.3	5.1	4.9	6.3	6.0	5.4
3	7.6	6.0	5.2	5.8	4.9	4.5	4.6	4.5	5.2	4.8	6.6	6.1	5.5
4	7.7	6.5	5.7	6.1	4.6	4.7	4.9	4.5	4.8	4.6	6.3	5.8	5.5
5	7.5	6.3	5.9	6.0	4.3	5.0	5.1	4.6	4.6	4.8	6.4	5.8	5.5
6	7.5	6.3	5.7	4.8	4.7	5.0	5.1	4.7	4.5	4.8	5.9	5.9	5.4
7	7.3	6.4	5.6	5.3	4.5	5.0	5.1	4.5	4.5	4.8	5.7	5.8	5.4
8	7.1	6.2	5.6	5.9	5.0	5.5	5.5	5.3	4.8	5.2	5.6	5.7	5.6
9	7.1	6.5	6.2	5.9	5.2	5.8	5.8	5.6	5.3	5.3	6.3	5.9	5.9
10	7.6	6.8	6.3	6.1	5.2	6.2	5.9	5.8	5.3	5.4	6.3	6.0	6.1
11	8.5	7.3	6.2	6.5	5.6	6.3	6.2	6.2	5.5	5.5	6.4	6.4	6.4
12	8.7	7.6	6.3	6.8	6.2	6.6	6.6	6.6	6.1	5.9	6.7	6.4	6.7
13	8.8	7.7	6.7	7.2	6.7	7.2	6.8	7.1	6.6	6.4	7.0	6.4	7.1
14	8.5	7.7	7.1	7.8	7.2	7.2	7.3	7.5	7.1	6.5	7.2	6.3	7.3
15	8.4	7.2	7.3	8.1	7.4	7.3	7.5	7.6	7.4	6.5	6.7	6.1	7.3
16	7.9	7.4	7.3	8.3	7.6	7.5	7.6	7.9	7.5	6.0	6.2	5.8	7.2
17	7.4	6.7	7.1	8.2	7.5	7.2	7.4	7.6	7.2	5.4	6.0	5.4	6.9
18	6.4	6.1	6.8	7.3	7.2	7.0	7.1	7.1	6.7	5.3	6.1	5.6	6.6
19	6.2	5.4	6.0	6.5	6.4	6.6	6.3	6.4	5.8	4.9	6.3	5.4	6.0
20	6.6	5.5	5.9	5.9	5.5	5.8	5.4	5.6	5.5	4.5	5.9	5.6	5.6
21	6.9	5.8	5.4	6.1	5.0	5.0	4.6	5.0	5.5	4.6	6.1	5.5	5.5
22	6.8	5.9	5.2	6.0	4.7	4.9	4.4	4.5	5.1	4.3	6.0	5.7	5.3
23	6.8	6.0	5.3	6.1	4.3	4.6	4.5	4.3	4.7	4.3	6.0	5.7	5.2
Mean	7.5	6.5	6.0	6.4	5.5	5.8	5.7	5.6	5.6	5.2	6.3	5.9	6.0

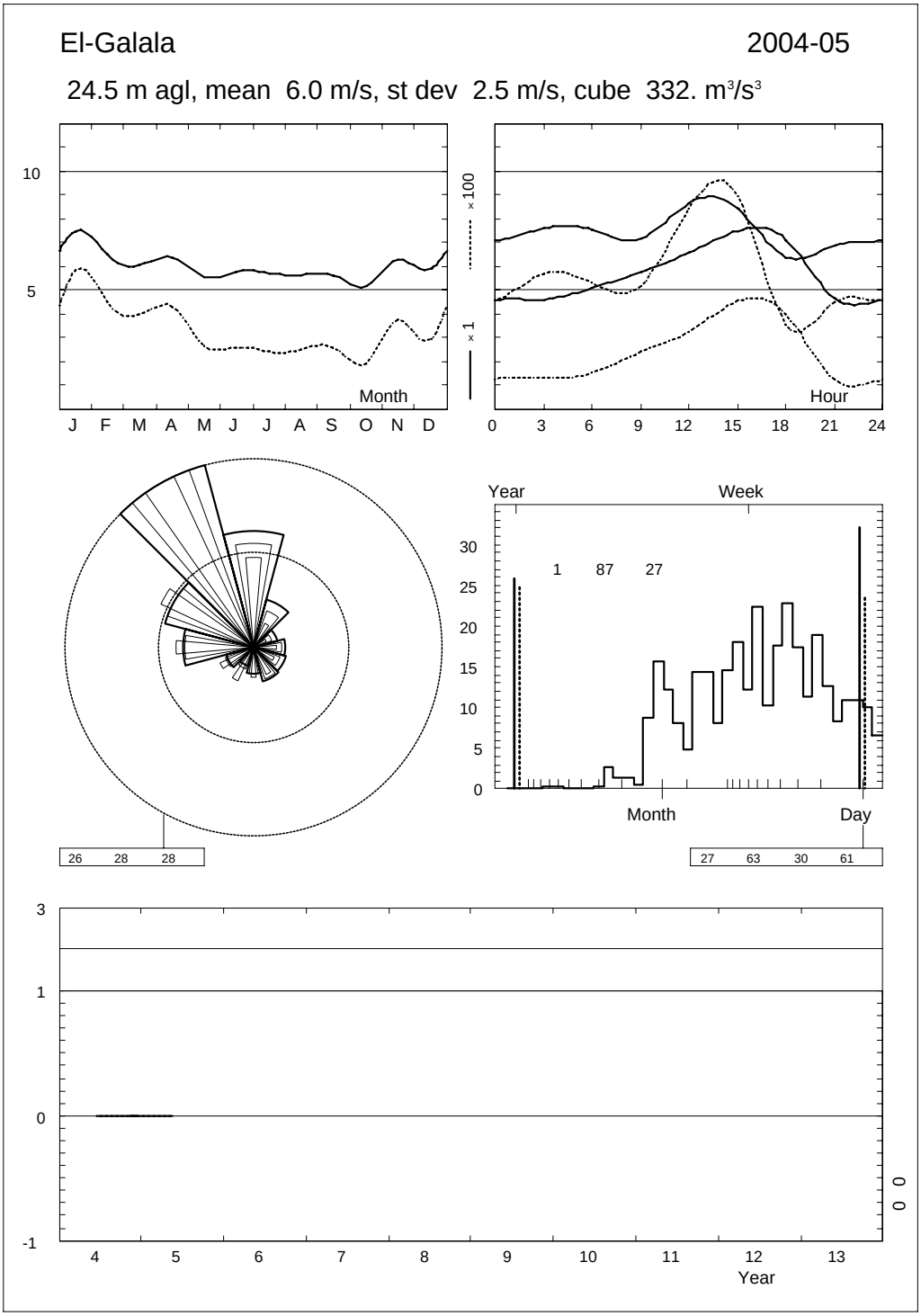

	Jan	Feb	Mar	Apr	May	Jun	Jul	Aug	Sep	Oct	Nov	Dec	Year
2004	—	—	—	—	—	5.8	5.7	5.6	5.6	5.2	6.3	5.9	5.7
2005	7.5	6.5	6.0	6.4	5.5	—	—	—	—	—	—	—	6.4
Mean	7.5	6.5	6.0	6.4	5.5	5.8	5.7	5.6	5.6	5.2	6.3	5.9	6.0

Roughness Class 0 ($z_0 = 0.0002$ m)

z	0	30	60	90	120	150	180	210	240	270	300	330	Total
10	6.8	6.0	6.2	6.6	6.7	7.2	7.6	8.4	8.4	7.7	7.8	7.6	7.3
	2.59	3.08	2.79	2.87	2.65	3.03	2.51	2.14	2.96	2.47	2.46	2.88	2.58
25	7.4	6.6	6.8	7.2	7.3	7.9	8.3	9.2	9.2	8.4	8.5	8.2	7.9
	2.67	3.18	2.88	2.96	2.73	3.12	2.58	2.20	3.05	2.55	2.54	2.97	2.65
50	7.9	7.0	7.3	7.7	7.8	8.4	8.9	9.9	9.8	9.0	9.1	8.9	8.5
	2.74	3.26	2.95	3.04	2.80	3.20	2.65	2.26	3.13	2.62	2.60	3.05	2.72
100	8.6	7.7	8.0	8.4	8.5	9.2	9.6	10.6	10.7	9.8	9.9	9.6	9.3
	2.65	3.16	2.86	2.94	2.71	3.10	2.57	2.20	3.04	2.54	2.52	2.96	2.64
200	9.5	8.5	8.8	9.3	9.4	10.1	10.7	11.7	11.8	10.8	11.0	10.6	10.2
	2.51	2.99	2.71	2.79	2.57	2.94	2.43	2.10	2.87	2.40	2.38	2.80	2.51
Freq.	15.2	7.9	4.0	4.5	4.9	5.1	3.7	2.9	3.9	9.3	13.4	25.1	100.0

Roughness Class 1 ($z_0 = 0.0300$ m)

z	0	30	60	90	120	150	180	210	240	270	300	330	Total
10	4.6	4.1	4.5	4.6	4.7	5.1	5.3	5.9	5.7	5.3	5.4	5.2	5.1
	2.28	2.60	2.29	2.40	2.25	2.55	1.98	1.87	2.47	2.03	2.08	2.42	2.18
25	5.5	4.9	5.3	5.5	5.6	6.1	6.4	7.1	6.8	6.3	6.4	6.2	6.0
	2.46	2.80	2.47	2.59	2.43	2.76	2.14	2.00	2.67	2.19	2.25	2.62	2.35
50	6.3	5.6	6.2	6.4	6.5	7.0	7.4	8.1	7.8	7.3	7.4	7.2	7.0
	2.76	3.15	2.78	2.91	2.73	3.10	2.41	2.21	3.00	2.46	2.53	2.94	2.62
100	7.5	6.6	7.3	7.5	7.7	8.3	8.7	9.6	9.3	8.6	8.8	8.5	8.3
	2.94	3.35	2.97	3.10	2.91	3.30	2.56	2.37	3.20	2.62	2.70	3.13	2.79
200	9.4	8.3	9.1	9.4	9.6	10.3	10.9	11.7	11.5	10.8	10.9	10.6	10.3
	2.81	3.21	2.83	2.96	2.78	3.15	2.45	2.27	3.05	2.50	2.57	2.99	2.67
Freq.	12.7	6.6	3.6	4.7	5.0	4.9	3.4	2.9	4.7	10.5	15.2	25.7	100.0

Roughness Class 2 ($z_0 = 0.1000$ m)

z	0	30	60	90	120	150	180	210	240	270	300	330	Total
10	4.0	3.6	3.9	4.0	4.1	4.4	4.7	5.2	4.9	4.6	4.7	4.5	4.4
	2.19	2.53	2.28	2.37	2.24	2.51	1.98	1.92	2.37	2.06	2.21	2.47	2.20
25	4.9	4.4	4.8	5.0	5.1	5.5	5.8	6.3	6.0	5.7	5.8	5.6	5.4
	2.34	2.70	2.44	2.53	2.40	2.68	2.12	2.04	2.53	2.21	2.36	2.64	2.35
50	5.7	5.1	5.6	5.8	5.9	6.4	6.8	7.4	7.0	6.7	6.8	6.5	6.4
	2.59	2.99	2.69	2.80	2.65	2.97	2.35	2.24	2.80	2.44	2.62	2.92	2.58
100	6.8	6.1	6.7	6.9	7.0	7.6	8.1	8.8	8.3	7.9	8.1	7.8	7.6
	2.85	3.29	2.96	3.08	2.92	3.26	2.58	2.46	3.08	2.69	2.87	3.21	2.83
200	8.4	7.5	8.2	8.5	8.7	9.4	10.0	10.7	10.3	9.8	10.0	9.6	9.3
	2.72	3.15	2.83	2.95	2.79	3.12	2.47	2.36	2.95	2.57	2.75	3.08	2.72
Freq.	12.2	6.3	3.7	4.7	5.0	4.8	3.3	3.1	5.2	10.9	16.3	24.6	100.0

Roughness Class 3 ($z_0 = 0.4000$ m)

z	0	30	60	90	120	150	180	210	240	270	300	330	Total
10	3.1	2.8	3.1	3.2	3.3	3.5	3.7	4.0	3.7	3.7	3.7	3.5	3.5
	2.22	2.41	2.27	2.33	2.32	2.47	1.98	1.98	2.27	2.12	2.32	2.49	2.23
25	4.1	3.7	4.0	4.2	4.3	4.6	4.9	5.3	4.9	4.8	4.9	4.7	4.6
	2.35	2.55	2.41	2.47	2.46	2.63	2.10	2.10	2.41	2.24	2.46	2.64	2.36
50	4.9	4.4	4.9	5.0	5.2	5.6	5.9	6.4	5.9	5.8	5.9	5.6	5.5
	2.55	2.78	2.62	2.68	2.67	2.85	2.28	2.27	2.62	2.44	2.68	2.87	2.56
100	5.9	5.3	5.8	6.0	6.2	6.7	7.2	7.7	7.1	7.0	7.0	6.7	6.6
	2.91	3.16	2.98	3.06	3.04	3.25	2.60	2.59	2.98	2.78	3.05	3.27	2.89
200	7.2	6.5	7.2	7.3	7.6	8.2	8.8	9.4	8.7	8.5	8.6	8.2	8.1
	2.80	3.04	2.87	2.94	2.93	3.13	2.51	2.49	2.87	2.68	2.94	3.15	2.79
Freq.	11.4	5.9	3.9	4.7	4.9	4.6	3.2	3.2	5.9	11.3	17.9	23.0	100.0

z	Class 0		Class 1		Class 2		Class 3	
m	ms^{-1}	Wm^{-2}	ms^{-1}	Wm^{-2}	ms^{-1}	Wm^{-2}	ms^{-1}	Wm^{-2}
10	6.4	254	4.5	97	3.9	64	3.1	31
25	7.1	326	5.4	156	4.8	113	4.1	67
50	7.6	398	6.2	222	5.7	170	4.9	111
100	8.2	516	7.4	357	6.7	272	5.9	181
200	9.1	724	9.1	704	8.3	523	7.2	336

Alexandria (62 318) Northwest Coast

31° 10′ 55.2″ N 29° 57′ 07.2″ E	UTM 35 E 781 337 m N 3 453 527 m	7 m

The site is located in the airport of Nouzha, more than one kilometer SE of the urban area of the city of Alexandria. The shortest distance to the coastline of the Mediterranean Sea is about 5 km in a northwesterly direction.

The observed data indicate that the mean wind speed in the 12-month period 2004-06 to 2005-05 is 99.2% of the mean value over the 10-year period 1995-2004.

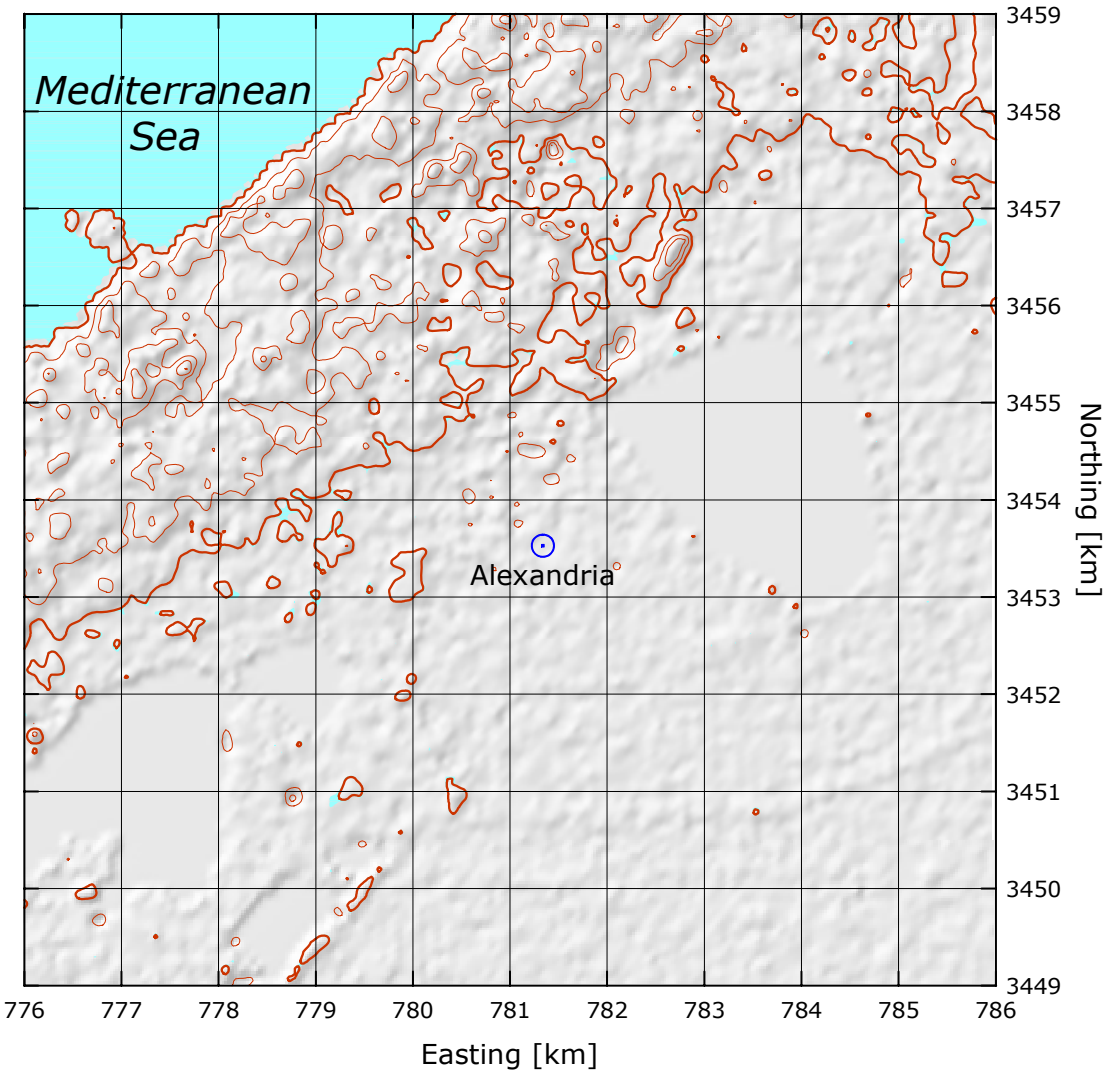

Sector	Input		Obstacles		Roughness		Orography		z_{0m}
0	0.0	0.0	−2.5	0.0	−4.6	0.0	−2.0	0.1	0.0040
30	0.0	0.0	0.0	0.0	9.1	0.0	−1.8	0.1	0.0340
60	0.0	0.0	−0.3	0.0	5.4	0.0	−1.6	0.0	0.0170
90	0.0	0.0	−1.5	0.0	6.0	0.0	−1.8	−0.1	0.0230
120	0.0	0.0	−0.2	0.0	8.2	0.0	−2.0	−0.1	0.0430
150	0.0	0.0	0.0	0.0	7.3	0.0	−2.0	0.0	0.0440
180	0.0	0.0	0.0	0.0	8.0	0.0	−1.9	0.1	0.0430
210	0.0	0.0	0.0	0.0	8.5	0.0	−1.8	0.1	0.0330
240	0.0	0.0	0.0	0.0	1.6	0.0	−1.7	0.0	0.0070
270	0.0	0.0	0.0	0.0	−2.8	0.0	−1.9	−0.1	0.0080
300	0.0	0.0	−0.7	0.0	−5.3	0.0	−2.0	−0.1	0.0030
330	0.0	0.0	−2.5	0.0	−6.3	0.0	−2.0	0.0	0.0020

Height of anemometer: 10.0 m a.g.l. 1995–2004

Sect	Freq	< 1	2	3	4	5	6	7	8	9	11	13	15	17	>17	*A*	*k*
0	16.8	63	70	120	158	190	210	130	44	10	5	1	0	0	0	5.0	2.97
30	8.2	92	97	183	165	158	156	94	37	12	5	0	0	0	0	4.5	2.26
60	5.6	173	182	232	170	122	67	34	14	5	1	0	0	0	0	3.2	1.74
90	4.2	188	202	226	164	117	64	27	11	0	2	0	0	0	0	3.1	1.74
120	3.6	298	248	192	101	79	50	25	4	2	1	0	0	0	0	2.4	1.37
150	2.5	308	212	227	98	92	29	20	7	5	1	0	0	0	0	2.5	1.42
180	3.9	257	245	255	110	62	31	20	10	8	3	0	0	0	0	2.6	1.42
210	3.6	147	180	208	142	108	79	63	29	18	20	4	2	0	0	3.7	1.46
240	3.6	85	101	127	117	98	107	117	81	50	81	27	7	2	0	5.8	1.88
270	4.8	53	60	88	90	121	152	145	99	87	70	26	7	1	0	6.5	2.40
300	16.1	27	34	70	108	151	211	190	112	50	40	8	1	0	0	6.2	3.13
330	27.0	18	25	62	107	173	250	218	90	35	19	2	0	0	0	6.0	3.70
Total	100.0	84	88	125	127	148	174	138	63	27	20	5	1	0	0	5.2	2.42

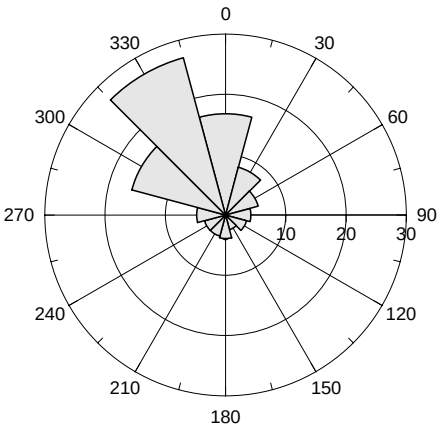

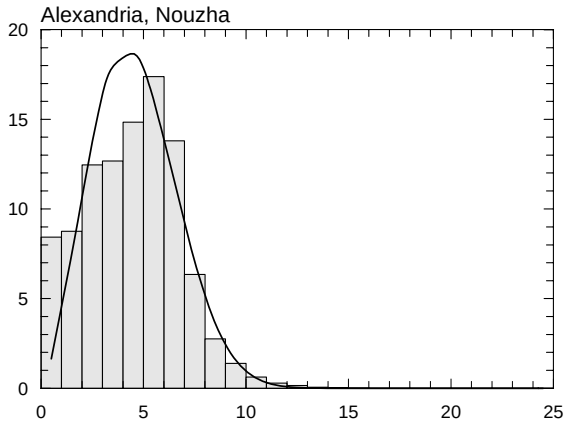

	Jan	Feb	Mar	Apr	May	Jun	Jul	Aug	Sep	Oct	Nov	Dec	Year
0	2.8	3.3	3.3	3.5	3.2	3.7	4.2	3.9	3.2	2.7	2.7	2.8	3.3
3	2.9	3.4	3.1	3.4	2.9	3.4	3.8	3.5	2.8	2.6	2.7	2.9	3.1
6	2.9	3.4	3.4	4.0	3.6	4.0	4.5	4.2	3.5	2.9	2.8	2.9	3.5
9	4.2	4.9	5.1	5.1	4.8	5.0	5.5	5.3	4.7	4.5	4.5	4.6	4.8
12	5.2	5.7	5.8	5.9	6.0	6.1	6.3	6.3	5.9	5.6	5.4	5.3	5.8
15	4.5	5.3	5.6	5.7	5.9	6.3	6.4	6.3	5.9	5.4	4.8	4.3	5.5
18	3.2	4.1	4.4	4.7	4.6	5.0	5.3	5.2	4.8	4.1	3.5	3.1	4.4
21	3.1	3.6	3.7	4.0	3.9	4.2	4.6	4.4	3.7	3.3	2.7	2.9	3.7
Mean	3.6	4.2	4.3	4.6	4.4	4.7	5.1	4.9	4.3	3.9	3.7	3.7	4.3

	Jan	Feb	Mar	Apr	May	Jun	Jul	Aug	Sep	Oct	Nov	Dec	Year
1995	2.0	3.4	3.2	4.4	3.8	3.5	4.9	5.5	4.6	3.7	4.2	3.2	3.9
1996	3.7	4.2	4.5	5.0	4.4	5.0	5.5	5.3	4.2	4.3	3.8	3.1	4.4
1997	3.3	4.3	4.7	4.9	4.2	4.9	5.2	4.4	4.5	3.8	3.1	3.4	4.2
1998	3.8	3.8	4.7	4.0	4.4	5.0	4.6	5.0	4.2	3.9	3.0	4.5	4.3
1999	3.7	4.1	4.4	4.4	4.6	5.8	4.9	4.5	4.1	3.9	3.8	3.6	4.3
2000	4.5	3.9	4.4	4.4	4.3	5.1	4.8	5.1	4.3	4.2	3.6	3.6	4.4
2001	3.2	4.4	3.9	4.5	5.4	5.0	5.3	4.2	4.3	3.9	3.9	3.9	4.3
2002	4.6	4.6	4.7	4.6	4.4	5.0	4.6	4.9	3.9	4.3	3.5	4.0	4.4
2003	3.7	5.7	5.0	5.1	4.6	4.6	6.1	4.9	4.9	3.9	3.6	4.6	4.7
2004	5.2	4.5	4.5	4.5	4.4	4.5	4.8	4.7	4.4	3.8	4.1	3.3	4.4
2005	4.2	4.5	4.2	4.5	4.5	—	—	—	—	—	—	—	—
Mean	3.6	4.2	4.3	4.6	4.4	4.7	5.1	4.9	4.3	3.9	3.7	3.7	4.3

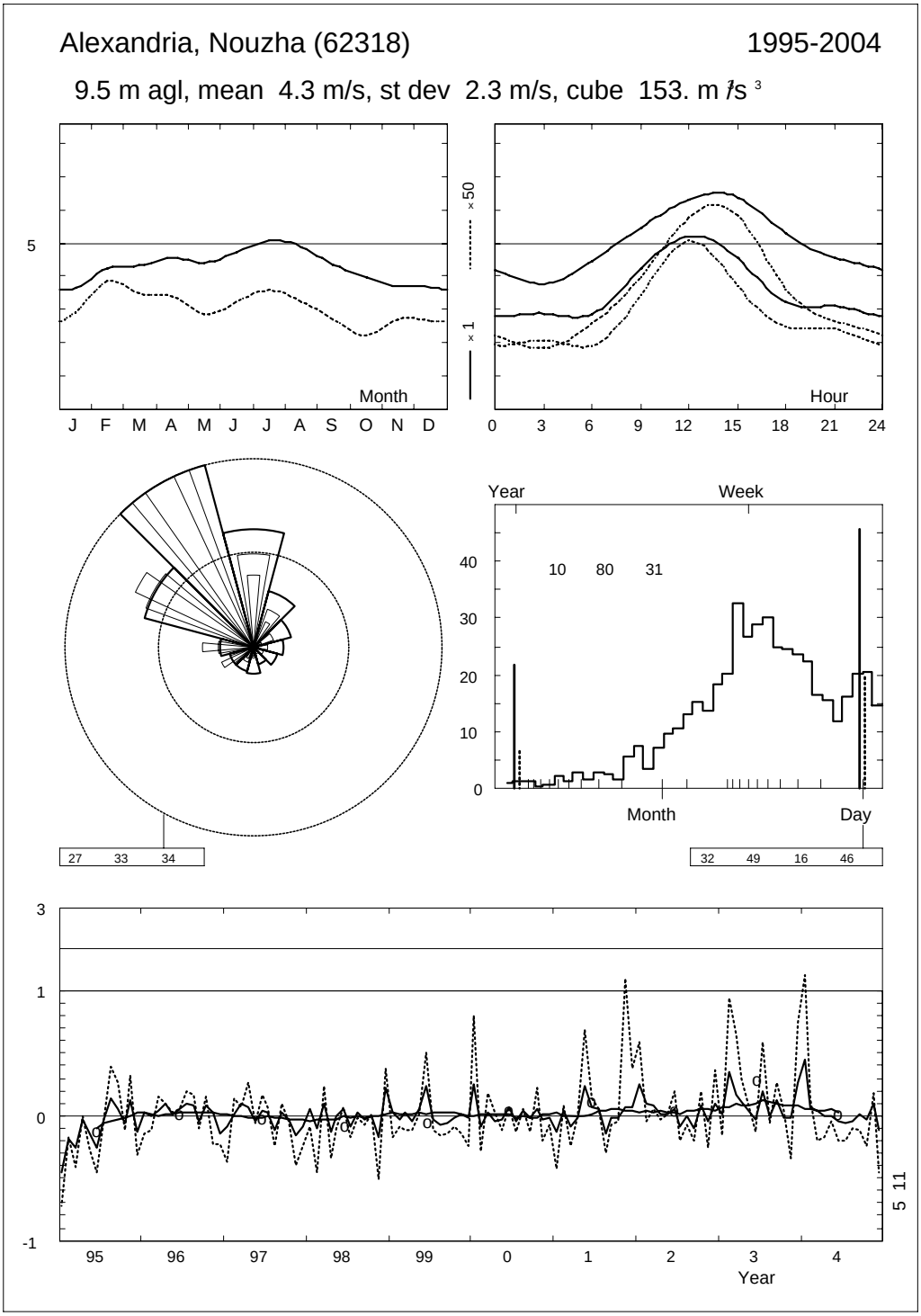
Alexandria, Nouzha (62318)
1995-2004
9.5 m agl, mean 4.3 m/s, st dev 2.3 m/s, cube 153. m ł/s 3
5
Month
J F M A M J J A S O N D
× 50
× 1
Hour
0 3 6 9 12 15 18 21 24
Year
Week
10 80 31
40
30
20
10
0
Month
Day
27 33 34
32 49 16 46
3
1
0
-1
95 96 97 98 99 0 1 2 3 4
Year
5 11

Roughness Class 0 ($z_0 = 0.0002$ m)

z	0	30	60	90	120	150	180	210	240	270	300	330	Total
10	7.0	6.3	4.7	4.2	3.7	3.5	3.7	4.7	7.0	8.6	8.0	7.6	6.7
	3.53	2.90	2.08	2.07	1.72	1.65	1.67	1.64	2.06	2.72	3.38	3.67	2.47
25	7.6	6.8	5.1	4.7	4.0	3.9	4.0	5.1	7.6	9.4	8.8	8.3	7.3
	3.64	3.00	2.15	2.14	1.77	1.71	1.73	1.69	2.13	2.81	3.49	3.79	2.53
50	8.2	7.3	5.5	5.0	4.3	4.2	4.3	5.5	8.2	10.1	9.4	8.9	7.8
	3.74	3.08	2.21	2.20	1.82	1.75	1.77	1.74	2.19	2.88	3.58	3.88	2.58
100	8.9	8.0	6.0	5.4	4.7	4.5	4.7	6.0	8.9	10.9	10.2	9.7	8.5
	3.62	2.98	2.13	2.13	1.76	1.69	1.72	1.68	2.12	2.79	3.47	3.76	2.52
200	9.8	8.8	6.6	6.0	5.2	5.0	5.1	6.6	9.8	12.1	11.3	10.7	9.4
	3.43	2.82	2.02	2.01	1.67	1.60	1.63	1.60	2.00	2.64	3.28	3.56	2.42
Freq.	18.6	9.9	6.1	4.5	3.7	2.8	3.6	3.7	3.7	4.6	13.9	25.0	100.0

Roughness Class 1 ($z_0 = 0.0300$ m)

z	0	30	60	90	120	150	180	210	240	270	300	330	Total
10	4.6	4.2	3.0	2.9	2.4	2.5	2.5	3.5	5.2	6.0	5.5	5.3	4.6
	2.72	2.19	1.70	1.72	1.37	1.42	1.41	1.47	1.89	2.37	2.92	3.08	2.15
25	5.5	5.0	3.6	3.5	2.9	3.0	3.1	4.3	6.2	7.2	6.6	6.3	5.5
	2.94	2.37	1.84	1.86	1.47	1.53	1.52	1.58	2.04	2.56	3.15	3.33	2.28
50	6.3	5.8	4.2	4.1	3.4	3.5	3.6	5.0	7.2	8.3	7.6	7.2	6.4
	3.31	2.67	2.06	2.08	1.65	1.72	1.71	1.77	2.29	2.88	3.54	3.74	2.49
100	7.5	6.8	4.9	4.8	4.0	4.2	4.3	5.9	8.6	9.8	9.0	8.6	7.6
	3.52	2.84	2.20	2.22	1.76	1.83	1.81	1.88	2.44	3.07	3.77	3.98	2.61
200	9.4	8.5	6.1	6.0	5.0	5.2	5.3	7.4	10.7	12.2	11.2	10.7	9.4
	3.37	2.71	2.10	2.12	1.68	1.75	1.73	1.80	2.33	2.93	3.60	3.80	2.52
Freq.	16.4	8.1	5.5	4.2	3.6	2.6	3.9	3.6	3.7	5.3	16.6	26.6	100.0

Roughness Class 2 ($z_0 = 0.1000$ m)

z	0	30	60	90	120	150	180	210	240	270	300	330	Total
10	4.0	3.6	2.6	2.5	2.1	2.2	2.3	3.2	4.6	5.1	4.8	4.6	4.0
	2.69	2.15	1.73	1.71	1.37	1.40	1.39	1.49	1.96	2.45	2.98	3.11	2.17
25	4.9	4.4	3.2	3.1	2.6	2.7	2.9	4.0	5.7	6.3	5.9	5.6	5.0
	2.87	2.30	1.85	1.83	1.47	1.50	1.49	1.59	2.10	2.62	3.19	3.33	2.29
50	5.8	5.2	3.8	3.7	3.1	3.2	3.4	4.7	6.7	7.4	6.9	6.6	5.8
	3.18	2.54	2.05	2.02	1.62	1.65	1.64	1.76	2.32	2.90	3.53	3.69	2.47
100	6.8	6.1	4.5	4.4	3.7	3.8	4.1	5.7	8.0	8.8	8.2	7.8	7.0
	3.49	2.80	2.25	2.22	1.78	1.81	1.80	1.93	2.55	3.19	3.87	4.05	2.64
200	8.4	7.6	5.6	5.4	4.6	4.7	5.0	7.0	9.9	10.9	10.1	9.6	8.6
	3.35	2.68	2.15	2.12	1.71	1.74	1.72	1.85	2.44	3.05	3.71	3.88	2.56
Freq.	15.6	7.9	5.4	4.1	3.5	2.7	3.8	3.6	3.8	6.3	17.5	25.8	100.0

Roughness Class 3 ($z_0 = 0.4000$ m)

z	0	30	60	90	120	150	180	210	240	270	300	330	Total
10	3.1	2.7	2.0	1.9	1.7	1.7	1.9	2.7	3.7	4.0	3.8	3.5	3.2
	2.62	2.08	1.68	1.63	1.41	1.40	1.36	1.54	2.03	2.53	2.97	2.98	2.15
25	4.1	3.6	2.7	2.6	2.2	2.2	2.5	3.5	4.9	5.2	4.9	4.6	4.2
	2.78	2.21	1.78	1.72	1.49	1.48	1.44	1.63	2.15	2.68	3.15	3.16	2.26
50	4.9	4.3	3.2	3.1	2.7	2.7	3.0	4.3	5.9	6.3	5.9	5.6	5.0
	3.02	2.40	1.93	1.87	1.62	1.60	1.56	1.76	2.33	2.91	3.42	3.43	2.40
100	5.9	5.2	3.9	3.8	3.3	3.3	3.7	5.2	7.1	7.5	7.1	6.7	6.1
	3.44	2.73	2.20	2.13	1.84	1.83	1.78	2.01	2.66	3.32	3.90	3.91	2.65
200	7.3	6.4	4.8	4.6	4.1	4.1	4.4	6.4	8.7	9.2	8.7	8.2	7.4
	3.31	2.63	2.12	2.05	1.78	1.76	1.71	1.94	2.56	3.20	3.76	3.77	2.58
Freq.	14.6	7.6	5.2	4.1	3.3	2.9	3.8	3.6	3.9	7.6	18.8	24.7	100.0

z	Class 0		Class 1		Class 2		Class 3	
m	ms^{-1}	Wm^{-2}	ms^{-1}	Wm^{-2}	ms^{-1}	Wm^{-2}	ms^{-1}	Wm^{-2}
10	5.9	201	4.1	75	3.6	50	2.8	24
25	6.5	260	4.9	123	4.4	89	3.7	53
50	7.0	318	5.7	177	5.2	136	4.5	88
100	7.5	411	6.7	288	6.2	219	5.4	145
200	8.3	573	8.4	566	7.6	421	6.6	268

Port Said

Northeast Coast

29° 16′ 49.4″ N 32° 36′ 03.3″ E	UTM 36 E 461 235 m N 3 239 117 m	1 m

The Port Said mast is situated about 7 km south of the town of Port Said, approximately 185 km from Cairo. The site is close to the Port Said road on the western side of the Suez Canal. The distance to the Suez Canal is about 400 m. There are no sheltering obstacles close to the mast. The mast is about 5 km from Manzala Lake. The surface is sandy and flat and homogeneous to the SW, W and NW; where there is an open area for cultivation, with a roughness length of about 0.02 m. The road is parallel to Suez Canal and on the eastern side of the mast.

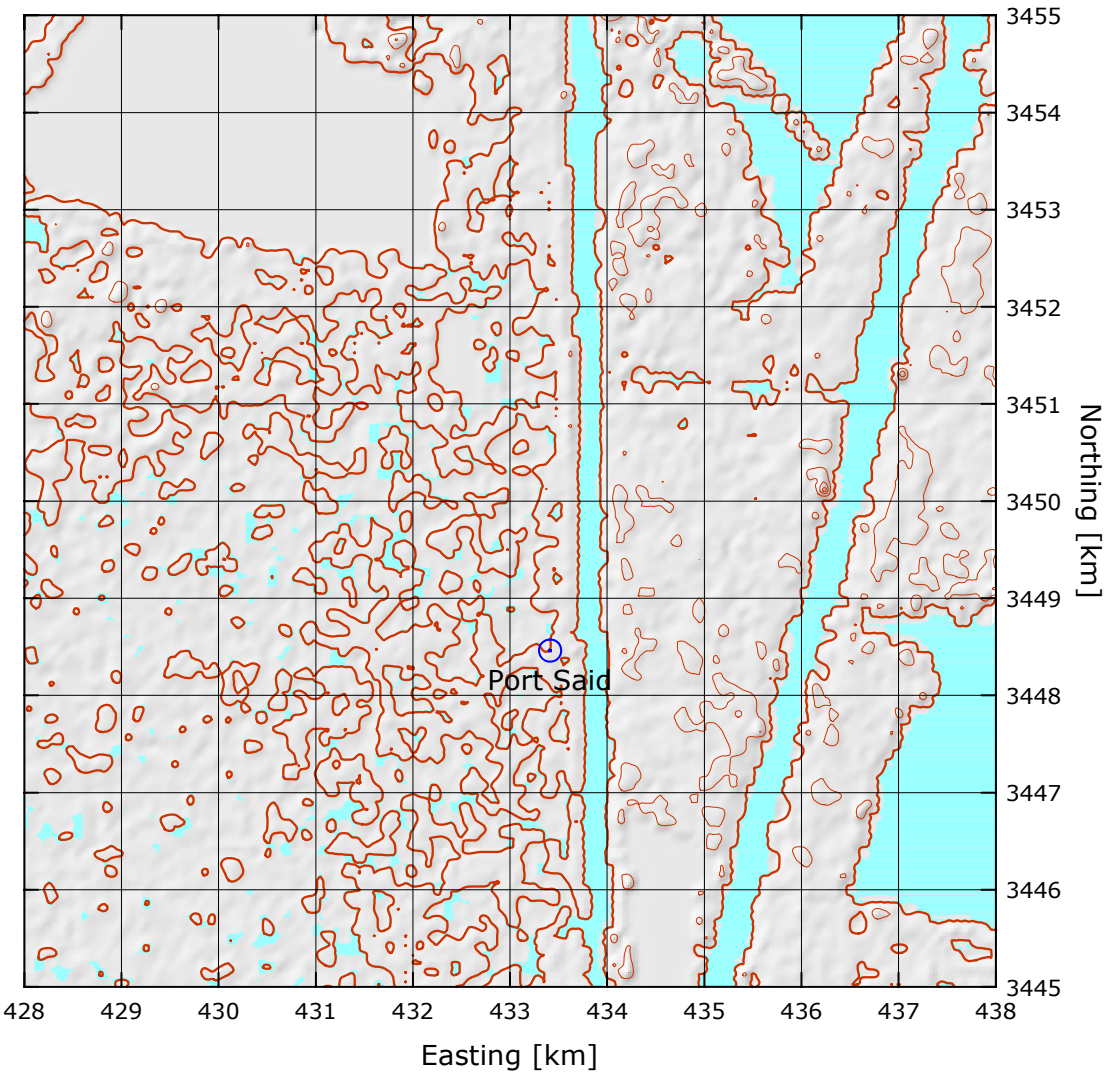

Sector	Input		Obstacles		Roughness		Orography		z_{0m}
0	0.0	0.0	0.0	0.0	0.0	0.0	0.5	0.4	0.0300
30	0.0	0.0	0.0	0.0	0.0	0.0	0.6	−0.3	0.0300
60	0.0	0.0	0.0	0.0	0.0	0.0	−0.2	−0.6	0.0300
90	0.0	0.0	0.0	0.0	0.0	0.0	−1.2	−0.4	0.0300
120	0.0	0.0	0.0	0.0	0.0	0.0	−1.4	0.3	0.0300
150	0.0	0.0	0.0	0.0	0.0	0.0	−0.5	0.6	0.0300
180	0.0	0.0	0.0	0.0	0.0	0.0	0.5	0.4	0.0300
210	0.0	0.0	0.0	0.0	0.0	0.0	0.6	−0.3	0.0300
240	0.0	0.0	0.0	0.0	0.0	0.0	−0.2	−0.6	0.0300
270	0.0	0.0	0.0	0.0	0.0	0.0	−1.2	−0.4	0.0300
300	0.0	0.0	0.0	0.0	0.0	0.0	−1.4	0.3	0.0300
330	0.0	0.0	0.0	0.0	0.0	0.0	−0.5	0.6	0.0300

Height of anemometer: 24.5 m a.g.l. 2004-05

Sect	Freq	< 1	2	3	4	5	6	7	8	9	11	13	15	17	>17	*A*	*k*
0	15.7	20	53	75	153	262	227	107	55	31	17	1	0	0	0	5.4	2.93
30	8.3	19	42	71	159	267	187	134	85	25	11	0	0	0	0	5.4	2.88
60	3.7	28	78	102	158	257	198	127	43	5	4	0	0	0	0	5.1	3.29
90	3.3	7	86	131	190	218	204	125	27	6	4	1	0	0	0	4.9	3.08
120	2.3	22	157	221	250	181	122	30	13	4	0	0	0	0	0	3.9	2.49
150	3.3	31	128	145	164	127	109	69	59	59	69	34	5	0	0	5.3	1.65
180	5.5	10	82	132	165	214	202	82	48	27	34	4	0	0	0	5.2	2.43
210	10.0	5	43	137	207	192	121	106	67	56	48	19	1	0	0	5.4	1.89
240	13.3	4	46	131	250	266	126	63	43	28	36	6	0	0	0	4.9	2.00
270	10.6	12	62	142	201	206	137	85	57	35	40	16	6	0	0	5.2	1.84
300	11.5	10	64	75	100	174	181	156	133	74	31	3	0	0	0	6.1	2.99
330	12.5	14	78	145	211	189	173	127	46	11	6	0	0	0	0	4.9	2.69
Total	100.0	13	64	116	183	220	168	106	63	34	26	6	1	0	0	5.3	2.32

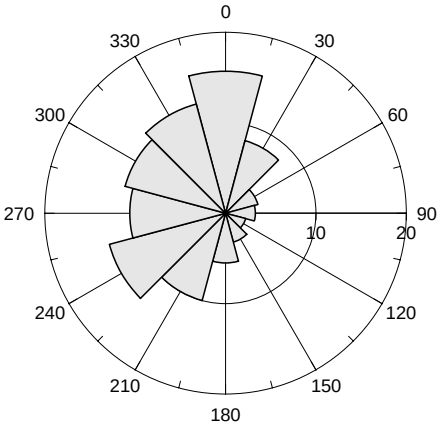

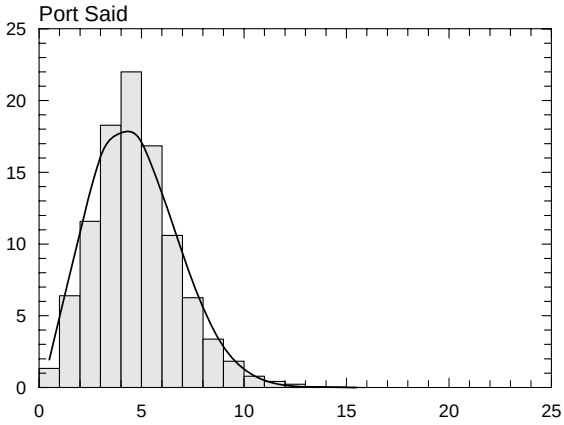

	Jan	Feb	Mar	Apr	May	Jun	Jul	Aug	Sep	Oct	Nov	Dec	Year
0	4.4	4.3	4.2	—	—	3.8	3.3	—	3.3	3.2	5.1	4.4	4.0
1	4.6	4.1	4.4	—	—	3.3	3.2	—	3.1	3.0	5.0	4.4	3.9
2	4.7	4.3	4.3	—	—	3.2	3.1	—	3.1	3.1	4.7	4.3	3.9
3	5.0	4.6	4.8	—	—	3.1	3.1	—	2.6	3.2	4.6	4.5	4.0
4	4.9	4.5	4.9	—	—	3.2	3.0	—	2.8	3.3	4.8	4.0	4.0
5	4.9	4.6	4.7	—	—	3.2	3.2	—	2.6	3.3	4.5	4.1	4.0
6	5.2	4.4	4.5	—	—	3.1	3.1	—	2.3	3.3	4.5	3.8	3.9
7	4.8	4.7	4.7	—	—	3.4	3.5	—	2.2	3.2	4.4	3.9	4.0
8	4.7	4.6	5.0	—	—	3.2	3.3	—	2.9	3.6	4.6	3.7	4.0
9	5.2	5.3	5.0	—	—	3.5	3.3	—	2.8	3.7	5.2	4.1	4.3
10	6.0	5.7	5.4	—	—	4.0	3.7	—	3.3	3.9	5.6	4.8	4.8
11	6.1	6.0	5.6	—	—	4.6	4.4	—	4.0	4.3	5.9	5.0	5.1
12	6.2	6.3	5.8	—	—	5.0	4.8	—	4.6	4.7	6.2	5.1	5.4
13	6.2	6.2	6.1	—	—	5.5	5.5	—	5.0	4.9	6.2	5.0	5.6
14	6.8	6.6	6.2	—	—	6.1	5.9	—	5.3	5.3	6.2	5.2	6.0
15	6.2	6.6	6.6	—	—	6.5	6.4	—	5.6	5.5	6.3	5.2	6.1
16	5.9	6.3	6.5	—	—	6.9	6.8	—	6.0	5.7	5.9	4.8	6.1
17	5.2	5.9	6.3	—	—	6.8	7.2	—	6.0	5.5	5.4	4.3	5.8
18	5.0	5.6	5.9	—	—	6.8	6.7	—	5.4	5.2	5.0	4.2	5.5
19	4.8	4.9	5.9	—	—	6.2	6.0	—	5.0	4.7	4.8	4.1	5.1
20	4.7	4.8	5.9	—	—	5.9	5.2	—	4.6	4.4	5.0	4.0	4.9
21	4.8	4.8	5.3	—	—	5.2	4.7	—	4.3	3.9	5.1	4.2	4.7
22	4.3	4.7	4.6	—	—	4.7	3.9	—	4.0	3.8	5.1	3.8	4.3
23	4.4	4.7	4.5	—	—	4.0	3.4	—	3.5	3.5	5.2	4.2	4.2
Mean	5.2	5.2	5.3	—	—	4.6	4.4	—	4.0	4.1	5.2	4.4	4.7

31° 04′ 57.7″ N 33° 49′ 41.0″ E	UTM 36 E 578 984 m N 3 439 060 m		34 m

The site is located in the airport of El Arish, in a wide valley oriented approx. NNW-SSE. The airport is surrounded by rural areas and desert. The built-up areas of El Arish are about 4 km to the north; the Mediterranean Sea is about 7 km to the north. Scattered low houses surround the site at near distance.

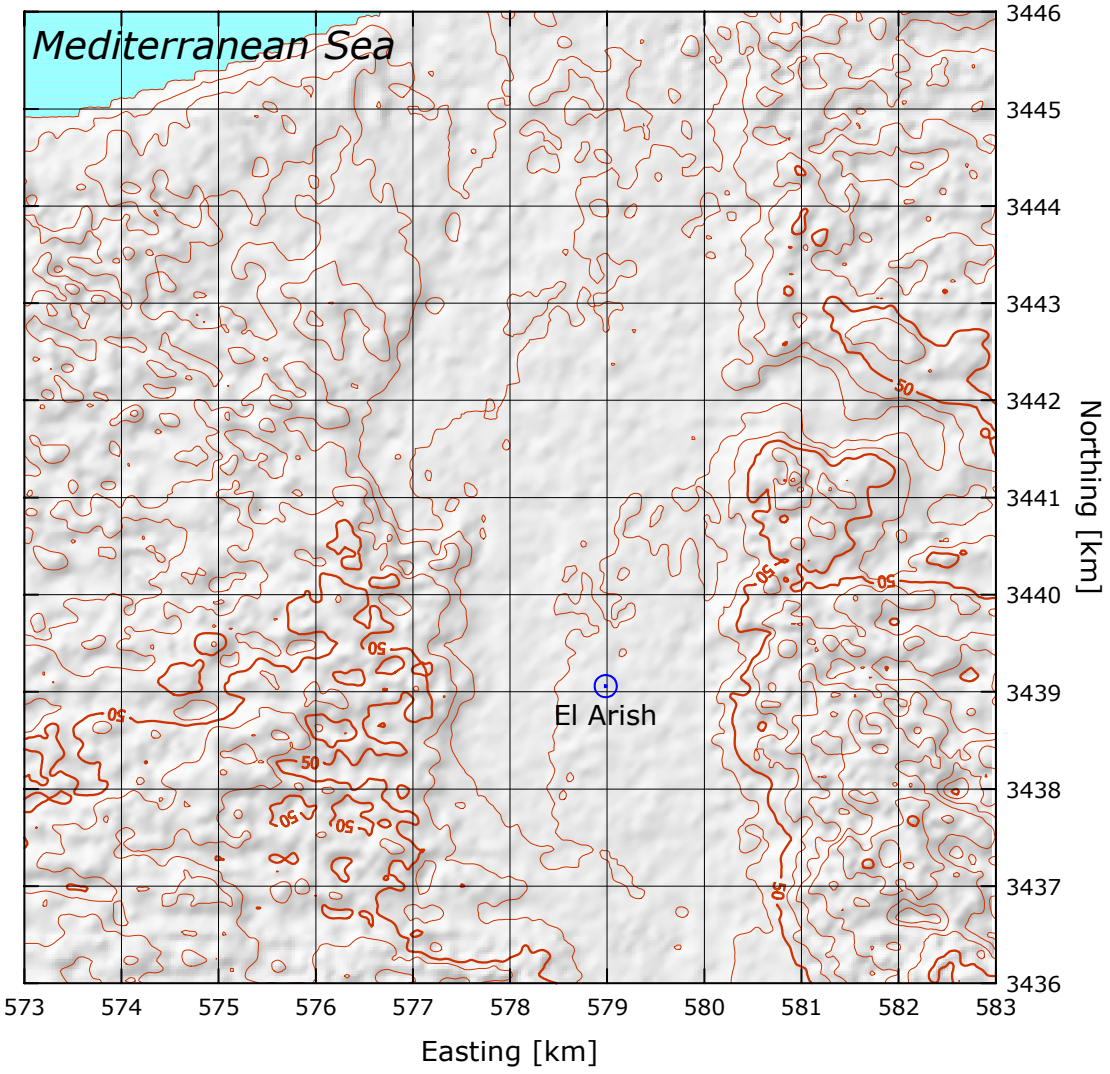

Sector	Input		Obstacles		Roughness		Orography		z_{0m}
0	0.0	0.0	−0.7	0.0	−9.6	0.0	0.2	−0.3	0.0070
30	0.0	0.0	0.0	0.0	−8.1	0.0	−0.5	−0.4	0.0050
60	0.0	0.0	−1.9	0.0	−3.4	0.0	−1.2	−0.1	0.0060
90	0.0	0.0	−2.1	0.0	0.0	0.0	−1.0	0.3	0.0050
120	0.0	0.0	−0.5	0.0	0.0	0.0	−0.3	0.4	0.0050
150	0.0	0.0	−16.7	0.0	−0.9	0.0	0.1	0.2	0.0110
180	0.0	0.0	−1.6	0.0	−1.8	0.0	0.1	−0.3	0.0130
210	0.0	0.0	0.0	0.0	−3.1	0.0	−0.6	−0.4	0.0090
240	0.0	0.0	−27.2	0.0	−6.2	0.0	−0.7	0.0	0.0090
270	0.0	0.0	−55.7	0.0	−6.6	0.0	−0.5	0.4	0.0080
300	0.0	0.0	−55.0	0.0	−10.9	0.0	0.1	0.4	0.0040
330	0.0	0.0	−32.3	0.0	−9.3	0.0	0.3	0.1	0.0080

Height of anemometer: 8.5 m a.g.l. 1995–2004

Sect	Freq	< 1	2	3	4	5	6	7	8	9	11	13	15	17	>17	*A*	*k*
0	14.0	238	113	187	213	145	78	21	3	1	0	0	0	0	0	3.3	2.09
30	6.8	242	116	180	207	127	85	32	8	1	2	0	0	0	0	3.4	1.95
60	2.3	372	189	149	141	86	49	9	2	2	0	0	0	0	0	2.3	1.39
90	2.1	425	221	151	99	47	31	17	4	2	2	0	0	0	2	2.0	0.95
120	2.2	430	218	191	84	39	25	10	2	2	0	0	0	0	0	1.9	1.27
150	10.5	369	211	229	112	53	15	7	2	1	1	0	0	0	0	2.2	1.48
180	12.8	508	199	150	69	35	18	6	5	4	3	1	0	0	0	1.6	1.02
210	6.5	495	150	108	77	68	37	24	17	5	15	2	1	1	0	1.9	0.93
240	9.0	233	113	145	131	111	83	59	44	29	36	10	5	0	0	4.0	1.41
270	8.1	216	133	164	142	113	86	52	41	27	17	5	2	0	0	3.8	1.47
300	9.3	219	124	172	165	123	94	53	25	12	12	1	0	0	0	3.7	1.67
330	16.5	144	107	234	266	149	68	24	6	2	1	0	0	0	0	3.6	2.21
Total	100.0	295	145	180	159	102	60	27	14	8	8	2	1	0	0	3.0	1.44

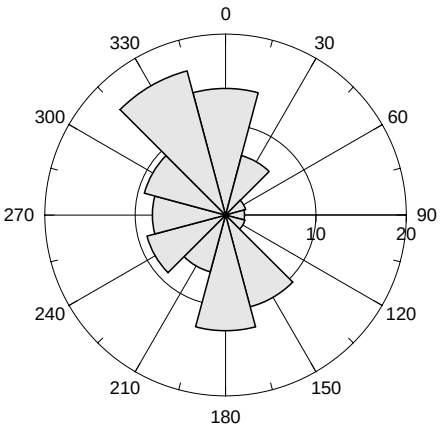

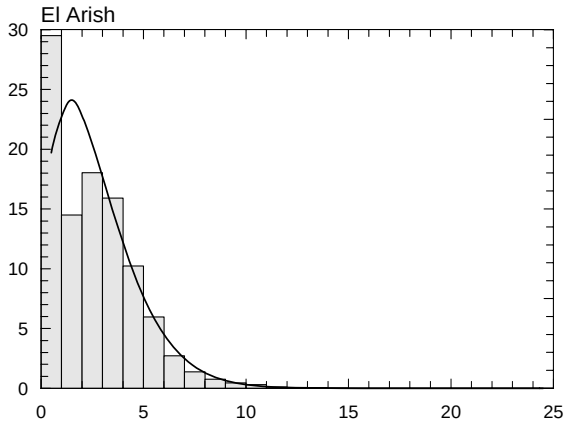

	Jan	Feb	Mar	Apr	May	Jun	Jul	Aug	Sep	Oct	Nov	Dec	Year
0	2.5	2.5	2.3	1.9	1.4	0.8	0.8	0.6	0.8	1.2	1.6	2.2	1.7
3	2.6	2.8	2.5	2.3	1.5	1.0	1.1	0.8	0.9	1.2	2.0	2.3	1.8
6	2.8	3.1	3.0	3.0	1.9	1.5	1.7	1.3	1.6	1.6	2.0	2.4	2.2
9	3.6	3.9	3.7	3.7	3.0	2.4	2.3	2.0	2.2	2.3	2.7	3.2	2.9
12	3.8	4.4	4.7	4.9	4.4	3.8	3.6	3.4	3.6	3.4	3.3	3.3	3.9
15	2.7	3.8	4.4	4.3	4.3	3.9	3.7	3.4	3.5	2.9	2.4	2.1	3.5
18	2.1	2.2	2.4	2.4	1.8	1.6	1.5	1.4	1.5	1.2	1.7	1.7	1.8
21	2.2	2.3	2.1	1.6	1.3	0.7	0.6	0.6	0.8	1.1	1.7	2.0	1.6
Mean	2.8	3.2	3.3	3.1	2.6	2.2	2.1	1.9	2.1	2.0	2.2	2.4	2.5

	Jan	Feb	Mar	Apr	May	Jun	Jul	Aug	Sep	Oct	Nov	Dec	Year
1995	2.7	4.0	3.6	3.9	3.1	2.6	2.9	2.5	2.3	1.8	2.6	1.9	2.8
1996	3.0	2.9	3.5	2.9	2.4	1.8	1.6	1.6	2.1	2.1	1.6	1.6	2.3
1997	1.9	3.5	3.1	3.0	2.5	2.1	2.1	1.8	2.0	1.9	2.1	2.6	2.4
1998	2.8	2.7	3.8	2.6	2.4	1.9	1.6	1.6	1.9	1.8	1.6	2.7	2.3
1999	2.1	2.3	2.4	2.5	1.9	2.1	1.8	1.5	1.7	1.6	1.6	1.7	1.9
2000	3.7	2.2	2.5	2.3	2.1	1.8	1.6	1.4	1.4	2.3	2.5	2.9	2.3
2001	2.5	3.1	2.6	3.2	3.5	2.7	2.4	2.1	2.0	2.0	2.8	3.0	2.7
2002	3.2	2.8	3.1	2.8	2.2	1.9	1.8	1.9	2.1	2.1	2.2	3.2	2.5
2003	2.7	4.7	4.1	3.7	2.8	2.4	2.6	2.0	2.4	2.6	2.4	3.1	3.0
2004	3.8	2.8	3.1	3.6	3.0	2.5	2.2	2.1	2.3	2.1	2.6	2.4	2.7
2005	3.4	3.7	3.4	3.2	3.0	—	—	—	—	—	—	—	—
Mean	2.8	3.2	3.3	3.1	2.6	2.2	2.1	1.9	2.1	2.0	2.2	2.4	2.5

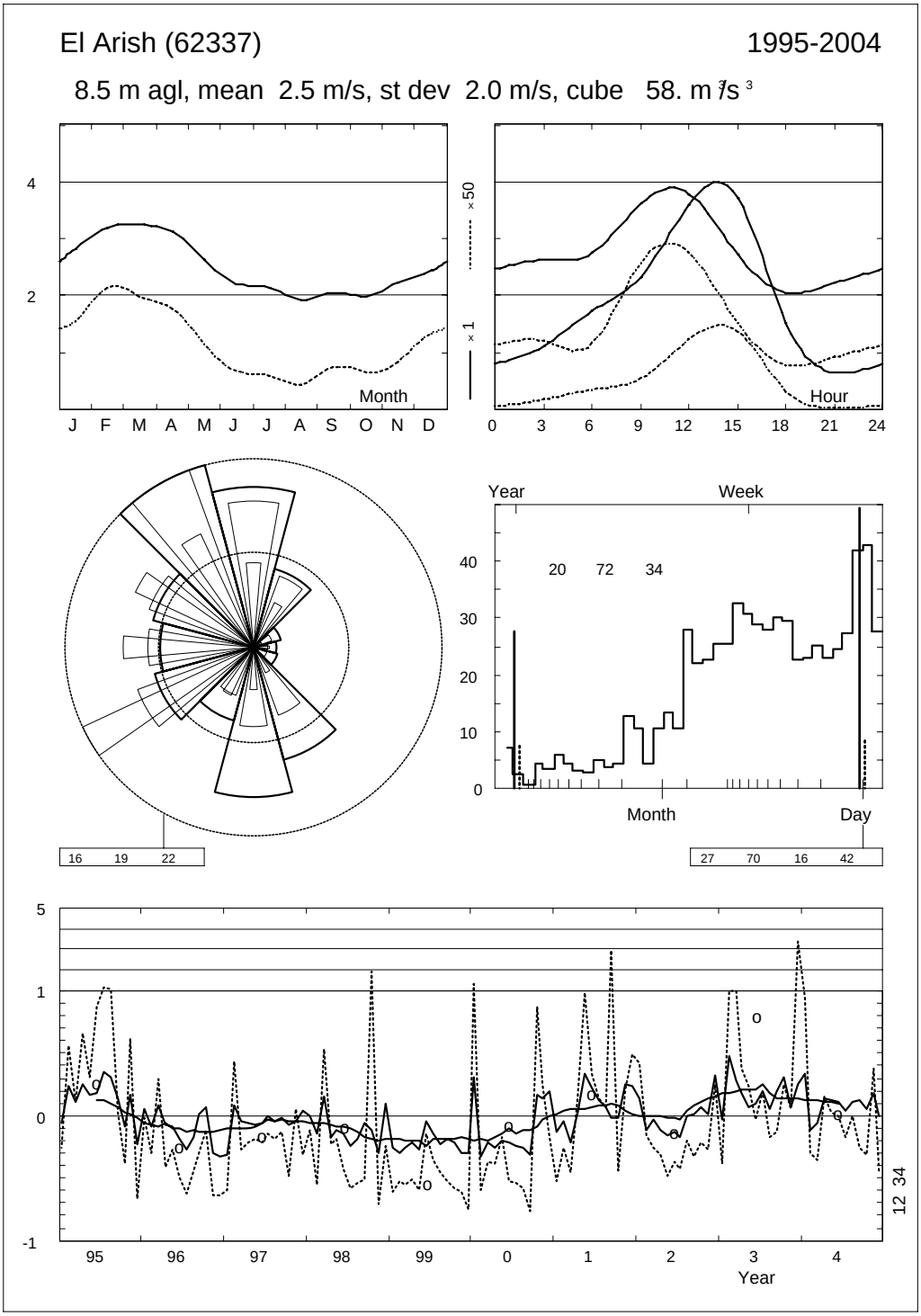
El Arish (62337)
1995-2004
8.5 m agl, mean 2.5 m/s, st dev 2.0 m/s, cube 58. m/s 3
4
2
Month
J F M A M J J A S O N D
× 50
× 1
Hour
0 3 6 9 12 15 18 21 24
Year
Week
20 72 34
40
30
20
10
0
Month
Day
16 19 22
27 70 16 42
5
1
0
-1
95 96 97 98 99 0 1 2 3 4
Year
12 34

Roughness Class 0 ($z_0 = 0.0002$ m)

z	0	30	60	90	120	150	180	210	240	270	300	330	Total
10	5.3	4.7	3.8	2.9	2.6	3.6	2.6	2.8	7.3	10.9	11.2	7.9	5.7
	2.20	2.34	1.85	1.19	1.42	1.75	1.27	1.11	1.48	1.47	1.74	2.15	1.17
25	5.8	5.2	4.2	3.2	2.9	4.0	2.9	3.0	8.0	11.9	12.2	8.7	6.2
	2.27	2.42	1.90	1.22	1.47	1.81	1.31	1.14	1.51	1.48	1.75	2.22	1.19
50	6.2	5.6	4.5	3.5	3.1	4.3	3.1	3.3	8.6	12.6	13.0	9.3	6.7
	2.33	2.48	1.95	1.25	1.51	1.85	1.34	1.17	1.54	1.49	1.77	2.28	1.21
100	6.7	6.0	4.8	3.7	3.3	4.6	3.3	3.5	9.1	13.4	13.8	10.1	7.2
	2.26	2.40	1.89	1.22	1.46	1.79	1.30	1.13	1.52	1.50	1.78	2.21	1.22
200	7.4	6.7	5.3	4.1	3.7	5.1	3.6	3.8	9.8	14.2	14.7	11.2	7.9
	2.14	2.27	1.79	1.15	1.38	1.70	1.24	1.08	1.48	1.48	1.75	2.09	1.22
Freq.	14.4	8.0	3.1	2.1	2.3	9.0	12.3	7.7	8.6	8.2	9.1	15.3	100.0

Roughness Class 1 ($z_0 = 0.0300$ m)

z	0	30	60	90	120	150	180	210	240	270	300	330	Total
10	3.3	3.3	2.2	1.8	1.9	2.4	1.6	2.2	5.6	8.4	7.5	5.1	3.9
	1.97	1.93	1.34	0.98	1.29	1.39	1.02	0.94	1.40	1.48	1.60	1.99	1.09
25	3.9	3.9	2.7	2.3	2.3	2.9	2.0	2.7	6.6	9.8	8.8	6.1	4.7
	2.13	2.09	1.45	1.05	1.39	1.50	1.09	1.01	1.45	1.50	1.63	2.15	1.13
50	4.6	4.6	3.2	2.7	2.8	3.3	2.4	3.3	7.5	10.9	9.9	7.0	5.4
	2.40	2.35	1.62	1.17	1.56	1.68	1.22	1.12	1.53	1.53	1.69	2.41	1.18
100	5.4	5.4	3.8	3.3	3.3	4.0	2.9	4.0	8.6	12.1	11.0	8.3	6.3
	2.55	2.50	1.72	1.24	1.66	1.79	1.29	1.19	1.64	1.58	1.79	2.57	1.26
200	6.7	6.7	4.7	4.0	4.1	5.0	3.5	4.8	9.9	13.4	12.4	10.4	7.6
	2.44	2.38	1.65	1.19	1.59	1.71	1.24	1.14	1.59	1.58	1.76	2.45	1.32
Freq.	13.2	6.4	2.4	2.1	3.1	10.8	12.0	6.6	8.7	8.2	10.0	16.6	100.0

Roughness Class 2 ($z_0 = 0.1000$ m)

z	0	30	60	90	120	150	180	210	240	270	300	330	Total
10	2.9	2.8	2.0	1.6	1.8	2.0	1.5	2.2	5.1	7.3	6.2	4.3	3.4
	1.93	1.90	1.33	1.01	1.33	1.35	1.02	0.98	1.39	1.50	1.54	1.94	1.10
25	3.6	3.5	2.5	2.1	2.2	2.5	1.9	2.8	6.2	8.8	7.5	5.3	4.2
	2.06	2.03	1.42	1.08	1.42	1.45	1.09	1.04	1.43	1.52	1.57	2.08	1.13
50	4.2	4.1	2.9	2.5	2.6	2.9	2.2	3.5	7.1	10.0	8.5	6.2	4.9
	2.28	2.25	1.56	1.18	1.57	1.60	1.20	1.14	1.49	1.54	1.62	2.30	1.17
100	5.0	4.9	3.5	3.0	3.2	3.5	2.7	4.2	8.2	11.2	9.7	7.4	5.8
	2.51	2.47	1.72	1.29	1.72	1.75	1.31	1.25	1.60	1.59	1.71	2.53	1.25
200	6.1	6.1	4.3	3.7	3.9	4.3	3.3	5.2	9.4	12.6	11.1	9.1	7.0
	2.40	2.36	1.64	1.24	1.65	1.68	1.25	1.20	1.57	1.61	1.71	2.42	1.31
Freq.	12.5	6.0	2.4	2.1	3.8	11.1	11.4	6.7	8.6	8.3	10.7	16.5	100.0

Roughness Class 3 ($z_0 = 0.4000$ m)

z	0	30	60	90	120	150	180	210	240	270	300	330	Total
10	2.3	2.2	1.5	1.3	1.5	1.5	1.2	2.1	4.2	5.7	4.5	3.2	2.7
	1.96	1.88	1.29	1.04	1.35	1.28	1.03	1.04	1.39	1.52	1.48	1.88	1.10
25	3.0	2.9	2.0	1.7	2.0	2.0	1.6	2.8	5.4	7.3	5.8	4.2	3.5
	2.08	1.99	1.37	1.10	1.43	1.35	1.08	1.09	1.42	1.54	1.51	1.99	1.13
50	3.6	3.5	2.5	2.1	2.4	2.4	2.0	3.5	6.5	8.6	6.9	5.1	4.2
	2.26	2.16	1.49	1.18	1.55	1.46	1.17	1.16	1.46	1.56	1.55	2.17	1.17
100	4.4	4.3	3.0	2.6	2.9	2.9	2.5	4.3	7.6	9.9	8.1	6.2	5.1
	2.57	2.46	1.69	1.34	1.76	1.66	1.32	1.31	1.53	1.60	1.63	2.47	1.24
200	5.3	5.2	3.7	3.2	3.6	3.6	3.0	5.1	8.8	11.4	9.4	7.6	6.1
	2.48	2.37	1.63	1.29	1.70	1.60	1.28	1.27	1.56	1.64	1.66	2.38	1.28
Freq.	11.6	5.4	2.3	2.2	4.9	11.5	10.5	6.9	8.4	8.5	11.6	16.3	100.0

z	Class 0		Class 1		Class 2		Class 3	
m	ms^{-1}	Wm^{-2}	ms^{-1}	Wm^{-2}	ms^{-1}	Wm^{-2}	ms^{-1}	Wm^{-2}
10	5.4	398	3.8	162	3.3	106	2.6	51
25	5.9	503	4.5	250	4.0	182	3.4	107
50	6.3	601	5.1	334	4.7	258	4.0	169
100	6.8	733	5.9	454	5.4	360	4.8	250
200	7.4	948	7.0	717	6.5	563	5.7	393

Nuweiba — Gulf of Aqaba

28° 58′ 53.2″ N 34° 41′ 06.8″ E	UTM 36 E 664 183 m N 3 207 100 m		10 m

The Nuweiba mast is situated inside the EMA met. station site, in the southeastern corner of the station site. It is situated very close to the coastline and the upwind is beach and water in the NE, E, SE and S sectors. The sandy surface is flat, homogeneous and smooth with a roughness of less than 0.01 m in all directions. There are some sheltering obstacles close to the mast: an old water desalination building is located on the western side; moreover, the main building of the EMA station is located to the north (in the main wind direction) with a height of about 5 m, and distance of about 100 m to N from the mast.

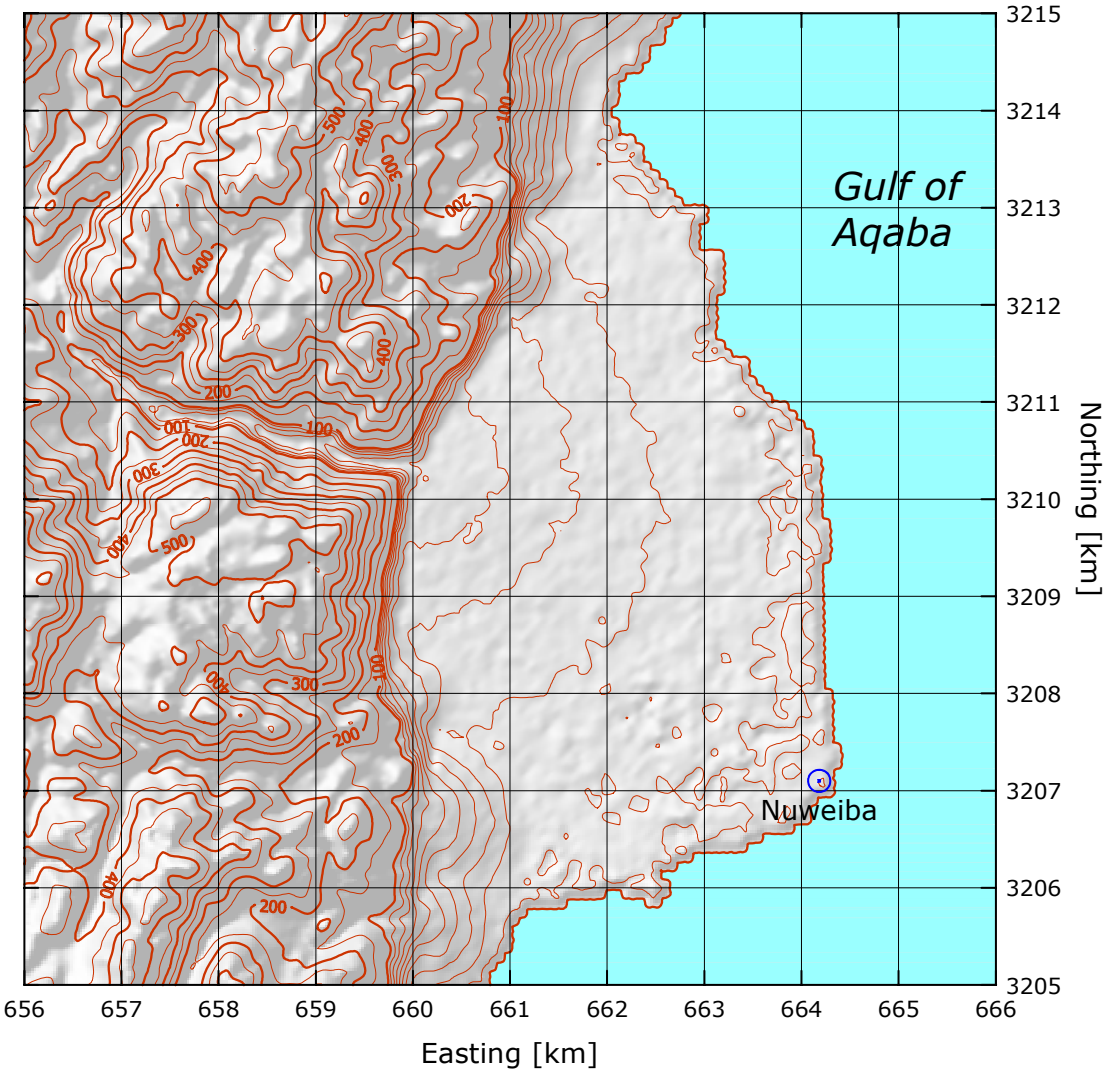

Sector	Input		Obstacles		Roughness		Orography		z_{0m}
0	0.0	0.0	0.0	0.0	−8.2	0.0	3.8	0.2	0.0010
30	0.0	0.0	0.0	0.0	0.0	0.0	2.5	−1.2	0.0000
60	0.0	0.0	0.0	0.0	0.0	0.0	−0.3	−1.5	0.0000
90	0.0	0.0	0.0	0.0	0.0	0.0	−2.1	−0.2	0.0000
120	0.0	0.0	0.0	0.0	0.0	0.0	−1.1	1.2	0.0000
150	0.0	0.0	0.0	0.0	0.0	0.0	1.6	1.4	0.0000
180	0.0	0.0	0.0	0.0	0.0	0.0	3.3	0.2	0.0000
210	0.0	0.0	0.0	0.0	2.7	0.0	2.5	−1.3	0.0010
240	0.0	0.0	0.0	0.0	−0.7	0.0	−0.6	−1.7	0.0040
270	0.0	0.0	0.0	0.0	−0.8	0.0	−2.7	−0.2	0.0060
300	0.0	0.0	0.0	0.0	−0.2	0.0	−1.4	1.5	0.0060
330	0.0	0.0	0.0	0.0	−6.6	0.0	1.8	1.8	0.0110

Height of anemometer: 24.5 m a.g.l. 2004-05

Sect	Freq	< 1	2	3	4	5	6	7	8	9	11	13	15	17	>17	*A*	*k*
0	15.6	5	30	80	184	259	243	126	49	17	8	0	0	0	0	5.3	3.34
30	28.0	3	21	60	151	239	214	153	87	41	27	4	0	0	0	5.8	2.84
60	29.8	3	19	60	101	130	153	161	132	110	105	25	1	0	0	7.0	2.92
90	4.4	91	302	206	103	89	71	45	49	20	22	3	0	0	0	3.3	1.29
120	0.9	147	403	305	80	34	26	5	0	0	0	0	0	0	0	2.3	1.75
150	0.4	96	275	356	179	64	27	3	0	0	0	0	0	0	0	2.8	2.26
180	0.8	39	241	304	155	115	66	23	14	14	25	4	0	0	0	3.3	1.36
210	3.2	42	172	138	57	35	34	39	51	74	199	113	36	9	0	7.7	2.02
240	0.9	71	205	210	85	49	58	75	56	61	79	50	0	0	0	4.8	1.39
270	0.4	91	345	175	134	99	79	26	26	15	9	0	0	0	0	3.1	1.43
300	1.6	33	150	135	63	117	157	119	86	68	57	15	1	0	0	5.9	2.30
330	13.9	5	24	34	42	84	163	215	225	137	69	2	0	0	0	7.2	4.55
Total	100.0	12	51	77	119	167	174	146	109	71	59	13	1	0	0	6.2	2.58

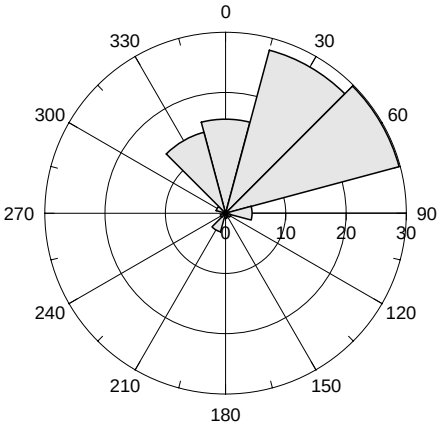

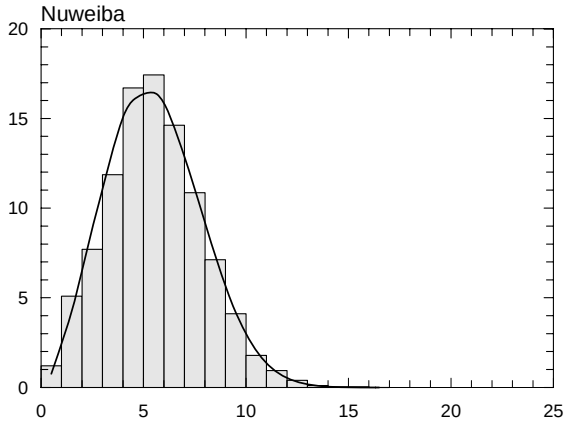

	Jan	Feb	Mar	Apr	May	Jun	Jul	Aug	Sep	Oct	Nov	Dec	Year
0	5.1	5.2	6.1	6.0	6.1	4.4	—	5.4	5.4	4.8	5.0	5.9	5.5
1	5.3	5.6	6.1	6.0	5.7	—	—	4.8	5.8	5.4	5.3	5.9	5.6
2	5.6	5.7	6.2	5.8	5.9	—	—	5.2	5.7	5.0	5.5	6.3	5.7
3	5.6	5.8	6.2	5.9	5.6	—	—	5.1	6.1	5.1	5.7	6.3	5.8
4	5.4	5.6	6.3	6.1	5.9	—	—	4.7	5.9	5.6	5.7	6.5	5.8
5	6.0	5.2	6.4	6.3	5.6	—	—	4.7	5.9	5.7	6.0	6.7	5.9
6	6.0	5.6	6.3	6.0	5.4	—	—	4.9	6.0	5.7	5.9	6.7	5.9
7	6.2	5.7	5.8	6.2	6.2	—	—	5.6	6.4	6.2	6.4	6.6	6.2
8	6.3	5.8	5.9	6.8	6.3	—	—	6.5	7.8	6.3	5.7	6.3	6.4
9	5.1	5.4	5.7	6.8	6.3	—	—	6.7	8.0	6.9	5.2	5.6	6.2
10	4.1	5.1	5.9	6.3	5.4	—	—	6.2	7.4	6.7	5.0	5.1	5.7
11	4.1	5.9	6.0	5.7	4.5	—	—	5.2	6.4	5.9	5.2	5.3	5.4
12	4.2	5.4	6.1	4.9	4.3	—	—	4.6	5.3	5.0	4.9	5.5	5.0
13	4.5	5.4	6.3	4.5	3.7	—	—	4.2	4.8	4.2	4.4	5.3	4.7
14	4.3	5.2	5.9	4.7	3.8	—	—	3.9	4.6	4.0	4.3	5.4	4.6
15	4.6	5.6	6.2	5.0	3.9	—	—	4.0	4.8	4.0	4.2	5.3	4.7
16	4.5	5.7	6.7	5.3	3.9	—	—	4.3	4.9	4.1	4.3	5.4	4.9
17	4.7	6.1	7.4	6.5	4.5	—	—	4.7	5.2	4.3	4.6	5.8	5.4
18	4.7	6.2	7.3	6.6	4.7	—	—	5.0	5.6	4.6	4.8	6.6	5.6
19	4.6	5.9	7.3	6.7	5.3	—	—	5.5	6.2	4.8	4.9	6.7	5.8
20	5.2	5.8	6.4	5.7	5.0	—	—	4.9	5.8	4.8	4.4	6.5	5.5
21	5.5	5.4	5.5	5.7	5.5	—	—	4.3	5.6	4.6	4.7	5.7	5.3
22	5.5	5.3	6.1	5.7	5.9	—	—	4.3	5.5	4.4	5.0	5.4	5.3
23	5.2	5.2	6.3	5.4	6.4	—	—	4.7	5.5	4.9	5.1	5.6	5.5
Mean	5.1	5.6	6.3	5.9	5.2	—	—	5.0	5.9	5.1	5.1	5.9	5.5

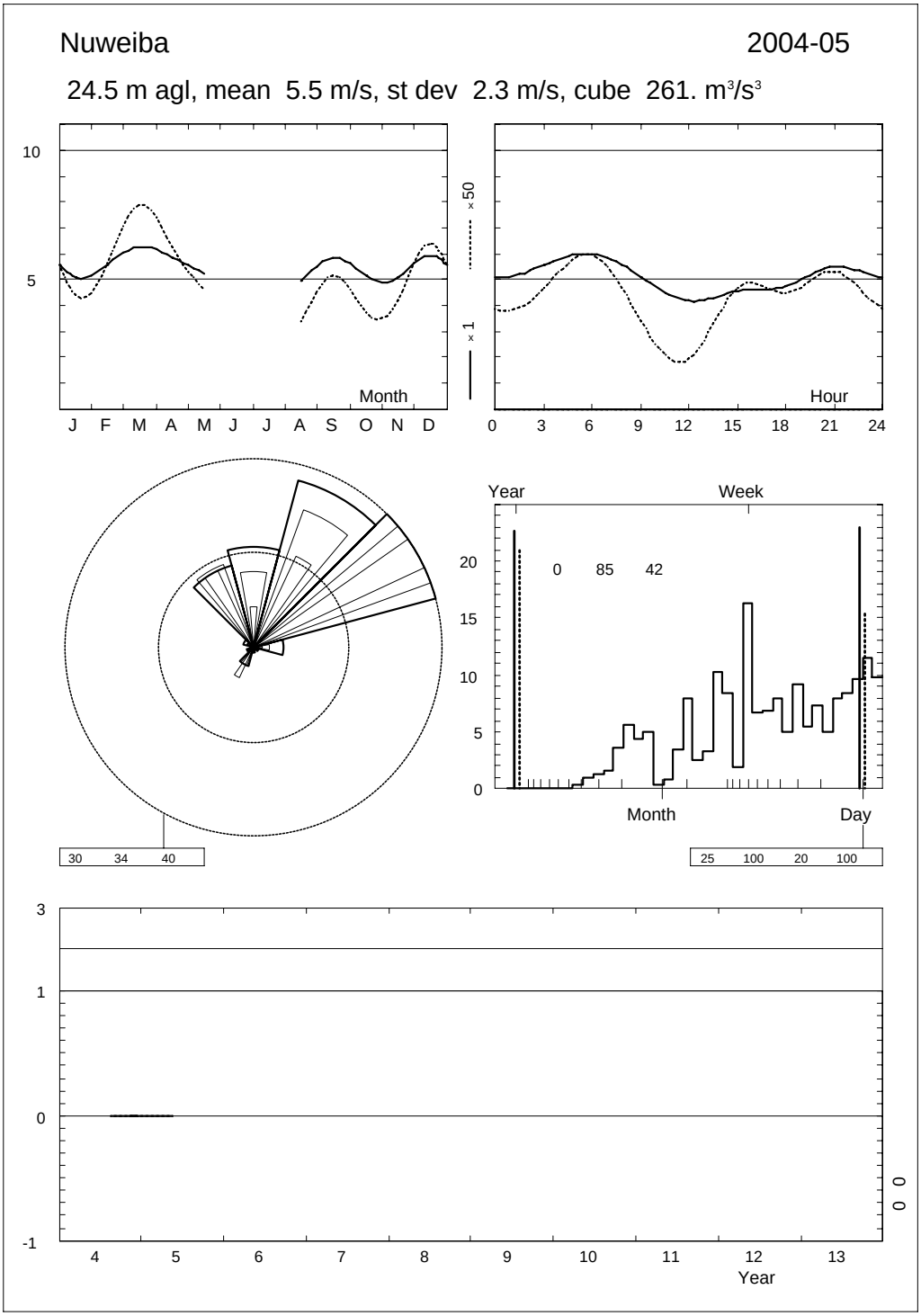

	Jan	Feb	Mar	Apr	May	Jun	Jul	Aug	Sep	Oct	Nov	Dec	Year
2004	—	—	—	—	—	—	—	5.0	5.9	5.1	5.1	5.9	5.4
2005	5.1	5.6	6.3	5.9	5.2	—	—	—	—	—	—	—	5.6
Mean	5.1	5.6	6.3	5.9	5.2	—	—	5.0	5.9	5.1	5.1	5.9	5.5

Roughness Class 0 ($z_0 = 0.0002$ m)

z	0	30	60	90	120	150	180	210	240	270	300	330	Total
10	5.6	5.2	6.4	4.6	2.4	2.5	3.0	7.1	5.9	4.0	7.0	8.5	6.1
	2.99	2.74	2.72	1.71	1.22	1.95	1.34	2.01	1.62	1.43	3.02	4.73	2.41
25	6.1	5.7	7.0	5.1	2.6	2.8	3.3	7.8	6.5	4.4	7.7	9.3	6.7
	3.08	2.83	2.81	1.76	1.26	2.01	1.38	2.07	1.67	1.48	3.12	4.88	2.47
50	6.5	6.2	7.5	5.4	2.8	3.0	3.5	8.4	7.0	4.7	8.2	9.9	7.2
	3.17	2.90	2.88	1.80	1.29	2.07	1.42	2.13	1.71	1.51	3.20	5.01	2.52
100	7.1	6.7	8.1	5.9	3.0	3.2	3.8	9.1	7.6	5.1	9.0	10.8	7.8
	3.06	2.81	2.79	1.75	1.25	2.00	1.37	2.06	1.65	1.47	3.10	4.85	2.46
200	7.8	7.4	9.0	6.5	3.3	3.6	4.2	10.0	8.3	5.6	9.9	12.0	8.6
	2.90	2.66	2.64	1.65	1.19	1.90	1.30	1.95	1.57	1.39	2.93	4.60	2.36
Freq.	14.8	26.4	30.0	6.6	1.2	0.5	0.8	2.9	1.1	0.5	2.2	12.9	100.0

Roughness Class 1 ($z_0 = 0.0300$ m)

z	0	30	60	90	120	150	180	210	240	270	300	330	Total
10	3.8	3.8	4.5	2.5	1.6	1.8	2.6	4.9	3.7	3.8	5.5	5.6	4.2
	2.61	2.13	2.29	1.19	1.50	1.31	0.95	1.67	1.28	1.69	3.18	3.34	2.09
25	4.5	4.5	5.3	3.1	1.9	2.2	3.2	5.9	4.5	4.6	6.5	6.7	5.1
	2.82	2.30	2.47	1.28	1.62	1.41	1.01	1.81	1.38	1.82	3.43	3.61	2.23
50	5.2	5.2	6.1	3.6	2.2	2.6	3.8	6.8	5.3	5.3	7.5	7.7	5.9
	3.17	2.59	2.78	1.43	1.81	1.58	1.13	2.03	1.55	2.04	3.86	4.05	2.46
100	6.1	6.2	7.3	4.4	2.6	3.1	4.6	8.1	6.4	6.3	8.9	9.1	7.0
	3.37	2.76	2.96	1.52	1.93	1.68	1.20	2.16	1.65	2.18	4.10	4.31	2.59
200	7.6	7.7	9.1	5.4	3.2	3.8	5.6	10.1	7.9	7.8	11.1	11.3	8.7
	3.22	2.63	2.83	1.45	1.85	1.60	1.15	2.06	1.58	2.08	3.92	4.12	2.49
Freq.	17.2	27.4	25.8	4.4	0.8	0.5	1.2	2.7	0.9	0.8	4.2	14.1	100.0

Roughness Class 2 ($z_0 = 0.1000$ m)

z	0	30	60	90	120	150	180	210	240	270	300	330	Total
10	3.3	3.4	3.9	2.2	1.4	1.7	2.5	4.3	3.2	3.6	4.8	4.7	3.7
	2.60	2.16	2.26	1.17	1.56	1.33	1.01	1.67	1.26	1.85	3.30	3.03	2.10
25	4.0	4.2	4.8	2.7	1.8	2.1	3.2	5.3	4.0	4.4	6.0	5.8	4.6
	2.78	2.31	2.41	1.24	1.67	1.42	1.07	1.79	1.35	1.98	3.54	3.24	2.22
50	4.7	4.9	5.6	3.2	2.1	2.5	3.9	6.2	4.7	5.2	6.9	6.8	5.3
	3.08	2.56	2.67	1.37	1.85	1.57	1.17	1.98	1.49	2.19	3.91	3.59	2.42
100	5.6	5.8	6.6	3.9	2.5	3.0	4.7	7.4	5.7	6.2	8.2	8.0	6.4
	3.38	2.81	2.94	1.50	2.03	1.72	1.28	2.18	1.63	2.41	4.29	3.94	2.62
200	6.9	7.2	8.2	4.8	3.0	3.7	5.7	9.1	7.0	7.6	10.2	9.9	7.9
	3.24	2.69	2.81	1.44	1.94	1.65	1.23	2.08	1.56	2.31	4.11	3.77	2.53
Freq.	18.3	27.7	23.7	4.0	0.8	0.6	1.4	2.5	0.9	0.9	5.1	14.3	100.0

Roughness Class 3 ($z_0 = 0.4000$ m)

z	0	30	60	90	120	150	180	210	240	270	300	330	Total
10	2.6	2.7	3.0	1.7	1.1	1.4	2.3	3.3	2.5	3.0	3.9	3.5	2.9
	2.56	2.12	2.19	1.20	1.52	1.44	1.12	1.67	1.26	1.98	3.37	2.72	2.09
25	3.4	3.6	4.0	2.3	1.5	1.9	3.1	4.4	3.3	3.9	5.1	4.6	3.8
	2.72	2.25	2.32	1.27	1.61	1.52	1.18	1.77	1.33	2.10	3.58	2.89	2.20
50	4.1	4.3	4.8	2.8	1.8	2.3	3.8	5.3	4.0	4.7	6.1	5.6	4.6
	2.96	2.44	2.52	1.37	1.74	1.65	1.27	1.92	1.44	2.28	3.88	3.14	2.37
100	4.9	5.2	5.7	3.5	2.2	2.8	4.7	6.5	4.9	5.6	7.3	6.7	5.6
	3.37	2.78	2.87	1.56	1.99	1.87	1.44	2.19	1.64	2.60	4.42	3.58	2.65
200	6.0	6.4	7.0	4.3	2.7	3.4	5.7	7.9	6.0	6.9	8.9	8.2	6.8
	3.24	2.68	2.77	1.51	1.91	1.81	1.39	2.11	1.58	2.50	4.26	3.45	2.56
Freq.	19.8	28.0	20.7	3.4	0.7	0.6	1.7	2.3	0.8	1.2	6.4	14.5	100.0

z	Class 0		Class 1		Class 2		Class 3	
m	ms^{-1}	Wm^{-2}	ms^{-1}	Wm^{-2}	ms^{-1}	Wm^{-2}	ms^{-1}	Wm^{-2}
10	5.4	157	3.8	60	3.3	39	2.6	19
25	5.9	202	4.5	96	4.0	70	3.4	42
50	6.4	247	5.2	138	4.7	106	4.1	70
100	6.9	321	6.2	223	5.7	169	5.0	113
200	7.6	447	7.7	441	7.0	325	6.1	210

Nabq

Gulf of Aqaba

28° 07′ 45.2″ N 34° 25′ 46.3″ E	UTM 36 E 640 395 m N 3 112 343 m		15 m

The Nabq mast is situated inside the Nabq restricted area after permission from EEAA in Sharm El-Sheikh. It is easy to enter the site from the south, north of the city of Sharm El-Sheikh. The mast is close to a small village called El-Gharghana, and near to an existing old NRG met. mast. The sandy surface is flat, homogeneous and smooth with a roughness length of about 0.01 m or less in all directions. There are no sheltering obstacles close to the mast, but a series of small hills (dunes) are located to the NW and N at a distance of about 700 m and a height of about 30 m.

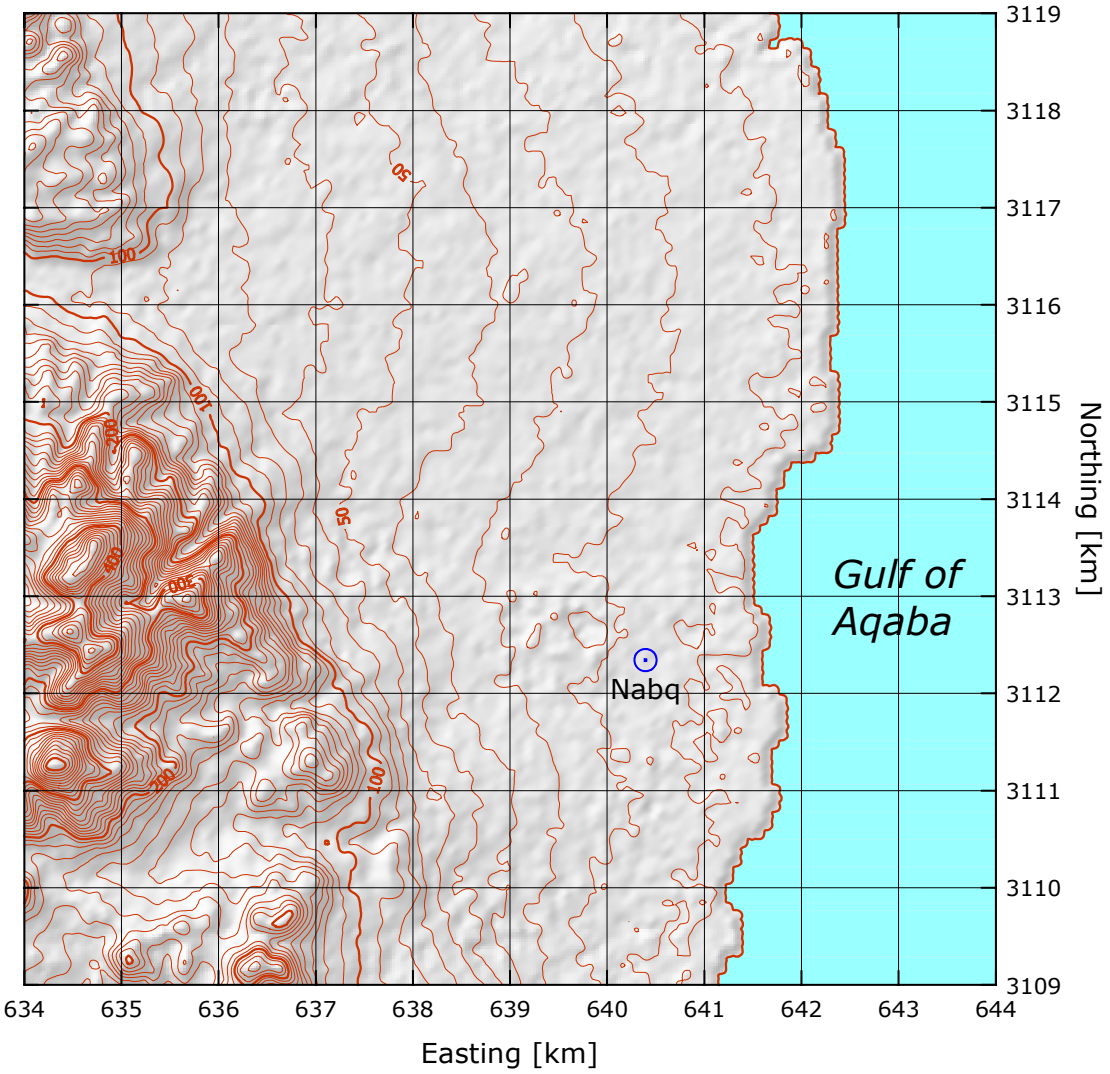

Sector	Input		Obstacles		Roughness		Orography		z_{0m}
0	0.0	0.0	0.0	0.0	−9.1	0.0	−0.5	−0.3	0.0040
30	0.0	0.0	0.0	0.0	−8.5	0.0	−1.5	−0.9	0.0010
60	0.0	0.0	0.0	0.0	−5.2	0.0	−2.9	−0.6	0.0000
90	0.0	0.0	0.0	0.0	−5.3	0.0	−3.3	0.2	0.0000
120	0.0	0.0	0.0	0.0	−7.1	0.0	−2.3	0.8	0.0000
150	0.0	0.0	0.0	0.0	−7.8	0.0	−0.8	0.6	0.0000
180	0.0	0.0	0.0	0.0	−2.3	0.0	−0.4	−0.3	0.0030
210	0.0	0.0	0.0	0.0	2.9	0.0	−1.8	−1.1	0.0120
240	0.0	0.0	0.0	0.0	3.8	0.0	−3.9	−0.9	0.0180
270	0.0	0.0	0.0	0.0	4.0	0.0	−4.4	0.3	0.0180
300	0.0	0.0	0.0	0.0	2.8	0.0	−2.9	1.2	0.0170
330	0.0	0.0	0.0	0.0	−3.9	0.0	−0.9	0.8	0.0110

Height of anemometer: 24.5 m a.g.l. 2004-05

Sect	Freq	< 1	2	3	4	5	6	7	8	9	11	13	15	17	>17	*A*	*k*
0	36.9	3	14	39	54	74	97	120	127	125	206	97	38	7	0	8.8	2.97
30	27.9	6	16	23	34	51	58	60	68	76	230	263	97	17	1	10.7	4.28
60	3.4	65	168	195	282	196	69	13	6	4	2	0	0	0	0	3.7	2.67
90	1.1	42	190	325	365	70	4	1	3	0	0	0	0	0	0	3.1	3.34
120	1.2	58	112	217	309	148	95	39	12	10	0	0	0	0	0	3.9	2.36
150	2.0	43	111	108	150	165	163	104	75	32	37	11	0	0	0	5.3	2.20
180	1.6	54	137	167	202	181	141	58	33	8	10	8	0	0	0	4.4	2.07
210	0.8	58	287	223	120	85	79	82	25	28	13	0	0	0	0	3.5	1.44
240	1.3	67	172	176	200	114	71	86	61	27	19	3	5	0	0	4.2	1.56
270	1.4	68	295	257	126	62	45	47	39	22	30	3	4	0	0	3.1	1.16
300	4.6	32	141	177	302	244	83	17	3	0	1	0	0	0	0	3.9	3.15
330	17.9	8	42	121	249	319	177	56	19	6	3	0	0	0	0	4.7	3.45
Total	100.0	13	46	76	117	128	99	78	73	70	142	109	41	7	0	7.7	2.04

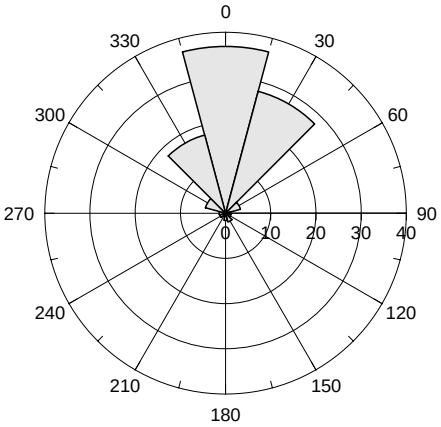

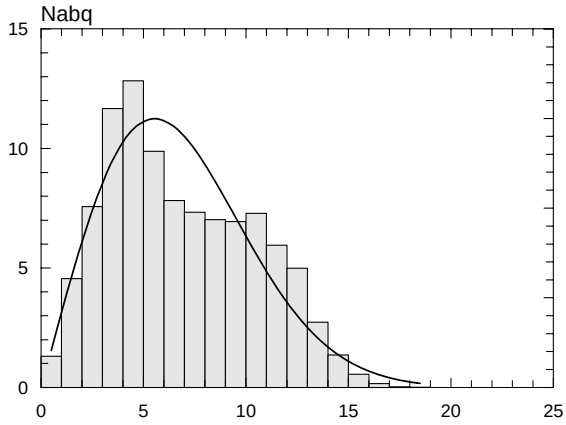

	Jan	Feb	Mar	Apr	May	Jun	Jul	Aug	Sep	Oct	Nov	Dec	Year
0	4.9	6.4	8.4	7.5	7.5	8.6	8.0	7.2	8.0	5.8	6.0	6.9	7.1
1	5.0	6.6	8.8	7.3	7.9	9.1	8.8	7.5	7.7	6.1	6.1	6.9	7.3
2	4.8	6.4	8.7	7.8	8.3	9.2	8.3	8.2	8.2	6.7	6.3	6.8	7.5
3	4.9	6.2	8.8	8.3	8.2	9.1	8.1	7.9	8.1	7.1	6.1	6.5	7.5
4	4.5	6.0	8.5	8.1	8.2	8.4	7.9	7.9	8.0	7.0	6.2	7.0	7.3
5	4.6	6.2	8.6	8.0	8.1	8.5	7.4	7.7	8.1	7.0	6.3	7.0	7.3
6	4.6	5.9	8.9	8.0	8.1	8.6	7.3	7.2	8.1	7.2	5.9	7.4	7.3
7	4.4	5.9	9.2	8.5	8.7	9.3	8.3	8.6	9.2	7.2	5.5	7.6	7.7
8	4.3	6.3	9.5	9.1	8.9	9.8	9.4	9.7	10.4	8.6	5.8	7.8	8.3
9	5.2	6.8	9.8	9.1	8.8	9.6	9.2	9.8	10.5	9.1	6.8	8.0	8.6
10	5.8	7.6	9.6	8.8	8.1	9.2	9.1	9.3	10.2	8.8	7.1	8.1	8.5
11	6.2	7.8	9.1	8.2	7.5	8.6	8.5	8.3	9.3	8.3	6.9	8.0	8.1
12	5.6	7.4	8.9	7.4	7.0	8.0	7.5	7.7	8.1	7.3	6.7	7.7	7.4
13	5.7	7.0	8.4	7.0	6.4	7.5	7.3	7.1	7.7	6.6	6.2	7.4	7.0
14	5.7	6.6	7.5	6.6	6.1	6.9	6.7	6.4	7.4	6.0	6.2	6.6	6.6
15	5.2	6.4	7.3	6.1	5.9	6.1	6.0	5.7	6.8	5.3	5.8	6.3	6.1
16	4.8	6.5	7.6	5.8	5.6	5.4	4.9	5.1	5.7	4.3	5.2	5.9	5.5
17	4.6	6.1	6.9	5.6	5.0	4.7	4.5	4.2	4.5	3.7	5.6	6.2	5.1
18	5.0	5.7	6.5	5.9	4.3	4.5	4.0	3.4	4.1	3.6	5.4	6.1	4.8
19	4.4	5.6	6.7	6.2	4.4	4.4	3.9	3.7	4.8	3.7	5.5	5.8	4.9
20	4.5	5.8	7.0	6.3	4.4	5.2	4.4	4.4	5.7	4.1	5.7	6.0	5.3
21	4.7	6.9	7.3	6.6	5.2	6.0	5.8	5.4	6.0	5.0	5.9	5.9	5.9
22	4.7	6.5	8.0	7.1	6.5	6.6	6.4	6.0	6.4	5.8	5.8	6.0	6.3
23	5.1	6.4	8.2	7.7	6.7	7.3	7.6	6.3	7.7	5.9	6.0	5.8	6.7
Mean	5.0	6.4	8.3	7.4	6.9	7.5	7.1	6.9	7.5	6.3	6.0	6.8	6.8

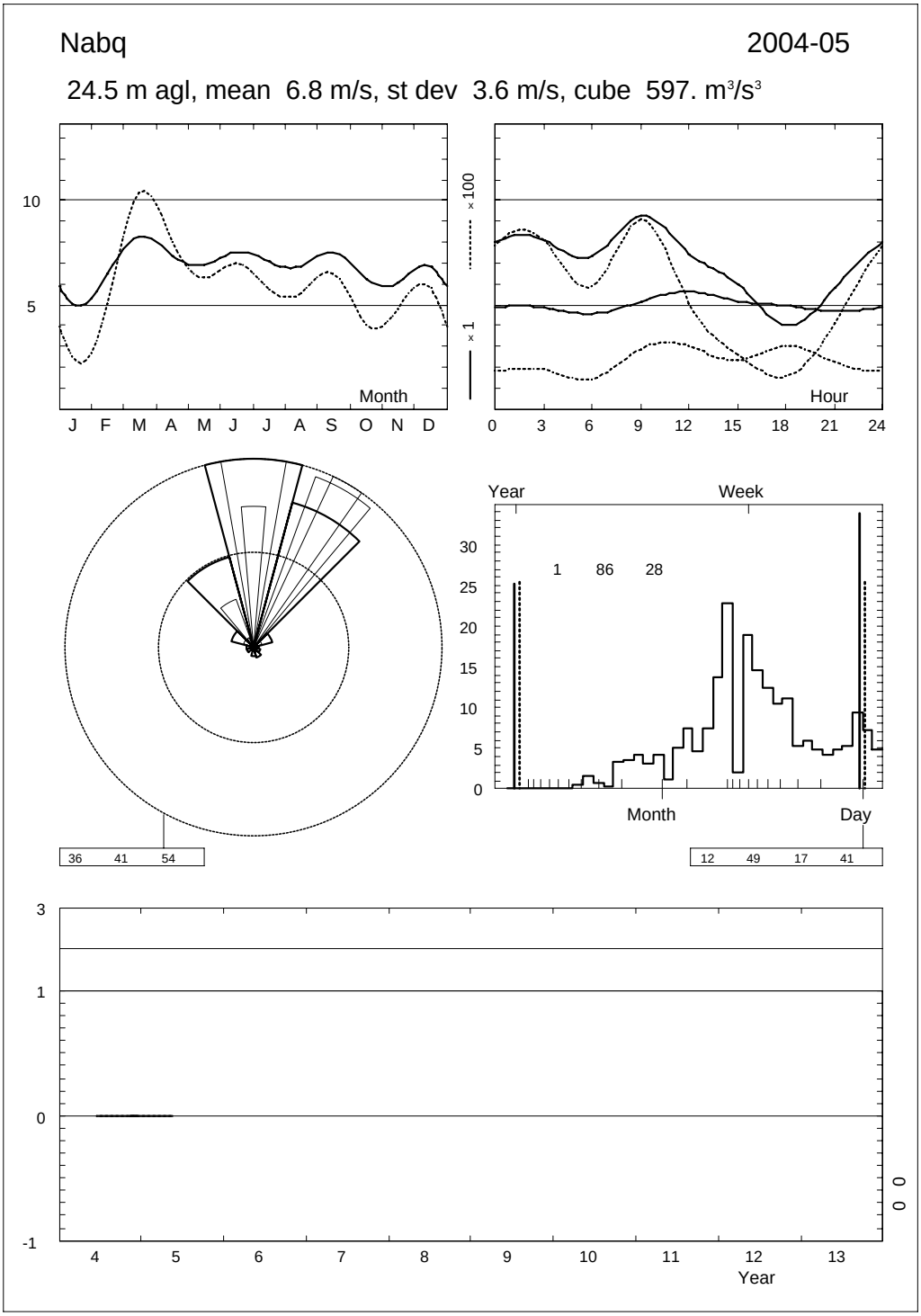

	Jan	Feb	Mar	Apr	May	Jun	Jul	Aug	Sep	Oct	Nov	Dec	Year
2004	—	—	—	—	—	7.5	7.1	6.9	7.5	6.3	6.0	6.8	6.9
2005	5.0	6.4	8.3	7.4	6.9	—	—	—	—	—	—	—	6.8
Mean	5.0	6.4	8.3	7.4	6.9	7.5	7.1	6.9	7.5	6.3	6.0	6.8	6.8

Roughness Class 0 ($z_0 = 0.0002$ m)

z	0	30	60	90	120	150	180	210	240	270	300	330	Total
10	10.2	11.4	7.4	3.6	4.0	5.4	4.8	4.2	4.9	4.1	4.7	5.6	8.9
	3.06	3.94	1.57	1.52	2.13	2.07	2.21	1.74	1.76	1.41	3.13	3.20	2.26
25	11.1	12.4	8.1	4.0	4.3	5.9	5.3	4.6	5.4	4.4	5.1	6.1	9.8
	3.13	4.03	1.61	1.56	2.19	2.13	2.28	1.79	1.82	1.46	3.23	3.30	2.29
50	11.9	13.3	8.7	4.3	4.7	6.3	5.7	5.0	5.8	4.8	5.5	6.6	10.4
	3.22	4.13	1.65	1.60	2.25	2.19	2.34	1.84	1.87	1.49	3.31	3.38	2.33
100	12.8	14.3	9.3	4.7	5.1	6.8	6.2	5.4	6.3	5.2	5.9	7.2	11.3
	3.14	4.04	1.62	1.55	2.18	2.12	2.26	1.79	1.81	1.45	3.21	3.28	2.31
200	14.1	15.6	10.1	5.1	5.6	7.6	6.8	5.9	6.9	5.7	6.6	7.9	12.3
	3.00	3.90	1.55	1.47	2.06	2.01	2.14	1.69	1.71	1.37	3.04	3.10	2.26
Freq.	34.0	28.9	6.6	1.5	1.2	1.9	1.6	0.9	1.2	1.5	4.6	16.2	100.0

Roughness Class 1 ($z_0 = 0.0300$ m)

z	0	30	60	90	120	150	180	210	240	270	300	330	Total
10	7.4	8.1	2.8	2.3	2.9	3.7	3.3	2.9	3.3	3.0	3.5	4.3	6.2
	2.80	3.54	1.01	2.21	1.60	1.75	1.82	1.40	1.44	1.44	2.72	1.64	2.01
25	8.7	9.6	3.4	2.8	3.5	4.5	3.9	3.5	4.0	3.6	4.2	5.2	7.4
	2.97	3.73	1.08	2.38	1.73	1.88	1.96	1.51	1.55	1.55	2.94	1.77	2.10
50	9.9	10.8	4.1	3.2	4.1	5.2	4.5	4.1	4.7	4.2	4.8	6.1	8.4
	3.25	4.03	1.21	2.68	1.94	2.12	2.21	1.69	1.74	1.74	3.31	1.99	2.24
100	11.6	12.5	4.9	3.8	4.8	6.2	5.4	4.9	5.6	5.0	5.7	7.2	9.8
	3.49	4.33	1.28	2.85	2.07	2.26	2.35	1.80	1.85	1.85	3.52	2.12	2.36
200	14.0	14.9	6.0	4.8	6.0	7.7	6.7	6.1	6.9	6.2	7.1	8.9	11.9
	3.35	4.18	1.22	2.72	1.97	2.15	2.24	1.72	1.77	1.77	3.36	2.02	2.34
Freq.	35.0	25.2	3.7	1.2	1.3	1.9	1.4	0.9	1.3	2.0	6.6	19.6	100.0

Roughness Class 2 ($z_0 = 0.1000$ m)

z	0	30	60	90	120	150	180	210	240	270	300	330	Total
10	6.5	7.0	2.4	2.1	2.7	3.2	2.8	2.6	2.8	2.7	3.1	4.0	5.4
	2.85	3.48	1.01	2.09	1.67	1.74	1.81	1.44	1.40	1.61	2.59	1.53	1.99
25	7.9	8.5	3.0	2.6	3.3	4.0	3.5	3.2	3.5	3.3	3.9	4.9	6.6
	3.00	3.64	1.07	2.23	1.78	1.87	1.94	1.53	1.50	1.72	2.78	1.63	2.06
50	9.1	9.8	3.7	3.1	3.9	4.7	4.1	3.8	4.2	3.9	4.5	5.8	7.6
	3.24	3.90	1.18	2.47	1.97	2.06	2.15	1.69	1.65	1.90	3.07	1.80	2.19
100	10.7	11.4	4.4	3.7	4.7	5.6	4.9	4.6	5.0	4.7	5.4	6.9	9.0
	3.56	4.28	1.29	2.72	2.17	2.26	2.36	1.86	1.81	2.09	3.38	1.98	2.34
200	12.9	13.6	5.4	4.5	5.8	6.9	6.1	5.7	6.1	5.8	6.6	8.6	10.8
	3.43	4.13	1.24	2.60	2.07	2.17	2.26	1.78	1.74	2.00	3.23	1.89	2.31
Freq.	34.3	23.4	3.5	1.2	1.4	1.9	1.4	0.9	1.3	2.3	7.7	20.9	100.0

Roughness Class 3 ($z_0 = 0.4000$ m)

z	0	30	60	90	120	150	180	210	240	270	300	330	Total
10	5.1	5.4	1.9	1.7	2.2	2.5	2.2	2.1	2.2	2.2	2.5	3.6	4.2
	2.92	3.39	1.04	1.78	1.61	1.70	1.74	1.42	1.37	1.81	2.71	1.72	2.03
25	6.7	7.1	2.6	2.2	2.9	3.3	2.9	2.8	2.9	2.9	3.3	4.7	5.5
	3.05	3.53	1.09	1.88	1.70	1.80	1.85	1.50	1.45	1.92	2.87	1.82	2.10
50	8.0	8.4	3.2	2.7	3.5	4.0	3.5	3.4	3.5	3.5	4.0	5.7	6.6
	3.25	3.74	1.18	2.04	1.85	1.96	2.01	1.63	1.57	2.08	3.12	1.97	2.21
100	9.5	9.9	4.0	3.2	4.2	4.8	4.3	4.1	4.2	4.2	4.8	6.9	7.9
	3.62	4.13	1.33	2.33	2.10	2.23	2.28	1.85	1.79	2.37	3.56	2.25	2.39
200	11.4	11.9	4.8	3.9	5.2	5.8	5.2	5.0	5.2	5.1	5.9	8.4	9.5
	3.55	4.08	1.29	2.24	2.03	2.15	2.20	1.79	1.72	2.28	3.43	2.17	2.38
Freq.	33.3	20.8	3.1	1.2	1.5	1.8	1.3	0.9	1.4	2.7	9.2	22.8	100.0

z	Class 0		Class 1		Class 2		Class 3	
m	ms^{-1}	Wm^{-2}	ms^{-1}	Wm^{-2}	ms^{-1}	Wm^{-2}	ms^{-1}	Wm^{-2}
10	7.9	518	5.5	191	4.7	126	3.7	60
25	8.6	667	6.5	308	5.8	223	4.9	131
50	9.3	808	7.5	438	6.8	333	5.9	217
100	10.0	1019	8.7	666	8.0	512	7.0	347
200	10.9	1358	10.5	1191	9.6	909	8.5	608

Katamaya

Gulf of Suez

29° 54′ 21.2″ N 31° 46′ 08.4″ E	UTM 36 E 381 156 m N 3 308 994 m	393 m

Katamia mast is situated north Cairo/Ain-Sokhna road about 52 km from Cairo. There are no sheltering obstacles close to the mast. The sandy surface is flat, homogeneous and smooth with a roughness of about 0.01 in all directions, a small hill is allocated in the N, NNE sectors of about 300 m distance and a height of about 20 m.

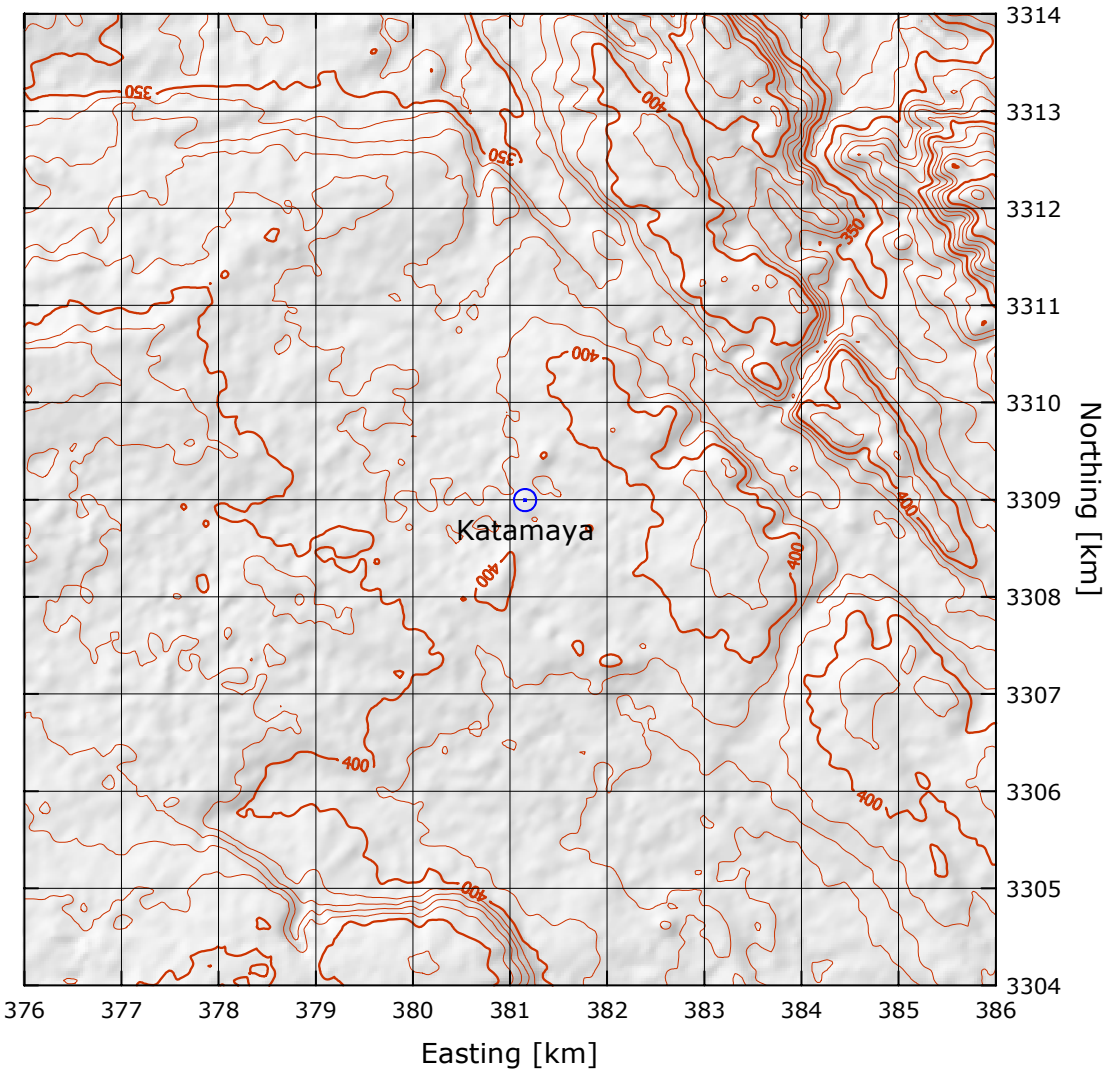

Sector	Input		Obstacles		Roughness		Orography		z_{0m}
0	0.0	0.0	0.0	0.0	0.0	0.0	1.4	−0.8	0.0050
30	0.0	0.0	0.0	0.0	0.0	0.0	−0.2	−0.7	0.0050
60	0.0	0.0	0.0	0.0	0.0	0.0	−0.8	0.2	0.0050
90	0.0	0.0	0.0	0.0	0.0	0.0	0.3	0.9	0.0050
120	0.0	0.0	0.0	0.0	0.0	0.0	1.9	0.7	0.0050
150	0.0	0.0	0.0	0.0	0.0	0.0	2.4	−0.1	0.0050
180	0.0	0.0	0.0	0.0	0.0	0.0	1.4	−0.8	0.0050
210	0.0	0.0	0.0	0.0	0.0	0.0	−0.2	−0.7	0.0050
240	0.0	0.0	0.0	0.0	0.0	0.0	−0.8	0.2	0.0050
270	0.0	0.0	0.0	0.0	0.0	0.0	0.3	0.9	0.0050
300	0.0	0.0	0.0	0.0	0.0	0.0	1.9	0.7	0.0050
330	0.0	0.0	0.0	0.0	0.0	0.0	2.4	−0.1	0.0050

Height of anemometer: 24.5 m a.g.l. 2004-05

Sect	Freq	<1	2	3	4	5	6	7	8	9	11	13	15	17	>17	*A*	*k*
0	24.2	9	45	71	104	154	179	176	128	79	53	2	0	0	0	6.4	3.11
30	18.6	9	36	57	114	168	184	169	132	73	54	3	0	0	0	6.3	3.04
60	10.3	17	61	71	117	168	177	166	119	58	47	0	0	0	0	6.1	2.97
90	3.1	63	196	191	166	138	115	88	27	10	5	2	1	0	0	4.1	1.91
120	1.5	54	265	213	167	110	66	77	32	3	7	7	0	0	0	3.6	1.56
150	3.9	22	127	137	177	148	168	140	42	20	10	8	1	0	0	5.0	2.31
180	3.5	33	138	137	198	128	133	90	49	27	46	21	1	0	0	5.0	1.76
210	1.9	57	150	98	72	94	115	104	57	46	126	42	32	6	0	6.5	1.76
240	4.5	22	96	69	60	108	162	158	146	74	66	32	5	1	1	6.8	2.67
270	7.5	19	85	114	97	108	157	166	94	63	59	33	4	0	0	6.4	2.44
300	7.8	19	113	133	131	154	176	124	74	44	23	6	1	0	0	5.4	2.43
330	13.2	14	85	110	123	162	160	138	115	58	26	6	0	0	0	5.8	2.62
Total	100.0	17	77	93	118	150	168	153	108	61	45	8	1	0	0	6.0	2.66

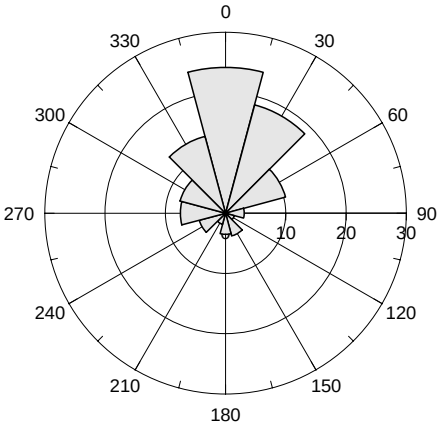

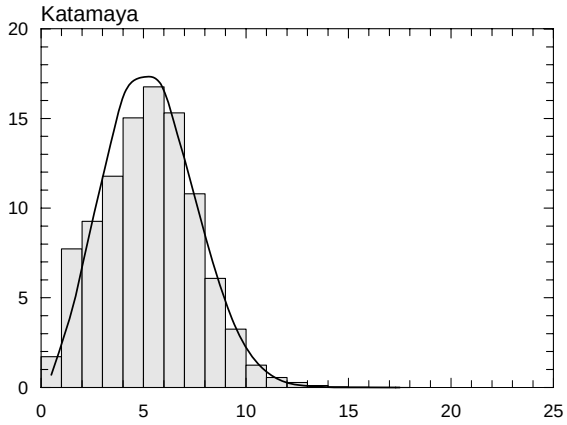

	Jan	Feb	Mar	Apr	May	Jun	Jul	Aug	Sep	Oct	Nov	Dec	Year
0	3.8	4.3	5.6	4.3	4.2	5.4	4.7	4.4	4.9	4.9	3.4	4.2	4.4
1	4.2	4.3	5.6	4.1	3.5	5.0	4.0	3.9	4.4	4.3	3.1	3.8	4.1
2	4.3	4.4	4.9	3.6	3.6	4.6	3.3	3.2	4.0	4.1	2.8	4.0	3.8
3	4.5	4.1	4.5	3.7	3.4	3.9	3.1	3.0	3.9	4.2	3.1	4.0	3.7
4	4.7	4.2	4.5	4.0	3.5	3.5	2.9	2.9	3.9	3.6	3.0	4.2	3.7
5	4.9	4.4	4.7	3.8	3.5	3.5	2.8	2.9	3.8	3.6	3.3	4.2	3.7
6	4.6	4.5	5.0	3.6	4.0	3.1	2.9	2.7	3.5	3.5	3.6	4.3	3.8
7	4.5	4.8	4.0	3.7	3.9	3.8	3.1	2.8	3.5	3.5	3.6	4.6	3.8
8	4.6	4.7	4.4	4.3	4.6	4.1	3.9	3.9	4.5	4.1	3.5	4.0	4.2
9	5.1	5.6	5.7	4.9	4.9	4.5	4.7	4.2	5.1	4.9	4.3	4.5	4.8
10	5.9	6.0	5.5	5.5	5.2	5.0	5.1	4.5	5.6	5.3	5.1	5.8	5.4
11	6.7	6.3	5.2	6.3	5.8	5.0	5.4	4.8	5.8	5.2	5.5	5.9	5.7
12	6.6	6.9	5.6	5.8	6.3	5.5	5.9	4.9	6.0	5.3	5.5	6.3	5.9
13	6.6	6.5	6.3	5.8	6.4	5.7	6.2	5.3	6.3	5.5	5.5	6.5	6.1
14	6.2	6.5	6.8	6.1	6.8	6.0	6.4	5.5	6.6	5.6	5.7	6.6	6.3
15	6.1	6.5	6.8	7.0	6.7	6.4	6.6	6.0	6.7	6.1	6.2	6.9	6.5
16	5.8	6.6	6.7	6.9	7.2	6.6	7.2	6.3	7.1	6.3	6.4	6.4	6.6
17	5.7	6.4	6.7	7.2	7.3	6.9	7.6	6.9	7.5	6.5	6.1	5.8	6.7
18	5.1	5.9	6.8	7.2	7.5	8.2	8.1	7.7	8.0	6.5	5.8	5.3	6.8
19	4.5	5.2	6.8	6.9	7.9	8.3	8.0	7.6	7.7	6.4	5.5	4.8	6.6
20	4.1	5.2	7.0	7.1	7.8	8.3	7.4	7.4	7.4	6.7	4.9	4.5	6.4
21	4.0	4.9	6.6	6.6	7.2	7.6	7.0	6.8	6.9	6.6	4.5	4.0	6.0
22	4.0	4.4	7.0	5.3	6.6	6.8	6.3	6.1	6.1	6.1	4.7	4.4	5.6
23	4.1	4.3	6.5	5.1	5.2	6.0	5.6	5.3	5.6	5.9	4.2	4.2	5.1
Mean	5.0	5.3	5.8	5.4	5.5	5.6	5.3	4.9	5.6	5.2	4.5	5.0	5.2

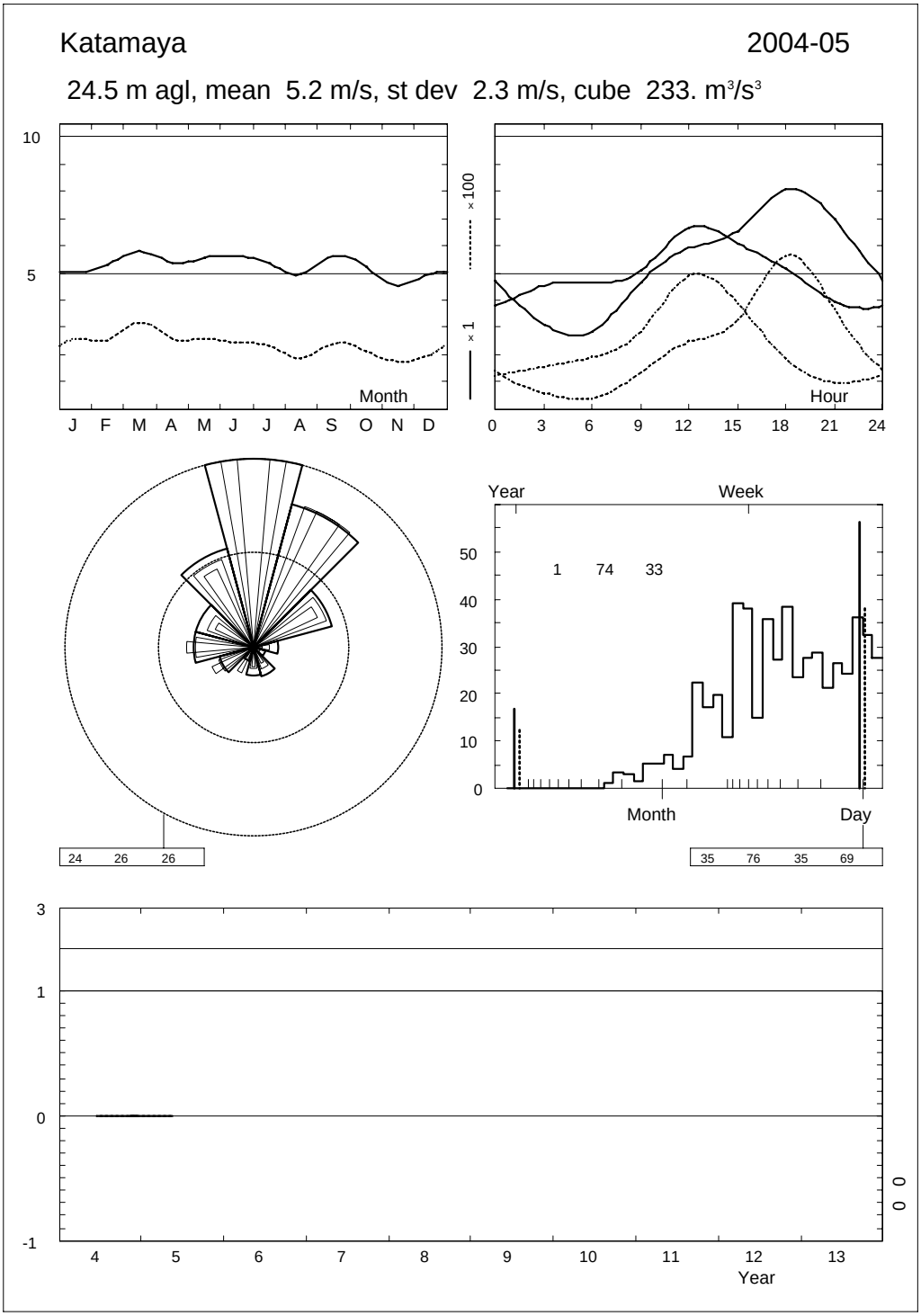

	Jan	Feb	Mar	Apr	May	Jun	Jul	Aug	Sep	Oct	Nov	Dec	Year
2004	—	—	—	—	—	5.6	5.3	4.9	5.6	5.2	4.5	5.0	5.1
2005	5.0	5.3	5.8	5.4	5.5	—	—	—	—	—	—	—	5.4
Mean	5.0	5.3	5.8	5.4	5.5	5.6	5.3	4.9	5.6	5.2	4.5	5.0	5.2

Roughness Class 0 ($z_0 = 0.0002$ m)

z	0	30	60	90	120	150	180	210	240	270	300	330	Total
10	6.7	6.8	6.6	5.2	4.0	5.2	5.3	6.5	7.3	6.8	5.9	6.0	6.4
	3.29	3.26	3.18	2.30	1.78	2.45	1.99	1.83	2.78	2.63	2.60	2.82	2.76
25	7.3	7.4	7.2	5.7	4.3	5.7	5.8	7.2	8.0	7.5	6.4	6.6	7.0
	3.40	3.36	3.28	2.37	1.83	2.53	2.05	1.89	2.87	2.72	2.68	2.91	2.85
50	7.8	8.0	7.8	6.1	4.7	6.1	6.2	7.7	8.6	8.1	6.9	7.1	7.5
	3.49	3.45	3.37	2.44	1.88	2.60	2.10	1.94	2.94	2.79	2.75	2.99	2.92
100	8.5	8.7	8.4	6.6	5.1	6.6	6.8	8.3	9.3	8.7	7.5	7.7	8.2
	3.38	3.34	3.26	2.36	1.82	2.51	2.03	1.88	2.85	2.70	2.67	2.89	2.83
200	9.4	9.6	9.3	7.3	5.6	7.3	7.5	9.2	10.3	9.7	8.3	8.5	9.0
	3.20	3.16	3.09	2.23	1.72	2.38	1.93	1.78	2.70	2.56	2.52	2.74	2.69
Freq.	22.4	19.7	11.7	4.1	1.7	3.5	3.5	2.2	4.3	7.2	7.7	12.1	100.0

Roughness Class 1 ($z_0 = 0.0300$ m)

z	0	30	60	90	120	150	180	210	240	270	300	330	Total
10	4.7	4.8	4.6	3.0	2.9	3.7	3.7	4.8	5.0	4.7	4.0	4.3	4.5
	2.79	2.76	2.63	1.71	1.55	2.02	1.60	1.71	2.35	2.19	2.20	2.43	2.34
25	5.6	5.7	5.4	3.6	3.5	4.4	4.5	5.8	6.0	5.6	4.8	5.2	5.3
	3.01	2.98	2.85	1.84	1.67	2.18	1.72	1.85	2.54	2.36	2.37	2.62	2.52
50	6.5	6.6	6.3	4.2	4.1	5.1	5.2	6.8	6.9	6.4	5.6	5.9	6.2
	3.39	3.35	3.20	2.07	1.88	2.45	1.94	2.08	2.86	2.65	2.67	2.95	2.81
100	7.7	7.8	7.4	5.0	4.8	6.0	6.2	8.0	8.2	7.6	6.6	7.0	7.3
	3.61	3.56	3.40	2.21	2.00	2.61	2.06	2.21	3.04	2.83	2.84	3.14	2.98
200	9.5	9.7	9.2	6.2	6.0	7.5	7.7	10.0	10.2	9.5	8.2	8.8	9.1
	3.44	3.40	3.25	2.10	1.91	2.49	1.97	2.11	2.90	2.70	2.71	3.00	2.85
Freq.	23.3	18.2	9.8	2.9	1.7	3.8	3.3	2.3	4.9	7.6	8.3	13.9	100.0

Roughness Class 2 ($z_0 = 0.1000$ m)

z	0	30	60	90	120	150	180	210	240	270	300	330	Total
10	4.1	4.1	3.9	2.6	2.7	3.2	3.3	4.2	4.3	4.0	3.5	3.8	3.9
	2.75	2.70	2.56	1.71	1.65	1.98	1.56	1.78	2.30	2.10	2.23	2.47	2.32
25	5.1	5.1	4.8	3.3	3.3	4.0	4.1	5.2	5.3	4.9	4.3	4.7	4.8
	2.94	2.89	2.75	1.83	1.77	2.12	1.67	1.90	2.46	2.25	2.39	2.64	2.47
50	5.9	6.0	5.7	3.8	3.9	4.6	4.8	6.2	6.2	5.7	5.1	5.5	5.6
	3.26	3.20	3.04	2.03	1.96	2.35	1.85	2.11	2.72	2.49	2.65	2.93	2.73
100	7.0	7.1	6.7	4.6	4.7	5.5	5.7	7.3	7.4	6.8	6.0	6.5	6.7
	3.58	3.52	3.34	2.23	2.15	2.58	2.03	2.31	2.99	2.74	2.91	3.22	2.98
200	8.6	8.7	8.3	5.6	5.8	6.8	7.1	9.1	9.1	8.4	7.5	8.0	8.2
	3.42	3.37	3.20	2.13	2.06	2.47	1.94	2.22	2.87	2.62	2.78	3.08	2.86
Freq.	22.9	17.5	9.2	2.8	1.9	3.7	3.2	2.5	5.2	7.7	8.7	14.9	100.0

Roughness Class 3 ($z_0 = 0.4000$ m)

z	0	30	60	90	120	150	180	210	240	270	300	330	Total
10	3.2	3.3	3.0	2.1	2.2	2.5	2.7	3.4	3.4	3.1	2.8	3.0	3.1
	2.75	2.70	2.47	1.67	1.70	1.92	1.58	1.91	2.29	2.06	2.19	2.48	2.31
25	4.2	4.3	4.0	2.7	2.9	3.3	3.5	4.4	4.4	4.0	3.7	4.0	4.0
	2.91	2.86	2.62	1.77	1.80	2.03	1.67	2.03	2.42	2.19	2.32	2.63	2.44
50	5.1	5.2	4.8	3.3	3.5	4.0	4.3	5.4	5.3	4.8	4.4	4.8	4.8
	3.17	3.11	2.85	1.92	1.96	2.21	1.81	2.20	2.63	2.38	2.52	2.86	2.65
100	6.1	6.2	5.8	4.0	4.2	4.8	5.2	6.5	6.4	5.8	5.3	5.8	5.8
	3.60	3.54	3.24	2.19	2.23	2.51	2.06	2.51	3.00	2.71	2.87	3.26	2.99
200	7.5	7.6	7.1	4.9	5.2	5.9	6.3	7.9	7.8	7.1	6.5	7.1	7.1
	3.47	3.41	3.12	2.11	2.15	2.42	1.99	2.41	2.89	2.61	2.77	3.14	2.89
Freq.	22.3	16.4	8.3	2.5	2.2	3.7	3.0	2.8	5.6	7.7	9.4	16.2	100.0

z	Class 0		Class 1		Class 2		Class 3	
m	ms^{-1}	Wm^{-2}	ms^{-1}	Wm^{-2}	ms^{-1}	Wm^{-2}	ms^{-1}	Wm^{-2}
10	5.7	168	4.0	63	3.4	42	2.7	20
25	6.2	216	4.7	103	4.3	75	3.6	45
50	6.7	264	5.5	148	5.0	113	4.3	74
100	7.3	343	6.5	239	5.9	181	5.2	121
200	8.0	478	8.1	471	7.3	349	6.3	225

29° 52′ 27.8″ N 32° 28′ 18.8″ E	UTM 36 E 449 002 m N 3 304 985 m	8 m

The El-Suez mast is situated along the western coast of the Sinai Peninsula, about 60 km S of the city of Suez and 18 km S of the town of El Sedr. The site is located just E of Ras Matarma. The distance to the coastline of the Gulf of Suez is about 500 m in a south-westerly direction. To the SE and S several one- and two-storey buildings are found, at distances of about 500 m. The surface to the NW and N is flat and level, and consists mostly of sand and pebbles with a roughness length of about 1 cm or less. Several hills and ridges occur to the NE, these reach about 100 m a.s.l. at a distance of about 4 km. The terrain appears to be a coastal plain and the mountains to the E are more than 10 km away; at 40 km they reach almost 1000 m a.s.l.

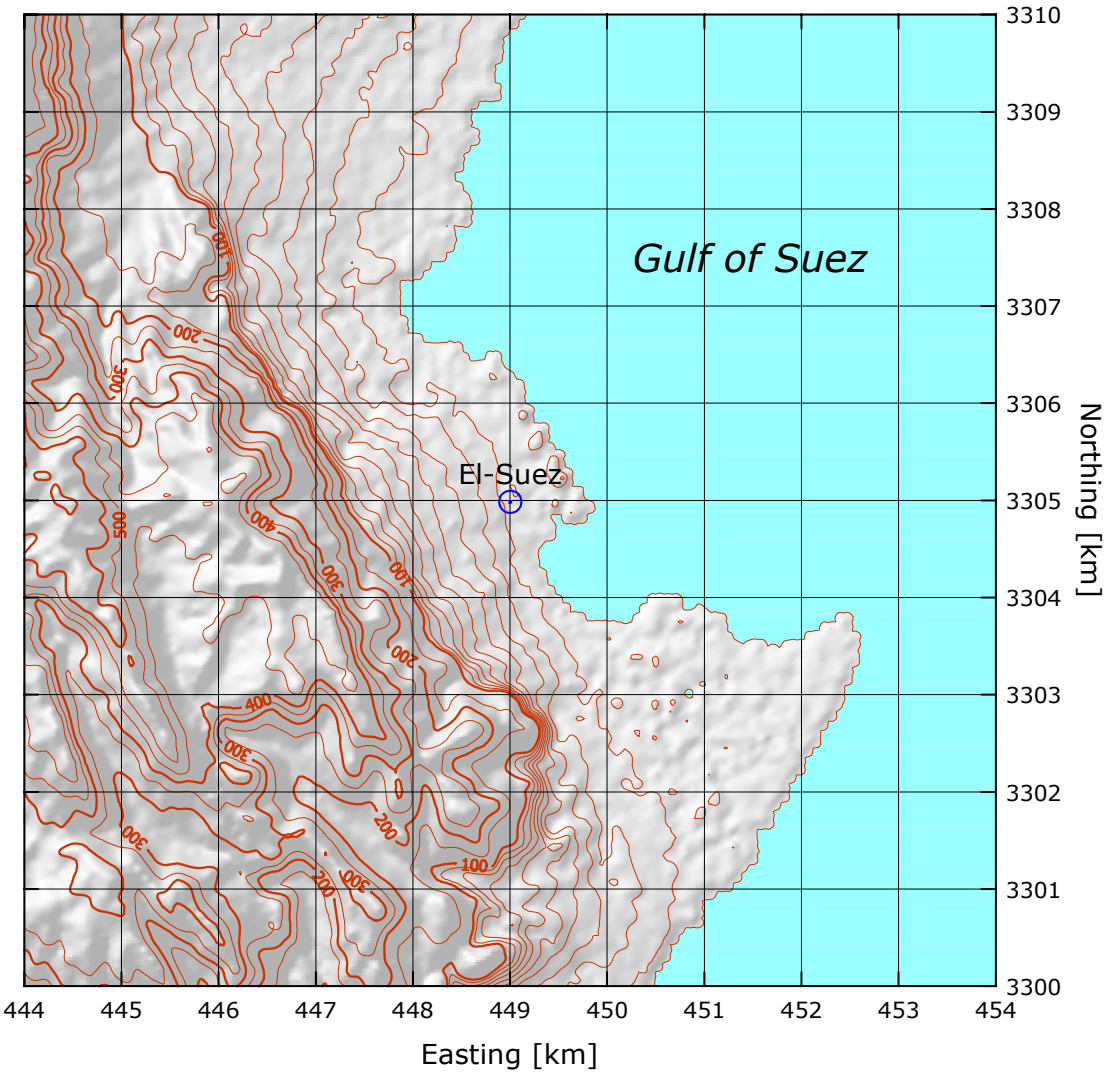

Sector	Input		Obstacles		Roughness		Orography		z_{0m}
0	0.0	0.0	−64.3	0.0	−4.1	0.0	0.4	−6.7	0.0120
30	0.0	0.0	−40.9	0.0	−7.7	0.0	−13.0	−9.5	0.0020
60	0.0	0.0	−18.9	0.0	−10.3	0.0	−24.4	−3.1	0.0010
90	0.0	0.0	−19.1	0.0	−14.1	0.0	−20.4	7.3	0.0000
120	0.0	0.0	−19.2	0.0	−10.0	0.0	−6.4	8.8	0.0000
150	0.0	0.0	−9.3	0.0	−13.3	0.0	3.1	2.2	0.0010
180	0.0	0.0	−18.8	0.0	−15.0	0.0	−1.2	−8.3	0.0030
210	0.0	0.0	−2.4	0.0	−2.8	0.0	−18.9	−13.2	0.0350
240	0.0	0.0	−8.4	0.0	0.0	0.0	−34.0	−3.6	0.0500
270	0.0	0.0	−55.3	0.0	0.0	0.0	−26.8	11.3	0.0500
300	0.0	0.0	−64.0	0.0	0.0	0.0	−7.4	11.5	0.0500
330	0.0	0.0	−64.0	0.0	−0.3	0.0	4.0	2.3	0.0430

Height of anemometer: 10.0 m a.g.l. 1995-2004

Sect	Freq	< 1	2	3	4	5	6	7	8	9	11	13	15	17	>17	*A*	*k*
0	44.0	16	25	72	101	122	216	201	150	67	27	1	0	0	0	6.4	3.67
30	8.7	21	41	119	155	139	203	183	96	30	13	2	0	0	0	5.7	3.29
60	1.8	32	78	270	243	161	118	67	27	2	2	0	0	0	0	4.1	2.23
90	2.0	42	109	294	221	140	128	42	16	2	5	0	0	0	0	3.9	2.09
120	1.5	34	99	282	167	162	128	76	25	15	12	0	0	0	0	4.2	2.06
150	2.4	21	49	139	139	135	163	136	130	47	36	3	3	0	0	5.9	2.63
180	3.6	12	35	109	112	81	156	141	133	97	82	28	9	3	0	6.9	2.52
210	1.6	10	21	98	126	94	162	124	112	85	94	43	27	5	0	7.0	2.10
240	1.2	5	19	86	116	113	181	133	104	107	89	39	3	1	4	6.9	2.33
270	2.5	10	32	120	112	127	183	125	100	72	82	23	9	4	1	6.5	2.16
300	4.6	6	25	181	187	176	193	114	74	22	19	2	0	1	0	5.3	2.58
330	26.2	7	18	78	133	151	225	185	129	53	19	2	0	0	0	6.1	3.49
Total	100.0	14	29	98	126	134	206	176	126	57	28	4	1	0	0	6.2	3.17

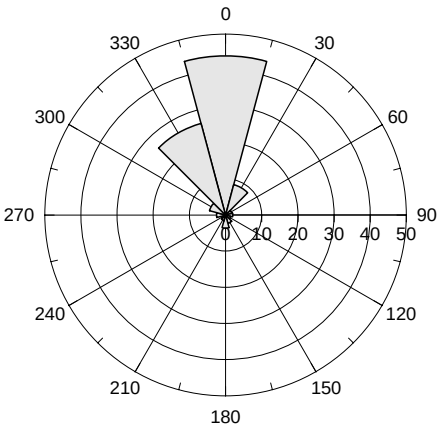

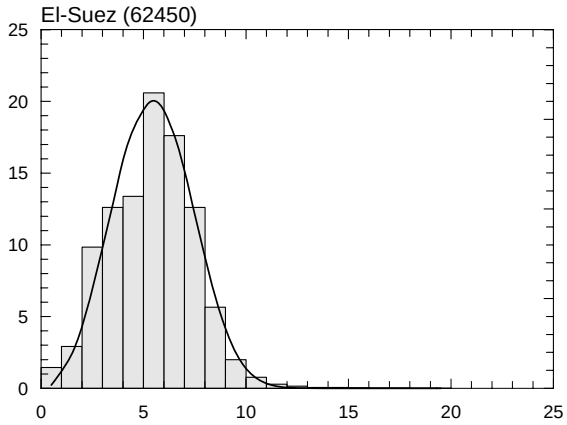

	Jan	Feb	Mar	Apr	May	Jun	Jul	Aug	Sep	Oct	Nov	Dec	Year
0	4.4	4.4	4.6	5.2	5.0	4.8	4.4	4.8	5.0	4.7	4.2	4.1	4.7
3	4.5	4.5	4.6	4.9	4.8	4.6	4.0	4.2	4.7	4.5	4.4	4.3	4.5
6	4.4	4.8	4.8	5.3	5.2	5.0	4.4	4.6	4.9	4.9	4.6	4.3	4.8
9	4.8	5.0	5.2	5.5	5.5	5.1	4.4	4.7	5.3	5.1	5.0	4.5	5.0
12	5.1	5.3	5.6	5.8	5.9	5.8	4.9	5.4	5.9	5.6	5.2	5.2	5.5
15	4.9	5.4	5.8	6.3	6.4	6.5	6.2	6.3	6.6	6.0	5.5	5.0	5.9
18	4.5	5.1	5.9	6.4	6.6	7.0	6.8	6.7	6.8	6.0	5.2	4.5	6.0
21	4.4	4.7	5.1	5.7	5.9	6.0	5.8	6.0	5.9	5.3	4.5	4.6	5.4
Mean	4.7	4.9	5.2	5.6	5.7	5.6	5.2	5.4	5.7	5.3	4.9	4.6	5.3

	Jan	Feb	Mar	Apr	May	Jun	Jul	Aug	Sep	Oct	Nov	Dec	Year
1995	3.6	4.7	4.4	4.9	5.3	4.9	4.1	4.7	5.1	4.9	4.9	3.8	4.7
1996	4.8	5.1	5.0	5.6	6.3	6.3	6.1	5.6	6.4	5.3	5.2	5.3	5.6
1997	5.1	5.2	4.9	5.7	5.3	4.9	4.7	4.7	5.7	4.5	4.5	4.1	5.0
1998	5.3	4.3	5.8	5.4	5.6	5.7	5.4	6.1	5.8	5.8	5.1	5.3	5.5
1999	4.6	5.7	5.6	5.7	6.6	5.7	5.6	5.5	6.1	5.8	5.2	4.7	5.6
2000	5.1	5.0	5.4	6.0	5.9	6.1	5.4	5.8	5.6	5.7	5.6	4.9	5.5
2001	4.2	4.3	5.8	5.8	5.8	6.1	5.5	5.6	5.5	5.0	4.6	5.0	5.3
2002	5.0	5.5	5.7	6.5	5.4	6.0	5.4	5.6	5.8	5.8	4.4	4.5	5.5
2003	4.4	4.9	4.7	6.0	5.3	5.4	5.0	5.3	5.4	5.2	4.8	4.6	5.1
2004	5.3	4.4	5.7	5.4	5.4	5.6	5.1	5.3	5.7	5.2	4.1	4.4	5.2
2005	5.0	4.6	5.6	5.5	5.4	—	—	—	—	—	—	—	—
Mean	4.7	4.9	5.2	5.6	5.7	5.6	5.2	5.4	5.7	5.3	4.9	4.6	5.3

El-Suez (62450) 1995-2004

10.0 m agl, mean 5.3 m/s, st dev 2.1 m/s, cube 217. m^3/s^3

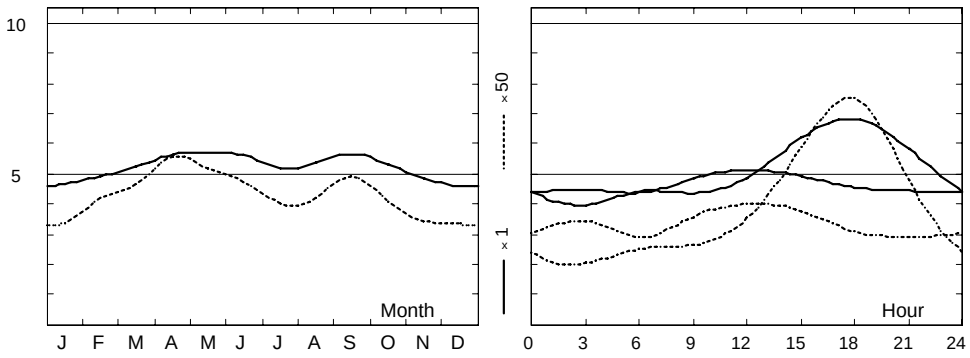

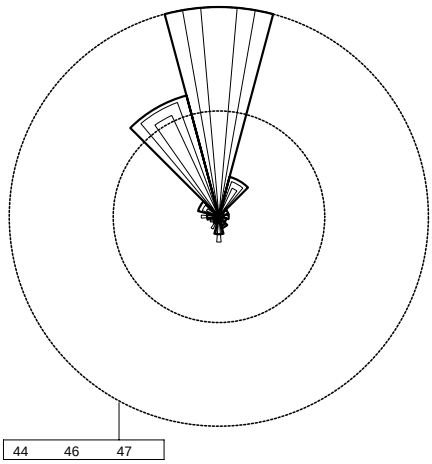

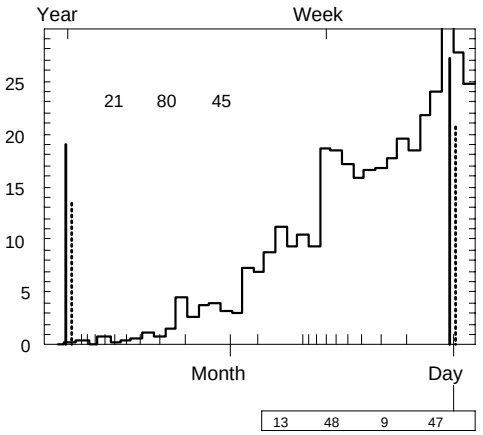

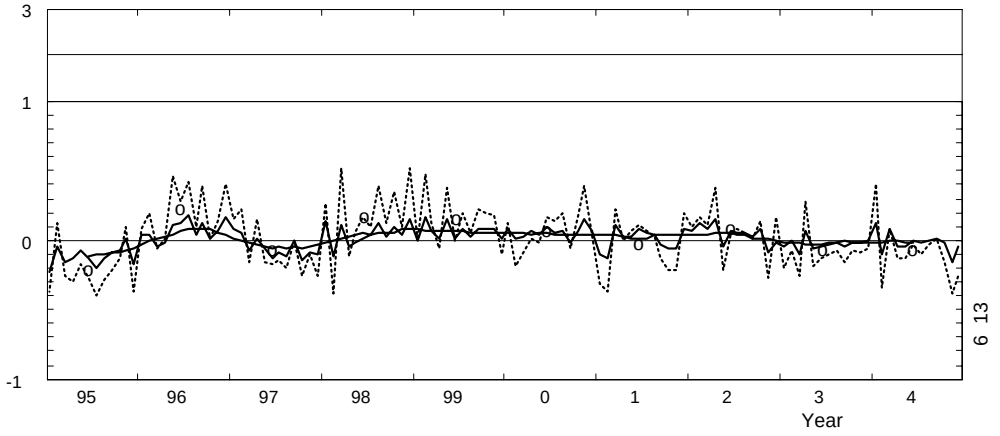

Roughness Class 0 ($z_0 = 0.0002$ m)

z	0	30	60	90	120	150	180	210	240	270	300	330	Total
10	8.7	9.5	9.5	7.6	7.1	7.8	11.2	13.6	15.6	12.5	9.9	8.9	9.5
	4.22	3.45	2.75	2.03	2.13	2.65	2.62	2.41	2.28	2.29	3.38	4.03	2.74
25	9.5	10.4	10.4	8.4	7.8	8.6	12.2	14.7	16.9	13.6	10.8	9.7	10.4
	4.36	3.55	2.82	2.09	2.19	2.73	2.65	2.43	2.29	2.31	3.48	4.16	2.80
50	10.2	11.1	11.1	9.0	8.4	9.2	13.0	15.7	17.9	14.4	11.6	10.4	11.2
	4.47	3.65	2.90	2.14	2.25	2.80	2.72	2.46	2.31	2.35	3.58	4.27	2.88
100	11.1	12.1	12.0	9.7	9.1	10.0	13.9	16.6	19.0	15.4	12.6	11.3	12.1
	4.33	3.53	2.82	2.08	2.18	2.71	2.68	2.46	2.32	2.35	3.47	4.13	2.88
200	12.3	13.4	13.2	10.7	10.0	11.0	15.0	17.8	20.2	16.4	13.9	12.5	13.3
	4.10	3.35	2.69	1.96	2.06	2.57	2.60	2.42	2.29	2.31	3.29	3.92	2.85
Freq.	31.8	20.7	6.0	2.5	1.6	1.7	2.4	2.4	2.0	3.6	8.2	17.0	100.0

Roughness Class 1 ($z_0 = 0.0300$ m)

z	0	30	60	90	120	150	180	210	240	270	300	330	Total
10	6.2	6.8	6.4	4.9	4.9	5.7	8.3	10.1	11.1	8.3	6.6	6.1	6.7
	3.48	2.99	1.99	1.71	1.82	2.12	2.40	2.28	2.12	2.15	3.10	3.50	2.42
25	7.3	8.1	7.6	5.9	5.9	6.9	9.7	11.7	12.9	9.8	7.9	7.3	7.9
	3.76	3.23	2.12	1.84	1.97	2.28	2.48	2.32	2.15	2.21	3.35	3.78	2.57
50	8.4	9.4	8.7	6.9	6.9	7.9	10.9	13.1	14.3	10.9	9.1	8.4	9.1
	4.22	3.63	2.32	2.07	2.21	2.57	2.62	2.38	2.18	2.31	3.76	4.24	2.82
100	10.0	11.1	10.2	8.2	8.1	9.4	12.4	14.5	15.9	12.3	10.7	9.9	10.7
	4.49	3.86	2.49	2.21	2.36	2.73	2.81	2.51	2.26	2.47	4.00	4.51	3.12
200	12.4	13.8	12.3	10.1	10.1	11.7	14.3	16.3	17.6	14.1	13.3	12.4	13.1
	4.29	3.69	2.38	2.10	2.25	2.61	2.73	2.48	2.26	2.41	3.82	4.31	3.22
Freq.	32.4	17.5	3.7	2.2	1.5	1.8	2.5	2.4	2.1	4.4	9.8	19.7	100.0

Roughness Class 2 ($z_0 = 0.1000$ m)

z	0	30	60	90	120	150	180	210	240	270	300	330	Total
10	5.4	5.9	5.5	4.3	4.3	5.2	7.3	8.8	9.4	7.0	5.7	5.3	5.8
	3.35	2.94	1.96	1.72	1.86	2.00	2.36	2.29	2.11	2.13	3.16	3.37	2.40
25	6.6	7.3	6.8	5.3	5.4	6.4	8.9	10.6	11.3	8.5	7.0	6.5	7.1
	3.58	3.15	2.06	1.84	1.99	2.13	2.43	2.33	2.13	2.19	3.39	3.61	2.53
50	7.7	8.5	7.8	6.2	6.3	7.5	10.1	12.1	12.8	9.7	8.1	7.6	8.3
	3.97	3.48	2.24	2.04	2.20	2.36	2.54	2.38	2.17	2.28	3.75	3.99	2.75
100	9.1	10.1	9.2	7.4	7.5	8.9	11.6	13.6	14.3	11.1	9.6	9.0	9.7
	4.35	3.82	2.46	2.24	2.42	2.59	2.75	2.48	2.24	2.47	4.12	4.38	3.06
200	11.3	12.5	11.1	9.2	9.3	11.0	13.4	15.4	16.1	12.8	11.9	11.1	11.9
	4.17	3.66	2.37	2.14	2.31	2.48	2.69	2.50	2.27	2.42	3.94	4.20	3.15
Freq.	31.0	16.3	3.6	2.2	1.6	1.8	2.5	2.3	2.3	4.8	10.6	21.1	100.0

Roughness Class 3 ($z_0 = 0.4000$ m)

z	0	30	60	90	120	150	180	210	240	270	300	330	Total
10	4.3	4.7	4.2	3.4	3.5	4.3	5.8	7.0	7.0	5.3	4.4	4.1	4.5
	3.26	2.92	1.90	1.73	1.90	1.99	2.33	2.29	2.07	2.17	3.06	3.30	2.39
25	5.6	6.1	5.5	4.5	4.6	5.6	7.6	9.1	9.0	6.8	5.7	5.4	5.9
	3.45	3.09	2.00	1.83	2.01	2.08	2.39	2.32	2.09	2.23	3.25	3.49	2.51
50	6.7	7.3	6.7	5.4	5.5	6.7	8.9	10.6	10.6	8.1	6.9	6.5	7.1
	3.75	3.35	2.13	1.99	2.19	2.23	2.47	2.36	2.12	2.33	3.53	3.80	2.68
100	8.1	8.8	7.9	6.5	6.6	8.0	10.4	12.3	12.2	9.5	8.3	7.8	8.5
	4.26	3.81	2.40	2.27	2.49	2.51	2.62	2.44	2.18	2.50	4.01	4.32	2.99
200	9.9	10.8	9.6	8.0	8.1	9.7	12.1	14.1	14.0	11.1	10.1	9.6	10.3
	4.11	3.68	2.34	2.19	2.40	2.45	2.66	2.50	2.24	2.52	3.87	4.17	3.08
Freq.	29.2	14.6	3.4	2.1	1.6	1.9	2.5	2.3	2.5	5.4	11.7	22.9	100.0

z	Class 0		Class 1		Class 2		Class 3	
m	ms^{-1}	Wm^{-2}	ms^{-1}	Wm^{-2}	ms^{-1}	Wm^{-2}	ms^{-1}	Wm^{-2}
10	8.5	555	5.9	205	5.1	134	4.0	65
25	9.3	715	7.0	331	6.3	240	5.3	142
50	10.0	868	8.1	476	7.4	361	6.3	235
100	10.8	1097	9.5	732	8.7	562	7.6	380
200	11.8	1467	11.7	1330	10.6	1002	9.2	662

Ras Sedr — Gulf of Suez

29° 25′ 57.8″ N 32° 47′ 25.5″ E	UTM 36 E 479 672 m N 3 255 947 m	6 m

The Ras Sedr mast is situated along the western coast of the Sinai Peninsula, about 60 km S of the city of Suez and 18 km S of the town of El Sedr. The site is located just E of Ras Matarma. The distance to the coastline of the Gulf of Suez is about 500 m in a south-westerly direction. To the SE and S several one- and two-storey buildings are found, at distances of about 500 m. The surface to the NW and N is flat and level, and consists mostly of sand and pebbles with a roughness length of about 1 cm or less. Several hills and ridges occur to the NE, these reach about 100 m a.s.l. at a distance of about 4 km. The terrain appears to be a coastal plain and the mountains to the E are more than 10 km away; at 40 km they reach almost 1000 m a.s.l.

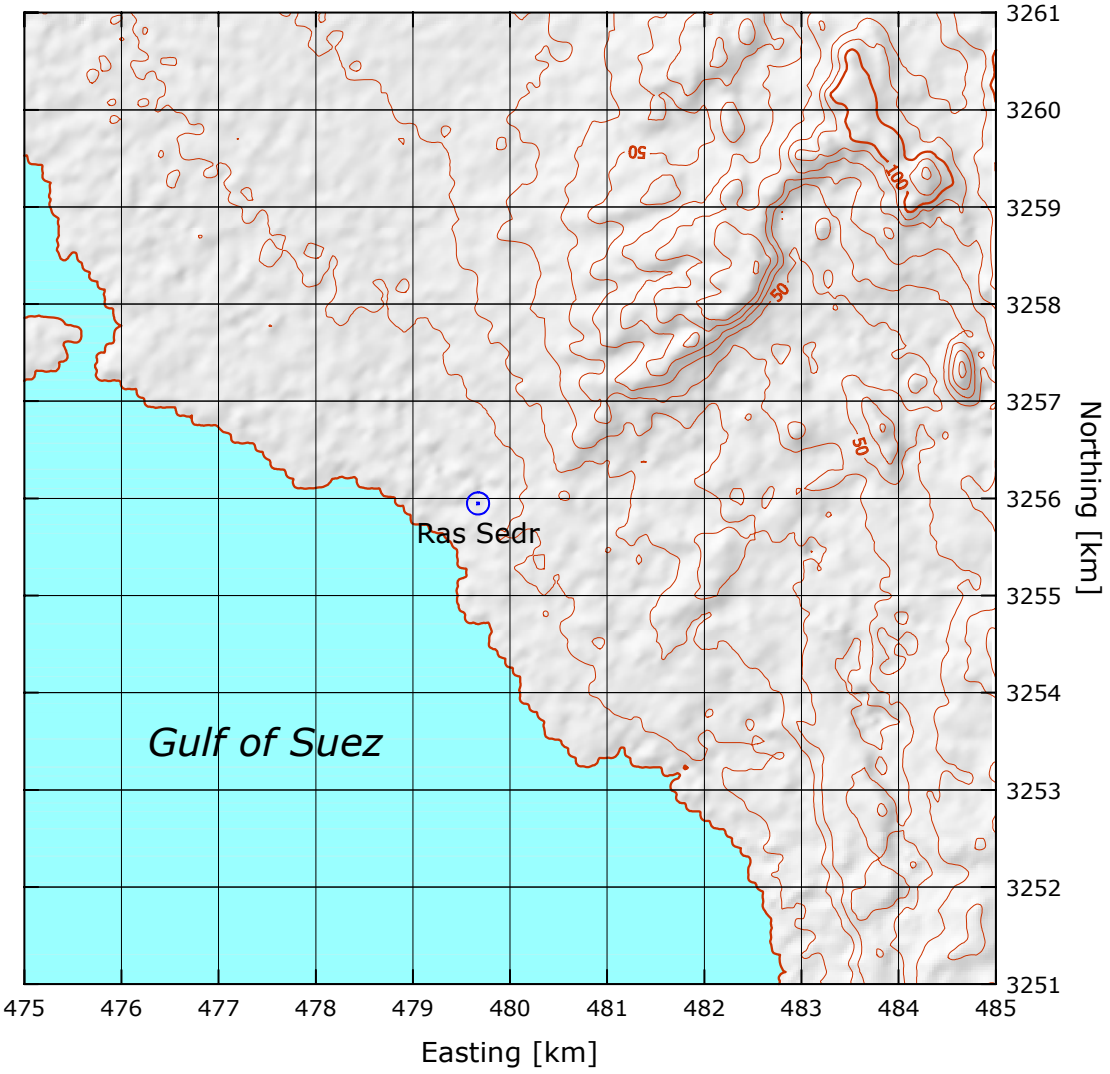

Sector	Input		Obstacles		Roughness		Orography		z_{0m}
0	0.0	0.0	0.0	0.0	0.0	0.0	0.0	−0.5	0.0030
30	0.0	0.0	0.0	0.0	0.0	0.0	−1.3	−0.8	0.0030
60	0.0	0.0	0.0	0.0	0.0	0.0	−2.4	−0.3	0.0030
90	0.0	0.0	0.0	0.0	0.0	0.0	−2.2	0.5	0.0030
120	0.0	0.0	0.0	0.0	0.0	0.0	−0.9	0.8	0.0030
150	0.0	0.0	0.0	0.0	−0.7	0.0	0.1	0.3	0.0010
180	0.0	0.0	0.0	0.0	−0.7	0.0	0.0	−0.4	0.0000
210	0.0	0.0	0.0	0.0	0.0	0.0	−1.1	−0.7	0.0000
240	0.0	0.0	0.0	0.0	0.0	0.0	−2.1	−0.3	0.0000
270	0.0	0.0	0.0	0.0	0.0	0.0	−2.0	0.4	0.0000
300	0.0	0.0	0.0	0.0	−3.2	0.0	−0.9	0.8	0.0010
330	0.0	0.0	0.0	0.0	−2.3	0.0	0.2	0.3	0.0010

Height of anemometer: 24.5 m a.g.l. 2000–2005

Sect	Freq	<1	2	3	4	5	6	7	8	9	11	13	15	17	>17	*A*	*k*
0	40.3	2	8	17	36	74	124	160	169	150	189	58	12	2	0	8.3	3.36
30	5.1	14	56	72	97	158	194	202	132	53	20	2	0	0	0	6.1	3.49
60	1.7	37	186	218	150	88	84	113	83	33	9	0	0	0	0	4.3	1.70
90	1.8	38	151	228	260	208	83	22	6	3	1	0	0	0	0	3.8	2.65
120	1.4	23	133	272	295	152	79	29	11	3	2	0	0	0	0	3.8	2.39
150	1.5	12	84	141	146	125	144	93	72	53	77	41	10	2	0	6.0	1.84
180	2.4	11	55	101	120	113	128	108	99	80	119	53	12	2	0	6.9	2.14
210	1.8	9	84	171	107	66	70	72	79	93	137	82	28	2	0	7.2	2.04
240	1.6	22	120	232	116	55	68	69	74	77	109	46	12	1	0	5.9	1.68
270	1.4	26	106	212	264	201	98	42	21	10	17	3	1	0	0	4.2	2.04
300	9.6	5	15	24	39	63	75	100	103	120	284	152	19	0	0	9.4	3.98
330	31.2	2	8	17	31	44	64	98	129	149	260	150	44	3	0	9.6	3.72
Total	100.0	6	25	44	57	75	100	125	133	128	194	89	21	2	0	8.5	3.06

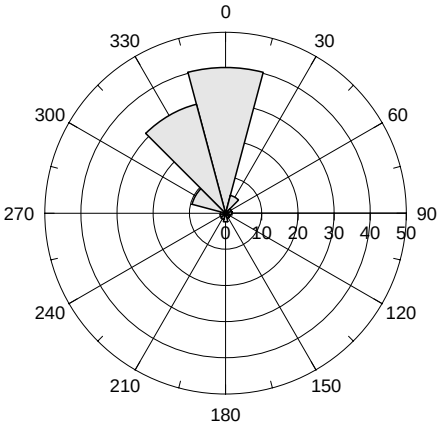

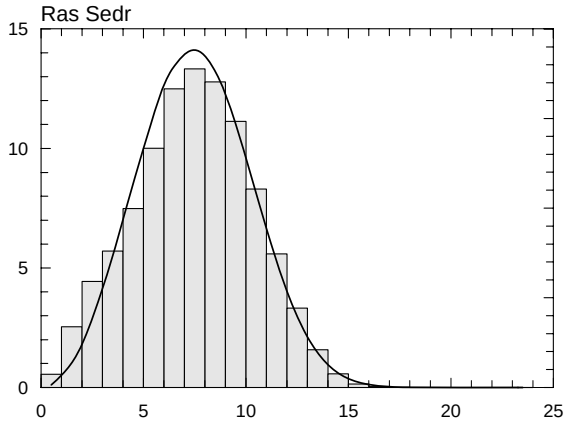

	Jan	Feb	Mar	Apr	May	Jun	Jul	Aug	Sep	Oct	Nov	Dec	Year
0	5.4	5.4	6.9	7.1	7.9	8.5	8.0	7.6	7.4	7.2	5.7	5.2	7.0
1	5.3	5.4	6.6	7.1	7.6	8.4	7.9	7.6	7.3	7.0	5.6	5.3	6.9
2	5.3	5.2	6.4	7.0	7.6	8.5	7.8	7.3	7.2	7.0	5.8	5.5	6.8
3	5.2	5.5	6.4	6.9	7.4	8.3	7.6	7.2	7.2	6.9	5.8	5.5	6.7
4	5.4	5.4	6.3	6.6	7.2	8.1	7.4	7.2	7.2	6.9	5.7	5.5	6.6
5	5.4	5.5	6.6	6.7	7.2	7.7	7.3	7.2	6.9	7.0	5.7	5.4	6.6
6	5.6	5.4	6.4	6.9	7.0	7.9	7.2	7.0	7.0	6.8	5.5	5.3	6.6
7	5.4	5.3	6.3	7.0	7.3	8.7	8.0	7.5	7.0	6.6	5.3	5.4	6.8
8	5.2	5.1	6.5	7.5	7.5	8.6	8.1	8.1	7.9	7.0	5.1	5.2	6.9
9	4.9	5.3	7.1	7.6	7.6	8.9	8.0	8.1	8.0	7.6	5.3	4.9	7.0
10	5.2	5.7	7.2	8.0	8.0	9.4	8.4	8.8	8.5	7.9	5.6	5.3	7.5
11	5.5	6.0	7.8	8.2	8.3	10.0	8.9	9.6	9.4	8.7	6.0	5.6	8.0
12	6.2	6.3	8.0	8.5	8.6	10.1	9.1	9.8	9.9	9.4	6.4	6.1	8.3
13	6.4	6.6	8.2	8.6	8.7	10.1	9.1	9.9	10.0	9.4	6.6	6.4	8.5
14	6.5	6.9	8.0	8.7	8.7	9.9	9.1	9.8	10.0	9.3	6.7	6.4	8.4
15	6.4	6.8	8.1	8.6	8.6	9.8	8.9	9.6	9.8	9.0	6.6	6.3	8.3
16	6.3	6.5	7.8	8.4	8.4	9.6	8.7	9.3	9.7	8.7	6.1	6.1	8.1
17	6.1	6.3	7.6	8.2	8.5	9.7	8.9	9.2	9.4	8.1	5.6	5.8	7.9
18	5.7	5.7	7.3	8.1	8.4	9.9	9.2	9.3	8.9	8.2	5.6	5.6	7.8
19	5.5	5.7	7.2	7.9	8.3	9.8	9.3	9.4	9.4	8.4	5.7	5.7	7.8
20	5.8	5.8	7.4	8.0	8.4	10.2	9.5	9.8	9.4	8.2	5.7	5.7	8.0
21	5.6	5.6	7.5	8.0	8.0	9.8	9.4	9.4	8.7	7.7	5.6	5.6	7.7
22	5.6	5.7	7.2	7.6	8.0	9.0	8.9	8.6	8.1	7.4	5.7	5.5	7.4
23	5.5	5.4	7.3	7.5	7.9	8.5	8.4	8.0	7.6	7.2	5.4	5.3	7.1
Mean	5.6	5.8	7.2	7.7	8.0	9.2	8.5	8.6	8.4	7.8	5.8	5.6	7.4

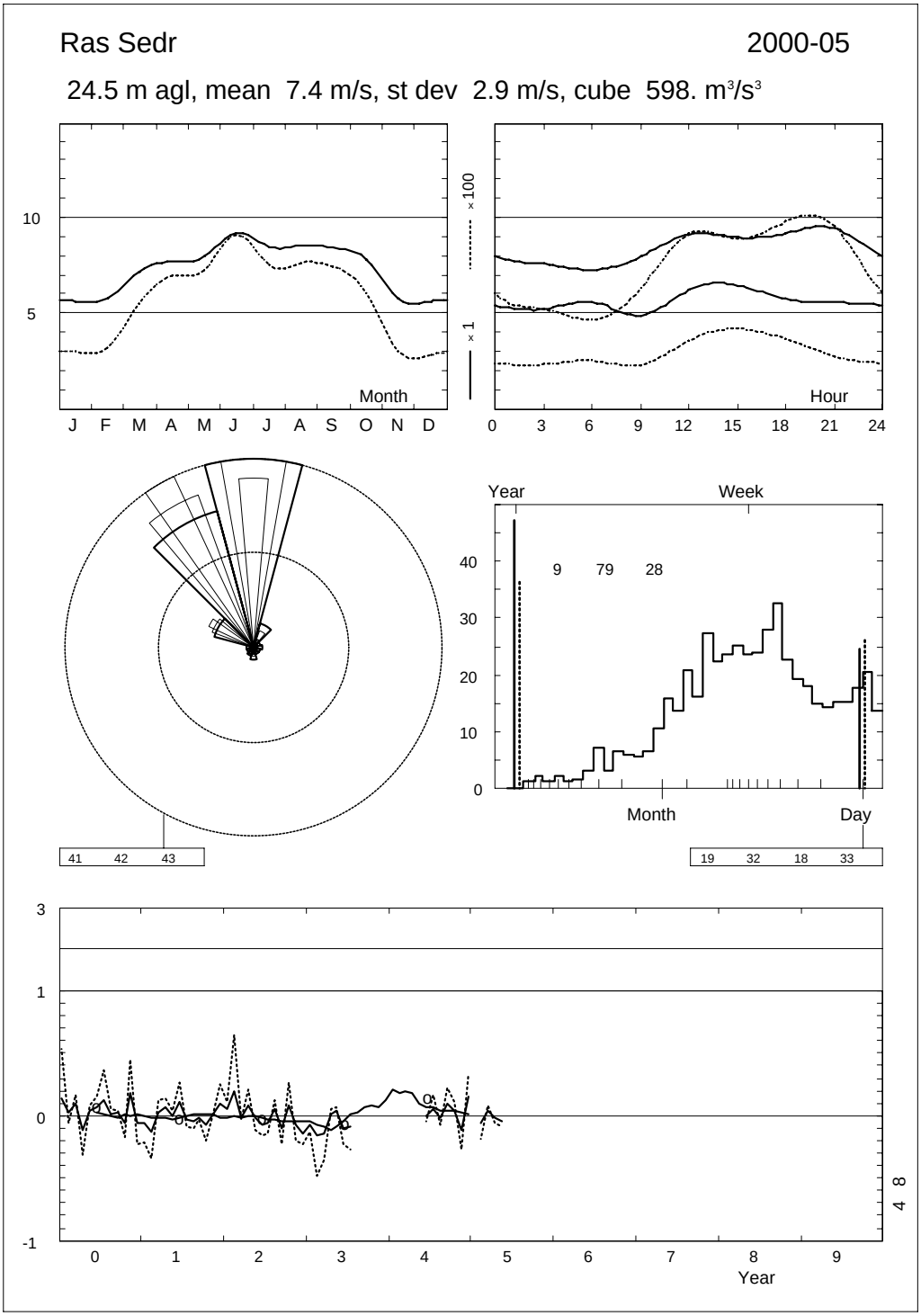

	Jan	Feb	Mar	Apr	May	Jun	Jul	Aug	Sep	Oct	Nov	Dec	Year
2000	6.4	5.9	7.9	6.8	8.2	9.7	9.5	8.7	8.6	7.4	6.8	5.3	7.7
2001	5.3	5.0	7.4	8.2	7.9	10.1	8.2	8.2	8.3	7.3	5.9	6.2	7.3
2002	5.9	6.9	7.0	8.3	7.8	8.5	8.0	9.0	7.6	8.5	5.4	4.8	7.3
2003	5.2	4.8	6.1	7.8	8.3	8.2	7.7	—	—	—	—	—	7.1
2004	—	—	—	—	—	9.1	9.0	8.4	9.2	8.2	5.1	6.5	8.0
2005	—	5.4	7.5	7.5	7.6	—	—	—	—	—	—	—	7.1
Mean	5.6	5.8	7.2	7.7	8.0	9.2	8.5	8.6	8.4	7.8	5.8	5.6	7.4

Roughness Class 0 ($z_0 = 0.0002$ m)

z	0	30	60	90	120	150	180	210	240	270	300	330	Total
10	8.8	7.4	5.3	4.1	4.0	5.8	6.4	6.7	5.6	4.3	9.5	9.9	8.6
	3.58	3.18	2.19	2.60	2.40	1.83	2.08	1.97	1.64	1.47	4.01	4.01	3.01
25	9.6	8.1	5.8	4.5	4.4	6.3	7.0	7.3	6.2	4.7	10.3	10.8	9.5
	3.70	3.28	2.26	2.69	2.48	1.89	2.14	2.03	1.69	1.52	4.13	4.13	3.08
50	10.3	8.7	6.2	4.8	4.7	6.8	7.5	7.8	6.6	5.1	11.1	11.6	10.1
	3.79	3.37	2.31	2.76	2.54	1.94	2.20	2.08	1.74	1.56	4.24	4.24	3.14
100	11.1	9.4	6.7	5.2	5.1	7.4	8.1	8.5	7.2	5.5	12.1	12.6	11.0
	3.67	3.26	2.24	2.67	2.46	1.88	2.13	2.02	1.69	1.51	4.11	4.11	3.07
200	12.4	10.5	7.4	5.8	5.7	8.1	9.0	9.4	7.9	6.0	13.4	13.9	12.2
	3.48	3.08	2.12	2.53	2.33	1.78	2.02	1.91	1.60	1.43	3.89	3.89	2.94
Freq.	38.9	8.0	2.1	1.8	1.4	1.5	2.3	1.9	1.7	1.6	9.5	29.3	100.0

Roughness Class 1 ($z_0 = 0.0300$ m)

z	0	30	60	90	120	150	180	210	240	270	300	330	Total
10	6.0	4.7	3.2	2.8	2.9	4.2	4.4	4.4	3.5	5.0	6.7	6.7	6.0
	2.97	2.74	1.62	2.24	1.56	1.62	1.73	1.58	1.29	1.72	3.28	3.21	2.59
25	7.2	5.7	3.8	3.4	3.5	5.0	5.3	5.4	4.3	5.9	7.9	8.0	7.2
	3.21	2.96	1.74	2.42	1.69	1.75	1.87	1.71	1.39	1.85	3.54	3.46	2.76
50	8.3	6.5	4.5	3.9	4.1	5.8	6.2	6.2	5.0	6.9	9.1	9.2	8.2
	3.60	3.33	1.96	2.72	1.89	1.96	2.10	1.92	1.55	2.08	3.97	3.89	3.04
100	9.8	7.7	5.3	4.7	4.9	6.9	7.3	7.4	6.0	8.2	10.8	10.9	9.8
	3.83	3.54	2.09	2.90	2.02	2.09	2.24	2.04	1.65	2.22	4.23	4.14	3.19
200	12.2	9.6	6.6	5.8	6.1	8.6	9.1	9.2	7.4	10.2	13.4	13.6	12.2
	3.66	3.38	1.99	2.77	1.92	1.99	2.13	1.95	1.58	2.12	4.04	3.96	3.08
Freq.	34.0	5.2	1.8	1.7	1.4	1.7	2.3	1.8	1.6	2.9	13.4	32.1	100.0

Roughness Class 2 ($z_0 = 0.1000$ m)

z	0	30	60	90	120	150	180	210	240	270	300	330	Total
10	5.2	4.1	2.8	2.5	2.7	3.7	3.9	3.8	3.0	4.8	5.8	5.8	5.2
	2.96	2.68	1.68	2.28	1.60	1.66	1.72	1.56	1.26	2.02	3.22	3.11	2.58
25	6.4	5.0	3.5	3.1	3.4	4.5	4.8	4.7	3.7	5.9	7.1	7.1	6.4
	3.17	2.87	1.80	2.44	1.71	1.77	1.84	1.66	1.35	2.16	3.44	3.33	2.74
50	7.5	5.9	4.1	3.6	4.0	5.3	5.6	5.6	4.5	6.9	8.3	8.3	7.5
	3.50	3.18	1.99	2.71	1.89	1.96	2.03	1.84	1.49	2.40	3.81	3.68	2.98
100	8.9	7.0	4.9	4.3	4.8	6.4	6.7	6.7	5.4	8.2	9.8	9.8	8.9
	3.85	3.49	2.19	2.97	2.07	2.15	2.24	2.02	1.63	2.63	4.18	4.04	3.21
200	11.0	8.6	6.0	5.3	5.9	7.9	8.3	8.2	6.6	10.1	12.2	12.1	11.0
	3.68	3.34	2.10	2.85	1.99	2.06	2.14	1.93	1.56	2.52	4.01	3.87	3.10
Freq.	31.2	4.9	1.9	1.7	1.4	1.7	2.2	1.8	1.6	3.6	15.0	32.9	100.0

Roughness Class 3 ($z_0 = 0.4000$ m)

z	0	30	60	90	120	150	180	210	240	270	300	330	Total
10	4.1	3.2	2.1	2.0	2.2	2.9	3.0	2.9	2.3	4.0	4.5	4.4	4.1
	2.90	2.60	1.66	2.09	1.52	1.67	1.69	1.53	1.26	2.34	3.19	3.09	2.58
25	5.4	4.2	2.8	2.6	2.9	3.8	4.0	3.9	3.1	5.2	6.0	5.8	5.4
	3.07	2.76	1.76	2.22	1.61	1.77	1.79	1.62	1.33	2.48	3.38	3.27	2.71
50	6.5	5.0	3.4	3.1	3.6	4.6	4.9	4.7	3.8	6.3	7.2	7.0	6.5
	3.34	3.00	1.91	2.41	1.74	1.92	1.95	1.75	1.44	2.70	3.67	3.55	2.91
100	7.7	6.0	4.1	3.7	4.3	5.6	5.9	5.7	4.6	7.6	8.6	8.4	7.8
	3.80	3.42	2.17	2.75	1.98	2.19	2.22	1.99	1.64	3.08	4.18	4.04	3.23
200	9.5	7.4	5.1	4.6	5.3	6.8	7.2	7.0	5.6	9.2	10.5	10.3	9.5
	3.67	3.29	2.09	2.65	1.91	2.11	2.14	1.92	1.58	2.96	4.03	3.90	3.14
Freq.	27.3	4.4	1.9	1.6	1.4	1.8	2.2	1.8	1.6	4.6	17.4	34.0	100.0

z	Class 0		Class 1		Class 2		Class 3	
m	ms^{-1}	Wm^{-2}	ms^{-1}	Wm^{-2}	ms^{-1}	Wm^{-2}	ms^{-1}	Wm^{-2}
10	7.7	395	5.3	142	4.6	93	3.6	45
25	8.5	512	6.4	233	5.7	169	4.8	99
50	9.1	628	7.4	342	6.7	259	5.8	167
100	9.8	811	8.8	558	8.0	421	6.9	277
200	10.9	1120	10.9	1092	9.8	806	8.5	513

Abu Darag NW — Gulf of Suez

29° 17′ 15.0″ N 32° 34′ 53.4″ E	UTM 36 E 459 351 m N 3 239 911 m	38 m

The Abu Darag NW mast is situated W of the Suez–Hurghada road, approximately 21 km N of Zafarana (map sheet: NH 36 F3c). The distance to the coastline of the Gulf of Suez is about 2.5 km in an easterly direction. There are no sheltering obstacles close to the mast. The surface consists mostly of sand dunes with a roughness length of less than 0.01 m. The terrain rises to the W and reaches 200 m at a distance of about 9 km. The highest peak to the NW (15 km) is about 700 m a.s.l. Further to the W (20 km) the North Galala Plateau rises to more than 1000 m a.s.l.

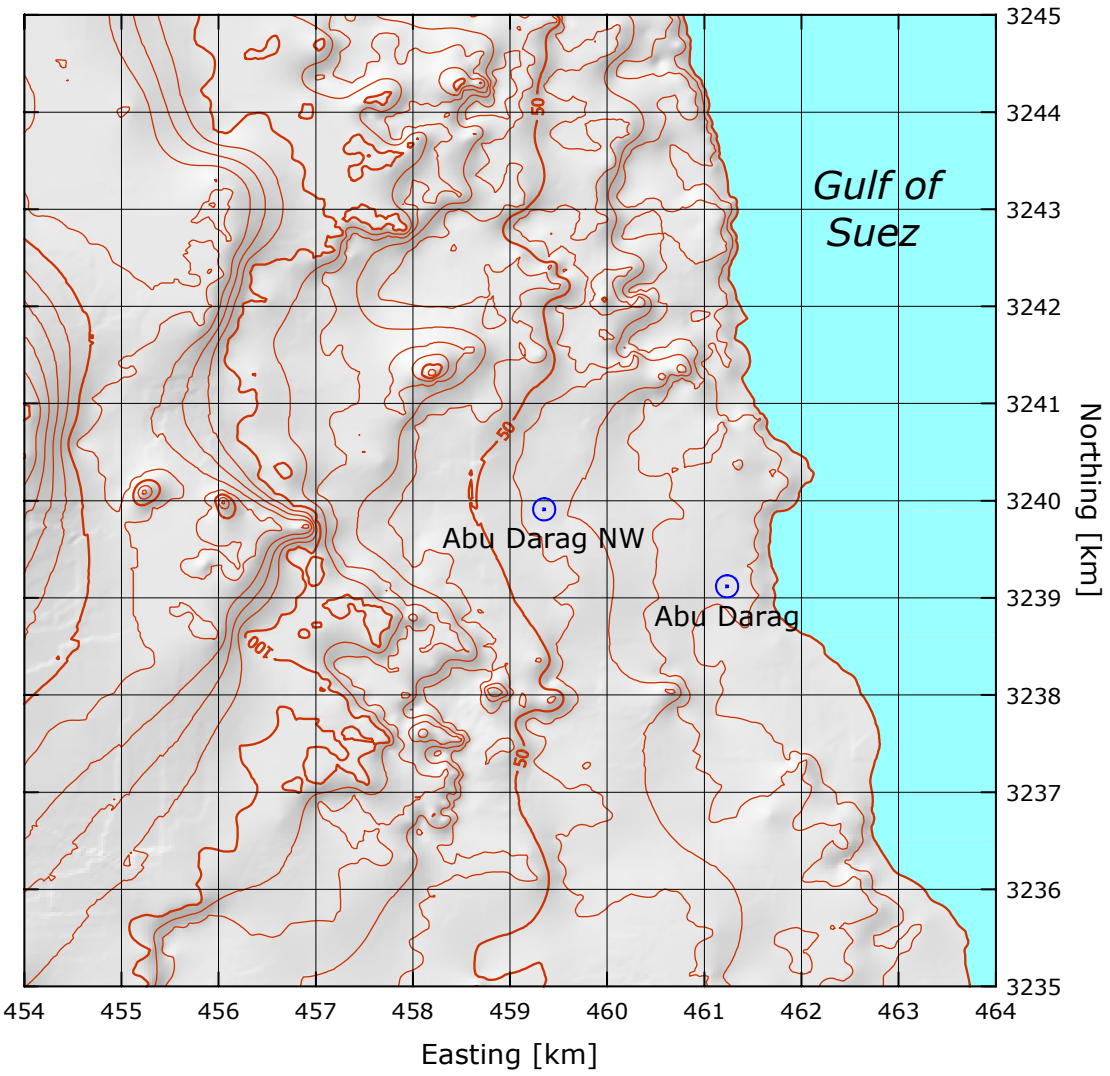

Sector	Input		Obstacles		Roughness		Orography		z_{0m}
0	0.0	0.0	0.0	0.0	−6.0	0.0	−2.0	0.2	0.0020
30	0.0	0.0	0.0	0.0	−4.7	0.0	−1.4	0.3	0.0010
60	0.0	0.0	0.0	0.0	−1.4	0.0	−0.8	0.1	0.0000
90	0.0	0.0	0.0	0.0	−1.1	0.0	−0.9	−0.2	0.0000
120	0.0	0.0	0.0	0.0	−1.9	0.0	−1.4	−0.3	0.0000
150	0.0	0.0	0.0	0.0	−3.2	0.0	−1.9	−0.1	0.0010
180	0.0	0.0	0.0	0.0	−1.6	0.0	−1.8	0.2	0.0050
210	0.0	0.0	0.0	0.0	−2.5	0.0	−1.3	0.3	0.0070
240	0.0	0.0	0.0	0.0	1.3	0.0	−1.0	0.0	0.0160
270	0.0	0.0	0.0	0.0	2.4	0.0	−1.2	−0.3	0.0140
300	0.0	0.0	0.0	0.0	4.2	0.0	−1.8	−0.3	0.0180
330	0.0	0.0	0.0	0.0	1.8	0.0	−2.0	0.0	0.0120

Height of anemometer: 47.5 m a.g.l. 2002–2003, 2004–05

Sect	Freq	<1	2	3	4	5	6	7	8	9	11	13	15	17	>17	*A*	*k*
0	61.4	1	5	11	18	29	46	78	113	143	297	180	67	13	1	10.3	3.92
30	5.0	16	42	59	116	160	173	152	124	88	59	11	0	0	0	6.4	2.78
60	1.7	39	118	216	225	207	122	51	18	3	1	0	0	0	0	4.1	2.52
90	0.7	73	197	275	242	136	58	17	2	1	0	0	0	0	0	3.3	2.28
120	0.6	56	154	235	217	148	88	58	16	17	10	1	0	0	0	3.9	1.90
150	1.6	29	79	115	105	106	86	83	65	74	98	73	50	33	6	7.3	1.67
180	2.0	37	102	140	142	122	96	81	60	52	59	42	39	16	11	6.0	1.39
210	2.0	36	104	159	140	138	98	80	79	58	74	27	4	0	0	5.5	1.72
240	5.4	15	37	51	63	76	96	119	143	129	180	72	15	3	1	8.2	3.06
270	1.8	32	119	151	115	120	118	115	96	59	52	17	4	1	1	5.7	1.98
300	1.3	54	186	236	178	98	80	68	51	19	19	7	4	1	0	3.9	1.45
330	16.5	5	24	42	44	54	63	71	95	103	235	172	75	15	1	9.9	3.38
Total	100.0	8	25	40	46	54	64	82	105	121	239	146	56	11	1	9.6	3.34

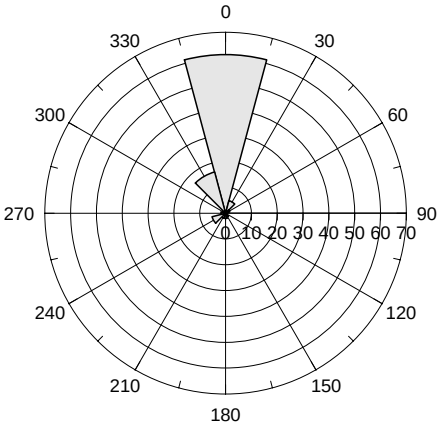

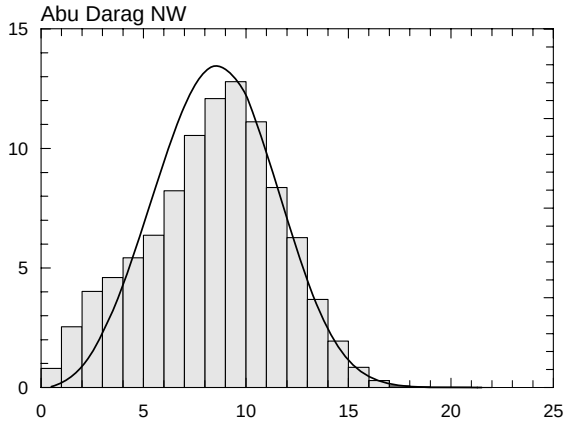

	Jan	Feb	Mar	Apr	May	Jun	Jul	Aug	Sep	Oct	Nov	Dec	Year
0	5.3	6.5	8.4	8.9	9.4	10.4	10.0	10.6	10.0	9.9	6.9	6.3	8.5
1	5.2	6.3	8.2	8.8	9.3	9.9	9.6	10.1	9.7	9.6	6.5	6.1	8.2
2	5.3	6.7	7.4	8.6	9.1	9.6	9.4	9.7	9.4	9.3	6.4	6.0	8.0
3	5.2	6.2	7.5	8.8	8.6	9.2	8.9	9.4	8.9	9.0	6.4	6.0	7.8
4	5.6	6.2	7.5	8.8	8.4	8.9	8.5	9.2	8.7	8.7	6.2	6.0	7.7
5	5.6	6.1	7.3	8.5	8.4	8.6	8.4	9.0	8.8	8.6	6.2	6.0	7.6
6	5.4	6.0	7.1	8.1	8.2	8.5	8.4	8.9	8.7	8.4	6.4	5.9	7.4
7	5.5	6.0	6.9	8.2	8.1	8.7	8.5	9.2	8.9	8.4	6.2	6.1	7.5
8	5.5	6.2	7.2	8.6	8.4	9.0	8.5	9.7	9.6	9.3	6.3	6.0	7.8
9	5.5	6.3	7.7	8.8	8.5	9.0	8.3	9.8	9.9	9.7	6.8	6.1	8.0
10	6.0	6.6	8.2	9.1	8.8	8.9	8.0	9.9	9.9	9.8	6.6	6.5	8.2
11	6.3	7.0	8.4	9.1	8.8	9.0	7.7	9.8	9.9	10.0	7.0	6.8	8.3
12	6.8	7.4	8.8	9.2	9.1	9.1	8.1	9.9	10.1	9.9	7.1	7.5	8.6
13	7.0	7.7	8.9	9.6	9.1	9.4	8.3	9.9	10.3	9.9	7.1	7.6	8.7
14	7.2	7.1	8.8	9.6	9.2	9.6	8.3	10.0	10.3	9.8	6.7	7.5	8.7
15	7.1	7.2	8.6	9.6	9.1	9.5	8.3	10.0	10.3	9.8	6.6	7.5	8.6
16	6.7	6.8	8.0	9.4	8.9	9.2	8.1	10.0	10.1	9.4	6.0	7.0	8.3
17	6.2	6.4	7.5	9.1	8.8	9.1	8.5	9.5	9.6	8.9	5.8	6.6	8.0
18	5.8	6.2	7.1	8.6	8.4	9.0	8.6	9.3	9.5	9.0	6.0	6.3	7.8
19	5.4	6.1	7.5	8.8	8.8	9.7	9.4	9.7	10.2	9.8	6.4	6.1	8.1
20	5.6	6.4	7.8	9.2	9.5	11.2	10.3	10.9	10.7	10.2	6.7	6.3	8.6
21	5.7	6.3	8.5	9.4	10.2	11.6	10.9	11.0	11.1	10.4	6.7	6.3	8.9
22	5.8	6.4	8.5	9.2	10.0	11.4	10.7	11.1	10.8	10.4	6.9	6.4	8.8
23	5.6	6.6	8.6	9.0	9.6	10.7	10.5	10.7	10.3	10.1	7.0	6.3	8.6
Mean	5.9	6.5	7.9	9.0	8.9	9.5	8.9	9.9	9.8	9.5	6.5	6.5	8.2

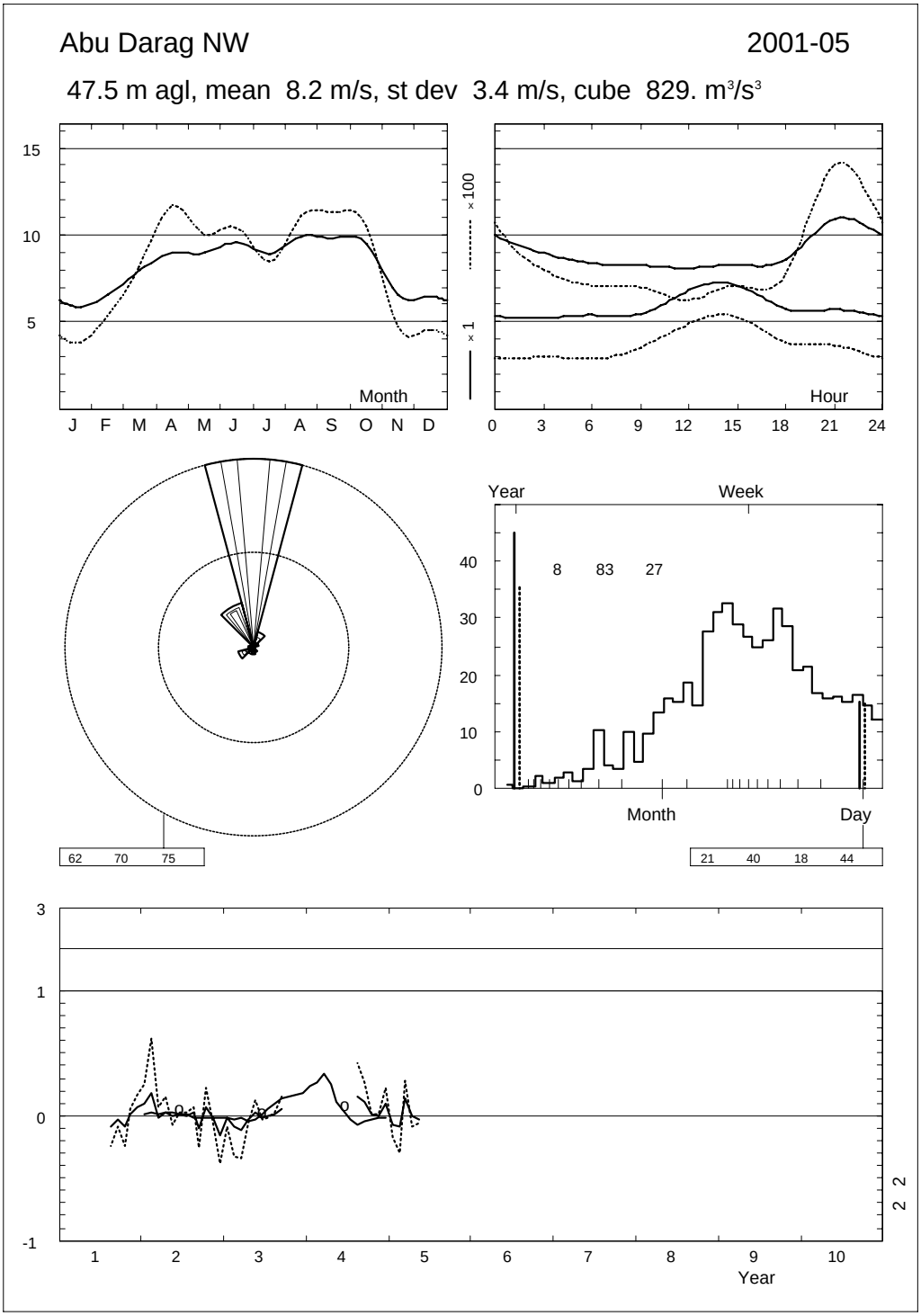

	Jan	Feb	Mar	Apr	May	Jun	Jul	Aug	Sep	Oct	Nov	Dec	Year
2001	—	—	—	—	—	—	—	9.1	9.5	8.7	6.6	6.9	8.0
2002	6.4	7.8	7.8	9.2	8.9	9.7	8.9	10.1	8.8	10.2	6.5	5.4	8.3
2003	5.8	5.9	7.0	8.7	9.2	9.4	8.9	10.0	10.3	—	—	—	8.3
2004	—	—	—	—	—	—	—	—	10.9	9.6	6.6	7.1	8.6
2005	5.4	5.9	9.0	9.0	8.7	—	—	—	—	—	—	—	7.6
Mean	5.9	6.5	7.9	9.0	8.9	9.5	8.9	9.9	9.8	9.5	6.5	6.5	8.2

Roughness Class 0 ($z_0 = 0.0002$ m)

z	0	30	60	90	120	150	180	210	240	270	300	330	Total
10	10.3	8.6	4.2	3.1	3.4	6.7	6.0	5.6	8.2	6.4	4.1	9.9	9.4
	3.70	2.59	1.92	2.07	1.76	1.53	1.37	1.62	2.91	2.07	1.45	3.30	2.81
25	11.2	9.4	4.6	3.4	3.8	7.4	6.6	6.1	9.0	7.0	4.5	10.8	10.3
	3.79	2.67	1.97	2.14	1.82	1.58	1.41	1.66	3.00	2.14	1.50	3.40	2.88
50	12.0	10.1	5.0	3.7	4.1	7.9	7.1	6.6	9.7	7.5	4.8	11.6	11.0
	3.90	2.74	2.03	2.19	1.87	1.62	1.44	1.71	3.08	2.19	1.54	3.49	2.94
100	13.0	11.0	5.4	4.0	4.4	8.6	7.6	7.1	10.5	8.1	5.2	12.6	11.9
	3.79	2.65	1.96	2.12	1.81	1.57	1.40	1.65	2.98	2.12	1.49	3.39	2.87
200	14.3	12.1	5.9	4.4	4.8	9.4	8.3	7.8	11.6	9.0	5.7	13.9	13.1
	3.62	2.51	1.86	2.01	1.71	1.50	1.34	1.57	2.82	2.01	1.41	3.22	2.77
Freq.	56.6	11.0	2.1	0.8	0.6	1.5	1.9	2.0	5.0	2.1	1.4	14.9	100.0

Roughness Class 1 ($z_0 = 0.0300$ m)

z	0	30	60	90	120	150	180	210	240	270	300	330	Total
10	7.2	4.1	2.5	2.1	2.6	4.5	3.9	4.3	5.7	3.8	5.3	7.0	6.6
	3.16	2.07	1.91	1.68	1.02	1.29	1.15	1.59	2.39	1.56	1.69	2.96	2.48
25	8.5	4.9	3.0	2.5	3.2	5.5	4.7	5.2	6.8	4.5	6.4	8.4	7.8
	3.37	2.24	2.06	1.81	1.09	1.38	1.24	1.71	2.58	1.69	1.83	3.17	2.63
50	9.7	5.7	3.5	3.0	3.8	6.4	5.6	6.0	7.8	5.3	7.4	9.6	9.0
	3.73	2.51	2.32	2.03	1.22	1.54	1.38	1.92	2.90	1.89	2.05	3.52	2.86
100	11.4	6.7	4.2	3.5	4.6	7.6	6.7	7.2	9.3	6.3	8.8	11.2	10.5
	3.99	2.68	2.47	2.17	1.29	1.64	1.47	2.04	3.10	2.01	2.19	3.76	3.02
200	14.0	8.4	5.2	4.3	5.7	9.3	8.3	8.9	11.6	7.8	11.0	13.8	12.9
	3.83	2.56	2.36	2.07	1.23	1.57	1.40	1.96	2.96	1.92	2.08	3.60	2.94
Freq.	55.0	4.5	1.6	0.7	0.7	1.7	2.0	2.4	4.9	1.7	3.1	21.7	100.0

Roughness Class 2 ($z_0 = 0.1000$ m)

z	0	30	60	90	120	150	180	210	240	270	300	330	Total
10	6.2	3.5	2.2	1.9	2.5	3.9	3.4	4.0	4.9	3.2	5.1	6.2	5.7
	3.15	2.05	1.90	1.63	1.00	1.27	1.18	1.71	2.35	1.52	1.98	3.04	2.49
25	7.6	4.4	2.7	2.3	3.1	4.8	4.3	5.0	6.1	4.0	6.3	7.6	7.0
	3.34	2.20	2.03	1.74	1.06	1.35	1.26	1.83	2.51	1.63	2.12	3.23	2.63
50	8.9	5.1	3.2	2.7	3.8	5.7	5.1	5.8	7.1	4.7	7.4	8.8	8.2
	3.65	2.43	2.25	1.93	1.17	1.47	1.38	2.03	2.78	1.80	2.35	3.54	2.83
100	10.4	6.1	3.8	3.3	4.6	6.8	6.2	7.0	8.4	5.6	8.8	10.3	9.6
	4.01	2.67	2.47	2.12	1.28	1.62	1.52	2.23	3.06	1.97	2.58	3.89	3.06
200	12.7	7.5	4.7	4.0	5.6	8.3	7.6	8.6	10.4	6.9	10.9	12.6	11.8
	3.85	2.56	2.37	2.03	1.22	1.55	1.46	2.13	2.92	1.89	2.47	3.73	2.97
Freq.	50.5	4.3	1.5	0.7	0.8	1.7	2.0	2.7	4.6	1.7	4.3	25.2	100.0

Roughness Class 3 ($z_0 = 0.4000$ m)

z	0	30	60	90	120	150	180	210	240	270	300	330	Total
10	4.9	2.7	1.7	1.5	2.2	3.0	2.7	3.4	3.8	2.4	4.3	4.8	4.5
	3.04	1.96	1.81	1.64	1.06	1.25	1.21	1.88	2.27	1.48	2.26	3.06	2.47
25	6.4	3.6	2.3	2.0	3.0	4.0	3.6	4.4	5.0	3.2	5.6	6.3	5.9
	3.21	2.07	1.92	1.74	1.12	1.31	1.28	1.99	2.40	1.56	2.39	3.22	2.59
50	7.6	4.3	2.8	2.5	3.7	4.8	4.4	5.3	6.0	3.9	6.8	7.6	7.0
	3.44	2.25	2.08	1.89	1.21	1.42	1.38	2.16	2.61	1.70	2.60	3.47	2.76
100	9.1	5.2	3.3	3.0	4.6	5.9	5.4	6.4	7.2	4.8	8.1	9.1	8.4
	3.90	2.56	2.37	2.15	1.37	1.60	1.57	2.46	2.97	1.93	2.96	3.93	3.06
200	11.0	6.3	4.1	3.7	5.6	7.1	6.5	7.9	8.9	5.8	9.9	11.0	10.2
	3.77	2.47	2.28	2.08	1.33	1.55	1.51	2.37	2.87	1.86	2.85	3.80	2.98
Freq.	44.2	3.9	1.3	0.7	0.9	1.8	2.0	3.1	4.2	1.6	6.1	30.2	100.0

z	Class 0		Class 1		Class 2		Class 3	
m	ms^{-1}	Wm^{-2}	ms^{-1}	Wm^{-2}	ms^{-1}	Wm^{-2}	ms^{-1}	Wm^{-2}
10	8.4	526	5.8	191	5.1	125	4.0	61
25	9.2	678	6.9	311	6.2	225	5.2	133
50	9.8	827	8.0	449	7.3	342	6.3	223
100	10.6	1058	9.4	709	8.6	543	7.5	364
200	11.7	1439	11.5	1334	10.5	1005	9.1	657

Abu Darag — Gulf of Suez

29° 16′ 49.4″ N 32° 36′ 03.3″ E	UTM 36 E 461 235 m N 3 239 117 m	12 m

The Abu Darag mast is situated about 100 m W of the Suez–Hurghada road, approximately 20 km N of Zafarana (map sheet: NH 36 F3c). The distance to the coastline of the Gulf of Suez is 500 m in an easterly direction. There are no sheltering obstacles close to the mast. The surface consists mostly of sand dunes with a roughness length of about 0.01 m. The terrain rises to the W and reaches 200 m at a distance of 7.5 km. The highest peak to the NW is about 700 m a.s.l. Further to the W (20 km) the North Galala Plateau rise to more than 1000 m a.s.l.

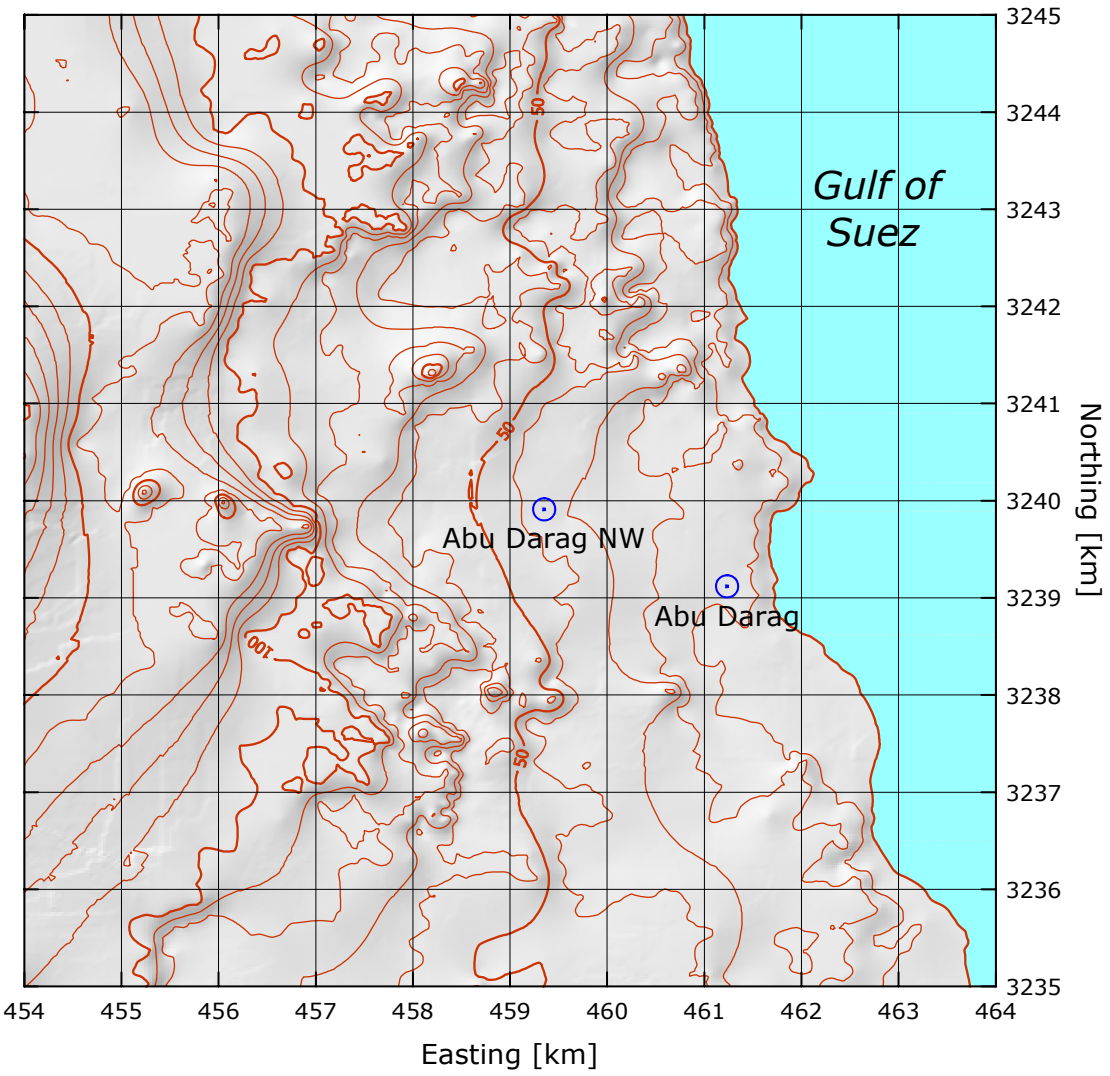

Sector	Input		Obstacles		Roughness		Orography		z_{0m}
0	0.0	0.0	0.0	0.0	−3.4	0.0	0.3	0.8	0.0010
30	0.0	0.0	0.0	0.0	−1.7	0.0	0.7	−0.4	0.0000
60	0.0	0.0	0.0	0.0	0.0	0.0	−0.9	−1.1	0.0000
90	0.0	0.0	0.0	0.0	0.0	0.0	−2.7	−0.8	0.0000
120	0.0	0.0	0.0	0.0	−0.5	0.0	−3.1	0.4	0.0000
150	0.0	0.0	0.0	0.0	−4.1	0.0	−1.6	1.2	0.0010
180	0.0	0.0	0.0	0.0	−0.1	0.0	0.2	0.8	0.0050
210	0.0	0.0	0.0	0.0	−0.2	0.0	0.6	−0.4	0.0050
240	0.0	0.0	0.0	0.0	2.5	0.0	−1.2	−1.3	0.0150
270	0.0	0.0	0.0	0.0	3.4	0.0	−3.3	−0.8	0.0130
300	0.0	0.0	0.0	0.0	4.9	0.0	−3.6	0.5	0.0150
330	0.0	0.0	0.0	0.0	1.3	0.0	−1.9	1.3	0.0110

Sect	Freq	<1	2	3	4	5	6	7	8	9	11	13	15	17	>17	*A*	*k*
0	62.8	1	4	7	13	22	38	62	92	123	291	225	100	21	2	10.9	4.11
30	8.1	6	19	38	71	94	111	125	127	127	194	73	15	1	0	8.2	3.04
60	1.5	26	104	244	252	185	104	53	15	7	8	1	0	0	0	4.1	2.17
90	0.7	40	178	343	243	126	48	17	4	0	1	1	0	0	0	3.3	2.15
120	0.6	40	157	228	230	154	85	46	29	18	9	4	0	0	0	4.0	1.82
150	1.2	22	84	104	95	91	86	88	86	82	103	86	52	16	6	7.6	1.88
180	1.1	31	130	164	140	104	87	69	57	45	71	52	30	14	7	5.7	1.37
210	1.7	28	133	174	167	129	89	70	58	47	67	31	7	1	0	5.0	1.52
240	4.0	17	64	87	99	100	98	100	94	93	138	75	25	9	3	7.6	2.15
270	2.4	39	109	121	102	100	103	111	91	72	81	43	18	6	4	6.5	1.86
300	1.6	56	190	245	209	132	64	37	29	17	14	4	1	0	0	3.7	1.59
330	14.2	6	22	46	61	61	59	68	78	90	211	185	92	21	1	10.1	3.25
Total	100.0	6	24	38	44	47	55	70	89	109	239	180	80	17	2	10.1	3.49

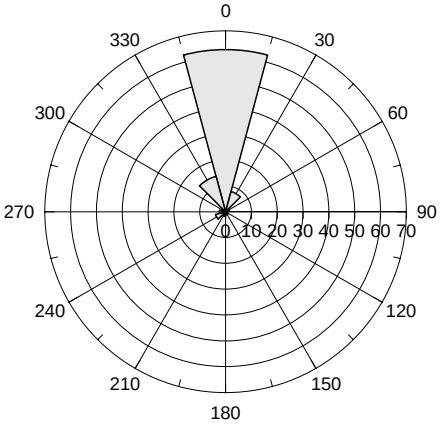

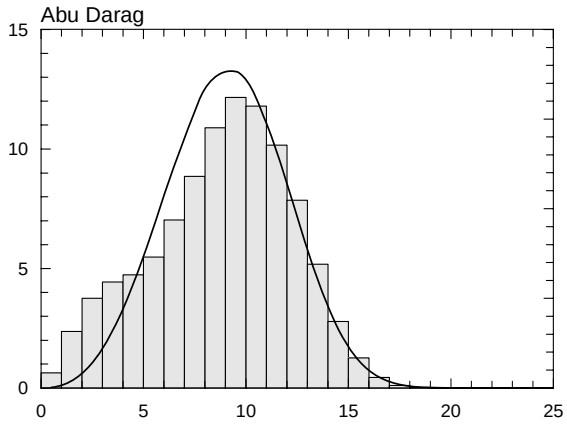

	Jan	Feb	Mar	Apr	May	Jun	Jul	Aug	Sep	Oct	Nov	Dec	Year
0	6.3	7.1	8.3	9.2	10.4	10.8	10.5	10.6	10.9	9.6	7.6	6.7	9.0
1	6.1	7.0	8.0	8.9	10.1	10.7	10.3	10.3	10.6	9.2	7.3	6.6	8.8
2	6.1	6.8	7.7	8.7	9.9	10.4	10.0	10.0	10.4	9.0	7.4	6.6	8.6
3	6.1	6.7	7.6	8.4	9.7	10.0	9.6	9.7	10.1	8.7	7.3	6.6	8.4
4	6.0	6.6	7.3	8.0	9.6	9.9	9.4	9.6	9.7	8.5	7.3	6.7	8.2
5	6.1	6.7	7.3	7.8	9.4	9.6	9.1	9.2	9.5	8.4	7.1	6.7	8.1
6	6.1	6.5	7.1	7.7	9.3	9.8	9.1	9.3	9.4	8.2	7.1	6.6	8.0
7	6.2	6.6	6.9	8.0	9.6	10.3	9.6	9.7	9.7	8.4	7.2	6.5	8.2
8	6.4	6.9	7.2	8.4	10.1	10.7	9.9	10.2	10.3	9.0	7.7	6.5	8.6
9	6.7	7.5	7.9	8.5	10.0	10.7	10.0	10.4	10.6	9.4	8.1	7.0	8.9
10	7.2	7.7	8.2	8.7	10.0	10.6	9.7	10.3	10.6	9.6	8.3	7.2	9.0
11	7.5	7.9	8.5	8.7	10.1	10.5	9.6	10.1	10.6	9.6	8.5	7.6	9.1
12	7.7	8.1	8.6	8.7	10.2	10.6	9.7	10.0	10.6	9.5	8.6	7.8	9.2
13	7.9	8.3	8.6	8.8	10.2	10.6	9.6	10.1	10.7	9.5	8.5	8.1	9.2
14	7.8	8.4	8.6	9.0	10.2	10.8	9.5	10.0	10.7	9.4	8.4	8.0	9.2
15	7.7	8.3	8.4	8.7	10.1	10.8	9.5	10.0	10.5	9.2	8.1	7.9	9.1
16	7.4	7.8	8.1	8.4	9.9	10.6	9.4	9.8	10.2	8.8	7.7	7.5	8.8
17	6.9	7.3	7.7	8.2	10.0	10.4	9.3	9.6	9.9	8.2	7.2	6.8	8.4
18	6.3	7.0	7.4	7.9	10.1	10.3	9.2	9.4	9.8	8.4	7.1	6.7	8.3
19	6.5	7.0	7.6	8.2	10.5	10.7	9.5	9.9	10.4	9.2	7.4	6.8	8.6
20	6.6	7.4	8.2	8.7	11.3	11.3	10.6	11.0	11.1	9.9	7.8	7.0	9.2
21	6.7	7.5	8.5	9.4	11.6	11.6	11.2	11.4	11.4	10.0	7.8	7.0	9.5
22	6.5	7.7	8.6	9.5	11.3	11.6	11.2	11.4	11.4	9.9	7.9	7.0	9.5
23	6.4	7.5	8.5	9.4	10.9	11.2	10.9	11.1	11.3	9.6	7.6	6.8	9.3
92-01	6.7	7.3	7.9	8.6	10.2	10.6	9.8	10.1	10.4	9.1	7.7	7.0	8.8

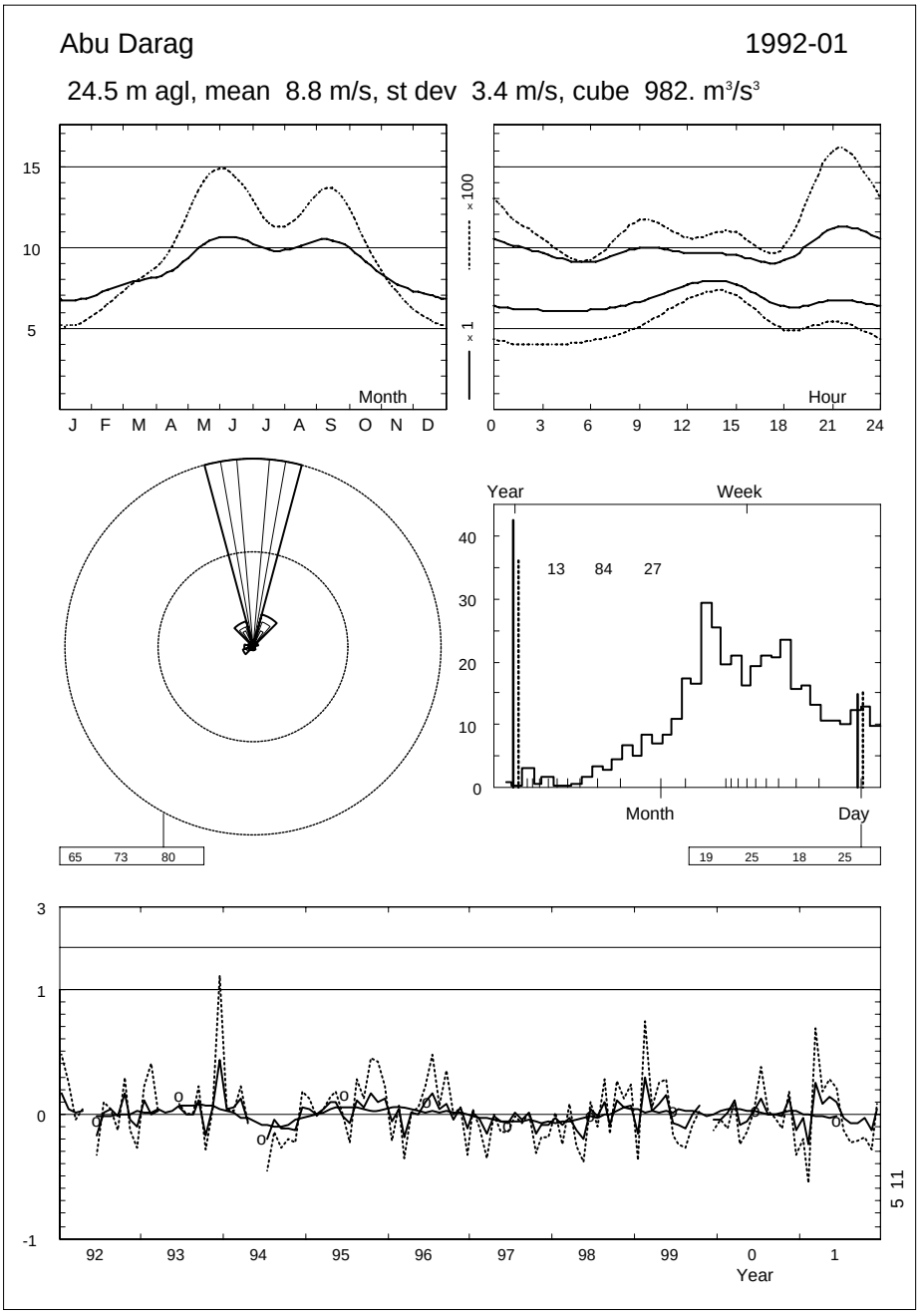

	Jan	Feb	Mar	Apr	May	Jun	Jul	Aug	Sep	Oct	Nov	Dec	Year
1991	—	—	8.3	8.3	10.2	10.1	10.2	9.8	11.5	9.5	8.4	6.4	9.3
1992	7.8	7.7	8.1	8.8	—	8.8	10.0	10.5	10.2	10.6	7.4	6.4	8.6
1993	7.5	7.3	8.1	—	—	11.1	9.8	10.1	11.6	7.6	8.2	10.1	9.4
1994	7.0	7.8	8.9	8.0	—	—	7.9	9.7	9.2	8.1	6.7	7.5	8.1
1995	7.0	7.3	8.2	9.4	11.1	10.4	9.1	11.2	11.0	10.7	8.5	7.9	9.3
1996	6.3	7.6	6.4	8.7	10.2	11.6	11.5	10.5	11.4	8.7	8.1	6.3	8.9
1997	6.8	7.1	6.6	8.5	9.6	9.9	10.0	9.7	10.5	7.7	7.0	6.4	8.3
1998	6.5	6.7	7.7	7.5	8.1	11.0	9.6	11.1	9.5	10.1	8.1	7.5	8.6
1999	5.7	9.5	8.1	9.3	11.7	9.9	8.9	9.0	10.4	9.7	—	6.7	8.9
2000	6.4	7.5	8.9	7.8	9.6	10.9	11.1	10.1	10.4	9.0	8.7	6.1	9.0
2001	6.5	5.5	9.9	9.3	11.5	11.7	9.6	9.4	9.7	8.9	6.8	7.3	8.6
2002	6.7	10.7	7.7	9.5	9.3	9.6	8.6	10.2	8.9	9.8	5.6	5.6	8.4
2003	5.9	—	7.5	8.7	7.4	9.0	8.2	10.1	7.5	—	—	—	8.2
2004	—	—	—	—	—	10.1	10.0	9.5	10.9	9.6	6.1	7.1	9.1
2005	5.7	6.0	9.0	8.9	8.5	—	—	—	—	—	—	—	7.8
92-01	6.7	7.3	7.9	8.6	10.2	10.6	9.8	10.1	10.4	9.1	7.7	7.0	8.8

Roughness Class 0 ($z_0 = 0.0002$ m)

z	0	30	60	90	120	150	180	210	240	270	300	330	Total
10	10.9	9.0	5.1	3.3	3.8	7.5	6.4	5.5	8.5	7.6	5.4	11.5	10.1
	4.17	3.05	1.64	1.82	1.59	1.81	1.53	1.62	2.30	2.08	1.38	3.63	3.04
25	11.8	9.9	5.6	3.7	4.2	8.2	7.0	6.0	9.3	8.3	5.9	12.6	11.1
	4.28	3.14	1.69	1.87	1.64	1.87	1.56	1.67	2.37	2.14	1.42	3.71	3.11
50	12.7	10.6	6.0	3.9	4.6	8.8	7.5	6.4	10.0	8.9	6.4	13.4	11.9
	4.40	3.23	1.74	1.92	1.68	1.92	1.61	1.72	2.43	2.20	1.46	3.81	3.18
100	13.7	11.5	6.5	4.3	4.9	9.5	8.1	7.0	10.8	9.7	6.9	14.4	12.8
	4.28	3.13	1.69	1.86	1.63	1.86	1.56	1.66	2.36	2.13	1.42	3.73	3.12
200	15.0	12.7	7.2	4.7	5.4	10.4	8.9	7.7	11.9	10.7	7.6	15.7	14.1
	4.10	2.96	1.60	1.76	1.54	1.77	1.49	1.58	2.24	2.01	1.34	3.60	3.02
Freq.	56.8	12.4	2.2	0.8	0.7	1.2	1.1	1.6	3.7	2.7	2.1	14.8	100.0

Roughness Class 1 ($z_0 = 0.0300$ m)

z	0	30	60	90	120	150	180	210	240	270	300	330	Total
10	7.6	5.3	2.8	2.3	2.9	5.1	4.1	4.2	5.9	5.0	6.2	8.0	7.1
	3.56	2.39	1.40	1.63	1.09	1.52	1.25	1.44	1.94	1.63	1.84	3.34	2.71
25	8.9	6.3	3.4	2.8	3.5	6.1	4.9	5.1	7.0	6.0	7.4	9.4	8.4
	3.80	2.58	1.50	1.76	1.17	1.63	1.35	1.56	2.09	1.76	1.94	3.52	2.86
50	10.2	7.3	4.0	3.2	4.2	7.1	5.8	5.9	8.1	6.9	8.4	10.7	9.6
	4.18	2.90	1.69	1.98	1.31	1.81	1.51	1.75	2.34	1.98	2.11	3.82	3.10
100	11.9	8.6	4.7	3.9	5.1	8.4	6.9	7.1	9.6	8.2	9.8	12.4	11.2
	4.47	3.09	1.79	2.11	1.39	1.94	1.60	1.86	2.49	2.11	2.27	4.10	3.28
200	14.5	10.7	5.8	4.8	6.2	10.4	8.5	8.8	11.9	10.3	11.8	14.8	13.7
	4.29	2.95	1.71	2.01	1.33	1.85	1.53	1.78	2.38	2.01	2.18	3.95	3.20
Freq.	53.5	7.0	1.5	0.7	0.7	1.2	1.2	1.9	3.7	2.5	3.9	22.2	100.0

Roughness Class 2 ($z_0 = 0.1000$ m)

z	0	30	60	90	120	150	180	210	240	270	300	330	Total
10	6.5	4.6	2.5	2.0	2.7	4.3	3.5	3.9	5.1	4.2	6.0	6.9	6.2
	3.55	2.33	1.44	1.50	1.07	1.47	1.27	1.52	1.92	1.58	2.17	3.42	2.73
25	8.0	5.6	3.1	2.5	3.4	5.4	4.4	4.9	6.3	5.2	7.3	8.4	7.6
	3.76	2.49	1.54	1.60	1.14	1.57	1.36	1.62	2.05	1.69	2.27	3.59	2.86
50	9.3	6.6	3.6	3.0	4.1	6.3	5.2	5.8	7.3	6.2	8.4	9.7	8.8
	4.09	2.76	1.70	1.77	1.26	1.72	1.50	1.79	2.26	1.87	2.44	3.86	3.07
100	10.9	7.8	4.3	3.5	4.9	7.6	6.3	6.9	8.7	7.4	9.8	11.3	10.3
	4.49	3.03	1.86	1.94	1.37	1.90	1.64	1.97	2.49	2.06	2.68	4.24	3.32
200	13.2	9.6	5.3	4.4	6.0	9.3	7.7	8.5	10.7	9.1	11.8	13.6	12.5
	4.32	2.90	1.78	1.86	1.31	1.82	1.58	1.88	2.38	1.97	2.59	4.09	3.24
Freq.	49.4	6.5	1.4	0.7	0.8	1.2	1.2	2.1	3.6	2.5	5.0	25.7	100.0

Roughness Class 3 ($z_0 = 0.4000$ m)

z	0	30	60	90	120	150	180	210	240	270	300	330	Total
10	5.1	3.5	1.9	1.7	2.4	3.3	2.7	3.3	3.9	3.2	5.0	5.4	4.9
	3.46	2.24	1.35	1.53	1.15	1.43	1.30	1.60	1.90	1.51	2.46	3.48	2.72
25	6.7	4.6	2.5	2.2	3.2	4.4	3.6	4.4	5.2	4.2	6.5	7.0	6.4
	3.63	2.38	1.42	1.62	1.22	1.51	1.37	1.69	2.01	1.60	2.56	3.64	2.84
50	8.0	5.6	3.0	2.7	4.0	5.3	4.4	5.3	6.2	5.1	7.7	8.3	7.6
	3.90	2.59	1.54	1.75	1.31	1.63	1.49	1.83	2.18	1.74	2.71	3.87	3.01
100	9.5	6.7	3.7	3.3	4.9	6.5	5.4	6.4	7.5	6.2	9.1	9.9	9.0
	4.40	2.95	1.76	1.99	1.49	1.85	1.69	2.09	2.49	1.97	2.99	4.31	3.32
200	11.4	8.2	4.4	4.0	5.9	7.8	6.6	7.8	9.2	7.6	10.9	11.9	10.9
	4.27	2.84	1.69	1.92	1.44	1.78	1.63	2.01	2.40	1.90	2.96	4.23	3.26
Freq.	43.5	5.7	1.3	0.7	0.8	1.2	1.3	2.4	3.5	2.4	6.6	30.7	100.0

z	Class 0		Class 1		Class 2		Class 3	
m	ms^{-1}	Wm^{-2}	ms^{-1}	Wm^{-2}	ms^{-1}	Wm^{-2}	ms^{-1}	Wm^{-2}
10	9.1	637	6.3	231	5.5	152	4.3	73
25	9.9	822	7.5	376	6.8	272	5.7	161
50	10.6	999	8.6	541	7.9	413	6.8	268
100	11.5	1266	10.1	840	9.3	648	8.1	437
200	12.6	1697	12.2	1528	11.2	1161	9.8	771

Zafarana, Mast 7 — Gulf of Suez

29° 10′ 22.2″ N 32° 37′ 44.9″ E	UTM 36 E 463 938 m N 3 227 191 m	18 m

Mast 7 is the reference met. station for the Egyptian-Danish Zafarana Wind Farm Project. The mast is situated just east of the wind farm site, approximately 7 km NNW of Zafarana (map sheet: NH 36 F3a). The distance to the coastline of the Gulf of Suez is about 2 km in an easterly direction. There are no sheltering obstacles close to the mast. The surface consists mostly of sand and gravel with a roughness length of less than 0.01 m. To the NW and S the wide valley is bordered by the North and South Galala Plateaus, respectively, which rise to more than 1000 m.

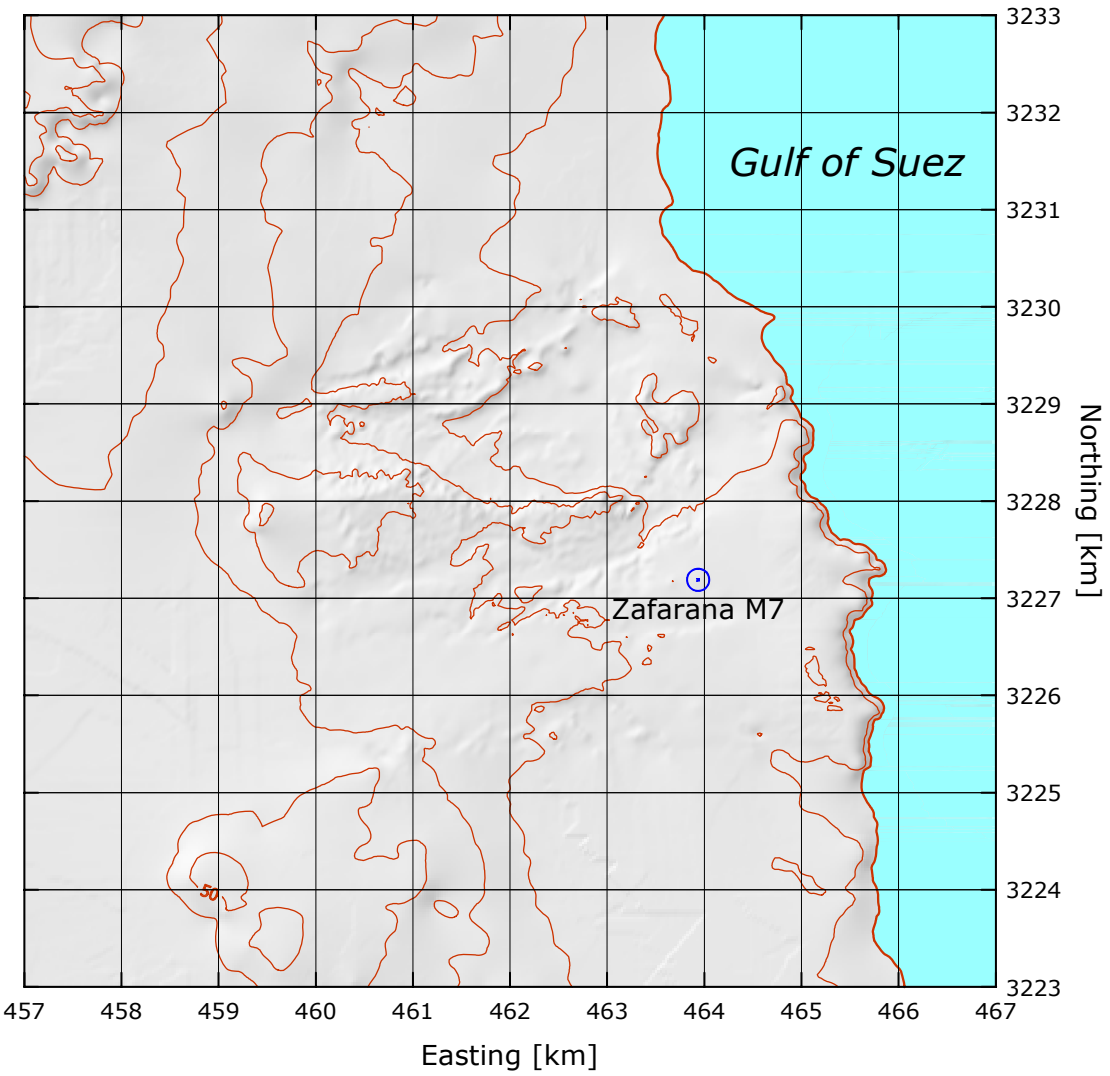

Sector	Input		Obstacles		Roughness		Orography		z_{0m}
0	0.0	0.0	0.0	0.0	−1.5	0.0	1.0	−0.3	0.0010
30	0.0	0.0	0.0	0.0	−0.6	0.0	0.3	−0.3	0.0000
60	0.0	0.0	0.0	0.0	0.0	0.0	−0.1	0.0	0.0000
90	0.0	0.0	0.0	0.0	−0.1	0.0	0.2	0.3	0.0000
120	0.0	0.0	0.0	0.0	−0.3	0.0	0.9	0.3	0.0000
150	0.0	0.0	0.0	0.0	−1.7	0.0	1.3	0.0	0.0000
180	0.0	0.0	0.0	0.0	−1.1	0.0	1.0	−0.3	0.0020
210	0.0	0.0	0.0	0.0	1.8	0.0	0.3	−0.4	0.0080
240	0.0	0.0	0.0	0.0	0.0	0.0	−0.1	0.0	0.0030
270	0.0	0.0	0.0	0.0	2.4	0.0	0.2	0.3	0.0060
300	0.0	0.0	0.0	0.0	1.7	0.0	0.9	0.4	0.0060
330	0.0	0.0	0.0	0.0	1.6	0.0	1.3	0.0	0.0060

Height of anemometer: 47.5 m a.g.l. 1998–2005

Sect	Freq	< 1	2	3	4	5	6	7	8	9	11	13	15	17	>17	*A*	*k*
0	74.1	0	2	4	9	14	25	40	61	89	261	259	160	61	14	12.0	4.18
30	4.7	7	27	56	97	124	154	149	127	112	115	27	4	0	0	7.1	2.79
60	1.1	32	106	195	224	187	157	67	18	8	2	2	0	0	0	4.4	2.43
90	0.5	28	126	295	291	152	72	32	4	0	1	0	0	0	0	3.7	2.50
120	0.7	13	104	181	224	193	112	78	43	16	13	9	10	5	0	4.7	1.67
150	1.7	14	53	66	82	107	101	101	88	62	121	89	61	31	26	8.3	1.78
180	0.7	14	69	165	165	146	89	75	52	60	58	38	27	25	18	5.8	1.29
210	0.4	18	119	219	225	135	105	56	37	29	37	7	5	5	3	4.4	1.40
240	3.0	6	27	56	73	72	84	95	107	112	214	105	31	13	5	8.9	2.79
270	5.7	6	23	51	91	124	144	146	128	100	125	44	11	4	3	7.4	2.42
300	1.8	11	75	200	284	238	111	41	20	9	7	4	1	0	0	4.3	2.28
330	5.7	6	29	72	106	124	109	89	81	85	143	87	54	14	2	8.0	2.09
Total	100.0	3	12	26	38	44	51	57	69	87	223	206	125	48	11	11.1	3.57

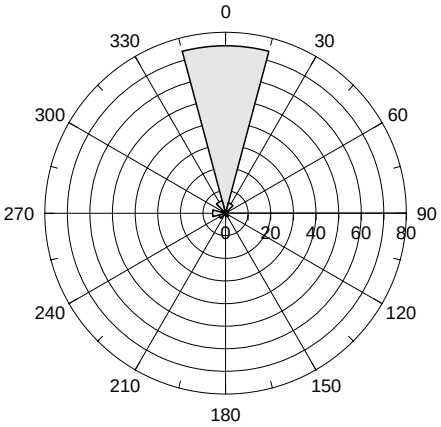

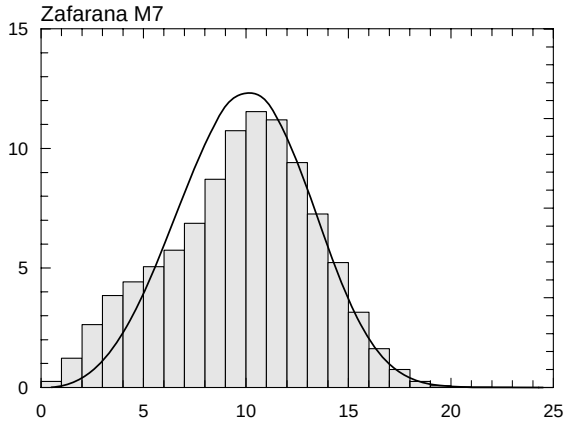

	Jan	Feb	Mar	Apr	May	Jun	Jul	Aug	Sep	Oct	Nov	Dec	Year
0	7.0	8.1	10.3	10.5	11.4	12.3	12.2	12.0	11.3	11.2	8.3	7.8	10.4
1	6.9	8.3	9.7	10.3	11.0	12.0	11.7	11.6	11.2	10.8	8.3	7.8	10.2
2	7.0	8.1	9.4	9.9	10.7	11.8	11.1	11.2	11.0	10.4	8.1	7.6	9.9
3	7.1	7.9	9.1	9.7	10.6	11.3	10.7	10.8	10.9	10.2	7.8	7.7	9.7
4	7.1	7.8	9.2	9.3	10.1	11.0	10.2	10.5	10.6	9.8	7.7	7.6	9.4
5	7.1	7.7	9.0	9.0	9.9	10.9	9.8	10.0	10.2	9.6	7.5	7.2	9.2
6	6.9	7.6	8.9	8.6	9.4	10.5	9.3	9.8	9.9	9.5	7.6	7.3	8.9
7	7.2	7.3	8.6	8.6	9.4	10.6	9.5	10.0	10.0	9.3	7.7	7.3	9.0
8	7.2	7.3	8.5	8.8	9.6	10.8	9.6	10.3	10.2	9.2	7.6	7.1	9.1
9	6.8	7.6	8.7	9.1	9.6	10.8	9.7	10.4	10.4	9.8	7.7	7.2	9.2
10	7.0	7.9	9.3	9.2	9.7	10.6	9.6	10.4	10.5	10.3	7.7	7.2	9.3
11	6.9	8.0	9.5	9.1	9.8	10.6	9.6	10.3	10.4	10.5	8.0	7.0	9.3
12	7.0	8.4	9.5	9.2	10.1	10.7	9.7	10.4	10.4	10.6	8.1	7.5	9.4
13	7.5	8.4	9.6	9.5	10.2	10.8	10.0	10.4	10.5	10.5	8.2	7.9	9.6
14	7.5	8.6	9.5	9.4	10.4	11.0	10.1	10.6	10.7	10.5	8.2	7.9	9.7
15	7.4	8.7	9.6	9.5	10.5	11.2	10.2	10.8	10.8	10.5	8.1	7.7	9.7
16	7.3	8.4	9.6	9.5	10.4	11.3	10.2	10.7	10.9	10.4	7.8	7.7	9.7
17	6.9	8.1	9.6	9.4	10.4	11.3	10.4	10.8	10.7	10.2	7.6	7.2	9.6
18	6.5	7.8	9.5	9.5	10.3	11.3	10.7	10.6	10.4	10.1	7.8	7.3	9.5
19	6.2	7.8	9.6	9.7	10.7	11.6	10.9	10.9	10.8	10.7	8.0	7.4	9.8
20	6.6	8.1	10.1	10.4	11.5	12.3	12.0	12.0	11.7	11.1	8.4	7.4	10.4
21	6.8	8.4	10.6	10.7	12.0	13.1	12.8	12.6	12.0	11.5	8.7	7.2	10.8
22	6.8	8.2	10.7	10.6	12.1	13.0	12.8	12.8	11.8	11.4	8.7	7.4	10.8
23	6.8	8.2	10.7	10.7	11.8	12.7	12.6	12.4	11.5	11.4	8.5	7.5	10.7
Mean	7.0	8.0	9.5	9.6	10.5	11.4	10.6	10.9	10.8	10.4	8.0	7.4	9.7

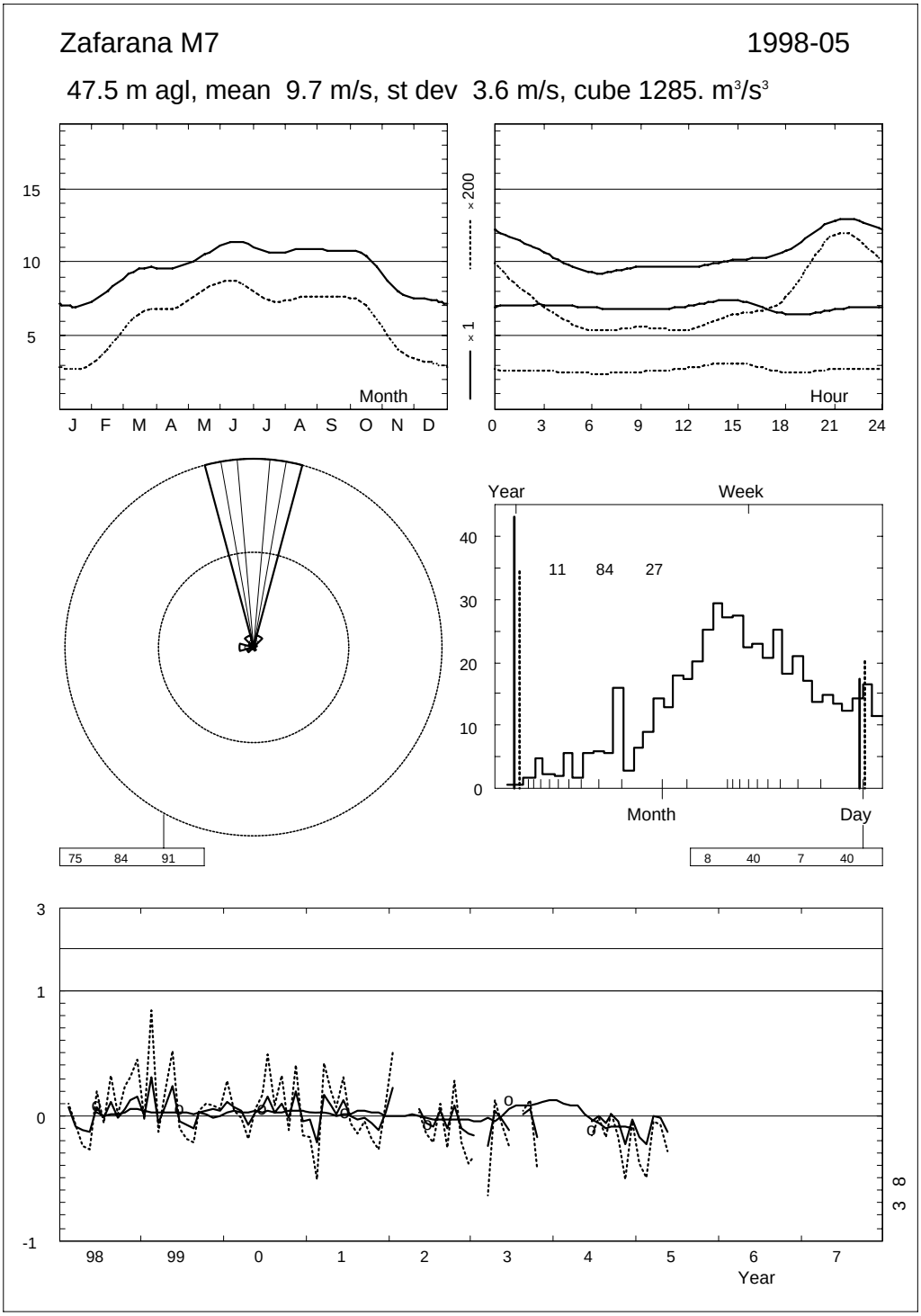

	Jan	Feb	Mar	Apr	May	Jun	Jul	Aug	Sep	Oct	Nov	Dec	Year
1998	—	8.6	8.8	8.5	9.1	12.1	10.5	12.2	10.6	11.0	9.0	8.6	9.9
1999	7.0	10.4	8.9	10.4	12.9	10.9	9.9	9.9	11.1	10.9	8.4	7.8	9.9
2000	7.7	8.6	9.9	8.9	10.8	12.2	12.3	11.2	11.8	10.2	9.6	7.1	9.9
2001	6.8	6.3	11.1	10.4	10.5	12.8	10.6	10.5	10.7	9.8	7.1	7.7	9.8
2002	8.6	—	—	—	11.1	10.8	9.8	11.4	9.7	11.2	7.2	6.4	9.5
2003	5.9	—	7.2	10.0	10.2	10.1	—	11.1	11.4	8.6	—	—	10.3
2004	—	—	—	—	—	10.8	10.6	10.2	10.9	9.9	6.2	7.2	9.4
2005	5.8	6.2	9.5	9.4	9.2	—	—	—	—	—	—	—	8.2
Mean	7.0	8.0	9.5	9.6	10.5	11.4	10.6	10.9	10.8	10.4	8.0	7.4	9.7

Roughness Class 0 ($z_0 = 0.0002$ m)

z	0	30	60	90	120	150	180	210	240	270	300	330	Total
10	10.6	8.9	4.5	3.3	4.0	7.1	5.6	4.3	8.3	7.0	4.5	7.3	9.6
	3.85	2.70	1.67	2.13	1.53	1.64	1.30	1.30	2.60	2.31	1.66	1.98	2.88
25	11.5	9.7	5.0	3.6	4.4	7.8	6.2	4.7	9.0	7.7	4.9	8.1	10.5
	3.94	2.78	1.72	2.20	1.58	1.69	1.33	1.34	2.68	2.38	1.71	2.04	2.94
50	12.3	10.4	5.3	3.8	4.7	8.4	6.7	5.1	9.7	8.2	5.3	8.6	11.3
	4.05	2.86	1.77	2.26	1.62	1.73	1.37	1.37	2.75	2.45	1.76	2.10	3.00
100	13.3	11.3	5.8	4.2	5.1	9.1	7.2	5.5	10.5	8.9	5.7	9.4	12.2
	3.95	2.77	1.72	2.18	1.57	1.68	1.33	1.33	2.67	2.37	1.70	2.03	2.94
200	14.6	12.5	6.3	4.6	5.6	9.9	7.8	6.0	11.7	9.9	6.3	10.4	13.4
	3.78	2.62	1.63	2.07	1.49	1.60	1.27	1.26	2.53	2.24	1.61	1.92	2.85
Freq.	68.5	10.3	1.5	0.6	0.7	1.6	0.8	0.4	2.8	5.5	2.1	5.3	100.0

Roughness Class 1 ($z_0 = 0.0300$ m)

z	0	30	60	90	120	150	180	210	240	270	300	330	Total
10	7.4	4.7	2.7	2.4	3.2	4.8	3.4	4.4	5.5	4.7	3.2	6.9	6.7
	3.29	1.83	1.85	1.63	1.11	1.38	1.03	1.51	2.04	1.88	1.20	2.92	2.58
25	8.7	5.6	3.2	2.8	3.9	5.8	4.1	5.4	6.5	5.7	3.9	8.2	8.0
	3.50	1.98	2.00	1.76	1.19	1.48	1.10	1.63	2.21	2.04	1.29	3.14	2.72
50	9.9	6.4	3.7	3.3	4.6	6.8	4.9	6.2	7.6	6.5	4.6	9.4	9.2
	3.85	2.22	2.24	1.98	1.33	1.65	1.22	1.83	2.48	2.29	1.44	3.50	2.96
100	11.6	7.7	4.4	3.9	5.5	8.1	5.9	7.4	8.9	7.8	5.6	11.1	10.7
	4.12	2.37	2.39	2.10	1.41	1.76	1.30	1.94	2.64	2.44	1.53	3.73	3.13
200	14.1	9.5	5.4	4.9	6.8	9.9	7.3	9.2	11.1	9.6	6.9	13.7	13.1
	3.95	2.26	2.28	2.01	1.35	1.68	1.24	1.85	2.52	2.33	1.46	3.57	3.04
Freq.	63.1	4.8	1.0	0.6	0.8	1.5	0.6	0.8	3.4	5.1	2.4	15.8	100.0

Roughness Class 2 ($z_0 = 0.1000$ m)

z	0	30	60	90	120	150	180	210	240	270	300	330	Total
10	6.4	4.0	2.3	2.1	2.9	4.2	2.9	4.2	4.6	4.0	3.0	6.2	5.9
	3.28	1.78	1.83	1.52	1.12	1.38	1.04	1.67	1.99	1.85	1.22	3.13	2.59
25	7.8	4.9	2.8	2.6	3.7	5.2	3.7	5.2	5.7	5.0	3.8	7.6	7.2
	3.46	1.90	1.96	1.63	1.19	1.47	1.10	1.79	2.13	1.98	1.30	3.33	2.72
50	9.1	5.8	3.3	3.1	4.4	6.2	4.5	6.1	6.7	5.9	4.6	8.8	8.3
	3.76	2.10	2.17	1.80	1.31	1.62	1.21	1.98	2.36	2.19	1.43	3.65	2.92
100	10.6	6.9	4.0	3.7	5.4	7.4	5.4	7.3	8.0	7.0	5.5	10.4	9.8
	4.13	2.31	2.38	1.97	1.43	1.78	1.33	2.17	2.59	2.40	1.57	4.01	3.16
200	12.9	8.5	4.9	4.5	6.6	9.0	6.6	9.0	9.9	8.6	6.7	12.7	12.0
	3.97	2.21	2.28	1.89	1.37	1.71	1.27	2.08	2.48	2.30	1.50	3.85	3.07
Freq.	57.7	4.4	1.0	0.6	0.9	1.4	0.6	1.0	3.7	4.8	2.7	21.1	100.0

Roughness Class 3 ($z_0 = 0.4000$ m)

z	0	30	60	90	120	150	180	210	240	270	300	330	Total
10	5.0	3.1	1.8	1.7	2.6	3.3	2.3	3.5	3.5	3.1	2.7	4.9	4.6
	3.23	1.74	1.75	1.44	1.18	1.38	1.06	1.84	1.96	1.79	1.30	3.21	2.58
25	6.5	4.1	2.3	2.2	3.4	4.3	3.1	4.6	4.7	4.1	3.5	6.4	6.0
	3.39	1.85	1.85	1.52	1.25	1.46	1.12	1.95	2.08	1.90	1.38	3.38	2.70
50	7.8	4.9	2.8	2.7	4.2	5.3	3.8	5.6	5.7	4.9	4.3	7.7	7.2
	3.63	2.01	2.01	1.65	1.35	1.57	1.21	2.12	2.26	2.06	1.49	3.63	2.87
100	9.3	5.9	3.4	3.3	5.2	6.4	4.8	6.8	6.8	6.0	5.3	9.2	8.6
	4.08	2.29	2.29	1.87	1.53	1.79	1.37	2.42	2.57	2.35	1.70	4.12	3.17
200	11.2	7.3	4.2	4.1	6.3	7.8	5.8	8.3	8.3	7.3	6.4	11.1	10.4
	3.97	2.21	2.21	1.81	1.48	1.72	1.32	2.33	2.47	2.26	1.64	3.98	3.10
Freq.	50.2	3.9	0.9	0.6	1.0	1.3	0.6	1.3	4.0	4.3	3.2	28.6	100.0

z	Class 0		Class 1		Class 2		Class 3	
m	ms^{-1}	Wm^{-2}	ms^{-1}	Wm^{-2}	ms^{-1}	Wm^{-2}	ms^{-1}	Wm^{-2}
10	8.6	558	6.0	201	5.2	133	4.1	64
25	9.4	720	7.1	327	6.4	238	5.4	141
50	10.1	876	8.2	472	7.4	360	6.4	235
100	10.9	1116	9.6	741	8.8	569	7.7	383
200	11.9	1504	11.7	1373	10.7	1038	9.3	685

Zafarana — Gulf of Suez

29° 06′ 48.7″ N 32° 36′ 38.9″ E	UTM 36 E 462 134 m N 3220 626 m	25 m

The Zafarana mast is situated about 80 m S of the Zafarana–El Wasta road, approximately 5 km W of Zafarana along this road (map sheet: NH 36 F3a). The distance to the coastline of the Gulf of Suez is 5000 m in an easterly direction. There are no sheltering obstacles close to the mast. The surface consists mostly of sand and gravel with a roughness length of less than 0.01 m. To the NW and S the wide valley is bordered by the North and South Galala Plateaus, respectively, which rise to more than 1000 m.

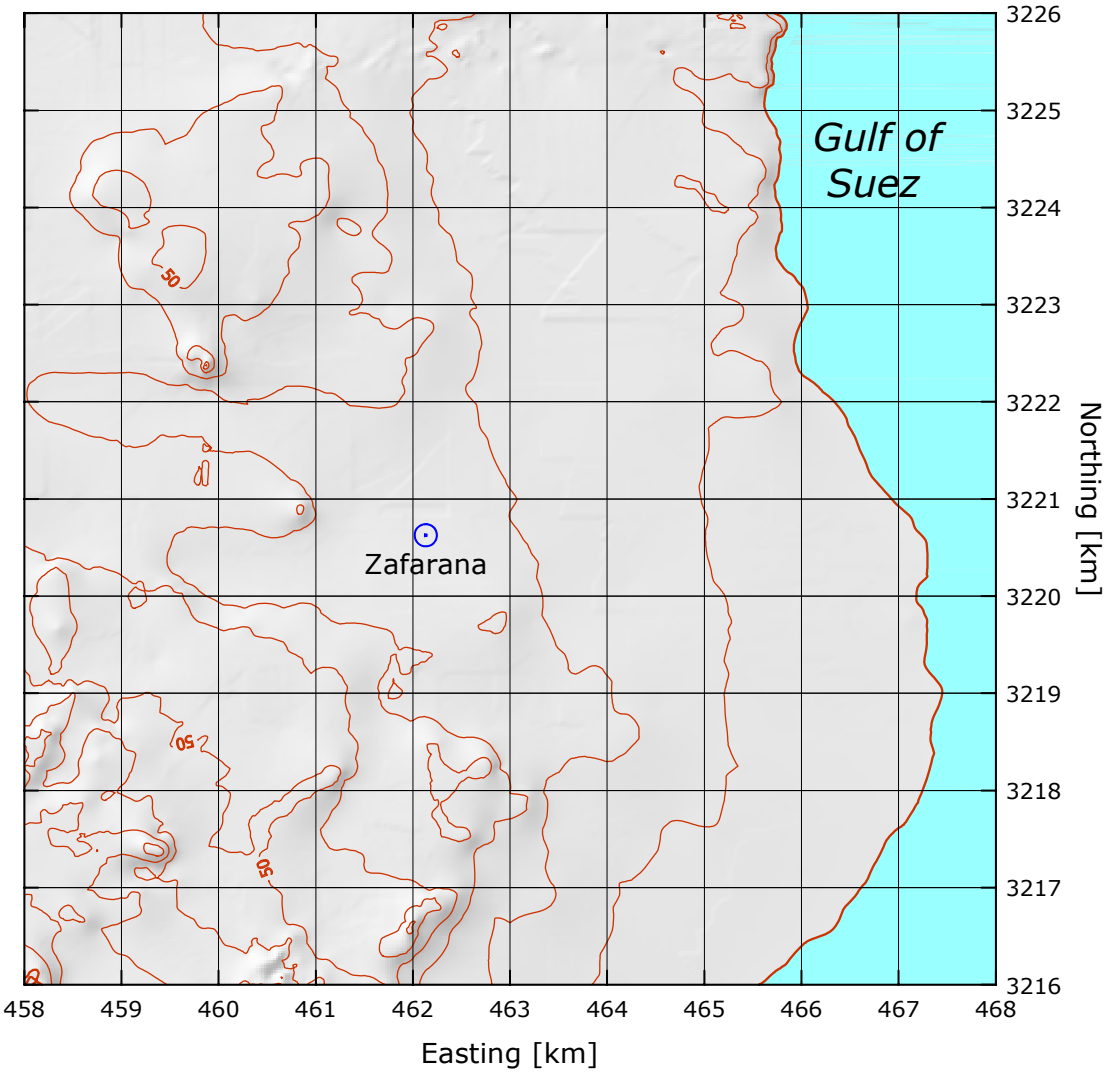

Sector	Input		Obstacles		Roughness		Orography		z_{0m}
0	0.0	0.0	0.0	0.0	−1.7	0.0	−1.9	−0.3	0.0020
30	0.0	0.0	0.0	0.0	−3.4	0.0	−1.5	0.5	0.0010
60	0.0	0.0	0.0	0.0	−3.7	0.0	−0.2	0.7	0.0010
90	0.0	0.0	0.0	0.0	−3.6	0.0	0.7	0.2	0.0010
120	0.0	0.0	0.0	0.0	−3.7	0.0	0.4	−0.5	0.0000
150	0.0	0.0	0.0	0.0	−3.8	0.0	−0.9	−0.7	0.0010
180	0.0	0.0	0.0	0.0	−1.1	0.0	−1.9	−0.3	0.0020
210	0.0	0.0	0.0	0.0	4.5	0.0	−1.8	0.5	0.0120
240	0.0	0.0	0.0	0.0	3.9	0.0	−0.4	0.8	0.0110
270	0.0	0.0	0.0	0.0	1.5	0.0	0.7	0.3	0.0030
300	0.0	0.0	0.0	0.0	4.2	0.0	0.4	−0.5	0.0060
330	0.0	0.0	0.0	0.0	1.0	0.0	−0.9	−0.8	0.0050

Sect	Freq	<1	2	3	4	5	6	7	8	9	11	13	15	17	>17	*A*	*k*
0	57.0	1	3	6	9	16	29	52	86	114	276	240	125	39	7	11.3	3.98
30	14.9	2	10	17	31	47	68	94	118	129	248	160	60	13	2	9.9	3.42
60	1.7	18	81	136	206	192	162	117	58	19	10	1	0	0	0	5.0	2.52
90	0.7	31	147	234	307	164	68	30	12	3	3	0	0	0	0	3.8	2.38
120	1.1	26	86	155	184	167	106	82	51	31	45	35	25	6	2	5.1	1.39
150	2.0	12	50	73	88	97	94	87	84	73	146	104	57	25	12	8.4	2.05
180	0.7	21	99	134	136	121	86	78	60	51	104	64	27	10	10	6.4	1.54
210	0.4	37	167	186	147	108	108	89	63	34	46	6	4	2	3	4.8	1.56
240	3.2	9	39	59	56	59	75	100	111	117	203	119	34	14	4	9.0	2.85
270	8.5	4	23	50	75	111	146	161	126	86	108	65	28	12	5	7.6	2.08
300	5.6	5	37	96	149	202	205	157	88	36	18	5	2	1	0	5.7	2.82
330	4.2	6	43	101	157	185	168	127	85	47	49	22	9	2	0	5.9	2.07
Total	100.0	3	16	30	44	56	67	80	93	102	217	174	86	26	5	10.2	3.19

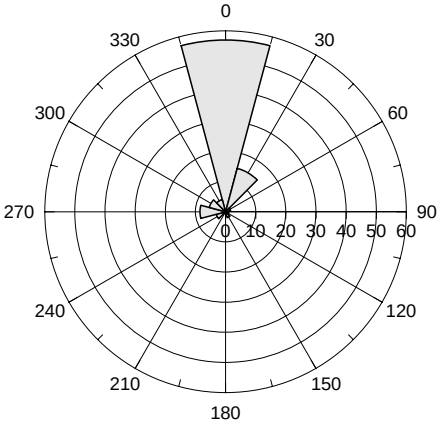

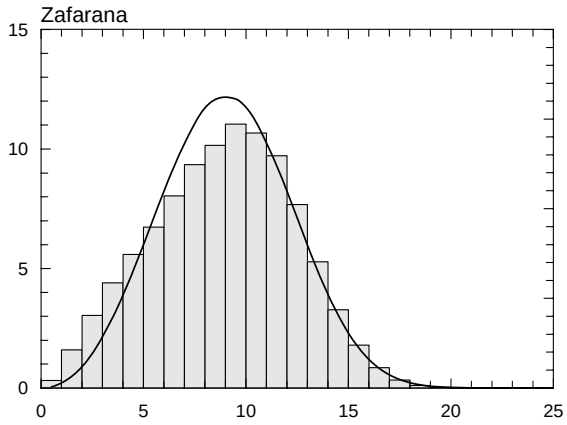

	Jan	Feb	Mar	Apr	May	Jun	Jul	Aug	Sep	Oct	Nov	Dec	Year
0	6.7	7.4	8.5	9.5	10.3	11.4	11.0	11.1	10.6	9.3	7.4	6.9	9.3
1	6.7	7.3	8.3	9.1	9.6	11.0	10.6	10.6	10.0	8.9	7.3	6.9	8.9
2	6.7	7.2	7.8	8.7	9.4	10.4	9.9	10.1	9.7	8.4	7.2	6.9	8.6
3	6.8	7.0	7.5	8.4	9.1	9.9	9.5	9.6	9.3	8.2	6.9	7.0	8.3
4	6.8	6.8	7.3	7.9	8.5	9.5	8.8	9.1	8.9	7.8	6.9	7.1	8.0
5	7.0	6.8	7.1	7.6	8.2	9.0	8.3	8.7	8.4	7.7	6.8	7.1	7.8
6	6.9	6.8	7.0	7.4	8.0	9.0	8.0	8.3	8.1	7.6	6.9	7.2	7.6
7	6.9	7.0	6.8	7.7	8.9	10.0	8.8	9.4	8.7	7.8	6.9	7.1	8.1
8	6.9	7.1	7.4	8.3	9.1	10.5	8.9	9.8	9.5	8.7	7.2	7.1	8.4
9	7.1	7.4	7.8	8.4	9.2	10.5	9.1	9.8	9.6	9.0	7.6	7.0	8.6
10	6.9	7.5	8.0	8.7	9.5	10.5	9.2	9.9	9.8	9.3	7.6	7.0	8.7
11	7.2	7.6	8.5	9.0	9.7	10.5	9.2	10.0	9.8	9.5	7.7	7.1	8.9
12	7.7	8.0	8.6	9.2	10.0	10.7	9.5	10.2	10.0	9.6	8.1	7.4	9.1
13	8.1	8.6	9.0	9.4	10.2	10.8	9.8	10.5	10.4	9.6	8.3	7.7	9.4
14	8.4	8.8	9.0	9.6	10.3	11.0	10.0	10.9	10.9	9.8	8.4	8.2	9.7
15	8.3	8.7	9.2	9.7	10.5	11.4	10.4	11.1	11.3	10.0	8.6	8.2	9.8
16	8.2	8.7	9.1	9.8	10.6	11.8	10.5	11.3	11.4	9.9	8.3	8.1	9.8
17	7.4	8.0	9.0	9.6	10.5	11.9	10.6	11.2	11.0	9.1	7.4	7.2	9.5
18	7.0	7.3	8.2	9.0	10.2	11.6	10.3	10.5	10.0	8.7	7.1	6.8	9.0
19	6.8	7.1	8.2	8.9	10.2	11.1	10.0	10.3	10.3	9.4	7.2	6.8	8.9
20	6.8	7.4	8.6	9.5	11.0	11.8	10.8	11.3	11.2	10.0	7.4	6.9	9.5
21	6.8	7.6	9.0	9.9	11.4	12.5	12.0	12.0	11.6	10.3	7.5	7.0	9.9
22	6.9	7.5	9.0	10.0	11.3	12.4	12.0	12.1	11.4	9.9	7.5	6.9	9.8
23	6.9	7.5	9.0	9.7	10.9	11.9	11.6	11.7	11.0	9.6	7.5	7.0	9.6
93-02	7.2	7.5	8.2	9.0	9.9	10.9	9.9	10.4	10.1	9.1	7.5	7.2	9.0

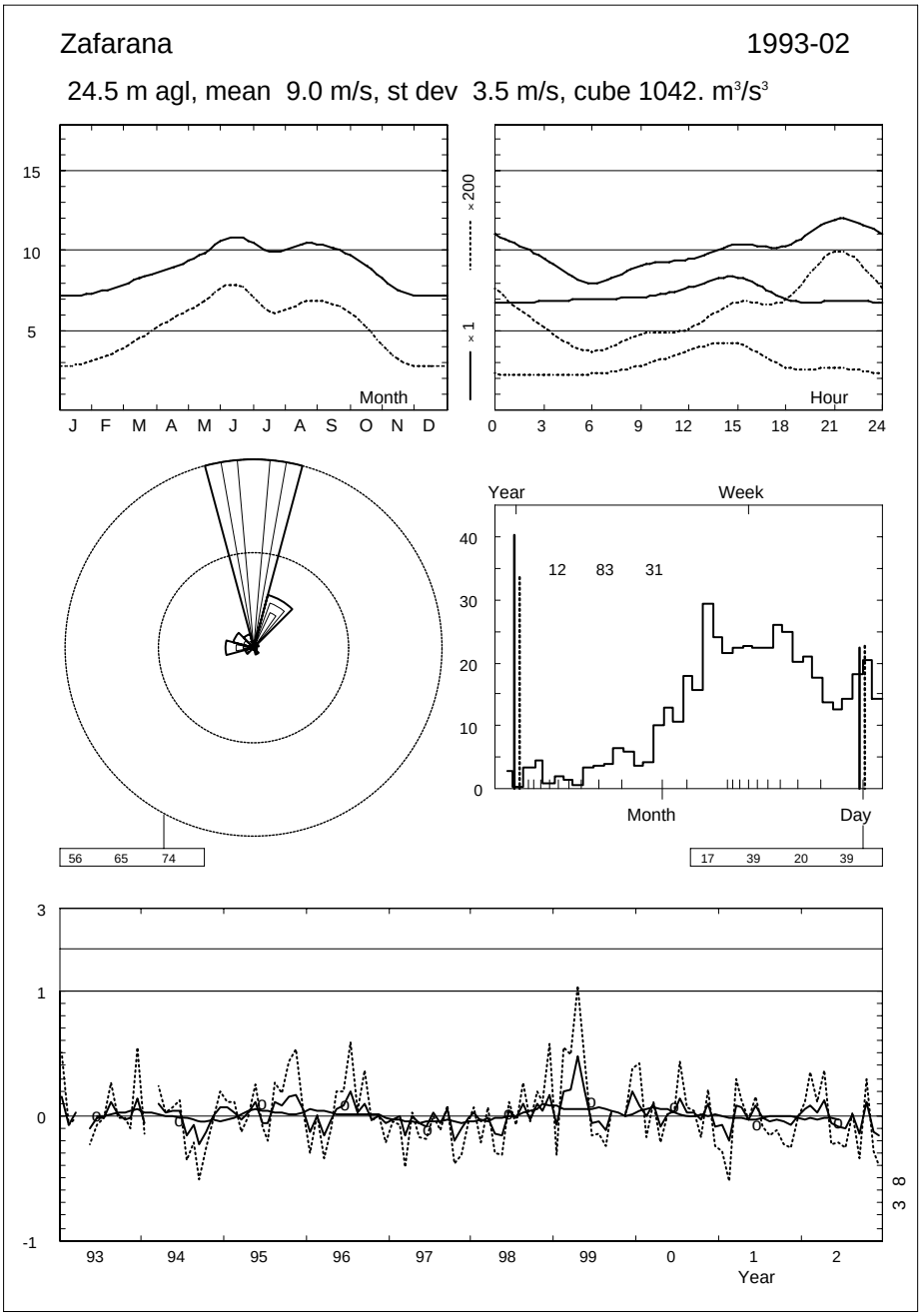

	Jan	Feb	Mar	Apr	May	Jun	Jul	Aug	Sep	Oct	Nov	Dec	Year
1991	—	—	8.6	8.4	9.7	—	8.8	10.1	11.6	9.0	8.2	7.2	9.1
1992	8.0	8.6	9.3	—	9.6	9.3	10.2	10.5	10.2	10.0	7.6	6.6	9.1
1993	8.3	7.0	8.4	—	8.9	10.6	9.8	11.5	10.3	8.8	7.4	8.2	9.0
1994	6.8	—	9.0	9.2	10.3	11.3	8.4	9.6	7.9	8.0	7.5	7.7	8.8
1995	7.6	7.7	8.0	9.2	11.0	10.3	9.4	11.5	10.9	10.5	8.7	7.5	9.4
1996	6.3	7.5	7.0	8.6	10.4	11.8	11.9	10.7	11.1	8.8	7.4	6.7	9.0
1997	6.9	7.5	6.9	9.0	9.2	9.9	10.1	9.8	10.6	7.3	6.7	7.1	8.5
1998	7.3	7.2	8.2	7.7	8.3	11.4	9.8	11.4	9.8	9.9	7.8	8.4	9.0
1999	6.6	9.1	10.0	13.2	11.8	10.2	9.4	9.2	10.4	—	7.6	8.6	9.5
2000	7.7	7.5	9.0	8.2	10.0	11.3	11.3	10.6	10.4	8.7	8.2	6.5	9.2
2001	6.6	6.0	9.0	9.5	9.5	11.8	9.8	9.9	9.8	8.7	6.9	7.2	8.7
2002	7.5	8.2	8.5	10.1	9.2	10.0	8.9	10.5	8.7	10.1	6.5	6.1	8.7
2003	6.1	6.8	7.6	9.2	9.0	9.4	8.8	10.4	6.5	—	—	—	8.4
2004	—	—	—	—	—	9.5	9.8	9.8	10.8	9.3	6.4	7.0	9.0
2005	6.1	6.1	8.8	8.8	8.7	—	—	—	—	—	—	—	7.7
93-02	7.2	7.5	8.2	9.0	9.9	10.9	9.9	10.4	10.1	9.1	7.5	7.2	9.0

Roughness Class 0 ($z_0 = 0.0002$ m)

z	0	30	60	90	120	150	180	210	240	270	300	330	Total
10	12.2	10.7	7.1	3.9	4.9	8.2	7.2	6.1	9.7	7.8	6.2	6.3	10.6
	4.24	3.56	1.91	2.20	1.37	1.97	1.72	1.72	3.02	2.26	2.71	2.30	2.86
25	13.3	11.6	7.8	4.3	5.4	9.0	7.9	6.7	10.6	8.6	6.8	6.9	11.6
	4.32	3.65	1.97	2.27	1.41	2.02	1.76	1.78	3.10	2.33	2.79	2.37	2.91
50	14.2	12.4	8.4	4.6	5.9	9.6	8.5	7.2	11.4	9.2	7.3	7.4	12.4
	4.44	3.75	2.02	2.33	1.45	2.08	1.81	1.83	3.19	2.40	2.87	2.44	2.97
100	15.2	13.4	9.1	5.0	6.3	10.4	9.2	7.8	12.3	10.0	7.9	8.1	13.3
	4.35	3.65	1.96	2.26	1.40	2.02	1.76	1.77	3.10	2.32	2.77	2.36	2.94
200	16.5	14.7	10.0	5.5	6.9	11.4	10.1	8.6	13.6	11.1	8.8	8.9	14.5
	4.21	3.50	1.85	2.13	1.33	1.93	1.68	1.68	2.95	2.20	2.63	2.23	2.88
Freq.	52.5	18.5	2.8	0.8	1.0	1.9	0.8	0.5	3.0	7.9	5.7	4.4	100.0

Roughness Class 1 ($z_0 = 0.0300$ m)

z	0	30	60	90	120	150	180	210	240	270	300	330	Total
10	8.6	7.0	3.4	2.7	3.8	5.8	4.6	5.4	6.3	5.3	4.2	7.5	7.5
	3.71	2.94	2.00	1.39	1.21	1.71	1.37	1.84	2.27	1.88	2.41	2.75	2.62
25	10.1	8.4	4.0	3.3	4.7	6.9	5.6	6.5	7.6	6.3	5.0	8.8	8.8
	3.88	3.15	2.17	1.49	1.30	1.82	1.47	1.99	2.44	2.03	2.60	2.91	2.74
50	11.4	9.6	4.7	3.8	5.5	7.9	6.5	7.6	8.7	7.3	5.8	10.0	10.0
	4.16	3.50	2.43	1.68	1.45	2.01	1.63	2.23	2.74	2.28	2.92	3.17	2.94
100	13.1	11.2	5.5	4.6	6.6	9.3	7.7	8.9	10.3	8.7	6.9	11.6	11.6
	4.47	3.74	2.59	1.78	1.54	2.15	1.74	2.38	2.92	2.42	3.12	3.40	3.13
200	15.4	13.9	6.9	5.7	8.1	11.3	9.5	11.1	12.8	10.8	8.5	14.0	13.9
	4.32	3.58	2.47	1.71	1.47	2.06	1.67	2.27	2.79	2.31	2.97	3.27	3.11
Freq.	51.7	13.1	1.5	0.8	1.2	1.8	0.7	0.9	4.0	8.0	5.3	11.1	100.0

Roughness Class 2 ($z_0 = 0.1000$ m)

z	0	30	60	90	120	150	180	210	240	270	300	330	Total
10	7.4	6.1	2.9	2.5	3.6	5.0	4.0	5.0	5.3	4.6	3.7	6.9	6.5
	3.70	2.88	1.97	1.37	1.26	1.70	1.37	2.00	2.16	1.92	2.35	3.15	2.64
25	9.0	7.5	3.6	3.1	4.5	6.1	4.9	6.2	6.6	5.6	4.5	8.4	7.9
	3.86	3.07	2.11	1.47	1.34	1.80	1.46	2.14	2.31	2.05	2.52	3.31	2.76
50	10.4	8.7	4.2	3.7	5.3	7.2	5.8	7.3	7.7	6.6	5.3	9.6	9.2
	4.10	3.37	2.33	1.62	1.48	1.96	1.60	2.37	2.56	2.27	2.79	3.54	2.93
100	12.0	10.2	5.0	4.4	6.4	8.5	7.0	8.7	9.1	7.9	6.3	11.2	10.7
	4.49	3.71	2.56	1.78	1.62	2.15	1.76	2.60	2.81	2.49	3.06	3.89	3.17
200	14.2	12.5	6.2	5.5	7.9	10.3	8.6	10.7	11.3	9.7	7.8	13.4	12.8
	4.35	3.55	2.45	1.71	1.56	2.07	1.68	2.49	2.69	2.39	2.93	3.76	3.14
Freq.	48.4	12.0	1.4	0.8	1.3	1.7	0.7	1.1	4.5	7.8	5.2	15.2	100.0

Roughness Class 3 ($z_0 = 0.4000$ m)

z	0	30	60	90	120	150	180	210	240	270	300	330	Total
10	5.8	4.7	2.2	2.0	3.0	3.9	3.1	4.1	4.1	3.5	2.9	5.6	5.1
	3.67	2.84	1.95	1.23	1.31	1.69	1.36	2.15	2.09	1.93	2.24	3.43	2.66
25	7.5	6.2	3.0	2.6	4.0	5.1	4.1	5.4	5.3	4.6	3.8	7.2	6.6
	3.80	3.00	2.06	1.30	1.39	1.77	1.44	2.28	2.22	2.05	2.37	3.57	2.76
50	8.9	7.4	3.6	3.2	4.9	6.2	5.0	6.6	6.4	5.6	4.6	8.6	7.9
	4.00	3.24	2.24	1.41	1.51	1.90	1.56	2.48	2.41	2.22	2.58	3.77	2.90
100	10.5	8.9	4.3	3.9	5.9	7.4	6.1	7.9	7.7	6.7	5.5	10.2	9.4
	4.37	3.68	2.56	1.60	1.71	2.15	1.77	2.83	2.74	2.53	2.94	4.15	3.15
200	12.5	10.8	5.3	4.8	7.2	8.9	7.4	9.7	9.5	8.2	6.8	12.1	11.2
	4.36	3.55	2.46	1.54	1.65	2.08	1.71	2.72	2.65	2.44	2.83	4.11	3.15
Freq.	43.8	10.5	1.3	0.8	1.4	1.6	0.6	1.4	5.1	7.4	5.0	20.9	100.0

z	Class 0		Class 1		Class 2		Class 3	
m	ms^{-1}	Wm^{-2}	ms^{-1}	Wm^{-2}	ms^{-1}	Wm^{-2}	ms^{-1}	Wm^{-2}
10	9.5	747	6.6	273	5.8	178	4.5	86
25	10.3	962	7.8	439	7.1	318	5.9	187
50	11.0	1163	9.0	625	8.2	476	7.1	310
100	11.9	1458	10.4	941	9.6	730	8.4	498
200	12.9	1908	12.5	1630	11.4	1256	10.0	850

St. Paul — Gulf of Suez

28° 48′ 12.6″ N 32° 44′ 23.5″ E	UTM 36 E 474 615 m N 3 186 243 m		17 m

The St. Paul mast is situated about 3 km south of Ras Azabarban, just west of the Zafarana–Ras Ghareb road (map sheet: NH 36 B6c). The road distance to Zafarana is about 40 km, to Ras Ghareb about 70 km. The distance to the coastline of the Gulf of Suez is about 1 km in a northeasterly direction. There are no sheltering obstacles close to the mast. The surface consists mostly of sand and gravel with a roughness length of less than 0.01 m.

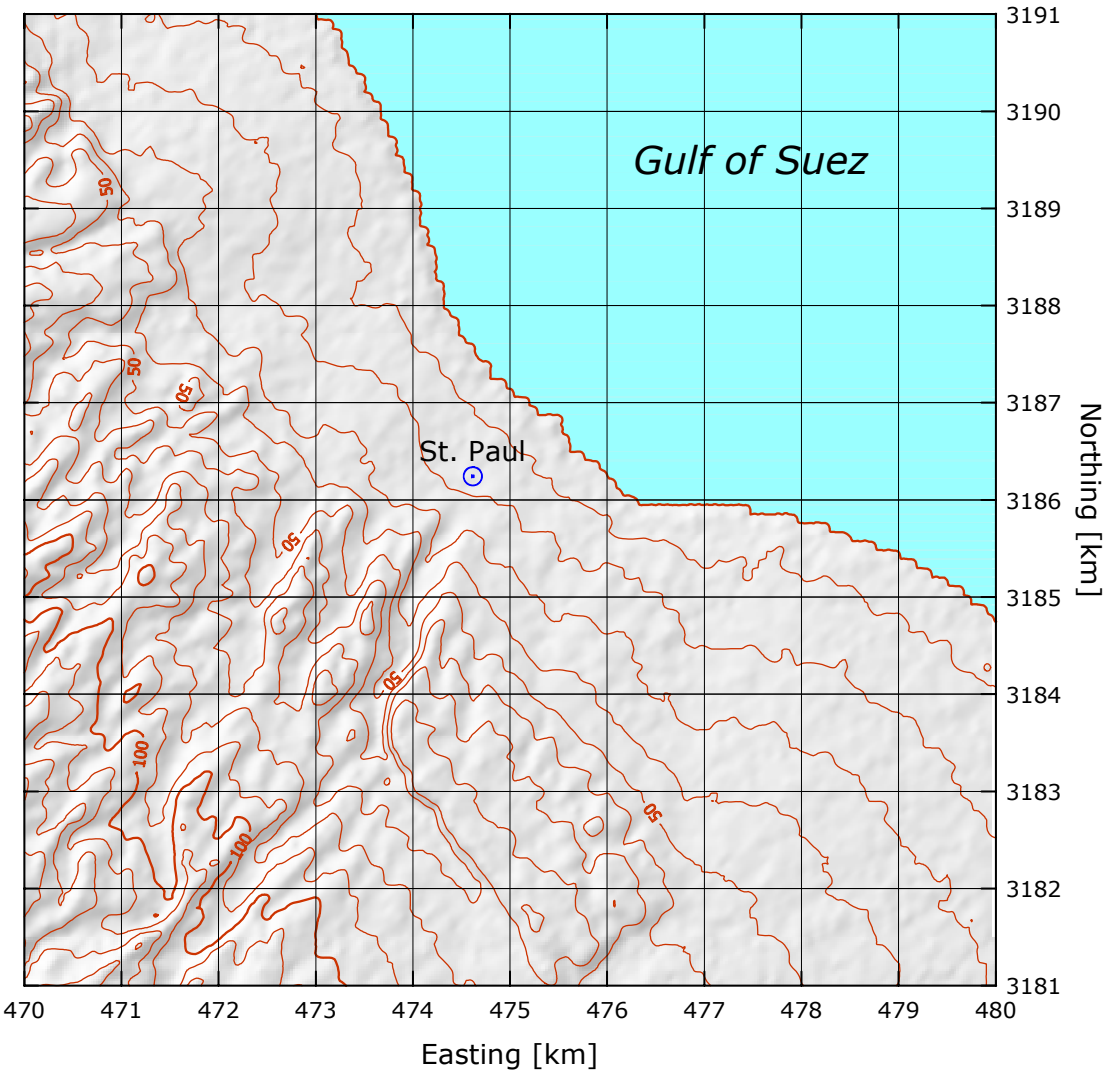

Sector	Input		Obstacles		Roughness		Orography		z_{0m}
0	0.0	0.0	0.0	0.0	−2.2	0.0	−2.1	−0.3	0.0000
30	0.0	0.0	0.0	0.0	−1.1	0.0	−2.4	0.0	0.0000
60	0.0	0.0	0.0	0.0	−1.4	0.0	−2.0	0.3	0.0000
90	0.0	0.0	0.0	0.0	−2.5	0.0	−1.4	0.3	0.0000
120	0.0	0.0	0.0	0.0	−3.7	0.0	−1.2	0.0	0.0010
150	0.0	0.0	0.0	0.0	0.0	0.0	−1.5	−0.4	0.0040
180	0.0	0.0	0.0	0.0	0.0	0.0	−2.3	−0.4	0.0050
210	0.0	0.0	0.0	0.0	0.0	0.0	−2.8	0.0	0.0050
240	0.0	0.0	0.0	0.0	0.0	0.0	−2.4	0.4	0.0050
270	0.0	0.0	0.0	0.0	0.0	0.0	−1.6	0.4	0.0050
300	0.0	0.0	0.0	0.0	0.0	0.0	−1.2	0.0	0.0050
330	0.0	0.0	0.0	0.0	−2.4	0.0	−1.5	−0.4	0.0020

Height of anemometer: 24.5 m a.g.l. 2000–2005

Sect	Freq	< 1	2	3	4	5	6	7	8	9	11	13	15	17	>17	*A*	*k*
0	19.3	2	10	25	43	59	78	95	126	149	251	124	31	4	0	9.3	3.67
30	2.1	25	102	211	218	142	123	79	47	27	25	2	0	0	0	4.5	1.87
60	1.5	34	110	215	258	196	132	46	5	1	2	0	0	0	0	4.1	2.63
90	1.0	23	115	180	218	215	162	69	16	2	0	0	0	0	0	4.4	2.81
120	0.9	18	78	110	109	91	93	61	45	45	105	108	74	52	12	8.0	1.67
150	1.4	9	59	74	97	100	82	68	74	85	153	100	65	26	7	8.6	2.15
180	1.4	25	134	155	168	167	134	79	47	34	45	9	2	0	0	5.0	1.87
210	2.2	21	90	154	193	235	170	66	30	19	14	2	1	3	1	4.9	2.27
240	2.3	30	150	266	281	117	77	44	15	8	9	3	2	0	0	3.8	1.82
270	3.3	18	114	229	251	209	106	31	17	9	10	3	1	1	0	4.2	2.09
300	13.5	4	21	41	73	117	152	149	156	135	133	17	1	0	0	7.4	3.31
330	51.0	1	4	7	10	17	33	60	98	135	310	220	85	19	1	10.8	4.18
Total	100.0	5	24	45	58	63	72	78	100	120	230	141	51	11	1	9.4	3.25

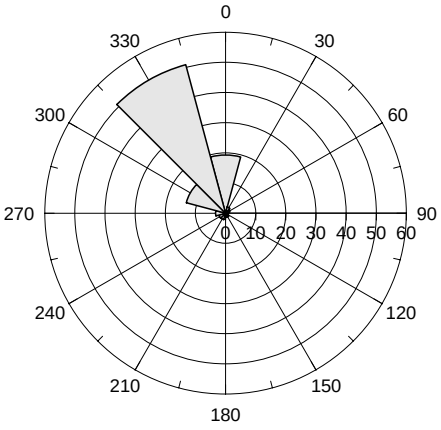

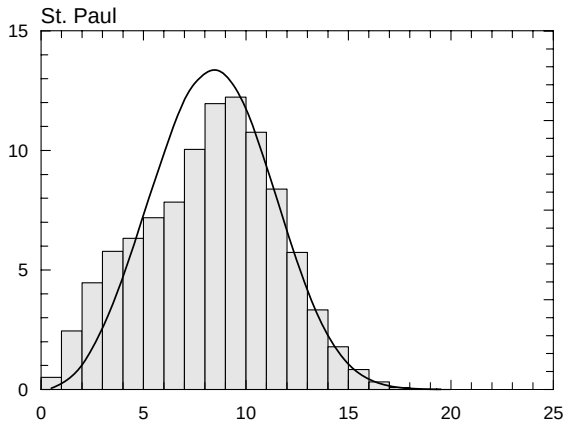

	Jan	Feb	Mar	Apr	May	Jun	Jul	Aug	Sep	Oct	Nov	Dec	Year
0	6.0	6.9	8.6	8.5	9.1	10.3	9.5	10.1	9.9	9.8	7.4	6.1	8.6
1	5.9	6.8	8.3	8.6	8.7	10.0	9.3	9.8	9.9	9.7	7.3	6.3	8.5
2	5.9	6.9	8.2	8.5	8.6	9.7	9.1	9.7	9.7	9.5	7.2	6.0	8.3
3	5.9	6.6	8.0	8.6	8.6	9.6	8.7	9.4	9.7	9.1	7.0	6.0	8.2
4	5.7	6.3	7.9	8.6	8.4	9.3	8.7	9.3	9.5	8.9	7.0	6.0	8.0
5	5.7	6.4	7.6	8.4	8.4	9.2	8.5	9.2	9.3	8.9	6.8	6.1	8.0
6	5.8	6.1	7.6	7.9	8.2	9.3	8.5	9.2	9.4	8.7	6.8	5.8	7.9
7	5.7	6.0	7.3	8.1	8.5	10.0	9.0	9.9	9.5	8.8	6.6	5.9	8.0
8	5.5	5.8	7.7	8.4	8.7	10.4	9.6	10.4	10.2	9.5	6.8	5.8	8.3
9	5.5	6.3	8.2	8.6	8.8	10.4	9.4	10.5	10.4	10.0	7.3	6.0	8.5
10	5.8	6.6	8.5	8.8	8.7	10.2	9.2	10.3	10.4	9.9	7.6	6.2	8.6
11	6.3	6.9	8.4	8.8	8.5	9.9	8.8	10.0	10.2	9.8	7.6	6.6	8.5
12	6.4	6.9	8.3	8.7	8.3	9.6	8.5	9.6	9.9	9.6	7.7	7.1	8.4
13	6.4	7.1	8.2	8.4	8.2	9.4	8.3	9.4	9.7	9.5	7.5	7.2	8.3
14	6.7	6.9	8.1	8.4	8.1	9.3	8.1	9.3	9.4	9.2	7.4	7.0	8.2
15	6.8	6.8	7.9	8.3	8.1	9.2	7.9	9.1	9.4	8.9	7.2	6.7	8.1
16	6.4	6.7	7.7	8.0	7.8	9.1	7.9	9.0	9.2	8.7	6.9	6.6	7.8
17	6.1	6.3	7.2	7.8	7.5	8.9	7.9	8.6	8.7	8.3	6.8	6.1	7.5
18	5.6	5.9	6.8	7.3	7.4	8.7	8.0	8.2	8.6	8.0	6.5	6.0	7.3
19	5.7	5.8	6.8	7.4	7.7	9.0	8.3	8.6	8.8	8.4	6.5	5.8	7.5
20	5.9	6.0	7.2	7.8	8.4	9.7	9.1	9.4	9.4	9.0	6.8	6.0	7.9
21	5.9	6.3	7.7	8.5	8.8	10.5	9.6	10.0	10.1	9.5	7.0	6.3	8.4
22	5.9	6.7	8.1	8.8	9.1	10.5	9.7	10.3	10.3	9.7	7.1	6.0	8.6
23	6.0	6.6	8.5	8.7	9.0	10.6	9.6	10.2	10.1	9.8	7.1	6.0	8.6
Mean	6.0	6.5	7.9	8.3	8.4	9.7	8.8	9.6	9.7	9.2	7.1	6.2	8.2

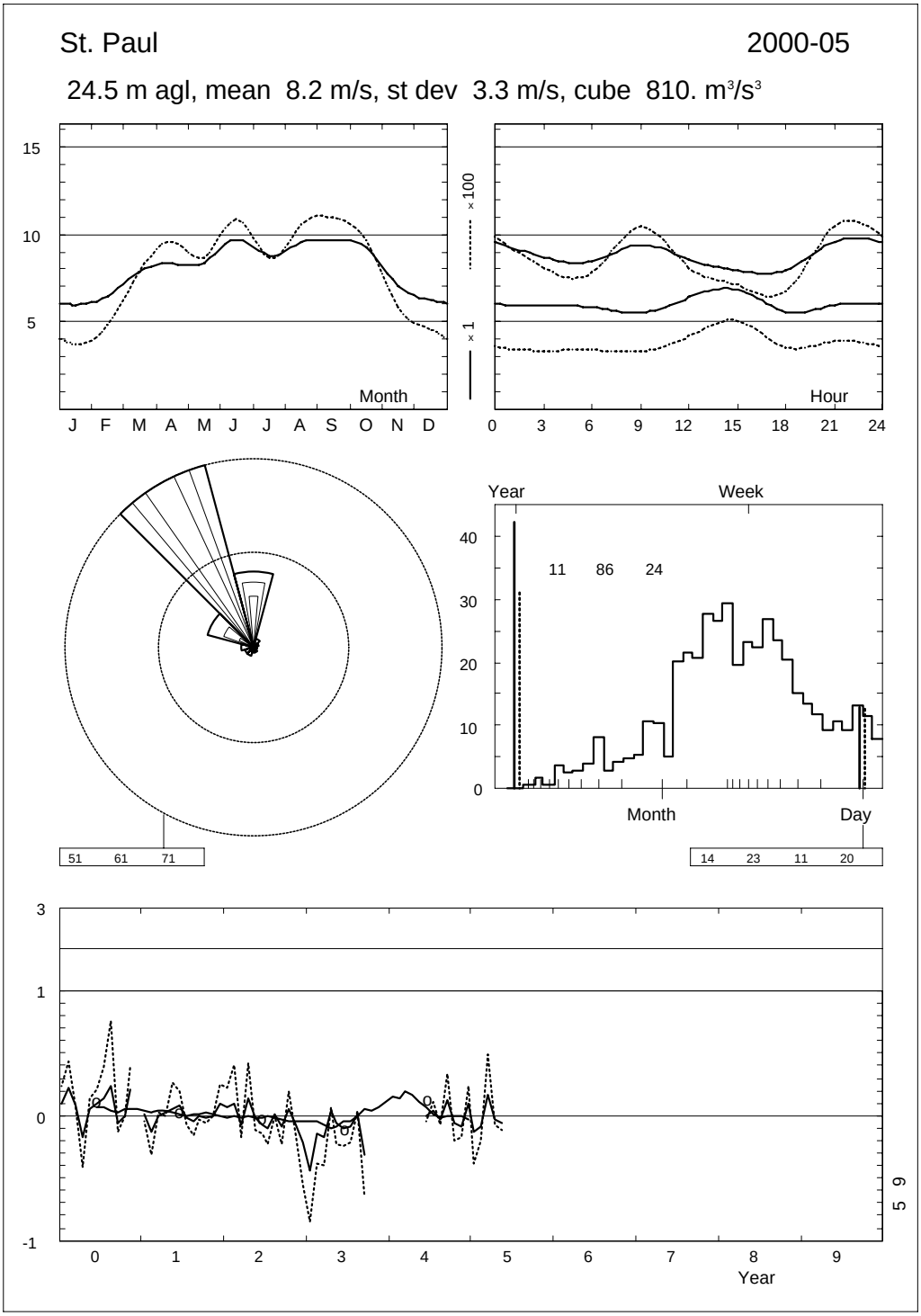

	Jan	Feb	Mar	Apr	May	Jun	Jul	Aug	Sep	Oct	Nov	Dec	Year
2000	6.6	8.0	8.5	6.9	8.8	10.6	10.1	11.8	9.1	9.1	8.5	—	8.7
2001	6.0	5.7	7.8	8.5	8.9	10.4	8.7	9.1	9.6	9.1	7.1	6.8	8.2
2002	6.4	7.1	7.3	9.4	8.3	9.0	7.9	9.6	8.9	9.8	6.5	4.9	8.0
2003	3.3	5.6	6.6	8.7	7.9	8.7	8.1	9.6	6.7	—	—	—	7.8
2004	—	—	—	—	—	9.6	9.2	9.3	10.9	8.7	6.4	6.8	8.7
2005	5.2	5.9	9.2	8.1	8.0	—	—	—	—	—	—	—	7.3
Mean	6.0	6.5	7.9	8.3	8.4	9.7	8.8	9.6	9.7	9.2	7.1	6.2	8.2

Roughness Class 0 ($z_0 = 0.0002$ m)

z	0	30	60	90	120	150	180	210	240	270	300	330	Total
10	9.4	6.5	4.0	4.2	7.9	9.3	5.7	5.4	4.2	4.6	8.0	11.5	9.7
	3.42	1.91	2.30	2.54	1.63	2.28	1.84	2.36	1.94	2.13	3.50	4.38	2.80
25	10.3	7.1	4.4	4.6	8.7	10.1	6.3	5.9	4.7	5.1	8.7	12.5	10.6
	3.53	1.97	2.37	2.62	1.67	2.33	1.90	2.44	2.01	2.19	3.61	4.48	2.85
50	11.1	7.6	4.7	4.9	9.3	10.8	6.7	6.3	5.0	5.4	9.3	13.4	11.3
	3.62	2.02	2.44	2.69	1.71	2.40	1.95	2.50	2.06	2.25	3.71	4.61	2.91
100	12.0	8.3	5.1	5.3	9.9	11.6	7.3	6.9	5.4	5.9	10.1	14.4	12.2
	3.51	1.96	2.36	2.60	1.68	2.34	1.89	2.42	1.99	2.18	3.59	4.50	2.87
200	13.3	9.1	5.6	5.9	10.7	12.7	8.1	7.6	6.0	6.5	11.2	15.7	13.4
	3.32	1.85	2.23	2.46	1.62	2.25	1.79	2.29	1.89	2.06	3.40	4.32	2.81
Freq.	22.2	3.6	1.5	1.0	0.9	1.3	1.4	2.1	2.3	3.3	12.5	47.6	100.0

Roughness Class 1 ($z_0 = 0.0300$ m)

z	0	30	60	90	120	150	180	210	240	270	300	330	Total
10	6.3	3.0	2.8	3.2	6.0	6.0	3.8	3.6	3.0	4.1	6.6	8.0	6.8
	2.92	1.44	2.06	1.28	1.64	1.78	1.72	1.93	1.67	1.76	2.83	3.79	2.55
25	7.5	3.6	3.3	3.8	7.2	7.1	4.6	4.3	3.5	4.9	7.8	9.5	8.0
	3.15	1.56	2.22	1.38	1.72	1.88	1.86	2.09	1.80	1.90	3.05	4.01	2.68
50	8.6	4.2	3.8	4.5	8.2	8.1	5.3	5.0	4.1	5.7	9.0	10.8	9.2
	3.54	1.75	2.50	1.54	1.85	2.06	2.08	2.35	2.03	2.14	3.43	4.37	2.88
100	10.2	5.1	4.5	5.4	9.4	9.5	6.3	5.9	4.9	6.7	10.7	12.4	10.8
	3.77	1.86	2.67	1.64	1.98	2.21	2.22	2.50	2.15	2.28	3.65	4.69	3.04
200	12.7	6.3	5.7	6.7	11.1	11.4	7.8	7.4	6.1	8.3	13.3	15.0	13.2
	3.60	1.78	2.54	1.57	1.92	2.12	2.12	2.38	2.06	2.18	3.49	4.51	3.01
Freq.	17.2	2.1	1.4	1.0	1.0	1.4	1.6	2.2	2.5	4.8	18.5	46.3	100.0

Roughness Class 2 ($z_0 = 0.1000$ m)

z	0	30	60	90	120	150	180	210	240	270	300	330	Total
10	5.4	2.7	2.5	2.7	5.3	4.9	3.3	3.1	2.7	3.9	6.0	6.9	5.9
	2.88	1.53	2.13	1.13	1.67	1.68	1.76	1.88	1.77	1.98	2.95	3.75	2.57
25	6.7	3.3	3.0	3.5	6.5	6.1	4.1	3.8	3.3	4.8	7.4	8.4	7.2
	3.09	1.63	2.28	1.20	1.75	1.77	1.88	2.01	1.89	2.12	3.15	3.94	2.69
50	7.8	3.9	3.5	4.1	7.5	7.1	4.8	4.4	3.9	5.6	8.6	9.7	8.4
	3.42	1.81	2.52	1.32	1.86	1.92	2.08	2.22	2.09	2.35	3.48	4.26	2.87
100	9.2	4.7	4.2	5.0	8.7	8.4	5.7	5.3	4.6	6.7	10.2	11.4	9.9
	3.76	1.98	2.77	1.45	2.04	2.11	2.29	2.45	2.29	2.58	3.82	4.67	3.07
200	11.4	5.8	5.2	6.1	10.4	10.1	7.1	6.5	5.7	8.3	12.6	13.7	12.0
	3.60	1.90	2.65	1.39	1.97	2.03	2.19	2.34	2.20	2.47	3.66	4.50	3.03
Freq.	15.8	2.0	1.4	0.9	1.0	1.4	1.6	2.2	2.6	5.7	21.4	43.9	100.0

Roughness Class 3 ($z_0 = 0.4000$ m)

z	0	30	60	90	120	150	180	210	240	270	300	330	Total
10	4.2	2.0	1.9	2.3	4.2	3.6	2.6	2.3	2.1	3.3	4.9	5.3	4.6
	2.88	1.48	2.03	1.07	1.73	1.58	1.81	1.83	1.69	2.20	3.15	3.65	2.58
25	5.6	2.7	2.5	3.0	5.5	4.8	3.4	3.1	2.8	4.3	6.5	7.0	6.1
	3.05	1.57	2.15	1.13	1.79	1.66	1.92	1.94	1.79	2.33	3.32	3.82	2.68
50	6.7	3.3	3.0	3.7	6.6	5.8	4.2	3.8	3.3	5.2	7.8	8.3	7.3
	3.32	1.70	2.34	1.22	1.90	1.78	2.09	2.11	1.94	2.53	3.58	4.07	2.83
100	8.0	4.0	3.7	4.6	7.8	6.9	5.0	4.5	4.0	6.3	9.2	9.9	8.7
	3.78	1.94	2.66	1.38	2.09	2.02	2.38	2.40	2.21	2.88	4.05	4.54	3.08
200	9.8	4.9	4.5	5.6	9.3	8.4	6.1	5.5	4.9	7.7	11.2	11.9	10.5
	3.64	1.87	2.56	1.33	2.07	1.96	2.29	2.32	2.13	2.78	3.92	4.45	3.04
Freq.	13.8	1.9	1.3	0.9	1.1	1.4	1.7	2.3	2.8	6.8	25.4	40.7	100.0

z	Class 0		Class 1		Class 2		Class 3	
m	ms^{-1}	Wm^{-2}	ms^{-1}	Wm^{-2}	ms^{-1}	Wm^{-2}	ms^{-1}	Wm^{-2}
10	8.6	575	6.0	206	5.2	135	4.1	65
25	9.4	743	7.2	337	6.4	244	5.4	144
50	10.1	904	8.2	488	7.5	371	6.5	241
100	10.9	1145	9.6	762	8.8	587	7.7	394
200	12.0	1531	11.8	1397	10.7	1062	9.4	699

Ras Ghareb — Gulf of Suez

28° 20′ 25.7″ N 33° 01′ 37.0″ E	UTM 36 E 502 641 m N 3 134 920 m		56 m

The Ras Ghareb mast is situated about 6 km WSW of the town of Ghareb (map sheet: NH 36 C1c). The distance to the coastline of the Gulf of Suez is also about 6 km in an east-northeasterly direction. There are no sheltering obstacles close to the mast. The surface consists mostly of sand and gravel with a roughness length of less than 0.01 m.

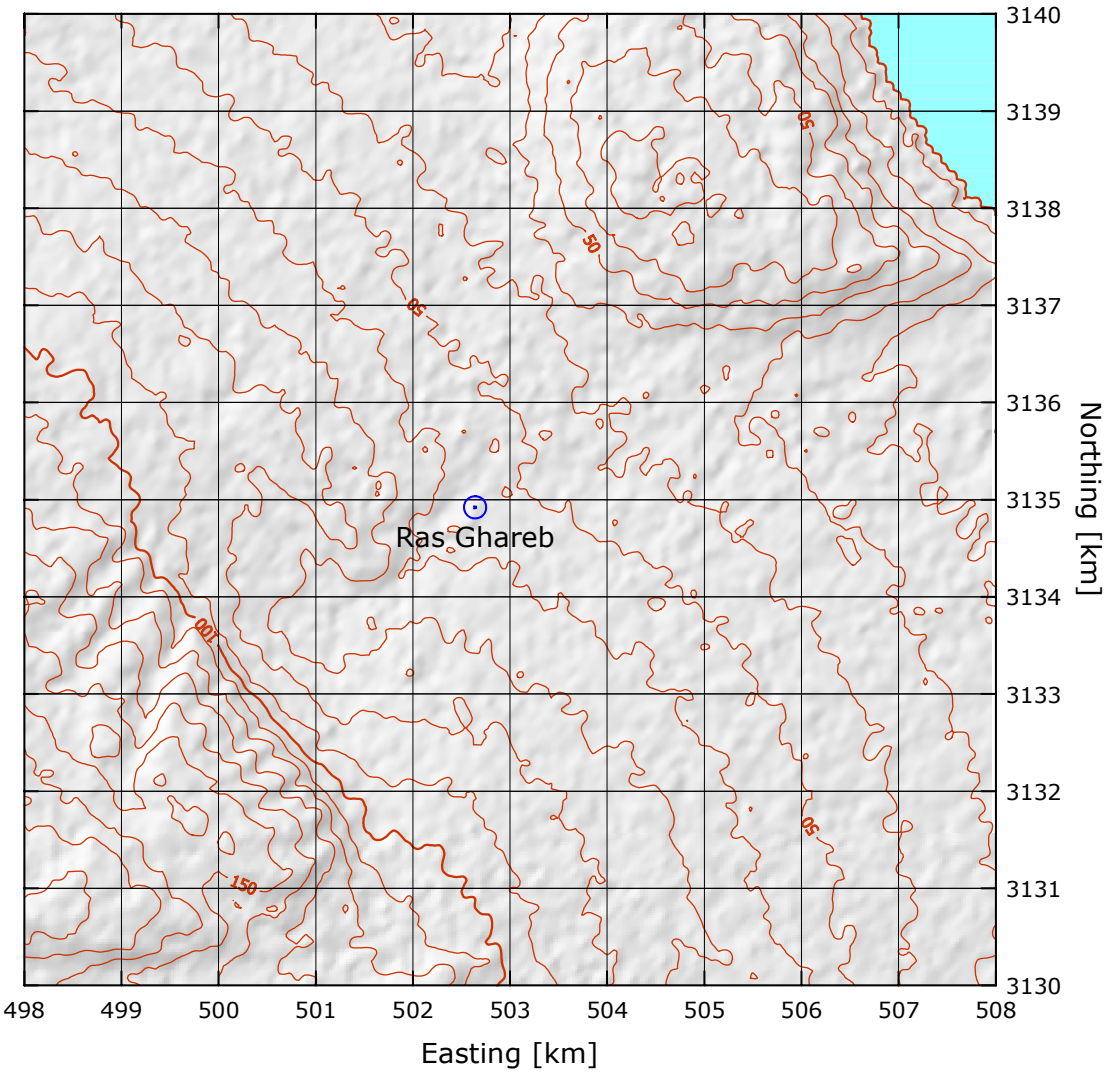

Sector	Input		Obstacles		Roughness		Orography		z_{0m}
0	0.0	0.0	0.0	0.0	−2.3	0.0	−0.1	−0.2	0.0010
30	0.0	0.0	0.0	0.0	−3.4	0.0	−0.7	−0.4	0.0010
60	0.0	0.0	0.0	0.0	−3.5	0.0	−1.3	−0.2	0.0010
90	0.0	0.0	0.0	0.0	−3.2	0.0	−1.3	0.2	0.0010
120	0.0	0.0	0.0	0.0	−2.1	0.0	−0.7	0.4	0.0010
150	0.0	0.0	0.0	0.0	0.0	0.0	−0.1	0.2	0.0030
180	0.0	0.0	0.0	0.0	0.0	0.0	−0.1	−0.2	0.0030
210	0.0	0.0	0.0	0.0	0.0	0.0	−0.8	−0.4	0.0030
240	0.0	0.0	0.0	0.0	0.0	0.0	−1.4	−0.2	0.0030
270	0.0	0.0	0.0	0.0	0.0	0.0	−1.4	0.2	0.0030
300	0.0	0.0	0.0	0.0	0.0	0.0	−0.7	0.4	0.0030
330	0.0	0.0	0.0	0.0	0.0	0.0	−0.1	0.2	0.0030

Height of anemometer: 24.5 m a.g.l. 2000–2005

Sect	Freq	< 1	2	3	4	5	6	7	8	9	11	13	15	17	>17	*A*	*k*
0	9.0	2	12	28	44	78	101	105	129	155	235	92	17	1	0	8.8	3.70
30	1.1	15	75	130	163	154	154	156	93	46	13	1	0	0	0	5.5	2.69
60	0.6	7	93	251	325	235	60	21	7	0	0	0	0	0	0	3.9	3.08
90	1.1	15	39	76	141	179	125	116	100	66	90	41	6	4	1	6.5	2.04
120	1.3	5	33	66	86	106	94	74	76	77	152	119	88	22	2	8.9	2.27
150	1.2	15	75	74	67	83	82	74	80	88	152	118	68	21	3	8.7	2.29
180	0.4	23	87	158	154	146	130	89	76	75	51	6	4	1	0	5.5	1.98
210	0.3	3	84	225	227	232	89	67	36	17	16	2	2	0	0	4.5	2.10
240	1.0	25	144	184	133	131	104	76	84	61	43	13	1	0	0	5.1	1.81
270	7.4	6	20	30	45	71	109	162	224	196	114	18	3	1	1	7.9	4.51
300	25.4	1	5	9	15	27	46	75	126	174	342	145	31	3	0	9.9	4.63
330	51.3	0	3	7	11	17	21	28	43	65	212	278	213	82	23	12.6	4.72
Total	100.0	2	10	19	26	37	47	61	88	111	231	193	121	43	12	11.0	3.40

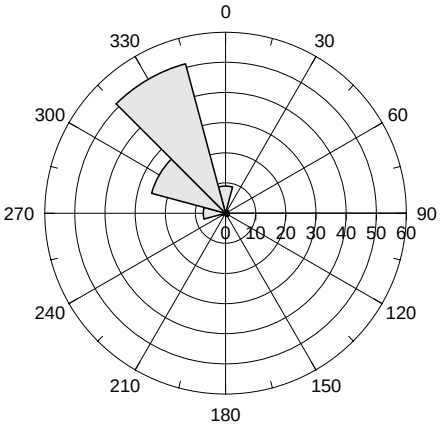

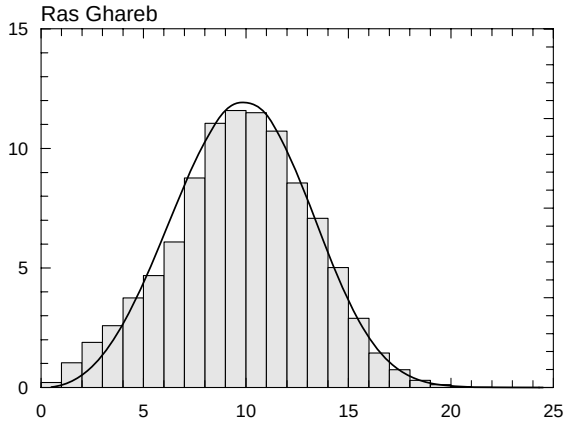

	Jan	Feb	Mar	Apr	May	Jun	Jul	Aug	Sep	Oct	Nov	Dec	Year
0	7.8	8.0	9.7	9.6	10.8	12.9	12.3	12.5	11.7	10.5	8.5	8.2	10.3
1	7.9	8.1	9.6	9.7	10.6	12.7	12.0	12.2	11.5	10.5	8.4	8.3	10.2
2	7.9	8.4	9.5	9.6	10.4	12.2	11.6	11.7	11.3	10.3	8.3	8.3	10.0
3	7.9	8.2	9.3	9.4	10.3	11.8	11.2	11.4	11.0	10.1	8.4	8.5	9.8
4	8.1	8.1	9.1	9.2	9.8	11.5	10.8	11.0	10.8	9.9	8.2	8.4	9.6
5	8.1	8.2	9.0	9.1	9.7	11.3	10.5	10.6	10.6	9.8	8.2	8.3	9.5
6	8.0	8.3	9.0	8.9	9.6	11.5	10.4	10.7	10.5	9.6	8.2	8.3	9.5
7	8.1	8.2	9.0	9.4	10.7	12.8	11.4	12.0	11.2	9.8	8.0	8.1	10.0
8	7.5	7.8	9.7	10.0	10.7	12.9	11.6	12.4	12.2	11.0	7.7	7.8	10.1
9	7.3	7.8	9.6	10.0	10.5	12.5	11.4	12.3	12.0	10.9	7.7	7.6	10.0
10	7.1	7.6	9.6	10.1	10.5	12.2	11.1	12.1	11.9	10.8	7.5	7.4	9.9
11	7.1	7.7	9.7	10.1	10.3	11.8	10.8	11.9	11.6	10.5	7.6	7.3	9.8
12	7.3	7.8	9.8	10.0	10.3	11.6	10.7	11.9	11.4	10.3	7.7	7.6	9.7
13	7.6	8.0	9.8	10.0	10.4	11.7	10.7	11.9	11.4	9.9	7.7	7.6	9.8
14	7.8	8.2	9.7	10.2	10.5	11.8	10.9	12.0	11.7	9.9	7.8	7.6	9.9
15	7.8	8.3	9.7	10.4	10.7	12.0	11.1	12.2	11.9	10.2	7.9	7.8	10.1
16	7.7	8.2	9.6	10.6	10.9	12.4	11.4	12.4	12.2	10.1	7.6	7.8	10.1
17	7.2	7.8	9.4	10.2	10.7	12.5	11.4	12.3	12.0	9.4	6.7	6.9	9.8
18	6.5	6.7	8.5	9.5	10.1	11.7	10.6	11.3	10.8	8.7	6.6	6.5	9.1
19	6.7	6.6	8.0	8.9	9.2	10.7	9.7	10.4	10.4	8.9	7.1	7.1	8.7
20	7.0	6.8	8.5	9.0	9.6	10.9	9.9	10.6	10.8	9.3	7.2	7.5	9.0
21	7.4	7.2	8.6	9.4	10.2	11.7	11.0	11.4	11.3	9.7	7.6	7.7	9.5
22	7.5	7.5	9.2	9.5	10.7	12.4	11.8	12.1	11.6	10.2	7.9	7.6	9.9
23	7.7	7.7	9.4	9.7	10.7	12.9	12.3	12.5	11.9	10.6	7.9	7.8	10.2
Mean	7.5	7.8	9.3	9.7	10.3	12.0	11.1	11.7	11.4	10.0	7.8	7.7	9.8

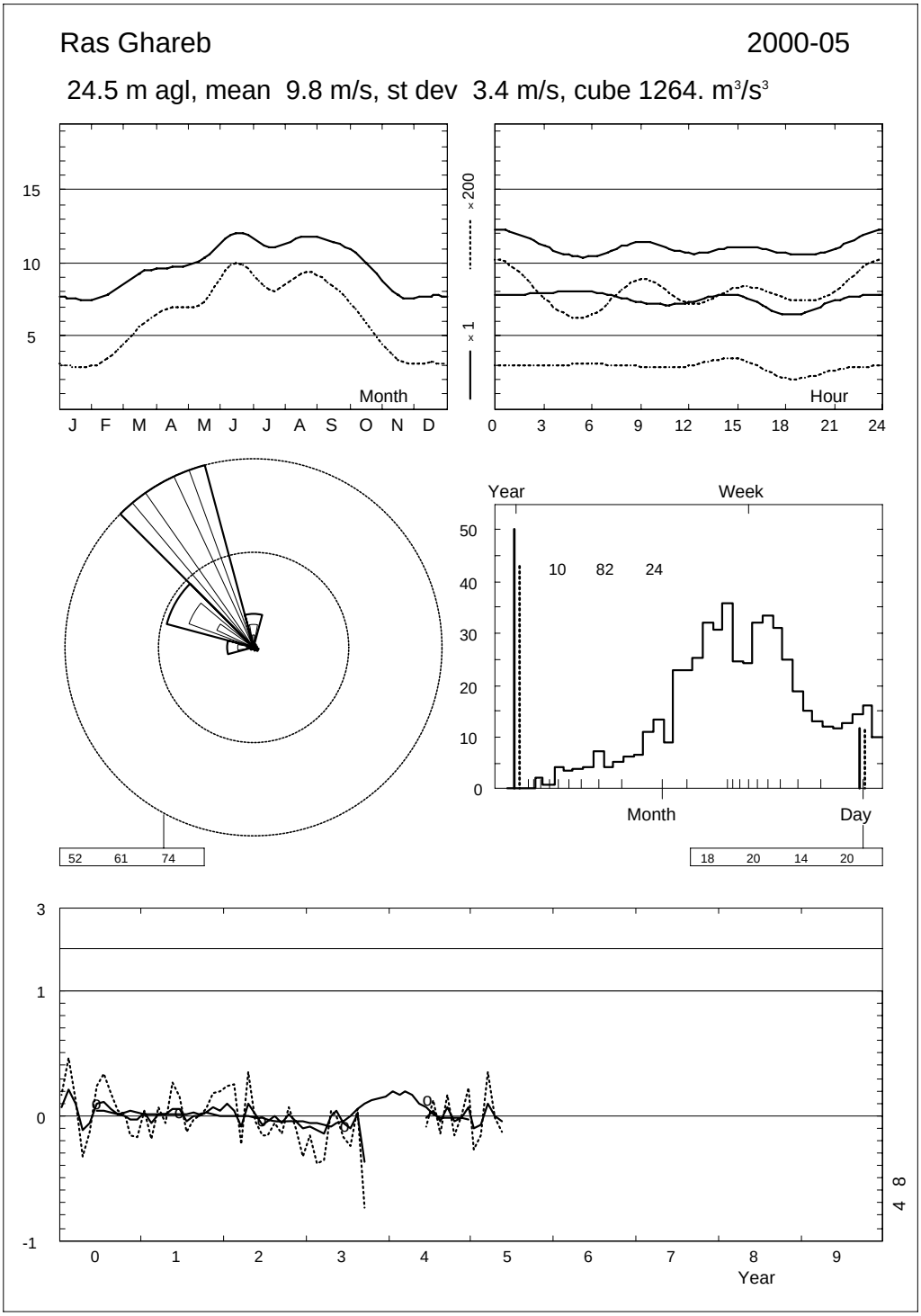

	Jan	Feb	Mar	Apr	May	Jun	Jul	Aug	Sep	Oct	Nov	Dec	Year
2000	8.1	9.4	10.2	8.6	9.7	13.1	12.3	12.3	11.6	10.0	7.5	7.5	10.2
2001	7.7	7.4	9.5	9.8	10.9	12.6	10.7	11.7	11.4	10.3	8.3	8.1	9.9
2002	8.2	8.1	8.5	10.7	10.5	11.2	10.7	11.6	10.8	10.1	7.4	6.9	9.6
2003	6.9	6.9	8.0	9.7	10.7	11.3	10.1	11.9	7.1	—	—	—	9.3
2004	—	—	—	—	—	11.7	11.6	11.1	12.2	9.5	7.7	8.3	10.4
2005	6.8	7.2	10.1	9.6	9.8	—	—	—	—	—	—	—	8.7
Mean	7.5	7.8	9.3	9.7	10.3	12.0	11.1	11.7	11.4	10.0	7.8	7.7	9.8

Roughness Class 0 ($z_0 = 0.0002$ m)

z	0	30	60	90	120	150	180	210	240	270	300	330	Total
10	10.5	7.1	4.2	6.5	9.1	9.1	6.3	4.8	5.4	8.4	10.4	13.1	11.5
	3.26	2.46	2.35	2.05	2.37	2.47	1.92	2.14	1.95	4.50	4.73	4.82	3.49
25	11.5	7.7	4.6	7.1	9.9	10.0	6.9	5.3	5.9	9.2	11.4	14.3	12.6
	3.34	2.54	2.43	2.11	2.43	2.53	1.98	2.21	2.01	4.64	4.87	4.90	3.55
50	12.3	8.3	4.9	7.7	10.6	10.7	7.4	5.7	6.4	9.8	12.2	15.2	13.4
	3.44	2.61	2.49	2.17	2.50	2.60	2.04	2.27	2.06	4.76	5.00	5.01	3.63
100	13.2	9.0	5.3	8.3	11.4	11.6	8.1	6.2	6.9	10.7	13.3	16.3	14.5
	3.35	2.53	2.42	2.10	2.44	2.54	1.97	2.20	2.00	4.62	4.85	4.94	3.62
200	14.5	10.0	5.9	9.2	12.5	12.7	8.9	6.8	7.6	11.9	14.7	17.7	15.7
	3.21	2.39	2.29	1.99	2.33	2.42	1.87	2.08	1.89	4.37	4.60	4.80	3.58
Freq.	12.3	1.8	0.6	1.0	1.3	1.2	0.5	0.3	0.9	7.1	24.2	48.8	100.0

Roughness Class 1 ($z_0 = 0.0300$ m)

z	0	30	60	90	120	150	180	210	240	270	300	330	Total
10	6.3	3.9	3.1	4.8	6.4	6.2	3.9	3.4	5.1	6.3	7.8	9.3	8.1
	3.22	2.03	1.51	1.71	2.07	2.04	1.77	1.69	2.60	3.38	3.52	4.32	3.13
25	7.5	4.7	3.7	5.8	7.6	7.4	4.7	4.1	6.1	7.6	9.2	10.9	9.5
	3.48	2.20	1.62	1.84	2.21	2.18	1.91	1.83	2.81	3.65	3.73	4.49	3.28
50	8.6	5.4	4.3	6.7	8.7	8.5	5.4	4.7	7.0	8.7	10.5	12.3	10.8
	3.91	2.47	1.82	2.07	2.43	2.41	2.15	2.06	3.15	4.10	4.08	4.76	3.51
100	10.2	6.4	5.1	8.0	10.2	10.0	6.5	5.6	8.3	10.3	12.2	14.0	12.5
	4.16	2.63	1.94	2.20	2.60	2.58	2.29	2.19	3.36	4.37	4.37	5.11	3.79
200	12.8	7.9	6.4	9.9	12.4	12.2	8.0	7.0	10.3	12.8	14.8	16.3	14.9
	3.98	2.51	1.85	2.10	2.50	2.47	2.19	2.09	3.21	4.17	4.20	4.96	3.83
Freq.	7.8	1.0	0.6	1.1	1.3	1.1	0.4	0.4	1.9	10.1	28.9	45.3	100.0

Roughness Class 2 ($z_0 = 0.1000$ m)

z	0	30	60	90	120	150	180	210	240	270	300	330	Total
10	5.5	3.3	2.8	4.3	5.6	5.3	3.4	3.0	4.7	5.7	7.0	8.1	7.0
	3.19	1.96	1.41	1.68	2.08	2.00	1.77	1.63	2.97	3.40	3.46	4.28	3.12
25	6.7	4.1	3.5	5.3	6.8	6.6	4.2	3.7	5.7	7.0	8.5	9.8	8.6
	3.42	2.10	1.51	1.80	2.20	2.13	1.90	1.75	3.19	3.63	3.62	4.42	3.25
50	7.8	4.8	4.1	6.2	7.9	7.7	4.9	4.3	6.7	8.1	9.8	11.2	9.9
	3.78	2.33	1.66	1.99	2.39	2.33	2.10	1.94	3.53	4.02	3.89	4.66	3.45
100	9.3	5.7	4.9	7.5	9.3	9.0	5.8	5.2	7.9	9.6	11.4	12.8	11.4
	4.15	2.56	1.82	2.19	2.63	2.56	2.31	2.13	3.87	4.41	4.27	5.08	3.76
200	11.5	7.1	6.1	9.2	11.3	11.0	7.2	6.4	9.8	11.9	13.6	15.0	13.6
	3.97	2.45	1.75	2.09	2.53	2.46	2.21	2.03	3.71	4.22	4.12	4.94	3.78
Freq.	7.2	1.0	0.7	1.1	1.3	1.0	0.4	0.4	2.5	11.5	30.8	42.1	100.0

Roughness Class 3 ($z_0 = 0.4000$ m)

z	0	30	60	90	120	150	180	210	240	270	300	330	Total
10	4.3	2.6	2.4	3.5	4.3	4.1	2.6	2.4	3.8	4.6	5.7	6.3	5.5
	3.15	1.94	1.52	1.70	2.08	1.96	1.79	1.65	3.05	3.50	3.53	4.13	3.12
25	5.6	3.4	3.2	4.6	5.7	5.4	3.5	3.2	4.9	6.0	7.3	8.1	7.2
	3.33	2.06	1.61	1.80	2.19	2.06	1.89	1.75	3.24	3.71	3.66	4.25	3.23
50	6.7	4.1	3.9	5.6	6.8	6.5	4.2	3.8	5.9	7.2	8.7	9.6	8.5
	3.62	2.24	1.75	1.96	2.35	2.22	2.06	1.90	3.52	4.03	3.87	4.44	3.40
100	8.1	4.9	4.8	6.8	8.2	7.8	5.1	4.7	7.1	8.7	10.3	11.3	10.1
	4.12	2.55	1.99	2.22	2.64	2.53	2.34	2.16	4.00	4.58	4.24	4.78	3.69
200	9.9	6.0	5.8	8.3	9.9	9.4	6.2	5.7	8.7	10.6	12.2	13.2	12.0
	3.97	2.46	1.92	2.15	2.57	2.44	2.26	2.08	3.86	4.41	4.21	4.81	3.75
Freq.	6.3	0.9	0.7	1.1	1.3	0.9	0.4	0.5	3.2	13.5	33.4	37.7	100.0

z	Class 0		Class 1		Class 2		Class 3	
m	ms^{-1}	Wm^{-2}	ms^{-1}	Wm^{-2}	ms^{-1}	Wm^{-2}	ms^{-1}	Wm^{-2}
10	10.4	891	7.2	319	6.3	209	4.9	100
25	11.3	1150	8.6	516	7.7	373	6.4	219
50	12.1	1393	9.7	738	8.9	560	7.7	364
100	13.0	1737	11.3	1102	10.3	854	9.1	585
200	14.2	2254	13.4	1865	12.3	1438	10.8	981

Gulf of El-Zayt NW

Gulf of Suez

27° 54′ 21.5″ N 33° 20′ 10.5″ E	UTM 36 E 533 090 m N 3 086 832 m	58 m

The Gulf of El-Zayt NW mast is situated about 19 km northwest of the main Gulf of El-Zayt station, approximately 90 km NNW of Hurghada (map sheet: NG 36 O4d). The distance to the coastline of the Gulf of Suez is about 15 km in a northerly direction. There are no sheltering obstacles close to the mast. The surface consists mostly of sand and gravel with a roughness length of less than 0.01 m.

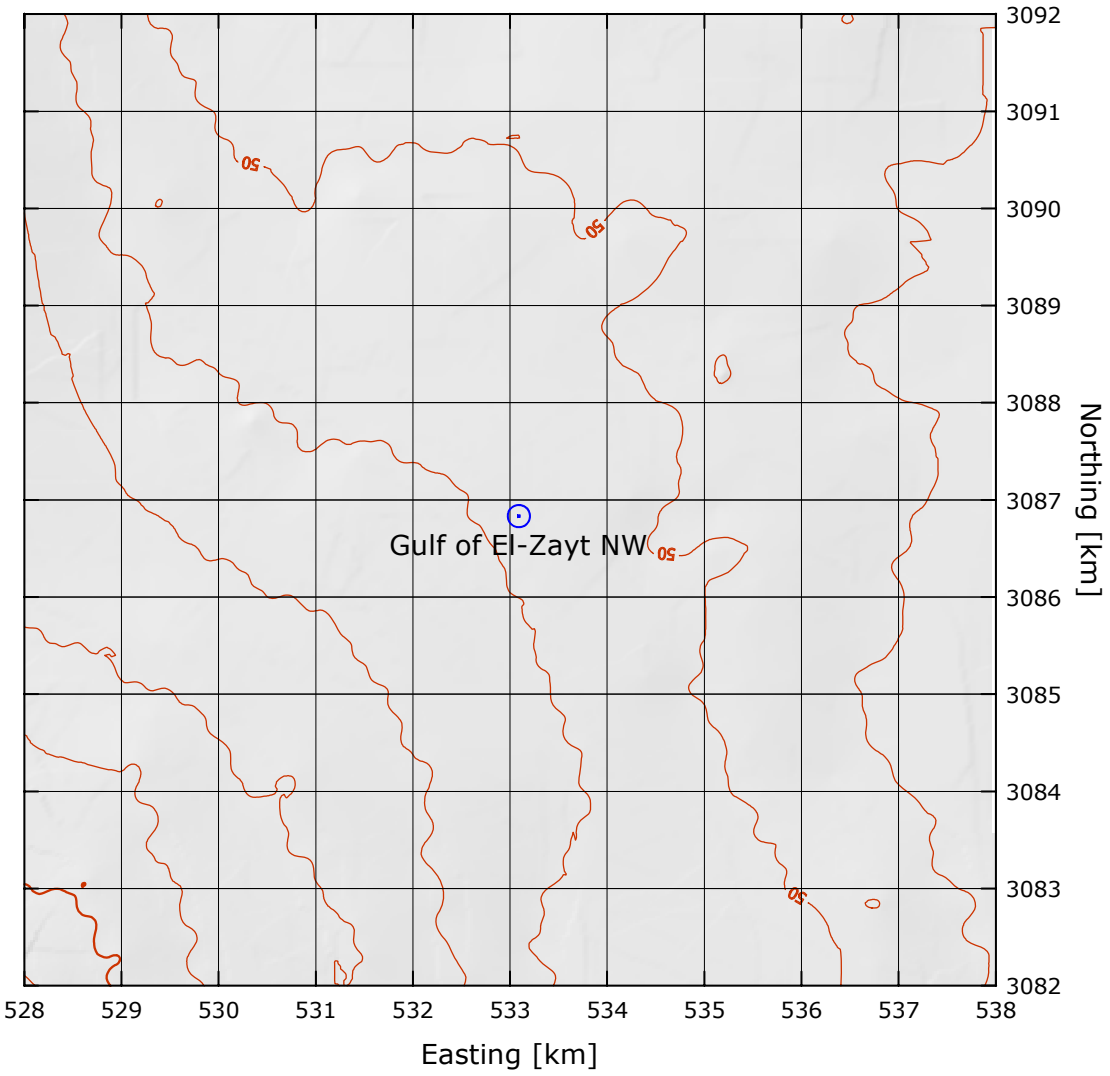

Sector	Input		Obstacles		Roughness		Orography		z_{0m}
0	0.0	0.0	0.0	0.0	−0.8	0.0	−0.3	−0.7	0.0010
30	0.0	0.0	0.0	0.0	−0.9	0.0	−1.5	−0.4	0.0010
60	0.0	0.0	0.0	0.0	−0.8	0.0	−1.6	0.3	0.0010
90	0.0	0.0	0.0	0.0	−0.6	0.0	−0.6	0.7	0.0010
120	0.0	0.0	0.0	0.0	−0.8	0.0	0.6	0.4	0.0010
150	0.0	0.0	0.0	0.0	−0.2	0.0	0.7	−0.3	0.0010
180	0.0	0.0	0.0	0.0	0.0	0.0	−0.3	−0.7	0.0010
210	0.0	0.0	0.0	0.0	0.0	0.0	−1.5	−0.4	0.0010
240	0.0	0.0	0.0	0.0	0.0	0.0	−1.6	0.3	0.0010
270	0.0	0.0	0.0	0.0	0.0	0.0	−0.6	0.7	0.0010
300	0.0	0.0	0.0	0.0	0.0	0.0	0.6	0.4	0.0010
330	0.0	0.0	0.0	0.0	0.0	0.0	0.7	−0.3	0.0010

Height of anemometer: 24.5 m a.g.l. 2000–2005

Sect	Freq	< 1	2	3	4	5	6	7	8	9	11	13	15	17	>17	*A*	*k*
0	3.9	20	52	59	84	135	148	145	114	73	107	50	12	0	0	7.0	2.33
30	0.5	65	192	177	122	175	134	87	33	11	3	0	0	0	0	4.2	2.16
60	0.2	124	367	227	124	97	51	7	3	0	0	0	0	0	0	2.6	1.64
90	0.3	85	241	236	200	111	75	38	8	4	3	0	0	0	0	3.3	1.84
120	2.2	15	72	92	123	119	138	132	93	60	100	45	10	0	0	6.6	2.14
150	2.2	18	58	86	87	125	143	138	102	75	86	66	16	0	0	6.9	2.18
180	0.4	55	229	180	140	134	122	48	49	34	7	2	0	0	0	4.1	1.77
210	0.4	78	268	198	146	105	96	85	22	2	0	0	0	0	0	3.5	1.72
240	0.9	57	145	114	117	120	160	129	85	33	34	6	0	0	0	5.3	2.28
270	2.9	22	56	65	83	125	146	180	163	90	54	11	3	2	0	6.7	3.11
300	49.4	1	7	14	19	23	32	42	55	68	194	233	185	96	31	12.4	4.08
330	36.7	2	8	14	17	22	26	34	50	67	203	253	201	83	22	12.4	4.43
Total	100.0	5	18	25	30	37	45	52	60	67	181	213	166	78	24	11.8	3.70

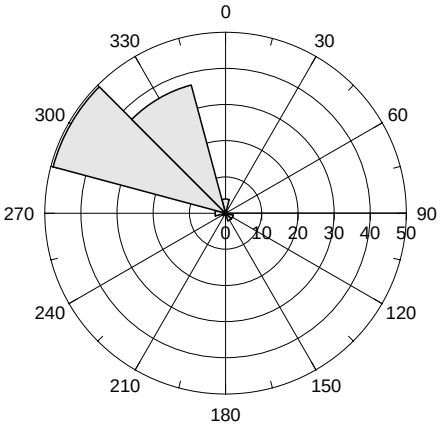

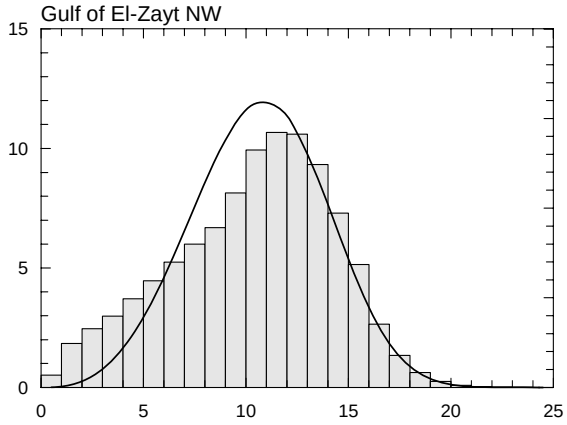

	Jan	Feb	Mar	Apr	May	Jun	Jul	Aug	Sep	Oct	Nov	Dec	Year
0	7.0	6.9	10.0	9.5	11.2	13.2	13.2	13.5	12.5	10.8	7.5	6.6	10.5
1	7.3	7.1	10.4	9.5	11.4	13.6	13.3	13.5	12.5	10.9	8.0	6.6	10.7
2	7.4	7.4	10.8	9.5	11.3	13.4	13.3	13.3	12.5	10.9	8.0	6.5	10.6
3	7.3	7.3	10.8	9.1	11.0	13.2	12.9	13.0	12.4	10.8	8.0	6.8	10.5
4	7.2	7.5	10.4	9.0	10.7	12.9	12.5	12.8	12.1	10.6	8.1	6.5	10.3
5	7.1	6.7	10.3	9.0	10.6	12.4	12.0	12.3	11.9	10.3	7.9	6.6	10.0
6	6.9	6.9	10.0	8.9	10.3	12.9	11.8	12.0	11.6	10.2	7.6	6.8	9.9
7	7.1	6.8	10.4	9.6	11.5	14.1	12.9	13.2	12.7	10.7	7.6	6.3	10.6
8	7.1	7.4	11.7	10.1	11.4	13.6	13.1	13.8	13.8	12.2	8.3	6.6	11.1
9	8.2	8.4	11.5	10.0	11.1	13.1	12.7	13.4	13.3	11.8	8.9	7.8	11.1
10	8.2	7.9	10.9	9.7	11.0	13.0	12.5	13.4	12.9	11.3	8.5	8.0	10.9
11	7.9	8.0	10.7	9.8	10.9	12.7	12.5	13.2	12.8	11.2	8.4	8.3	10.7
12	7.9	8.5	10.7	10.0	10.8	12.5	12.4	13.0	12.5	10.8	8.4	8.2	10.7
13	7.9	8.5	10.6	10.2	10.8	12.4	12.1	13.0	12.4	10.5	8.4	8.5	10.6
14	8.0	8.2	10.6	10.4	10.8	12.3	12.1	13.2	12.5	10.4	8.7	8.3	10.7
15	8.5	8.3	10.6	10.4	10.9	12.4	12.0	13.2	12.5	10.4	8.7	8.4	10.7
16	8.9	8.5	10.5	10.5	11.1	12.5	12.1	13.2	12.4	10.3	8.5	8.3	10.7
17	8.4	8.0	10.3	10.5	11.1	12.3	11.8	12.8	11.9	9.5	7.8	7.5	10.4
18	7.4	6.8	9.3	9.8	10.5	11.7	11.4	11.9	11.0	8.7	7.2	7.0	9.6
19	7.1	6.6	8.5	8.8	9.6	10.7	10.5	10.9	10.5	8.4	7.2	7.0	9.0
20	6.9	6.7	8.8	8.8	9.3	10.6	9.9	10.8	10.7	8.8	6.9	7.1	9.0
21	7.0	6.6	9.3	8.9	9.9	11.1	10.4	11.3	11.1	9.6	6.9	6.9	9.3
22	7.0	6.0	9.7	9.3	10.4	11.8	11.5	11.9	11.8	10.0	6.9	6.6	9.7
23	6.9	6.2	9.9	9.6	10.9	12.6	12.4	12.8	12.2	10.4	7.3	6.5	10.2
Mean	7.5	7.4	10.3	9.6	10.8	12.5	12.1	12.7	12.2	10.4	7.9	7.2	10.3

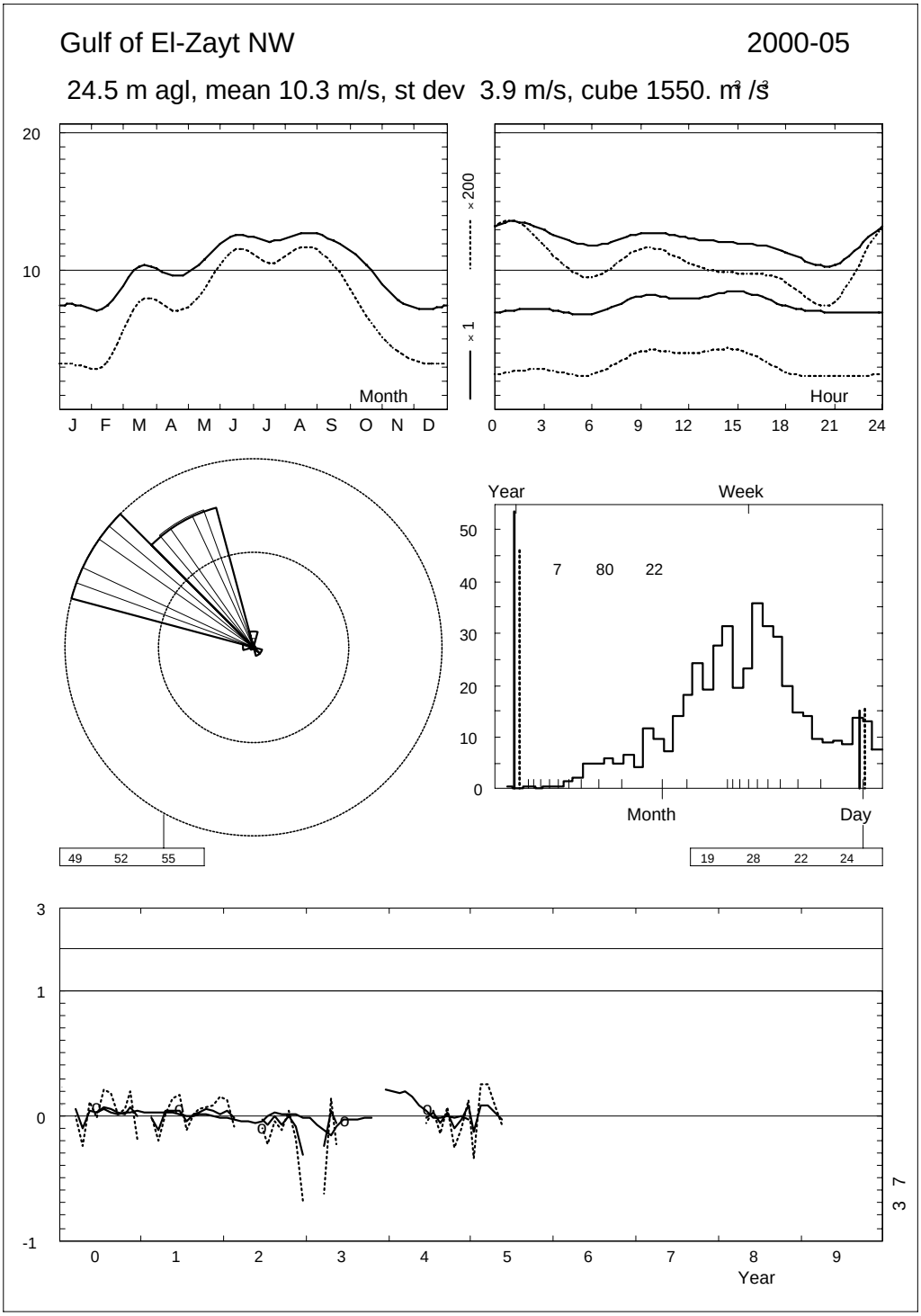

	Jan	Feb	Mar	Apr	May	Jun	Jul	Aug	Sep	Oct	Nov	Dec	Year
2000	8.2	—	10.9	8.7	11.2	12.9	13.0	13.3	12.4	10.5	8.5	7.2	10.6
2001	—	7.3	9.1	9.9	11.2	13.0	11.5	12.9	12.5	10.9	8.3	7.4	10.4
2002	7.8	7.3	—	—	—	12.1	11.3	12.7	11.3	10.4	7.2	5.0	9.9
2003	—	—	7.7	10.0	10.1	—	—	—	—	—	—	—	10.0
2004	—	—	—	—	—	12.4	12.4	12.0	12.5	9.4	7.6	7.8	10.7
2005	6.6	8.1	11.1	9.9	10.4	—	—	—	—	—	—	—	9.5
Mean	7.5	7.4	10.3	9.6	10.8	12.5	12.1	12.7	12.2	10.4	7.9	7.2	10.3

Roughness Class 0 ($z_0 = 0.0002$ m)

z	0	30	60	90	120	150	180	210	240	270	300	330	Total
10	9.1	5.6	2.9	3.7	6.5	6.8	4.9	3.6	5.4	7.9	12.3	12.3	11.6
	2.40	1.87	1.61	1.65	2.26	2.32	1.87	1.82	2.44	2.09	4.27	4.63	3.42
25	10.0	6.1	3.2	4.0	7.1	7.5	5.4	4.0	5.9	8.6	13.4	13.4	12.7
	2.46	1.93	1.66	1.71	2.33	2.39	1.92	1.88	2.51	2.16	4.35	4.72	3.47
50	10.7	6.6	3.4	4.3	7.6	8.0	5.8	4.3	6.4	9.3	14.3	14.3	13.5
	2.53	1.98	1.71	1.75	2.40	2.46	1.97	1.93	2.58	2.22	4.46	4.85	3.54
100	11.5	7.1	3.7	4.7	8.3	8.7	6.3	4.6	6.9	10.0	15.4	15.4	14.5
	2.47	1.92	1.65	1.70	2.32	2.38	1.91	1.87	2.50	2.15	4.38	4.76	3.51
200	12.6	7.9	4.1	5.1	9.2	9.6	6.9	5.1	7.7	11.1	16.7	16.7	15.8
	2.36	1.82	1.57	1.61	2.20	2.25	1.81	1.77	2.36	2.03	4.24	4.60	3.43
Freq.	6.0	0.7	0.2	0.3	2.1	2.2	0.6	0.4	0.9	3.6	46.3	36.7	100.0

Roughness Class 1 ($z_0 = 0.0300$ m)

z	0	30	60	90	120	150	180	210	240	270	300	330	Total
10	5.2	3.2	2.0	3.6	4.6	4.7	2.9	2.9	4.6	7.9	8.7	8.6	8.2
	1.79	1.73	1.35	1.53	1.91	1.93	1.52	1.59	1.78	2.90	3.84	4.08	3.13
25	6.2	3.8	2.4	4.3	5.4	5.6	3.5	3.5	5.5	9.3	10.2	10.1	9.6
	1.93	1.87	1.46	1.65	2.06	2.09	1.64	1.72	1.92	3.04	4.01	4.28	3.26
50	7.2	4.4	2.9	5.0	6.3	6.5	4.1	4.1	6.4	10.5	11.6	11.5	10.9
	2.17	2.10	1.63	1.85	2.31	2.35	1.84	1.93	2.16	3.28	4.29	4.60	3.47
100	8.6	5.3	3.4	6.0	7.5	7.7	4.9	4.8	7.6	12.1	13.2	13.1	12.5
	2.31	2.24	1.73	1.97	2.47	2.50	1.96	2.05	2.30	3.53	4.61	4.93	3.70
200	10.7	6.6	4.2	7.4	9.3	9.6	6.1	6.0	9.4	14.4	15.6	15.6	14.9
	2.21	2.13	1.66	1.88	2.35	2.38	1.87	1.96	2.20	3.40	4.46	4.76	3.65
Freq.	3.7	0.5	0.2	0.7	2.2	1.9	0.5	0.5	1.4	11.2	46.5	30.8	100.0

Roughness Class 2 ($z_0 = 0.1000$ m)

z	0	30	60	90	120	150	180	210	240	270	300	330	Total
10	4.6	2.7	1.9	3.3	4.0	4.1	2.5	2.7	4.1	7.0	7.6	7.5	7.1
	1.83	1.63	1.38	1.62	1.91	1.92	1.52	1.64	1.76	3.15	3.86	4.01	3.15
25	5.6	3.3	2.3	4.1	4.9	5.0	3.1	3.3	5.1	8.6	9.2	9.1	8.6
	1.95	1.74	1.48	1.73	2.04	2.05	1.62	1.76	1.89	3.28	4.01	4.18	3.26
50	6.6	3.9	2.8	4.9	5.8	5.9	3.7	3.9	6.0	9.9	10.5	10.4	10.0
	2.16	1.92	1.63	1.92	2.26	2.27	1.79	1.94	2.09	3.50	4.26	4.44	3.44
100	7.9	4.7	3.3	5.8	6.9	7.0	4.4	4.6	7.2	11.4	12.1	12.1	11.5
	2.37	2.12	1.79	2.10	2.49	2.50	1.97	2.13	2.29	3.84	4.66	4.86	3.72
200	9.7	5.8	4.1	7.2	8.5	8.7	5.4	5.7	8.8	13.6	14.3	14.3	13.7
	2.27	2.03	1.72	2.01	2.38	2.39	1.88	2.04	2.20	3.71	4.51	4.71	3.66
Freq.	3.4	0.4	0.2	0.8	2.2	1.7	0.4	0.5	1.7	14.7	45.5	28.4	100.0

Roughness Class 3 ($z_0 = 0.4000$ m)

z	0	30	60	90	120	150	180	210	240	270	300	330	Total
10	3.6	2.1	1.6	2.8	3.1	3.2	2.0	2.2	3.4	5.6	5.9	5.8	5.6
	1.84	1.65	1.46	1.69	1.90	1.88	1.53	1.70	1.80	3.37	3.83	3.90	3.14
25	4.7	2.8	2.1	3.6	4.1	4.2	2.6	2.9	4.5	7.3	7.7	7.6	7.2
	1.95	1.75	1.54	1.79	2.01	2.00	1.62	1.80	1.90	3.50	3.96	4.05	3.24
50	5.7	3.3	2.5	4.4	5.0	5.0	3.1	3.5	5.4	8.7	9.1	9.0	8.6
	2.12	1.90	1.67	1.95	2.19	2.17	1.76	1.95	2.07	3.69	4.16	4.26	3.39
100	6.9	4.1	3.1	5.3	6.0	6.1	3.8	4.2	6.5	10.3	10.7	10.6	10.1
	2.41	2.16	1.90	2.22	2.49	2.47	2.01	2.22	2.36	4.04	4.53	4.66	3.66
200	8.4	4.9	3.8	6.5	7.3	7.4	4.7	5.2	8.0	12.2	12.7	12.6	12.0
	2.32	2.08	1.83	2.13	2.40	2.38	1.93	2.14	2.27	4.01	4.52	4.64	3.67
Freq.	2.9	0.4	0.2	1.0	2.2	1.5	0.4	0.6	2.0	19.6	44.1	24.9	100.0

z	Class 0		Class 1		Class 2		Class 3	
m	ms^{-1}	Wm^{-2}	ms^{-1}	Wm^{-2}	ms^{-1}	Wm^{-2}	ms^{-1}	Wm^{-2}
10	10.4	916	7.3	329	6.4	215	5.0	103
25	11.4	1181	8.6	531	7.8	384	6.5	225
50	12.2	1428	9.8	756	8.9	575	7.7	373
100	13.1	1775	11.3	1122	10.4	872	9.1	598
200	14.2	2295	13.4	1883	12.3	1460	10.9	1001

Gulf of El-Zayt

Gulf of Suez

27° 47′ 23.9″ N 33° 28′ 23.3″ E	UTM 36 E 546 610 m N 3 074 027 m	14 m

The Gulf of El-Zayt mast is situated just W of the Hurghada–Zafarana road, approximately 60 km NNW of Hurghada along this road (map sheet: NG 36 O4d). The distance to the coastline of the Gulf of El-Zayt is 1300 m in a northeasterly direction. There are no sheltering obstacles close to the mast. The surface consists mostly of sand and gravel with a roughness length of less than 0.01 m.

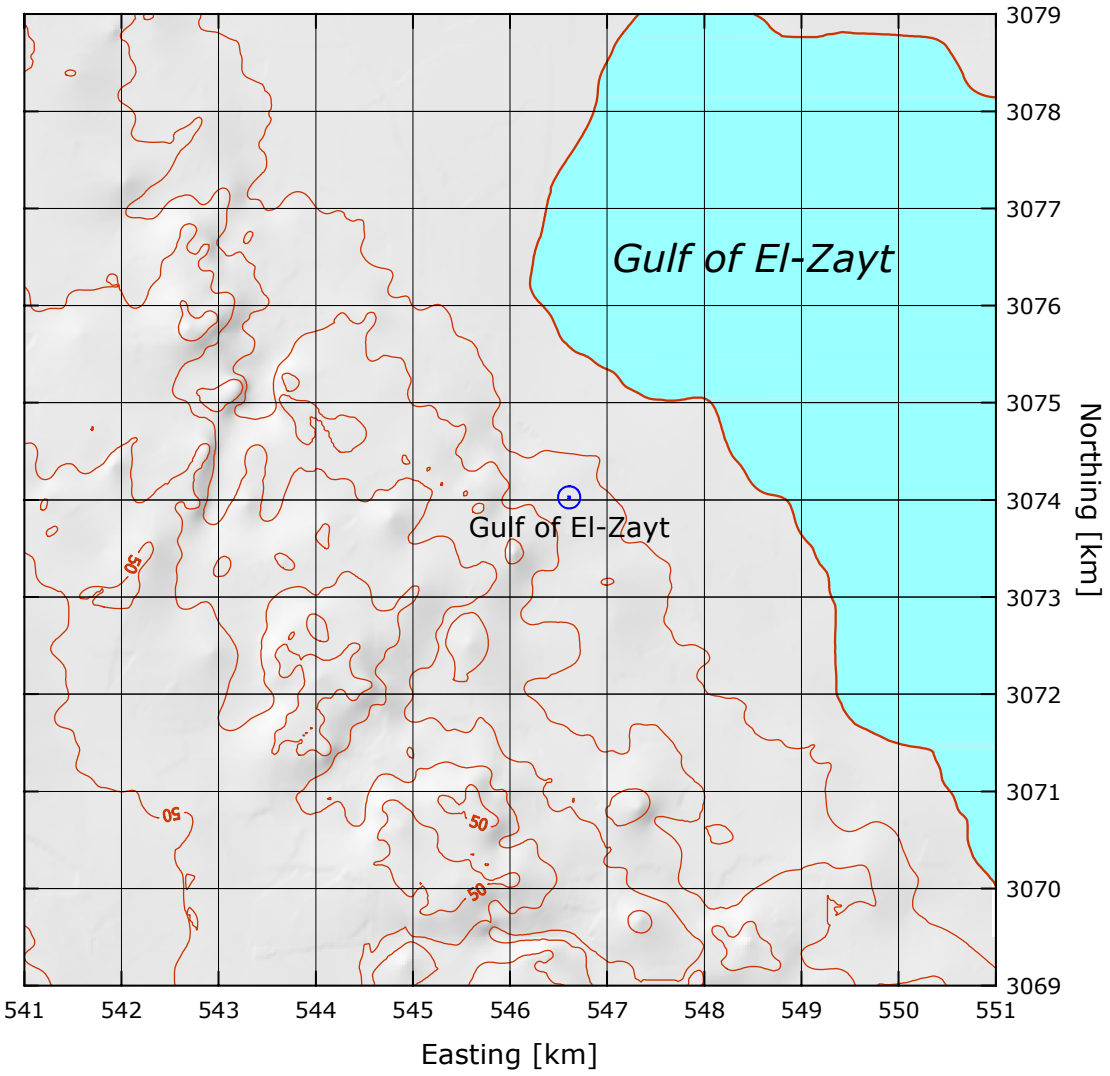

Sector	Input		Obstacles		Roughness		Orography		z_{0m}
0	0.0	0.0	0.0	0.0	0.3	0.0	0.1	−1.1	0.0010
30	0.0	0.0	0.0	0.0	−0.4	0.0	−1.9	−0.9	0.0010
60	0.0	0.0	0.0	0.0	−1.7	0.0	−2.6	0.2	0.0010
90	0.0	0.0	0.0	0.0	−2.7	0.0	−1.4	1.1	0.0000
120	0.0	0.0	0.0	0.0	−3.5	0.0	0.6	0.9	0.0000
150	0.0	0.0	0.0	0.0	−2.0	0.0	1.3	−0.2	0.0010
180	0.0	0.0	0.0	0.0	0.0	0.0	0.1	−1.1	0.0030
210	0.0	0.0	0.0	0.0	0.0	0.0	−2.0	−1.0	0.0030
240	0.0	0.0	0.0	0.0	0.0	0.0	−2.8	0.2	0.0030
270	0.0	0.0	0.0	0.0	0.0	0.0	−1.5	1.1	0.0030
300	0.0	0.0	0.0	0.0	0.0	0.0	0.6	0.9	0.0030
330	0.0	0.0	0.0	0.0	0.0	0.0	1.3	−0.2	0.0030

Sect	Freq	<1	2	3	4	5	6	7	8	9	11	13	15	17	>17	*A*	*k*
0	7.5	6	26	43	48	47	56	62	76	93	198	191	126	25	1	10.4	3.31
30	0.7	45	172	261	254	138	69	34	16	6	3	0	0	0	0	3.7	2.04
60	0.6	43	171	233	249	126	88	59	26	3	1	1	0	0	0	3.8	2.03
90	1.8	21	61	113	184	233	193	126	52	13	4	0	0	0	0	5.1	3.06
120	2.6	12	58	93	120	145	151	136	107	99	70	9	1	0	0	6.3	2.59
150	1.6	31	84	116	153	181	158	126	72	43	31	5	0	0	0	5.4	2.38
180	1.1	50	159	183	198	183	127	59	24	6	6	4	1	0	0	4.2	2.09
210	0.3	64	176	231	248	148	74	18	23	11	2	0	0	4	0	3.8	1.76
240	0.4	52	148	135	135	105	112	96	75	65	64	8	5	0	0	5.4	1.85
270	1.8	30	84	74	62	67	108	159	194	107	82	25	8	1	0	7.2	3.25
300	30.3	2	9	13	18	28	41	55	73	90	220	199	166	70	16	11.7	3.57
330	51.3	1	7	14	22	35	40	46	54	64	169	213	200	100	34	12.5	4.02
Total	100.0	5	19	29	37	47	52	57	65	73	172	185	162	74	23	11.5	3.29

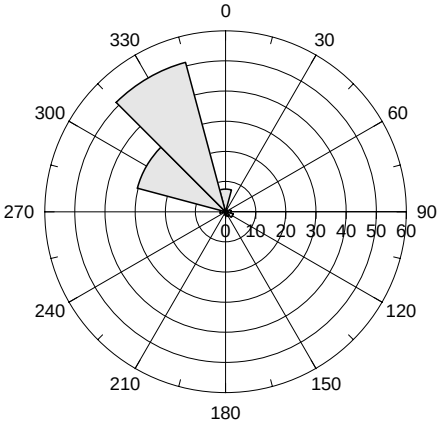

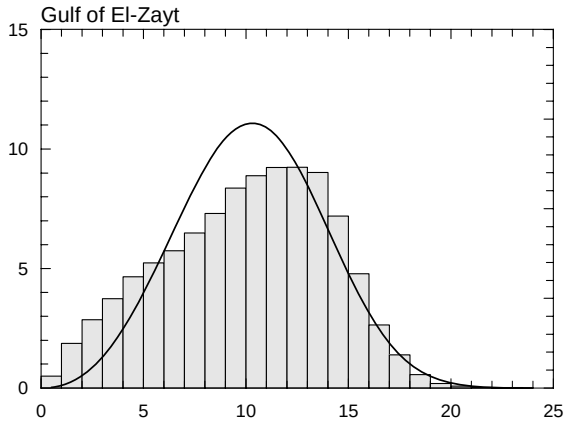

	Jan	Feb	Mar	Apr	May	Jun	Jul	Aug	Sep	Oct	Nov	Dec	Year
0	7.4	7.8	7.9	9.0	10.1	12.5	12.2	12.9	12.1	10.1	8.1	7.1	10.0
1	7.4	8.0	8.0	9.3	10.3	12.7	12.5	13.1	12.3	10.2	8.3	7.1	10.2
2	7.4	8.0	8.1	9.5	10.3	12.8	12.7	13.0	12.3	10.3	8.3	7.1	10.2
3	7.5	8.1	8.3	9.4	10.2	12.5	12.3	12.7	12.2	10.2	8.1	7.2	10.1
4	7.5	8.1	8.3	9.4	10.1	12.2	11.9	12.4	12.0	10.1	8.3	7.2	10.0
5	7.5	8.1	8.0	9.2	10.1	11.8	11.5	12.0	11.7	10.0	8.3	7.1	9.8
6	7.4	8.0	8.1	9.0	10.1	12.3	11.4	11.9	11.7	10.0	8.2	7.0	9.8
7	7.4	7.8	8.2	9.8	11.6	14.2	13.2	13.6	13.0	10.5	8.2	7.0	10.6
8	7.3	8.6	9.4	10.3	11.7	14.0	13.2	13.9	14.0	11.9	9.2	7.0	11.1
9	8.8	9.6	9.6	10.0	11.2	13.4	12.5	13.5	13.3	11.4	9.9	8.4	11.1
10	8.8	9.3	9.3	9.7	10.9	12.8	12.1	13.0	12.5	10.5	9.2	8.4	10.7
11	8.3	8.9	9.1	9.6	10.7	12.6	11.9	12.7	12.1	10.1	8.6	8.1	10.4
12	8.1	8.7	9.1	9.8	10.5	12.4	11.6	12.6	11.9	10.0	8.3	7.9	10.3
13	8.4	8.7	9.4	9.7	10.6	12.4	11.4	12.6	11.8	9.8	8.3	8.1	10.3
14	8.7	8.7	9.4	9.8	10.5	12.5	11.5	12.8	11.9	9.6	8.4	8.3	10.4
15	8.7	9.0	9.6	9.9	10.7	12.7	11.8	13.1	12.1	9.7	8.4	8.3	10.5
16	8.8	9.3	9.6	10.0	10.7	13.0	12.1	13.3	12.2	9.8	8.5	8.4	10.7
17	8.4	9.2	9.3	10.1	10.7	12.8	11.9	13.1	12.1	9.7	7.7	7.5	10.4
18	7.4	7.9	8.4	9.3	10.0	12.2	11.4	12.1	11.1	8.6	7.1	7.0	9.6
19	7.4	7.5	7.6	8.3	9.0	11.1	10.0	10.8	10.5	8.4	7.0	7.2	8.9
20	7.5	7.7	7.5	8.1	8.9	10.8	9.6	10.6	10.7	8.6	7.4	7.6	8.9
21	7.6	7.7	7.7	8.0	9.1	11.2	9.9	10.9	11.1	9.1	7.5	7.3	9.1
22	7.4	7.8	7.7	8.2	9.7	11.6	10.7	11.7	11.6	9.5	7.6	7.1	9.4
23	7.4	7.9	7.8	8.6	10.1	12.2	11.7	12.4	11.8	9.8	7.7	7.2	9.7
Mean	7.9	8.3	8.6	9.3	10.3	12.5	11.7	12.5	12.0	9.9	8.2	7.5	10.1

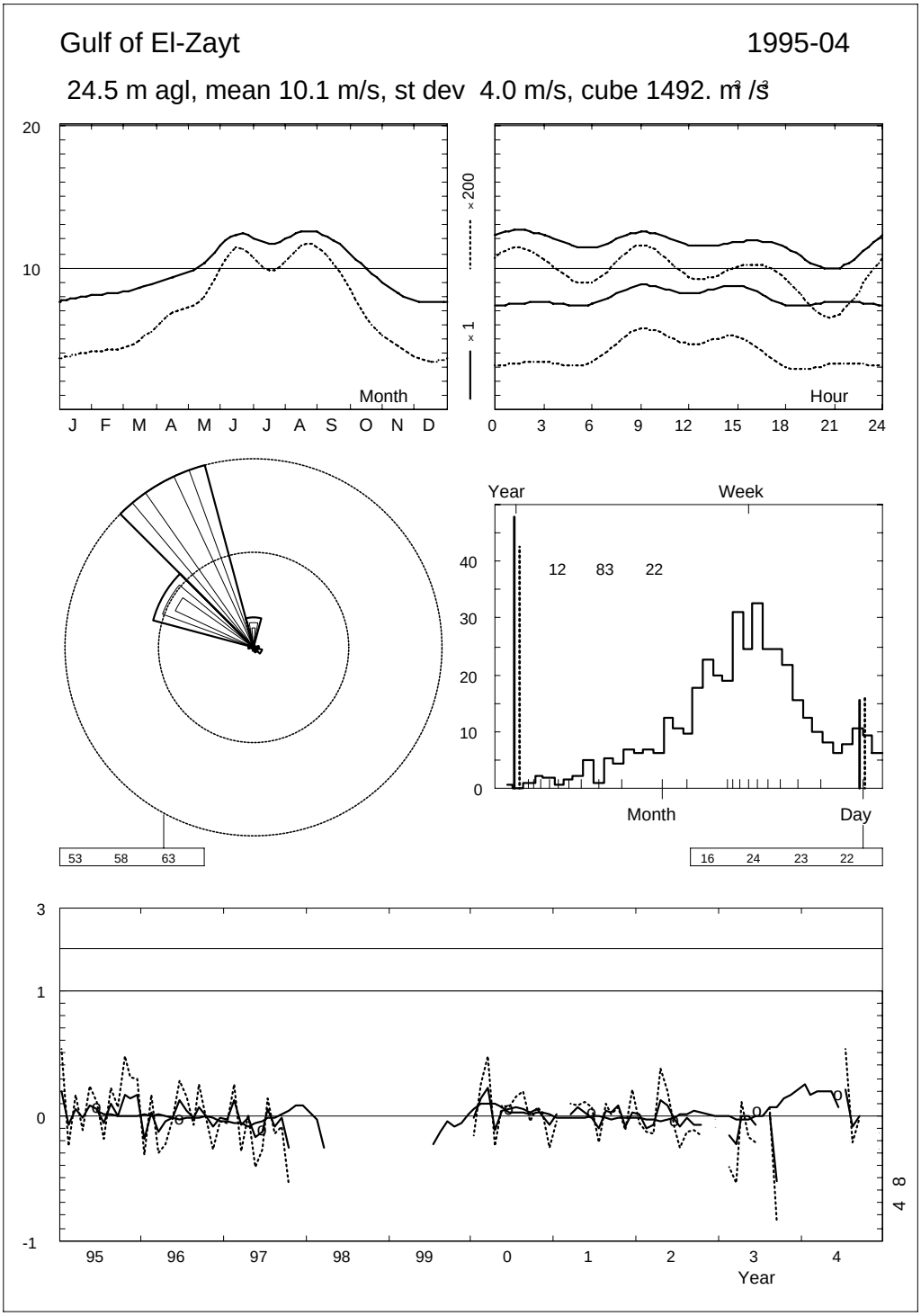

	Jan	Feb	Mar	Apr	May	Jun	Jul	Aug	Sep	Oct	Nov	Dec	Year
1995	9.4	7.6	9.0	9.2	11.1	13.0	11.1	13.8	12.0	11.6	9.3	8.8	10.5
1996	6.4	8.4	7.4	8.9	10.2	13.9	12.3	12.3	12.8	9.9	7.5	7.3	9.8
1997	7.7	9.2	7.9	9.2	8.5	10.8	12.3	11.5	11.8	7.4	—	—	9.6
2000	7.8	9.3	10.5	8.3	10.7	13.0	12.5	13.3	12.2	10.5	8.2	7.0	10.4
2001	7.9	3.6	8.6	9.9	10.6	12.1	10.5	13.1	12.3	10.7	7.4	7.8	10.1
2002	8.0	7.4	8.0	10.5	11.2	11.9	10.6	12.2	11.1	9.2	—	7.3	9.9
2003	—	6.9	6.6	9.4	10.3	11.4	—	12.7	5.7	—	—	—	10.1
2004	—	—	—	—	—	15.7	14.2	11.5	11.9	10.1	—	6.4	10.8
2005	6.0	7.5	10.4	9.5	10.2	—	—	—	—	—	—	—	8.7
Mean	7.9	8.2	8.5	9.3	10.3	12.3	11.7	12.5	11.9	9.9	8.2	7.5	10.1

Roughness Class 0 ($z_0 = 0.0002$ m)

z	0	30	60	90	120	150	180	210	240	270	300	330	Total
10	11.4	7.2	4.0	5.0	6.1	5.6	4.6	4.1	5.8	9.3	12.2	12.8	11.8
	3.55	1.69	1.74	2.83	2.55	2.55	2.26	1.94	1.99	2.40	3.81	4.26	3.21
25	12.4	7.9	4.3	5.5	6.7	6.1	5.0	4.5	6.3	10.1	13.3	14.0	12.8
	3.62	1.73	1.79	2.92	2.63	2.63	2.33	2.01	2.05	2.46	3.87	4.33	3.25
50	13.2	8.5	4.7	5.9	7.2	6.6	5.4	4.9	6.8	10.8	14.1	14.9	13.7
	3.72	1.78	1.84	2.99	2.71	2.70	2.39	2.06	2.10	2.53	3.97	4.44	3.31
100	14.2	9.2	5.1	6.4	7.8	7.1	5.8	5.3	7.4	11.7	15.2	15.9	14.7
	3.65	1.73	1.78	2.90	2.62	2.62	2.31	1.99	2.03	2.47	3.90	4.37	3.28
200	15.5	10.0	5.6	7.1	8.6	7.9	6.4	5.8	8.1	12.8	16.5	17.2	15.9
	3.51	1.65	1.69	2.74	2.48	2.47	2.19	1.88	1.93	2.36	3.78	4.24	3.22
Freq.	11.2	1.5	0.6	1.8	2.5	1.6	1.2	0.4	0.5	2.6	27.9	48.2	100.0

Roughness Class 1 ($z_0 = 0.0300$ m)

z	0	30	60	90	120	150	180	210	240	270	300	330	Total
10	7.5	2.9	3.0	3.7	4.2	3.8	3.1	2.9	5.3	7.9	8.7	9.1	8.3
	2.97	1.03	1.87	2.18	2.11	2.09	1.84	1.46	1.84	2.75	3.44	3.78	2.92
25	8.9	3.6	3.6	4.4	5.1	4.5	3.7	3.5	6.4	9.3	10.2	10.6	9.8
	3.15	1.10	2.01	2.35	2.28	2.25	1.99	1.57	1.99	2.88	3.59	3.93	3.03
50	10.1	4.3	4.2	5.1	5.8	5.2	4.3	4.1	7.4	10.5	11.5	12.0	11.0
	3.45	1.22	2.26	2.64	2.56	2.53	2.24	1.76	2.24	3.10	3.83	4.17	3.20
100	11.7	5.2	4.9	6.0	6.9	6.2	5.1	4.9	8.8	12.0	13.1	13.6	12.6
	3.70	1.30	2.41	2.81	2.73	2.70	2.38	1.87	2.38	3.33	4.11	4.48	3.40
200	14.2	6.4	6.1	7.4	8.6	7.7	6.3	6.1	10.9	14.3	15.4	15.9	14.9
	3.55	1.24	2.30	2.69	2.60	2.58	2.27	1.79	2.27	3.22	3.98	4.34	3.37
Freq.	7.2	0.9	0.8	2.0	2.4	1.5	1.0	0.4	0.8	6.7	32.7	43.6	100.0

Roughness Class 2 ($z_0 = 0.1000$ m)

z	0	30	60	90	120	150	180	210	240	270	300	330	Total
10	6.5	2.5	2.7	3.2	3.7	3.2	2.7	2.7	4.9	7.0	7.6	7.9	7.2
	2.94	1.02	2.02	2.09	2.10	2.03	1.87	1.48	1.91	2.94	3.49	3.77	2.93
25	7.9	3.2	3.4	4.0	4.5	4.0	3.3	3.3	6.0	8.5	9.2	9.5	8.8
	3.10	1.08	2.16	2.24	2.25	2.17	2.00	1.58	2.05	3.06	3.62	3.90	3.02
50	9.2	3.8	4.0	4.7	5.3	4.7	3.9	4.0	7.1	9.8	10.6	10.9	10.1
	3.36	1.19	2.39	2.48	2.49	2.40	2.21	1.75	2.26	3.26	3.83	4.12	3.18
100	10.7	4.6	4.7	5.6	6.3	5.5	4.7	4.7	8.4	11.3	12.1	12.5	11.6
	3.69	1.30	2.63	2.72	2.74	2.63	2.43	1.92	2.49	3.56	4.18	4.49	3.42
200	12.9	5.7	5.8	6.9	7.8	6.8	5.8	5.8	10.4	13.4	14.3	14.7	13.7
	3.55	1.25	2.51	2.61	2.62	2.52	2.32	1.84	2.38	3.45	4.06	4.36	3.38
Freq.	6.6	0.9	0.9	2.0	2.3	1.5	0.9	0.4	1.0	8.8	34.3	40.4	100.0

Roughness Class 3 ($z_0 = 0.4000$ m)

z	0	30	60	90	120	150	180	210	240	270	300	330	Total
10	5.1	2.0	2.2	2.6	2.8	2.5	2.1	2.2	4.0	5.6	6.0	6.1	5.6
	2.90	1.07	2.13	2.07	2.06	2.03	1.81	1.44	1.95	3.07	3.51	3.71	2.92
25	6.6	2.7	2.9	3.4	3.7	3.3	2.8	2.9	5.2	7.3	7.8	7.9	7.3
	3.04	1.13	2.26	2.19	2.18	2.15	1.92	1.53	2.06	3.18	3.63	3.83	3.01
50	7.9	3.3	3.5	4.1	4.5	4.0	3.4	3.5	6.3	8.6	9.2	9.4	8.7
	3.24	1.22	2.46	2.38	2.37	2.34	2.09	1.65	2.24	3.34	3.80	4.00	3.13
100	9.3	4.1	4.3	5.0	5.4	4.8	4.1	4.3	7.6	10.2	10.8	11.0	10.2
	3.63	1.38	2.80	2.71	2.70	2.67	2.38	1.88	2.55	3.65	4.11	4.31	3.35
200	11.2	5.0	5.2	6.1	6.6	5.8	5.0	5.2	9.3	12.0	12.7	13.0	12.1
	3.55	1.33	2.70	2.62	2.60	2.57	2.29	1.81	2.46	3.64	4.12	4.33	3.38
Freq.	5.8	0.8	1.1	2.1	2.2	1.4	0.8	0.4	1.3	11.8	36.4	35.9	100.0

z	Class 0		Class 1		Class 2		Class 3	
m	ms^{-1}	Wm^{-2}	ms^{-1}	Wm^{-2}	ms^{-1}	Wm^{-2}	ms^{-1}	Wm^{-2}
10	10.6	977	7.4	356	6.4	232	5.0	111
25	11.5	1258	8.7	571	7.8	412	6.5	241
50	12.3	1516	9.9	805	9.0	613	7.8	397
100	13.2	1876	11.3	1174	10.4	917	9.2	632
200	14.3	2407	13.3	1924	12.3	1504	10.9	1038

Hurghada WETC — Red Sea

27° 18′ 59.3″ N 33° 42′ 03.5″ E	UTM 36 E 569 352 m N 3 021 683 m	13 m

The Hurghada mast is situated at the Wind Energy Technology Center of NREA, about 275 m SW of the Zafarana–Hurghada road and approximately 12.5 km N of Hurghada (map sheet: NG 36 O2c). The distance to the coastline of the Red Sea is about one km towards the NE. There were no sheltering obstacles close to the mast during the period when data were collected. The surface consists mostly of sand with a roughness length of less than 0.01 m. The station is situated on a coastal plateau which rises gently towards the SW, where it reaches 300 m a.s.l. at a distance of 20 km. Further to the SW the mountains rise to more than 1000 m. To the NW the terrain rises abruptly at a distance of 10 km – to heights of almost 200 m.

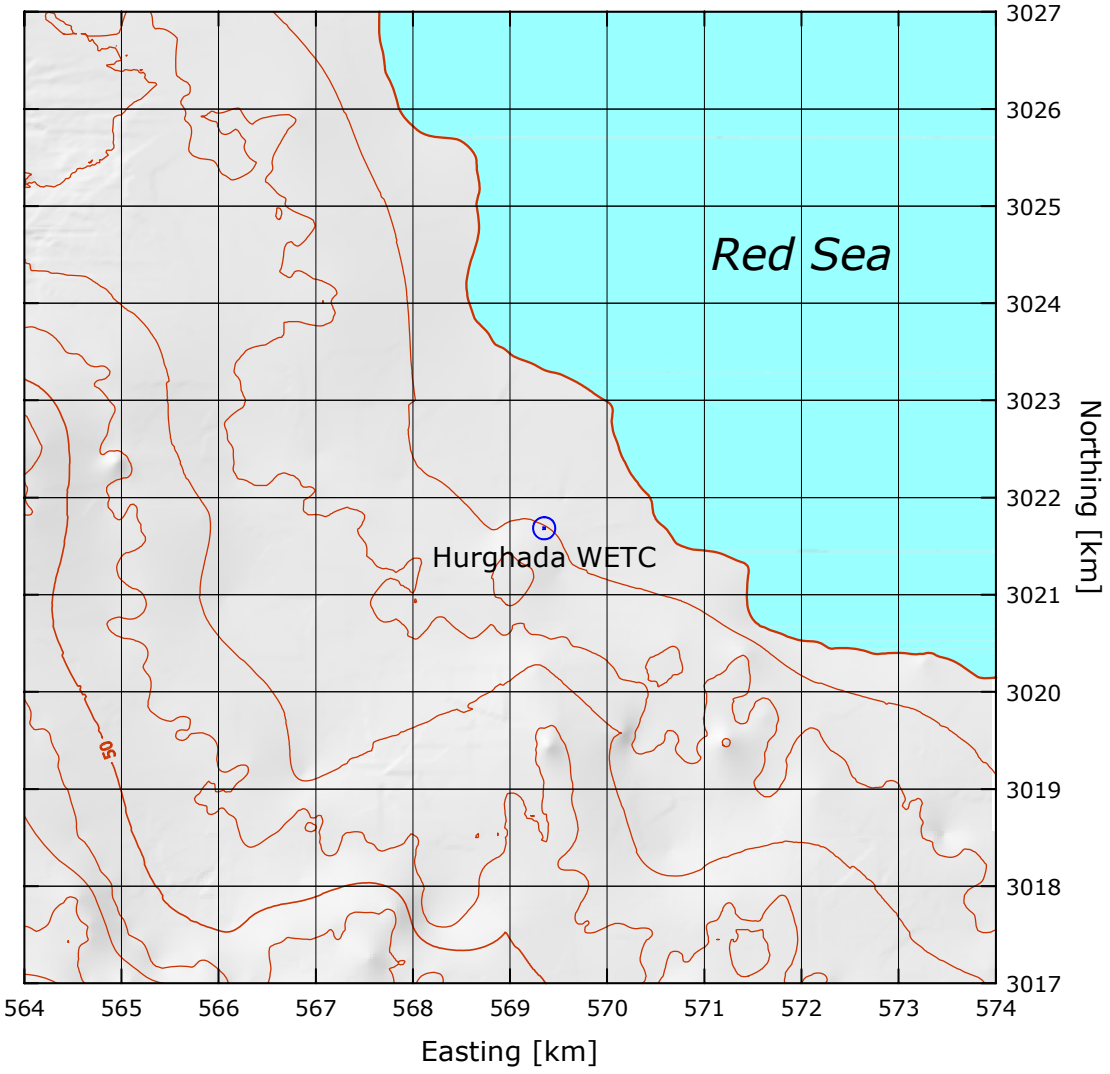

Sector	Input		Obstacles		Roughness		Orography		z_{0m}
0	0.0	0.0	0.0	0.0	0.0	0.0	−1.6	0.1	0.0010
30	0.0	0.0	0.0	0.0	0.0	0.0	−1.1	0.5	0.0010
60	0.0	0.0	0.0	0.0	0.0	0.0	−0.2	0.4	0.0010
90	0.0	0.0	0.0	0.0	0.0	0.0	0.0	−0.1	0.0010
120	0.0	0.0	0.0	0.0	0.0	0.0	−0.5	−0.5	0.0010
150	0.0	0.0	0.0	0.0	0.0	0.0	−1.4	−0.4	0.0010
180	0.0	0.0	0.0	0.0	0.0	0.0	−1.6	0.1	0.0010
210	0.0	0.0	0.0	0.0	0.0	0.0	−1.1	0.5	0.0010
240	0.0	0.0	0.0	0.0	0.0	0.0	−0.2	0.4	0.0010
270	0.0	0.0	0.0	0.0	0.0	0.0	0.0	−0.1	0.0010
300	0.0	0.0	0.0	0.0	0.0	0.0	−0.5	−0.5	0.0010
330	0.0	0.0	0.0	0.0	0.0	0.0	−1.4	−0.4	0.0010

Height of anemometer: 24.5 m a.g.l. 1992–2001, 2004–05

Sect	Freq	<1	2	3	4	5	6	7	8	9	11	13	15	17	>17	*A*	*k*
0	19.4	7	20	30	43	62	82	104	121	135	243	124	26	4	0	9.1	3.49
30	6.3	18	51	88	141	158	137	130	104	80	77	15	1	0	0	6.2	2.40
60	2.6	38	106	169	265	229	117	53	18	4	0	0	0	0	0	4.2	2.73
90	1.8	36	123	141	184	179	144	103	57	21	11	0	0	0	0	4.8	2.33
120	1.3	44	141	193	178	152	107	71	48	25	29	10	1	0	0	4.5	1.72
150	1.0	40	153	185	202	163	106	53	31	26	22	6	10	3	0	4.4	1.55
180	0.7	49	199	209	188	155	89	51	37	17	4	0	0	0	0	3.9	1.87
210	0.9	59	199	248	213	149	84	33	9	4	1	0	0	0	0	3.6	2.07
240	8.6	10	51	84	124	178	228	206	95	16	5	2	0	0	0	5.8	3.70
270	16.8	8	40	81	117	149	179	189	133	60	33	8	2	0	0	6.3	3.04
300	19.0	7	33	64	91	104	122	134	130	104	128	57	20	5	1	7.6	2.49
330	21.7	6	22	36	46	53	66	84	109	123	237	147	55	14	2	9.6	3.29
Total	100.0	11	41	67	93	109	121	127	112	90	134	69	21	5	1	7.6	2.32

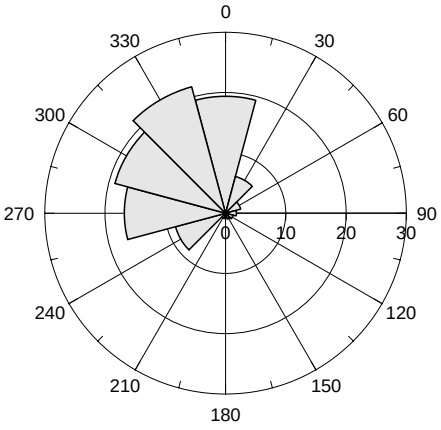

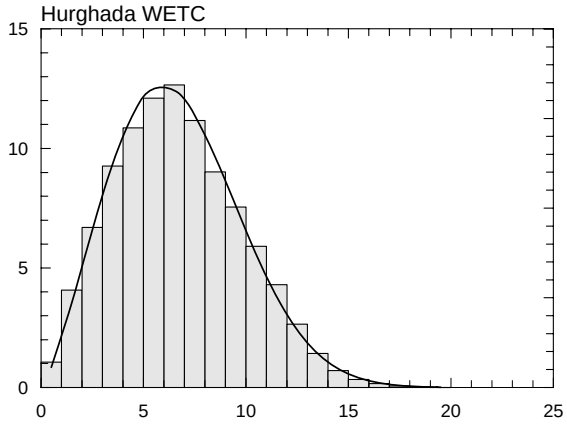

	Jan	Feb	Mar	Apr	May	Jun	Jul	Aug	Sep	Oct	Nov	Dec	Year
0	6.3	6.3	6.2	6.0	6.0	6.5	6.4	6.8	5.5	5.1	5.7	6.2	6.1
1	6.3	6.3	6.1	5.9	5.9	5.9	6.2	6.4	5.4	5.0	5.8	6.2	6.0
2	6.5	6.3	6.0	5.8	5.5	5.8	5.9	6.2	5.0	4.9	5.7	6.2	5.9
3	6.5	6.4	6.0	5.8	5.3	5.5	5.8	5.9	5.1	5.0	5.9	6.3	5.8
4	6.6	6.6	6.1	6.0	5.3	5.5	5.6	5.7	4.9	4.9	6.0	6.5	5.8
5	6.7	6.5	6.2	5.9	5.3	5.5	5.5	5.8	5.1	4.9	5.9	6.5	5.8
6	6.6	6.3	6.0	5.7	5.4	5.4	5.5	5.5	5.1	4.8	5.9	6.4	5.7
7	6.6	6.5	6.0	5.5	5.8	6.5	6.1	6.2	5.4	4.6	5.7	6.4	6.0
8	6.3	6.3	6.1	5.9	6.7	8.5	7.6	7.6	7.0	5.2	5.1	6.0	6.5
9	6.2	6.7	6.9	7.0	7.9	9.2	8.2	8.9	8.9	7.1	5.7	5.6	7.3
10	6.5	7.4	7.8	7.5	8.0	9.2	8.4	9.0	9.2	8.0	6.5	6.0	7.7
11	7.1	8.0	8.2	7.8	7.8	9.1	8.2	8.8	8.7	7.8	7.0	6.7	7.9
12	7.4	8.2	8.2	7.8	7.8	9.1	8.1	8.7	8.8	7.7	7.0	7.1	7.9
13	7.5	8.2	8.3	7.9	7.7	9.0	8.1	8.7	8.5	7.4	6.9	7.2	7.9
14	7.5	8.2	8.3	7.8	7.6	8.9	7.7	8.5	8.5	7.2	6.8	7.2	7.8
15	7.4	8.2	8.2	7.5	7.3	8.8	7.5	8.3	8.1	7.1	6.6	7.1	7.6
16	7.4	8.0	7.9	7.3	6.9	8.5	7.1	7.9	7.7	6.6	6.3	6.9	7.4
17	7.1	7.6	7.7	6.9	6.8	8.6	6.8	7.4	7.4	6.2	5.8	6.5	7.0
18	6.7	7.1	7.3	6.7	6.5	8.7	6.7	7.4	7.5	6.2	5.8	6.5	6.9
19	6.5	6.8	7.1	6.3	6.7	8.7	6.6	7.6	7.6	6.3	5.8	6.5	6.9
20	5.9	6.4	6.7	6.3	7.1	9.0	7.1	7.8	7.4	5.6	5.1	5.5	6.6
21	5.6	5.8	6.2	5.7	6.0	7.9	6.4	6.7	6.4	4.8	5.2	5.6	6.0
22	5.8	5.9	6.2	5.3	5.4	6.7	5.7	6.1	5.9	5.1	5.4	5.9	5.8
23	6.3	6.2	6.1	5.6	5.7	6.5	6.1	6.4	5.7	5.1	5.6	6.1	6.0
Mean	6.6	6.9	6.9	6.5	6.5	7.6	6.8	7.3	6.9	5.9	6.0	6.4	6.7

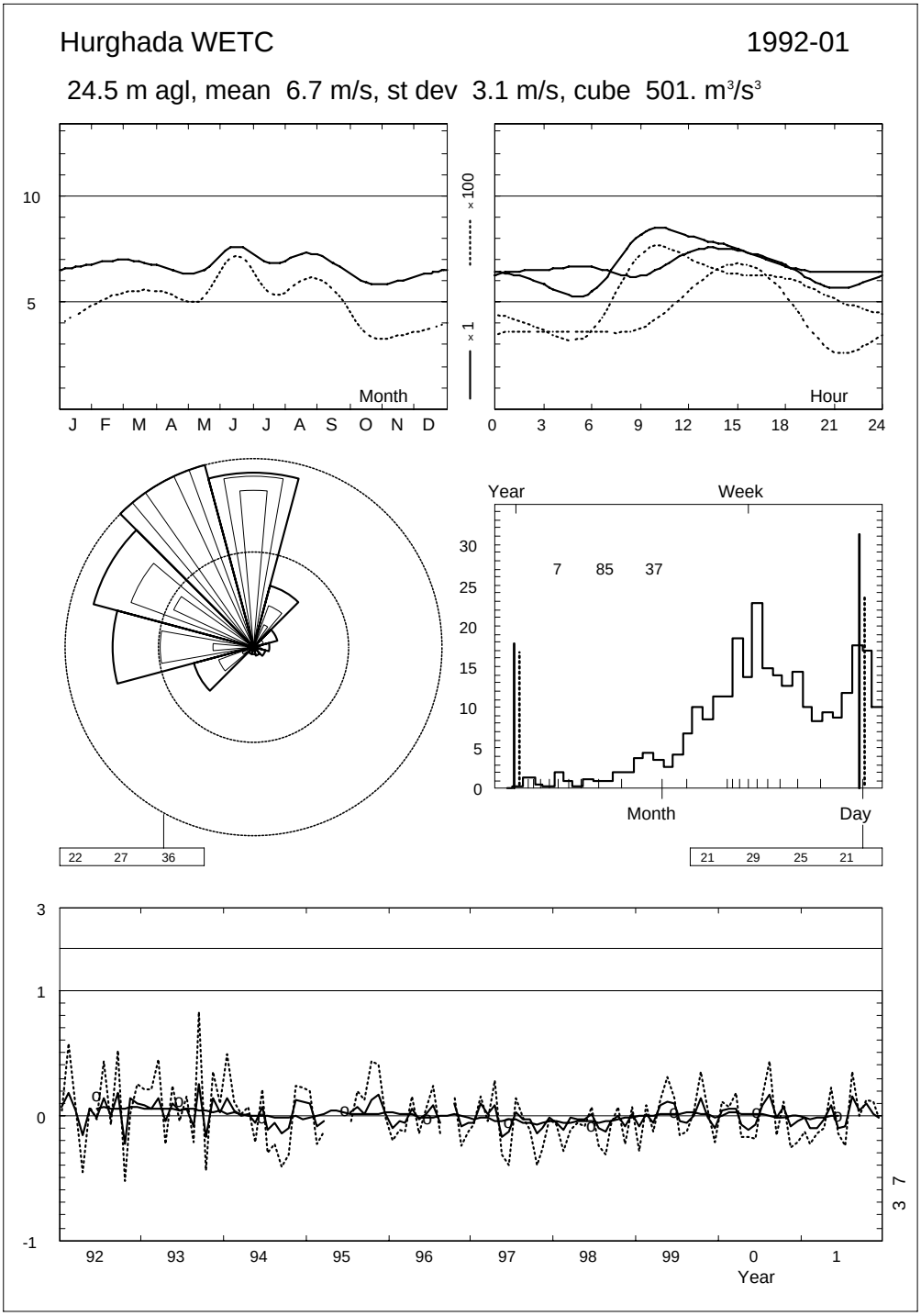

	Jan	Feb	Mar	Apr	May	Jun	Jul	Aug	Sep	Oct	Nov	Dec	Year
1992	7.1	8.2	7.2	5.5	6.9	7.5	7.7	7.2	8.1	4.5	6.8	6.9	7.1
1993	7.2	7.2	7.9	6.2	7.2	7.9	7.2	6.6	8.6	4.9	6.8	6.6	7.0
1994	7.6	7.2	6.9	6.6	6.2	8.1	6.0	6.8	5.8	5.3	6.7	7.1	6.7
1995	7.2	6.3	6.5	—	—	—	7.0	7.8	6.9	6.7	7.0	6.5	6.9
1996	6.0	6.6	6.5	6.9	6.4	7.7	7.3	6.8	—	6.5	5.4	6.0	6.6
1997	6.3	7.6	7.0	7.0	5.4	6.6	7.0	7.1	6.6	5.1	5.3	6.3	6.4
1998	6.3	6.2	6.8	6.2	6.3	7.7	6.1	6.4	6.5	5.9	5.5	6.4	6.4
1999	6.1	7.0	6.5	7.0	7.3	8.4	6.5	6.9	6.8	6.7	5.9	5.7	6.7
2000	6.9	7.3	7.3	6.0	5.7	7.1	7.4	8.5	6.7	6.3	5.4	6.0	6.8
2001	6.5	6.2	6.2	6.2	7.0	6.8	6.2	8.4	7.1	6.5	6.0	6.3	6.7
2004	—	—	—	—	—	7.2	7.0	6.8	8.1	4.7	5.5	6.1	6.5
2005	6.3	—	7.4	6.5	6.7	—	—	—	—	—	—	—	6.7
Mean	6.6	6.9	6.9	6.5	6.5	7.6	6.8	7.3	6.9	5.9	6.0	6.4	6.7

Roughness Class 0 ($z_0 = 0.0002$ m)

z	0	30	60	90	120	150	180	210	240	270	300	330	Total
10	9.2	6.7	4.5	4.7	4.6	4.5	4.0	3.9	5.7	6.2	7.5	9.6	7.7
	3.69	2.50	2.44	2.47	1.88	1.67	1.95	2.17	3.79	3.21	2.63	3.41	2.55
25	10.1	7.3	4.9	5.2	5.0	4.9	4.4	4.2	6.3	6.8	8.2	10.5	8.4
	3.80	2.58	2.51	2.54	1.94	1.72	2.01	2.24	3.91	3.31	2.72	3.52	2.60
50	10.8	7.9	5.2	5.5	5.4	5.3	4.8	4.5	6.7	7.3	8.9	11.2	9.1
	3.90	2.65	2.58	2.61	1.99	1.77	2.06	2.29	4.01	3.40	2.79	3.62	2.65
100	11.8	8.6	5.7	6.0	5.8	5.7	5.2	4.9	7.3	7.9	9.6	12.2	9.8
	3.78	2.56	2.50	2.53	1.92	1.71	2.00	2.22	3.88	3.29	2.70	3.50	2.60
200	13.0	9.5	6.3	6.7	6.4	6.3	5.7	5.4	8.1	8.8	10.6	13.5	10.9
	3.58	2.43	2.36	2.40	1.82	1.62	1.89	2.10	3.68	3.12	2.56	3.31	2.49
Freq.	19.7	7.0	2.8	1.8	1.3	1.0	0.8	1.0	8.1	16.1	18.7	21.7	100.0

Roughness Class 1 ($z_0 = 0.0300$ m)

z	0	30	60	90	120	150	180	210	240	270	300	330	Total
10	6.3	4.2	3.0	3.3	3.1	3.0	2.8	3.6	4.1	4.5	5.5	6.7	5.3
	2.97	2.04	2.24	1.97	1.52	1.41	1.69	2.43	2.88	2.42	2.25	2.94	2.23
25	7.5	5.1	3.6	4.0	3.8	3.7	3.3	4.3	4.9	5.4	6.6	8.0	6.4
	3.21	2.20	2.42	2.13	1.63	1.52	1.82	2.63	3.11	2.61	2.43	3.17	2.37
50	8.6	5.8	4.1	4.6	4.4	4.3	3.8	4.9	5.6	6.2	7.6	9.2	7.4
	3.61	2.47	2.72	2.40	1.84	1.71	2.04	2.95	3.49	2.94	2.73	3.56	2.58
100	10.2	6.9	4.9	5.4	5.2	5.1	4.6	5.8	6.7	7.4	9.1	10.9	8.7
	3.84	2.63	2.90	2.56	1.96	1.81	2.17	3.14	3.72	3.13	2.91	3.79	2.70
200	12.8	8.6	6.1	6.8	6.5	6.3	5.7	7.2	8.3	9.2	11.3	13.5	10.9
	3.67	2.52	2.76	2.44	1.87	1.73	2.08	3.00	3.55	2.99	2.78	3.62	2.61
Freq.	17.4	5.6	2.4	1.7	1.2	0.9	0.8	2.3	9.9	16.9	19.2	21.5	100.0

Roughness Class 2 ($z_0 = 0.1000$ m)

z	0	30	60	90	120	150	180	210	240	270	300	330	Total
10	5.4	3.6	2.7	2.9	2.8	2.7	2.4	3.2	3.6	4.0	4.9	5.8	4.6
	2.92	2.03	2.28	1.94	1.55	1.46	1.71	2.59	2.81	2.32	2.28	2.92	2.22
25	6.7	4.5	3.3	3.6	3.4	3.3	3.0	4.0	4.4	4.9	6.1	7.1	5.7
	3.13	2.17	2.44	2.08	1.65	1.56	1.82	2.77	3.01	2.49	2.44	3.13	2.35
50	7.8	5.3	3.8	4.2	4.0	3.9	3.5	4.6	5.2	5.8	7.1	8.3	6.7
	3.47	2.41	2.70	2.30	1.83	1.73	2.02	3.07	3.34	2.76	2.70	3.47	2.54
100	9.3	6.3	4.6	5.0	4.8	4.7	4.2	5.5	6.1	6.8	8.4	9.9	8.0
	3.81	2.65	2.97	2.53	2.01	1.90	2.22	3.37	3.67	3.03	2.97	3.81	2.72
200	11.4	7.7	5.7	6.1	5.9	5.8	5.2	6.8	7.6	8.5	10.4	12.2	9.8
	3.64	2.53	2.84	2.42	1.92	1.82	2.12	3.23	3.51	2.90	2.84	3.64	2.63
Freq.	16.3	5.3	2.4	1.6	1.2	0.9	0.8	3.0	10.6	17.0	19.4	21.3	100.0

Roughness Class 3 ($z_0 = 0.4000$ m)

z	0	30	60	90	120	150	180	210	240	270	300	330	Total
10	4.2	2.8	2.1	2.3	2.2	2.0	1.9	2.6	2.8	3.2	4.0	4.5	3.6
	2.81	2.00	2.16	1.90	1.53	1.44	1.72	2.67	2.67	2.29	2.33	2.96	2.22
25	5.5	3.7	2.8	3.0	2.8	2.7	2.5	3.4	3.7	4.2	5.2	5.9	4.8
	2.99	2.12	2.29	2.02	1.62	1.53	1.83	2.83	2.83	2.42	2.47	3.14	2.33
50	6.6	4.4	3.3	3.6	3.5	3.3	3.0	4.1	4.5	5.1	6.3	7.1	5.8
	3.24	2.31	2.49	2.19	1.76	1.65	1.98	3.07	3.07	2.63	2.69	3.41	2.49
100	7.9	5.3	4.0	4.3	4.2	4.0	3.6	4.9	5.4	6.1	7.6	8.5	6.9
	3.69	2.63	2.83	2.50	2.00	1.88	2.26	3.50	3.50	3.00	3.06	3.88	2.74
200	9.7	6.5	4.9	5.3	5.1	4.9	4.4	6.0	6.6	7.5	9.2	10.4	8.5
	3.56	2.53	2.73	2.40	1.92	1.81	2.18	3.37	3.37	2.89	2.95	3.74	2.67
Freq.	14.8	4.9	2.2	1.6	1.2	0.9	0.8	3.9	11.6	17.2	19.7	21.1	100.0

z	Class 0		Class 1		Class 2		Class 3	
m	ms^{-1}	Wm^{-2}	ms^{-1}	Wm^{-2}	ms^{-1}	Wm^{-2}	ms^{-1}	Wm^{-2}
10	6.8	306	4.7	112	4.1	73	3.2	35
25	7.5	396	5.7	182	5.1	132	4.2	78
50	8.1	484	6.5	265	5.9	201	5.1	130
100	8.7	626	7.8	430	7.1	325	6.2	214
200	9.7	870	9.7	845	8.7	624	7.5	396

Hurghada (62 463) Red Sea

27° 11′ 05.1″ N 33° 48′ 07.9″ E	UTM 36 E 579 462 m N 3 007 152 m	12 m

The site is located in Hurghada International Airport which is located 5 km southwest of the city of Hurghada. The airport buildings and hangars occur in a sector from north to east. Further away, there are many tourists villages to the northeast, east and south-east. The distance to the Red Sea is about 2-3 km in an easterly direction. There is a mountain ridge to the west, oriented approx. 150-330 degrees from north, about 20 km from the site.

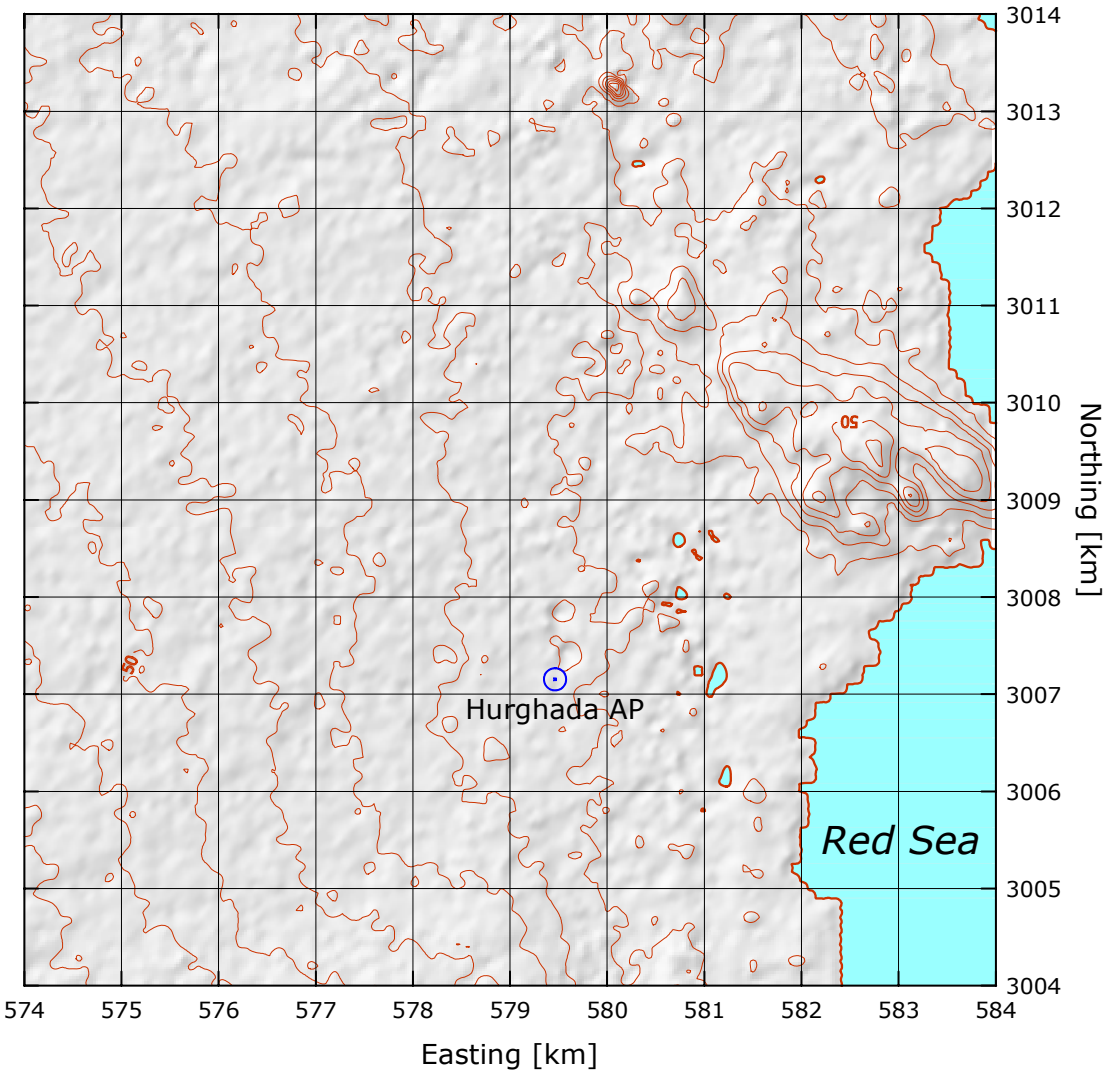

Sector	Input		Obstacles		Roughness		Orography		z_{0m}
0	0.0	0.0	−5.0	0.0	−1.1	0.0	0.8	−0.5	0.0000
30	0.0	0.0	−1.3	0.0	−1.3	0.0	−0.6	−1.0	0.0000
60	0.0	0.0	−9.5	0.0	−1.4	0.0	−2.1	−0.5	0.0000
90	0.0	0.0	−8.4	0.0	−1.5	0.0	−2.1	0.5	0.0000
120	0.0	0.0	−3.0	0.0	−1.5	0.0	−0.7	1.0	0.0000
150	0.0	0.0	−3.4	0.0	−1.5	0.0	0.8	0.5	0.0000
180	0.0	0.0	−1.0	0.0	0.0	0.0	0.8	−0.5	0.0010
210	0.0	0.0	0.0	0.0	0.0	0.0	−0.6	−1.0	0.0010
240	0.0	0.0	−1.3	0.0	0.0	0.0	−2.1	−0.5	0.0010
270	0.0	0.0	−1.5	0.0	0.0	0.0	−2.2	0.5	0.0010
300	0.0	0.0	−0.5	0.0	0.0	0.0	−0.7	1.0	0.0010
330	0.0	0.0	0.0	0.0	0.0	0.0	0.8	0.5	0.0010

Height of anemometer: 10.0 m a.g.l. 1995–2004

Sect	Freq	< 1	2	3	4	5	6	7	8	9	11	13	15	17	>17	*A*	*k*
0	23.1	5	14	36	47	60	96	117	127	122	224	123	26	3	0	8.9	3.23
30	2.6	21	71	200	143	169	184	107	62	30	10	3	0	0	0	5.1	2.53
60	0.9	32	193	290	259	133	75	17	0	0	0	0	0	0	0	3.4	2.42
90	1.5	42	103	280	284	152	82	38	14	4	0	0	0	0	0	3.8	2.32
120	2.8	31	103	212	187	112	135	108	68	19	21	3	0	0	0	4.7	1.94
150	1.1	63	187	254	141	135	104	72	14	9	14	6	0	0	0	3.8	1.65
180	0.5	104	233	350	184	43	49	31	6	0	0	0	0	0	0	2.9	1.84
210	0.5	111	225	309	168	107	20	27	20	0	0	13	0	0	0	3.1	1.37
240	1.2	52	153	247	305	138	74	11	13	3	3	3	0	0	0	3.7	2.27
270	11.7	10	26	57	84	90	176	199	145	124	75	13	1	0	0	7.0	3.36
300	27.5	3	11	29	55	97	188	231	165	118	84	16	2	0	0	7.2	3.38
330	26.7	3	12	36	60	76	134	146	132	120	178	85	16	3	0	8.3	2.84
Total	100.0	9	27	60	74	86	143	161	131	109	132	57	11	1	0	7.6	2.66

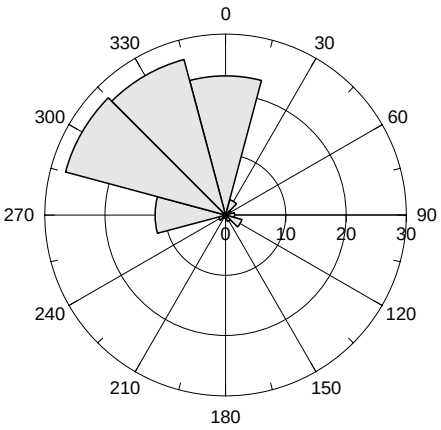

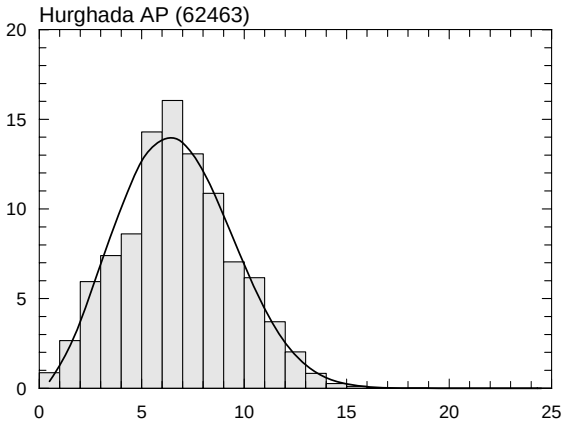

	Jan	Feb	Mar	Apr	May	Jun	Jul	Aug	Sep	Oct	Nov	Dec	Year
0	5.9	6.1	5.9	6.1	6.3	7.3	6.7	7.1	6.8	6.1	6.0	5.8	6.3
3	6.0	6.2	5.9	6.1	5.7	6.4	6.0	6.2	6.2	6.0	6.0	6.0	6.1
6	6.0	6.4	6.5	6.7	7.1	7.8	7.1	7.5	7.1	6.6	6.2	6.0	6.8
9	6.6	7.0	7.4	7.7	8.2	9.3	8.4	9.4	9.2	8.0	6.5	6.4	7.9
12	6.6	7.1	7.6	7.8	7.7	8.8	7.9	9.2	8.6	7.7	6.2	6.3	7.6
15	6.0	6.6	6.9	6.8	6.8	8.0	6.7	8.0	7.5	6.3	5.3	5.5	6.7
18	5.4	5.5	5.6	5.9	6.0	6.9	5.8	6.5	6.4	5.5	5.0	5.1	5.8
21	5.6	5.6	5.5	5.8	6.0	6.9	5.9	6.3	6.3	5.9	5.5	5.5	5.9
Mean	6.0	6.3	6.4	6.6	6.8	7.7	6.8	7.5	7.3	6.5	5.8	5.8	6.6

	Jan	Feb	Mar	Apr	May	Jun	Jul	Aug	Sep	Oct	Nov	Dec	Year
1995	7.0	5.9	6.5	6.6	7.0	7.8	7.1	8.6	7.4	7.4	7.0	6.4	7.1
1996	5.5	6.2	6.2	6.7	6.9	8.8	7.1	7.5	7.6	6.7	5.1	5.6	6.7
1997	5.7	6.7	6.0	6.4	5.4	6.7	7.0	6.2	6.3	4.4	4.6	4.9	5.9
1998	5.1	5.0	5.5	5.3	5.6	7.0	5.5	6.1	6.5	5.4	4.8	5.4	5.6
1999	5.0	6.7	6.1	6.6	7.5	8.1	6.4	6.5	7.3	7.5	6.0	5.6	6.6
2000	6.2	7.2	7.5	6.3	7.1	8.0	7.8	8.6	7.5	6.6	5.7	6.0	7.1
2001	6.3	6.4	6.5	7.4	7.6	7.7	7.3	9.2	8.1	7.6	6.5	6.4	7.3
2002	7.1	6.2	6.1	7.7	7.5	8.1	6.4	7.0	7.0	6.6	5.7	5.7	6.8
2003	5.5	6.5	6.9	6.8	5.7	7.5	6.5	7.9	8.0	6.4	6.7	6.0	6.7
2004	5.7	6.5	7.0	6.3	6.8	7.1	7.0	6.7	6.9	5.7	5.4	5.4	6.4
2005	5.0	5.7	6.6	6.1	6.1	—	—	—	—	—	—	—	—
Mean	6.0	6.3	6.4	6.6	6.8	7.7	6.8	7.5	7.3	6.5	5.8	5.8	6.6

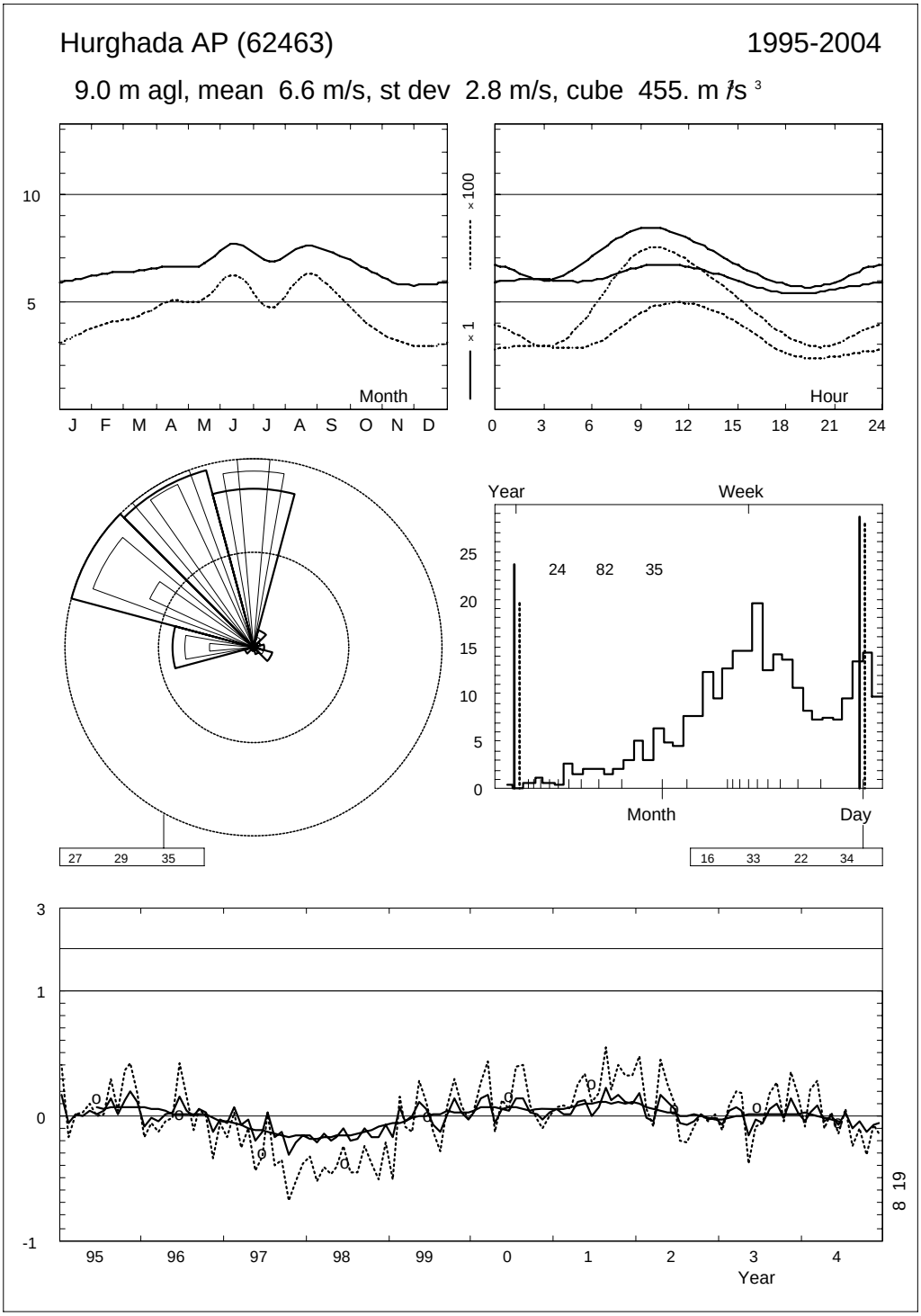
Hurghada AP (62463)
1995-2004
9.0 m agl, mean 6.6 m/s, st dev 2.8 m/s, cube 455. m ł/s 3
10
5
Month
J F M A M J J A S O N D
× 100
× 1
Hour
0 3 6 9 12 15 18 21 24
Year
Week
25
20
15
10
5
0
24 82 35
Month
Day
27 29 35
16 33 22 34
3
1
0
-1
95 96 97 98 99 0 1 2 3 4
Year
8 19

Roughness Class 0 ($z_0 = 0.0002$ m)

z	0	30	60	90	120	150	180	210	240	270	300	330	Total
10	10.1	6.6	4.3	4.4	5.1	4.2	3.3	3.5	4.2	8.0	8.1	9.0	8.5
	3.65	2.11	2.20	2.24	2.01	1.75	2.04	1.61	2.54	3.89	3.84	3.33	2.96
25	11.0	7.3	4.7	4.8	5.5	4.6	3.6	3.8	4.6	8.8	8.8	9.8	9.3
	3.76	2.17	2.27	2.31	2.07	1.81	2.10	1.66	2.62	4.01	3.96	3.44	3.03
50	11.8	7.8	5.0	5.2	5.9	5.0	3.9	4.1	4.9	9.4	9.4	10.6	9.9
	3.87	2.23	2.33	2.37	2.12	1.85	2.16	1.70	2.69	4.12	4.06	3.53	3.09
100	12.8	8.5	5.4	5.6	6.4	5.4	4.2	4.4	5.4	10.2	10.3	11.4	10.8
	3.75	2.16	2.26	2.30	2.06	1.79	2.09	1.65	2.61	3.99	3.94	3.42	3.02
200	14.1	9.4	6.0	6.2	7.1	5.9	4.6	4.8	5.9	11.3	11.4	12.7	11.9
	3.56	2.04	2.14	2.18	1.95	1.70	1.98	1.56	2.47	3.78	3.73	3.24	2.90
Freq.	22.5	3.5	1.0	1.5	2.7	1.1	0.5	0.5	1.2	12.1	27.2	26.1	100.0

Roughness Class 1 ($z_0 = 0.0300$ m)

z	0	30	60	90	120	150	180	210	240	270	300	330	Total
10	7.0	4.2	3.0	3.2	3.5	2.8	2.4	2.7	4.9	5.6	5.8	6.4	5.9
	3.00	1.81	1.96	1.71	1.65	1.45	1.71	1.71	2.55	3.30	3.10	2.83	2.59
25	8.3	5.0	3.6	3.8	4.2	3.4	2.8	3.2	5.8	6.7	6.9	7.7	7.0
	3.23	1.96	2.11	1.84	1.78	1.56	1.85	1.85	2.75	3.57	3.35	3.06	2.76
50	9.5	5.8	4.1	4.4	4.8	4.0	3.3	3.8	6.7	7.7	7.9	8.8	8.1
	3.62	2.20	2.37	2.07	2.00	1.76	2.08	2.08	3.10	4.01	3.76	3.44	3.04
100	11.2	6.9	4.9	5.2	5.7	4.7	3.9	4.5	8.0	9.1	9.3	10.4	9.6
	3.86	2.34	2.53	2.20	2.13	1.87	2.21	2.21	3.29	4.26	4.00	3.67	3.19
200	14.0	8.6	6.1	6.5	7.1	5.8	4.8	5.5	9.9	11.3	11.6	13.0	11.9
	3.69	2.23	2.41	2.10	2.04	1.78	2.11	2.11	3.15	4.08	3.82	3.50	3.08
Freq.	18.6	2.6	1.1	1.8	2.4	1.0	0.5	0.6	3.5	15.5	27.1	25.2	100.0

Roughness Class 2 ($z_0 = 0.1000$ m)

z	0	30	60	90	120	150	180	210	240	270	300	330	Total
10	6.0	3.6	2.6	2.8	3.0	2.4	2.0	2.4	4.4	4.9	5.0	5.6	5.1
	2.99	1.78	1.97	1.69	1.63	1.43	1.57	1.74	2.73	3.33	3.03	2.86	2.60
25	7.4	4.4	3.2	3.4	3.7	3.0	2.5	3.0	5.4	6.0	6.2	6.9	6.3
	3.19	1.90	2.11	1.80	1.75	1.53	1.68	1.86	2.92	3.57	3.24	3.06	2.75
50	8.6	5.2	3.8	4.0	4.3	3.5	2.9	3.5	6.4	7.0	7.2	8.1	7.4
	3.53	2.10	2.34	1.99	1.93	1.69	1.86	2.06	3.24	3.95	3.59	3.38	2.99
100	10.2	6.2	4.5	4.8	5.2	4.2	3.5	4.1	7.6	8.3	8.6	9.6	8.8
	3.88	2.31	2.57	2.19	2.12	1.85	2.04	2.26	3.56	4.34	3.94	3.72	3.22
200	12.6	7.7	5.6	5.9	6.4	5.2	4.3	5.1	9.3	10.2	10.6	11.9	10.8
	3.71	2.21	2.46	2.10	2.03	1.77	1.96	2.17	3.40	4.15	3.78	3.56	3.11
Freq.	17.0	2.4	1.2	1.9	2.2	0.9	0.5	0.7	4.4	16.7	27.0	24.9	100.0

Roughness Class 3 ($z_0 = 0.4000$ m)

z	0	30	60	90	120	150	180	210	240	270	300	330	Total
10	4.7	2.8	2.1	2.2	2.3	1.9	1.7	1.9	3.6	3.8	4.0	4.5	4.0
	2.96	1.73	1.91	1.70	1.63	1.43	1.71	1.81	2.99	3.33	2.94	2.88	2.61
25	6.2	3.7	2.7	3.0	3.1	2.5	2.2	2.5	4.7	5.0	5.2	5.9	5.3
	3.14	1.83	2.02	1.79	1.73	1.51	1.81	1.92	3.17	3.53	3.11	3.06	2.74
50	7.4	4.4	3.3	3.6	3.7	3.0	2.7	3.0	5.7	6.0	6.3	7.1	6.4
	3.41	1.99	2.20	1.95	1.88	1.64	1.97	2.08	3.44	3.83	3.38	3.32	2.93
100	8.9	5.3	4.0	4.3	4.5	3.7	3.3	3.7	6.8	7.2	7.6	8.5	7.6
	3.88	2.27	2.51	2.22	2.14	1.87	2.24	2.37	3.92	4.36	3.85	3.78	3.25
200	10.8	6.5	4.8	5.3	5.5	4.4	4.0	4.5	8.3	8.8	9.2	10.4	9.3
	3.74	2.19	2.41	2.14	2.06	1.80	2.16	2.28	3.78	4.20	3.71	3.65	3.16
Freq.	14.9	2.2	1.2	2.1	2.0	0.8	0.5	0.8	5.8	18.5	26.8	24.4	100.0

z	Class 0		Class 1		Class 2		Class 3	
m	ms^{-1}	Wm^{-2}	ms^{-1}	Wm^{-2}	ms^{-1}	Wm^{-2}	ms^{-1}	Wm^{-2}
10	7.5	373	5.2	135	4.5	88	3.6	42
25	8.3	483	6.3	221	5.6	160	4.7	94
50	8.9	592	7.2	324	6.6	245	5.7	158
100	9.6	763	8.6	527	7.8	400	6.8	264
200	10.6	1054	10.7	1030	9.7	763	8.3	487

Kosseir (62 465) Red Sea

26° 06′ 44.0″ N 34° 15′ 21.5″ E	UTM 36 E 625 582 m N 2 888 716 m		29 m

The Kosseir meteorological station was moved in 2001; the data analyzed here are from the new site only. The site is situated to the west of the city of Kosseir, at a distance of approximately 2 km from the city center. The distance to the Red Sea is about 2 km in a northeasterly direction. There is a mountain ridge of 1500 m elevation, the foothills of this mountain occur about 3 km to the west of the site.

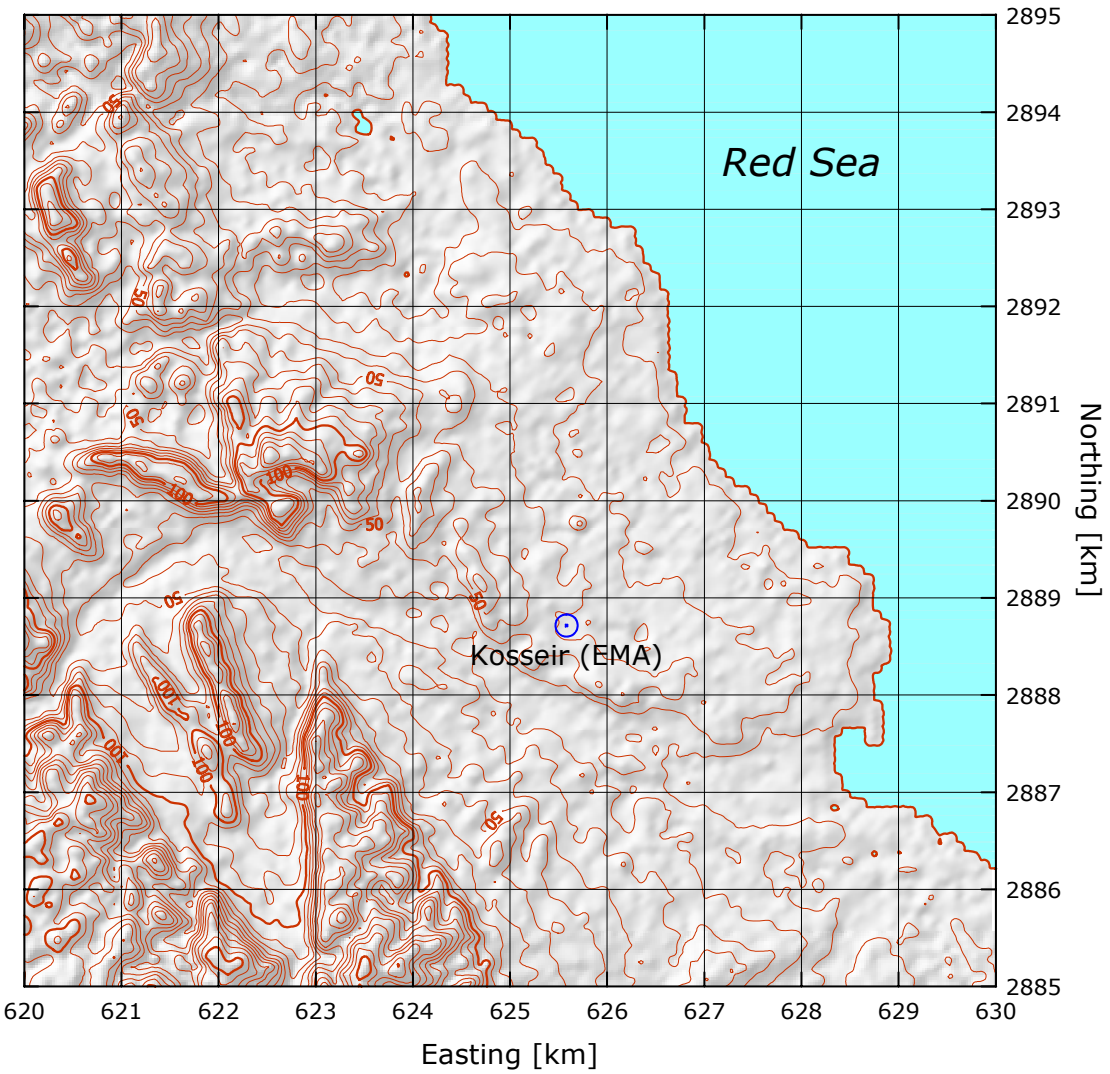

Sector	Input		Obstacles		Roughness		Orography		z_{0m}
0	0.0	0.0	0.0	0.0	−8.0	0.0	−1.4	0.8	0.0010
30	0.0	0.0	0.0	0.0	−17.7	0.0	−0.8	0.1	0.0010
60	0.0	0.0	0.0	0.0	−20.7	0.0	−0.6	−1.0	0.0010
90	0.0	0.0	0.0	0.0	−20.7	0.0	−2.4	−1.6	0.0010
120	0.0	0.0	0.0	0.0	−13.8	0.0	−4.0	−0.2	0.0010
150	0.0	0.0	0.0	0.0	−2.5	0.0	−3.0	0.7	0.0060
180	0.0	0.0	0.0	0.0	0.0	0.0	−1.6	0.8	0.0100
210	0.0	0.0	0.0	0.0	0.0	0.0	−0.8	0.1	0.0100
240	0.0	0.0	0.0	0.0	0.0	0.0	−1.4	−0.7	0.0100
270	0.0	0.0	0.0	0.0	0.0	0.0	−2.8	−0.8	0.0100
300	0.0	0.0	0.0	0.0	0.0	0.0	−3.7	−0.1	0.0100
330	0.0	0.0	0.0	0.0	0.0	0.0	−3.0	0.7	0.0100

Height of anemometer: 10.0 m a.g.l. 2001–2005

Sect	Freq	< 1	2	3	4	5	6	7	8	9	11	13	15	17	>17	*A*	*k*
0	29.3	8	18	68	116	168	187	169	129	74	53	7	2	0	0	6.4	2.90
30	3.9	26	75	183	313	187	111	41	39	14	8	2	0	0	0	4.2	2.04
60	1.5	78	142	251	294	139	70	21	5	0	0	0	0	0	0	3.6	2.58
90	1.4	113	163	270	220	110	45	56	17	6	0	0	0	0	0	3.4	1.85
120	1.2	78	143	202	215	140	117	59	26	20	0	0	0	0	0	4.0	2.04
150	0.9	86	159	218	218	118	45	100	45	9	0	0	0	0	0	3.8	1.82
180	1.0	135	373	333	63	63	24	0	8	0	0	0	0	0	0	2.4	1.73
210	1.6	156	290	342	109	45	40	10	0	5	5	0	0	0	0	2.6	1.64
240	4.2	58	136	320	299	98	43	19	9	8	6	0	4	0	0	3.5	1.84
270	10.7	37	118	362	257	101	64	30	12	7	9	1	1	0	0	3.5	1.74
300	19.2	16	51	255	310	118	71	63	54	32	25	4	1	0	0	4.0	1.49
330	25.0	9	27	104	173	188	168	135	88	54	42	9	3	0	0	5.8	2.38
Total	100.0	23	59	175	204	149	128	104	75	43	33	5	2	0	0	5.1	2.03

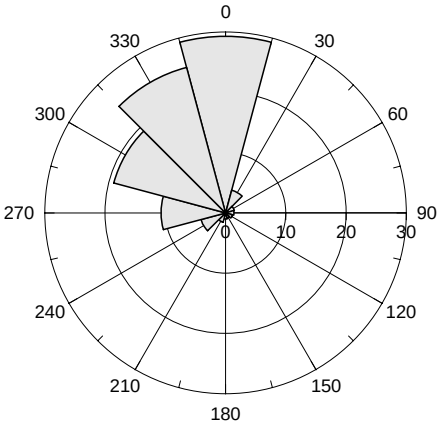

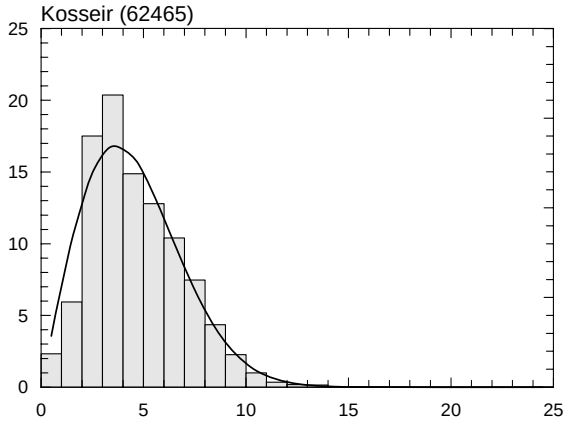

	Jan	Feb	Mar	Apr	May	Jun	Jul	Aug	Sep	Oct	Nov	Dec	Year
0	3.6	3.7	3.9	4.1	3.2	3.2	2.9	3.2	3.8	3.4	3.8	3.6	3.6
3	3.8	4.0	4.2	4.3	3.9	3.8	3.6	3.9	4.7	4.2	4.3	3.8	4.0
6	4.2	4.4	4.9	4.9	4.9	5.6	5.1	5.6	6.3	5.1	4.8	4.0	5.0
9	5.6	5.6	6.7	6.3	6.2	6.5	6.4	6.7	7.1	6.7	6.3	5.5	6.3
12	5.5	5.8	6.3	6.1	5.6	5.7	5.5	6.0	6.4	6.2	6.3	5.8	5.9
15	4.4	4.7	5.0	4.8	4.3	4.4	3.9	4.4	4.9	4.4	4.8	4.4	4.6
18	3.4	3.4	3.6	3.4	3.0	2.8	2.6	2.8	3.4	2.8	3.5	3.4	3.2
21	3.5	3.5	3.6	3.1	2.5	2.6	2.2	2.6	3.0	3.0	3.6	3.5	3.1
Mean	4.3	4.4	4.8	4.6	4.2	4.4	4.1	4.5	5.0	4.5	4.7	4.3	4.5

	Jan	Feb	Mar	Apr	May	Jun	Jul	Aug	Sep	Oct	Nov	Dec	Year
2001	4.1	4.3	4.3	4.6	4.4	4.5	4.3	5.1	5.3	5.4	5.0	4.3	4.6
2002	5.1	5.1	4.4	4.7	4.8	4.6	4.2	4.8	5.1	4.8	5.1	4.4	4.8
2003	4.5	3.8	4.1	4.7	3.5	4.0	3.7	4.2	5.1	4.0	4.7	3.9	4.2
2004	3.6	4.8	5.9	4.5	4.4	4.4	4.1	3.9	4.4	4.0	4.0	4.5	4.4
2005	3.9	4.0	5.2	4.8	3.9	—	—	—	—	—	—	—	4.4
Mean	4.3	4.4	4.8	4.6	4.2	4.4	4.1	4.5	5.0	4.5	4.7	4.3	4.5

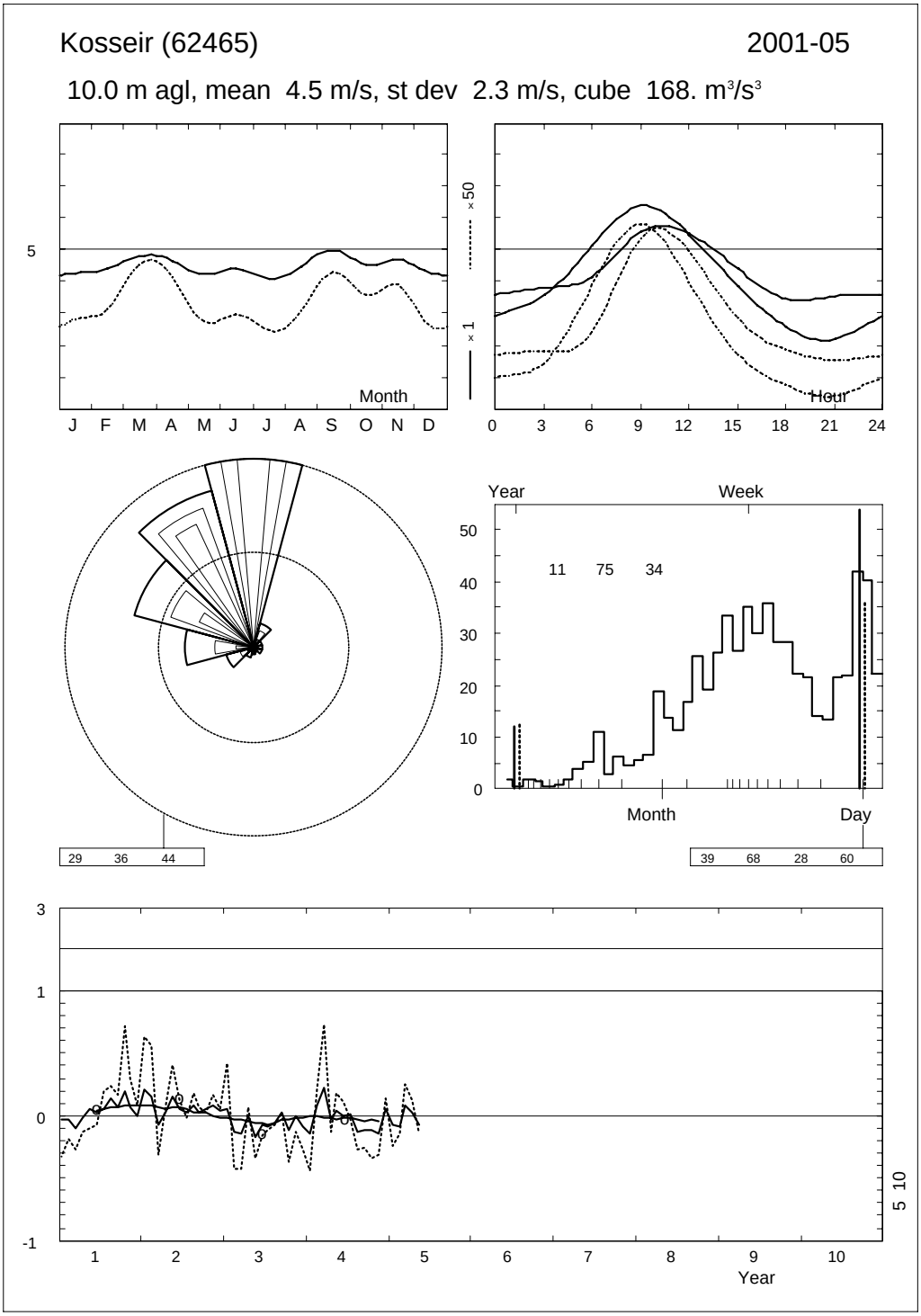
Kosseir (62465)
2001-05
10.0 m agl, mean 4.5 m/s, st dev 2.3 m/s, cube 168. m³/s³
5
Month
J F M A M J J A S O N D
× 50
× 1
Hour
0 3 6 9 12 15 18 21 24
29 36 44
Year
Week
11 75 34
50
40
30
20
10
0
Month
Day
39 68 28 60
3
1
0
-1
1 2 3 4 5 6 7 8 9 10
Year
5 10

Roughness Class 0 ($z_0 = 0.0002$ m)

z	0	30	60	90	120	150	180	210	240	270	300	330	Total
10	7.6	6.4	5.0	4.8	5.3	5.2	3.4	3.5	4.7	4.8	5.5	7.8	6.6
	2.97	2.33	2.40	1.96	2.15	2.18	1.89	1.90	2.16	2.07	1.78	2.76	2.22
25	8.3	7.0	5.5	5.3	5.8	5.7	3.7	3.8	5.1	5.2	6.1	8.5	7.2
	3.07	2.40	2.47	2.02	2.22	2.25	1.95	1.96	2.23	2.13	1.83	2.85	2.28
50	8.9	7.6	5.9	5.7	6.3	6.1	4.0	4.1	5.5	5.6	6.5	9.1	7.7
	3.15	2.47	2.54	2.07	2.28	2.31	2.00	2.01	2.29	2.19	1.88	2.92	2.33
100	9.7	8.2	6.4	6.1	6.8	6.6	4.3	4.4	5.9	6.1	7.1	9.9	8.4
	3.05	2.39	2.46	2.01	2.21	2.24	1.94	1.95	2.22	2.12	1.82	2.83	2.26
200	10.7	9.1	7.1	6.8	7.5	7.3	4.8	4.9	6.6	6.7	7.8	10.9	9.3
	2.88	2.26	2.33	1.90	2.09	2.12	1.83	1.85	2.10	2.01	1.72	2.68	2.16
Freq.	28.4	6.5	1.8	1.4	1.3	0.9	1.0	1.5	3.8	9.9	18.5	24.9	100.0

Roughness Class 1 ($z_0 = 0.0300$ m)

z	0	30	60	90	120	150	180	210	240	270	300	330	Total
10	5.3	3.8	3.4	3.3	3.7	3.3	2.3	2.7	3.2	3.5	4.1	5.5	4.6
	2.53	1.81	2.06	1.61	1.82	1.67	1.67	1.69	1.77	1.70	1.62	2.41	1.94
25	6.3	4.6	4.0	4.0	4.5	4.0	2.8	3.2	3.9	4.2	5.0	6.6	5.5
	2.73	1.96	2.23	1.73	1.96	1.81	1.80	1.82	1.91	1.84	1.74	2.60	2.06
50	7.3	5.3	4.6	4.7	5.2	4.7	3.2	3.8	4.5	4.8	5.8	7.6	6.3
	3.07	2.20	2.51	1.95	2.21	2.03	2.02	2.04	2.15	2.06	1.96	2.93	2.28
100	8.6	6.3	5.5	5.6	6.2	5.5	3.8	4.4	5.4	5.7	6.9	9.0	7.5
	3.27	2.34	2.67	2.07	2.35	2.16	2.15	2.17	2.29	2.20	2.08	3.12	2.40
200	10.7	7.8	6.8	6.9	7.7	6.9	4.7	5.5	6.7	7.1	8.5	11.2	9.4
	3.12	2.24	2.55	1.98	2.24	2.06	2.06	2.08	2.19	2.10	1.99	2.97	2.31
Freq.	25.7	3.5	1.5	1.4	1.2	0.9	1.1	1.9	4.9	11.7	20.2	26.0	100.0

Roughness Class 2 ($z_0 = 0.1000$ m)

z	0	30	60	90	120	150	180	210	240	270	300	330	Total
10	4.6	3.3	2.9	2.9	3.2	2.8	2.0	2.4	2.9	3.1	3.9	4.8	4.0
	2.54	1.88	1.92	1.62	1.78	1.66	1.65	1.72	1.84	1.65	1.81	2.48	1.99
25	5.7	4.1	3.6	3.7	4.0	3.5	2.5	3.0	3.6	3.8	4.8	5.9	5.0
	2.72	2.01	2.05	1.73	1.91	1.78	1.76	1.85	1.97	1.77	1.94	2.66	2.11
50	6.6	4.8	4.2	4.3	4.7	4.1	2.9	3.5	4.2	4.5	5.6	6.9	5.8
	3.02	2.22	2.27	1.92	2.12	1.97	1.95	2.04	2.18	1.96	2.14	2.94	2.29
100	7.8	5.8	5.0	5.1	5.6	4.9	3.5	4.2	5.0	5.3	6.7	8.2	6.9
	3.31	2.44	2.50	2.10	2.32	2.16	2.14	2.24	2.40	2.15	2.35	3.23	2.48
200	9.7	7.1	6.2	6.3	6.9	6.1	4.3	5.2	6.1	6.6	8.2	10.1	8.6
	3.17	2.34	2.39	2.01	2.22	2.07	2.05	2.15	2.29	2.05	2.26	3.10	2.40
Freq.	23.6	3.3	1.5	1.4	1.2	0.9	1.1	2.1	5.5	12.4	20.6	26.2	100.0

Roughness Class 3 ($z_0 = 0.4000$ m)

z	0	30	60	90	120	150	180	210	240	270	300	330	Total
10	3.6	2.6	2.3	2.4	2.5	2.0	1.6	2.0	2.2	2.6	3.1	3.8	3.2
	2.53	1.96	1.92	1.67	1.84	1.53	1.73	1.68	1.77	1.79	1.86	2.55	2.01
25	4.7	3.5	3.0	3.1	3.3	2.7	2.1	2.6	3.0	3.4	4.1	5.0	4.2
	2.68	2.07	2.04	1.77	1.95	1.62	1.83	1.78	1.87	1.89	1.97	2.71	2.12
50	5.7	4.2	3.7	3.8	4.1	3.3	2.6	3.1	3.6	4.1	5.0	6.0	5.0
	2.91	2.25	2.21	1.92	2.12	1.76	1.99	1.93	2.03	2.06	2.14	2.94	2.27
100	6.8	5.1	4.4	4.6	4.9	4.0	3.1	3.8	4.3	5.0	6.0	7.2	6.1
	3.31	2.57	2.52	2.19	2.41	2.01	2.27	2.20	2.32	2.34	2.44	3.35	2.53
200	8.4	6.2	5.4	5.6	6.0	4.9	3.8	4.6	5.3	6.1	7.4	8.8	7.4
	3.19	2.47	2.43	2.11	2.32	1.94	2.19	2.12	2.23	2.26	2.35	3.23	2.46
Freq.	20.7	3.0	1.5	1.4	1.2	1.0	1.2	2.4	6.3	13.5	21.2	26.6	100.0

z	Class 0		Class 1		Class 2		Class 3	
m	ms^{-1}	Wm^{-2}	ms^{-1}	Wm^{-2}	ms^{-1}	Wm^{-2}	ms^{-1}	Wm^{-2}
10	5.8	210	4.1	81	3.6	53	2.8	26
25	6.4	270	4.9	130	4.4	95	3.7	56
50	6.9	328	5.6	185	5.2	142	4.5	93
100	7.4	428	6.7	297	6.2	227	5.4	151
200	8.2	601	8.3	588	7.6	436	6.6	281

Kosseir — Red Sea

25° 49′ 56.2″ N 34° 25′ 33.0″ E	UTM 36 E 642 905 m N 2 857 885 m	25 m

The Kosseir mast is situated close to Ras Abu Aweid, about 34 km SSE of the city of Kosseir. The distance to the coastline of the Red Sea is about one km to the northeast. There are no sheltering obstacles close to the mast. The surface consists mostly of sand, gravel and stones with a roughness length of about 0.01 m or less. The station is situated on a coastal plateau which rises gently towards the SW, where it reaches 300 m a.s.l. at a distance of about 10 km. Further to the SW the mountains rise to more than 1000 m.

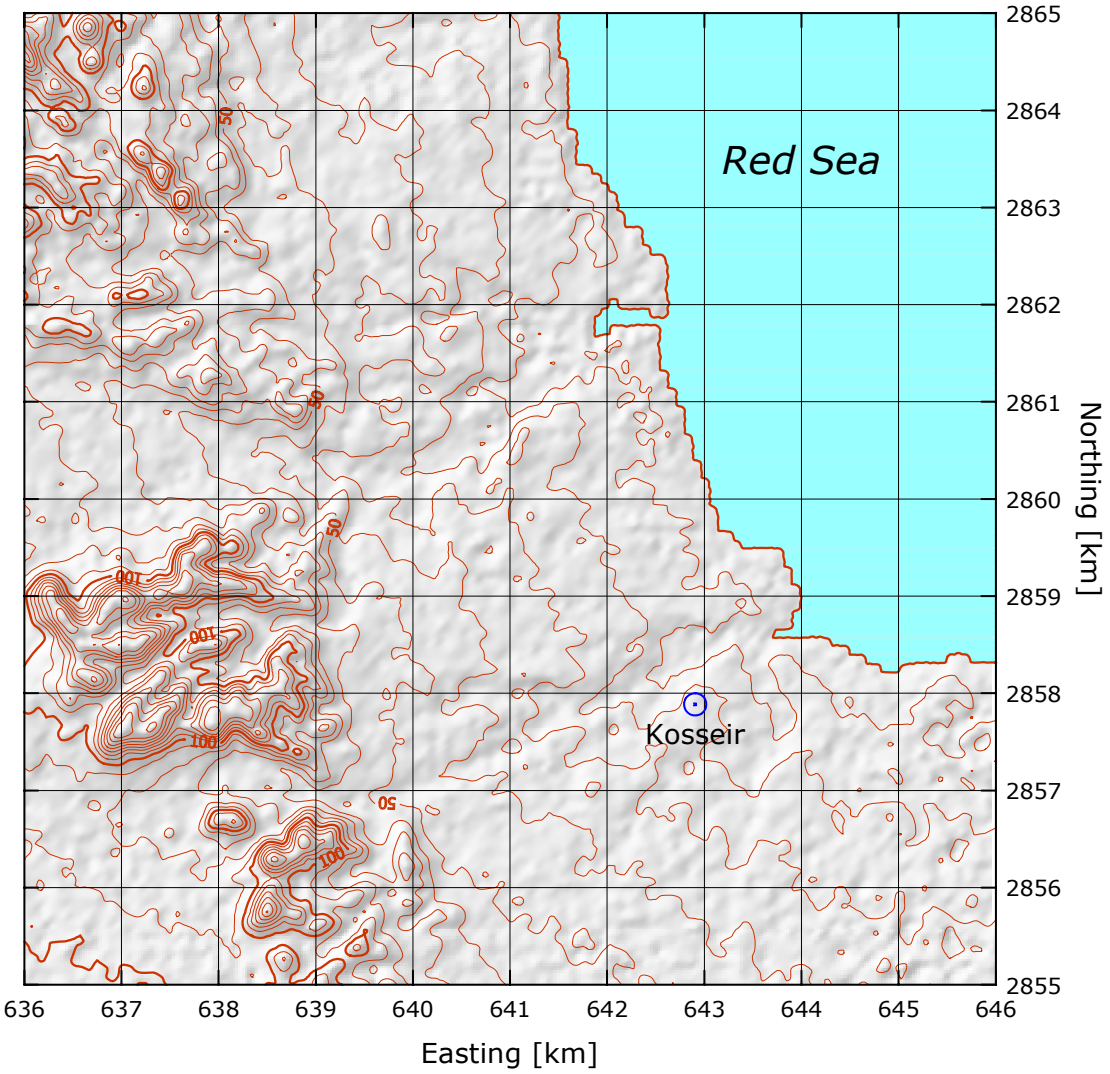

Sector	Input		Obstacles		Roughness		Orography		z_{0m}
0	0.0	0.0	0.0	0.0	−4.2	0.0	1.3	−0.8	0.0000
30	0.0	0.0	0.0	0.0	−3.2	0.0	0.6	0.2	0.0000
60	0.0	0.0	0.0	0.0	−2.6	0.0	1.9	1.0	0.0000
90	0.0	0.0	0.0	0.0	−3.5	0.0	3.8	0.8	0.0000
120	0.0	0.0	0.0	0.0	−3.4	0.0	4.3	−0.2	0.0010
150	0.0	0.0	0.0	0.0	1.9	0.0	2.9	−1.0	0.0070
180	0.0	0.0	0.0	0.0	1.7	0.0	1.1	−0.8	0.0070
210	0.0	0.0	0.0	0.0	0.0	0.0	0.4	0.2	0.0070
240	0.0	0.0	0.0	0.0	−0.6	0.0	1.7	1.0	0.0080
270	0.0	0.0	0.0	0.0	−1.1	0.0	3.6	0.8	0.0070
300	0.0	0.0	0.0	0.0	0.0	0.0	4.3	−0.2	0.0090
330	0.0	0.0	0.0	0.0	0.0	0.0	3.0	−1.0	0.0090

Height of anemometer: 24.5 m a.g.l. 2001-05

Sect	Freq	< 1	2	3	4	5	6	7	8	9	11	13	15	17	>17	*A*	*k*
0	22.1	9	22	33	55	91	127	167	174	160	138	23	1	0	0	7.7	3.72
30	3.3	34	101	143	233	266	158	54	8	2	0	0	0	0	0	4.4	3.25
60	1.9	80	173	183	193	224	119	26	2	0	0	0	0	0	0	3.8	2.58
90	1.6	48	155	147	132	161	126	90	57	36	39	9	1	0	0	5.0	1.95
120	1.6	47	142	130	151	125	99	56	39	51	100	44	16	0	0	5.3	1.48
150	1.2	59	257	227	176	117	72	32	16	12	23	9	0	0	0	3.5	1.45
180	0.6	48	285	343	191	84	23	19	0	0	6	0	0	0	0	3.0	1.85
210	0.8	49	191	346	244	113	23	18	4	4	2	2	1	2	2	3.3	1.63
240	4.1	26	120	258	309	206	52	16	6	3	2	1	0	1	0	3.8	2.58
270	21.7	11	57	116	183	202	157	130	82	31	25	5	1	0	0	5.4	2.36
300	21.0	9	31	69	116	180	220	193	105	48	26	4	0	0	0	6.1	3.29
330	20.3	8	24	43	62	78	92	96	116	133	225	101	20	2	0	8.7	3.29
Total	100.0	15	51	86	122	146	141	131	104	81	90	28	5	1	0	6.5	2.32

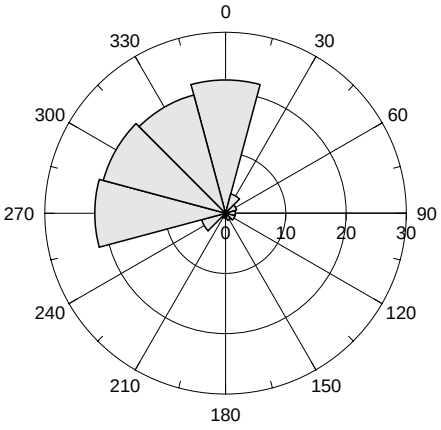

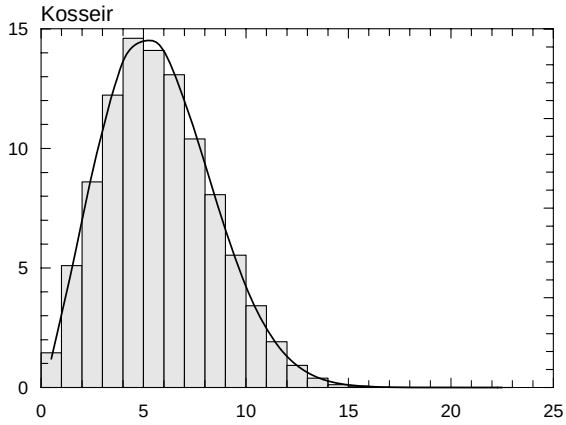

	Jan	Feb	Mar	Apr	May	Jun	Jul	Aug	Sep	Oct	Nov	Dec	Year
0	5.4	4.6	4.1	4.4	4.3	3.5	2.9	3.7	4.4	3.9	4.1	4.6	4.2
1	5.5	4.9	4.7	4.4	4.4	3.9	3.1	4.0	4.9	4.0	4.1	4.8	4.4
2	5.7	5.2	4.8	4.7	4.7	4.5	3.7	4.5	5.3	4.1	4.3	4.7	4.7
3	5.7	5.4	5.0	5.0	5.3	4.8	4.1	5.1	5.6	4.3	4.4	4.9	5.0
4	5.7	5.3	5.2	5.3	5.6	5.1	4.2	5.3	5.7	4.3	4.5	4.9	5.1
5	5.8	5.5	5.0	5.4	5.8	5.7	5.2	5.7	5.9	4.4	4.4	4.8	5.3
6	5.7	5.5	5.3	5.2	5.7	6.1	5.2	5.9	6.0	4.7	5.2	5.2	5.5
7	5.9	5.7	5.2	5.6	6.9	7.4	6.5	6.7	6.6	4.8	5.5	5.4	6.0
8	5.7	5.7	6.1	7.0	8.2	9.1	8.3	8.9	8.7	6.2	5.8	5.6	7.1
9	6.3	6.6	7.0	7.8	8.6	9.3	8.9	9.3	9.6	7.5	6.5	6.2	7.9
10	6.8	6.7	7.6	8.0	8.6	9.0	8.7	9.1	9.7	8.1	7.2	6.3	8.0
11	7.1	6.9	7.9	8.1	8.4	8.6	8.4	8.9	9.3	8.2	7.5	6.4	8.0
12	7.3	7.0	8.0	8.0	8.3	8.2	7.8	8.3	8.9	8.1	7.6	6.7	7.9
13	7.0	7.0	7.8	7.9	7.7	7.7	7.1	7.8	8.1	7.5	7.6	6.5	7.5
14	7.0	7.0	7.4	7.3	7.0	6.9	6.3	6.9	7.1	6.8	7.1	6.5	7.0
15	6.6	6.5	6.8	6.8	6.1	6.2	5.5	6.1	6.2	5.9	6.4	6.1	6.3
16	5.9	5.7	6.1	6.1	5.4	5.5	4.7	5.4	5.5	4.7	5.4	5.4	5.5
17	4.8	4.9	5.3	5.5	4.6	4.7	3.9	4.8	4.7	3.6	3.8	4.4	4.6
18	4.1	3.9	4.3	4.5	4.1	4.1	3.1	4.0	4.1	2.8	3.3	3.4	3.8
19	3.8	3.3	3.7	3.9	3.5	3.3	2.7	3.5	3.9	2.7	3.3	3.5	3.4
20	4.1	3.5	3.6	3.8	3.6	3.4	2.5	3.4	4.0	2.7	3.7	3.7	3.5
21	4.6	3.8	3.5	3.9	4.0	3.5	2.8	3.5	4.0	3.2	3.9	4.0	3.7
22	4.8	4.0	3.8	4.2	4.1	3.6	3.0	3.7	4.1	3.5	4.1	4.4	3.9
23	5.1	4.5	4.0	4.3	4.3	3.5	3.0	3.6	4.2	3.6	4.2	4.5	4.0
Mean	5.7	5.4	5.5	5.7	5.8	5.7	5.1	5.7	6.1	5.0	5.2	5.1	5.5

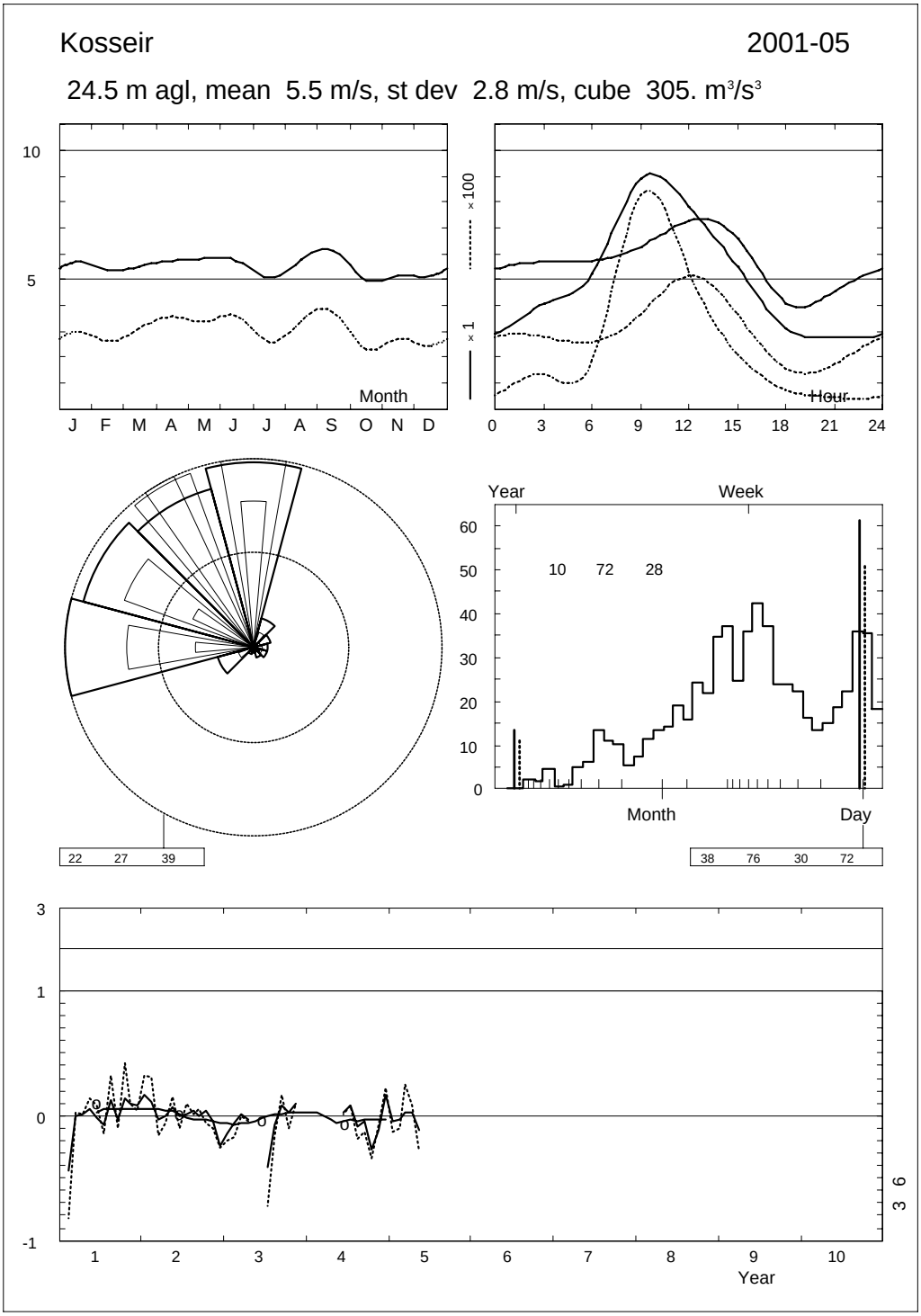

	Jan	Feb	Mar	Apr	May	Jun	Jul	Aug	Sep	Oct	Nov	Dec	Year
2001	—	3.0	5.5	5.8	6.1	5.7	4.7	6.5	5.9	5.7	5.7	5.5	5.7
2002	6.7	6.0	5.3	5.7	6.2	5.7	5.1	5.9	6.1	5.2	4.9	3.8	5.5
2003	4.9	5.0	5.6	5.5	—	—	2.9	5.3	6.6	5.1	5.7	—	5.4
2004	—	—	—	—	—	5.9	5.5	5.3	5.8	3.6	4.6	6.0	5.3
2005	5.5	5.2	5.7	5.9	5.1	—	—	—	—	—	—	—	5.4
Mean	5.7	5.4	5.5	5.7	5.8	5.7	5.1	5.7	6.1	5.0	5.2	5.1	5.5

Roughness Class 0 ($z_0 = 0.0002$ m)

z	0	30	60	90	120	150	180	210	240	270	300	330	Total
10	7.6	5.5	3.8	4.5	5.2	4.0	3.2	3.6	4.4	5.7	6.4	9.1	6.8
	3.34	2.05	2.40	1.87	1.56	1.52	1.74	1.83	2.31	2.54	3.40	3.23	2.43
25	8.3	6.0	4.1	5.0	5.7	4.3	3.5	4.0	4.8	6.3	7.0	9.9	7.5
	3.45	2.11	2.47	1.93	1.61	1.56	1.79	1.89	2.39	2.62	3.51	3.33	2.48
50	8.9	6.4	4.4	5.3	6.2	4.7	3.8	4.3	5.1	6.7	7.5	10.6	8.0
	3.54	2.17	2.54	1.98	1.65	1.60	1.84	1.94	2.45	2.69	3.60	3.42	2.53
100	9.7	7.0	4.8	5.8	6.7	5.1	4.1	4.6	5.6	7.3	8.1	11.5	8.7
	3.42	2.10	2.46	1.92	1.60	1.55	1.78	1.88	2.37	2.60	3.48	3.31	2.47
200	10.7	7.7	5.3	6.4	7.3	5.6	4.5	5.1	6.2	8.1	9.0	12.8	9.6
	3.24	1.99	2.33	1.81	1.51	1.47	1.69	1.78	2.25	2.46	3.30	3.13	2.37
Freq.	22.3	5.4	2.1	1.6	1.5	1.2	0.7	0.9	4.3	19.5	20.4	20.2	100.0

Roughness Class 1 ($z_0 = 0.0300$ m)

z	0	30	60	90	120	150	180	210	240	270	300	330	Total
10	5.2	3.0	2.6	3.3	3.5	2.6	2.3	2.8	3.4	4.1	4.7	6.3	4.7
	2.90	2.10	1.81	1.51	1.29	1.34	1.65	1.77	1.91	2.26	2.51	2.81	2.15
25	6.2	3.7	3.1	3.9	4.2	3.1	2.8	3.3	4.1	4.9	5.7	7.6	5.7
	3.13	2.26	1.96	1.63	1.38	1.44	1.78	1.91	2.06	2.44	2.71	3.04	2.29
50	7.1	4.2	3.6	4.6	4.9	3.7	3.2	3.8	4.7	5.7	6.5	8.7	6.6
	3.52	2.55	2.20	1.83	1.55	1.62	2.00	2.15	2.32	2.74	3.05	3.42	2.49
100	8.4	5.0	4.3	5.5	5.9	4.4	3.8	4.6	5.6	6.7	7.7	10.3	7.8
	3.75	2.71	2.34	1.94	1.65	1.72	2.13	2.29	2.47	2.92	3.24	3.64	2.60
200	10.4	6.2	5.3	6.8	7.3	5.4	4.8	5.7	6.9	8.4	9.6	12.8	9.7
	3.58	2.59	2.23	1.86	1.58	1.64	2.03	2.19	2.36	2.79	3.10	3.47	2.52
Freq.	20.0	3.3	1.8	1.5	1.5	1.1	0.7	1.4	6.9	21.1	20.2	20.5	100.0

Roughness Class 2 ($z_0 = 0.1000$ m)

z	0	30	60	90	120	150	180	210	240	270	300	330	Total
10	4.5	2.6	2.3	2.8	2.9	2.2	2.0	2.5	3.1	3.6	4.2	5.4	4.1
	2.85	2.04	1.75	1.44	1.24	1.32	1.55	1.85	1.92	2.34	2.30	2.77	2.13
25	5.5	3.2	2.9	3.5	3.6	2.8	2.5	3.1	3.8	4.5	5.2	6.7	5.1
	3.05	2.18	1.87	1.54	1.33	1.41	1.66	1.98	2.05	2.51	2.47	2.97	2.25
50	6.4	3.8	3.4	4.2	4.3	3.3	2.9	3.6	4.4	5.2	6.1	7.8	5.9
	3.38	2.42	2.07	1.70	1.46	1.56	1.83	2.19	2.27	2.78	2.73	3.28	2.43
100	7.6	4.5	4.0	5.0	5.2	3.9	3.5	4.3	5.3	6.2	7.2	9.2	7.1
	3.71	2.65	2.28	1.86	1.60	1.71	2.01	2.41	2.49	3.05	3.00	3.61	2.60
200	9.4	5.6	5.0	6.2	6.4	4.8	4.3	5.3	6.5	7.7	8.9	11.4	8.7
	3.55	2.54	2.18	1.78	1.54	1.63	1.93	2.30	2.38	2.92	2.87	3.45	2.52
Freq.	18.5	3.2	1.8	1.5	1.5	1.0	0.7	1.8	8.3	21.0	20.1	20.8	100.0

Roughness Class 3 ($z_0 = 0.4000$ m)

z	0	30	60	90	120	150	180	210	240	270	300	330	Total
10	3.5	2.0	1.9	2.3	2.2	1.8	1.7	2.0	2.5	2.9	3.5	4.2	3.2
	2.77	2.04	1.67	1.43	1.26	1.38	1.72	1.81	2.08	2.39	2.27	2.72	2.13
25	4.6	2.7	2.5	3.0	3.0	2.4	2.2	2.6	3.3	3.8	4.5	5.4	4.3
	2.94	2.17	1.77	1.51	1.33	1.47	1.82	1.91	2.20	2.53	2.40	2.88	2.24
50	5.5	3.2	3.0	3.7	3.7	2.9	2.7	3.1	4.0	4.6	5.5	6.6	5.1
	3.19	2.35	1.92	1.64	1.44	1.59	1.98	2.08	2.39	2.75	2.62	3.13	2.39
100	6.6	3.9	3.6	4.5	4.5	3.5	3.2	3.8	4.9	5.5	6.6	7.9	6.2
	3.63	2.68	2.19	1.87	1.63	1.81	2.26	2.37	2.72	3.13	2.98	3.57	2.64
200	8.1	4.8	4.4	5.5	5.4	4.3	4.0	4.6	5.9	6.7	8.0	9.6	7.6
	3.50	2.58	2.11	1.80	1.58	1.74	2.17	2.28	2.62	3.02	2.87	3.44	2.57
Freq.	16.3	3.0	1.7	1.5	1.4	1.0	0.8	2.2	10.3	20.8	19.9	21.1	100.0

z	Class 0		Class 1		Class 2		Class 3	
m	ms^{-1}	Wm^{-2}	ms^{-1}	Wm^{-2}	ms^{-1}	Wm^{-2}	ms^{-1}	Wm^{-2}
10	6.0	218	4.2	81	3.6	53	2.9	26
25	6.6	282	5.0	131	4.5	95	3.8	57
50	7.1	345	5.8	190	5.3	145	4.6	95
100	7.7	446	6.9	309	6.3	233	5.5	155
200	8.5	621	8.6	607	7.8	448	6.7	287

Farafra (62 423) — Western Desert

27° 03′ 29.3″ N 27° 59′ 20.7″ E	UTM 35 E 598 085 m N 2 993 260 m	74 m

The Farafra mast is situated about 1.5 km east of the town of Farafra. Flat desert terrain surrounds the station except for the town of Farafra and a few small hills about 1 km to the northwest of the station. The only other nearby disturbances are: a rather open fence no closer than 45 m from the mast, the main building (30 m × 30 m × 9 m) at 85 m distance to the east of the measuring mast, and a small building (10 m × 10 m × 4 m) for balloon measurements which is located about 80 m southeast of the mast. Further to the W (about 6 km) and to the NNW (about 7 km) one finds the agricultural areas of the oasis.

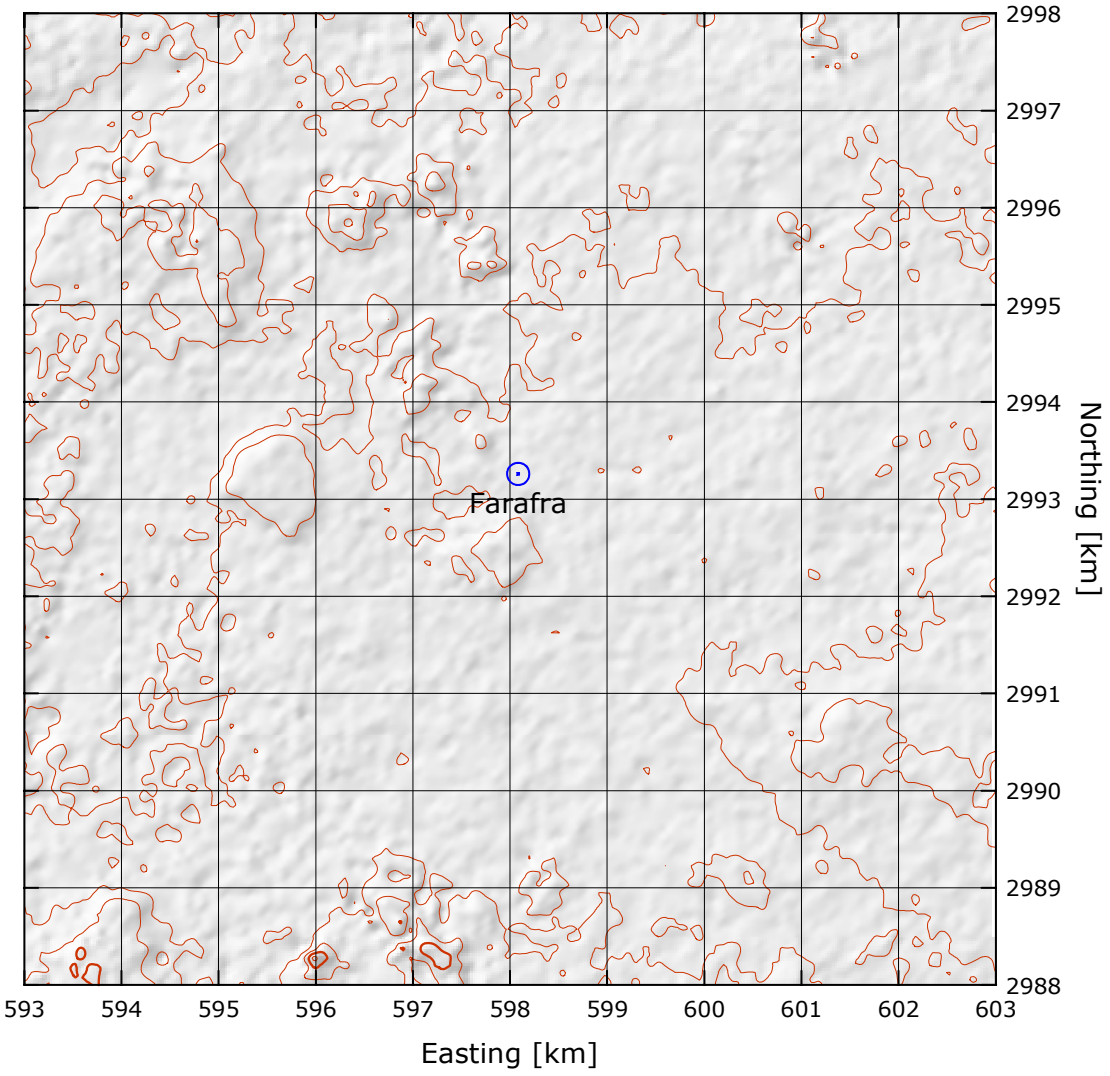

Sector	Input		Obstacles		Roughness		Orography		z_{0m}
0	0.0	0.0	0.0	0.0	0.0	0.0	0.2	0.3	0.0100
30	0.0	0.0	0.0	0.0	0.0	0.0	0.4	−0.1	0.0100
60	0.0	0.0	−6.6	0.0	0.0	0.0	−0.1	−0.4	0.0100
90	0.0	0.0	−17.9	0.0	0.0	0.0	−0.8	−0.3	0.0100
120	0.0	0.0	−2.9	0.0	0.0	0.0	−0.9	0.1	0.0100
150	0.0	0.0	−11.9	0.0	0.0	0.0	−0.4	0.4	0.0100
180	0.0	0.0	0.0	0.0	0.0	0.0	0.2	0.3	0.0100
210	0.0	0.0	0.0	0.0	0.0	0.0	0.4	−0.1	0.0100
240	0.0	0.0	0.0	0.0	0.5	0.0	−0.1	−0.4	0.0120
270	0.0	0.0	0.0	0.0	7.6	0.0	−0.6	−0.3	0.0390
300	0.0	0.0	0.0	0.0	1.0	0.0	−0.9	0.1	0.0130
330	0.0	0.0	0.0	0.0	5.2	0.0	−0.4	0.4	0.0270

Height of anemometer: 6.0 m a.g.l. 2003–05

Sect	Freq	< 1	2	3	4	5	6	7	8	9	11	13	15	17	>17	*A*	*k*
0	32.9	37	82	210	218	199	114	73	43	16	8	0	0	0	0	4.5	2.21
30	7.2	79	123	239	246	151	103	26	23	8	2	0	0	0	0	3.8	2.17
60	2.8	168	222	325	151	92	18	0	18	5	0	0	0	0	0	2.8	1.80
90	2.0	205	235	290	161	64	45	0	0	0	0	0	0	0	0	2.7	1.97
120	2.2	184	235	282	159	82	35	18	6	0	0	0	0	0	0	2.8	1.81
150	3.6	118	223	231	203	133	46	14	7	0	11	14	0	0	0	3.4	1.52
180	3.8	214	298	191	125	63	49	26	20	3	10	0	0	0	0	2.6	1.29
210	7.1	124	253	300	154	68	52	32	4	7	7	0	0	0	0	2.9	1.52
240	5.2	180	336	233	92	51	22	36	19	17	10	2	0	0	0	2.5	1.14
270	3.9	159	189	220	123	90	45	65	52	36	19	3	0	0	0	3.5	1.33
300	6.9	107	148	184	181	125	71	62	53	38	29	2	0	2	0	4.2	1.55
330	22.5	43	85	293	222	122	106	80	36	9	5	0	0	0	0	4.0	1.91
Total	100.0	84	143	243	195	136	86	57	32	14	8	1	0	0	0	3.9	1.79

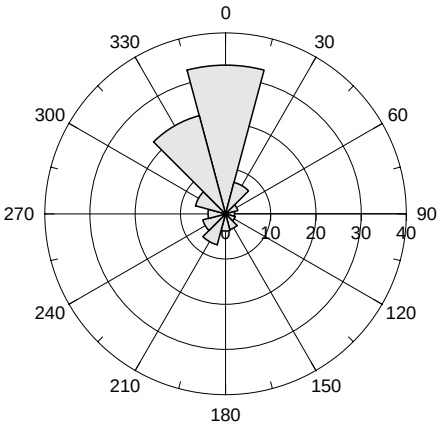

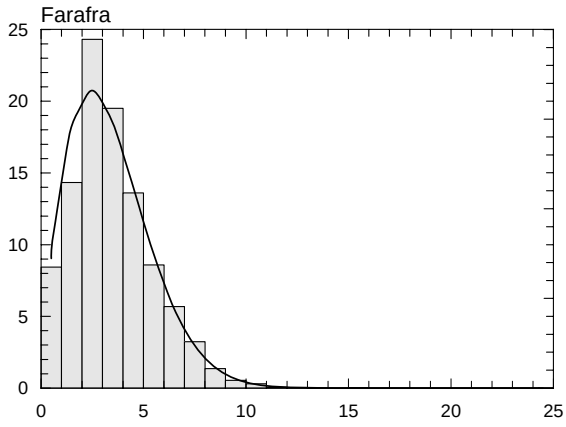

	Jan	Feb	Mar	Apr	May	Jun	Jul	Aug	Sep	Oct	Nov	Dec	Year
0	2.6	2.3	3.0	3.0	2.9	2.7	3.1	2.3	2.8	2.7	2.4	2.1	2.7
3	2.6	2.1	2.6	3.0	2.8	3.2	3.0	2.8	2.7	2.5	2.3	2.1	2.6
6	2.5	1.9	2.3	2.5	2.2	2.4	2.8	2.3	2.7	2.2	2.0	2.1	2.3
9	3.0	2.8	3.3	3.3	3.3	3.1	3.0	3.2	3.5	2.9	3.1	2.4	3.1
12	4.6	3.9	4.6	4.5	4.2	3.9	4.2	5.0	5.0	4.1	4.1	3.7	4.3
15	5.2	4.2	5.0	4.9	5.1	5.3	5.5	6.1	6.1	5.0	4.4	3.8	5.0
18	3.2	3.1	4.3	4.8	5.3	5.9	4.7	4.5	4.4	3.1	2.7	2.5	4.0
21	2.6	2.3	3.1	3.1	3.3	3.0	2.7	3.0	3.0	2.6	2.2	2.0	2.7
Mean	3.3	2.8	3.4	3.6	3.5	3.7	3.6	3.7	3.8	3.2	2.9	2.6	3.3

	Jan	Feb	Mar	Apr	May	Jun	Jul	Aug	Sep	Oct	Nov	Dec	Year
2003	—	—	—	—	—	—	3.7	3.9	4.0	3.1	3.3	2.6	3.4
2004	3.2	2.8	3.7	3.5	3.9	3.7	3.6	3.5	3.6	3.2	2.6	2.6	3.3
2005	3.3	2.8	3.4	3.7	3.3	—	—	—	—	—	—	—	3.3
Mean	3.3	2.8	3.4	3.6	3.5	3.7	3.6	3.7	3.8	3.2	2.9	2.6	3.3

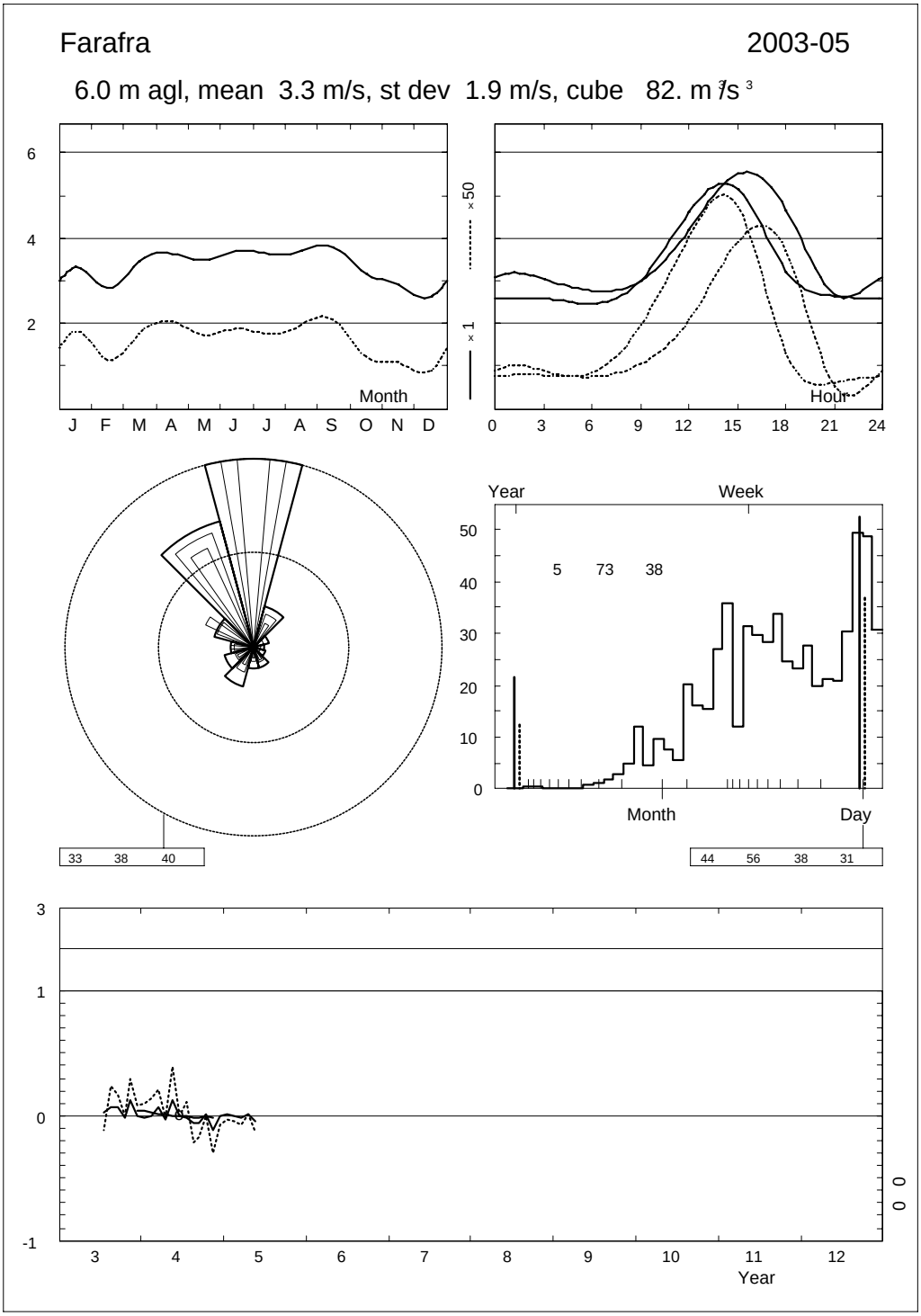
Farafra
2003-05
6.0 m agl, mean 3.3 m/s, st dev 1.9 m/s, cube 82. m/s³
6
4
2
Month
J F M A M J J A S O N D
× 50
× 1
Hour
0 3 6 9 12 15 18 21 24
33 38 40
Year
Week
50
40
30
20
10
0
5 73 38
Month
Day
44 56 38 31
3
1
0
-1
3 4 5 6 7 8 9 10 11 12
Year
0 0

Roughness Class 0 ($z_0 = 0.0002$ m)

z	0	30	60	90	120	150	180	210	240	270	300	330	Total
10	6.3	5.8	4.7	4.6	4.3	5.4	4.2	4.2	3.9	5.0	6.2	6.1	5.7
	2.64	2.58	2.24	2.28	2.19	1.83	1.61	1.83	1.47	1.51	1.87	2.30	2.11
25	6.9	6.4	5.2	5.0	4.7	5.9	4.6	4.7	4.3	5.5	6.7	6.7	6.2
	2.73	2.66	2.31	2.35	2.26	1.88	1.66	1.88	1.51	1.55	1.93	2.38	2.17
50	7.4	6.8	5.5	5.4	5.0	6.4	5.0	5.0	4.6	6.0	7.2	7.2	6.7
	2.80	2.73	2.37	2.42	2.31	1.94	1.71	1.94	1.55	1.59	1.98	2.44	2.22
100	8.1	7.4	6.0	5.8	5.4	6.9	5.4	5.4	5.0	6.4	7.8	7.8	7.2
	2.71	2.64	2.29	2.34	2.24	1.87	1.65	1.87	1.50	1.54	1.92	2.36	2.15
200	8.9	8.2	6.6	6.5	6.0	7.6	5.9	6.0	5.5	7.1	8.7	8.6	8.0
	2.56	2.50	2.17	2.21	2.12	1.78	1.56	1.78	1.42	1.46	1.82	2.24	2.05
Freq.	30.8	11.8	3.6	2.1	2.2	3.3	3.8	6.4	5.5	4.2	6.6	19.8	100.0

Roughness Class 1 ($z_0 = 0.0300$ m)

z	0	30	60	90	120	150	180	210	240	270	300	330	Total
10	4.4	3.8	3.0	3.2	3.0	3.8	2.7	2.9	2.6	3.8	4.2	4.2	3.9
	2.25	2.20	1.78	1.93	1.74	1.54	1.35	1.54	1.17	1.39	1.62	1.95	1.78
25	5.3	4.5	3.7	3.9	3.6	4.5	3.2	3.5	3.1	4.6	5.1	5.1	4.7
	2.43	2.38	1.92	2.08	1.88	1.66	1.45	1.66	1.26	1.49	1.75	2.11	1.92
50	6.1	5.2	4.2	4.5	4.1	5.3	3.8	4.1	3.7	5.4	5.9	5.9	5.5
	2.73	2.67	2.15	2.35	2.11	1.86	1.63	1.87	1.40	1.68	1.96	2.37	2.13
100	7.2	6.2	5.0	5.3	4.9	6.3	4.5	4.9	4.4	6.4	7.0	6.9	6.5
	2.91	2.85	2.29	2.50	2.24	1.98	1.73	1.99	1.49	1.78	2.09	2.52	2.26
200	9.0	7.7	6.2	6.6	6.1	7.8	5.6	6.1	5.5	8.0	8.7	8.6	8.0
	2.78	2.72	2.19	2.38	2.14	1.89	1.65	1.90	1.42	1.71	2.00	2.41	2.17
Freq.	31.2	6.8	2.7	2.0	2.2	3.7	4.0	6.9	5.1	4.1	7.9	23.3	100.0

Roughness Class 2 ($z_0 = 0.1000$ m)

z	0	30	60	90	120	150	180	210	240	270	300	330	Total
10	3.9	3.3	2.7	2.8	2.7	3.2	2.4	2.6	2.4	3.4	3.7	3.8	3.4
	2.27	2.15	1.85	1.92	1.70	1.51	1.39	1.57	1.20	1.41	1.71	2.05	1.82
25	4.8	4.0	3.4	3.5	3.4	3.9	3.0	3.2	3.0	4.2	4.6	4.6	4.3
	2.43	2.30	1.99	2.05	1.81	1.62	1.49	1.68	1.28	1.51	1.83	2.19	1.94
50	5.6	4.7	3.9	4.1	4.0	4.7	3.5	3.8	3.5	5.0	5.4	5.4	5.0
	2.69	2.54	2.20	2.27	2.01	1.79	1.64	1.86	1.41	1.66	2.03	2.43	2.13
100	6.6	5.6	4.7	4.8	4.7	5.6	4.2	4.6	4.3	5.9	6.5	6.4	6.0
	2.96	2.79	2.42	2.49	2.21	1.97	1.80	2.04	1.55	1.82	2.22	2.67	2.32
200	8.2	6.9	5.8	5.9	5.8	6.9	5.2	5.6	5.3	7.3	8.0	8.0	7.4
	2.83	2.67	2.31	2.39	2.11	1.88	1.73	1.95	1.49	1.74	2.13	2.55	2.23
Freq.	29.0	6.5	2.6	2.0	2.4	3.7	4.3	6.7	5.0	4.4	9.3	24.2	100.0

Roughness Class 3 ($z_0 = 0.4000$ m)

z	0	30	60	90	120	150	180	210	240	270	300	330	Total
10	3.0	2.6	2.1	2.2	2.2	2.4	1.9	2.0	1.9	2.7	2.9	3.0	2.7
	2.26	2.21	1.75	1.87	1.60	1.47	1.44	1.45	1.17	1.49	1.79	2.12	1.82
25	4.0	3.4	2.8	2.8	2.9	3.2	2.5	2.6	2.5	3.6	3.8	3.9	3.6
	2.40	2.34	1.85	1.97	1.69	1.56	1.52	1.54	1.24	1.58	1.90	2.25	1.92
50	4.8	4.1	3.4	3.4	3.5	3.8	3.1	3.2	3.1	4.4	4.7	4.7	4.3
	2.61	2.54	2.01	2.15	1.83	1.69	1.65	1.67	1.34	1.71	2.06	2.44	2.08
100	5.8	4.9	4.1	4.1	4.2	4.7	3.8	3.8	3.8	5.3	5.6	5.7	5.2
	2.97	2.89	2.29	2.44	2.09	1.92	1.87	1.90	1.52	1.95	2.35	2.78	2.34
200	7.1	6.0	4.9	5.1	5.2	5.7	4.6	4.7	4.6	6.5	6.9	6.9	6.4
	2.86	2.79	2.21	2.36	2.01	1.85	1.81	1.83	1.47	1.88	2.26	2.68	2.26
Freq.	25.9	5.9	2.5	2.1	2.5	3.8	4.7	6.5	4.8	4.8	11.2	25.4	100.0

z	Class 0		Class 1		Class 2		Class 3	
m	ms^{-1}	Wm^{-2}	ms^{-1}	Wm^{-2}	ms^{-1}	Wm^{-2}	ms^{-1}	Wm^{-2}
10	5.0	141	3.5	56	3.1	37	2.4	18
25	5.5	180	4.2	89	3.8	65	3.2	39
50	5.9	219	4.8	124	4.4	96	3.8	63
100	6.4	287	5.7	197	5.3	151	4.6	100
200	7.1	406	7.1	392	6.5	294	5.6	187

Kharga — Western Desert

25° 46′ 20.3″ N 30° 39′ 40.1″ E	UTM 36 E 265 442 m N 2 852 551 m	102 m

The Kharga mast is situated just west of the Asyut – Kharga road, in a wide (more than 10 km) valley about 35 km north of the oasis and town of Kharga. The site is close to the HT power line connecting Kharga to the national grid. The nearby surroundings consist of a flat and fairly homogeneous desert surface. The surface is a mixture of sand, gravel and stones with a roughness length of about 1 cm or less. There are no sheltering obstacles close to the mast.

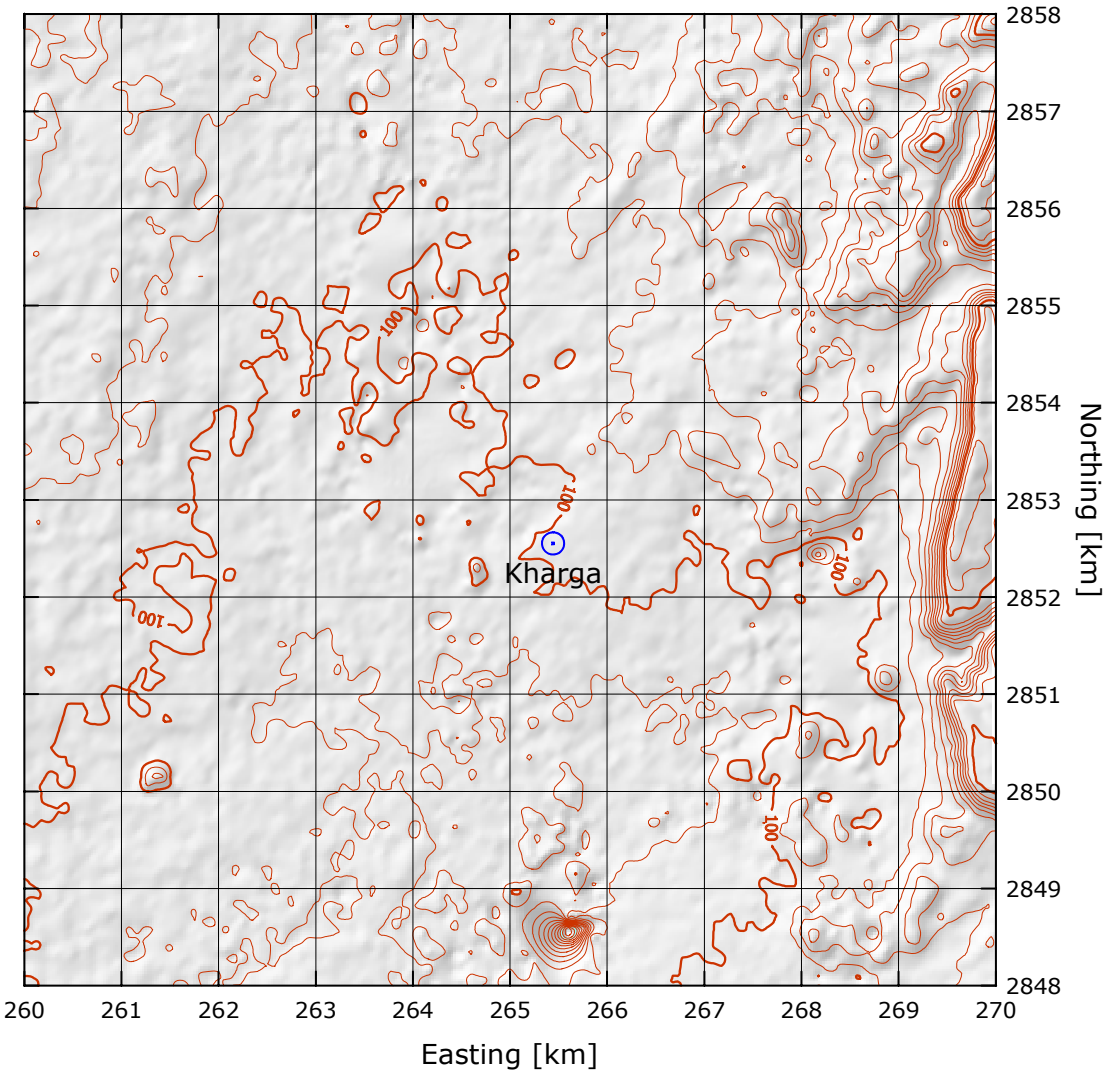

Sector	Input		Obstacles		Roughness		Orography		z_{0m}
0	0.0	0.0	0.0	0.0	0.0	0.0	2.1	−1.2	0.0050
30	0.0	0.0	0.0	0.0	0.0	0.0	−1.0	−1.9	0.0050
60	0.0	0.0	0.0	0.0	0.0	0.0	−3.7	−0.7	0.0050
90	0.0	0.0	0.0	0.0	0.0	0.0	−3.2	1.3	0.0050
120	0.0	0.0	0.0	0.0	0.0	0.0	0.0	1.9	0.0050
150	0.0	0.0	0.0	0.0	0.0	0.0	2.6	0.7	0.0050
180	0.0	0.0	0.0	0.0	0.0	0.0	2.1	−1.2	0.0050
210	0.0	0.0	0.0	0.0	0.0	0.0	−1.0	−1.9	0.0050
240	0.0	0.0	0.0	0.0	0.0	0.0	−3.7	−0.7	0.0050
270	0.0	0.0	0.0	0.0	0.0	0.0	−3.2	1.3	0.0050
300	0.0	0.0	0.0	0.0	0.0	0.0	0.0	1.9	0.0050
330	0.0	0.0	0.0	0.0	0.0	0.0	2.6	0.7	0.0050

Height of anemometer: 24.5 m a.g.l. 2004-05

Sect	Freq	<1	2	3	4	5	6	7	8	9	11	13	15	17	>17	*A*	*k*
0	45.2	3	14	34	74	129	151	151	133	96	139	61	15	1	0	7.6	2.57
30	1.8	64	192	138	160	188	82	44	33	47	43	9	0	0	0	4.5	1.72
60	0.7	152	226	129	124	128	84	41	27	36	53	0	0	0	0	3.9	1.46
90	0.6	138	314	155	119	144	51	21	8	12	23	15	0	0	0	3.2	1.26
120	0.8	59	330	250	166	91	47	25	10	10	11	0	0	0	0	3.0	1.48
150	1.2	62	248	267	149	87	83	36	6	12	27	22	0	0	0	3.4	1.24
180	2.4	38	202	298	193	131	66	30	33	6	3	0	0	0	0	3.5	1.77
210	0.8	91	428	269	131	56	13	10	2	0	0	0	0	0	0	2.4	1.74
240	0.6	97	436	243	101	50	39	22	13	0	0	0	0	0	0	2.4	1.40
270	0.7	69	263	186	118	125	87	53	57	36	5	0	0	0	0	3.8	1.61
300	3.3	23	84	118	132	175	174	114	88	39	43	8	1	0	0	5.6	2.36
330	42.0	2	11	31	70	115	132	146	145	124	160	51	10	2	1	7.9	2.95
Total	100.0	10	39	54	82	124	136	137	126	99	133	49	11	1	0	7.4	2.58

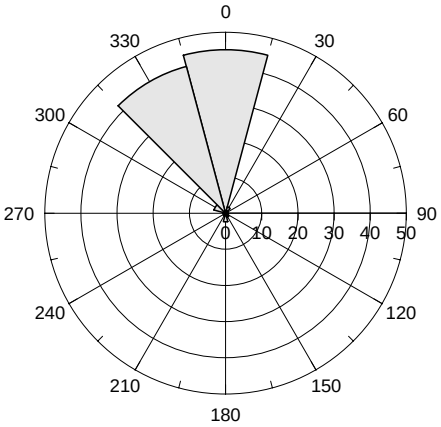

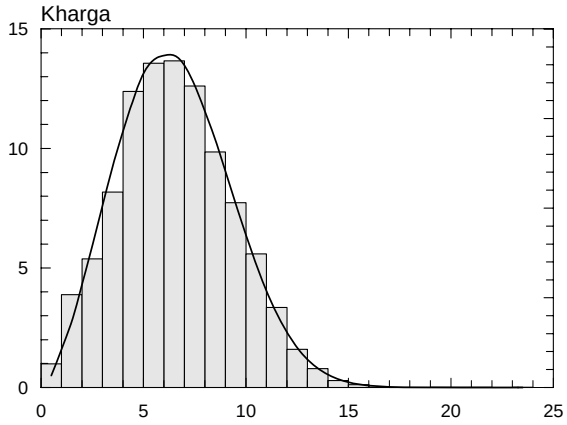

	Jan	Feb	Mar	Apr	May	Jun	Jul	Aug	Sep	Oct	Nov	Dec	Year
0	4.1	5.0	6.0	7.7	5.9	5.7	5.5	4.9	6.5	7.4	5.5	5.5	5.8
1	4.6	5.4	6.6	7.3	6.6	6.1	5.8	5.2	7.0	7.5	5.6	5.5	6.1
2	4.7	5.3	6.5	7.5	6.6	6.2	5.8	5.6	7.4	7.7	6.2	5.4	6.2
3	4.5	5.5	6.9	7.0	6.1	6.6	6.4	5.7	7.1	8.2	5.9	6.1	6.4
4	4.6	5.9	7.0	6.9	6.2	7.0	6.7	5.7	7.5	8.2	6.0	6.0	6.5
5	4.5	5.6	6.6	7.2	5.8	6.7	6.4	6.1	7.1	8.0	5.7	5.7	6.3
6	4.3	5.8	6.7	7.2	6.2	7.1	6.8	6.2	7.4	7.8	5.2	6.1	6.4
7	4.2	5.5	7.0	7.4	6.6	7.6	7.3	6.5	8.3	8.0	4.8	5.6	6.6
8	4.3	5.4	7.1	7.5	6.6	7.7	7.3	6.5	8.7	8.2	5.6	5.3	6.7
9	4.7	5.7	7.6	7.8	7.0	7.9	7.3	7.0	8.9	8.5	5.9	5.3	7.0
10	4.8	5.5	8.3	7.5	6.7	8.2	7.9	7.7	9.2	8.5	6.2	5.4	7.2
11	5.3	5.7	8.2	7.4	6.9	8.0	7.7	7.7	9.0	8.3	6.4	5.3	7.2
12	5.1	5.9	8.0	7.3	7.0	8.0	7.6	7.9	8.7	8.0	6.7	5.4	7.1
13	5.5	5.9	7.7	7.5	7.4	8.2	7.5	8.1	8.7	7.6	6.6	5.6	7.2
14	5.5	5.9	8.2	7.7	7.6	8.3	7.5	8.0	8.4	7.6	6.6	5.9	7.3
15	6.1	5.9	8.6	7.6	8.0	8.6	7.6	8.1	8.9	8.0	6.8	6.2	7.5
16	5.8	5.9	8.6	8.5	8.4	8.7	7.7	8.6	9.2	8.1	6.6	6.0	7.7
17	5.2	5.7	8.3	8.3	8.1	8.8	8.2	8.5	8.5	7.2	5.8	5.4	7.3
18	4.6	5.4	7.1	7.2	7.1	7.6	7.4	7.2	6.9	6.5	5.3	5.1	6.5
19	4.4	4.7	6.5	6.8	6.1	6.1	6.2	6.1	5.9	6.4	4.6	4.8	5.7
20	4.0	4.5	5.8	6.7	5.8	5.8	5.5	5.0	6.2	6.7	4.7	4.7	5.5
21	3.8	4.9	6.0	6.5	6.4	5.8	5.4	5.2	6.1	6.7	4.8	5.2	5.6
22	4.5	4.7	6.5	6.6	5.6	5.8	5.4	5.1	6.3	7.0	4.7	5.3	5.6
23	4.2	4.6	6.1	7.0	5.5	5.8	5.3	4.6	6.4	7.3	5.3	5.5	5.6
Mean	4.7	5.4	7.2	7.3	6.7	7.2	6.8	6.6	7.7	7.6	5.7	5.5	6.5

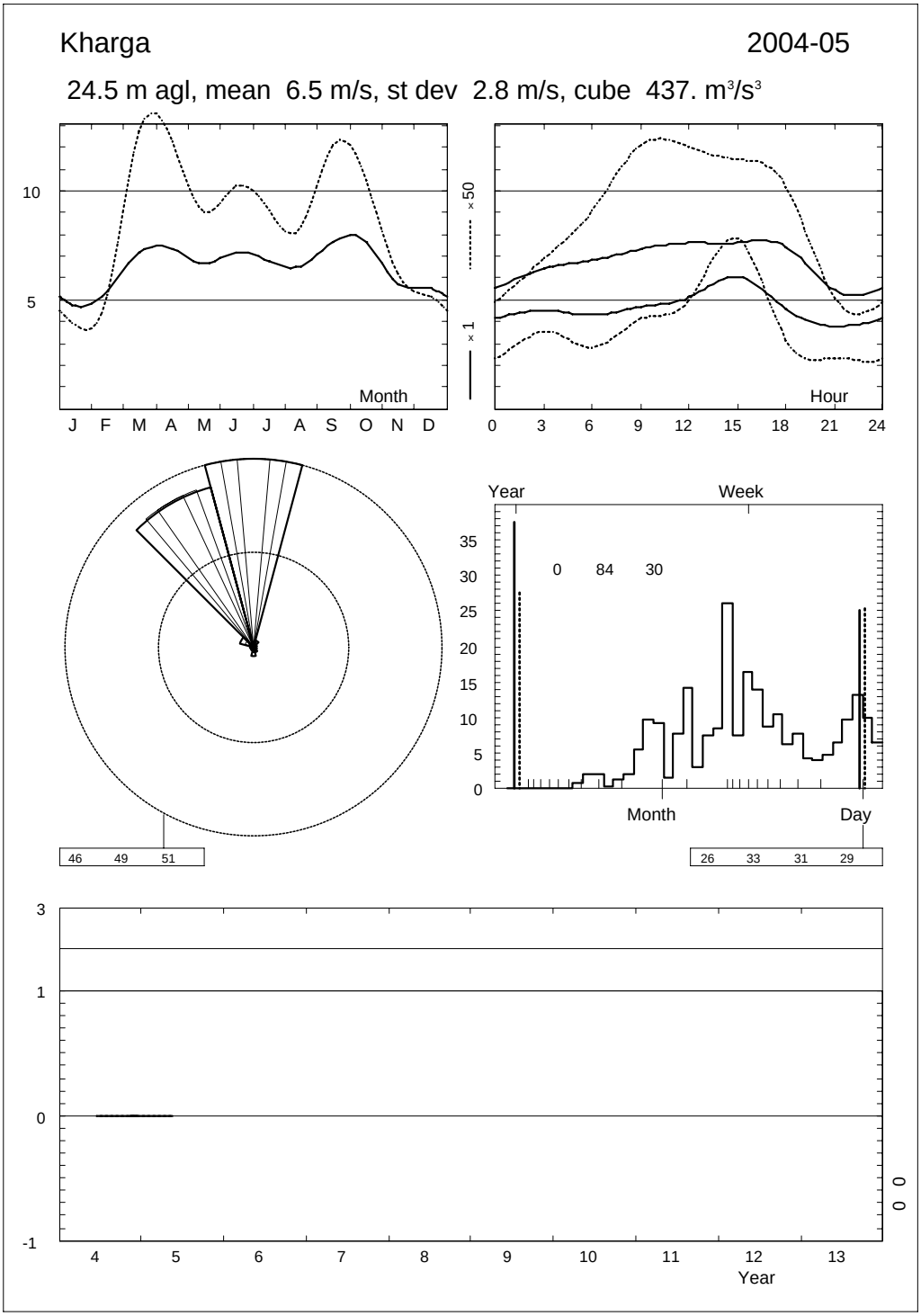

	Jan	Feb	Mar	Apr	May	Jun	Jul	Aug	Sep	Oct	Nov	Dec	Year
2004	—	—	—	—	—	7.2	6.8	6.6	7.7	7.6	5.7	5.5	6.7
2005	4.7	5.4	7.2	7.3	6.7	—	—	—	—	—	—	—	6.3
Mean	4.7	5.4	7.2	7.3	6.7	7.2	6.8	6.6	7.7	7.6	5.7	5.5	6.5

Roughness Class 0 ($z_0 = 0.0002$ m)

z	0	30	60	90	120	150	180	210	240	270	300	330	Total
10	8.1	7.6	5.6	3.7	3.3	3.6	3.7	3.0	2.8	4.5	6.9	8.2	7.7
	2.82	2.60	1.82	1.41	1.51	1.35	1.85	1.79	1.58	1.80	2.47	3.17	2.61
25	8.8	8.3	6.1	4.1	3.6	3.9	4.1	3.3	3.0	5.0	7.5	9.0	8.4
	2.91	2.68	1.87	1.46	1.55	1.40	1.91	1.85	1.63	1.86	2.55	3.27	2.68
50	9.4	8.9	6.6	4.4	3.9	4.2	4.3	3.6	3.3	5.3	8.1	9.7	9.1
	2.99	2.75	1.92	1.49	1.60	1.43	1.96	1.90	1.68	1.90	2.62	3.35	2.74
100	10.3	9.7	7.1	4.8	4.2	4.6	4.7	3.9	3.5	5.8	8.8	10.5	9.8
	2.89	2.67	1.86	1.45	1.54	1.38	1.90	1.84	1.62	1.85	2.54	3.24	2.66
200	11.4	10.7	7.8	5.2	4.6	5.0	5.2	4.3	3.9	6.4	9.7	11.6	10.9
	2.74	2.52	1.76	1.37	1.47	1.31	1.80	1.74	1.54	1.75	2.40	3.07	2.54
Freq.	42.7	9.0	1.2	0.7	0.8	1.1	2.1	1.1	0.6	0.9	4.4	35.4	100.0

Roughness Class 1 ($z_0 = 0.0300$ m)

z	0	30	60	90	120	150	180	210	240	270	300	330	Total
10	5.6	4.8	3.0	2.4	2.3	2.5	2.6	2.0	2.0	3.9	5.2	5.7	5.3
	2.35	1.87	1.35	1.20	1.33	1.24	1.68	1.51	1.23	1.75	2.32	2.62	2.24
25	6.7	5.8	3.7	3.0	2.8	3.1	3.1	2.4	2.4	4.6	6.2	6.8	6.4
	2.54	2.02	1.46	1.29	1.43	1.33	1.81	1.63	1.32	1.89	2.50	2.83	2.40
50	7.7	6.7	4.3	3.5	3.3	3.6	3.6	2.8	2.9	5.4	7.2	7.9	7.4
	2.86	2.27	1.63	1.44	1.60	1.49	2.04	1.83	1.48	2.12	2.81	3.18	2.66
100	9.1	7.9	5.1	4.2	4.0	4.3	4.3	3.3	3.4	6.4	8.5	9.3	8.7
	3.04	2.42	1.73	1.53	1.71	1.59	2.17	1.95	1.57	2.26	3.00	3.38	2.81
200	11.3	9.9	6.3	5.2	4.9	5.4	5.4	4.1	4.2	7.9	10.6	11.6	10.9
	2.90	2.31	1.66	1.46	1.63	1.52	2.07	1.87	1.50	2.16	2.86	3.23	2.70
Freq.	39.3	3.7	0.8	0.7	0.8	1.3	2.1	0.9	0.6	1.3	8.4	40.1	100.0

Roughness Class 2 ($z_0 = 0.1000$ m)

z	0	30	60	90	120	150	180	210	240	270	300	330	Total
10	4.9	4.2	2.6	2.1	2.0	2.2	2.2	1.8	1.8	3.6	4.7	5.0	4.6
	2.37	1.87	1.33	1.17	1.23	1.24	1.58	1.56	1.22	1.86	2.40	2.60	2.25
25	6.0	5.2	3.2	2.6	2.5	2.7	2.7	2.2	2.3	4.4	5.7	6.1	5.7
	2.54	1.99	1.42	1.25	1.31	1.33	1.69	1.67	1.30	1.99	2.58	2.78	2.39
50	7.0	6.1	3.8	3.1	2.9	3.2	3.2	2.6	2.8	5.2	6.7	7.1	6.7
	2.81	2.21	1.57	1.38	1.45	1.46	1.87	1.84	1.43	2.20	2.85	3.08	2.62
100	8.3	7.2	4.6	3.7	3.5	3.9	3.8	3.1	3.3	6.2	8.0	8.5	8.0
	3.08	2.43	1.72	1.51	1.58	1.60	2.05	2.03	1.57	2.42	3.13	3.38	2.83
200	10.3	8.9	5.7	4.6	4.3	4.8	4.7	3.8	4.1	7.7	9.9	10.5	9.9
	2.95	2.32	1.65	1.45	1.52	1.54	1.96	1.94	1.50	2.31	3.00	3.23	2.73
Freq.	36.0	3.4	0.8	0.7	0.8	1.4	2.0	0.8	0.7	1.6	11.3	40.4	100.0

Roughness Class 3 ($z_0 = 0.4000$ m)

z	0	30	60	90	120	150	180	210	240	270	300	330	Total
10	3.8	3.2	2.0	1.7	1.7	1.8	1.8	1.4	1.7	3.0	3.7	3.9	3.7
	2.38	1.83	1.31	1.27	1.34	1.38	1.69	1.59	1.36	1.92	2.48	2.55	2.26
25	5.0	4.3	2.7	2.3	2.2	2.4	2.3	1.9	2.2	3.9	4.9	5.1	4.8
	2.52	1.94	1.39	1.34	1.42	1.46	1.79	1.69	1.44	2.03	2.63	2.71	2.38
50	6.1	5.2	3.2	2.8	2.8	2.9	2.8	2.3	2.7	4.7	5.9	6.1	5.8
	2.74	2.10	1.51	1.45	1.54	1.59	1.95	1.83	1.56	2.21	2.86	2.94	2.56
100	7.3	6.2	4.0	3.4	3.3	3.5	3.4	2.8	3.3	5.7	7.1	7.3	7.0
	3.12	2.40	1.71	1.65	1.75	1.81	2.22	2.08	1.77	2.51	3.26	3.35	2.87
200	8.9	7.6	4.8	4.1	4.1	4.3	4.2	3.4	4.1	6.9	8.7	9.0	8.5
	3.01	2.31	1.65	1.59	1.69	1.74	2.14	2.01	1.71	2.42	3.14	3.22	2.78
Freq.	31.5	3.1	0.8	0.7	0.9	1.5	1.8	0.8	0.7	2.1	15.3	40.8	100.0

z	Class 0		Class 1		Class 2		Class 3	
m	ms^{-1}	Wm^{-2}	ms^{-1}	Wm^{-2}	ms^{-1}	Wm^{-2}	ms^{-1}	Wm^{-2}
10	6.9	302	4.7	112	4.1	73	3.2	36
25	7.5	389	5.7	181	5.1	131	4.3	77
50	8.1	475	6.6	261	6.0	199	5.1	129
100	8.7	616	7.8	422	7.1	320	6.2	211
200	9.7	860	9.7	833	8.8	615	7.6	392

Dakhla South — Western Desert

24° 37′ 19.0″ N 29° 06′ 22.8″ E	UTM 35 E 713 227 m N 2 724 721 m	365 m

The Dakhla South mast is situated in the Western Desert, just west of the Dakhla – Shark El-Ouinat road, approximately 106 km south of the town of Dakhla along this road. The station is equipped with a satellite transmitter, which makes it able to provide online data. There are no sheltering obstacles close to the mast. The surface consists mostly of very smooth uniform sand with a roughness length of less than 0.001 m.

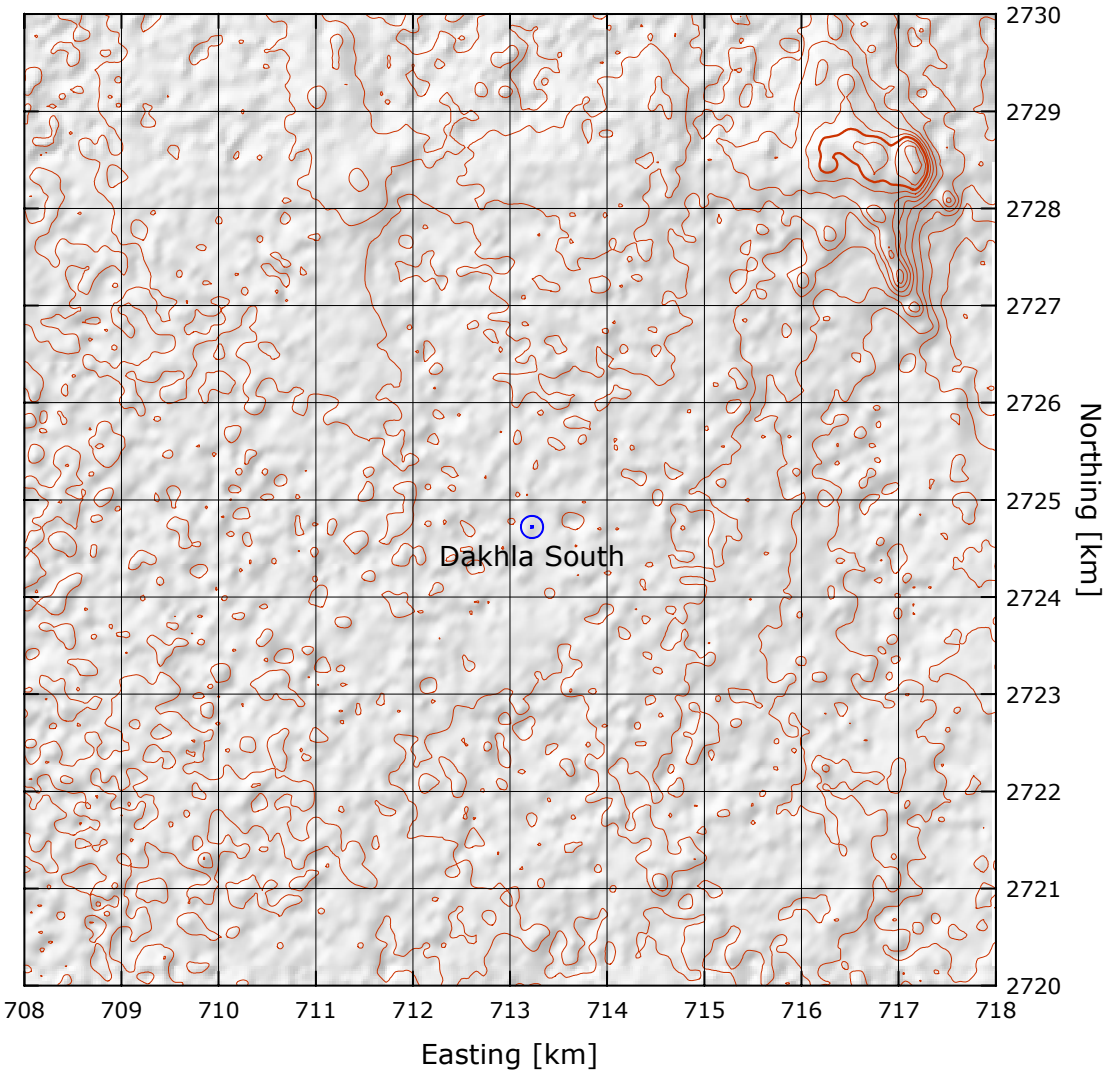

Sector	Input		Obstacles		Roughness		Orography		z_{0m}
0	0.0	0.0	0.0	0.0	0.0	0.0	−0.3	−0.6	0.0010
30	0.0	0.0	0.0	0.0	0.0	0.0	−0.6	0.3	0.0010
60	0.0	0.0	0.0	0.0	0.0	0.0	0.6	0.9	0.0010
90	0.0	0.0	0.0	0.0	0.0	0.0	2.0	0.6	0.0010
120	0.0	0.0	0.0	0.0	0.0	0.0	2.3	−0.3	0.0010
150	0.0	0.0	0.0	0.0	0.0	0.0	1.1	−0.9	0.0010
180	0.0	0.0	0.0	0.0	0.0	0.0	−0.3	−0.6	0.0010
210	0.0	0.0	0.0	0.0	0.0	0.0	−0.6	0.3	0.0010
240	0.0	0.0	0.0	0.0	0.0	0.0	0.6	0.9	0.0010
270	0.0	0.0	0.0	0.0	0.0	0.0	2.0	0.6	0.0010
300	0.0	0.0	0.0	0.0	0.0	0.0	2.3	−0.3	0.0010
330	0.0	0.0	0.0	0.0	0.0	0.0	1.1	−0.9	0.0010

Height of anemometer: 24.5 m a.g.l. 2004-05

Sect	Freq	< 1	2	3	4	5	6	7	8	9	11	13	15	17	>17	*A*	*k*
0	54.4	3	10	17	31	71	132	198	204	156	144	29	5	0	0	7.9	3.75
30	6.0	18	65	111	152	179	187	121	71	45	44	6	0	0	0	5.6	2.46
60	3.0	17	102	161	184	166	155	107	78	26	5	0	0	0	0	4.9	2.44
90	1.5	39	162	209	187	137	118	85	48	13	2	0	0	0	0	4.2	2.02
120	0.8	32	249	356	185	59	42	58	11	7	0	0	0	0	0	3.0	1.55
150	1.2	45	201	285	209	95	56	60	42	7	0	0	0	0	0	3.5	1.70
180	1.8	20	177	225	244	111	152	44	17	9	0	0	0	0	0	3.9	2.13
210	1.5	10	130	216	260	162	94	81	22	22	2	0	0	0	0	4.2	2.08
240	0.9	56	207	231	242	155	93	11	4	0	0	0	0	0	0	3.5	2.43
270	1.5	11	158	167	188	149	106	93	57	35	29	5	2	0	0	4.7	1.86
300	4.4	3	36	88	105	138	147	159	135	82	83	21	2	1	0	6.7	2.78
330	23.0	1	9	26	57	119	178	207	177	123	84	15	4	0	0	7.3	3.42
Total	100.0	6	33	52	70	99	144	179	167	121	105	20	4	0	0	7.3	3.34

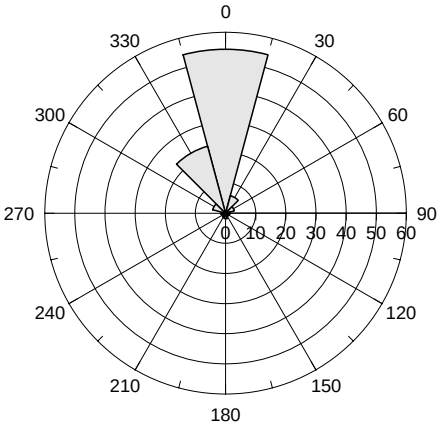

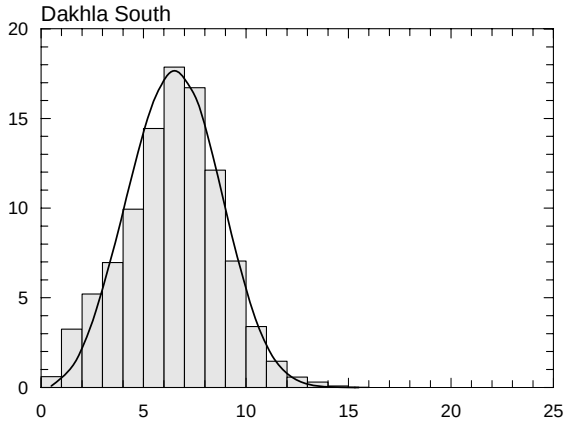

	Jan	Feb	Mar	Apr	May	Jun	Jul	Aug	Sep	Oct	Nov	Dec	Year
0	5.1	5.7	—	—	6.7	6.8	6.1	6.1	7.0	7.5	6.2	5.6	6.3
1	5.3	5.5	—	—	6.7	6.6	6.2	5.9	6.9	7.8	6.4	5.5	6.3
2	5.3	5.2	—	—	6.5	6.2	6.3	6.0	7.2	7.6	5.8	5.4	6.2
3	5.4	5.5	—	—	6.2	6.3	6.3	5.8	7.0	7.7	6.0	5.4	6.2
4	5.2	5.3	—	—	6.2	6.7	5.9	6.0	7.2	7.7	5.9	5.2	6.1
5	5.3	4.7	—	—	6.0	6.7	6.2	5.8	7.1	7.6	6.1	5.5	6.1
6	5.3	4.7	—	—	6.1	6.3	5.9	5.7	6.8	7.6	5.9	5.4	6.0
7	5.3	4.8	—	—	5.7	6.2	5.6	5.3	6.2	7.2	5.8	5.0	5.7
8	5.0	4.2	—	—	5.5	6.6	5.6	5.3	6.5	6.8	5.2	4.9	5.6
9	5.0	4.2	—	—	6.3	6.9	6.0	5.9	7.3	7.5	5.5	4.8	6.0
10	6.2	5.5	—	—	6.3	7.2	6.3	6.1	8.3	7.9	5.9	5.3	6.5
11	6.5	5.6	—	—	6.3	7.3	6.3	6.2	8.6	8.1	5.9	5.2	6.6
12	6.3	5.7	—	—	5.8	7.0	6.4	6.6	8.5	8.0	5.8	5.3	6.6
13	6.4	5.9	—	—	6.0	6.9	6.7	6.7	8.1	7.6	5.7	5.1	6.5
14	6.4	5.8	—	—	5.7	7.0	6.7	6.9	7.9	7.5	5.9	5.1	6.5
15	6.3	5.4	—	—	5.8	7.4	6.8	7.1	7.9	7.5	6.0	5.4	6.6
16	6.5	5.7	—	—	6.4	7.6	6.9	7.1	8.1	7.6	6.2	5.6	6.8
17	6.4	5.8	—	—	6.7	8.0	7.4	7.6	8.2	8.1	6.6	5.8	7.1
18	6.0	5.9	—	—	6.9	8.3	7.9	7.9	8.4	7.8	6.6	5.9	7.2
19	5.8	5.6	—	—	7.0	8.2	7.6	7.4	7.7	7.7	6.5	6.4	7.0
20	5.5	5.8	—	—	7.0	7.7	7.2	6.7	7.5	7.8	6.6	6.3	6.8
21	5.8	5.7	—	—	7.1	7.5	6.8	6.9	7.5	7.9	6.6	6.1	6.8
22	5.8	5.8	—	—	7.1	7.3	6.7	6.3	7.1	7.6	6.3	5.6	6.6
23	5.6	5.2	—	—	7.2	7.1	6.3	6.4	7.0	7.7	6.1	5.4	6.4
Mean	5.7	5.4	—	—	6.4	7.1	6.5	6.4	7.5	7.7	6.1	5.5	6.4

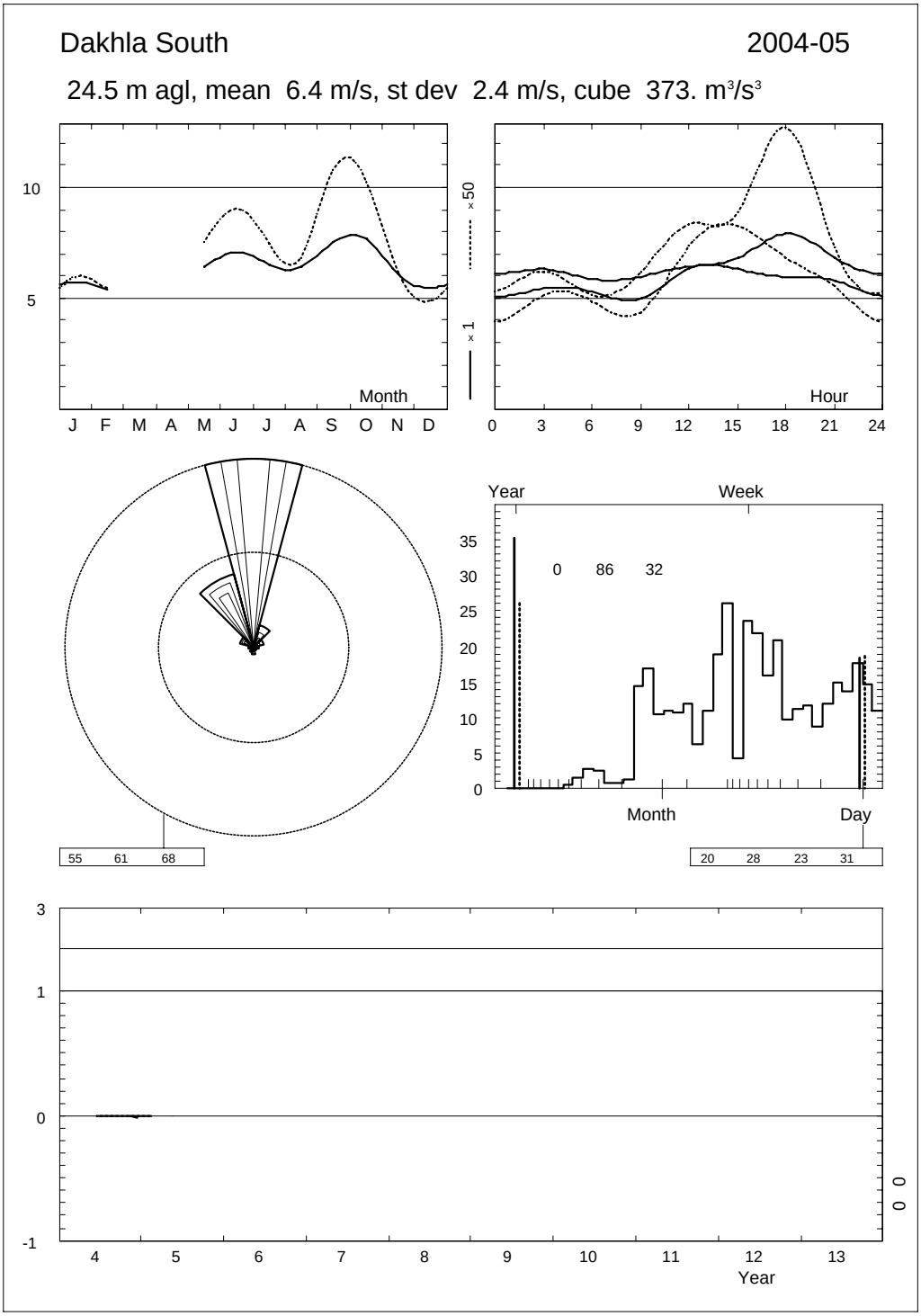

	Jan	Feb	Mar	Apr	May	Jun	Jul	Aug	Sep	Oct	Nov	Dec	Year
2004	—	—	—	—	—	7.1	6.5	6.4	7.5	7.7	6.1	5.5	6.7
2005	5.7	5.4	—	—	6.4	—	—	—	—	—	—	—	5.8
Mean	5.7	5.4	—	—	6.4	7.1	6.5	6.4	7.5	7.7	6.1	5.5	6.4

Roughness Class 0 ($z_0 = 0.0002$ m)

z	0	30	60	90	120	150	180	210	240	270	300	330	Total
10	7.7	6.2	4.8	4.1	3.0	3.4	3.8	4.1	3.5	4.5	6.4	7.0	7.0
	3.86	2.75	2.54	2.17	1.72	1.78	2.26	2.24	2.39	1.95	2.84	3.58	3.03
25	8.4	6.8	5.3	4.5	3.3	3.7	4.2	4.5	3.8	4.9	7.0	7.6	7.6
	3.98	2.84	2.62	2.24	1.77	1.83	2.33	2.31	2.47	2.01	2.93	3.70	3.11
50	9.1	7.3	5.7	4.8	3.6	4.0	4.5	4.8	4.1	5.3	7.5	8.2	8.2
	4.09	2.92	2.69	2.30	1.82	1.88	2.40	2.37	2.53	2.06	3.01	3.79	3.17
100	9.8	7.9	6.2	5.2	3.9	4.3	4.9	5.2	4.5	5.8	8.1	8.9	8.9
	3.96	2.82	2.60	2.23	1.76	1.82	2.32	2.29	2.45	2.00	2.91	3.67	3.09
200	10.9	8.8	6.8	5.8	4.3	4.8	5.4	5.8	5.0	6.4	9.0	9.9	9.9
	3.75	2.67	2.46	2.11	1.67	1.72	2.20	2.17	2.32	1.89	2.76	3.48	2.96
Freq.	53.4	8.2	3.1	1.5	0.8	1.2	1.8	1.5	1.0	1.4	4.1	21.8	100.0

Roughness Class 1 ($z_0 = 0.0300$ m)

z	0	30	60	90	120	150	180	210	240	270	300	330	Total
10	5.4	3.8	3.3	2.7	2.1	2.5	2.7	2.8	2.6	3.7	4.7	5.0	4.9
	3.27	2.13	2.08	1.75	1.47	1.66	1.91	1.88	1.76	1.89	2.75	3.01	2.66
25	6.4	4.6	3.9	3.3	2.6	3.0	3.3	3.4	3.2	4.4	5.6	6.0	5.8
	3.53	2.31	2.24	1.88	1.59	1.79	2.06	2.03	1.89	2.04	2.97	3.25	2.83
50	7.4	5.3	4.5	3.8	3.0	3.5	3.8	3.9	3.7	5.1	6.4	6.9	6.7
	3.97	2.59	2.52	2.12	1.79	2.01	2.32	2.28	2.13	2.30	3.34	3.65	3.11
100	8.7	6.3	5.4	4.5	3.6	4.1	4.5	4.6	4.3	6.1	7.6	8.2	7.9
	4.22	2.76	2.69	2.26	1.90	2.14	2.47	2.43	2.26	2.45	3.55	3.88	3.26
200	10.9	7.8	6.7	5.6	4.4	5.1	5.6	5.8	5.4	7.6	9.5	10.2	9.9
	4.03	2.64	2.56	2.15	1.81	2.04	2.36	2.32	2.16	2.34	3.39	3.71	3.15
Freq.	45.7	5.7	2.7	1.3	0.9	1.3	1.8	1.4	1.0	2.0	7.7	28.5	100.0

Roughness Class 2 ($z_0 = 0.1000$ m)

z	0	30	60	90	120	150	180	210	240	270	300	330	Total
10	4.7	3.3	2.8	2.3	1.9	2.2	2.4	2.5	2.4	3.3	4.1	4.4	4.2
	3.21	2.16	2.10	1.71	1.45	1.66	1.97	1.94	1.73	1.96	2.78	3.12	2.67
25	5.7	4.1	3.5	2.9	2.3	2.7	3.0	3.1	2.9	4.1	5.0	5.5	5.2
	3.44	2.31	2.25	1.83	1.55	1.78	2.11	2.07	1.85	2.10	2.97	3.34	2.83
50	6.7	4.8	4.1	3.4	2.8	3.2	3.5	3.6	3.4	4.8	5.9	6.4	6.1
	3.81	2.56	2.49	2.02	1.71	1.96	2.33	2.29	2.04	2.32	3.29	3.70	3.07
100	7.9	5.7	4.9	4.1	3.3	3.8	4.2	4.3	4.1	5.8	7.0	7.6	7.2
	4.18	2.81	2.73	2.22	1.88	2.15	2.56	2.52	2.25	2.55	3.61	4.06	3.30
200	9.8	7.1	6.1	5.0	4.1	4.7	5.2	5.3	5.1	7.1	8.6	9.4	8.9
	4.00	2.69	2.62	2.13	1.79	2.06	2.46	2.41	2.15	2.44	3.46	3.89	3.19
Freq.	41.8	5.4	2.6	1.3	0.9	1.4	1.7	1.3	1.1	2.2	9.2	31.1	100.0

Roughness Class 3 ($z_0 = 0.4000$ m)

z	0	30	60	90	120	150	180	210	240	270	300	330	Total
10	3.7	2.6	2.2	1.8	1.6	1.8	1.9	1.9	1.9	2.7	3.3	3.5	3.3
	3.19	2.14	2.03	1.70	1.67	1.76	1.86	1.79	1.63	2.07	2.86	3.17	2.68
25	4.8	3.4	2.9	2.4	2.1	2.3	2.5	2.5	2.5	3.6	4.3	4.6	4.4
	3.38	2.27	2.15	1.80	1.76	1.87	1.97	1.90	1.73	2.19	3.03	3.36	2.81
50	5.8	4.1	3.5	2.9	2.6	2.8	3.0	3.0	3.0	4.3	5.1	5.6	5.3
	3.67	2.46	2.34	1.96	1.92	2.03	2.14	2.06	1.88	2.38	3.30	3.65	3.01
100	6.9	5.0	4.2	3.5	3.1	3.4	3.6	3.6	3.7	5.2	6.2	6.7	6.3
	4.18	2.81	2.67	2.23	2.18	2.31	2.44	2.35	2.14	2.72	3.76	4.15	3.33
200	8.4	6.1	5.2	4.3	3.8	4.1	4.4	4.4	4.5	6.4	7.6	8.2	7.7
	4.03	2.71	2.57	2.15	2.10	2.22	2.35	2.26	2.06	2.62	3.62	4.00	3.24
Freq.	36.2	5.0	2.4	1.2	1.0	1.5	1.7	1.3	1.1	2.6	11.4	34.8	100.0

z	Class 0		Class 1		Class 2		Class 3	
m	ms^{-1}	Wm^{-2}	ms^{-1}	Wm^{-2}	ms^{-1}	Wm^{-2}	ms^{-1}	Wm^{-2}
10	6.3	209	4.3	75	3.8	49	3.0	24
25	6.8	270	5.2	123	4.6	89	3.9	53
50	7.4	332	6.0	181	5.4	138	4.7	89
100	8.0	429	7.1	296	6.5	225	5.7	150
200	8.8	592	8.8	579	8.0	428	6.9	276

Shark El-Ouinat (62 425) Western Desert

22° 34′ 41.2″ N 28° 43′ 13.6″ E	UTM 35 E 676 875 m N 2 497 839 m	271 m

The site is located at the Shark El-Ouinat airport, the location is near a tourist village. The site is 320 km from Dakhla City in south-west direction. It is located in a flat and open sandy area. The observations are taken 12 hours per day from 7 UT to 19 UT. Because of the bias introduced by the missing night-time observations, the regional wind climate is not calculated and shown here.

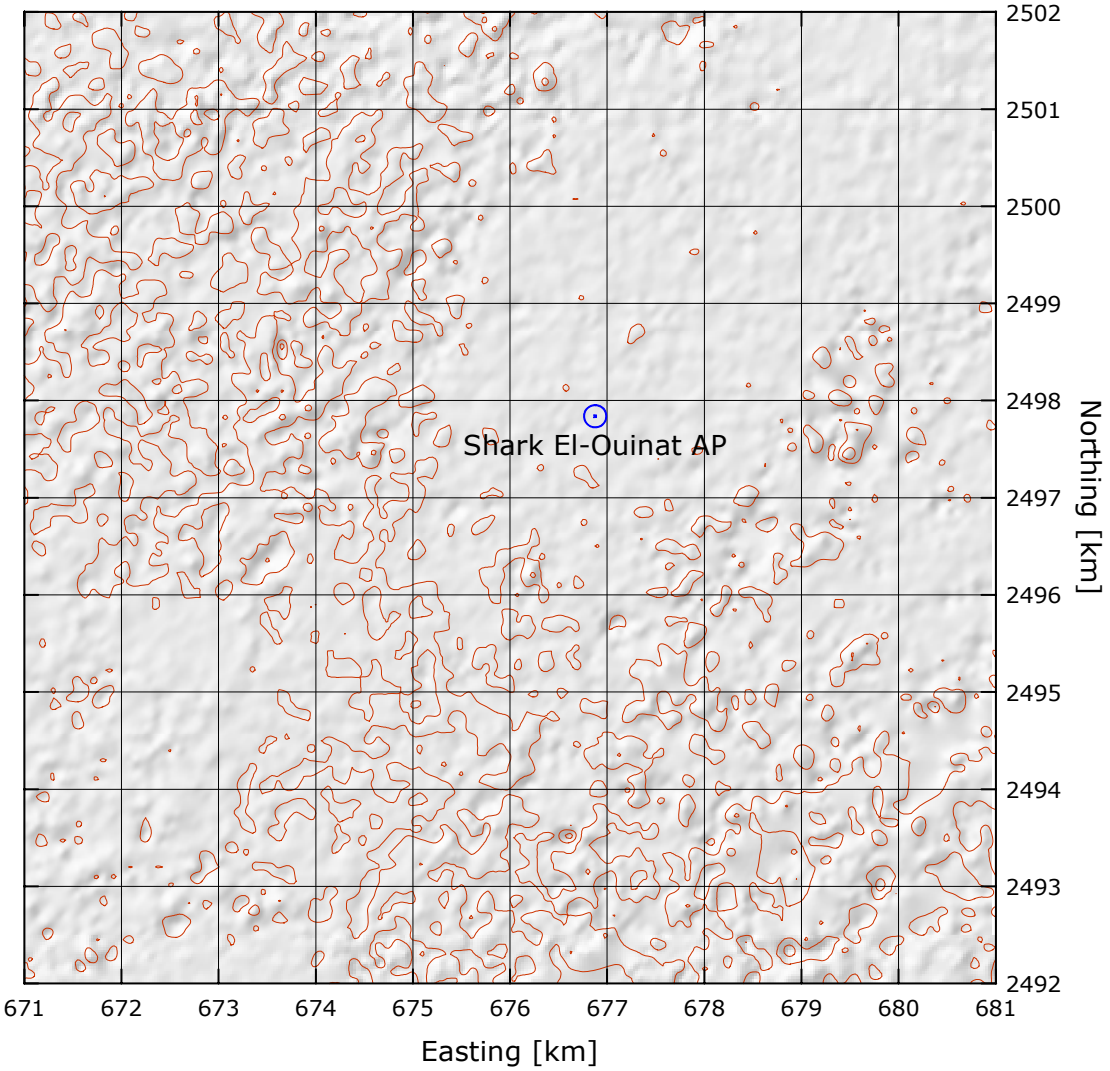

Sector	Input		Obstacles		Roughness		Orography		z_{0m}
0	0.0	0.0	0.0	0.0	−0.7	0.0	1.4	0.4	0.0000
30	0.0	0.0	0.0	0.0	0.0	0.0	1.7	−0.1	0.0010
60	0.0	0.0	0.0	0.0	0.0	0.0	1.1	−0.5	0.0010
90	0.0	0.0	0.0	0.0	0.0	0.0	0.2	−0.4	0.0010
120	0.0	0.0	0.0	0.0	0.0	0.0	−0.2	0.1	0.0010
150	0.0	0.0	0.0	0.0	0.0	0.0	0.4	0.5	0.0010
180	0.0	0.0	0.0	0.0	0.0	0.0	1.4	0.4	0.0010
210	0.0	0.0	0.0	0.0	0.0	0.0	1.7	−0.1	0.0010
240	0.0	0.0	0.0	0.0	0.0	0.0	1.1	−0.5	0.0010
270	0.0	0.0	0.0	0.0	−0.7	0.0	0.2	−0.4	0.0000
300	0.0	0.0	0.0	0.0	−2.6	0.0	−0.2	0.1	0.0010
330	0.0	0.0	0.0	0.0	0.3	0.0	0.5	0.5	0.0010

Height of anemometer: 10.0 m a.g.l. 2000–05

Sect	Freq	< 1	2	3	4	5	6	7	8	9	11	13	15	17	>17	*A*	*k*
0	47.1	6	11	41	61	83	151	160	158	124	141	44	12	7	1	7.9	2.84
30	25.0	4	7	45	45	77	144	161	180	129	155	36	13	3	0	8.0	3.17
60	5.3	6	9	56	93	130	174	174	170	96	78	11	0	4	0	7.0	3.09
90	3.0	4	3	99	73	132	192	152	165	113	53	13	0	0	0	6.7	3.06
120	0.7	48	45	272	91	30	151	242	60	30	30	0	0	0	0	5.5	2.58
150	0.8	2	26	131	131	79	131	210	184	53	0	53	0	0	0	6.7	2.93
180	1.4	23	36	114	128	185	143	114	71	71	57	14	43	0	0	6.1	1.82
210	0.8	28	51	128	102	102	102	51	179	51	102	77	26	0	0	7.2	2.06
240	0.6	3	32	97	161	161	129	97	129	64	129	0	0	0	0	6.3	2.40
270	1.6	32	44	275	175	100	137	50	100	75	12	0	0	0	0	4.9	1.91
300	2.4	17	8	139	197	172	172	139	57	33	57	0	8	0	0	5.6	2.29
330	11.4	9	14	89	117	122	159	146	134	91	87	21	10	2	0	6.9	2.55
Total	100.0	7	11	60	73	94	152	156	156	114	125	34	11	5	1	7.6	2.82

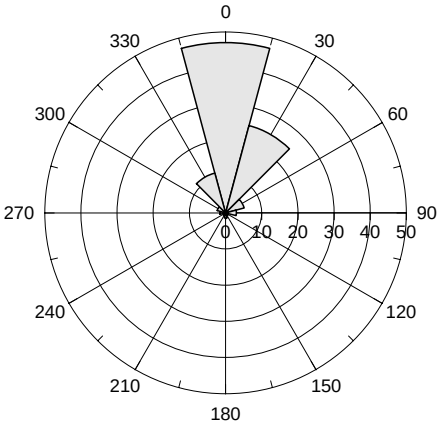

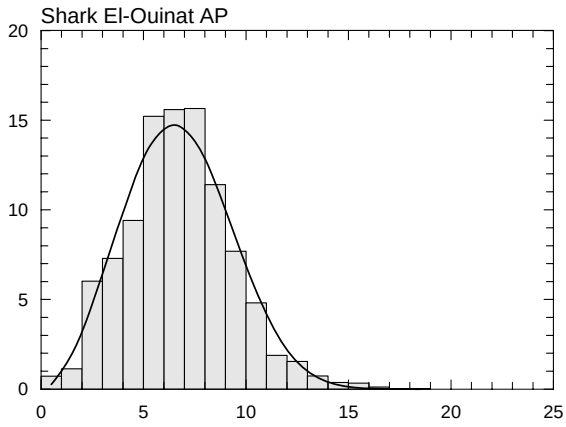

	Jan	Feb	Mar	Apr	May	Jun	Jul	Aug	Sep	Oct	Nov	Dec	Year
0	—	—	—	—	—	—	—	—	—	—	—	—	—
3	—	—	—	6.4	—	—	—	—	—	—	—	—	—
6	4.9	5.4	5.9	7.0	6.9	6.5	5.5	5.5	6.6	6.4	5.5	4.4	5.9
9	6.5	7.1	7.5	7.5	7.5	6.8	6.0	6.3	8.0	7.5	6.4	6.0	6.9
12	6.2	6.9	7.6	7.0	7.0	6.6	6.1	6.2	7.8	7.2	6.7	5.8	6.8
15	5.8	6.7	7.0	6.9	6.8	6.7	6.0	5.9	6.8	6.2	5.4	4.8	6.3
18	—	—	—	—	—	7.2	—	—	—	—	—	—	—
21	—	—	—	—	—	—	—	—	—	—	—	—	—
Mean	5.9	6.6	7.1	7.1	7.1	6.7	5.9	6.0	7.4	6.9	6.1	5.4	6.5

	Jan	Feb	Mar	Apr	May	Jun	Jul	Aug	Sep	Oct	Nov	Dec	Year
2001	6.2	6.8	7.6	8.0	7.1	7.3	6.8	6.2	8.5	7.9	6.9	6.4	7.1
2002	7.8	7.5	6.9	8.1	7.6	7.5	6.4	5.6	6.6	6.7	5.2	4.9	6.7
2003	4.7	5.8	5.8	5.7	6.8	5.3	4.9	6.3	6.9	6.1	6.6	5.0	5.8
2004	5.2	6.5	8.2	6.6	6.7	6.5	5.5	5.9	7.8	7.1	5.9	5.2	6.4
2005	5.7	5.2	6.3	5.6	5.1	—	—	—	—	—	—	—	—
Mean	5.9	6.6	7.1	7.1	7.1	6.7	5.9	6.0	7.4	6.9	6.1	5.4	6.5

22° 27′ 31.2″ N 28° 41′ 51.1″ E	UTM 35 E 674 669 m N 2 484 585 m		270 m

The Shark Ouinat mast is situated about 8 km south the airport of Shark El-Ouinat and about 16 km north of the village of Al-Ain. This station is also equipped with a satellite transmitter, which makes it able to provide online data. A few buildings and an oil station are located NE, E, SE of the mast. The surface consists mostly of sand and gravel with a roughness length less than about 0.01 m.

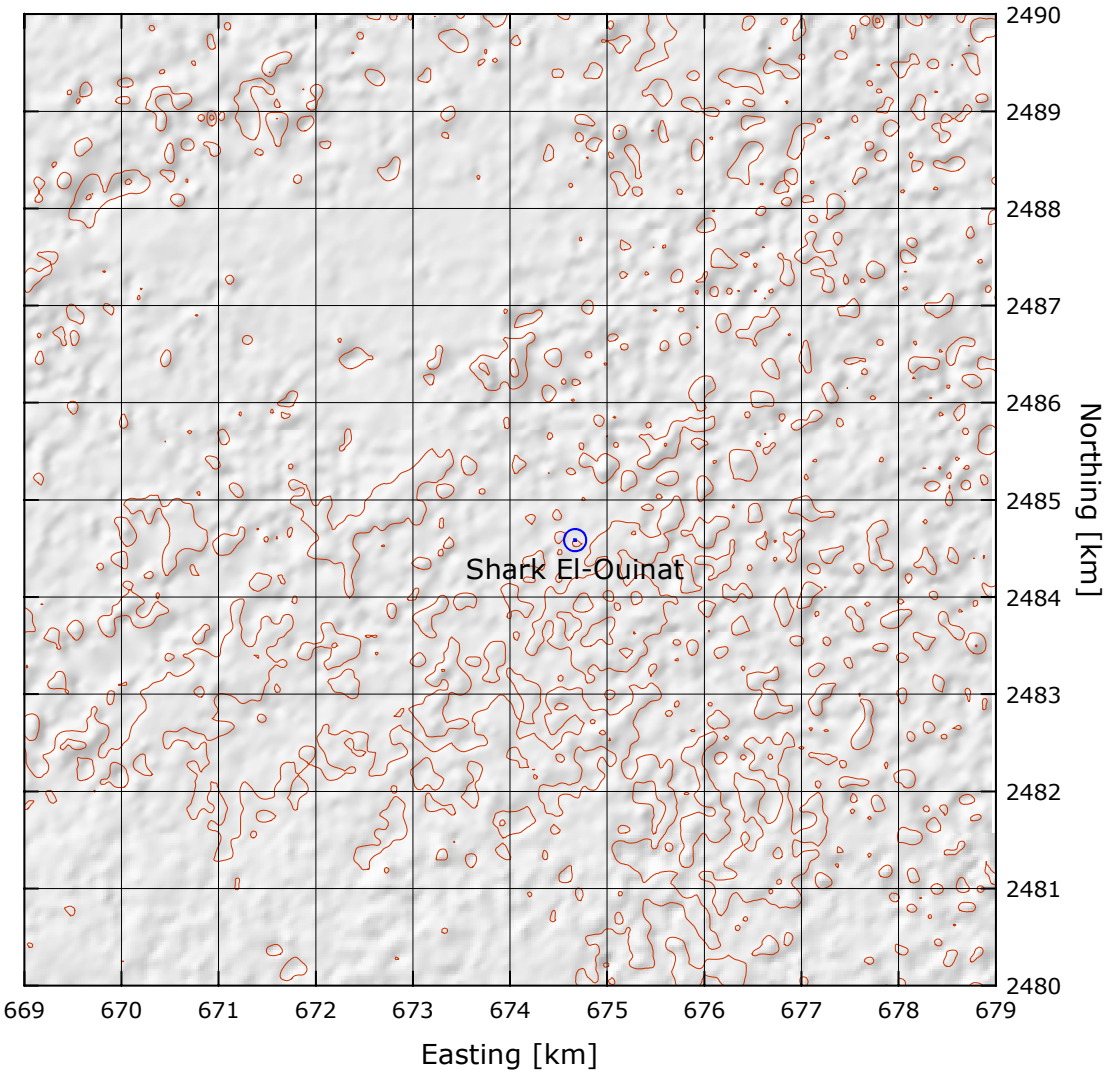

Sector	Input		Obstacles		Roughness		Orography		z_{0m}
0	0.0	0.0	0.0	0.0	−0.7	0.0	1.4	0.4	0.0000
30	0.0	0.0	0.0	0.0	0.0	0.0	1.7	−0.1	0.0010
60	0.0	0.0	0.0	0.0	0.0	0.0	1.1	−0.5	0.0010
90	0.0	0.0	0.0	0.0	0.0	0.0	0.2	−0.4	0.0010
120	0.0	0.0	0.0	0.0	0.0	0.0	−0.2	0.1	0.0010
150	0.0	0.0	0.0	0.0	0.0	0.0	0.4	0.5	0.0010
180	0.0	0.0	0.0	0.0	0.0	0.0	1.4	0.4	0.0010
210	0.0	0.0	0.0	0.0	0.0	0.0	1.7	−0.1	0.0010
240	0.0	0.0	0.0	0.0	0.0	0.0	1.1	−0.5	0.0010
270	0.0	0.0	0.0	0.0	−0.7	0.0	0.2	−0.4	0.0000
300	0.0	0.0	0.0	0.0	−2.6	0.0	−0.2	0.1	0.0010
330	0.0	0.0	0.0	0.0	0.3	0.0	0.5	0.5	0.0010

Height of anemometer: 24.5 m a.g.l. 2000–03

Sect	Freq	< 1	2	3	4	5	6	7	8	9	11	13	15	17	>17	*A*	*k*
0	45.8	1	7	14	38	75	162	237	190	125	114	30	6	0	0	7.6	3.15
30	11.7	3	21	49	93	120	166	205	151	82	85	20	5	0	0	7.0	3.06
60	3.2	8	65	99	137	140	161	162	119	64	34	12	0	0	0	6.1	2.76
90	1.2	20	119	213	188	171	114	76	68	28	3	0	0	0	0	4.5	2.11
120	0.9	4	84	130	190	178	161	80	90	59	19	6	0	0	0	5.3	2.27
150	1.0	7	78	133	194	155	72	81	109	91	48	13	15	4	0	5.6	1.77
180	0.8	5	90	138	121	124	100	119	68	107	58	58	12	0	0	6.4	1.97
210	0.5	0	146	243	190	146	77	69	8	40	20	32	28	0	0	4.3	1.26
240	0.5	22	103	255	192	114	103	111	59	18	22	0	0	0	0	4.4	1.81
270	1.0	11	109	180	231	203	128	88	33	6	11	0	0	0	0	4.5	2.32
300	2.9	8	57	155	187	169	178	109	100	22	12	3	0	0	0	5.3	2.57
330	30.4	2	8	28	51	93	210	271	183	84	55	12	2	0	0	7.1	3.72
Total	100.0	2	18	39	65	96	175	229	171	98	82	21	5	0	0	7.2	3.29

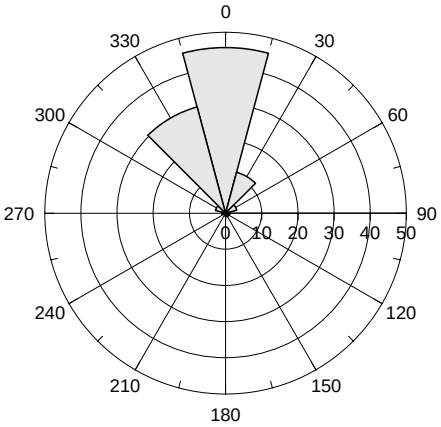

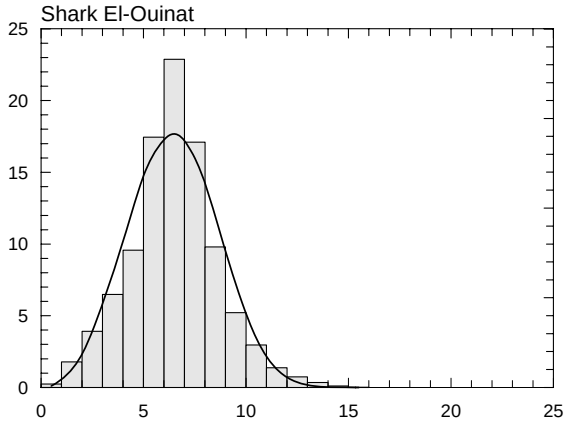

	Jan	Feb	Mar	Apr	May	Jun	Jul	Aug	Sep	Oct	Nov	Dec	Year
0	6.1	6.3	6.7	6.7	7.2	6.6	5.9	6.6	7.3	7.2	6.5	5.6	6.5
1	6.2	6.1	6.6	6.7	7.1	6.6	6.0	6.5	7.2	7.2	6.5	5.7	6.5
2	6.2	6.1	6.6	6.7	7.0	6.6	6.0	6.4	6.9	7.0	6.4	5.8	6.5
3	6.1	6.0	6.6	6.8	6.9	6.5	6.0	6.4	6.9	6.9	6.4	5.8	6.4
4	6.0	5.8	6.5	6.6	6.8	6.3	6.0	6.3	6.8	6.8	6.3	5.6	6.3
5	6.0	5.8	6.3	6.4	6.6	6.3	5.9	6.1	6.6	6.5	6.1	5.5	6.2
6	6.0	5.6	6.3	6.3	6.3	6.0	5.7	6.0	6.4	6.2	5.9	5.6	6.0
7	5.8	5.5	6.2	6.2	6.2	5.6	5.5	5.7	6.2	6.0	5.8	5.6	5.9
8	5.7	5.4	5.7	6.5	6.8	6.2	5.8	5.9	6.5	6.3	5.9	5.4	6.0
9	5.6	5.7	6.1	7.6	7.9	7.2	6.8	7.0	8.0	7.4	6.3	5.2	6.7
10	6.3	6.7	7.1	8.0	8.1	7.4	7.0	7.5	8.5	8.0	6.9	5.7	7.3
11	6.9	7.1	7.1	7.7	7.7	6.9	6.4	7.3	8.3	8.0	6.9	6.2	7.2
12	6.8	6.9	6.8	7.3	7.4	6.2	5.8	6.8	8.1	7.5	6.6	6.1	6.9
13	6.5	6.5	6.5	7.0	7.0	6.0	5.6	6.7	7.9	7.4	6.3	5.9	6.6
14	6.2	6.2	6.2	6.8	6.8	6.0	5.7	6.9	7.7	7.5	6.2	5.8	6.5
15	6.3	6.3	6.1	6.7	6.6	6.3	5.8	7.2	7.7	7.5	6.2	5.8	6.5
16	6.4	6.3	6.1	6.8	6.8	6.4	6.1	7.3	7.8	7.7	6.3	5.9	6.7
17	6.4	6.2	6.1	7.0	6.9	6.7	6.2	7.5	8.0	7.8	6.3	5.8	6.7
18	5.9	6.1	5.9	7.0	7.0	6.7	6.3	7.6	7.8	7.2	5.8	5.4	6.6
19	5.5	5.7	5.5	6.5	6.5	6.2	5.9	6.8	7.0	6.6	5.8	5.3	6.1
20	5.6	5.7	5.5	6.2	6.3	5.8	5.5	6.1	6.7	6.7	6.0	5.4	6.0
21	5.9	5.9	5.9	6.3	6.6	6.0	5.6	6.2	7.0	6.8	6.2	5.5	6.2
22	6.0	6.0	6.3	6.6	6.9	6.3	5.6	6.5	7.3	7.1	6.3	5.4	6.4
23	6.0	6.1	6.6	6.7	7.1	6.5	5.9	6.5	7.3	7.2	6.5	5.5	6.5
Mean	6.1	6.1	6.3	6.8	6.9	6.4	6.0	6.7	7.3	7.1	6.3	5.6	6.5

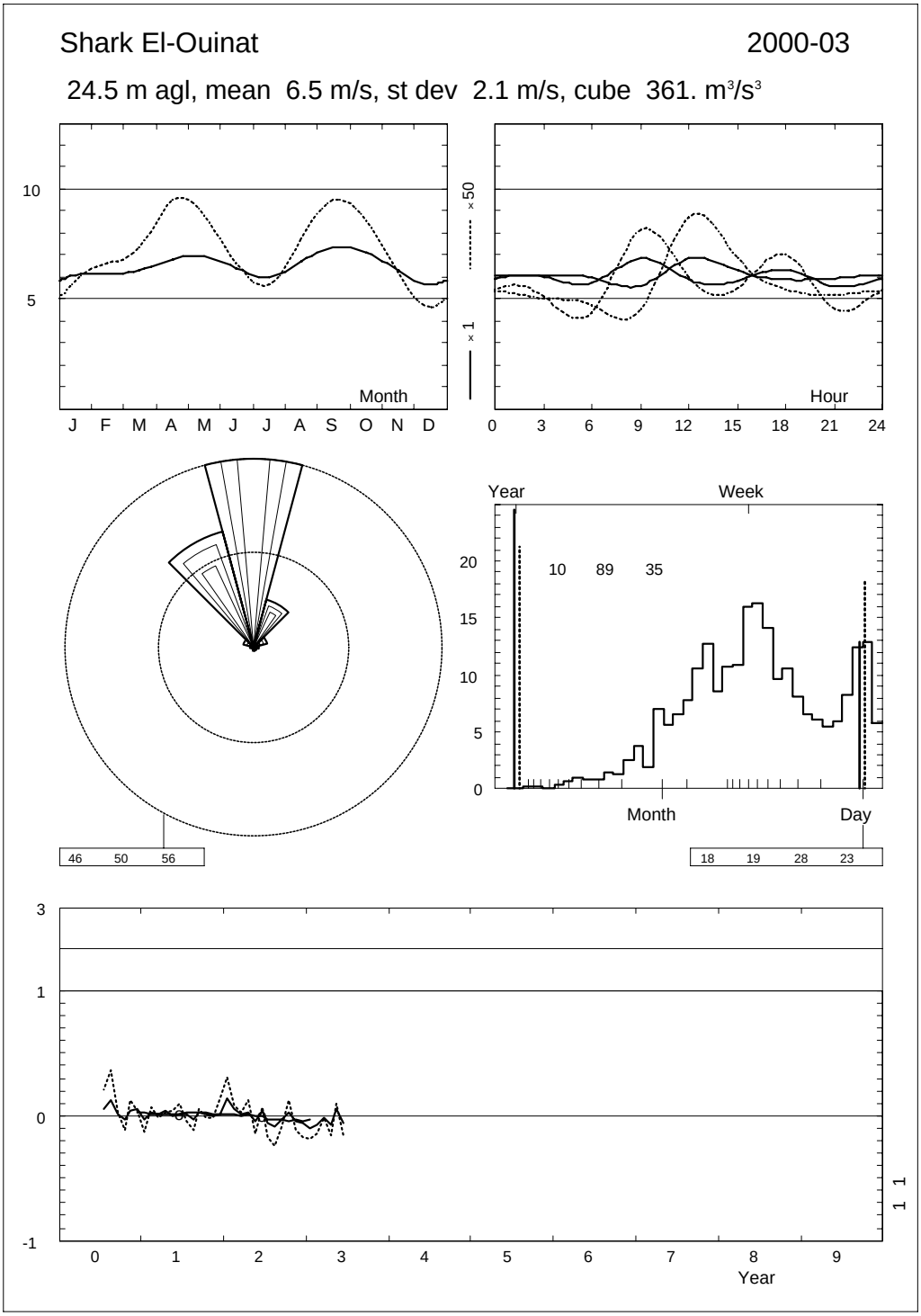

	Jan	Feb	Mar	Apr	May	Jun	Jul	Aug	Sep	Oct	Nov	Dec	Year
2000	—	—	—	—	—	—	6.3	7.5	7.4	6.9	6.5	5.9	6.7
2001	5.9	6.2	6.4	7.1	6.9	6.5	6.0	6.4	7.6	7.1	6.3	5.7	6.5
2002	6.9	6.4	6.3	7.0	6.6	6.6	5.6	6.1	7.1	7.3	6.0	5.3	6.4
2003	5.5	5.7	6.2	6.3	7.3	6.0	—	—	—	—	—	—	6.2
Mean	6.1	6.1	6.3	6.8	6.9	6.4	6.0	6.7	7.3	7.1	6.3	5.6	6.5

Roughness Class 0 ($z_0 = 0.0002$ m)

z	0	30	60	90	120	150	180	210	240	270	300	330	Total
10	7.2	6.8	5.9	4.5	5.1	5.5	6.1	4.3	4.3	4.2	5.4	7.0	6.9
	3.29	3.18	2.90	2.22	2.37	1.85	2.04	1.37	1.91	2.22	2.63	3.81	3.15
25	7.9	7.4	6.5	5.0	5.6	6.0	6.7	4.7	4.7	4.6	5.9	7.7	7.5
	3.39	3.28	3.00	2.29	2.44	1.91	2.11	1.40	1.97	2.29	2.71	3.94	3.24
50	8.5	7.9	7.0	5.3	6.0	6.4	7.1	5.1	5.1	4.9	6.3	8.2	8.1
	3.48	3.37	3.08	2.35	2.50	1.96	2.16	1.44	2.02	2.36	2.78	4.04	3.32
100	9.2	8.6	7.6	5.8	6.5	7.0	7.7	5.5	5.5	5.4	6.9	8.9	8.8
	3.37	3.26	2.98	2.28	2.42	1.90	2.10	1.40	1.96	2.28	2.70	3.91	3.22
200	10.2	9.5	8.4	6.4	7.2	7.7	8.6	6.0	6.0	5.9	7.6	9.9	9.7
	3.19	3.08	2.82	2.15	2.29	1.80	1.98	1.33	1.85	2.16	2.55	3.71	3.06
Freq.	44.8	12.7	3.6	1.3	0.9	1.0	0.8	0.5	0.5	1.0	3.1	29.8	100.0

Roughness Class 1 ($z_0 = 0.0300$ m)

z	0	30	60	90	120	150	180	210	240	270	300	330	Total
10	5.0	4.6	4.0	3.2	3.6	3.9	4.0	2.8	3.0	3.2	4.5	4.9	4.8
	2.67	2.62	2.31	1.86	1.85	1.63	1.64	1.19	1.74	1.85	2.88	2.93	2.62
25	5.9	5.5	4.8	3.8	4.3	4.7	4.9	3.5	3.6	3.8	5.4	5.8	5.7
	2.88	2.82	2.50	2.01	1.99	1.76	1.77	1.28	1.87	1.99	3.11	3.17	2.81
50	6.8	6.3	5.5	4.4	5.0	5.4	5.7	4.1	4.1	4.5	6.2	6.7	6.5
	3.24	3.17	2.81	2.25	2.24	1.98	1.99	1.43	2.10	2.24	3.50	3.56	3.15
100	8.1	7.5	6.5	5.2	6.0	6.5	6.7	4.9	4.9	5.3	7.4	8.0	7.8
	3.45	3.38	2.99	2.40	2.39	2.11	2.12	1.52	2.24	2.39	3.72	3.79	3.34
200	10.1	9.4	8.1	6.5	7.4	8.0	8.4	6.1	6.1	6.6	9.2	9.9	9.7
	3.29	3.23	2.86	2.29	2.28	2.01	2.02	1.46	2.14	2.28	3.56	3.62	3.20
Freq.	38.8	9.9	2.9	1.2	0.9	1.0	0.7	0.5	0.6	1.4	8.5	33.6	100.0

Roughness Class 2 ($z_0 = 0.1000$ m)

z	0	30	60	90	120	150	180	210	240	270	300	330	Total
10	4.4	4.0	3.4	2.8	3.1	3.4	3.4	2.6	2.6	2.9	4.0	4.3	4.2
	2.80	2.54	2.29	1.90	1.76	1.61	1.57	1.26	1.83	1.88	2.89	3.08	2.71
25	5.4	4.9	4.2	3.5	3.9	4.2	4.3	3.2	3.2	3.5	4.9	5.3	5.1
	3.00	2.72	2.46	2.04	1.88	1.72	1.68	1.35	1.96	2.01	3.10	3.30	2.89
50	6.3	5.8	5.0	4.1	4.6	4.9	5.0	3.8	3.8	4.2	5.8	6.2	6.0
	3.32	3.02	2.72	2.26	2.08	1.90	1.85	1.49	2.17	2.23	3.42	3.65	3.18
100	7.4	6.8	5.9	4.8	5.4	5.9	6.0	4.6	4.5	5.0	6.8	7.3	7.1
	3.65	3.31	2.99	2.48	2.28	2.09	2.04	1.63	2.39	2.45	3.76	4.01	3.47
200	9.2	8.4	7.3	6.0	6.7	7.3	7.4	5.6	5.6	6.1	8.4	9.1	8.8
	3.49	3.17	2.86	2.37	2.19	2.00	1.95	1.56	2.29	2.35	3.60	3.84	3.33
Freq.	36.0	9.3	2.7	1.2	1.0	1.0	0.7	0.5	0.7	1.6	10.7	34.7	100.0

Roughness Class 3 ($z_0 = 0.4000$ m)

z	0	30	60	90	120	150	180	210	240	270	300	330	Total
10	3.4	3.1	2.7	2.2	2.5	2.8	2.7	2.0	2.0	2.3	3.2	3.4	3.3
	2.89	2.56	2.21	1.93	1.81	1.71	1.55	1.27	1.77	1.96	3.12	3.17	2.80
25	4.5	4.1	3.5	3.0	3.3	3.6	3.5	2.6	2.7	3.1	4.2	4.5	4.3
	3.07	2.71	2.34	2.04	1.92	1.80	1.64	1.34	1.88	2.08	3.31	3.36	2.96
50	5.4	4.9	4.2	3.6	4.0	4.4	4.3	3.2	3.2	3.7	5.1	5.4	5.2
	3.33	2.95	2.54	2.22	2.09	1.96	1.78	1.45	2.04	2.26	3.60	3.65	3.20
100	6.5	5.9	5.1	4.3	4.9	5.3	5.2	4.0	3.9	4.4	6.1	6.4	6.2
	3.79	3.36	2.89	2.53	2.38	2.23	2.03	1.65	2.32	2.57	4.09	4.16	3.61
200	7.9	7.3	6.2	5.3	5.9	6.5	6.3	4.8	4.8	5.4	7.4	7.9	7.6
	3.66	3.24	2.79	2.44	2.29	2.15	1.96	1.59	2.24	2.48	3.94	4.01	3.49
Freq.	32.2	8.3	2.5	1.1	1.0	0.9	0.6	0.5	0.7	1.9	13.9	36.3	100.0

z	Class 0		Class 1		Class 2		Class 3	
m	ms^{-1}	Wm^{-2}	ms^{-1}	Wm^{-2}	ms^{-1}	Wm^{-2}	ms^{-1}	Wm^{-2}
10	6.2	196	4.2	71	3.7	47	2.9	22
25	6.7	253	5.1	116	4.6	84	3.9	50
50	7.2	311	5.9	169	5.4	129	4.6	84
100	7.9	401	7.0	275	6.4	209	5.6	139
200	8.7	556	8.7	539	7.9	400	6.9	257

Asswan (62 414) — Western Desert

23° 57′ 55.1″ N 32° 49′ 30.4″ E	UTM 36 E 482 207 m N 2 650 398 m	193 m

The Asswan mast is situated in the international airport of Asswan, about 2 km SW of the town of Sahara City. Lake Nasser is found to the east and south, at distances of about 3–5 km, and the high dam is located about 5 km to the east of the site. There are several sheltering obstacles (airport buildings) close to the mast, in the NE, SE and SW directions. The airport area itself is also characterized by a higher roughness length than the surrounding sandy desert. The terrain is mostly flat or slightly undulating, except to the NE where the Nile valley is located – about 5 km from the site.

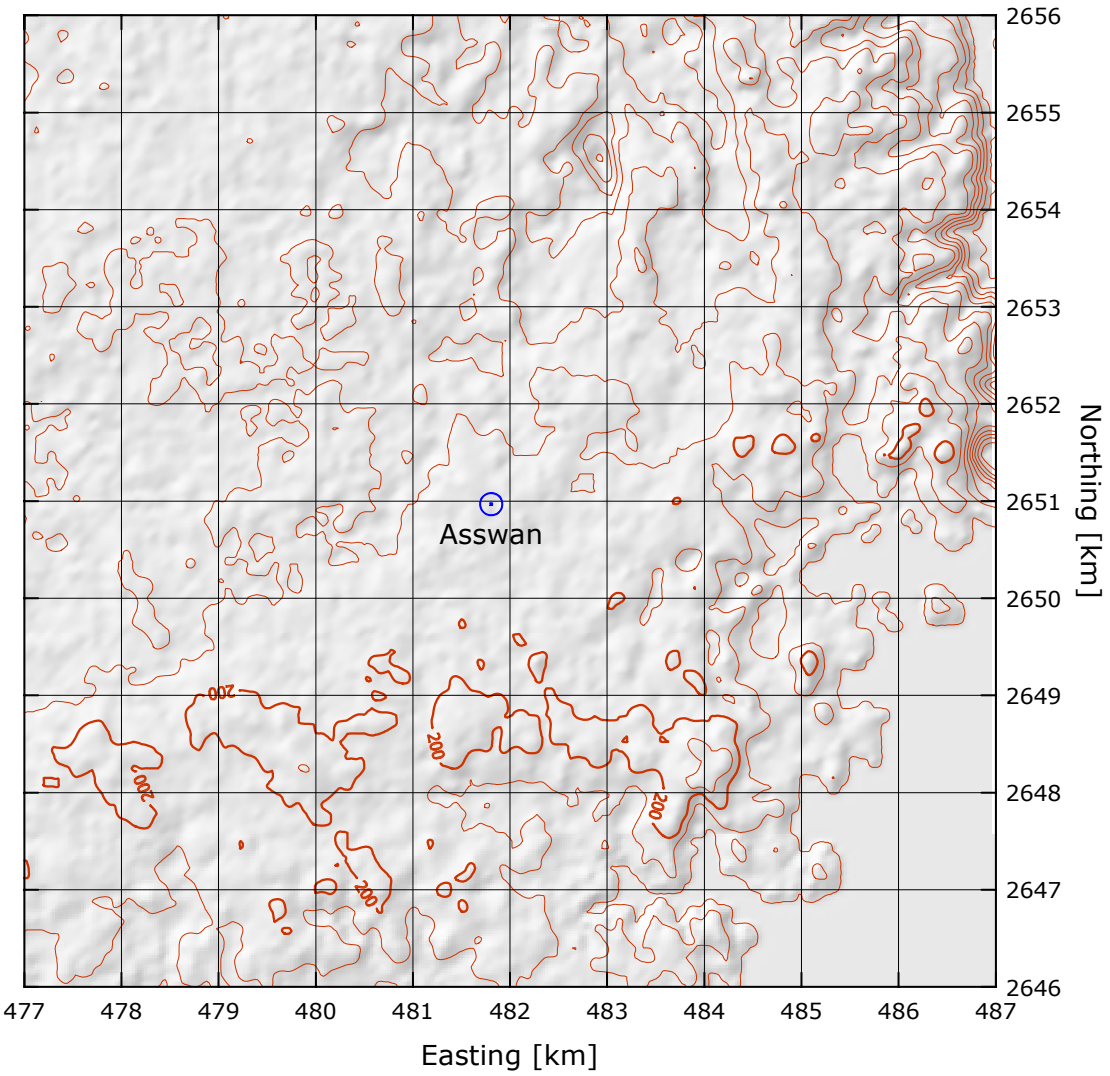

Sector	Input		Obstacles		Roughness		Orography		z_{0m}
0	0.0	0.0	−2.9	0.0	−6.8	0.0	0.3	0.9	0.0060
30	0.0	0.0	−8.3	0.0	−7.8	0.0	1.6	0.3	0.0060
60	0.0	0.0	−0.4	0.0	−5.7	0.0	1.3	−0.5	0.0080
90	0.0	0.0	−1.5	0.0	−6.3	0.0	−0.2	−0.8	0.0020
120	0.0	0.0	−0.1	0.0	−4.2	0.0	−1.2	−0.3	0.0020
150	0.0	0.0	−1.7	0.0	−7.4	0.0	−1.0	0.5	0.0010
180	0.0	0.0	−5.2	0.0	−8.8	0.0	0.4	0.8	0.0010
210	0.0	0.0	−16.9	0.0	−5.9	0.0	1.5	0.3	0.0030
240	0.0	0.0	−15.1	0.0	−3.1	0.0	1.3	−0.5	0.0040
270	0.0	0.0	−7.8	0.0	−1.3	0.0	0.0	−0.8	0.0050
300	0.0	0.0	−0.2	0.0	−3.2	0.0	−1.1	−0.3	0.0050
330	0.0	0.0	−8.0	0.0	−6.2	0.0	−1.0	0.6	0.0060

Height of anemometer: 10.0 m a.g.l. 1995-2004

Sect	Freq	< 1	2	3	4	5	6	7	8	9	11	13	15	17	>17	*A*	*k*
0	47.3	6	33	126	211	191	187	142	59	29	13	3	0	0	0	5.3	2.70
30	9.9	12	62	204	236	182	156	111	26	9	2	0	0	0	0	4.6	2.49
60	1.2	70	145	263	228	137	95	30	13	11	8	0	0	0	0	3.7	1.94
90	0.9	37	158	245	245	150	86	38	21	7	14	0	0	0	0	3.9	1.90
120	1.1	51	174	253	154	147	125	68	9	16	4	0	0	0	0	3.9	1.95
150	1.5	19	67	179	178	160	169	154	44	23	6	0	0	0	0	5.0	2.65
180	1.2	29	111	242	209	186	104	67	28	11	12	0	0	0	0	4.2	2.09
210	1.0	36	103	249	207	193	85	75	24	13	10	6	0	0	0	4.2	1.97
240	1.1	42	103	212	141	160	148	98	50	33	13	0	0	0	0	4.8	2.20
270	2.8	20	71	120	153	161	137	156	76	60	41	4	1	0	0	5.7	2.39
300	10.6	12	41	80	141	151	209	177	88	53	37	8	1	1	1	6.1	2.76
330	21.4	9	40	99	165	171	196	175	77	39	23	5	1	0	0	5.8	2.85
Total	100.0	11	46	132	193	179	181	145	60	32	17	3	1	0	0	5.4	2.61

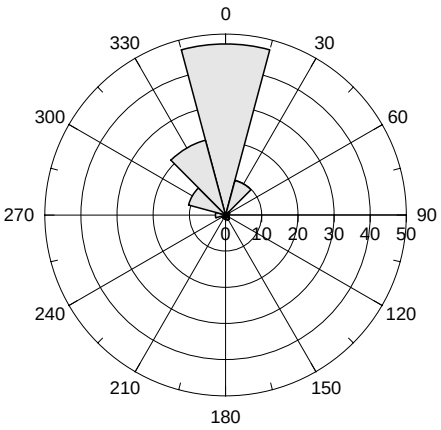

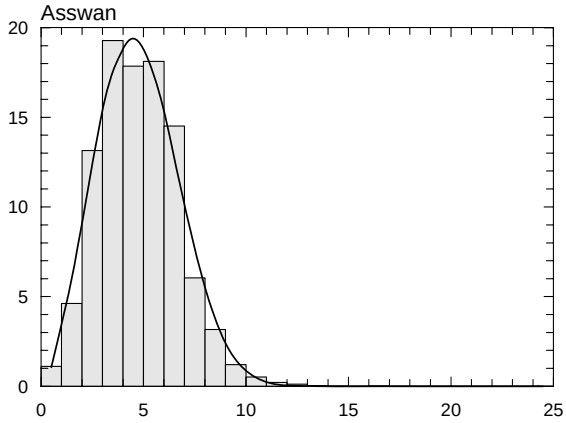

	Jan	Feb	Mar	Apr	May	Jun	Jul	Aug	Sep	Oct	Nov	Dec	Year
0	3.9	4.0	3.9	4.2	4.4	4.4	4.0	4.1	4.4	4.4	3.9	3.8	4.1
3	3.9	3.9	3.8	4.0	3.9	3.9	3.5	3.6	4.2	4.2	3.8	3.5	3.8
6	3.8	3.9	4.1	4.7	4.7	4.8	4.2	4.3	4.8	4.7	3.9	3.4	4.3
9	5.1	5.4	5.1	5.2	5.2	5.5	5.1	5.7	5.5	5.1	4.7	4.7	5.2
12	4.9	5.3	5.1	5.3	5.5	5.5	5.6	6.0	4.8	4.6	4.3	4.4	5.1
15	5.1	5.5	5.6	5.6	5.7	5.8	6.0	6.3	5.2	4.8	4.5	4.5	5.4
18	4.4	4.7	4.7	4.8	5.0	5.2	5.2	5.2	4.9	4.6	4.2	3.9	4.7
21	4.0	4.1	4.3	4.6	4.7	5.1	4.6	4.5	4.5	4.5	4.1	3.8	4.4
Mean	4.4	4.6	4.6	4.8	4.9	5.0	4.8	5.0	4.8	4.6	4.2	4.0	4.6

	Jan	Feb	Mar	Apr	May	Jun	Jul	Aug	Sep	Oct	Nov	Dec	Year
1995	5.6	5.3	4.9	4.9	5.6	5.2	5.3	5.5	4.8	5.3	5.0	4.4	5.2
1996	3.9	4.5	5.0	5.1	5.0	5.4	5.2	5.0	5.3	5.4	4.4	4.4	4.9
1997	4.8	5.3	4.8	5.2	4.5	4.9	5.0	5.2	5.3	4.5	3.9	4.8	4.8
1998	4.6	4.6	5.2	4.9	5.0	5.4	4.8	5.3	5.4	5.1	4.4	4.9	5.0
1999	5.2	5.7	4.9	5.9	5.6	5.9	5.0	5.3	5.1	4.9	4.3	3.9	5.1
2000	4.1	4.6	4.9	4.2	4.9	4.8	5.0	5.0	4.3	4.1	3.6	3.9	4.4
2001	3.9	4.1	3.9	4.8	4.5	5.0	4.5	5.0	4.6	4.6	4.3	3.6	4.4
2002	3.8	4.1	3.9	4.7	4.7	4.8	4.0	4.3	4.6	4.2	3.8	3.6	4.2
2003	3.6	3.9	4.0	4.4	4.3	4.5	4.6	4.5	4.5	4.0	3.7	3.3	4.1
2004	3.3	3.5	3.9	4.0	4.2	4.2	4.1	4.0	3.9	3.4	3.7	3.3	3.8
2005	3.3	3.7	3.8	4.4	4.1	—	—	—	—	—	—	—	—
Mean	4.4	4.6	4.6	4.8	4.9	5.0	4.8	5.0	4.8	4.6	4.2	4.0	4.6

Asswan (62414) 1995-2004

6.0 m agl, mean 4.6 m/s, st dev 2.0 m/s, cube 164. m ł/s ³

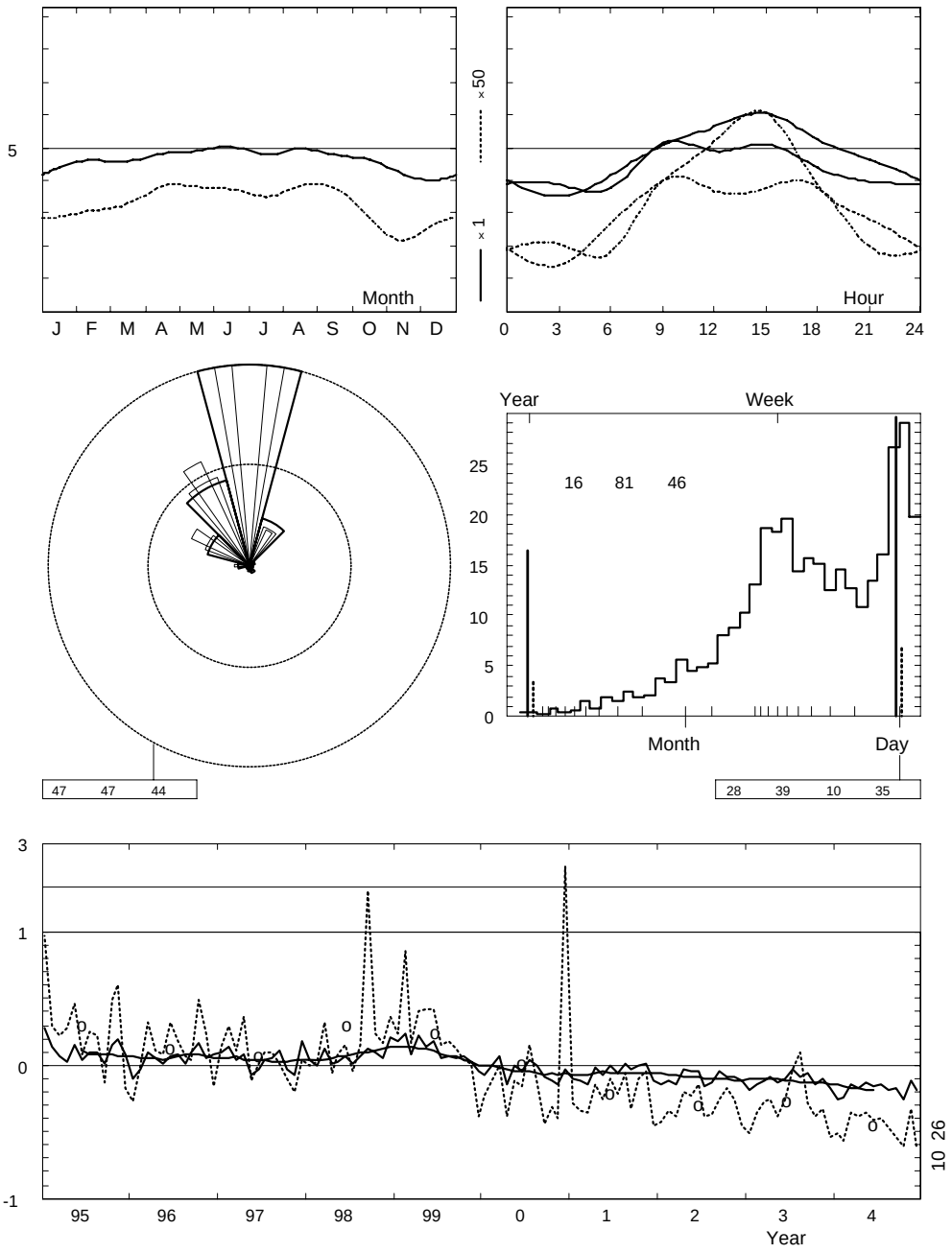

Roughness Class 0 ($z_0 = 0.0002$ m)

z	0	30	60	90	120	150	180	210	240	270	300	330	Total
10	7.5	7.0	5.9	4.9	4.7	5.9	5.5	6.3	7.0	7.8	8.0	8.4	7.5
	3.18	3.04	2.49	2.22	2.08	2.63	2.33	2.22	2.55	2.85	3.21	3.33	2.98
25	8.2	7.6	6.4	5.4	5.1	6.5	6.0	6.8	7.6	8.5	8.8	9.2	8.2
	3.28	3.13	2.57	2.29	2.14	2.72	2.40	2.29	2.63	2.94	3.31	3.44	3.07
50	8.8	8.2	6.9	5.8	5.5	6.9	6.5	7.4	8.2	9.2	9.4	9.9	8.9
	3.37	3.22	2.64	2.35	2.20	2.79	2.46	2.35	2.71	3.02	3.40	3.53	3.15
100	9.5	8.9	7.5	6.3	6.0	7.5	7.0	8.0	8.9	9.9	10.2	10.8	9.6
	3.26	3.12	2.56	2.28	2.13	2.70	2.38	2.27	2.62	2.93	3.29	3.42	3.05
200	10.6	9.8	8.3	7.0	6.6	8.3	7.8	8.8	9.8	11.0	11.3	11.9	10.6
	3.09	2.95	2.42	2.16	2.01	2.56	2.26	2.15	2.48	2.77	3.12	3.24	2.90
Freq.	43.7	13.8	2.2	0.9	1.1	1.5	1.2	1.0	1.0	2.6	9.9	21.1	100.0

Roughness Class 1 ($z_0 = 0.0300$ m)

z	0	30	60	90	120	150	180	210	240	270	300	330	Total
10	5.2	4.7	3.6	3.4	3.4	4.1	3.8	4.4	5.0	5.4	5.6	5.7	5.2
	2.65	2.49	1.93	1.86	1.82	2.22	1.87	1.87	2.21	2.46	2.69	2.72	2.52
25	6.2	5.6	4.3	4.1	4.1	4.9	4.6	5.3	6.0	6.5	6.7	6.8	6.3
	2.87	2.69	2.09	2.01	1.96	2.40	2.03	2.01	2.38	2.66	2.91	2.94	2.72
50	7.1	6.4	4.9	4.7	4.7	5.7	5.3	6.2	6.9	7.5	7.7	7.8	7.2
	3.22	3.02	2.35	2.26	2.21	2.70	2.28	2.26	2.69	2.99	3.27	3.31	3.03
100	8.4	7.6	5.8	5.6	5.6	6.7	6.3	7.3	8.1	8.9	9.1	9.3	8.5
	3.43	3.21	2.50	2.40	2.35	2.87	2.42	2.41	2.86	3.18	3.48	3.52	3.21
200	10.5	9.5	7.3	7.0	7.0	8.4	7.8	9.1	10.1	11.1	11.4	11.6	10.6
	3.28	3.07	2.38	2.29	2.24	2.74	2.31	2.30	2.73	3.04	3.33	3.37	3.08
Freq.	42.0	8.7	1.2	0.9	1.2	1.5	1.1	1.0	1.3	3.7	12.0	25.3	100.0

Roughness Class 2 ($z_0 = 0.1000$ m)

z	0	30	60	90	120	150	180	210	240	270	300	330	Total
10	4.5	4.1	3.1	3.0	3.1	3.6	3.3	3.9	4.4	4.8	4.9	4.9	4.6
	2.66	2.53	1.95	1.86	1.86	2.16	1.86	1.88	2.22	2.54	2.71	2.67	2.53
25	5.5	5.0	3.8	3.7	3.8	4.4	4.1	4.8	5.4	5.8	6.0	6.0	5.6
	2.85	2.71	2.08	1.99	1.99	2.31	1.99	2.01	2.38	2.72	2.90	2.86	2.70
50	6.4	5.9	4.5	4.3	4.5	5.2	4.9	5.6	6.3	6.8	7.1	7.0	6.5
	3.15	2.99	2.31	2.20	2.21	2.56	2.20	2.22	2.63	3.01	3.22	3.17	2.97
100	7.7	7.0	5.3	5.1	5.3	6.1	5.8	6.7	7.5	8.1	8.4	8.3	7.8
	3.46	3.29	2.54	2.42	2.42	2.81	2.42	2.45	2.89	3.30	3.53	3.48	3.24
200	9.5	8.6	6.6	6.3	6.6	7.6	7.1	8.3	9.3	10.0	10.4	10.3	9.6
	3.31	3.15	2.43	2.31	2.32	2.69	2.32	2.34	2.77	3.16	3.38	3.33	3.11
Freq.	39.0	8.0	1.1	0.9	1.2	1.5	1.1	1.0	1.4	4.4	12.9	27.4	100.0

Roughness Class 3 ($z_0 = 0.4000$ m)

z	0	30	60	90	120	150	180	210	240	270	300	330	Total
10	3.5	3.2	2.5	2.3	2.5	2.8	2.7	3.1	3.5	3.7	3.9	3.7	3.6
	2.65	2.48	1.97	1.87	1.94	2.12	1.88	1.91	2.24	2.57	2.68	2.62	2.51
25	4.6	4.2	3.2	3.1	3.3	3.7	3.5	4.1	4.6	4.9	5.1	4.9	4.7
	2.81	2.63	2.09	1.98	2.05	2.25	1.99	2.03	2.38	2.72	2.84	2.78	2.66
50	5.6	5.1	3.9	3.7	4.0	4.4	4.3	4.9	5.5	5.9	6.1	5.9	5.6
	3.06	2.86	2.27	2.15	2.23	2.44	2.16	2.20	2.59	2.96	3.09	3.02	2.88
100	6.7	6.1	4.7	4.5	4.8	5.3	5.2	5.9	6.6	7.1	7.3	7.1	6.8
	3.48	3.26	2.59	2.45	2.54	2.79	2.46	2.51	2.95	3.37	3.51	3.44	3.26
200	8.2	7.4	5.7	5.5	5.9	6.5	6.3	7.2	8.1	8.6	8.9	8.7	8.3
	3.35	3.14	2.49	2.36	2.45	2.69	2.37	2.42	2.84	3.25	3.39	3.32	3.15
Freq.	34.7	7.0	1.1	1.0	1.2	1.4	1.1	1.0	1.6	5.3	14.3	30.2	100.0

z	Class 0		Class 1		Class 2		Class 3	
m	ms^{-1}	Wm^{-2}	ms^{-1}	Wm^{-2}	ms^{-1}	Wm^{-2}	ms^{-1}	Wm^{-2}
10	6.7	264	4.6	97	4.0	63	3.2	31
25	7.4	340	5.6	157	5.0	113	4.2	67
50	7.9	417	6.4	228	5.8	173	5.0	112
100	8.6	540	7.6	371	7.0	280	6.1	185
200	9.5	750	9.5	729	8.6	536	7.4	342

Abu Simbel — Western Desert

22° 25′ 49.1″ N 31° 33′ 25.7″ E	UTM 36 E 351 509 m N 2 481 171 m	198 m

The Abu Simbel mast is situated about 8 km NNW of the airport of Abu Simbel. Lake Nasser is located to the east of the site, but at a distance of about 7–10 km or more. The terrain consists mostly of flat uniform sandy desert, but with some rocky outcrops or 'hills' to the east and south – some of these are several tens of meters high. To the north and west the terrain is very open and there are no hills or other obstacles.

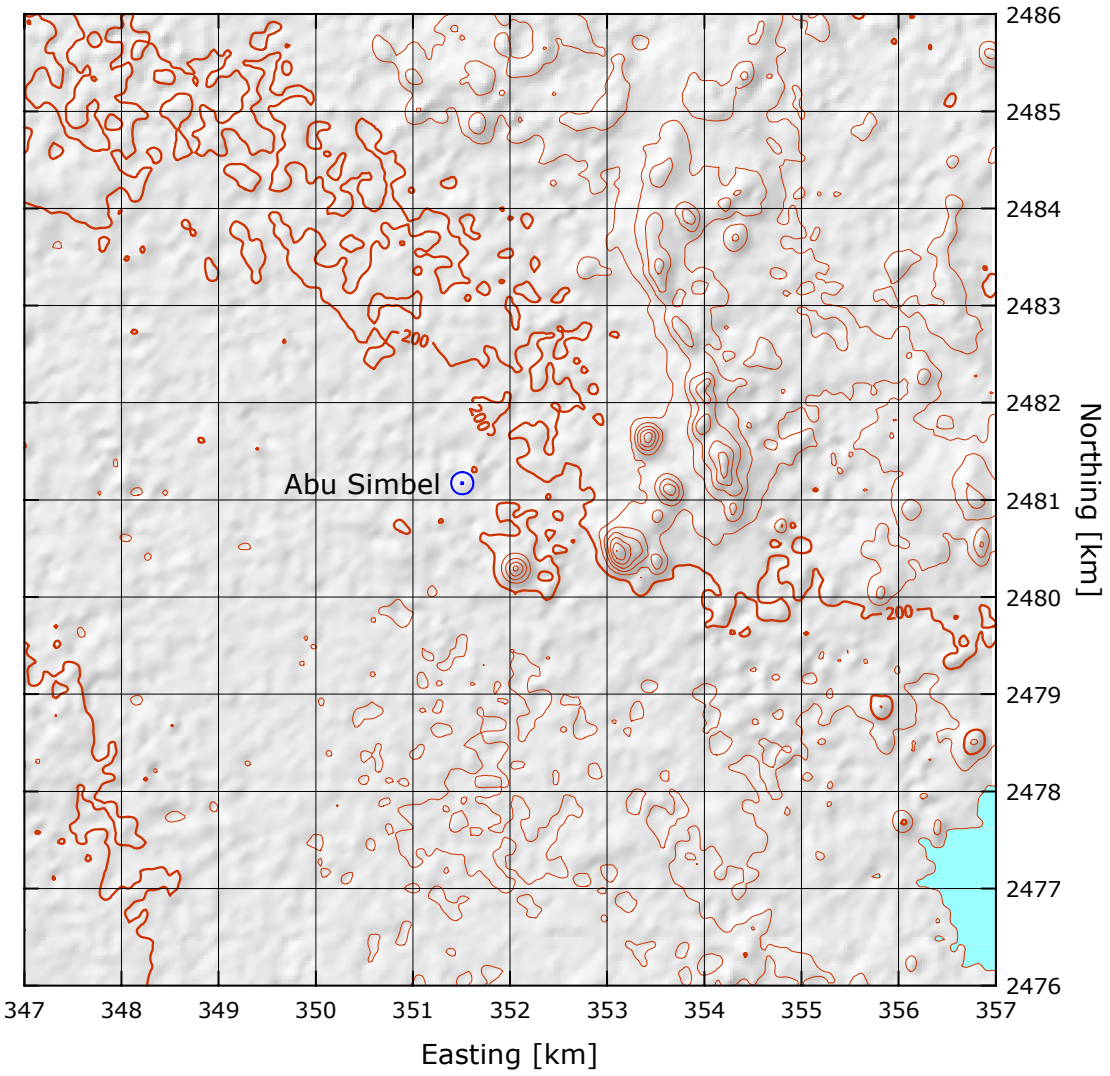

Sector	Input		Obstacles		Roughness		Orography		z_{0m}
0	0.0	0.0	0.0	0.0	0.0	0.0	1.0	−0.7	0.0050
30	0.0	0.0	0.0	0.0	0.0	0.0	−0.2	−0.4	0.0050
60	0.0	0.0	0.0	0.0	0.0	0.0	−0.3	0.3	0.0050
90	0.0	0.0	0.0	0.0	−2.0	0.0	0.7	0.7	0.0030
120	0.0	0.0	0.0	0.0	−4.1	0.0	1.8	0.4	0.0010
150	0.0	0.0	0.0	0.0	−1.2	0.0	2.0	−0.3	0.0030
180	0.0	0.0	0.0	0.0	0.0	0.0	1.0	−0.7	0.0050
210	0.0	0.0	0.0	0.0	0.0	0.0	−0.2	−0.4	0.0050
240	0.0	0.0	0.0	0.0	0.0	0.0	−0.3	0.3	0.0050
270	0.0	0.0	0.0	0.0	0.0	0.0	0.7	0.7	0.0050
300	0.0	0.0	0.0	0.0	0.0	0.0	1.9	0.4	0.0050
330	0.0	0.0	0.0	0.0	0.0	0.0	2.0	−0.3	0.0050

Height of anemometer: 24.5 m a.g.l. 2004-05

Sect	Freq	<1	2	3	4	5	6	7	8	9	11	13	15	17	>17	*A*	*k*
0	40.4	8	38	64	88	117	159	157	148	107	92	21	2	0	0	7.0	2.97
30	11.1	5	57	113	154	182	179	132	89	50	32	7	1	0	0	5.7	2.53
60	8.5	7	54	99	156	177	207	137	86	46	28	3	0	0	0	5.7	2.84
90	2.4	40	138	146	204	175	136	100	31	26	3	0	0	0	0	4.5	2.29
120	0.9	90	184	232	239	164	44	16	7	16	9	0	0	0	0	3.6	1.97
150	0.3	51	251	393	229	71	6	0	0	0	0	0	0	0	0	2.9	2.78
180	0.4	110	371	221	74	55	62	52	55	0	0	0	0	0	0	2.7	1.21
210	0.5	105	447	179	133	33	32	53	19	0	0	0	0	0	0	2.4	1.28
240	0.5	215	401	205	95	23	20	18	8	8	8	0	0	0	0	2.1	1.15
270	1.5	113	396	202	124	78	51	21	3	7	6	0	0	0	0	2.6	1.37
300	5.9	48	161	166	137	131	134	100	82	23	14	3	0	0	0	4.7	2.06
330	27.5	8	43	74	88	109	146	179	173	109	65	5	0	0	0	6.8	3.54
Total	100.0	15	65	90	110	128	155	149	130	85	62	11	1	0	0	6.4	2.76

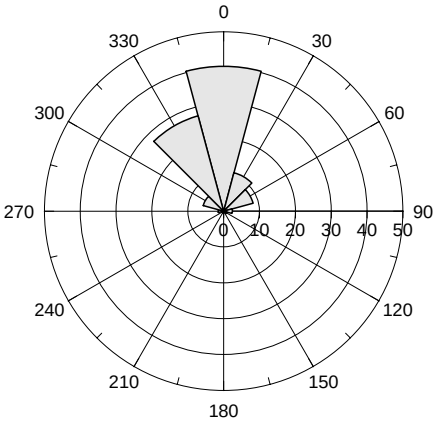

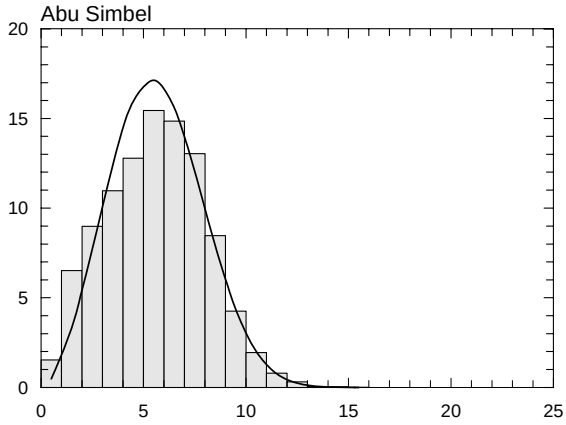

	Jan	Feb	Mar	Apr	May	Jun	Jul	Aug	Sep	Oct	Nov	Dec	Year
0	4.7	6.2	6.5	7.5	6.9	6.5	4.1	5.5	7.3	6.6	6.1	5.3	6.1
1	4.3	5.7	6.4	7.0	6.6	6.2	4.3	4.9	7.0	6.7	6.4	4.9	5.9
2	4.1	5.4	5.6	6.9	6.3	5.8	3.8	4.9	6.1	6.0	5.8	4.7	5.4
3	3.7	5.0	5.2	6.6	5.6	5.0	3.5	4.3	5.8	5.5	5.1	4.4	5.0
4	4.0	4.9	4.8	6.0	4.6	4.8	3.3	4.0	5.2	5.3	4.5	4.5	4.7
5	4.0	4.8	4.2	5.2	4.4	4.3	3.1	3.6	5.2	4.9	4.7	4.5	4.4
6	3.6	4.4	4.1	4.9	4.2	3.9	2.5	3.1	4.6	4.6	4.6	4.6	4.1
7	3.2	3.7	3.9	5.1	3.9	3.8	2.5	3.0	4.5	4.7	4.0	4.0	3.9
8	3.1	4.3	4.4	5.9	5.2	5.1	3.8	4.2	6.0	5.9	4.2	3.8	4.7
9	3.8	5.2	4.9	6.6	5.7	5.6	4.6	5.4	7.0	6.8	5.5	4.3	5.5
10	4.5	6.0	5.4	6.7	6.1	5.8	5.4	5.8	7.3	6.5	6.0	5.3	5.9
11	5.2	5.9	5.3	6.6	5.7	5.6	5.5	5.6	6.6	5.9	5.8	5.2	5.7
12	5.1	5.4	5.3	6.3	5.7	5.2	5.3	5.7	6.3	5.9	5.8	5.2	5.6
13	4.9	5.4	5.3	6.2	5.8	5.2	5.5	5.7	6.1	5.7	5.5	5.1	5.5
14	5.0	5.3	5.7	6.1	5.7	5.2	5.7	6.2	6.2	5.4	5.7	5.5	5.6
15	5.3	5.3	5.7	6.3	6.1	5.3	6.4	6.6	6.4	5.5	5.8	5.5	5.8
16	5.3	5.7	6.0	6.9	6.1	5.6	6.2	6.8	6.8	5.8	6.1	5.4	6.1
17	5.5	5.9	6.3	6.9	6.1	6.1	6.3	7.2	7.4	6.0	6.4	5.1	6.3
18	5.4	5.7	6.5	6.7	6.8	6.6	6.5	7.3	7.2	5.8	5.9	4.7	6.3
19	5.1	5.9	6.3	6.5	6.5	6.6	6.4	6.3	6.9	6.3	6.2	5.3	6.2
20	5.1	6.1	6.0	6.5	6.1	6.0	6.1	5.6	7.1	6.4	6.6	5.6	6.1
21	5.4	6.2	6.4	7.2	6.6	6.6	5.7	5.3	7.3	6.9	6.6	5.1	6.3
22	5.1	6.0	6.7	7.0	7.0	6.0	5.3	5.2	7.2	6.9	6.4	5.3	6.2
23	5.0	6.2	6.8	7.1	7.1	6.3	4.6	5.4	7.1	7.0	6.2	4.9	6.1
Mean	4.6	5.4	5.6	6.4	5.9	5.5	4.9	5.3	6.4	6.0	5.7	4.9	5.5

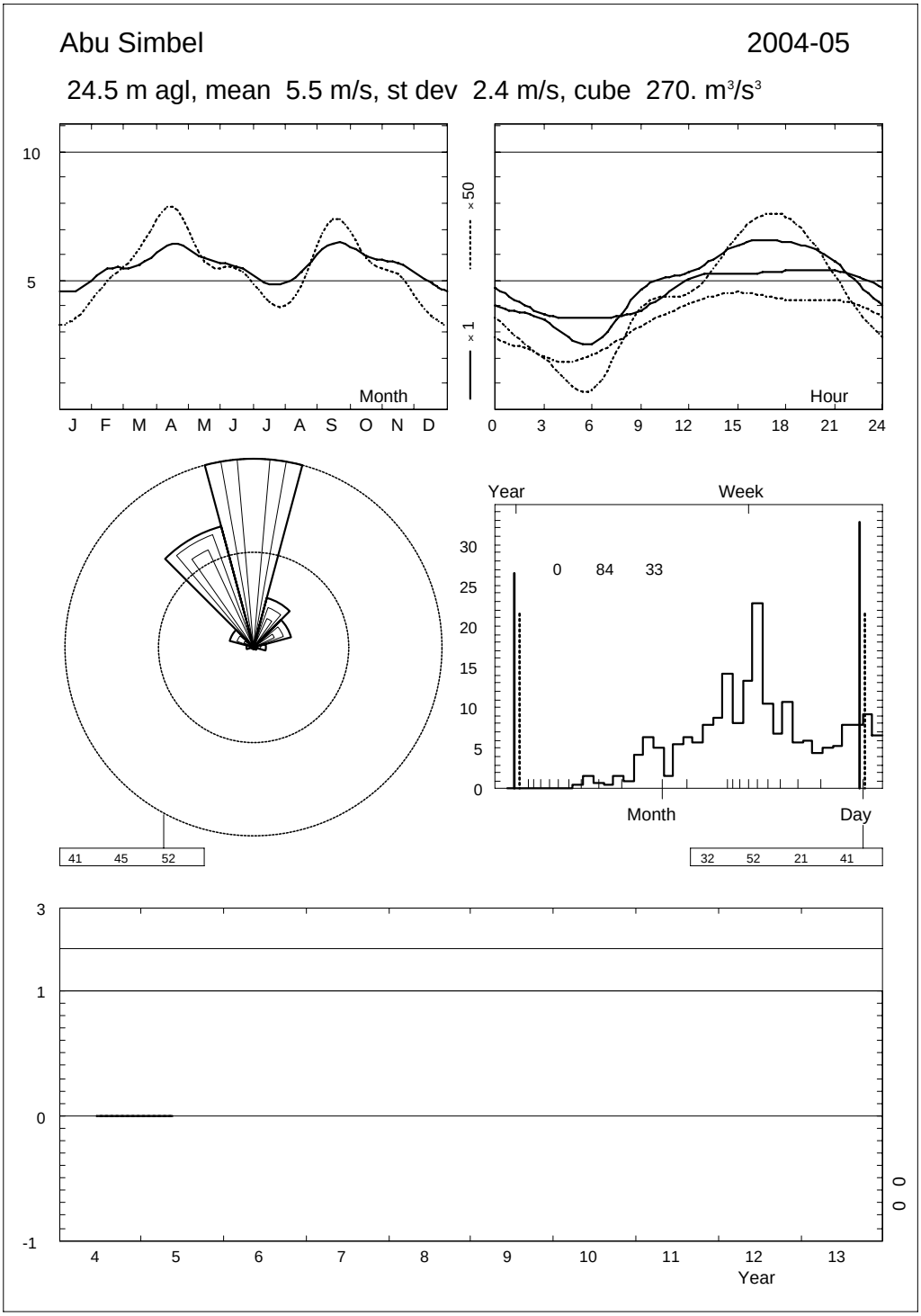

	Jan	Feb	Mar	Apr	May	Jun	Jul	Aug	Sep	Oct	Nov	Dec	Year
2004	—	—	—	—	—	5.5	4.9	5.3	6.4	6.0	5.7	4.9	5.5
2005	4.6	5.4	5.6	6.4	5.9	—	—	—	—	—	—	—	5.6
Mean	4.6	5.4	5.6	6.4	5.9	5.5	4.9	5.3	6.4	6.0	5.7	4.9	5.5

Roughness Class 0 ($z_0 = 0.0002$ m)

z	0	30	60	90	120	150	180	210	240	270	300	330	Total
10	7.4	6.6	6.2	5.2	3.9	3.1	2.9	2.7	2.4	2.9	5.0	7.2	6.8
	3.24	2.78	2.94	2.55	2.06	2.40	1.37	1.40	1.29	1.47	2.19	3.75	2.84
25	8.1	7.2	6.8	5.7	4.3	3.4	3.2	3.0	2.6	3.2	5.4	7.8	7.4
	3.34	2.87	3.03	2.63	2.12	2.47	1.41	1.44	1.33	1.51	2.26	3.87	2.92
50	8.7	7.7	7.2	6.1	4.6	3.7	3.5	3.2	2.8	3.5	5.9	8.4	7.9
	3.43	2.94	3.11	2.70	2.18	2.54	1.44	1.48	1.36	1.55	2.32	3.97	2.98
100	9.5	8.4	7.9	6.7	5.0	4.0	3.7	3.5	3.1	3.8	6.3	9.1	8.6
	3.32	2.85	3.01	2.62	2.11	2.46	1.40	1.44	1.32	1.51	2.25	3.85	2.90
200	10.5	9.3	8.7	7.4	5.5	4.4	4.1	3.8	3.4	4.1	7.0	10.1	9.6
	3.14	2.70	2.85	2.47	2.00	2.33	1.33	1.36	1.25	1.43	2.13	3.64	2.77
Freq.	38.5	15.2	9.0	3.1	1.0	0.4	0.4	0.5	0.5	1.5	5.3	24.5	100.0

Roughness Class 1 ($z_0 = 0.0300$ m)

z	0	30	60	90	120	150	180	210	240	270	300	330	Total
10	5.2	4.3	4.3	3.3	2.5	2.1	2.0	1.8	1.8	2.4	4.1	5.0	4.7
	2.66	2.29	2.49	2.01	1.69	1.95	1.15	1.19	1.18	1.35	2.15	3.01	2.43
25	6.1	5.2	5.1	3.9	3.0	2.5	2.4	2.2	2.2	3.0	4.8	6.0	5.6
	2.88	2.48	2.69	2.17	1.82	2.10	1.24	1.28	1.27	1.46	2.32	3.25	2.60
50	7.1	6.0	5.9	4.6	3.5	2.9	2.8	2.6	2.5	3.5	5.6	6.9	6.5
	3.23	2.79	3.03	2.44	2.04	2.37	1.38	1.44	1.42	1.63	2.61	3.65	2.88
100	8.4	7.1	7.0	5.4	4.2	3.5	3.4	3.2	3.0	4.1	6.6	8.1	7.7
	3.44	2.97	3.22	2.60	2.18	2.52	1.47	1.53	1.51	1.74	2.78	3.88	3.03
200	10.4	8.8	8.7	6.7	5.2	4.3	4.2	3.9	3.8	5.1	8.2	10.1	9.5
	3.29	2.83	3.08	2.48	2.08	2.40	1.41	1.46	1.44	1.66	2.65	3.71	2.92
Freq.	37.0	11.5	7.9	2.2	0.8	0.3	0.4	0.5	0.6	2.1	8.1	28.4	100.0

Roughness Class 2 ($z_0 = 0.1000$ m)

z	0	30	60	90	120	150	180	210	240	270	300	330	Total
10	4.5	3.8	3.7	2.9	2.2	1.8	1.7	1.7	1.6	2.3	3.7	4.4	4.1
	2.65	2.30	2.43	2.04	1.67	1.71	1.17	1.27	1.25	1.40	2.31	3.02	2.44
25	5.5	4.6	4.5	3.5	2.7	2.2	2.2	2.1	2.0	2.8	4.6	5.4	5.0
	2.84	2.46	2.60	2.19	1.79	1.83	1.25	1.36	1.33	1.50	2.47	3.23	2.59
50	6.4	5.4	5.3	4.2	3.2	2.7	2.6	2.5	2.4	3.4	5.4	6.3	5.9
	3.15	2.72	2.88	2.42	1.98	2.02	1.38	1.50	1.47	1.66	2.74	3.58	2.84
100	7.6	6.4	6.3	4.9	3.8	3.2	3.1	3.0	2.9	4.0	6.4	7.4	7.0
	3.46	2.99	3.17	2.66	2.18	2.22	1.51	1.64	1.61	1.82	3.01	3.93	3.08
200	9.4	8.0	7.8	6.1	4.7	3.9	3.8	3.7	3.6	5.0	7.9	9.2	8.6
	3.31	2.87	3.03	2.55	2.08	2.12	1.44	1.57	1.54	1.74	2.88	3.76	2.96
Freq.	34.7	11.3	7.4	2.1	0.7	0.4	0.4	0.5	0.8	2.5	9.8	29.4	100.0

Roughness Class 3 ($z_0 = 0.4000$ m)

z	0	30	60	90	120	150	180	210	240	270	300	330	Total
10	3.5	3.0	2.9	2.2	1.7	1.5	1.4	1.3	1.3	2.0	3.1	3.4	3.2
	2.62	2.28	2.35	1.95	1.67	1.73	1.28	1.23	1.26	1.53	2.47	2.90	2.42
25	4.6	3.9	3.8	2.9	2.2	2.0	1.9	1.7	1.8	2.6	4.0	4.5	4.2
	2.78	2.41	2.50	2.06	1.77	1.83	1.35	1.30	1.33	1.62	2.62	3.08	2.55
50	5.5	4.7	4.5	3.5	2.7	2.4	2.3	2.1	2.1	3.2	4.8	5.4	5.1
	3.02	2.62	2.71	2.24	1.92	1.99	1.46	1.41	1.44	1.76	2.85	3.34	2.74
100	6.6	5.6	5.4	4.2	3.3	2.9	2.9	2.6	2.6	3.8	5.8	6.5	6.1
	3.44	2.99	3.09	2.56	2.19	2.27	1.66	1.60	1.63	2.00	3.24	3.81	3.07
200	8.1	6.9	6.7	5.2	4.0	3.6	3.5	3.1	3.2	4.7	7.1	8.0	7.5
	3.31	2.88	2.98	2.46	2.10	2.19	1.60	1.54	1.57	1.93	3.12	3.67	2.97
Freq.	31.5	10.9	6.7	1.9	0.7	0.3	0.4	0.5	0.9	3.0	12.2	30.9	100.0

z	Class 0		Class 1		Class 2		Class 3	
m	ms^{-1}	Wm^{-2}	ms^{-1}	Wm^{-2}	ms^{-1}	Wm^{-2}	ms^{-1}	Wm^{-2}
10	6.0	195	4.2	71	3.6	47	2.8	23
25	6.6	252	5.0	116	4.5	84	3.7	50
50	7.1	308	5.8	168	5.2	128	4.5	84
100	7.7	399	6.8	273	6.2	207	5.5	138
200	8.5	555	8.5	537	7.7	396	6.7	255

Intentionally left blank

8 Design wind conditions

In addition to the predicted wind climate – i.e. the wind rose and the sector-wise distributions of mean wind speed – other wind conditions may be important for the design of a wind turbine or wind farm. Below, a brief summary and some examples are given with respect to the extreme wind climate, the gustiness of the wind and the turbulence intensity.

Other atmospheric or flow characteristics may be important as well; as an example the Wind Atlas for the Gulf of Suez (Mortensen et al., 2003) provides information on atmospheric pressure, solar radiation, air and surface temperatures, atmospheric stability and wind speed profiles for this region.

8.1 Extreme wind speeds

It has been shown in Chapter 7 that the two-parameter Weibull distribution usually gives a good fit to observed wind speed data. However, when it comes to the highest wind speeds, these are statistically very uncertain and other distribution functions must be employed in extreme wind analysis. In general, the Weibull distribution should not be used for the estimation of frequencies of occurrence much below 1% (Troen and Petersen, 1989), i.e. 10-min wind-speed values occurring several hundred times in one year.

The wind climate of extreme wind speeds is often characterized by the so-called '*n*th-year return wind', i.e. the 10-min mean wind speed which on the average will be exceeded once in a period of *n* years. Below we have tried to estimate the 10-, 20- and 50-year wind speeds at the long-term stations Abu Darag, Zafarana and Hurghada WETC. It should be borne in mind, however, that the wind speed records at these stations are only about 10-15 years long, and that the data recovery rates are between 80 and 90%. Estimates of extreme wind speeds from such time-series should be treated with great care and used only as a rough guideline.

The highest 10-min wind speeds recorded during the measurement period at the three stations are: 25.04 ms^{-1} at Abu Darag, 25.58 ms^{-1} at Zafarana, and 24.81 ms^{-1} at Hurghada WETC. In order to estimate wind speeds with a longer return period, we follow the procedures outlined in Jensen and Nielsen (1989), Jensen et al. (1992), Jørgensen et al. (2005), see also Cook (1985).

It is assumed that the double exponential so-called Gumbel distribution can be used to represent the frequency of extreme wind speed events. For each year we now find the highest 10-min wind speed measured at e.g. Zafarana. We then obtain 15 extreme wind speeds. These are ranked according to their value, from 1 for the lowest wind speed to 15 for the highest, and assigned a probability, *P*, calculated as:

$$P = \frac{m}{N+1} \qquad m = 1,\ldots,N \tag{8-1}$$

where *m* is the rank and *N* the size of the sample, in this case 15. The same procedure is carried out for each sector. Figure 8-1 shows a plot of the monthly extreme wind speeds versus the return period.

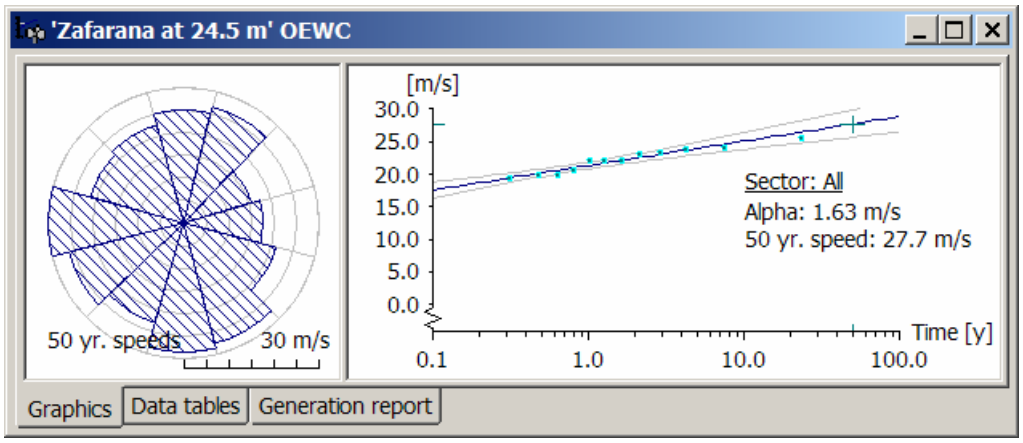

Figure 8-1. Yearly extreme 10-min wind speeds at Zafarana for each of twelve wind direction sectors (rose plot). Graph to the right shows the Gumbel fit to the observations irrespective of direction. The straight line shown corresponds to $u = \alpha\, x + \beta$, with $\alpha = 1.63$. The software in question is the WAsP Climate Analyst (Jørgensen et al., 2005).

The points shown in Figure 8-1 deviate somewhat from the linear least-squares fit. This is also the case for the other two stations, and could, at least partly, be related to the low data recovery rate in some months. The value of the regression line for $m = 15$ is 26.3 ms^{-1}, slightly higher than the value actually observed.

Fifty-year extreme wind speeds for each sector are shown in Figure 8-2.

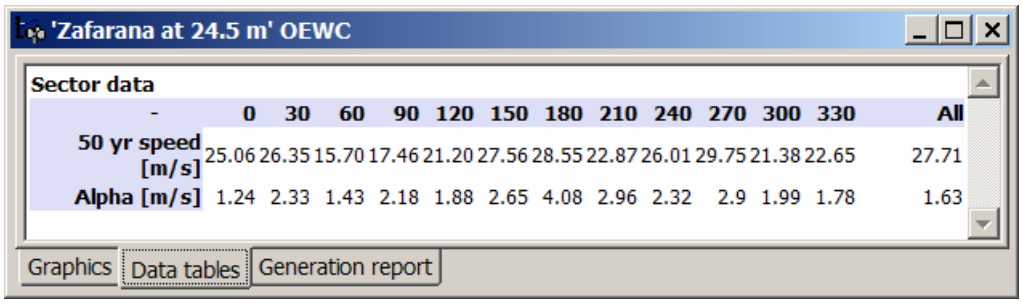

-	0	30	60	90	120	150	180	210	240	270	300	330	All
50 yr speed [m/s]	25.06	26.35	15.70	17.46	21.20	27.56	28.55	22.87	26.01	29.75	21.38	22.65	27.71
Alpha [m/s]	1.24	2.33	1.43	2.18	1.88	2.65	4.08	2.96	2.32	2.9	1.99	1.78	1.63

Figure 8-2. Sector-wise extreme wind speeds at Zafarana. Due to the short time-series and the fitting procedure employed, the extreme wind speed in e.g. sector 270 is slightly higher than the omni-directional extreme wind speed. The software in question is the WAsP Climate Analyst (Jørgensen et al., 2005).

According to Jensen et al. (1992) this fit may be used to extrapolate from one 'return period', T_1, to another, T_2, in the following way:

$$u_2 = u_1 + \alpha \ln \frac{T_2}{T_1} \tag{8-2}$$

Inserting $u_1 = 25.7$, $T_1 = 15$ years, and $T_2 = 20$ years, we get an estimate of the 20-year wind at Zafarana of 26.2 ms^{-1}. With $T_2 = 50$ we get an estimate of the 50-year wind of 27.7 ms^{-1}. Since we have used the 25-m wind speeds for the analysis, the same height also applies to these estimates.

The measured and estimated extreme 10-min wind speeds at Abu Darag, Zafarana and Hurghada WETC are shown in the table below. The highest sector-wise 50-y extreme wind speed is given in the right-most column (U_{50s}).

Station	R [%]	U_m [ms^{-1}]	U_e [ms^{-1}]	U_{10} [ms^{-1}]	U_{20} [ms^{-1}]	U_{50} [ms^{-1}]	U_{50s} [ms^{-1}]
Abu Darag	82.5	25.04	24.1	23.5	24.5	25.9	29.2
Zafarana	85.2	25.58	25.7	25.1	26.2	27.7	29.8
Hurghada WETC	79.6	24.81	21.3	21.0	22.2	23.8	26.8

In conclusion, the distributions of monthly extreme wind speeds at the three stations are apparently not represented very well by the double exponential function. Consequently, the estimated 10-minute wind speeds given above may be quite uncertain and should be treated accordingly. Reanalysis of the extreme wind speeds can readily be carried out from the wind speed data in the meteorological data base.

8.2 Gustiness of the wind

In addition to the mean wind speed, the wind speed processor also determines a gust wind speed, u_g, and a lull wind speed, u_l, within each 10-min observation period, see Appendix A. The mean, gust and lull speeds are measured at the top level of the wind atlas masts only.

Gust wind speeds

The gust wind speed is obtained as the maximum 2-second continuous block average within each 10-min averaging period. This value is in general larger than the 10-min mean value and the relative excess provides a measure of the gustiness or turbulence intensity in the atmospheric surface layer.

In order to illustrate the distribution of gusts we define the *relative gust amplitude*, a, following Jensen and Kristensen (1989):

$$a = \frac{u_g - U}{U} \tag{8-3}$$

where U is the mean wind speed over the 10-min period in which the gust speed is obtained. The distribution of relative gust amplitudes at Zafarana for the 1-y period from June 2004 to May 2005 is shown in Figure 8-3. The highest 2-sec gust speed recorded at Zafarana in this period was 24 ms^{-1}.

The median value of the relative gust amplitude in Figure 8-3 is 0.20, corresponding to a gust wind speed which is about 20% higher than the mean wind speed.

Lull wind speeds

The lull wind speed is obtained as the minimum 2-second continuous block average within each 10-min averaging period. This value is in general smaller than the 10-min mean value and the relative excursion from the mean value provides a measure of the turbulence intensity in the atmospheric surface layer.

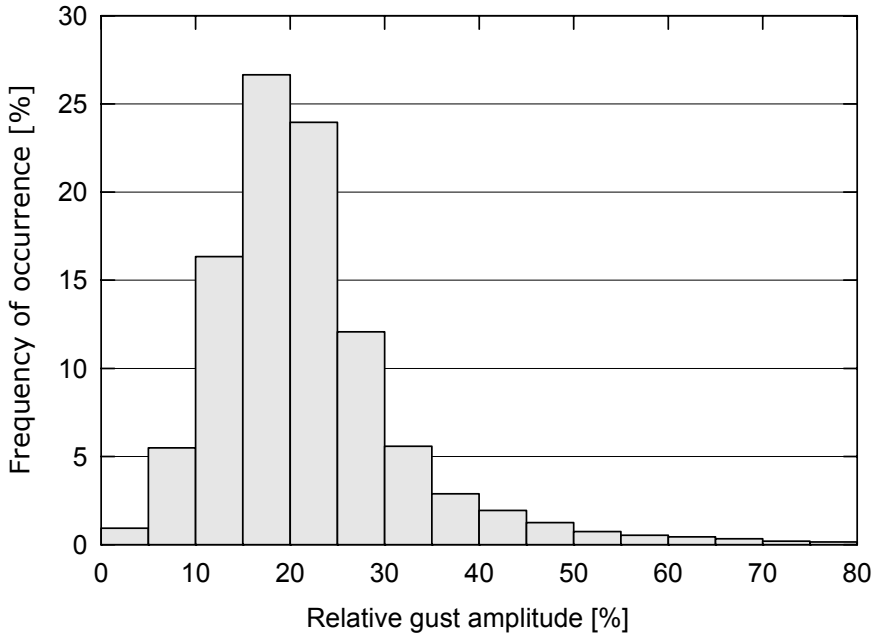

Figure 8-3. Distribution of relative gust amplitudes at the Zafarana mast, measured 24.5 m above ground level.

We can use the definition of gust amplitude for lull wind speeds as well; the lull wind speeds then simply correspond to negative relative gust amplitudes. The distribution of relative gust amplitudes for lull wind speeds at Zafarana is shown in Figure 8-4.

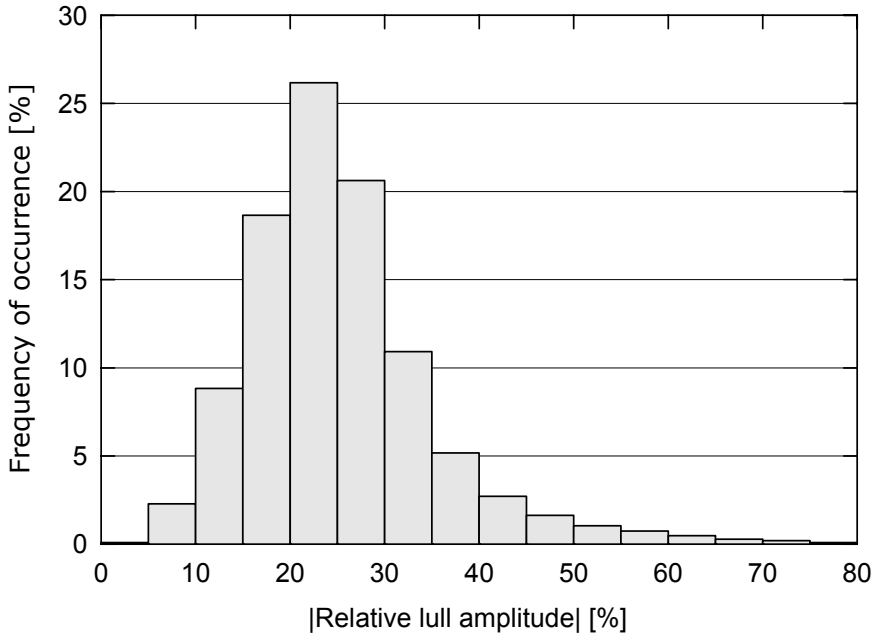

Figure 8-4. Distribution of relative lull amplitudes at the Zafarana mast, measured 24.5 m above ground level. For convenience, the absolute value of the amplitudes has been plotted.

The median value of the relative lull amplitude in Figure 8-4 is -0.24, corresponding to a lull wind speed which is about 24% lower than the mean wind speed.

8.3 Turbulence characteristics

Except for the gust and lull measurements presented in the preceding section, the wind speed data reported in this Atlas are mean wind speeds, corresponding to an averaging time of 10 minutes (one hour for Shark El-Ouinat). Consequently, these data contain no information about wind fluctuations over periods shorter than the averaging time. These faster fluctuations do however contribute to the theoretical wind power density and it can be shown (Troen and Petersen, 1989) that this contribution is approximately proportional to the square of the turbulence intensity, e.g.:

$$\overline{E} = \frac{1}{2}\rho \overline{u}^3 (1 + 3i^2) \tag{8-4}$$

where $\overline{E}$ is mean wind power density, ρ is air density, $\overline{u}$ is mean wind speed, and i is the turbulence intensity ($i \equiv \sigma_u / \overline{u}$). For homogeneous surface roughness and neutral conditions the turbulence intensity can be estimated as $i = [\ln(z/z_0)]^{-1}$. With a height of 25 m and a typical roughness length of 0.001 m the turbulence intensity is then about 10% and the term $3i^2$ in Eq. (4) about 3%.

In practice, however, the contribution of turbulence should in most cases not be added to the estimated power production of a sizeable wind turbine (Troen and Petersen, 1989). This is because the power curve itself is usually referred to 10-min mean wind speeds and so contains part of the contribution already. Furthermore, the effect of turbulence is diminished by the finite response time of the rotor system and the lack of lateral and vertical coherence in the wind field over the rotor disk.

The turbulence characteristics are important for the loads and fatigue life of a wind turbine. Table 8-1 presents average turbulence intensities for the 1-y period from June 2004 to May 2005 at the 22 wind atlas stations. The measurements were taken at 25 m a.g.l. (47 m a.g.l. for Abu Darag NW and Zafarana M7) and averaged in 1 ms^{-1} bins. Reanalysis of the turbulence characteristics can readily be carried out from the wind speed data in the meteorological data base.

For other sites and heights, as well as other applications, the turbulence characteristics must be estimated from the wind speed values, using information on the terrain surface roughness, height above ground level and atmospheric stability; as described by e.g. Panofsky and Dutton (1984) or Mann et al. (2002).

Table 8-1. Measured turbulence intensities at 25 (or 47) m a.g.l. at 22 wind atlas stations: Weibull A- and k-parameters, mean wind speed U, mean turbulence intensities I_5, I_{10} and I_{15} at 5, 10 and 15 ms^{-1}, respectively. The averaging period is 10 minutes, except for Shark El-Ouinat where it is 60 minutes. Values calculated from less than 10 observations are given in parentheses.

Region/Station	***A*** [ms^{-1}]	***k***	***U*** [ms^{-1}]	I_5 [%]	I_{10} [%]	I_{15} [%]
Northwest Coast						
El-Mathany	6.4	2.33	5.7	10.3	10.7	12.5
Ras El-Hekma	7.2	2.23	6.4	10.1	9.8	9.9
El-Galala	6.7	2.41	5.9	9.4	10.5	11.1
Northeast Coast						
Port Said	5.3	2.32	4.7	11.0	11.6	(13.2)
Gulf of Aqaba						
Nuweiba	6.2	2.58	5.6	11.2	8.4	(6.8)
Nabq	7.7	2.04	6.8	10.2	9.8	9.8
Gulf of Suez						
Katamaya	6.0	2.66	5.4	11.6	10.2	11.3
Ras Sedr	8.5	3.06	7.6	8.8	8.0	8.5
Abu Darag NW (47 m)	9.6	3.34	8.6	10.2	9.9	10.2
Abu Darag	10.1	3.50	9.1	10.1	10.5	10.6
Zafarana M7 (47 m)	11.1	3.57	10.0	11.7	10.0	8.9
Zafarana	10.2	3.19	9.1	9.9	8.2	8.9
Saint Paul	9.4	3.25	8.5	8.5	8.7	8.7
Ras Ghareb	11.0	3.40	9.9	10.5	7.6	7.9
Gulf of El-Zayt NW	11.8	3.70	10.7	10.4	8.2	8.2
Gulf of El-Zayt	11.5	3.29	10.3	9.9	8.0	8.4
Red Sea						
Hurghada WETC	7.6	2.32	6.7	10.3	10.0	10.2
Kosseir	6.4	2.28	5.6	8.8	10.1	10.7
Western Desert						
Kharga	7.4	2.57	6.6	10.1	9.6	8.6
Dakhla South	7.3	3.31	6.6	10.3	8.4	(9.9)
Shark El-Ouinat	7.2	3.29	6.5	13.1	11.0	10.0
Abu Simbel	6.4	2.76	5.7	10.8	9.3	(8.2)

9 References

Adrian, G. (1994). Zur Dynamik des Windfeldes über orographisch gegliedertem Gelände, Ber. Deutschen Wetterdienstes 188, Offenbach am Main 1994. 142 pp.

Adrian, G. and F. Fiedler (1991). Simulation of unstationary wind and temperature fields over complex terrain and comparison with observations. Beitr. Phys. Atmosph. 64, 27-48.

Bowen, A.J. and N.G. Mortensen (1996). Exploring the limits of WAsP: the Wind Atlas Analysis and Application Program. Proceedings of the 1996 European Union Wind Energy Conference, Göteborg, Sweden, May 20-24, 584-587.

Busch, N.E., O. Christensen, L. Kristensen, L. Lading and S.E. Larsen (1980). Cups, vanes, propellers and laser anemometers. Air-Sea Interaction–Instruments and Methods, Plenum Press, New York, 11-46.

Businger, J. (1973). Turbulent transfer in the atmospheric surface layer. In: Workshop on Micrometeorology. Ed. by D.A. Haugen. American Meteor. Soc., Boston, Mass. 67-100.

Chamberlain, A.C. (1983). Roughness lengths of sea, sand, and snow. Boundary-Layer Meteorol. 25, 405-409.

Charnock, H. (1955). Wind stress on a water surface. Quart. J. Roy. Meteor. Soc. 81, 639-640.

Cook, N.J. (1985). The designer's guide to wind loading of building structures. Part 1: Background, damage survey, wind data and structural classification. Butterworths, London, 1985. 371 pp.

Dyer, A.J. (1974). A review of flux-profile relationships. Boundary-Layer Meteorol. 7, 363-372.

Egyptian Meteorological Authority (1996). Climatic Atlas of Egypt. Egyptian Meteorological Authority, Cairo. 160 pp.

Elliot, D.L., C.G. Holladay, D.S. Renne and M.N. Schwartz (1986). Wind energy resource analysis for Egypt. Batelle, Pacific Northwest Laboratories, Richland, Washington. 35 pp. + 1 appendix.

Elliott, D.L., D.S. Renne and K. Bassyouni (1987). Wind energy resource assessment of Egypt. Proceedings of the Sixth ASME Wind Energy Symposium, Dallas, Texas, 1987, vol. 3, 215-216.

Essa, K.S.M. and M. Embaby (2005). Statistical evaluation of wind energy at Inshas, Egypt. Wind Engineering 29, 83-88.

Farr, T.G., M. Kobrick, 2000, Shuttle Radar Topography Mission produces a wealth of data, Amer. Geophys. Union Eos, v. 81, p. 583-585.

Frank, H.P. (2000). Wind Simulations for the Gulf of Suez with KAMM. Risø National Laboratory, Roskilde.

Frank, H.P. and L. Landberg (1997a). Modelling the wind climate of Ireland. Boundary-Layer Meteorol. 85, 359-378.

Frank, H.P. and L. Landberg (1997b). Numerical simulation of the Irish wind climate and comparison with wind atlas data, Proceedings of the European Wind Energy Conference, Dublin, Ireland, 6-9 October 1997, pp. 309-312.

Frey-Buness, F., D. Heimann and R. Sausen, (1995). A statistical-dynamical downscaling procedure for global climate simulations, Theor. Appl. Climatol. 50, 117-131.

Golder, D. (1972). Relations among stability parameters in the surface layer. Boundary-Layer Meteorol. 3, 47-58.

Griffiths, J.F. and H. Soliman (1972). The Northern Desert (Sahara). In: World Survey of Climatology Volume 10 (The climates of Africa, ed. J.F. Griffiths), 75-132. Elsevier, Amsterdam.

Hansen, J.C. and S.E. Larsen (1991). Site selection and sketch design for Hurghada Wind Energy Technology Centre and Demonstration Wind Farm. Risø National Laboratory, Roskilde. 97 pp.

Hansen, J.C. and U. Said Said (1993). A preliminary wind resource assessment at Ras Abu Darag and Zafarana. Internal project document. Risø National Laboratory and New and Renewable Energy Authority, 9 pp.

Hansen, J.C., N.G. Mortensen and U. Said Said (1999). Wind resource modelling for micro-siting–validation at a 60-MW wind farm site. In: Wind energy for the next millennium. Proceedings. 1999 European wind energy conference (EWEC '99), Nice (FR), 1-5 Mar 1999. Petersen, E.L.; Hjuler Jensen, P.; Rave, K.; Helm, P.; Ehmann, H. (eds.), (James and James Science Publishers, London, 1999) p. 1181-1184.

Jackson, P.S. and J.C.R. Hunt (1975). Turbulent wind flow over a low hill. Quart. J. Roy. Meteor. Soc. 101, 929-955.

Jensen, N.O, E.L. Petersen and I. Troen (1984). Extrapolation of mean wind statistics with special regard to wind energy applications. World Meteorological Organization, WCP-86. 85 pp.

Jensen, N.O. and L. Kristensen (1989). Gust statistics for the Great Belt Region. Risø-M-2828. 21 pp.

Jensen, N.O. and B. Nielsen (1989). Extreme values of wind speeds over the Great Belt region. Risø–M-2829. 23 pp.

Jensen, N.O., J. Mann and L. Kristensen (1992). Aspects of the natural wind of relevance to large bridges. In: Aerodynamics of large bridges, A. Larsen (ed.), Balkema, Rotterdam, 25-32.

Jørgensen, H.E., D.N. Heathfield, J. Mann, M. Nielsen and N.G. Mortensen (2005). WAsP Engineering User's Guide. Risø-I-2391(EN). 70 pp.

Kalnay, E., M. Kanamitsu, R. Kistler, W. Collins, D. Deaven, L. Gandin, M. Iredell, S. Saha, G. White, J. Woollen, Y. Zhu, A. Leetmaa, R. Reynolds, M. Chelliah, W. Ebisuzaki, W. Higgins, J. Janowiak, K. C. Mo, C. Ropelewski, J. Wang, R. Jenne, and D. Joseph (1996). The NCEP/NCAR 40-year reanalysis project, Bull. Amer. Meteor. Soc. 77, 437-471.

Klemp, J.B. and D.R. Durran (1983). An upper boundary condition permitting internal gravity wave radiation in numerical mesoscale models. Mon. Wea. Rev. 1983 vol. 111, 430-444.

Kristensen, L. (1993). The cup anemometer and other exciting instruments. Risø-R-615(EN). 82 pp.

Kristensen, L. (1998). Cup anemometer behavior in turbulent environments. J. Atmos. Ocean. Tecnol. 15, 5-17.

Kristensen, L. (1999). The perennial cup anemometer. Wind Energy 2, 59-75.

Kristensen, L. and Ole F. Hansen (2002). Distance Constant of the Risø Cup Anemometer. Risø-R-1320(EN). 25 pp.

Landberg, L., S. Frandsen, K. Thomsen, S. Larsen, J. Mann, N.O. Jensen and N.G. Mortensen (2001). Site assessment – a guide. Report UVE 51171/98-0035, Risø National Laboratory, Roskilde, 31 pp.

Larsen, S.E. and J.C. Hansen (1991). Wind assessment at the Red Sea coast area–site survey, station descriptions and planning of supplementary measurements. Risø National Laboratory, Roskilde. 27 pp.

Lockwood, J.G. (1974). World climatology–an environmental approach. Edward Arnold, London. 330 pp.

Manes, A., M. Rindsberger and L. Segal (1980). Wind power resources in Israel and eastern Mediterranean. Ministry of Transport, Israel Meteorological Service, Bet-Dagan, Israel. 177 p + 2 appendices.

Mann, J., S. Ott, B.H. Jørgensen and H.P. Frank (2002). WAsP Engineering 2000. Risø-R-1356(EN). Risø National Laboratory, Roskilde. 90 pp.

Mobarak, A. (1992). Generation of electric power from large wind farms at the Gulf of Suez area. Report, Cairo University, Cairo. 170 pp.

Mobarak, A., A. El-Mallah and M.A. Serag El-Din (1982). Wind energy in Egypt. Report, Cairo University, Cairo. 150 pp.

Mortensen, N.G. and G. Jensen (1986). Radiation screens for temperature measurement (Strålingsskærme for temperaturmåling). In Danish. Vejret 28: 19-24.

Mortensen, N.G. and G. Jensen (1987). One step forward and two steps back. The story of a radiation screen (Et skridt frem og to tilbage. Historien om en strålingsskærm). In Danish. Vejret 33: 13-15.

Mortensen, N.G. and E.L. Petersen (1997). Influence of topographical input data on the accuracy of wind flow modelling in complex terrain. Proceedings of the 1997 European Wind Energy Conference, Dublin, Ireland, October 6-9, 317-320.

Mortensen, N.G., L. Landberg, I. Troen, E.L. Petersen, O. Rathmann and M. Nielsen (2004). WAsP Utility programs. Risø-I-2261(EN). Risø National Laboratory, Roskilde. 52 pp.

Mortensen, N.G. and U.S. Said (1996). Wind Atlas for the Gulf of Suez. Measurements and modelling 1991-95. ISBN 87-550-2143-3. Risø National Laboratory, Roskilde; New and Renewable Energy Authority, Cairo. 114 pp.

Mortensen, N.G., U. Said Said, H.P. Frank, L. Georgy, C.B. Hasager, M. Akmal, J.C. Hansen and A. Abdel Salam (2003). Wind Atlas for the Gulf of Suez. Measurements and Modelling 1991-2001. New and Renewable Energy Authority, Cairo, and Risø National Laboratory, Roskilde. ISBN 87-550-3195-1. 196 pp.

Mortensen, N.G., A.M. El-Asrag, M.A.M. Sayed, M.A.A. Hussein and A.M. Awad (2004). Preliminary Wind Atlas for Egypt. Egyptian Meteorological Authority, Cairo, and Risø National Laboratory, Roskilde. 189 pp.

Mortensen, N.G., D.N. Heathfield, L. Myllerup, L. Landberg and O. Rathmann (2005). Wind Atlas Analysis and Application Program: WAsP 8 Help Facility. Risø National Laboratory, Roskilde, Denmark. 335 topics. ISBN 87-550-3457-8.

Nof, D. and N. Paldor (1994). Statistics of wind over the Red Sea with application to the Exodus question. J. Appl. Met. 33, 1017-1025.

Oberhettinger, F. (1973). Fourier expansions. A collection of formulas. Academic Press, New York and London. 64 pp.

Owen, P.R. (1964). Saltation of uniform sand grains in air. J. Fluid Mech. 20, 225-242.

Palmén, E. (1951). The rôle of atmospheric disturbances in the general circulation. Quart. J. Roy. Meteor. Soc. 77, 337-354.

Panofsky, H.A. (1973). Tower micrometeorology. In: Workshop on micrometeorology. Ed. D.A. Haugen, American Meteorological Society, Boston, Mass., 151-176.

Panofsky, H. A. and Dutton, J. A. (1984). Atmospheric turbulence. Models and methods for engineering applications. John Wiley and Sons, New York, 1984. 397 pp.

Perera, M.D. (1981). Shelter behind two-dimensional solid and porous fences. J. Wind Engin. and Industrial Aerodyn. 8, 93-104.

Rao, K.S., J.C. Wyngaard and D.R. Coté (1974). The structure of the two-dimensional internal boundary layer over a sudden change of surface roughness. J. Atmos. Sci. 26, 432-440.

Rasmussen, K.R. and H.E. Mikkelsen (1991). Wind tunnel observations of aeolian transport rates. Acta Mechanica 1, 135-144.

Rasmussen, K.R., J.D. Iversen and P. Rautaheimo (1995). Saltation and wind-flow interaction in a variable slope wind tunnel. To be published in Geomorphology.

Renne, D.S. and B.D. Holst (1985). Wind characteristics for wind energy use in Egypt – workshop. BN-SA-2237. Batelle, Pacific Northwest Laboratories, Richland, Washington. 120 pp.

Renne, D.S. and B.D. Holst (1985). Wind characteristics for wind energy use in Egypt – seminar. BN-SA-2238. Batelle, Pacific Northwest Laboratories, Richland, Washington. 88 pp.

Renne, D.S., D.L. Elliott, B.D. Holst and K. El-Bassyouni (1986). Wind energy resource assessment activities in Egypt. Proceedings of the European Wind Energy Association Conference and Exhibition, Rome, October 7-9, 1986, 299-304.

Rossby C.-G. and R.B. Montgomery (1935). The layer of frictional influence in wind and ocean currents. Papers in Phys. Oceanogr. Meteor., MIT and Woods Hole Oceanogr. Inst., III no. 3. 101 pp.

Scharl, G. (1988). Results of the wind measurements on the Sinai peninsula, Report 4, December 1986–January 1988.

Sempreviva, A.M., S.E. Larsen, N.G. Mortensen and I. Troen (1990). Response of neutral boundary layers to changes of roughness. Boundary-Layer Meteorology 50: 205-225.

Troen, I. and A.F. de Baas (1986). A spectral diagnostic model for wind flow simulation in complex terrain. Proceedings of the European Wind Energy Association Conference and Exhibition, Rome, October 7-9, 1986, 243-249.

Troen, I. and E.L. Petersen (1989). European Wind Atlas. Risø National Laboratory, Roskilde. 656 pp. ISBN 87-550-1482-8.

Walmsley, J.L., J.R. Salmon and P.A. Taylor (1982). On the application of a model of boundary-layer flow over low hills to real terrain. Boundary-Layer Meteorol. 23, 17-46.

Weibull, W. (1951). A statistical distribution function of wide applicability. J. Appl. Mech. 18, 293-297.

Wood, N. (1995). The onset of separation in neutral, turbulent flow over hills. Boundary-Layer Meteorology 76, 137-164.

9.1 Web pages and ftp sites

Coastline Extractor.
National Geophysical Data Center (NGDC).
rimmer.ngdc.noaa.gov/mgg/coast/getcoast.html

Egyptian Meteorological Authority, Cairo, Egypt.
www.nwp.gov.eg/

Global Land Cover Classification (GLCC).
United States Geological Survey (USGS).
edcsns17.cr.usgs.gov/glcc/

Google Earth – Home.
Google Inc.
earth.google.com

GTOPO30 – Global Topographic Data.
United States Geological Survey (USGS).
edcdaac.usgs.gov/gtopo30/gtopo30.asp

NCEP/NCAR Global Reanalysis Data.
Climate Diagnostics Centre.
www.cdc.noaa.gov/cdc/reanalysis/

New and Renewable Energy Authority, Cairo, Egypt.
www.nrea.gov.eg/

Risø National Laboratory, Roskilde, Denmark.
www.risoe.dk/vea

Shuttle Radar Topography Mission.
NASA, Jet Propulsion Laboratory.
www2.jpl.nasa.gov/srtm (web page)
ftp://e0srp01u.ecs.nasa.gov/srtm/version2 (ftp site)

SRTM Water Body Data.
NASA, Jet Propulsion Laboratory.
www2.jpl.nasa.gov/srtm (web page)
ftp://e0srp01u.ecs.nasa.gov/srtm/version2 (ftp site)

WAsP – the Wind Atlas Analysis and Application Program.
Risø National Laboratory.
www.wasp.dk

WAsP Engineering.
Risø National Laboratory.
www.waspengineering.dk

Wind Atlases of the World – the World of Wind Atlases.
Risø National Laboratory.
www.windatlas.dk

A The meteorological stations

The meteorological instrumentation used for the 22 wind atlas stations was supplied by Aanderaa Instruments and the Wind Energy Department at Risø. It consists of a data logger with a data storage unit, as well as sensors to measure wind speed, wind direction, air temperature, atmospheric pressure and solar radiation. The sensors and data logger are mounted on 24- or 47-m high triangular, lattice towers, see Figure A-1.

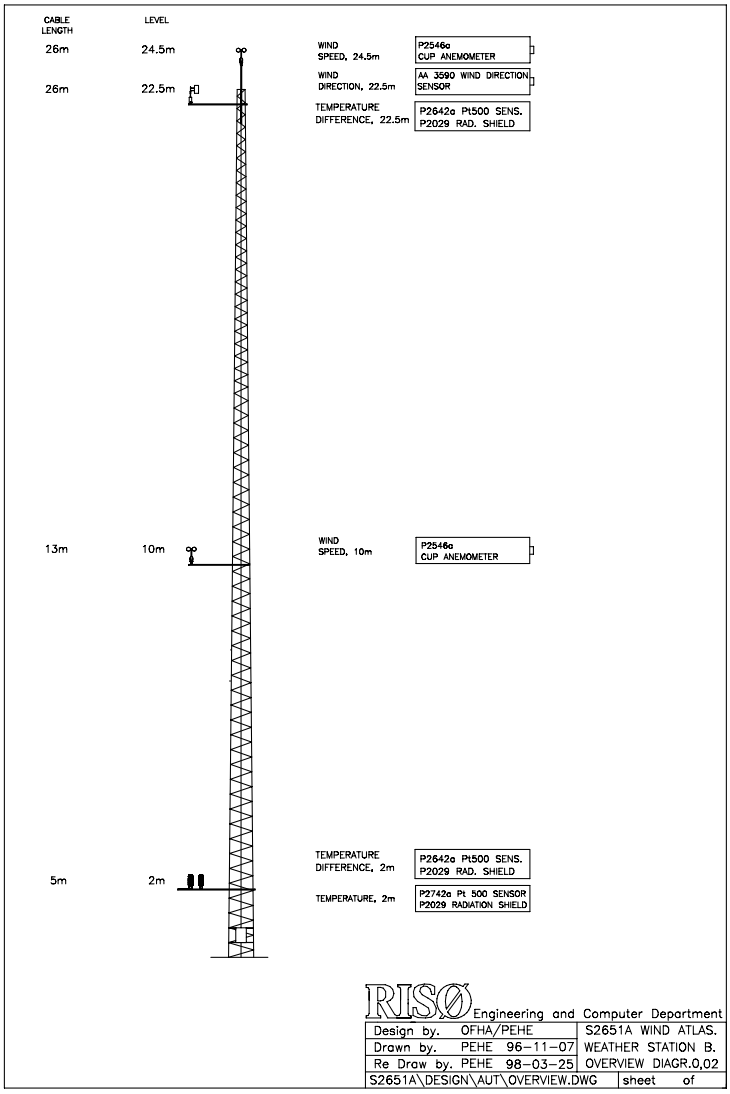

Figure A-1. Sketch of the meteorological mast and instrumentation at Hurghada Wind Energy Technology Centre. A solar radiation sensor and barometer are also mounted at this station.

A.1 Wind atlas stations 2004-05

Table A-1 provides an overview of the parameters measured at each of the 10 wind atlas stations erected and employed for the 2004-05 measuring campaign. The ten possible parameters are: wind speed (U_{10} and U_{25}), standard deviation of wind speed (S_{25}), gust wind speed (G_{25}), lull wind speed (L_{25}), mean wind direction (D_{25}), air temperature (T_2), air temperature gradient (ΔT), atmospheric pressure (B) and short-wave solar radiation (S_i).

Table A-1. Configuration of the 10 wind atlas stations employed from 2004-05.

Station	U_{10}	U_{25}	S_{25}	G_{25}	L_{25}	D_{25}	T_2	ΔT	B	S_i
El-Mathany	●	●	●	●	●	●	n/a	n/a	n/a	n/a
Ras El-Hekma	n/a	●	●	●	●	●	n/a	n/a	n/a	n/a
El-Galala	●	●	●	●	●	●	n/a	n/a	n/a	n/a
Port Said	n/a	●	●	●	●	●	n/a	n/a	n/a	n/a
Katamaya	●	●	●	●	●	●	n/a	n/a	n/a	●
Nuweiba	n/a	●	●	●	●	●	●	n/a	n/a	n/a
Nabq	n/a	●	●	●	●	●	n/a	n/a	n/a	●
Kharga	●	●	●	●	●	●	●	n/a	●	n/a
Abu Simbel	●	●	●	●	●	●	●	n/a	●	n/a
Dakhla South	●	●	●	●	●	●	●	n/a	●	n/a

A.2 Long-term wind atlas stations

The set-up and configuration of 10 long-term stations: Ras Sedr, Abu Darag, Zafarana, St. Paul, Ras Ghareb, Gulf of El-Zayt NW, Gulf of El-Zayt, Hurghada WETC, Kosseir and Shark El-Ouinat were described by Mortensen et al. (2003). Table A-2 provides an overview of the instrumentation used and the parameters measured at each of these 10 long-term stations.

Table A-2. Configuration of the 10 long-term wind atlas stations.

Station	U_{10}	U_{25}	S_{25}	G_{25}	L_{25}	D_{25}	T_2	ΔT	B	S_i
Ras Sedr	n/a	●	●	●	●	●	●	n/a	n/a	n/a
Abu Darag	●	●	●	●	●	●	●	●	●	n/a
Zafarana	n/a	●	●	●	●	●	●	n/a	n/a	n/a
St. Paul	n/a	●	●	●	●	●	n/a	n/a	n/a	n/a
Ras Ghareb	●	●	●	●	●	●	●	●	●	n/a
Gulf of El-Zayt NW	●	●	●	●	●	●	●	n/a	n/a	n/a
Gulf of El-Zayt	●	●	●	●	●	●	●	●	●	n/a
Hurghada WETC	n/a	●	●	●	●	●	●	●	●	n/a
Kosseir	●	●	●	●	●	●	●	n/a	n/a	n/a
Shark-El-Ouinat	●	●	●	●	●	●	●	n/a	●	n/a

In addition to these 10 stations, the atlas contains data from two auxiliary stations in the Zafarana area, see Table A-3. These masts are 45 m high, plus a top pole.

Table A-3. Configuration of two auxiliary stations in the Gulf of Suez.

Station	U_{25}	U_{47}	S_{47}	G_{47}	L_{47}	D_{45}	T_2	ΔT	B	S_i
Abu Darag NW	n/a	●	●	●	●	●	n/a	n/a	n/a	n/a
Zafarana M7	●	●	●	●	●	●	●	n/a	●	n/a

The Wind Atlas for Egypt project has thus erected and operated 22 wind atlas stations for the investigation of the Egyptian wind resources; a more detailed description of the instrumentation of these stations is given below.

In addition, eight meteorological stations operated by the Egyptian Meteorological Authority (EMA) have been employed for the study; these stations are instrumented according to WMO requirements and are described elsewhere.

A.3 Station instrumentation

The data logger used at the wind atlas stations is the Aanderaa Sensor Scanning Unit 3010 or the Aanderaa Sensor Scanning Unit 3660. These 10-bit data loggers scan, read and store up to 12/18 channels of Aanderaa sensors. Other sensors can also be used provided they are interfaced properly. The sampling interval (and averaging time) used here is 10 minutes and a built-in quartz clock triggers the scanning. The accuracy of the data logger is ±1 data bit.

Data are stored on site in an Aanderaa Data Storing Unit 2990. This portable, reusable, solid-state memory module can store about 65,500 ten-bit data words and further features a preset-able, real-time clock for recording of date/time information. Data stored in the DSU are transferred to a PC-computer by means of a DSU Reader 2995.

Wind speed

Wind speed is measured with cup anemometers of the Risø-70 type (Busch et al, 1980), manufactured by the Wind Energy Department at Risø (P2546a). This anemometer features a lightweight 3-cup rotor and is a sturdy, yet fast-responding anemometer. The calibration is linear with an offset ('starting speed') of approx. 0.2 ms^{-1}. The distance constant is about 1.8 m (Kristensen and Hansen, 2002).

The response characteristics and associated errors of this anemometer were reviewed by Kristensen (1993, 1998, 1999). Kristensen discusses four types of overspeeding: i) *u*-bias or 'overspeeding', causing too high measured wind speeds because the cup anemometer responds more quickly to an increase in the wind speed than to a decrease of the same magnitude; ii) *v*-bias or the so-called DP-error (data processing 'error') which accounts for the fact that the cup anemometer is not a vector instrument, but measures the mean of the total horizontal wind speed; iii) *w*-bias and iv) stress-bias which are equal to zero only if the anemometer has an ideal cosine response.

The cup anemometer biases are proportional to $(\sigma_u/U)^2$, $(\sigma_v/U)^2$, $(\sigma_w/U)^2$ and $\langle uw \rangle/U^2$, respectively. The errors associated with these biases (i.e. *i*, *iii* and *iv*) are for the Risø-70 anemometer of the order of 1% and can be neglected in most applications (Kristensen, 1993). The wind speed measurements reported here are therefore thought to be accurate to within ±1% of the actual reading above about 5 ms^{-1}, and to ±0.05 ms^{-1} below 5 ms^{-1} (Busch et al, 1980).

A Risø wind speed processor (type P2706a) is used to measure the output pulse rate from the cup anemometer and to calculate the mean wind speed, the standard deviation of wind speed, the gust wind speed and the lull wind speed. The gust and lull wind speeds are the maximum and minimum values, respectively, of the wind speed in a 2-second window, which is updated continuously during the averaging period.

Wind direction

Wind direction is measured with Aanderaa wind vanes, type 3590. This sensor consists of a light wind vane pivoted on top of a cylindrical housing. A magnet on the wind vane couples the vane movement to a compass inside the housing. Wind direction is measured every second by four Hall elements and a micro-controller calculates the mean wind direction for the 10-min averaging period. According to Aanderaa

Instruments, the threshold speed is less than 0.3 ms^{-1}, the operating temperature range is from -40°C to 50°C and the accuracy is better than ±5 degrees.

Air temperature

Air temperature is measured with Risø pt-500 resistance temperature sensors (type P2742a) mounted in Aanderaa 4011 radiation screens. The sensor is formed as an ohmic halfbridge and the sensing element is a 500 Ω platinum resistor. The measuring range is from -44°C to 49°C with a resolution of 0.1°C. The time constant of the sensor is about one minute; the accuracy depends entirely on the experimental set-up – in particular the efficiency of shielding of the sensor from radiation.

The radiation screen is a small, cylindrical, Thaller-type shield made from 9 stacked plastic plates. The plates are shiny-white on the outside and matte-black on the inside. It is a so-called passive shield, ventilated only by ambient airflow. Field comparisons of several active and passive radiation shields have shown (Mortensen and Jensen; 1986, 1987) this shield to be superior to the traditional Stevenson screen and comparable to active shields under most atmospheric conditions. Tests over grass-covered surfaces indicate that the average temperature differences between the Aanderaa screen and active screens are less than 0.1°C for wind speeds above 2-3 ms^{-1}. At lower wind speeds, the radiation error increases with decreasing wind speed and errors of up to one or more degrees may be experienced in calm weather and very high solar insolation. These effects are probably augmented over sandy surfaces, which have a higher albedo than grass.

Temperature difference

Temperature difference is measured by two coupled Risø pt-500 temperature sensors (type 2642), both mounted in Aanderaa 4011 radiation shields. The resolution of this set-up is about 0.05°C and the accuracy in the temperature gradient is better than stated above for absolute temperature, since the errors in the two levels are of the same order.

Atmospheric pressure

Barometric pressure is measured with an Aanderaa air pressure transducer 2810. The sensing element is a small, 4×4 mm^2 silicon chip. A thin membrane in the central area of this chip is exposed to atmospheric pressure on one side and to vacuum on the other. The membrane is furnished with four diffused resistors that form a Wheatstone bridge, providing an output signal proportional to the atmospheric pressure. The sensor acts as an absolute pressure-sensing device with a measuring range of 920-1080 hPa and a resolution of 0.2 hPa. The operating temperature range is from -40°C to 47°C and the accuracy is ±0.2 hPa according to the manufacturer.

Solar radiation

Solar and sky short-wave radiation is measured with an Aanderaa solar radiation sensor 2770. The sensor employs a high-sensitivity thermistor bridge, which measures the temperature rise of a black surface under a glass dome. The sensor measures the radiation in the wavelength range 0.3 to 2.5 μm with a resolution of 4 Wm^{-2} and accuracy better than ±20 Wm^{-2}.

B The meteorological data base

The meteorological measurements from the 22 wind atlas stations are stored in yearly, sequential ASCII data files with one observation (scan) per file record. The numbers in one record are separated by at least one blank character and can thus be read with either a fixed or free-format statement, e.g.:

```
52551  9.22 10.37  1.38 13.41  7.03 349  15.7   0.13 1018.5    4 200112312235
52552 10.21 11.23  1.15 13.25  7.65 351  15.6   0.13 1018.3    4 200112312245
52553 10.84 12.01  1.09 14.65  8.89 347  15.7   0.19 1018.5    4 200112312255
52554 10.80 11.85  1.26 14.81  8.58 346  15.6   0.13 1017.8    4 200112312305
52555 11.63 12.79  0.97 15.28  9.52 347  15.6   0.19 1017.8    4 200112312315
52556 10.90 12.16  1.34 15.12  9.05 348  15.6   0.13 1017.8    4 200112312325
52557 11.76 12.94  1.32 16.06  9.21 346  15.5   0.13 1017.5    4 200112312335
52558 11.76 13.10  1.36 16.21  9.83 344  15.5   0.19 1017.3    4 200112312345
52559 11.99 13.33  1.38 15.90  9.98 346  15.5   0.08 1017.5    4 200112312355
```

The contents and format of the 2000-05 data files are specified in Table B-1 below. The same format is used for all data files regardless of the station configuration. Missing channels or data are flagged by so-called dummy values.

Table B-1. Format of the meteorological data files from the 12 wind atlas stations 2000-04. The flag values are used for missing or erroneous observations in the data file – also when a parameter has not been measured at all at the station.

#	Parameter	Symbol	Height	Units	Format	Flag
1	Scan number	N	n/a	n/a	I5	n/a
2	Wind speed	U_{10}	10	[ms^{-1}]	F6.2	99.99
3	Wind speed	U_{25}	25	[ms^{-1}]	F6.2	99.99
4	Std. deviation	S_{25}	25	[ms^{-1}]	F6.2	99.99
5	Gust speed	G_{25}	25	[ms^{-1}]	F6.2	99.99
6	Lull speed	L_{25}	25	[ms^{-1}]	F6.2	99.99
7	Wind direction	D_{25}	25	[deg]	I4	999
8	Air temperature	T_2	2	[°C]	F6.1	999.9
9	Temp. gradient	ΔT		[°C]	F7.2	999.99
10	Atm. pressure	B	2	[hPa]	F7.1	9999.9
11	Solar radiation	S_i	2	[Wm^{-2}]	I5	9999
12	Date/time group	n/a	n/a	n/a	I13	n/a

Scan number The scan number is the number of the observation within the year in question. The first observation in a given year is recorded at 00:05 on the first day of the year (e.g. 199501010005) and is given the number 0 (zero). The scan number thus takes values between 0 and 52,559 (or 52,703 for leap years).

Wind speed The mean wind speed, standard deviation of wind speed, gust speed and lull speed are given in meters per second with a resolution of 0.01 ms^{-1}. The speed indication in calm conditions is equivalent to the offset in the linear calibration of the anemometer in question – this value is different for each anemometer, but usually about 0.1-0.2 ms^{-1}.

Wind direction Wind directions are given in degrees (0-360°) relative to the geographic north direction. For the 2000-05 data at the 22 stations, wind directions are

calculated as averages over the 10 min. scanning interval – based on 1-Hz direction measurements. For the pre-2000 data at Abu Darag, Zafarana, Gulf of El-Zayt and Hurghada, the wind directions are instantaneous values, measured every 10 minutes.

Air temperature The air temperatures are given in degrees Celsius with a resolution of 0.1°C.

Air temperature gradient The vertical profile of air temperature measured at some stations is given in degrees with a resolution of 0.01°C.

Atmospheric pressure The atmospheric pressure measured at some stations is given in hPa with a resolution of 0.1 hPa. Pressures have not been reduced to mean sea level.

Solar radiation The solar radiation measured at Katamaya and Nabq is given in Watts per square meter with a resolution of one Watt per square meter.

Date/time group The date/time group refers to local time (Egyptian Standard Time = UTC + 2 hours) and contains 12 digits: CCYYMMDDhhmm, e.g. 199112312105 means December 31, 1991, at 21:05.

B.1 Formats used for 1991-99 data

Long-term data measured from 1991-99 exist for four Wind Atlas stations in the Gulf of Suez: Abu Darag, Zafarana, Gulf of El-Zayt and Hurghada. The formats used for these data are specified in Table B-2 and Table B-3 below.

Table B-2. Format of the meteorological data measured 1991-99 at Abu Darag, Zafarana and Gulf of El-Zayt. The flag value is also used for missing values in the data file. The two wind speeds are independent signals from the same cup anemometer.

#	Parameter	Symbol	Height	Units	Format	Flag
1	Scan number	N	n/a	n/a	I5	n/a
2	Wind speed	U_{25}	25	[ms^{-1}]	F6.2	99.99
3	Wind speed	U_{25}	25	[ms^{-1}]	F6.2	99.99
4	Wind direction	D_{25}	25	[deg]	I4	999
5	Air temperature	T_2	2	[°C]	F6.1	999.9
6	Date/time group	n/a	n/a	n/a	I13	n/a

Table B-3. Format of the meteorological data measured 1991-99 at Hurghada WETC. The flag value is also used for missing values in the data file.

#	Parameter	Symbol	Height	Units	Format	Flag
1	Scan number	N	n/a	n/a	I5	n/a
2	Wind speed	U_{10}	10	[ms^{-1}]	F6.2	99.99
3	Wind speed	U_{25}	25	[ms^{-1}]	F6.2	99.99
4	Wind direction	D_{25}	25	[deg]	I4	999
5	Air temperature	T_2	2	[°C]	F6.1	999.9
6	Temp. gradient	ΔT	24-2	[°C]	F7.2	999.99
7	Gust speed	G_{25}	25	[ms^{-1}]	F6.2	99.99
8	Atm. Pressure	B	1.5	[hPa]	F7.1	9999.9
9	Date/time group	n/a	n/a	n/a	I13	n/a

C Cup anemometer calibration facility

Regular maintenance and calibration of the anemometers are necessary prerequisites for obtaining accurate and reliable measurements of mean wind speed, turbulence intensity, gust wind speed and lull wind speed – not least when the measurements are used for wind resource assessment or power performance verification. NREA alone has almost 50 cup anemometers that need rehabilitation and recalibration at regular intervals, say, every 2-3 years.

A cup anemometer rehabilitation and recalibration facility was therefore established at the Hurghada Wind Energy Technology Center (WETC) as part of the Wind Atlas for Egypt project. The purpose of this facility is to enable NREA to rehabilitate and recalibrate their cup anemometers, i.e. to establish an accurate relation between the ambient wind speed and the anemometer output.

Figure C-1. Cup anemometer calibration facility at Hurghada WETC: upwind fetch to the NW (left) and details of the cup anemometer set-up (right).

At the calibration facility, up to 10 test cup anemometers are mounted on a horizontal boom, with a reliable reference anemometer in the center position, see Figure C-1. The reference instrument is calibrated in a certified wind tunnel, so for this anemometer the relation between wind speed and anemometer output is well known. By comparing the 10 test anemometers with the reference anemometer, similar relations can be established for the test anemometers. These relations can subsequently be used in the calibration software that is set up for each met. station operated by NREA.

This methodology has two important requirements in order to provide reliable calibration expressions for the cup anemometers:

- The comparisons should be made over such a long period of time – and range of wind speeds – that the calibrations are statistically stable and reliable. This

period is dependent on the wind climate (i.e. location and season), and range from a few weeks to more than a month.

- The anemometers must experience the same wind conditions in each of the 10-min data-collecting intervals. Therefore, only a narrow range of wind directions can be used and the upwind terrain (fetch) in this sector must be completely flat and uniform. At Hurghada WETC a 30°-degree sector from 323° to 353° is used.

In the siting of an anemometer calibration facility, the following additional requirements should be taken into account:

- The boom should be erected perpendicular to the prevailing wind direction, in most cases perpendicular to the direction of the mean wind vector.
- The upwind fetch must be as flat and uniform as possible, i.e. have the same land-use and terrain surface roughness length. If we require that the wind at the height of the anemometers (10 m above ground level) should be in equilibrium with the upstream terrain surface, there should be no changes of roughness within at least 100 times this height. Adding a safety margin of 50%, the upwind surface should then be uniform within at least 1500 m from the calibration facility.
- There should be no sheltering obstacles close to the calibration facility, especially in the upwind sector.
- The facility should be easily accessible for operation and maintenance.
- The facility should preferably be fenced in and/or guarded, to protect the instruments and accurate set-up from any changes caused by human activity.
- Any fence in the upwind direction must interfere as little as possible with the wind flow.

Results obtained so far from this in-situ calibration facility show that the calibration expressions are sufficiently reliable and accurate for wind resource assessment.

D WAsP version and configuration

The WAsP modelling results reported in this atlas were obtained using the most recent version of the *Wind Atlas Analysis and Application Program*, version 8.03.0012, 2005). This program, as well as the underlying wind atlas methodology, is described in some detail by Troen and Petersen (1989). Details of setting up and running the software are given by Mortensen *et al*. (2005). The standard configuration of the WAsP program has been used throughout the report.

In addition, the WAsP Observed Wind Climate Wizard version 2.0.62, the WAsP Climate Analyst version 1.01.0036, the WAsP Map Editor version 8.2.0.191 and the WAsP Utility Programs version 3.1 have been used.

The *Wind Atlas for Egypt* is the result of an investigation of the climatic wind conditions over the entire land area of the Arab Republic of Egypt.

The investigation was conducted from 1998-2005 by the New and Renewable Energy Authority, the Egyptian Meteorological Authority and Risø National Laboratory under the sponsorship of the governments of Egypt and Denmark.

The Atlas is an attempt to provide an updated overview of the wind-climatological conditions over Egypt, based on reliable wind data and employing contemporary meso- and micro-scale meteorological models. It further seeks to provide an up-to-date methodology for applying the wind statistics and model results for the purpose of wind resource assessment and siting of wind turbines and wind farms.

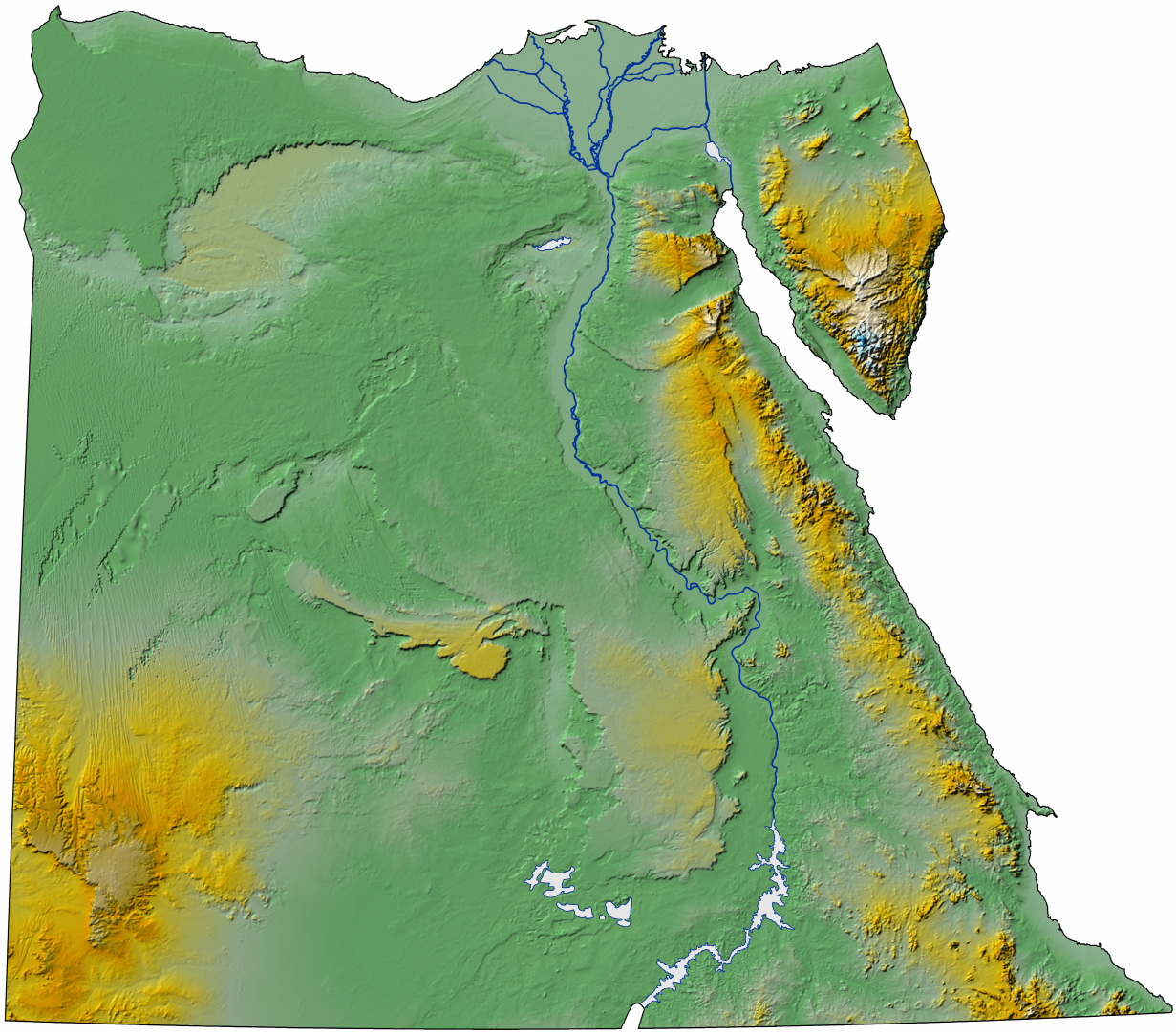

Wind Atlas for Egypt
ISBN 87-550-3493-4